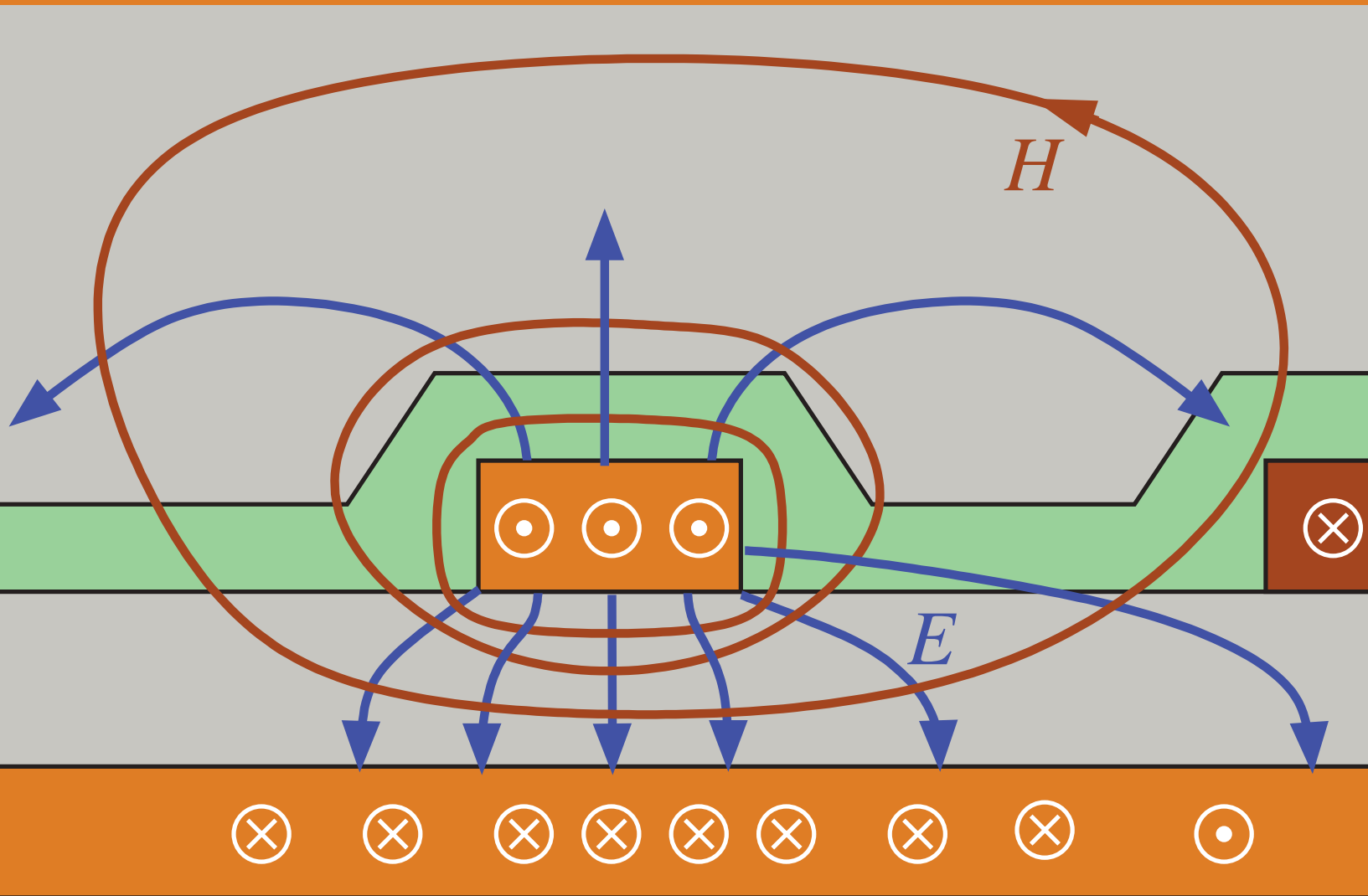


Volume 2

MICROWAVE AND RF DESIGN TRANSMISSION LINES



Michael Steer

Third Edition

Microwave and RF Design

Transmission Lines

Volume 2

Third Edition

Michael Steer

Microwave and RF Design *Transmission Lines*

Volume 2

Third Edition

Michael Steer

Copyright © 2019 by M.B. Steer

Citation: Steer, Michael. *Microwave and RF Design: Transmission Lines*. Volume 2. (Third Edition), NC State University, 2019. doi: <https://doi.org/10.5149/9781469656939> Steer

This work is licensed under a Creative Commons Attribution-NonCommercial 4.0 International license (CC BY-NC 4.0). To view a copy of the license, visit <http://creativecommons.org/licenses>.

ISBN 978-1-4696-5692-2 (paperback)
ISBN 978-1-4696-5693-9 (open access ebook)

Published by NC State University

NC STATE UNIVERSITY

Distributed by the University of North Carolina Press
www.uncpress.org

Printing: 1

To Conor and all my grandchildren

Preface

The book series *Microwave and RF Design* is a comprehensive treatment of radio frequency (RF) and microwave design with a modern “systems-first” approach. A strong emphasis on design permeates the series with extensive case studies and design examples. Design is oriented towards cellular communications and microstrip design so that lessons learned can be applied to real-world design tasks. The books in the Microwave and RF Design series are:

- Microwave and RF Design: Radio Systems, Volume 1
- Microwave and RF Design: Transmission Lines, Volume 2
- Microwave and RF Design: Networks, Volume 3
- Microwave and RF Design: Modules, Volume 4
- Microwave and RF Design: Amplifiers and Oscillators, Volume 5

The length and format of each is suitable for automatic printing and binding.

Rationale

The central philosophy behind this series’s popular approach is that the student or practicing engineer will develop a full appreciation for RF and microwave engineering and gain the practical skills to perform system-level design decisions. Now more than ever companies need engineers with an ingrained appreciation of systems and armed with the skills to make system decisions. One of the greatest challenges facing RF and microwave engineering is the increasing level of abstraction needed to create innovative microwave and RF systems. This book series is organized in such a way that the reader comes to understand the impact that system-level decisions have on component and subsystem design. At the same time, the capabilities of technologies, components, and subsystems impact system design. The book series is meticulously crafted to intertwine these themes.

Audience

The book series was originally developed for three courses at North Carolina State University. One is a final-year undergraduate class, another an introductory graduate class, and the third an advanced graduate class. Books in the series are used as supplementary texts in two other classes. There are extensive case studies, examples, and end of chapter problems ranging from straight-forward to in-depth problems requiring hours to solve. A companion book, *Fundamentals of Microwave and RF Design*, is more suitable for an undergraduate class yet there is a direct linkage between the material in this book and the series which can then be used as a career-long reference text. I believe it is completely understandable for senior-level students where a microwave/RF engineering course is offered. The book series is a comprehensive RF and microwave text and reference, with detailed index, appendices, and cross-references throughout. Practicing engineers will find the book series a valuable systems primer, a refresher as needed, and a

reference tool in the field. Additionally, it can serve as a valuable, accessible resource for those outside RF circuit engineering who need to understand how they can work with RF hardware engineers.

Organization

This book is a volume in a five volume series on RF and microwave design. The first volume in the series, *Microwave and RF Design: Radio Systems*, addresses radio systems mainly following the evolution of cellular radio. A central aspect of microwave engineering is distributed effects considered in the second volume of this book series, *Microwave and RF Design: Transmission Lines*. Here transmission lines are treated as supporting forward- and backward-traveling voltage and current waves and these are related to electromagnetic effects. The third volume, *Microwave and RF Design: Networks*, covers microwave network theory which is the theory that describes power flow and can be used with transmission line effects. Topics covered in *Microwave and RF Design: Modules*, focus on designing microwave circuits and systems using modules introducing a large number of different modules. Modules is just another term for a network but the implication is that it is packaged and often available off-the-shelf. Other topics that are important in system design using modules are considered including noise, distortion, and dynamic range. Most microwave and RF designers construct systems using modules developed by other engineers who specialize in developing the modules. Examples are filter and amplifier modules which once designed can be used in many different systems. Much of microwave design is about maximizing dynamic range, minimizing noise, and minimizing DC power consumption. The fifth volume in this series, *Microwave and RF Design: Amplifiers and Oscillators*, considers amplifier and oscillator design and develops the skills required to develop modules.

Volume 1: Microwave and RF Design: Radio Systems

The first book of the series covers RF systems. It describes system concepts and provides comprehensive knowledge of RF and microwave systems. The emphasis is on understanding how systems are crafted from many different technologies and concepts. The reader gains valuable insight into how different technologies can be traded off in meeting system requirements. I do not believe this systems presentation is available anywhere else in such a compact form.

Volume 2: Microwave and RF Design: Transmission Lines

This book begins with a chapter on transmission line theory and introduces the concepts of forward- and backward-traveling waves. Many examples are included of advanced techniques for analyzing and designing transmission line networks. This is followed by a chapter on planar transmission lines with microstrip lines primarily used in design examples. Design examples illustrate some of the less quantifiable design decisions that must be made. The next chapter describes frequency-dependent transmission line effects and describes the design choices that must be taken to avoid multimoding. The final chapter in this volume addresses coupled-lines. It is shown how to design coupled-line networks that exploit this distributed effect to realize novel circuit functionality and how to design networks that minimize negative effects. The modern treatment of transmission lines in this volume emphasizes planar circuit design and the practical aspects of designing

around unwanted effects. Detailed design of a directional coupler is used to illustrate the use of coupled lines. Network equivalents of coupled lines are introduced as fundamental building blocks that are used later in the synthesis of coupled-line filters. The text, examples, and problems introduce the often hidden design requirements of designing to mitigate parasitic effects and unwanted modes of operation.

Volume 3: Microwave and RF Design: Networks

Volume 3 focuses on microwave networks with descriptions based on S parameters and $ABCD$ matrices, and the representation of reflection and transmission information on polar plots called Smith charts. Microwave measurement and calibration technology are examined. A sampling of the wide variety of microwave elements based on transmission lines is presented. It is shown how many of these have lumped-element equivalents and how lumped elements and transmission lines can be combined as a compromise between the high performance of transmission line structures and the compactness of lumped elements. This volume concludes with an in-depth treatment of matching for maximum power transfer. Both lumped-element and distributed-element matching are presented.

Volume 4: Microwave and RF Design: Modules

Volume 4 focuses on the design of systems based on microwave modules. The book considers the wide variety of RF modules including amplifiers, local oscillators, switches, circulators, isolators, phase detectors, frequency multipliers and dividers, phase-locked loops, and direct digital synthesizers. The use of modules has become increasingly important in RF and microwave engineering. A wide variety of passive and active modules are available and high-performance systems can be realized cost effectively and with stellar performance by using off-the-shelf modules interconnected using planar transmission lines. Module vendors are encouraged by the market to develop competitive modules that can be used in a wide variety of applications. The great majority of RF and microwave engineers either develop modules or use modules to realize RF systems. Systems must also be concerned with noise and distortion, including distortion that originates in supposedly linear elements. Something as simple as a termination can produce distortion called passive intermodulation distortion. Design techniques are presented for designing cascaded systems while managing noise and distortion. Filters are also modules and general filter theory is covered and the design of parallel coupled line filters is presented in detail. Filter design is presented as a mixture of art and science. This mix, and the thought processes involved, are emphasized through the design of a filter integrated throughout this chapter.

Volume 5: Microwave and RF Design: Amplifiers and Oscillators

The fifth volume presents the design of amplifiers and oscillators in a way that enables state-of-the-art designs to be developed. Detailed strategies for amplifiers and voltage-controlled oscillators are presented. Design of competitive microwave amplifiers and oscillators are particularly challenging as many trade-offs are required in design, and the design decisions cannot be reduced to a formulaic flow. Very detailed case studies are presented and while some may seem quite complicated, they parallel the level of sophistication required to develop competitive designs.

Case Studies

A key feature of this book series is the use of real world case studies of leading edge designs. Some of the case studies are designs done in my research group to demonstrate design techniques resulting in leading performance. The case studies and the persons responsible for helping to develop them are as follows.

1. Software defined radio transmitter.
2. High dynamic range down converter design. This case study was developed with Alan Victor.
3. Design of a third-order Chebyshev combline filter. This case study was developed with Wael Fathelbab.
4. Design of a bandstop filter. This case study was developed with Wael Fathelbab.
5. Tunable Resonator with a varactor diode stack. This case study was developed with Alan Victor.
6. Analysis of a 15 GHz Receiver. This case study was developed with Alan Victor.
7. Transceiver Architecture. This case study was developed with Alan Victor.
8. Narrowband linear amplifier design. This case study was developed with Dane Collins and National Instruments Corporation.
9. Wideband Amplifier Design. This case study was developed with Dane Collins and National Instruments Corporation.
10. Distributed biasing of differential amplifiers. This case study was developed with Wael Fathelbab.
11. Analysis of a distributed amplifier. This case study was developed with Ratan Bhatia, Jason Gerber, Tony Kwan, and Rowan Gilmore.
12. Design of a WiMAX power amplifier. This case study was developed with Dane Collins and National Instruments Corporation.
13. Reflection oscillator. This case study was developed with Dane Collins and National Instruments Corporation.
14. Design of a C-Band VCO. This case study was developed with Alan Victor.
15. Oscillator phase noise analysis. This case study was developed with Dane Collins and National Instruments Corporation.

Many of these case studies are available as captioned YouTube videos and qualified instructors can request higher resolution videos from the author.

Course Structures

Based on the adoption of the first and second editions at universities, several different university courses have been developed using various parts of what was originally one very large book. The book supports teaching two or three classes with courses varying by the selection of volumes and chapters. A standard microwave class following the format of earlier microwave texts can be taught using the second and third volumes. Such a course will benefit from the strong practical design flavor and modern treatment of measurement technology, Smith charts, and matching networks. Transmission line propagation and design is presented in the context of microstrip technology providing an immediately useful skill. The subtleties of multimoding are also presented in the context of microstrip lines. In such

a class the first volume on microwave systems can be assigned for self-learning.

Another approach is to teach a course that focuses on transmission line effects including parallel coupled-line filters and module design. Such a class would focus on Volumes 2, 3 and 4. A filter design course would focus on using Volume 4 on module design. A course on amplifier and oscillator design would use Volume 5. This course is supported by a large number of case studies that present design concepts that would otherwise be difficult to put into the flow of the textbook.

Another option suited to an undergraduate or introductory graduate class is to teach a class that enables engineers to develop RF and microwave systems. This class uses portions of Volumes 2, 3 and 4. This class then omits detailed filter, amplifier, and oscillator design.

The fundamental philosophy behind the book series is that the broader impact of the material should be presented first. Systems should be discussed up front and not left as an afterthought for the final chapter of a textbook, the last lecture of the semester, or the last course of a curriculum.

The book series is written so that all electrical engineers can gain an appreciation of RF and microwave hardware engineering. The body of the text can be covered without strong reliance on this electromagnetic theory, but it is there for those who desire it for teaching or reader review. The book is rich with detailed information and also serves as a technical reference.

The Systems Engineer

Systems are developed beginning with fuzzy requirements for components and subsystems. Just as system requirements provide impetus to develop new base technologies, the development of new technologies provides new capabilities that drive innovation and new systems. The new capabilities may arise from developments made in support of other systems. Sometimes serendipity leads to the new capabilities. Creating innovative microwave and RF systems that address market needs or provide for new opportunities is the most exciting challenge in RF design. The engineers who can conceptualize and architect new RF systems are in great demand. This book began as an effort to train RF systems engineers and as an RF systems resource for practicing engineers. Many RF systems engineers began their careers when systems were simple. Today, appreciating a system requires higher levels of abstraction than in the past, but it also requires detailed knowledge or the ability to access detailed knowledge and expertise. So what makes a systems engineer? There is not a simple answer, but many partial answers. We know that system engineers have great technical confidence and broad appreciation for technologies. They are both broad in their knowledge of a large swath of technologies and also deep in knowledge of a few areas, sometimes called the “T” model. One book or course will not make a systems engineer. It is clear that there must be a diverse set of experiences. This book series fulfills the role of fostering both high-level abstraction of RF engineering and also detailed design skills to realize effective RF and microwave modules. My hope is that this book will provide the necessary background for the next generation of RF systems engineers by stressing system principles immediately, followed by core RF technologies. Core technologies are thereby covered within the context of the systems in which they are used.

Supplementary Materials

Supplementary materials available to qualified instructors adopting the book include PowerPoint slides and solutions to the end-of-chapter problems. Requests should be directed to the author. Access to downloads of the books, additional material and YouTube videos of many case studies are available at <https://www.lib.ncsu.edu/do/open-education>

Acknowledgments

Writing this book has been a large task and I am indebted to the many people who helped along the way. First I want to thank the more than 1200 electrical engineering graduate students who used drafts and the first two editions at NC State. I thank the many instructors and students who have provided feedback. I particularly thank Dr. Wael Fathelbab, a filter expert, who co-wrote an early version of the filter chapter. Professor Andreas Cangellaris helped in developing the early structure of the book. Many people have reviewed the book and provided suggestions. I thank input on the structure of the manuscript: Professors Mark Wharton and Nuno Carvalho of Universidade de Aveiro, Professors Ed Delp and Saul Gelfand of Purdue University, Professor Lynn Carpenter of Pennsylvania State University, Professor Grant Ellis of the Universiti Teknologi Petronas, Professor Islam Eshrah of Cairo University, Professor Mohammad Essaadi and Dr. Otman Aghzout of Abdelmalek Essaadi Univeristy, Professor Jianguo Ma of Guangdong University of Technology, Dr. Jayesh Nath of Apple, Mr. Sony Rowland of the U.S. Navy, and Dr. Jonathan Wilkerson of Lawrence Livermore National Laboratories, Dr. Josh Wetherington of Vadum, Dr. Glen Garner of Vadum, and Mr. Justin Lowry who graduated from North Carolina State University.

Many people helped in producing this book. In the first edition I was assisted by Ms. Claire Sideri, Ms. Susan Manning, and Mr. Robert Lawless who assisted in layout and production. The publisher, task master, and chief coordinator, Mr. Dudley Kay, provided focus and tremendous assistance in developing the first and second editions of the book, collecting feedback from many instructors and reviewers. I thank the Institution of Engineering and Technology, who acquired the original publisher, for returning the copyright to me. This open access book was facilitated by John McLeod and Samuel Dalzell of the University of North Carolina Press, and by Micah Vandergrift and William Cross of NC State University Libraries. The open access ebooks are host by NC State University Libraries.

The book was produced using LaTeX and open access fonts, line art was drawn using xfig and inkscape, and images were edited in gimp. So thanks to the many volunteers who developed these packages.

My family, Mary, Cormac, Fiona, and Killian, gracefully put up with my absence for innumerable nights and weekends, many more than I could have ever imagined. I truly thank them. I also thank my academic sponsor, Dr. Ross Lampe, Jr., whose support of the university and its mission enabled me to pursue high risk and high reward endeavors including this book.

Michael Steer
North Carolina State University
Raleigh, North Carolina
mbs@ncsu.edu

List of Trademarks

3GPP® is a registered trademark of the European Telecommunications Standards Institute.

802® is a registered trademark of the Institute of Electrical & Electronics Engineers .

APC-7® is a registered trademark of Amphenol Corporation.

AT&T® is a registered trademark of AT&T Intellectual Property II, L.P.

AWR® is a registered trademark of National Instruments Corporation.

AWRDE® is a trademark of National Instruments Corporation.

Bluetooth® is a registered trademark of the Bluetooth Special Interest Group.

GSM® is a registered trademark of the GSM MOU Association.

Mathcad® is a registered trademark of Parametric Technology Corporation.

MATLAB® is a registered trademark of The MathWorks, Inc.

NEC® is a registered trademark of NEC Corporation.

OFDMA® is a registered trademark of Runcom Technologies Ltd.

Qualcomm® is a registered trademark of Qualcomm Inc.

Teflon® is a registered trademark of E. I. du Pont de Nemours.

RFMD® is a registered trademark of RF Micro Devices, Inc.

SONNET® is a trademark of Sonnet Corporation.

Smith is a registered trademark of the Institute of Electrical and Electronics Engineers.

Touchstone® is a registered trademark of Agilent Corporation.

WiFi® is a registered trademark of the Wi-Fi Alliance.

WiMAX® is a registered trademark of the WiMAX Forum.

All other trademarks are the properties of their respective owners.

Contents

Preface	v
1 Introduction to Distributed Microwave Circuits	1
1.1 Introduction	1
1.2 Book Outline	2
1.3 Chapter Outline	5
1.4 Distributed Circuits	6
1.5 Maxwell's Equations	7
1.5.1 Point Form of Maxwell's Equations	8
1.5.2 Moments and Polarization	10
1.5.3 Field Intensity and Flux Density	11
1.5.4 Maxwell's Equations in Phasor Form	14
1.5.5 Integral Form of Maxwell's Equations	15
1.6 Electric and Magnetic Field Laws	16
1.6.1 Ampere's Circuital Law	16
1.6.2 Biot-Savart Law	16
1.6.3 Gauss's Law	17
1.6.4 Faraday's Law	18
1.7 Electromagnetic Fields in Dielectrics and Metals	19
1.7.1 Electromagnetic Fields in a Dielectric	19
1.7.2 Refractive Index	19
1.7.3 Electromagnetic Fields in a Metal	20
1.8 Electric and Magnetic Walls	21
1.8.1 Electric Wall	21
1.8.2 Magnetic Wall	23
1.9 Fields in Lossy Media	24
1.9.1 Lossy Dielectrics	24
1.9.2 Lossy Conductors	26
1.10 Summary	29
1.11 References	30
1.12 Exercises	30
1.12.1 Exercises By Section	32
1.12.2 Answers to Selected Exercises	32
1.A Mathematical Foundations	33
1.A.1 Angles of a Triangle	33
1.A.2 Trigonometric Identities	34
1.A.3 Trigonometric Derivatives	34
1.A.4 Complex Numbers and Phasors	34
1.A.5 Vector Operators	36
1.A.6 Hyperbolic Functions and Complex Numbers	39
1.A.7 Volumes and Areas	40
1.A.8 Series Expansions	40
1.A.9 Trigonometric Series Expansions	41
1.A.10 Special Polynomials	42

1.A.11	Matrix Operations	43
1.A.12	Interpolation	44
1.A.13	Circles on the Complex Plane	45
1.A.14	Bilinear Transform	46
1.A.15	Quadratic and Cubic Equations	48
1.A.16	Kron's Method: Network Condensation	48
2	Transmission Lines	51
2.1	Introduction	51
2.1.1	When Must a Line be Considered a Transmission Line	52
2.1.2	Movement of a Signal on a Transmission Line	52
2.2	Transmission Line Theory	55
2.2.1	Transmission Line RLGC Model	55
2.2.2	Derivation of Transmission Line Properties	56
2.2.3	Relationship of RLGC parameters to Permittivity and Permeability of a Medium	59
2.2.4	Dimensions of γ , α , and β	61
2.2.5	Lossless Transmission Line	62
2.2.6	Coaxial Line	62
2.2.7	Microstrip Line	65
2.2.8	Summary	66
2.3	The Lossless Terminated Line	66
2.3.1	Total Voltage and Current on the Line	67
2.3.2	Forward- and Backward-Traveling Pulses	69
2.3.3	Input Reflection Coefficient of a Lossless Line	71
2.3.4	Input Impedance of a Lossless Line	73
2.3.5	Standing Waves and Voltage Standing Wave Ratio	73
2.3.6	Summary	78
2.4	Special Lossless Line Configurations	78
2.4.1	Short Length of Short-Circuited Line	79
2.4.2	Short Length of Open-Circuited Line	79
2.4.3	Short-Circuited Stub	79
2.4.4	Open-Circuited Stub	82
2.4.5	Electrically Short Lossless Line	83
2.4.6	Quarter-Wave Transformer	85
2.4.7	Summary	87
2.5	The Lossy Terminated Line	87
2.5.1	Input Reflection Coefficient of a Lossy Line	87
2.5.2	Input Impedance of a Long Lossy Line	87
2.5.3	Input Impedance of a Lossy Line	88
2.5.4	Attenuation on a Low-Loss Line	89
2.5.5	Power Flow on a Terminated Lossy Line	90
2.5.6	Lossy Transmission Line Dispersion	91
2.5.7	Design of a Dispersionless Lossy Line	92
2.5.8	Summary	92
2.6	Reflections at Interfaces	92
2.6.1	Power Flow and Return Loss	93
2.6.2	Maximum Power Transfer Theorem	94
2.6.3	A Single Interface	96
2.6.4	Bounce Diagram	98
2.6.5	Theory of Small Reflections	102

2.7	Models of Transmission Lines	105
2.7.1	Circuit Models of Transmission Lines	105
2.7.2	$ABCD$ (Chain) Parameters of a Transmission Line . . .	108
2.8	Two-Conductor Transmission Lines	110
2.9	Coaxial Line	111
2.9.1	Characteristic Impedance of a Coaxial Line	111
2.9.2	Electromagnetic Fields on a Realistic Coaxial Line . . .	114
2.10	Summary	115
2.11	References	116
2.12	Exercises	117
2.12.1	Exercises By Section	122
2.12.2	Answers to Selected Exercises	122
2.A	Physical Constants and Material Properties	123
2.A.1	SI Units	123
2.A.2	Greek Alphabet and Additional Characters	127
2.A.3	Conductors, Dielectrics, and Magnetic Materials	127
3	Planar Transmission Lines	131
3.1	Introduction	131
3.2	Substrates	132
3.2.1	Dielectric Effect	133
3.2.2	Dielectric Loss Tangent, $\tan \delta$	133
3.2.3	Magnetic Material Effect	134
3.2.4	Substrates for Planar Transmission Lines	134
3.3	Planar Transmission Line Structures	135
3.3.1	Microstrip	136
3.3.2	Coplanar Waveguide	137
3.3.3	Coplanar Strip and Differential Line	137
3.3.4	Stripline	137
3.3.5	Embedded Differential Line	138
3.4	Modeling of Transmission Lines	138
3.5	Microstrip Transmission Lines	139
3.5.1	Microstrip Line in the Quasi-TEM Approximation . .	139
3.5.2	Input Impedance of a Shorted Microstrip Line Mod- eled using a Field Solver	140
3.5.3	Effective Permittivity and Characteristic Impedance	143
3.5.4	Filling Factor	148
3.5.5	Microstrip Resistance	148
3.5.6	Microstrip Conductance	149
3.6	Microstrip Design Formulas	150
3.6.1	High Impedance	150
3.6.2	Low Impedance	151
3.7	Stripline	151
3.7.1	Characteristic Impedance of a Stripline	152
3.7.2	Attenuation on a Stripline	153
3.7.3	Design Formulas for a Stripline	155
3.8	Coplanar Waveguide	155
3.8.1	Effective Permittivity and Characteristic Impedance of CPW	156
3.8.2	Loss of CPW lines	157

3.8.3	CPW Structures	157
3.8.4	Differential Line and Coplanar Strip	158
3.8.5	Summary	159
3.9	Summary	159
3.10	References	160
3.11	Exercises	161
3.11.1	Exercises by Section	164
3.11.2	Answers to Selected Exercises	164
4	Extraordinary Transmission Line Effects	165
4.1	Introduction	165
4.2	Frequency-Dependent Characteristics	166
4.2.1	Material Dependency	166
4.2.2	Frequency-Dependent Charge Distribution	166
4.2.3	Current Bunching	167
4.2.4	Skin Effect and Internal Conductor Inductance	169
4.2.5	Skin Effect and Line Resistance	171
4.2.6	Dielectric Dispersion	173
4.2.7	Summary	174
4.3	High-Frequency Properties of Microstrip Lines	174
4.3.1	Frequency-Dependent Loss	175
4.3.2	Field Simulations	176
4.3.3	Summary	178
4.4	Multimoding on Transmission Lines	178
4.5	Parallel-Plate Waveguide	179
4.5.1	Electromagnetic Derivation	180
4.5.2	Multimoding and Electric and Magnetic Walls	182
4.6	Microstrip Operating Frequency Limitations	183
4.6.1	Microstrip Dielectric Mode (Slab Mode)	185
4.6.2	Higher-Order Microstrip Mode	186
4.6.3	Transverse Microstrip Resonance	187
4.6.4	Summary	189
4.7	High-Frequency Considerations for Coplanar Waveguide	189
4.8	High-Frequency Considerations for Stripline	190
4.9	Power Losses and Parasitic Effects	191
4.10	Lines on Semiconductor Substrates	192
4.10.1	Modes on the MIS (MOS) Line	194
4.11	Summary	195
4.12	References	196
4.13	Exercises	197
4.13.1	Exercises by Section	201
4.13.2	Answers to Selected Exercises	201
5	Coupled Lines and Applications	203
5.1	Introduction	203
5.2	Physics of Coupling	204
5.3	Coupled Transmission Line Theory	208
5.3.1	Summary	210
5.4	Low-Frequency Capacitance Model of Coupled Lines	210
5.4.1	Capacitance Matrix Extraction	212
5.5	Symmetric Coupled Transmission Lines	213

5.5.1	Odd-Mode and Even-Mode Capacitances	215
5.6	Formulas for Characteristic Impedance of Coupled Microstrip Lines	217
5.6.1	Even-Mode Coupled-Line Parameters	218
5.6.2	Odd-Mode Coupled-Line Parameters	218
5.6.3	System Impedance of Coupled Lines	219
5.6.4	Discussion	219
5.6.5	Summary	223
5.7	Terminated Coupled Lines	223
5.7.1	Reflectionless Condition	223
5.8	Directional Coupler	227
5.8.1	Design Equations for a Directional Coupler	229
5.8.2	Directional Coupler With Lumped Capacitors	230
5.8.3	Physical Design of a Pair of Coupled Lines	230
5.8.4	The Lange Coupler	234
5.9	Models of Parallel Coupled Lines	235
5.9.1	Chain Matrix Model of Coupled Lines	235
5.9.2	$ABCD$ Parameters of Coupled-Line Sections	236
5.9.3	Synthesis of Specific Coupled-Line Connections	236
5.9.4	Model Using Even- and Odd-Mode Lines	238
5.9.5	Alternative Coupled-Line Model	240
5.9.6	Approximate Synthesis from the Coupled-Line Model	242
5.10	Differential and Common Modes	243
5.11	Common Impedance Coupling	246
5.12	Summary	246
5.13	References	248
5.14	Exercises	249
5.14.1	Exercises by Section	251
5.14.2	Answers to Selected Exercises	251
6	Waveguides	253
6.1	Introduction	253
6.2	The Rectangular Wave Equation	254
6.3	Parallel-Plate Waveguide	257
6.3.1	TEM Mode	257
6.3.2	TM Mode	259
6.3.3	TE Mode	261
6.3.4	Summary	262
6.4	Rectangular Waveguide	262
6.4.1	TM Modes	263
6.4.2	TE Modes	265
6.4.3	Practical Rectangular Waveguide	266
6.4.4	Rectangular Waveguide Components	268
6.5	Summary	274
6.6	References	275
6.7	Exercises	276
6.7.1	Exercises by Section	277
Index	279

Introduction to Distributed Microwave Circuits

1.1	Introduction	1
1.2	Book Outline	2
1.3	Chapter Outline	5
1.4	Distributed Circuits	6
1.5	Maxwell's Equations	7
1.6	Electric and Magnetic Field Laws	16
1.7	Electromagnetic Fields and Materials	19
1.8	Electric and Magnetic Walls	21
1.9	Fields in Lossy Mediums	24
1.10	Summary	29
1.11	References	30
1.12	Exercises	30
1.A	Appendix: Mathematical Foundations	33

1.1 Introduction

The universe has a speed limit, the finite speed of causality or c , the speed of light, which is embodied in Maxwell's equations and in the special theory of relativity. The result of this is that a cause, say a voltage, in one part of a circuit produces an effect, say a current, in another part of the circuit after a delay. When using circuits at low frequencies the impact of this delay is insignificant as the effect occurs long before there is even the slightest discernible change in the cause. However the delay is important at microwave and higher frequencies. Electromagnetic (EM) radiation travels 30 cm in a nanosecond in free space. Thus a circuit operating at 1 GHz that is 1 cm across will just see an appreciable affect due to the finite speed of the EM signal which, of course, is how the voltage and current "communicate." The impact will be more significant at higher frequencies and if the EM signal travels in a dielectric as a dielectric reduces the speed of light.

A microwave engineer must design circuits to manage this finite delay, but what is particularly interesting is that the effect gives rise to an enormous number of useful circuit elements that have no analog at lower frequencies. Whole circuits, and quite complex circuits at that, can be designed by exploiting distributed effects. This book explores the design of circuits with transmission lines and introduces effects, such as coupling from one

transmission line to another, that can be exploited to build novel circuits.

This book is the second volume in a series on microwave and RF design. The first volume in the series addresses radio systems [1] mainly following the evolution of cellular radio. The third volume [2] covers microwave network theory which is the theory that describe power flow and can be used to describe transmission line effects. Topics covered in this volume include scattering parameters, Smith charts, and matching networks that enable maximum power transfer. The fourth volume [3] focuses on designing microwave circuits and systems using modules introducing a large number of different modules. Modules is just another term for a network but the implication is that is packaged and often available off-the-shelf. Other topics in this chapter that are important in system design using modules are considered including noise, distortion, and dynamic range. Most microwave and RF designers construct systems using modules developed by other engineers who specialize in developing the modules. Examples are filter and amplifier chip modules which once designed can be used in many different systems. Much of microwave design is about maximizing dynamic range, minimizing noise, and minimizing DC power consumption. The fifth volume in this series [4] considers amplifier and oscillator design and develops the skills required to develop modules.

The books in the Microwave and RF Design series are:

- Microwave and RF Design: Radio Systems
- Microwave and RF Design: Transmission Lines
- Microwave and RF Design: Networks
- Microwave and RF Design: Modules
- Microwave and RF Design: Amplifiers and Oscillators

1.2 Book Outline

The telegraphist's equations, used to analyze transmission lines, and their interpretations are presented in Chapter 2 where transmission line theory is presented. This leads to the analysis of terminated transmission lines with key results being how these can be used as circuit elements to realize narrow-band inductors and capacitors. The chapter concludes by developing circuit models of transmission lines that are suitable for use in circuit simulators and in designing circuits using transmission lines.

Chapters 2–6 describe transmission lines and the exploitation of transmission effects that are used in RF and microwave engineering. One of the aspects that distinguishes design at a few tens of megahertz and below from design above a few megahertz up to a terahertz is that at low frequencies design proceeds with the assumption that circuit elements and indeed whole circuits exist at a point and there is no time-of-flight, e.g. speed-of-light, limitation to a voltage and current at one point in a circuit instantaneously impacting the voltage and current anywhere else in the circuit. As the frequency of operation of a circuit increases, the effect of the finite speed of light becomes significant and distributed effects often need to be considered.

Chapter 3 focuses on a class of transmission lines called planar lines which are lines usually fabricated starting with a low loss dielectric substrate with metal sheets on both sides. The most important planar transmission line is the microstrip line shown in Figure 1-1. This is the most widely used

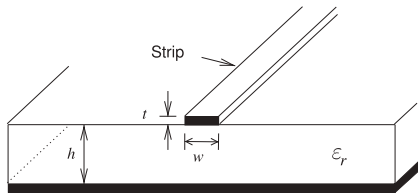


Figure 1-1: Microstrip transmission line.

interconnect at microwave frequencies. The strip of the line is formed by patterning the top conductor and etching away the unwanted metal. The defining distinction between a microstrip line, and any planar transmission line, and a trace on a printed circuit board is that at microwave frequencies attention must be given to providing a signal return path and maintaining as uniform an environment as possible for the electric and magnetic fields. Any discontinuity will introduce reflections of EM energy. This may actually be desired when implementing circuit elements but if not it is important that geometrical uniformity be maintained. Considering the microstrip line, see Figure 1-1, the width, w , of the strip and the thickness, h , of the substrate define the ratio of the voltage and current signals traveling along the microstrip line. This ratio is called the characteristic impedance of the line and it is critical for reliable signal transmission, i.e., good signal integrity, that the cross-sectional geometry be the same along the line as then the characteristic impedance of the line is constant.

While simple in concept, planar transmission lines needed to be invented. As well as conceptualizing a transmission line that can be realized by etching a planar metallic conductor on the printed circuit board, it is essential to provide the analytic tools that enable the propagation characteristics of the line to be calculated and enable structures such as couplers and filters to be synthesized using planar transmission lines. The origins of microstrip trace back to developments in the early 1940s, beginning with a coaxial line with a flat center conductor forming a rectangular coaxial line [5]. At that time printed circuit boards were being used for low-frequency circuits. In 1949 these came together when Barrett reasoned that the thick center conductor of the rectangular coaxial transmission line could be very thin with little effect on the properties of the line. This then meant that low-frequency printed circuit board techniques could be employed in microwave circuits and the transmission line system became known as stripline [5, 6].

The conceptual evolution of stripline is shown in Figure 1-2. The stripline configuration is developed by sandwiching a metallic strip between two metal-clad dielectric sheets. As initially envisioned, the strip could be stamped out or silk-screened using silver ink. Today it is most common to begin with a continuous metallic sheet bonded to one or both sides of a dielectric sheet. A pattern of an etch resistant material is then photolithographically defined on the sheet and the strip pattern appears after etching. The next advance in 1952 when Grieg and Engelmann removed one of stripline's ground planes thus becoming microstrip [7]. With an invention it is not sufficient to simply describe a structure, in this case understanding had to be provided as evidenced by presenting design equations for the electrical properties of the line. The essential electrical properties of a transmission line are its characteristic impedance, the ratio of the traveling voltage and current waves on the line, and its propagation constant, which relates to the speed of propagation of the voltage and current

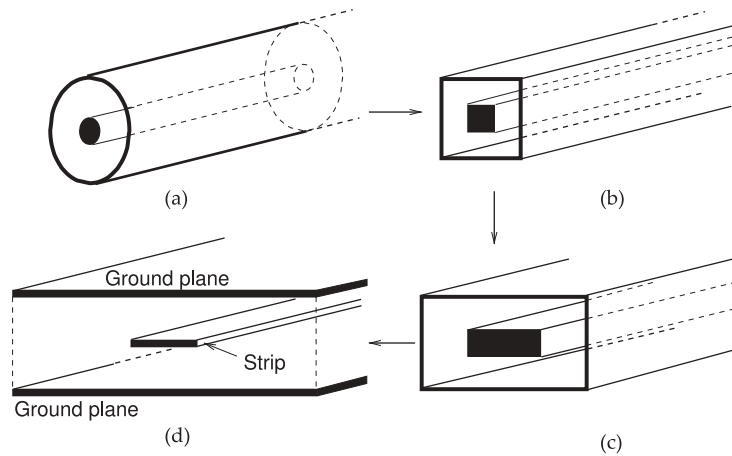


Figure 1-2: Evolution of the stripline transmission line: (a) coaxial line with a round center conductor; (b) square coaxial line with a square flat center conductor; (c) rectangular coaxial line with a flat center conductor; and (d) stripline.

waves on the lines.

Planar lines are not ideal transmission lines and undesired effects must be anticipated and design adjusted to reduce their occurrence or impact. These extraordinary effects are considered in Chapter 4. Understanding and anticipating these effects is really where the art of microwave design comes into play. Many of the effects occur when dimensions are too large but at the same time manufacturability improves when dimensions are large, so a design trade-off is required. Rarely is a design successful on the first pass. Thus it is important for a microwave engineer to interpret undesirable results and know what to modify in a design. It is difficult to do measurements at microwave frequencies as anything that is introduced in a measurement, e.g. a probe, will have significant impact on a circuit. Often a few indirect measurements, some analysis, and great intuition is required to correctly identify and hence resolve design issues.

Chapter 4 begins by considering frequency-dependent characteristics of planar lines and then moves on to developing analysis equations and design concepts for microstrip lines at high frequencies. As the transverse dimensions of a planar line approach a wavelength, say greater than a tenth of a wavelength, it is possible for the EM signal to travel down the line in two (or more field) orientations called modes and these travel at different velocities and corrupt a signal. Multimoding is nearly always undesirable so understanding the origins of multiple modes and designing to avoid multiple modes is an important consideration. However in some situations these modes are exploited, e.g. in realizing a small area inductor on an RFIC.

When two planar lines are close to each other the fields of one line can be in the vicinity of the other line and the lines are coupled. A portion of the energy of a signal traveling on one of the lines can appear on the other line. Many circuit elements can be developed by exploiting parallel coupled lines (PCLs). Chapter 5 begins by presenting the physics of coupling and then a generalization of the telegraphist's equations for coupled transmission lines. Design approaches and circuit models are developed and the circuit models enable the synthesis of microwave designs using parallel coupled lines. Several PCL circuit elements are presented but many more will be described in other volumes of this book series.

The final chapter of this volume, Chapter 6, discusses rectangular waveguides. Instead of 'rectangular waveguide' just the term 'waveguide'

is usually used with the understanding that reference is being made to a rectangular waveguide. This is a little confusing because really all transmission lines guide waves and so are waveguides. A rectangular waveguide is a very different type of transmission line that confines the EM fields inside a rectangular metal pipe. These are important elements starting at low microwave frequencies, 1 GHz and above, as they can carry very powerful signals with very little loss. They are almost always used in radar and similar high power applications. Waveguides are also very important at higher frequencies even when power levels are relatively low. They are often used at 15 GHz and above as they have very little loss while the loss of coaxial lines grows tremendously with frequency. With waveguides it is very difficult to use voltage and current concepts except over very narrow fractional bandwidths, a few percent at most. This means that it is very difficult to do circuit design using waveguides.

1.3 Chapter Outline

The chapter begins by considering distributed circuits in Section 1.4 and identifying the types of structures to be considered in this book. Then Section 1.5 revisits Maxwell's equations from a perspective different from the way it was (almost certainly) introduced to the reader. It is assumed that the reader has a knowledge of Maxwell's equations which are nearly always introduced following a treatment of the static field laws: Biot-Savart law, Ampere's circuital law, Gauss's law, Gauss's law for magnetism, and Faraday's law. The classic treatment follows the historical time line and then Maxwell's equations are introduced. It was almost as though Maxwell's equations were derived from the static field laws but that was never stated because they were not. Maxwell's equations represent a separate physical insight. Maxwell's equations cannot be derived from the static field laws, however the static field laws can be derived from Maxwell's equations. Maxwell had remarkable insight and interpreted the physical world in an amazing way and this places him among the greatest physicists of all time. He touched on relativity and quantum field theory in imagining that the electric and magnetic fields, and light, formed a two-component field where the spatial derivative of one component was related to the time derivative of the other. He imagined that this relationship imposed a cosmic speed limit. The components of Maxwell's field are the electric and magnetic fields but the insight was much more fundamental than that.

The next section, Section 1.6, demonstrates that all of the early static field laws can be derived from Maxwell's equation. Maxwell unified what seemed to be a number of unconnected observations but at the time many suspected that there was an underlying reality. The next few sections derive some important short-hand techniques that are useful in working with distributed circuits and in particular transmission lines. Section 1.7 describes how the EM fields interact with lossless materials. It is no secret that Maxwell's equations are fiendishly difficult to work with unless great simplifications are made. While tremendous computational EM analysis tools are available the design engineer needs insight. One of the critical pieces of insight that guides microwave engineers is to imagine a magnetic wall analogous to a conductor which is an electric wall. A magnetic wall is approximated at the interface of two dielectrics. The concepts of electric and magnetic walls

analyzed in Section 1.8 provide an insight that is particularly useful to the microwave engineer is developed. These results will be used throughout the chapters in this book. Actual dielectrics and conductors are lossy so the effect of loss is considered in Section 1.9. Examples of how insight and fortuitous use of geometry, symmetries, and physical insight can be used in EM calculations are given in Section 1.9. Generally only particular structures with the requisite symmetries and simple geometry are used in design because if a structure is too difficult to analyze then the important intuitive insight is hard to acquire.

The final part of this chapter is an appendix on mathematical foundations with the required essentials of trigonometric expansions, mathematical identities, complex arithmetic, Butterworth and Chebyshev polynomials used in matching network and filter design, the properties of circles on a complex plane are used in dealing with complex numbers plotted on a polar plot, Kron's method used in network condensation and thus in simplifying designs, and the mathematics of random processes which are used in working with digitally modulated signals and with noise. Everything in this appendix is used somewhere in this book series.

1.4 Distributed Circuits

RF and microwave engineering has as its basis transmission line effects also known as distributed effects. As is well known, the voltage and current at one point, A, cannot instantaneously affect the voltage and current at another spatially separated point B. However if points A and B in a circuit are sufficiently close then a circuit can nearly always be treated as a lumped element circuit. What constitutes sufficiently close is related to the distance between A and B, d , compared to a wavelength, λ . If $d < \lambda/100$ then nearly always the circuit can be considered as being lumped. If $d \geq \lambda/10$ then distributed effects, limitations imposed by the finite time-of-flight, must be considered and the circuit is always regarded as being distributed. When d is between $\lambda/100$ and $\lambda/10$ then it is not clear whether the circuit must be regarded as distributed or can be regarded as lumped. It is of course much simpler to analyze and design with lumped-element circuits.

Distributed and transmission-line effects are synonymous. While a distributed circuit may be difficult to analyze, distributed effects can be exploited to realize a very large array of elements that usually have no equivalent at lower frequencies. For example, the fields from two adjacent transmission lines can overlap so that part of the signal (energy) from one of the lines appears on the other. This could be a problem in some situations but can be used to couple some of the power from one line onto another. Many novel circuit elements are based on this coupling effect.

Distributed effects and transmission line effects result from a signal, voltage or current, at one point in space not being able to instantaneously change the voltage and current at another point in space. To be more physical, voltage and current can be replaced by electric and magnetic field. The finite speed of light is encapsulated in Maxwell's equations which were developed between 1861 and 1862 [8, 9]. For microwave engineers Maxwell's equations are the most convenient and complete description of reality. They are the classical limit of a more fundamental theory called quantum electrodynamics. Maxwell's equations are important to the

physical understanding of transmission line effects and distributed effects, but in reality are very difficult to manipulate and use in calculations. What are much more useful are the transmission line equations, or telegrapher's equations, developed by Heaviside in 1887 [10].

The telegrapher's equations use voltage and current which are related to the integral of electric field and integral of magnetic field respectively. The telegrapher's equations relate the time derivative of voltage (or current) to the spatial variation of current (or voltage). This is analogous to how Maxwell's equations relate the electric and magnetic fields. Heaviside also introduced the concept of phasors with the result that the four dimensions of Maxwell's equations, time and three spatial dimensions, are reduced to just one spatial dimension, along the length of a transmission line. Microwave designers, as with all circuit designers, is that they design based on lumped-element circuits that are naturally described by voltage and current. What is particularly important about the telegrapher's equations is that they enable direct relationship of transmission line circuits to lumped-element circuits. Never-the-less the telegraphist's equations are not always sufficient to understand distributed circuits so (sometimes reluctantly) microwave engineers must have working familiarity with Maxwell's equations to understand every situation that can be encountered. Putting this another way, microwave engineers want to express circuit quantities as voltage and currents rather than electric and magnetic fields but are always aware that microwave circuits are intricately connected to electric and magnetic fields and energy is stored in electric and magnetic fields. The telegraphist's equations provide a link between the voltage/current and EM field worlds and introduce concepts of traveling wave voltages and currents which further aid the connection.

1.5 Maxwell's Equations

In this and following sections, EM theory is presented in a form that aids in the understanding of distributed effects, such as propagation on transmission lines, coupling of transmission lines, and how transmission line effects can be used to realize components with unique functionality. While this is a review of material that most readers have previously learned, it is presented in a slightly different form than is usual. The treatment begins with Maxwell's equations and not the static field laws. This is not the way EM theory is initially presented.

Maxwell's equations are a remarkable insight and the early field laws can be derived from them. Most importantly, Maxwell's equations describe the propagation of an EM field. Maxwell's equations are presented in point form in Section 1.5.1 and in integral form in Section 1.5.5. From these, the early electric and magnetic field laws are derived. The effect of boundary conditions are introduced in Section 1.8 to arrive at implications for multimoding on transmission lines. Multimoding is almost always undesirable, and in designing transmission line structures so that multimoding is avoided, it is necessary to have rules that establish when multimoding can occur.

1.5.1 Point Form of Maxwell's Equations

The characteristics of EM fields are described by Maxwell's equations:

$$\nabla \times \bar{\mathcal{E}} = -\frac{\partial \bar{\mathcal{B}}}{\partial t} - \bar{\mathcal{J}}_m \quad (1.1) \quad \nabla \times \bar{\mathcal{H}} = \frac{\partial \bar{\mathcal{D}}}{\partial t} + \bar{\mathcal{J}} \quad (1.3)$$

$$\nabla \cdot \bar{\mathcal{D}} = \rho_V \quad (1.2) \quad \nabla \cdot \bar{\mathcal{B}} = \rho_{mV}, \quad (1.4)$$

where μ is called the permeability of the medium and ε is called the permittivity of the medium. (The left-hand side of Equation (1.1) is read as “curl E” and the left-hand side of Equation (1.2) as “div E.”) They are the property of a medium and describe the ability to store magnetic energy and electric energy. The other quantities in Equations (1.1)–(1.4) are

- $\bar{\mathcal{E}}$, the **electric field**, with units of volts per meter (V/m), a time-varying vector
- $\bar{\mathcal{D}}$, the **electric flux density**, with units of coulombs per square meter (C/m²)
- $\bar{\mathcal{H}}$, the three-dimensional **magnetic field**, with units of amperes per meter (A/m)
- $\bar{\mathcal{B}}$, the **magnetic flux density**, with units of teslas (T)
- $\bar{\mathcal{J}}$, the **electric current density**, with units of amperes per square meter (A/m²)
- ρ_V , the **electric charge density**, with units of coulombs per cubic meter (C/m³)
- ρ_{mV} , the **magnetic charge density**, with units of webers per cubic meter (Wb/m³)
- $\bar{\mathcal{J}}_m$ is the **magnetic current density**, with units of webers per second per square meter (Wb · s⁻¹ · m⁻²).

Magnetic charges do not exist, but their introduction in Maxwell's equations through the **magnetic charge density**, ρ_{mV} , and the **magnetic current density**, $\bar{\mathcal{J}}_m$, introduce an aesthetically appealing symmetry. Maxwell's equations are differential equations, and as with most differential equations, their solution is obtained with particular boundary conditions that here are imposed by conductors. Electric conductors (i.e., electric walls) support electric charges and hence electric current. By analogy, magnetic walls support magnetic charges and magnetic currents. Magnetic walls also provide boundary conditions to be used in the solution of Maxwell's equations. The notion of magnetic walls is important in RF and microwave engineering, as they are approximated by the boundary between two dielectrics of different permittivity. The greater the difference in permittivity, the more closely the boundary approximates a magnetic wall. As a result, the analysis of many structures with different dielectrics can be simplified, aiding in intuitive understanding.

The fields in Equations (1.1)–(1.4) are three-dimensional fields, e.g.,

$$\bar{\mathcal{E}} = \mathcal{E}_x \hat{x} + \mathcal{E}_y \hat{y} + \mathcal{E}_z \hat{z}, \quad (1.5)$$

where \hat{x} , \hat{y} , and \hat{z} are the unit vectors (having a magnitude of 1) in the x , y and z directions, respectively. \mathcal{E}_x , \mathcal{E}_y , and \mathcal{E}_z are the electric field components in the x , y , and z directions, respectively.

The symbols and units used with the various field quantities and some of the other symbols to be introduced soon are given in Table 1-1. $\bar{\mathcal{B}}$ and $\bar{\mathcal{H}}$, and $\bar{\mathcal{D}}$ and $\bar{\mathcal{E}}$ are related to each other by the properties of the medium embodied

Table 1-1: Quantities used in Maxwell's equations. Magnetic charge and current are introduced in establishing boundary conditions, especially at dielectric interfaces. The SI units of other quantities used in RF and microwave engineering are given in Table 2-1.

Symbol	SI unit	SI unit	Name and base units
E	volts per meter	V/m	electric field intensity base unit: $\text{kg} \cdot \text{m} \cdot \text{s}^{-3} \cdot \text{A}^{-1}$
H	amps per meter	A/m	magnetic field intensity
D	coulombs per square meter	C/m ²	$D = \epsilon E$, electric flux density base unit: $\text{A} \cdot \text{s} \cdot \text{m}^{-2}$
B	tesla, webers per square meter	T	$B = \mu H$, magnetic flux density base unit: $\text{kg} \cdot \text{s}^{-2} \cdot \text{A}^{-1}$
I	amp	A	electric current
M	amps per meter	A/m	magnetization base unit: $\text{A} \cdot \text{m}^{-1}$
q_e	coulomb	C	electric charge base unit: $\text{A} \cdot \text{s}$
q_m	weber	Wb	magnetic charge base unit: $\text{kg} \cdot \text{m}^2 \cdot \text{s}^{-2} \cdot \text{A}^{-1}$
ψ_e	coulomb	C	electric flux base unit: $\text{A} \cdot \text{s}$
ψ_m	weber	Wb	magnetic flux base unit: $\text{kg} \cdot \text{m}^2 \cdot \text{s}^{-2} \cdot \text{A}^{-1}$
ρ_V	coulombs per cubic meter	C/m ³	charge density base unit: $\text{A} \cdot \text{s} \cdot \text{m}^{-3}$
ρ_S	coulombs per square meter	C/m ²	surface charge density base unit: $\text{A} \cdot \text{s} \cdot \text{m}^{-2}$
ρ_{mV}	webers per cubic meter	Wb/m ³	magnetic charge density base unit: $\text{kg} \cdot \text{m}^{-1} \cdot \text{s}^{-2} \cdot \text{A}^{-1}$
ρ_{mS}	webers per square meter	Wb/m ²	surface magnetic charge density base unit: $\text{kg} \cdot \text{s}^{-2} \cdot \text{A}^{-1}$
J	amps per square meter	A/m ²	electric current density
J_S	amps per meter	A/m	surface electric current density
J_m	webers per second per square meter	Wb \cdot s ⁻¹ \cdot m ⁻²	magnetic current density base unit: $\text{kg} \cdot \text{s}^{-3} \cdot \text{A}^{-1}$
J_{mS}	webers per second per meter	Wb \cdot s ⁻¹ \cdot m ⁻¹	surface magnetic current density base unit: $\text{kg} \cdot \text{m}^{-1} \cdot \text{s}^{-3} \cdot \text{A}^{-1}$
S	square meters	m ²	surface
V	cubic meters	m ³	volume
ϵ	farads per meter	F/m	permittivity base unit: $\text{kg}^{-1} \cdot \text{m}^{-3} \cdot \text{A}^2 \cdot \text{s}^4$
μ	henry per meter	H/m	permeability base unit: $\text{kg} \cdot \text{m} \cdot \text{s}^{-2} \cdot \text{A}^{-2}$
dS	square meter	m ²	incremental area
$d\ell$	meter	m	incremental length
dV	cubic meter	m ³	incremental volume
\oint_C			integral around a closed contour
\oint_S			integral over a closed surface
\int_V			volume integral

in μ and ε :

$$\vec{B} = \mu \vec{H} \quad (1.6) \quad \vec{D} = \varepsilon \vec{E}. \quad (1.7)$$

The quantity μ is called the **permeability** and describes the ability to store **magnetic energy** in a region. The permeability in free space (or vacuum) is denoted μ_0 and the magnetic flux and magnetic field are related as (where $\mu_0 = 4\pi \times 10^{-7} \text{ H/m}$)

$$\vec{B} = \mu_0 \vec{H}. \quad (1.8)$$

1.5.2 Moments and Polarization

In this subsection the response of materials to electric and magnetic fields are described. In a later section there will be a more specific discussion about the interaction of dielectrics and metals to electric fields. The main purpose here is to define electric and magnetic polarization vectors.

Material Response to an Applied Electric Field

The generation of electric moments is the atomic-level response of a material to an applied electric field. With an atom the center of negative charge, the center of the electron cloud, and the center of the positive charge, the nucleus, overlap. When an electric field is applied the centers of positive and negative charge separate and electrical energy additional to that stored in free space is stored in a manner very similar to potential energy storage in a stretched spring. The separation of charge (charge by distance) forms an electric dipole which has an electric dipole moment \vec{p} having the SI units of $\text{C} \cdot \text{m}$ or $\text{A} \cdot \text{s} \cdot \text{m}$. The same occurs with solids but now the centers of positive and negative charge could be separated even without an external electric field and the material is said to be polarized. If there are n electric dipole moments \vec{p} per unit volume (in SI per m^3), then the polarization density (or electric polarization or simply polarization) is

$$\vec{P} = n\vec{p}. \quad (1.9)$$

which has the SI units of C/m^2 . \vec{P} has the same units and has the same effect as the electric flux density \vec{D} . In a homogeneous, linear, isotropic material, \vec{P} is proportional to the applied electric field intensity \vec{E} . A homogenous material has the same average properties everywhere and an isotropic material looks the same in all directions. Materials that are not isotropic are called anisotropic and most commonly these are crystals that have asymmetrical unit cells so that the separation of charge, the electric energy stored by this separation of charge (the strength of the spring) in response to an applied field depends on direction. As a result

$$\vec{P} = \check{\chi}_e \varepsilon_0 \vec{E} \quad (1.10)$$

where $\check{\chi}_e$ is called the electric susceptibility of the material. The electric susceptibility has been written as a tensor, a 3×3 matrix that relates the three directions of \vec{E} to the three possible directions of \vec{P} . For an amorphous solid or a crystal with high unit cell symmetry, the nine elements of $\check{\chi}_e$ are the same and so the tensor notation is dropped and χ_e is used as a scalar.

Material Response to an Applied Magnetic Field

All materials contain electrons each having a charge and a spin. The charges produce an electric field and the spin produces a magnetic field. The magnetic field produced by an electron is almost that which would be produced by a mechanically spinning charge, although there is no actual mechanical rotation. Spin is a quantum mechanical property. Still it is very hard to avoid using the rotating charge analogy. The spin of an electron points in a particular direction and in most materials these spins are randomly arranged and cancel each other out so that there is no net magnetic effect. Some materials can be magnetized by a large externally applied magnetic field and the spins are then permanently aligned even when the external magnetic field is removed. Sometimes the alignment is established by crystal geometry.

Consider a magnetic material without permanent magnetization. When a magnetic field is applied to these materials the electron spin vector tends to rotate and energy is stored. The ability to store magnetic energy above that which would be stored in vacuum is described by the concept of relative permeability.

The response of a material to an applied magnetic field is not directly analogous to the response to an applied electric field because of the fundamental difference in the source of magnetic moments. In most materials the magnetic moment of one electron is paired with an electron occupying the same orbital with a magnetic moment in the opposite direction so that there is no net magnetic moment. In magnetic materials there are some orbitals that do not have a pair of electrons so that there is a net magnetic moment. Additional energy is stored when the net magnetic moments are rotated away from their preferred long-term direction by an externally applied magnetic field \vec{H} . This is like storing energy in a spring. It is as though there is an additional magnetic field called the magnetic polarization which has a particular density. The net magnetic polarization density is denoted \vec{M} which has the SI units of A/m and

$$\vec{M} = \tilde{\chi}_m \vec{H} \quad (1.11)$$

where $\tilde{\chi}_m$ is called the magnetic susceptibility of the material and in general can be a 3×3 matrix. The relative permeability is defined as

$$\tilde{\mu}_r = 1 + \tilde{\chi}_m. \quad (1.12)$$

Summary

A vacuum can store electric and magnetic energy. Materials can store additional energy and the propensity relative to vacuum is described by the relative permittivity and permeability, respectively, of the material.

1.5.3 Field Intensity and Flux Density

Permeability, μ , is generally a scalar, but in magnetic materials it can be a 3×3 matrix called a **dyadic** tensor with the relative permeability tensor being $\tilde{\mu}_r$. Then

$$\vec{B} = \mu_0(\vec{H} + \vec{M}) \quad (1.13)$$

where $\bar{\mathcal{M}}$ is the magnetization of the material. Introducing phasors

$$\bar{B} = \mu_0(\bar{H} + \check{\chi}_m \bar{\mathcal{H}}) = \mu_0 \check{\mu}_r \bar{H} \quad (1.14)$$

$$\begin{bmatrix} \mathcal{B}_x \\ \mathcal{B}_y \\ \mathcal{B}_z \end{bmatrix} = \check{\mu}_r \begin{bmatrix} \mathcal{H}_x \\ \mathcal{H}_y \\ \mathcal{H}_z \end{bmatrix} = \begin{bmatrix} \mu_{xx} & \mu_{xy} & \mu_{xz} \\ \mu_{yx} & \mu_{yy} & \mu_{yz} \\ \mu_{zx} & \mu_{zy} & \mu_{zz} \end{bmatrix} \begin{bmatrix} \mathcal{H}_x \\ \mathcal{H}_y \\ \mathcal{H}_z \end{bmatrix}. \quad (1.15)$$

The direction-dependent property indicated by this dyadic results from alignment of electron spins in a material. However, in most materials there is no alignment of spins and $\mu = \mu_0$. The **relative permeability**, μ_r , refers to the ratio of permeability of a material to its value in a vacuum:

$$\mu_r = \frac{\mu}{\mu_0}. \quad (1.16)$$

So $\mu_r > 1$ indicates that a material can store more magnetic energy than can a vacuum in a given volume.

The other material quantity is the **permittivity**, ε , which is denoted ε_0 , and in a vacuum

$$\mathcal{D} = \varepsilon_0 \mathcal{E}, \quad (1.17)$$

where $\varepsilon_0 = 8.854 \times 10^{-12} \text{ F}\cdot\text{m}^{-1}$. The **relative permittivity**, ε_r , refers to the ratio of permeability of a material to its value in a vacuum:

$$\varepsilon_r = \frac{\varepsilon}{\varepsilon_0}. \quad (1.18)$$

So $\varepsilon_r > 1$ indicates that a material can store more electric energy in a volume than can be stored in a vacuum. In some calculations it is useful to introduce an **electric polarization**, \mathcal{P}_e . Then

$$\mathcal{D} = \varepsilon \mathcal{E} = \varepsilon_0 \mathcal{E} + \mathcal{P}_e, \quad (1.19)$$

and so the polarization vector is

$$\mathcal{P}_e = (\varepsilon - \varepsilon_0) \mathcal{E} = \varepsilon_0 \chi_e \mathcal{E}, \quad (1.20)$$

where χ_e is called the **electric susceptibility**.

Some materials require a dyadic form of ε . This usually indicates a dependence on crystal symmetry, and the relative movement of charge centers in different directions when an E field is applied. Some commonly used microwave substrates, such as sapphire, have permittivities that are direction dependent rather than having full **dyadic permittivity**. A material in which the permittivity is a function of direction is called an anisotropic material or is said to have **dielectric anisotropy**. In an isotropic material the permittivity is the same in all directions; the material has **dielectric isotropy**. Most materials are isotropic.

Maxwell's original equations were put in the form of Equations (1.1)–(1.4) by the mathematician Oliver Heaviside from the less convenient form Maxwell originally used. The above equations are called the point form of Maxwell's equations, relating the field components to each other and to charge and current density at a point.

Maxwell's equations have three types of derivatives. First, there is the time derivative, $\partial/\partial t$. Then there are two spatial derivatives: $\nabla \times$, called curl, capturing the way a field circulates spatially (or the amount that it curls up on itself); and $\nabla \cdot$, called the div operator, describing the spreading out of a field (i.e., its divergence). **Curl** and **div** have different forms in different coordinate systems, and in the rectangular system can be expanded as ($\mathbf{A} = A_x \hat{\mathbf{x}} + A_y \hat{\mathbf{y}} + A_z \hat{\mathbf{z}}$)

$$\nabla \times \mathbf{A} = \left(\frac{\partial A_z}{\partial y} - \frac{\partial A_y}{\partial z} \right) \hat{\mathbf{x}} + \left(\frac{\partial A_x}{\partial z} - \frac{\partial A_z}{\partial x} \right) \hat{\mathbf{y}} + \left(\frac{\partial A_y}{\partial x} - \frac{\partial A_x}{\partial y} \right) \hat{\mathbf{z}} \quad (1.21)$$

$$\text{and} \quad \nabla \cdot \mathbf{A} = \frac{\partial A_x}{\partial x} + \frac{\partial A_y}{\partial y} + \frac{\partial A_z}{\partial z}. \quad (1.22)$$

Curl and div in cylindrical and spherical coordinates are given in Equations (1.134), (1.135), (1.143), and (1.144). Studying Equation (1.21) you will see that curl, $\nabla \times$, describes how much a field circles around the x , y , and z axes. That is, the curl describes how a field circulates on itself. So Equation (1.1) relates the amount an electric field circulates on itself to changes of the B field in time (and modified by the magnetic current). So a spatial derivative of electric fields is related to a time derivative of the magnetic field. Also in Equation (1.3), the spatial derivative of the magnetic field is related to the time derivative of the electric field (and modified by the electric current). These are the key elements that result in self-sustaining propagation.

Div, $\nabla \cdot$, describes how a field spreads out from a point. So the presence of net electric charge (say, on a conductor) will result in the electric field spreading out from a point (see Equation (1.2)). The magnetic field (Equation (1.4)) can never diverge from a point, which is a result of magnetic charges not existing. A magnetic wall approximation describes an open circuit and then effectively magnetic charges terminate the magnetic field. What actually happens in free space or on a transmission line depends on boundary conditions, and in the case of transmission lines, the dimensions involved.

How fast a field varies with time, $\partial \mathbf{B}/\partial t$ and $\partial \mathbf{E}/\partial t$, depends on frequency. The more interesting property is how fast a field can change spatially, $\nabla \times \mathbf{E}$ and $\nabla \times \mathbf{H}$ —this depends on wavelength relative to geometry. So if the cross-sectional dimensions of a transmission line are much less than a wavelength (say, less than $\lambda/4$), then it will be impossible for the fields to curl up on themselves and so there will be only one or, in some cases, no solutions to Maxwell's equations.

EXAMPLE 1.1 Energy Storage

Consider a material with a relative permittivity of 65 and a relative permeability of 1000. There is a static electric field E of 1 kV/m. How much energy is stored in the E field in a 10 cm^3 volume of the material?

Solution:

Energy stored in a static electric field $= \int_V \bar{D} \cdot \bar{E} \cdot dv$:

$D = \varepsilon E$ and field is constant (uniform)

$$\text{Energy stored} = \varepsilon E^2 \times (\text{volume}) = 65\varepsilon_0 \cdot (10^3)^2 \cdot (10 \cdot 10^{-6}) = 5.75 \cdot 10^{-9} \text{ J} = 5.75 \text{ nJ}.$$

The complete calculation using SI units is

$$\begin{aligned} \text{Energy stored} &= 65(8.854 \cdot 10^{-12} \cdot \text{F} \cdot \text{m}^{-1}) (10^3 \cdot \text{V} \cdot \text{m}^{-1})^2 \cdot (10 \cdot 10^{-6} \cdot \text{m}^3) \\ &= 65(8.854 \cdot 10^{-12} \cdot \text{kg}^{-1} \cdot \text{m}^{-3} \cdot \text{A}^2 \cdot \text{s}^4) \cdot (10^3 \cdot \text{kg} \cdot \text{m}^2 \cdot \text{A}^{-1} \cdot \text{s}^{-3} \cdot \text{m}^{-1})^2 \cdot (10^{-5} \cdot \text{m}^3) \\ &= 65 \cdot 8.854 \cdot 10^{-12} \cdot 10^6 \cdot 10^{-5} \cdot \text{kg} \cdot \text{m}^2 \cdot \text{s}^{-2} = 5.75 \cdot 10^{-9} \cdot \text{kg} \cdot \text{m}^2 \cdot \text{s}^{-2} \\ &= 5.75 \cdot 10^{-9} \text{ J} = 5.75 \text{ nJ}. \end{aligned}$$

EXAMPLE 1.2 Polarization Vector

A time-varying electric field in the x direction has a strength of 100 V/m and a frequency of 10 GHz. The medium has a relative permittivity of 10. What is the polarization vector? Express this vector in the time domain?

Solution:

$$\bar{D} = \varepsilon \bar{E} = \varepsilon_0 \bar{E} + \bar{P}_e.$$

The polarization vector is

$$\bar{P}_e = (\varepsilon - \varepsilon_0) \bar{E} = (10 - 1) \varepsilon_0 \bar{E} = 9\varepsilon_0 \bar{E}.$$

Now $\bar{E} = 100 \cos(2 \cdot \pi \cdot 10^{10} t) \hat{x}$
and $\varepsilon_0 = 8.85 \cdot 10^{-12}$, so

$$\begin{aligned} \bar{P}_e &= 9 (8.85 \times 10^{-12}) \cdot (100) \cos(6.28 \times 10^{10} t) \hat{x} \\ &= 79.7 \times 10^{-10} \cdot \cos(6.28 \times 10^{10} t) \hat{x} \\ &= 7.79 \cos(6.28 \times 10^{10} t) \hat{x} \text{ nC/m}^2. \end{aligned} \tag{1.23}$$

1.5.4 Maxwell's Equations in Phasor Form

Phasors reduce the dimensionality of Maxwell's equations by replacing a time derivative by a complex scalar. The phasor form is used with a sinusoidally varying quantity so, for example, an x -directed electric field in rectangular coordinates,

$$\bar{E} = |E_x| \cos(\omega t + \phi) \hat{x}, \tag{1.24}$$

is represented as the phasor

$$E_x = |E_x| e^{j\phi} \hat{x}. \tag{1.25}$$

The full three-dimensional electric field is

$$\bar{\mathcal{E}} = |E_x| \cos(\omega t + \phi_x) \hat{\mathbf{x}} + |E_y| \cos(\omega t + \phi_y) \hat{\mathbf{y}} + |E_z| \cos(\omega t + \phi_z) \hat{\mathbf{z}} \quad (1.26)$$

and has the phasor form

$$\bar{E} = |E_x| e^{j\phi_x} \hat{\mathbf{x}} + |E_y| e^{j\phi_y} \hat{\mathbf{y}} + |E_z| e^{j\phi_z} \hat{\mathbf{z}}. \quad (1.27)$$

To express Maxwell's equations in phasor form, the full complex form of Equation (1.26) must be considered. Using Equation (1.94), Equation (1.26) becomes

$$\begin{aligned} \bar{\mathcal{E}} = & \frac{1}{2} (|E_x| e^{j\phi_x} \hat{\mathbf{x}} + |E_y| e^{j\phi_y} \hat{\mathbf{y}} + |E_z| e^{j\phi_z} \hat{\mathbf{z}}) e^{j\omega t} \\ & + \frac{1}{2} (|E_x| e^{-j\phi_x} \hat{\mathbf{x}} + |E_y| e^{-j\phi_y} \hat{\mathbf{y}} + |E_z| e^{-j\phi_z} \hat{\mathbf{z}}) e^{-j\omega t} \end{aligned} \quad (1.28)$$

with the time derivative

$$\begin{aligned} \frac{\partial \mathbf{E}}{\partial t} = & \frac{1}{2} j\omega (|E_x| e^{j\phi_x} \hat{\mathbf{x}} + |E_y| e^{j\phi_y} \hat{\mathbf{y}} + |E_z| e^{j\phi_z} \hat{\mathbf{z}}) e^{j\omega t} \\ & - \frac{1}{2} j\omega (|E_x| e^{-j\phi_x} \hat{\mathbf{x}} + |E_y| e^{-j\phi_y} \hat{\mathbf{y}} + |E_z| e^{-j\phi_z} \hat{\mathbf{z}}) e^{-j\omega t}. \end{aligned} \quad (1.29)$$

Equation (1.29) has the phasor form (from the $e^{j\omega t}$ component)

$$\frac{2}{e^{j\omega t}} \left\{ \begin{array}{l} e^{j\omega t} \\ \text{component of} \end{array} \frac{\partial \bar{\mathcal{E}}}{\partial t} \right\} = j\omega (|E_x| e^{j\phi_x} \hat{\mathbf{x}} + |E_y| e^{j\phi_y} \hat{\mathbf{y}} + |E_z| e^{j\phi_z} \hat{\mathbf{z}}). \quad (1.30)$$

Noting this, **Maxwell's equations in phasor form**, from Equations (1.1)–(1.4), are

$$\nabla \times \bar{E} = -j\omega \bar{B} - \bar{J}_m \quad (1.31)$$

$$\nabla \times \bar{H} = j\omega \bar{D} + \bar{J} \quad (1.32)$$

$$\nabla \cdot \bar{D} = \rho_V \quad (1.33)$$

$$\nabla \cdot \bar{B} = \rho_{mV}. \quad (1.34)$$

1.5.5 Integral Form of Maxwell's Equations

It is sometimes more convenient to use the integral forms of Maxwell's equations, and Equations (1.1)–(1.4) become

$$\oint_s \nabla \times \bar{\mathcal{E}} \cdot d\mathbf{s} = \oint_C \bar{\mathcal{E}} \cdot d\mathbf{\ell} = - \oint_s \frac{\partial \bar{B}}{\partial t} \cdot d\mathbf{s} - \oint_s \bar{J}_m \cdot d\mathbf{s} \quad (1.35)$$

$$\oint_s \nabla \times \bar{H} \cdot d\mathbf{s} = \oint_C \bar{H} \cdot d\mathbf{\ell} = \int_s \frac{\partial \bar{D}}{\partial t} \cdot d\mathbf{s} + \bar{I} \quad (1.36)$$

$$\int_v \nabla \cdot \bar{D} \, dv = \oint_s \bar{D} \cdot d\mathbf{s} = \int_V \rho_v \, dv = Q_{\text{enclosed}} \quad (1.37)$$

$$\int_v \nabla \cdot \bar{B} \, dv = \oint_s \bar{B} \cdot d\mathbf{s} = 0, \quad (1.38)$$

where Q_{enclosed} is the total charge in the volume enclosed by the surface, S . The subscript S on the integral indicates a surface integral and the circle

on the integral sign indicates that the integral is over a closed surface. Two mathematical identities were used in developing Equations (1.35)–(1.38). The first identity is **Stoke's theorem**, which states that for any vector field \mathbf{X} ,

$$\oint_{\ell} \mathbf{X} \cdot d\ell \equiv \oint_s (\nabla \times \mathbf{X}) \cdot ds. \quad (1.39)$$

So the contour integral of X around a closed contour, C (with incremental length vector $d\ell$), is the integral of $\nabla \times X$ over the surface enclosed by the contour and ds is the incremental area multiplied by a unit vector normal to the surface. This identity is used in Equations (1.35) and (1.36). The **divergence theorem** is the other identity and is used in Equations (1.37) and (1.38). For any vector field \mathbf{X} , the divergence theorem states that

$$\oint_s \mathbf{X} \cdot ds = \int_v \nabla \cdot \mathbf{X} \, dv. \quad (1.40)$$

That is, the volume integral of $\nabla \cdot \mathbf{X}$ is equal to the closed surface integral of \mathbf{X} .

Using phasors the integral-based forms of Maxwell's equations become

$$\oint_C \bar{E} \cdot d\ell = -j\omega \oint_s \bar{B} \cdot ds - \oint_s \bar{J}_m \cdot ds \quad (1.41)$$

$$\oint_C \bar{H} \cdot d\ell = j\omega \oint_s \bar{D} \cdot ds + \bar{I} \quad (1.42)$$

$$\oint_s \bar{D} \cdot ds = \int_V \rho_v \, dv = Q_{\text{enclosed}} \quad (1.43)$$

$$\oint_s \bar{B} \cdot ds = 0, \quad (1.44)$$

1.6 Electric and Magnetic Field Laws

Before Maxwell's equations were postulated, several laws of electromagnetics were known. These are the Biot–Savart law, Ampere's circuital law, Gauss's law, Gauss's law for magnetism, and Faraday's law. The laws are for specific circumstances and mostly for static fields. In this section they are derived from Maxwell's equations.

1.6.1 Ampere's Circuital Law

Ampere's circuital law, often called just Ampere's law, relates direct current and the static magnetic field \bar{H} . The relationship is based on Figure 1-3. In the static situation, $\partial \bar{D} / \partial t = 0$, and so one of Maxwell's equations, Equation (1.36), reduces to

$$\oint_{\ell} \bar{H} \cdot d\ell = I_{\text{enclosed}}. \quad (1.45)$$

This is Ampere's circuital law.

1.6.2 Biot–Savart Law

The Biot–Savart law relates current to static magnetic field. With $\partial \bar{D} / \partial t = 0$, Equation (1.3) becomes

$$\nabla \times \bar{H} = \bar{J}. \quad (1.46)$$

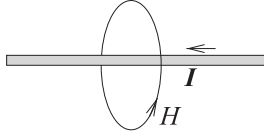


Figure 1-3: Diagram illustrating Ampere's law. Ampere's law relates the current on a wire to the magnetic field around it.

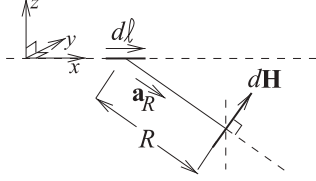


Figure 1-4: Diagram illustrating the Biot-Savart law. The Biot-Savart law relates current to magnetic field.

In Cartesian coordinates,

$$\nabla \times \bar{H} = \left(\frac{\partial H_z}{\partial y} - \frac{\partial H_y}{\partial z} \right) \hat{x} + \left(\frac{\partial H_x}{\partial z} - \frac{\partial H_z}{\partial x} \right) \hat{y} + \left(\frac{\partial H_y}{\partial x} - \frac{\partial H_x}{\partial y} \right) \hat{z}, \quad (1.47)$$

and if the current is confined to a thin wire as shown in Figure 1-4, $\nabla \times \bar{H}$ reduces to an operation along the wire, but also with vector information. So the first step in the development of the Biot-Savart law, Equation (1.46), is simplified to (ignoring vector information for now)

$$\frac{\partial H}{\partial \ell} = \frac{I}{4\pi R^2}. \quad (1.48)$$

With vector information and moving the infinitesimal length of wire, $d\ell$, from the left side of the equation to the right, the final form of the Biot-Savart law is obtained:

$$d\bar{H} = \frac{I d\ell \times \hat{a}_R}{4\pi R^2}, \quad (1.49)$$

which has the units of amps per meter in the SI system. In Equation (1.49), I is current, $d\ell$ is a length increment of a filament of current I , \hat{a}_R is the unit vector in the direction from the current filament to the magnetic field, and R is the distance between the filament and the magnetic field increment. So Equation (1.49) is saying that a filament of current produces a magnetic field at a point. The total static magnetic field from a current on a wire or surface can be found by modeling the wire or surface as a number of current filaments, and the total magnetic field at a point is obtained by summing up the contributions from each filament.

1.6.3 Gauss's Law

The third law is Gauss's law, which relates the static electric flux density vector, \bar{D} , to charge. With reference to Figure 1-5, Gauss's law in integral form is

$$\oint_s \bar{D} \cdot d\bar{v} = Q_{\text{enclosed}}, \quad (1.50)$$

which states that the integral of the electric flux density vector, \bar{D} , is equal to the total charge enclosed by the surface, Q_{enclosed} . This is just the integral form of the third Maxwell equation (Equation (1.37)).

Figure 1-5: Diagram illustrating Gauss's law. Charges are distributed in the volume enclosed by the closed surface. An incremental area is described by the vector ds which is normal to the surface and whose magnitude is the area of the incremental area.

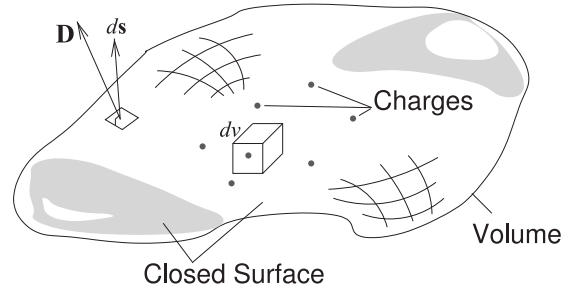
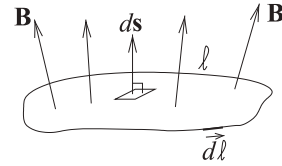


Figure 1-6: Diagram illustrating Faraday's law. The contour ℓ encloses the surface.



There is a similar law called Coulomb's law which says that the magnitude of the force between two stationary point charges is directly proportional to the product of the magnitudes of charges and inversely proportional to the square of the distance between them. This law can be derived from Gauss's law but is less general. Coulomb's law applies only to stationary charges whereas with Gauss's law the charges can be moving.

Gauss's law has also been used for magnetic field where it is called Gauss's law for magnetism. In integral form Gauss's law for magnetism is

$$\oint_s \vec{B} \cdot d\vec{s} = 0, \quad (1.51)$$

where \vec{B} , is the static magnetic flux density. This law is the same as saying that there are no magnetic charges. "Gauss's law for magnetism" is a name that is not universally used and many people simply say that there are no magnetic charges.

1.6.4 Faraday's Law

Faraday's law relates a time-varying magnetic field to an induced voltage drop, V , which is now understood to be $\oint_{\ell} \vec{E} \cdot d\vec{\ell}$, that is, the closed contour integral of the electric field,

$$V = \oint_{\ell} \vec{E} \cdot d\vec{\ell} = - \oint_s \frac{\partial \vec{B}}{\partial t} \cdot d\vec{s}, \quad (1.52)$$

and this has the units of volts in the SI unit system. This is just the first of Maxwell's equations in integral form (see Equation (1.35)). The operation described in Equation (1.52) is illustrated in Figure 1-6.

1.7 Electromagnetic Fields in Dielectrics and Metals

The discussion in this section follows the description by Max Born [11] (who was instrumental in the development of quantum mechanics). Extensions are made to relate quantum descriptions to effects important to microwave engineering. In particular the descriptions here relate phenomena at the discrete particle level to continuum properties such as permittivity, ϵ .

1.7.1 *Electromagnetic Fields in a Dielectric*

A dielectric has no electrons that are free to move through a material under the influence of an electric field. When an EM field is incident on a dielectric the electric field moves charge centers. For a crystal these charge centers are at the scale of the lattice, and for composite materials like plastics the centers are at the molecular scale. With some materials, which we know as materials having high permittivity, the charge centers are normally separated but by less than the intra-atom spacing. With all dielectric materials, the major impact of an applied electric field is movement of the charge centers, alternately moving them apart and moving them together as the applied electric field alternates. Now being a dielectric, the charges cannot move freely through the material and the energy that is transferred to the charges is stored as electric potential energy in stretched bonds or, sometimes, as a distorted lattice (such as with the piezoelectric effect). This energy storage is much like storing mechanical energy in a spring. Now the charges move and thus excite an electric field of their own. However the charges move sluggishly and so the phase of the EM signal they produce is out of phase with respect to an externally applied alternating EM field. The charge centers are moving the fastest at the peak of the applied sinusoidal field and the net effect is a 90° phase lag.

Another phenomenon is that the combined effect of the reradiated fields from the moving charge centers produces an EM wave with the same frequency as the applied field but with a smaller phase velocity (smaller because the phase velocity is averaged over many paths). The oscillating charge centers radiate in all directions (which is called scattering) and so some of the EM energy will be scattered in the direction from which the applied EM wave came.

An ideal dielectric has no loss. That is, there is no dielectric relaxation loss associated with heating as the charge centers move, and there is no conductivity due to moving free charges in the dielectric.

1.7.2 *Refractive Index*

Dielectrics were first characterized by their refractive index long before the concept of EM waves and permittivity were developed. The refractive index, n , of a medium is defined as the ratio of the speed of light (i.e., of an EM wave) in a vacuum, c , of an EM wave to the phase velocity, v_p , of the wave in the medium:

$$n = \frac{c}{v_p} = \frac{1}{\sqrt{\epsilon_0 \mu_0}} \frac{\sqrt{\epsilon \mu}}{1}. \quad (1.53)$$

For a loss-free medium $n = \sqrt{\epsilon_r \mu_r}. \quad (1.54)$

For a lossy medium the complex index of refraction is

$$\tilde{n} = n + j\kappa, \quad (1.55)$$

where n is called the refractive index and is directly related to the phase velocity, v_p , and κ is called the extinction coefficient, which describes loss when the EM wave propagates through the material.

Conversion between refractive index and permittivity is as follows [12, 13]; the complex permittivity

$$\varepsilon = \varepsilon_1 + j\varepsilon_2 = (n + j\kappa)^2, \quad (1.56)$$

$$\text{where } \varepsilon_1 = n^2 - \kappa^2 \quad \text{and} \quad \varepsilon_2 = 2n\kappa. \quad (1.57)$$

The components of the complex index of refraction are then

$$n = \sqrt{\frac{\sqrt{\varepsilon_1^2 + \varepsilon_2^2} + \varepsilon_1}{2}} \quad \text{and} \quad \kappa = \sqrt{\frac{\sqrt{\varepsilon_1^2 + \varepsilon_2^2} - \varepsilon_1}{2}}. \quad (1.58)$$

The permittivity is just the square of the (complex) refractive index in a nonmagnetic medium ($\mu_r = 1$). The refractive index is used with optics and the permittivity is used when working with Maxwell's equations and with electronics.

The refractive index, and thus permittivity, of a dielectric can vary significantly between microwave and optical frequencies, a result of how quickly different types of charge centers can move. For water at 20°C and at the standard optical wavelength of 589 nm (the yellow doublet sodium D-line), $n = 1.333$ ($\epsilon_r = 1.78$) [14]. At 1 GHz $n = 8.94$ ($\epsilon_r = 80$) [15].

1.7.3 Electromagnetic Fields in a Metal

The discussion here refers to the behavior of EM fields in metals at frequencies from DC to 10 THz. Above these frequencies the EM wave changes direction much faster than electrons can move. Metals have a large number of free charges that can move through a metal under the influence of an electric field. On transmission lines the energy is contained in the EM fields between metal guides, and electric and magnetic fields are present at the surface of the metal. The main effect of the EM fields at the surface of the metal is to accelerate the free electrons at the surface, with the electrons accelerating in the direction opposite to that of the electric field. While some of the EM energy propagates into the metal, the overwhelming effect is transfer of energy from the EM photons to kinetic energy of the free electrons. There is also some transfer of energy to the bound electrons, however, this effect is smaller as the bound electrons are shielded by the sea of free electrons. Electrons have mass and accelerate relatively slowly. Even when the electric field is reversed, the electrons will continue moving considerably in the same direction as the electric field before reversing. The moving and accelerating electrons also produce electric fields of their own that in turn influence the movement of other electrons. Electrons are sluggish and their position is almost 180° out of phase with the applied E field. The net effect is that the electric field produced by the electrons almost completely cancels

Table 1-2: Electromagnetic properties of metals at optical frequencies. (n and κ are measured, ε_1 and ε_2 are derived using Equation (1.57).

Metal	Photon energy (eV)	Wavelength, λ (μm)	Frequency f (THz)	n	κ	ε_1	ε_2
Gold	0.1	12.398	24.197	8.17	82.83	-6794	1353
Copper	0.1	12.398	24.197	29.69	71.57	-4240	4250
Aluminum	0.1	12.398	24.197	98.595	203.7	-31 663	40 168

the incoming electric field. It is therefore almost meaningless to talk about the (group or phase) velocity of the EM fields in the metal. The overriding effect is transfer of energy to moving electrons that eventually make the lattice move and transfer their energy to the lattice, producing heat.

The accelerating electrons radiate electric field in all directions and in turn this field accelerates other electrons. There is also a damping force as the free electrons collide with atoms. So there is a rapidly diminishing component of the EM field that travels through the metal at the speed of light. Rather than energy being stored in the electric field through the movement of charge centers as in dielectrics, electric energy in the forward-propagating field is almost entirely lost in the scattering and collision processes. So at microwave frequencies the effective permittivity of a metal is almost entirely imaginary (corresponding to loss), and this imaginary component of the relative permittivity is 8–10 orders of magnitude greater than the real component, which is believed to be 1 [16]. The real component of the relative permittivity is 1 because the charge centers are masked by the sea of free electrons. It is not possible to directly measure the real part of the permittivity of metals at microwave frequencies. An ideal conductor has infinite conductivity, so there are no EM fields inside the metal and net charges are confined to the surface of the conductor. At optical frequencies metals are known to have a negative permittivity (see Table 1-2).

1.8 Electric and Magnetic Walls

The boundaries imposed by conductors and the interface between dielectrics define the mode structure (i.e., orientation of the fields) supported by a transmission line. Understanding the fields at the interfaces provides the intuition required to understand the operational frequency limits of distributed structures such as transmission lines.

1.8.1 Electric Wall

An electric wall is formed by an ideal conductor, as shown in Figure 1-7, where there are electric charges at the surface of the conductor. Consider that the conductor in Figure 1-7(a) carries a current of density J and charge of density ρ_V . As the conductivity of the conductor goes to infinity, the conductor becomes a perfect conductor and forms an electric wall, as shown in Figure 1-7(b). The current and charge now occupy the very skin of the conductor at the interface to the region above which there is either free space or a dielectric. The behavior of the fields at the interface can be understood

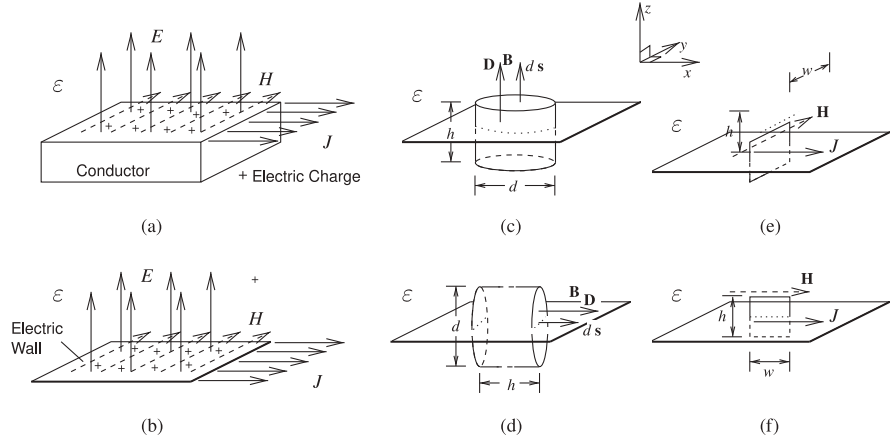


Figure 1-7: Properties of an electric wall: (a) the electrical field is perpendicular to a conductor and the magnetic field is parallel to it and is orthogonal to the current; (b) a conductor can be approximated by an electric wall; (c) cylinder used in deriving the normal electric field; (d) cylinder used in showing that the tangential electric field is zero; (e) contour used in deriving the tangential magnetic field in the y direction; and (f) contour used in deriving the z - and x -directed magnetic fields (they are zero).

by considering the integration surfaces and volumes shown in Figure 1-7(c and d). The cylinder in Figure 1-7(c) with height h and diameter d enables Gauss's law (Equation (1.50)) to be applied. As $h \rightarrow 0$ (h approaching zero), Equation (1.50) yields

$$\oint_s \bar{D} \cdot d\mathbf{s} = D_z \frac{1}{4} \pi d^2 = \int_v \rho_v \cdot dv = Q_{\text{enclosed}} = \rho_S \frac{1}{4} \pi d^2, \quad (1.59)$$

where ρ_S is the surface charge density (in SI units of C/m^2) and so

$$D_z = \rho_S. \quad (1.60)$$

Now considering the cylinder in Figure 1-7(d), again as $h \rightarrow 0$,

$$\begin{aligned} \oint_s \bar{D} \cdot d\mathbf{s} &= D_x \frac{1}{4} \pi d^2 = \int_v \rho_v \cdot dv = Q_{\text{enclosed}} \\ &= \rho_S \pi d h \rightarrow 0. \end{aligned} \quad (1.61)$$

$$\text{That is, } D_x = 0. \quad (1.62)$$

Changing the orientation of the cylinder, it can be seen that

$$D_y = 0. \quad (1.63)$$

So the electric field is normal to the surface of the conductor.

The properties of the magnetic field at the electric wall can be deduced from Faraday's circuital law and the Biot-Savart law (Equation (1.49)). Consider the rectangular contour shown in Figure 1-7(e) with height h and width w . With $h \rightarrow 0$, only the y -directed component of the magnetic field will contribute to the static magnetic field integral of Faraday's law, so from

Equation (1.52),

$$\oint_{\ell} \bar{\mathbf{H}} \cdot d\ell = H_y w = I_{\text{enclosed}} = J_S w, \quad (1.64)$$

where J_S is the surface current density (with SI units of A/m) and

$$H_y = J_S. \quad (1.65)$$

For the field oriented in the x direction, the rectangular contour shown in Figure 1-7(f) can be used, but now no current is enclosed by the contour, so that with $h \rightarrow 0$,

$$\oint_{\ell} \bar{\mathbf{H}} \cdot d\ell = H_x w = I_{\text{enclosed}} = 0 \quad (1.66)$$

$$\text{and} \quad H_x = 0. \quad (1.67)$$

H_z has not yet been considered. Again, using the rectangle in Figure 1-7(f) and with $w \rightarrow 0$,

$$\oint_{\ell} \mathbf{H} \cdot d\ell = H_z h = I_{\text{enclosed}} = 0 \quad (1.68)$$

$$\text{and} \quad H_z = 0. \quad (1.69)$$

This could also have been derived from the Biot–Savart law (Equation (1.49)). Immediately above the electric wall $R \rightarrow 0$ and only the filament of current immediately below the magnetic field contributes. Thus a_R is normal to the surface so that \mathbf{H} will be perpendicular to the current, but in the plane of the current.

Gathering the results together, the EM fields immediately above the electric wall have the following properties:

The E field is perpendicular to the electric wall. The H field is parallel to the electric wall.

$D_{\text{normal}} = \rho_S$, the surface charge density. $H_{\text{parallel}} = J_S$, the surface current density.

1.8.2 Magnetic Wall

A true magnetic wall does not exist, but it is approximated by the interface between two dielectrics (as shown in Figure 1-8) when the permittivity of the dielectrics differ so that $\varepsilon_2 \gg \varepsilon_1$. Considering the top dielectric region, the magnetic wall model can then be introduced at the interface between the two dielectrics, complete with magnetic charges and magnetic current density, M . The situation is analogous to the electric wall situation with the roles of the electric and magnetic fields interchanged. The EM fields immediately above the magnetic wall have the following properties:

The H field is perpendicular to the magnetic wall. The E field is parallel to the magnetic wall.

$H_{\text{normal}} = \rho_{mS}$, the surface magnetic charge density. $E_{\text{parallel}} = J_{mS}$, the surface magnetic current density.

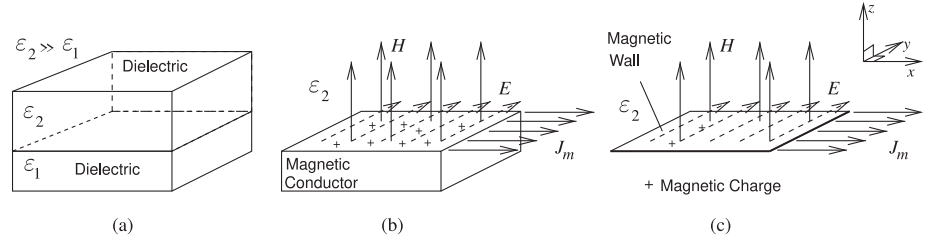


Figure 1-8: Properties of the EM field at a magnetic wall: (a) the interface of two dielectrics of contrasting permittivities approximates a magnetic wall with the magnetic field perpendicular to the interface and the electric field parallel to it; (b) the dielectric with lower permittivity can be approximated as a magnetic conductor; and (c) the magnetic conductor forms a magnetic wall at the interface with the material with higher permittivity.

Table 1-3: Properties of electric and magnetic walls.

	Electric field	Magnetic field
Electric wall	Normal	Parallel
Magnetic wall	Parallel	Normal

What constitutes a good magnetic wall is subject to debate, as the contrast between dielectrics is not as great as the contrast between the conductivity of a good conductor and that of a good dielectric. However, it is an essential concept in understanding the coupling of signals and approximating transmission lines to yield intuitive understanding.

The summary that is used in the text to understand multimoding is given in Table 1-3.

1.9 Fields in Lossy Mediums

Lossy mediums result in power loss of EM fields. In RF and microwave systems materials are ideally either perfect conductors or perfect dielectrics. In practice, conductors and dielectrics have finite conductivity and dielectrics have another type of loss called dielectric relaxation loss. Dielectric relaxation loss is due to heating that can result from the movement of charge centers in a material.

1.9.1 Lossy Dielectrics

In a lossy dielectric there can be both current flow and relaxation loss. Current flow results from applied electric field and is described by the **conductivity**, σ , of the material. **Relaxation loss** results from polarization of the material and the transfer of energy to the lattice of the material as the electric field changes direction. This is also referred to as **dielectric damping**. The polarization vector describes the additional energy storage capacity of a material (above that of vacuum) in response to an applied electric field. The capacity is described by the electric susceptibility, χ_e , in Equation (1.20). In phasor form, loss is captured by a complex χ_e or a **complex permittivity**:

$$\varepsilon = \varepsilon' - j\varepsilon'' = \varepsilon(1 + \chi_e). \quad (1.70)$$

Both current and relaxation respond to an applied electric field. In phasor form, Maxwell's curl equation for a magnetic field, Equation (1.32), becomes

$$\begin{aligned}\nabla \times \bar{H} &= j\omega \bar{D} + \bar{J} = j\omega \varepsilon \bar{E} + \sigma \bar{E} = j\omega(\varepsilon' - j\varepsilon'')\bar{E} + \sigma \bar{E} \\ &= j\omega \varepsilon' \bar{E} + (\sigma + \omega \varepsilon'')\bar{E} \\ &= j\omega \left(\varepsilon' - j\varepsilon'' - j\frac{\sigma}{\omega} \right) \bar{E}.\end{aligned}\quad (1.71)$$

In the above, $\omega \varepsilon'$ describes the ability to store electric energy, $\omega \varepsilon''$ describes dielectric damping loss, and σ describes conductivity loss. At a single frequency, damping and conductivity losses are indistinguishable and so the term $(\omega \varepsilon'' + \sigma)$ is taken as the effective conductivity. The effective (complex) relative permittivity is

$$\varepsilon_e = \left(\varepsilon' - j\varepsilon'' - j\frac{\sigma}{\omega} \right) \frac{1}{\varepsilon_0}. \quad (1.72)$$

Another quantity that describes loss is the **loss tangent**, $\tan \delta$, which is the ratio of power lost to energy stored:

$$\tan \delta = \frac{\omega \varepsilon'' + \sigma}{\omega \varepsilon'}. \quad (1.73)$$

For many dielectric materials used with EM structures, $\tan \delta$ is approximately independent of frequency up to 100s of gigahertz, so it is commonly used to characterize the dielectric loss of a material. Most exceptions are semiconductors such as silicon which can have appreciable **conductive loss**. The frequency independence of $\tan \delta$ indicates that conductivity loss is negligible.

EXAMPLE 1.3 Electromagnetic Wave Propagation in a Lossy Dielectric

Consider a plane EM wave propagating in a medium with permittivity ε and permeability μ . The complex permittivity measured at two frequencies is experimentally characterized by the relative permittivity ($\varepsilon/\varepsilon_0$) of the real, $\Re\{\varepsilon/\varepsilon_0\}$, and imaginary, $\Im\{\varepsilon/\varepsilon_0\}$, parts as follows:

Measured relative permittivity:

Frequency	Real part	Imaginary part
1 GHz	1.9	-0.0490
2 GHz	1.9	-0.0314

Measured relative permeability:

Frequency	Real part	Imaginary part
1 GHz	1.9	-0.001
2 GHz	1.9	-0.001

Since there is an imaginary part of the dielectric constant, there could be loss due to either dielectric damping or finite material conductivity, or both. When characterizing materials, it is only possible to distinguish the contribution to the measured imaginary part of the permittivity by considering the experimentally derived imaginary permittivity at two different frequencies.

- Determine the dielectric loss tangent at 1 GHz.
- Determine the relative dielectric damping factor at 1 GHz (the part of the permittivity due to dielectric damping).
- What is the conductivity of the dielectric?
- What is the magnetic conductivity of the medium?

Solution:

(a) At 1 GHz, $\varepsilon = \varepsilon_r \varepsilon_0$, and the measured relative permittivity is

$$\varepsilon_r = 1.9 - j0.049 = \varepsilon'_{r,e} - j\varepsilon''_{r,e}, \quad (1.74)$$

where $\varepsilon'_{r,e}$ and $\varepsilon''_{r,e}$ are the effective (measured) values of ε'_r and ε''_r obtained from measurement. Now $\varepsilon'_e = \varepsilon'_r$, but the imaginary permittivity includes the effect of dielectric conductivity, σ , as well as of dielectric damping, which is described by ε'' alone. That is,

$$\varepsilon''_e = \varepsilon'' + \frac{\sigma}{\omega} \cdot \varepsilon_r = \varepsilon''_{r,e} = 0.0490 \quad \text{and} \quad \tan \delta = 0.0490/1.9 = 0.0258.$$

(b) The imaginary relative permittivity is found by noting that $\varepsilon''_{r,e} = \varepsilon''_r + \sigma/\omega$ and $\omega\varepsilon''_r + \sigma = \omega\varepsilon''_{r,e}$. Let $\omega_1 = 2\pi$ (1 GHz). Then

$$\begin{aligned} \omega_2 &= 2\omega_1 \\ \omega_1\varepsilon''_{r,e} \text{ (1 GHz)} &= \omega_1\varepsilon''_r + \sigma = \omega_1 \cdot 0.0490 \quad (\text{A}) \end{aligned}$$

$$\omega_2\varepsilon''_{r,e} \text{ (2 GHz)} = \omega_2\varepsilon''_r + \sigma = \omega_2 \cdot 0.0314$$

$$2\omega_1\varepsilon''_e + \sigma = 2\omega_1(0.0314) \quad (\text{B})$$

$$(\text{B}) - (\text{A}) \rightarrow \omega_1\varepsilon''_r = \omega_1[0.0628 - 0.0490]$$

$$\varepsilon''_r = 0.0138 \text{ (at all frequencies).}$$

(c) Recall that $\varepsilon''_{r,e} = \varepsilon''_r + \sigma/\omega$.

At 1 GHz, $\omega = 2\pi \times 10^9$, $\varepsilon''_{r,e} = 0.0490$, $\varepsilon''_r = 0.0138$, so

$$\sigma = \omega(\varepsilon''_{r,e} - \varepsilon''_r) = 2 \cdot \pi \cdot 10^9 (0.0490 - 0.0138) = 0.221 \cdot 10^9 \text{ S/m} = 221 \text{ MS/m}.$$

(d) Magnetic conductivity is nonexistent, thus magnetic conductivity is zero.

1.9.2 Lossy Conductors

Perfect conductors would have infinite conductivity, but since the conductivity of real conductors is finite, EM fields penetrate into the interior of a conductor. Still the energy stored in the current is much greater than the (dielectric) electric energy storage capability, $\sigma \gg \omega\varepsilon'$, and the losses from conductivity are much higher than dielectric loss, $\sigma \gg \omega\varepsilon''$, so that the effective relative permittivity from Equation (1.72) is

$$\varepsilon_e = \left(\varepsilon' - j\varepsilon'' - j\frac{\sigma}{\omega} \right) \frac{1}{\varepsilon_0} \approx \left(-j\frac{\sigma}{\omega} \right) \frac{1}{\varepsilon_0} \approx \left(\frac{\sigma}{j\omega} \right) \frac{1}{\varepsilon_0}. \quad (1.75)$$

For most conductors the permeability is μ_0 and the working permittivity is

$$\varepsilon = \varepsilon_e \varepsilon_0 = \frac{\sigma}{j\omega}. \quad (1.76)$$

The propagation constant of the field in a conductor is

$$\gamma = \alpha + j\beta \approx j\omega\sqrt{\mu\varepsilon} \approx j\omega\sqrt{\mu} \sqrt{\frac{\sigma}{j\omega}} \approx (1 + j) \sqrt{\frac{\omega\mu\sigma}{2}}. \quad (1.77)$$

So $\alpha = \sqrt{\omega\mu\sigma/2}$. The EM field in the conductor reduces in amplitude as $e^{-\alpha x}$ after a distance x . Thus the field reduces to $1/e$ of its value after a distance called the skin depth, δ_s :

$$\delta_s = \sqrt{\frac{2}{\omega\mu\sigma}}. \quad (1.78)$$

If the amplitude of the electric field at the surface of a conductor is $A(0)$, after a distance δ_s the amplitude of the electric field will have the amplitude

$$\begin{aligned} A(\delta_s) &= e^{-\alpha x} = e^{-\left(\sqrt{\omega\mu\sigma/2}\sqrt{2/\omega\mu\sigma}\right)} \\ &= e^{-1}. \end{aligned} \quad (1.79)$$

Table 1-4 lists the skin depth and phase velocities of conductors commonly used in microwave circuits. The resistivity values here are those of a single crystal. The phase velocity, v_p , is calculated from the propagation constant β . From Equation (1.77), $\beta = \sqrt{\omega\mu\sigma/2}$.

Now $v_p = \omega/\beta$, so that

$$v_p = \frac{\omega}{\beta} = \frac{\omega\sqrt{2}}{\sqrt{\omega\mu\sigma}} = \sqrt{\frac{2\omega}{\mu\sigma}}. \quad (1.80)$$

This can be simplified further if the relative permeability of the material is 1, as then $\mu = \mu_0 = 4\pi 10^{-7}$ H/m. If SI units are used for f and σ :

$$v_p = \sqrt{\frac{2\omega}{\mu_0\sigma}} = \sqrt{\frac{4\pi f}{4\pi 10^{-7}\sigma}} = \sqrt{\frac{10^7 f}{\sigma}}. \quad (1.81)$$

From Table 1-4 note that the skin depth at gigahertz frequencies is close to the thickness of microstrip lines which are often only a few microns thick. Also the speed of an EM wave in a conductor is very slow. The speed of EM in copper (ideal), for example, is 0.004% of the speed of light in a vacuum.

Table 1-4: Skin depth and effective phase velocity at 1 GHz of several conductors commonly used in microwave circuits.

Material	Electrical conductivity, σ (MS.m ⁻¹)	Skin depth, δ at 1 GHz (μ m)	Phase velocity, v_p at 1 GHz (km/s)
1 GHz			
Aluminum (crystal)	37.7	2.59	16.3
Aluminum (2 \times resistivity)	18.9	3.66	23.0
Copper (single crystal)	59.6	2.06	13.0
Copper (2 \times resistivity)	29.8	2.92	18.3
Gold (single crystal)	45.2	2.37	14.9
Gold (2 \times resistivity)	22.6	3.35	21.0
Silver (single crystal)	63.0	2.01	12.6
Silver (2 \times resistivity)	31.5	2.84	17.8
Titanium (single crystal)	0.238	32.6	200
Titanium (2 \times resistivity)	0.119	46.1	290

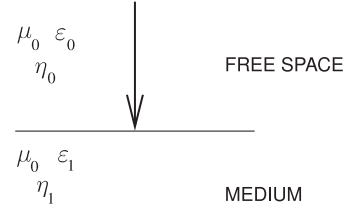


Figure 1-9: Two regions used in Example 1.4.

EXAMPLE 1.4

Electromagnetic Calculations

This example provides a review of basic EM theory. In Figure 1-9, a plane wave in free space is normally incident on a lossless medium occupying a half space with a dielectric constant of 16. Calculate the electric field reflection coefficient at the interface referred to the medium.

Solution:

Since it is not explicitly stated, assume $\mu_1 = \mu_0$. (This should be done in general since μ_0 is the default value for μ , as most materials have unity relative permeability.) The characteristic impedance of a medium is $\eta = \sqrt{\mu/\epsilon}$. Now η is used for characteristic impedance (also called wave impedance) of a TEM propagating wave in a medium. It is used instead of Z_0 , which is generally reserved for the characteristic impedance of transmission lines. The electric field reflection coefficient is

$$\Gamma^E = \frac{\eta_1 - \eta_0}{\eta_1 + \eta_0} = \frac{\eta_1/\eta_0 - 1}{\eta_1/\eta_0 + 1}$$

$$\frac{\eta_1}{\eta_0} = \sqrt{\frac{\mu_0}{\epsilon_1}} \cdot \sqrt{\frac{\epsilon_0}{\mu_0}} = \sqrt{\frac{\epsilon_0}{\epsilon_1}} = \sqrt{\frac{1}{16}} = \frac{1}{4},$$

so

$$\Gamma^E = \frac{1/4 - 1}{1/4 + 1} = \frac{1 - 4}{1 + 4} = -\frac{3}{5} = -0.6.$$

EXAMPLE 1.5

Intuitive Solution of Electromagnetic Problems

This example provides an intuitive way of solving an EM problem. A plane wave in free space is normally incident on a lossless medium occupying a half space with a dielectric constant of 16. What is the magnetic field reflection coefficient?

Solution:

There are two ways to answer this question. An intuitive approach will be used first.

Intuitively $|\Gamma^H| = |\Gamma^E|$.

With $\vec{\mathcal{E}}$ and $\vec{\mathcal{H}}$ being vectors, the Poynting vector $\vec{\mathcal{E}} \times \vec{\mathcal{H}}$ points in the direction of propagation for a plane wave, since the reflected wave is in the opposite direction to the incident wave, thus

$$\text{sign}(\Gamma^H) = -\text{sign}(\Gamma^E).$$

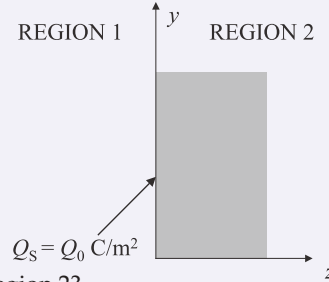
Therefore $\Gamma^H = -\Gamma^E = +0.6$. (Γ^E was calculated in Example 1.4.)

Now the second approach. The formula for the magnetic field reflection coefficient is

$$\Gamma_H = \frac{\eta_1 - \eta_2}{\eta_1 + \eta_2} = \frac{1 - \eta_2/\eta_1}{1 + \eta_2/\eta_1} = \frac{1 - 1/4}{1 + 1/4} = \frac{3}{5} = 0.6.$$

EXAMPLE 1.6**Wave Impedance and Propagation Constant**

A 4 GHz time-varying EM field is traveling in the $+z$ direction in Region 1 and is normally incident on another material in Region 2. The boundary between the two regions is in the $z = 0$ plane. The permittivity of Region 1 is $\varepsilon_1 = \varepsilon_0$ and that of Region 2 is $\varepsilon_2 = (4 - j0.4)\varepsilon_0$. For both regions, $\mu_1 = \mu_2 = \mu_0$. The phasor of the forward-traveling electric field (i.e., the incident field) is $\mathbf{E}^+ = 100 \hat{y}$, and the phase is normalized with respect to $z = 0$.



What are the wave impedance and propagation constant of Region 2?

Solution:

The wave impedance is

$$\begin{aligned} \eta &= \sqrt{\frac{\mu}{\varepsilon}} = \sqrt{\frac{\mu_0}{\varepsilon_0}} \sqrt{\frac{\mu_r}{\varepsilon_r}} = \eta_0 \sqrt{\frac{\mu_r}{\varepsilon_r}} = 377 \sqrt{\frac{1}{(4 - j0.4)}} \Omega \\ &= 187.8 + j9.4 \Omega. \end{aligned} \quad (1.82)$$

The propagation constant is

$$\begin{aligned} \gamma &= j\omega \sqrt{\mu \varepsilon} = j\omega \sqrt{\mu_0 \varepsilon_0} \sqrt{\mu_r \varepsilon_r} \\ &= j4 \cdot 2\pi \cdot 10^9 \cdot \sqrt{4\pi \cdot 10^{-7} \cdot 8.854 \cdot 10^{-12}} \sqrt{4 - j0.4} = (8.4 + j167.9) \text{ m}^{-1}. \end{aligned} \quad (1.83)$$

1.10 Summary

This introductory chapter provided the background for the following chapters on distributed effects. A review of Maxwell's equations and their implications was presented. The notable change in the way these were presented here to the first time they are introduced in electromagnetics courses is the first time the static electric and magnetic field laws are presented and then Maxwell's equations are covered almost as though there was a continuous derivation. However Maxwell's equations cannot be derived from the static laws even with some additional insight. Instead Maxwell's equations embed the quantum field theory that there are two inseparable component fields which we call electric and magnetic fields, and the fundamental relativity effect of the finite speed of light which results from relating the spatial derivative of each of the field components to the time derivative of the other component. The insight places Maxwell among the ten greatest physicists of all time.

The finite speed for electromagnetic radiation is at the core of microwave engineering. At microwave frequencies the finite speed at which information can move means that microwave circuit design is quite different from low frequency circuit design, and the distributed and electromagnetic coupling effects lead to a large number of microwave circuit components that provide a very rich design space.

1.11 References

- [1] M. Steer, *Microwave and RF Design, Radio Systems*, 3rd ed. North Carolina State University, 2019.
- [2] —, *Microwave and RF Design, Networks*, 3rd ed. North Carolina State University, 2019.
- [3] —, *Microwave and RF Design, Modules*, 3rd ed. North Carolina State University, 2019.
- [4] —, *Microwave and RF Design, Amplifiers and Oscillators*, 3rd ed. North Carolina State University, 2019.
- [5] R. Barrett, "Microwave printed circuits—a historical survey," *IRE Trans. on Microwave Theory and Techniques*, vol. 3, no. 2, pp. 1–9, Mar. 1955.
- [6] R. M. Barrett, "Microwave printed circuits—the early years," *IEEE Trans. on Microwave Theory and Techniques*, vol. 32, no. 9, pp. 983–990, Sep. 1984.
- [7] D. Grieg and H. Engelmann, "Microstrip—a new transmission technique for the kilomegacycle range," *Proc. IRE*, vol. 40, no. 12, pp. 1644–1650, Dec. 1952.
- [8] J. Maxwell, *A Treatise on Electricity and Magnetism*. Clarendon Press (Reprinted, Oxford University Press, 1998), 1873.
- [9] J. Rautio, "Maxwell's legacy," *IEEE Microwave Magazine*, vol. 6, no. 2, pp. 46–53, Jun. 2005.
- [10] O. Heaviside, "Electromagnetic induction and its propagation," *Electrician*, Jun. 1887.
- [11] M. Born and E. Wolf, "Two-dimensional diffraction of a plane wave by a half-plane," in *Principles of Optics: Electromagnetic Theory of Propagation, Interference, and Diffraction of Light*, 7th ed. Cambridge University Press, 1999, section 11.5.
- [12] F. Wooten, *Optical Properties of Solids*. Academic Press, 1972.
- [13] J. Waever and H. Frederikse, "Optical properties of selected elements," in *CRC Handbook of Chemistry and Physics*, 1972.
- [14] E. Hecht, *Optics*. Addison-Wesley, 2002.
- [15] "International Council for Science: Committee on Data for Science and Technology." [Online]. Available: <http://www.codata.org/resources/databases/index.html>
- [16] J.-M. Lourtioz, H. Benisty, V. Berger, J.-M. Gerard, D. Maystre, and A. Tchebnokov, *Photonic Crystals: Towards Nanoscale Photonic Devices*. Springer, 2005.
- [17] A. Stogryn, "Equations for calculating the dielectric constant of saline water (correspondence)," *IEEE Trans. on Microwave Theory and Techniques*, vol. 19, no. 8, pp. 733–736, Aug. 1971.
- [18] H. Marshall, V. Mechenova, and V. Yakovlev, "Computer modeling of microwave high power loads," in *Proc. 36th Microwave Power Symp.*, Apr. 2001.
- [19] S. Ponnusamy and H. Silverman, "Bilinear transformations and mappings," in *Complex Variables with Applications*. Birkhäuser, 2006, pp. 61–90.
- [20] W. Press, S. Teukolsky, W. Vetterling, and B. Flannery, *Numerical recipes in C+: the art of scientific computing*. Cambridge University Press, 2009.
- [21] P. Honnell, "Kron's methods and the theoretical foundation of the matrix computer," *Journal of the Franklin Institute*, vol. 286, no. 6, pp. 566–571, Dec. 1968.
- [22] H. Brown, *Solution of Large Networks by Matrix Methods*. Wiley-Interscience, 1975.
- [23] G. Kron, *Tensor Analysis of Networks*. John Wiley and Sons, 1939.

1.12 Exercises

1. The plane wave electric field of a radar pulse propagating in free space in the z direction is given by (with $\omega_0 \gg \pi/(2\tau)$)

$$\bar{\mathcal{E}}(t) = \begin{cases} A \cos\left(\frac{\pi t}{2\tau}\right) \cos(\omega_0 t) \hat{\mathbf{x}} & -\tau \leq t \leq \tau \\ 0 & \text{otherwise,} \end{cases}$$
 - (a) Sketch $\bar{\mathcal{E}}(t)$ over the interval $-1.5\tau \leq t \leq 1.5\tau$.
 - (b) What is, $\bar{\mathcal{H}}(t)$.
 - (c) What is the Poynting vector, $\bar{\mathcal{S}}(t)$.
 - (d) Determine the total energy density in the pulse (in units of J/m^2).
2. Consider a material with a relative permittivity of 72, a relative permeability of 1, and a static electric field (E) of 1 kV/m. How much energy is stored in the E field in a 10 cm^3 volume of the material? [Parallels Example 1.1]
3. A time-varying electric field in the x direction has a strength of 1 kV/m and a frequency of 1 GHz. The medium has a relative permittivity of 70. What is the time-domain polarization vector? [Parallels Example 1.2]

4. A medium has a dielectric constant of 20. What is the index of refraction?
5. Consider a plane EM wave propagating in a medium with a permittivity ϵ and permeability μ . The complex permittivity measured at two frequencies is characterized by the relative permittivity (ϵ/ϵ_0) of the real $\Re\{\epsilon/\epsilon_0\}$ and imaginary parts $\Im\{\epsilon/\epsilon_0\}$ as follows:

Measured relative permittivity:

Frequency	Real part	Imaginary part
1 GHz	3.8	-0.05
10 GHz	4.0	-0.03

Measured relative permeability:

Frequency	Real Part	Imaginary Part
1 GHz	0.999	-0.001
10 GHz	0.998	-0.001

Since there is an imaginary part of the dielectric constant there could be either dielectric damping or material conductivity, or both. [Parallels Example 1.3]

- (a) Determine the dielectric loss tangent at 10 GHz.
- (b) Determine the relative dielectric damping factor at 10 GHz (the part of the permittivity due to dielectric damping).
- (c) What is the conductivity of the dielectric at 10 GHz?
6. A medium has a relative permittivity of 13 and supports a 5.6 GHz EM signal. By default, if not specified otherwise, a medium is lossless and will have a relative permeability of 1.
- (a) Calculate the characteristic impedance of an EM plane wave.
- (b) Calculate the propagation constant of the medium.
7. A plane wave in free space is normally incident on a lossless medium occupying a half space with a dielectric constant of 12. [Parallels Example 1.4]
- (a) Calculate the electric field reflection coefficient referred to the interface medium.

- (b) What is the magnetic field reflection coefficient?

8. Water, or more specifically tap water or sea water, has a complex dielectric constant resulting from two effects: conductivity resulting from dissolved ions in the water leading to charge carriers that can conduct current under the influence of an electric field, and dielectric loss resulting from rotation or bending of the water molecules themselves under the influence of an electric field. The rotation or bending of the water molecules results in motion of the water molecules and thus heat. The relative permittivity is

$$\epsilon_{wr} = \epsilon'_{wr} - j\epsilon''_{wr} \quad (1.84)$$

and the real and imaginary components are

$$\epsilon'_{wr} = \epsilon_{w00} + \frac{\epsilon_{w0} - \epsilon_{w00}}{1 + (2\pi f\tau_w)^2} \quad (1.85)$$

$$\epsilon''_{wr} = \frac{2\pi f\tau_w(\epsilon_{w0} - \epsilon_{w00})}{1 + (2\pi f\tau_w)^2} + \frac{\sigma_i}{2\pi\epsilon_0 f}, \quad (1.86)$$

where f is frequency, $\epsilon_0 = 8.854 \times 10^{-12}$ F/m is the permittivity magnitude, and $\epsilon_{w00} = 4.9$ is the high-frequency limit of ϵ_r and is known to be independent of salinity and is also that of pure deionized water. The other quantities are τ_w , the relaxation time of water; ϵ_{w0} , the static relative dielectric constant of water (which for pure water at 0°C is equal to 87.13); and σ_i , the ionic conductivity of the water. At 5°C and for tap water with a salinity of 0.03 (in parts per thousand by weight) [17, 18], $\epsilon_{w0} = 85.9$, $\tau_w = 14.6$ ps, and $\sigma_i = 0.00548$ S/m.

- (a) Calculate and then plot the real and imaginary dielectric constant of water over the frequency range from DC to 40 GHz for tap water at 5°C. You should see two distinct regions. Identify the part of the imaginary dielectric constant graph that results from ionic conductivity and the part of the graph that relates to dielectric relaxation.
- (b) Consider a plane wave propagating in water. Determine the attenuation constant and the propagation constant of the wave at 500 MHz.

- (c) Consider a plane wave propagating in water. Determine the attenuation constant and the propagation constant of the wave at 2.45 GHz.
 - (d) Consider a plane wave propagating in water. Determine the attenuation constant and the propagation constant of the wave at 22 GHz.
 - (e) Again considering the plane wave in water, calculate the loss factor over a distance of 1 cm at 2.45 GHz. Express your answer in terms of decibels.
 - (f) Consider a plane wave making normal incidence from above into a bucket of tap water that is 1 m deep so that you do not need to consider the reflection at the bottom of the bucket. Calculate the reflection coefficient of the incident plane wave at 2.45 GHz referred to the air immediately above the surface of the water.
 - (g) Again consider the situation in (f), but this time with the plane wave incident on the air–water interface from the water side, calculate the reflection coefficient of the incident wave at 2.45 GHz referred to the water immediately below the surface of the water.
 - (h) If the bucket in (f) and (g) is 0.5 cm deep you will need to consider the reflection at the bottom of the bucket. Consider that the bottom of the bucket is a perfect conductor. Draw the bounce diagram for calculating the reflection of the plane wave in air. Determine the total reflection coefficient of the plane wave (referred to the air immediately above the surface of the water) by using the bounce diagram.
 - (i) Repeat (h) using the formula for multiple reflections.
9. A 4 GHz time-varying EM field is traveling in the $+z$ direction in Region 1 and is incident on another material in Region 2. The permittivity of Region 1 is $\epsilon_1 = \epsilon_0$ and that of Region 2 is $\epsilon_2 = (4 - j0.04)\epsilon_0$. For both regions $\mu_1 = \mu_2 = \mu_0$. [Parallels Example 1.6]
 - (a) What is the characteristic impedance (or wave impedance) in Region 2?
 - (b) What is the propagation constant in Region 1?
 10. A 4 GHz time-varying EM field is traveling in the $+z$ direction in Region 1 and is normally incident on another material in Region 2. The boundary between the two regions is in the $z = 0$ plane. The permittivity of Region 1 is $\epsilon_1 = \epsilon_0$, and that of Region 2 is $\epsilon_2 = 4\epsilon_0$. For both regions, $\mu_1 = \mu_2 = \mu_0$. The phasor of the forward-traveling electric field (i.e., the incident field) is $\mathbf{E}^+ = 100 \hat{\mathbf{y}}$ V/m and the phase is normalized with respect to $z = 0$. $Q_0 = 0$. [Parallels Example 1.6]
 - (a) What is the wave impedance of Region 1?
 - (b) What is the wave impedance of Region 2?
 - (c) What is the electric field reflection coefficient at the boundary?
 - (d) What is the magnetic field reflection coefficient at the boundary?
 - (e) What is the electric field transmission coefficient at the boundary?
 - (f) What is the power transmitted into Region 2?
 - (g) What is the power reflected from the boundary back into Region 1?

1.12.1 Exercises By Section

[†]challenging, [‡]very challenging

§1.5 1[†], 2[†], 3[†]

§1.7 4, 5[†]

§1.9 6, 7[†], 8[‡], 9[†], 10[†]

1.12.2 Answers to Selected Exercises

4 4.47

8(c) $\gamma = 49 + j468 \text{ m}^{-1}$

9 $0.84 + j168 \text{ m}^{-1}$

Appendix

1.A Mathematical Foundations

1.A.1	Angles of a Triangle	33
1.A.2	Trigonometric Identities	34
1.A.3	Trigonometric Derivatives	34
1.A.4	Complex Numbers and Phasors	34
1.A.5	Del (∇) Vector Operator	36
1.A.6	Hyperbolic Functions and Complex Numbers	39
1.A.7	Volumes and Areas	40
1.A.8	Series Expansions	40
1.A.9	Trigonometric Series Expansions	41
1.A.10	Special Polynomials	42
1.A.11	Matrix Operations	43
1.A.12	Interpolation	44
1.A.13	Circles on the Complex Plane	45
1.A.14	Bilinear Transform	46
1.A.15	Quadratic Equation	48
1.A.16	Kron's Method: Network Condensation	48

1.A.1 Angles of a Triangle

The law of cosines relates the angles and lengths of the sides of the triangle in Figure 1-10(a):

$$c^2 = a^2 + b^2 - 2ab \cos(\gamma) \quad (1.87)$$

$$\cos(\alpha) = \frac{b^2 + c^2 - a^2}{2bc}, \quad \cos(\beta) = \frac{a^2 + c^2 - b^2}{2ac}, \quad \cos(\gamma) = \frac{a^2 + b^2 - c^2}{2ab}. \quad (1.88)$$

Referring to the right-angle triangle in Figure 1-10(b):

$$\sin(x) = \frac{\text{opposite}}{\text{hypotenuse}}, \quad \cos(x) = \frac{\text{adjacent}}{\text{hypotenuse}}, \quad \tan(x) = \frac{\text{opposite}}{\text{adjacent}}. \quad (1.89)$$

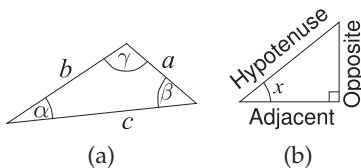


Figure 1-10: Triangles: (a) triangle with sides having lengths a , b , and c , and angles α , β , and γ ; and (b) right-angle triangle.

1.A.2 Trigonometric Identities

$$\text{if } \sin(\theta) = x \text{ then } \theta = \arcsin(x) \quad \text{if } \cos(\theta) = x \text{ then } \theta = \arccos(x) \quad (1.90)$$

$$\text{if } \tan(\theta) = x \text{ then } \theta = \arctan(x) \quad (1.91)$$

$$\sin(-x) = -\sin x \quad \cos(-x) = \cos x \quad \tan(-x) = -\tan x \quad (1.92)$$

$$\csc(-x) = -\csc x \quad \sec(-x) = \sec x \quad \cot(-x) = -\cot x \quad (1.93)$$

$$\cos(x) = \frac{1}{2}(e^{jx} + e^{-jx}) \quad \sin(x) = \frac{1}{2j}(e^{-jx} - e^{jx}) \quad (1.94)$$

$$\sin x = 1/\csc x \quad \cos x = 1/\sec x \quad \tan x = 1/\cot x \quad (1.95)$$

$$\tan x = \sin x / \cos x \quad (1.96)$$

$$\sin^2 x + \cos^2 x = 1 \quad 1 + \tan^2 x = \sec^2 x \quad 1 + \cot^2 x = \csc^2 x \quad (1.97)$$

$$\sin\left(x - \frac{\pi}{2}\right) = -\cos x \quad \cos\left(x - \frac{\pi}{2}\right) = \sin x \quad \tan\left(x - \frac{\pi}{2}\right) = -\cot x \quad (1.98)$$

$$\sin\left(x + \frac{\pi}{2}\right) = \cos x \quad \cos\left(x + \frac{\pi}{2}\right) = -\sin x \quad \tan\left(x + \frac{\pi}{2}\right) = -\cot x \quad (1.99)$$

$$\sin\left(\frac{\pi}{2} - x\right) = \cos x \quad \cos\left(\frac{\pi}{2} - x\right) = \sin x \quad \tan\left(\frac{\pi}{2} - x\right) = \cot x \quad (1.100)$$

$$\csc\left(x - \frac{\pi}{2}\right) = -\sec x \quad \sec\left(x - \frac{\pi}{2}\right) = \csc x \quad \cot\left(x - \frac{\pi}{2}\right) = -\tan x \quad (1.101)$$

$$\csc\left(x + \frac{\pi}{2}\right) = \sec x \quad \sec\left(x + \frac{\pi}{2}\right) = -\csc x \quad \cot\left(x + \frac{\pi}{2}\right) = -\tan x \quad (1.102)$$

$$\csc\left(\frac{\pi}{2} - x\right) = \sec x \quad \sec\left(\frac{\pi}{2} - x\right) = \csc x \quad \cot\left(\frac{\pi}{2} - x\right) = \tan x \quad (1.103)$$

$$\sin(2x) = 2 \sin x \cos x \quad \cos(2x) = \cos^2(x) - \sin^2(x) \quad (1.104)$$

$$\tan(2x) = \frac{2 \tan x}{1 - \tan^2 x} \quad \cot(2x) = \frac{1}{2}[\cot(x) - \tan(x)] \quad (1.105)$$

$$\sin^2 x = \frac{1}{2}[1 - \cos(2x)] \quad \cos^2 x = \frac{1}{2}[1 + \cos(2x)] \quad \tan^2 x = \frac{1 - \cos(2x)}{1 + \cos(2x)} \quad (1.106)$$

$$\tan(x + y) = \frac{\tan(x) + \tan(y)}{1 - \tan(x)\tan(y)} \quad \tan(x - y) = \frac{\tan(x) - \tan(y)}{1 + \tan(x)\tan(y)} \quad (1.107)$$

$$\sin x + \sin y = 2 \sin\left(\frac{x+y}{2}\right) \cos\left(\frac{x-y}{2}\right) \quad \sin x - \sin y = 2 \cos\left(\frac{x+y}{2}\right) \sin\left(\frac{x-y}{2}\right) \quad (1.108)$$

$$\cos x + \cos y = 2 \cos\left(\frac{x+y}{2}\right) \cos\left(\frac{x-y}{2}\right) \quad \cos x - \cos y = -2 \sin\left(\frac{x+y}{2}\right) \sin\left(\frac{x-y}{2}\right) \quad (1.109)$$

$$\sin x \sin y = \frac{1}{2}[\cos(x - y) - \cos(x + y)] \quad \sin x \cos y = \frac{1}{2}[\sin(x + y) + \sin(x - y)] \quad (1.110)$$

$$\cos x \cos y = \frac{1}{2}[\cos(x - y) + \cos(x + y)] \quad \cos x \sin y = \frac{1}{2}[\sin(x + y) - \sin(x - y)] \quad (1.111)$$

1.A.3 Trigonometric Derivatives

$$\begin{aligned} \frac{d}{dx} \sin(x) &= \cos(x) & \frac{d}{dx} \cos(x) &= -\sin(x) & \frac{d}{dx} \tan(x) &= \sec^2(x) \\ \frac{d}{dx} \csc(x) &= -\csc(x) \cot(x) & \frac{d}{dx} \sec(x) &= \sec(x) \tan(x) & \frac{d}{dx} \cot(x) &= -\csc^2(x) \end{aligned} \quad (1.112)$$

1.A.4 Complex Numbers and Phasors

A complex number z is an ordered pair of two real numbers x and y , and a complex number has a special meaning when working in the frequency domain. The rectangular form of the complex number is $z = x + jy$, where $j = \sqrt{-1}$ is an imaginary number.¹ The polar form of the complex number $z = r\angle\phi$ relates directly to the amplitude and phase of a cosinusoid. In determining phase, reference is made to a cosinusoid of the form $u(t) = r \cos(\omega t + \phi)$, as this has a value of r when the radian frequency $\omega = 0$ (i.e., at DC). The cosinusoid is shown as the solid line in Figure 1-11(a), where r is the amplitude and ϕ is the phase of the cosinusoid. The cosinusoid can be presented as the complex valued function

$$f(t) = ze^{j\omega t}, \quad \text{where} \quad z = re^{j\phi} \quad (1.113)$$

¹ Outside electrical engineering i (i without the dot) is used for $\sqrt{-1}$, but this is replaced by j (j without the dot) in electrical engineering to avoid confusion with the usage of i for current.

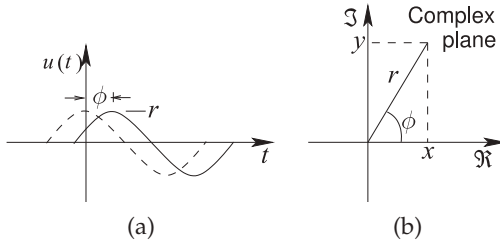


Figure 1-11: Sinusoidal signal representations: (a) waveform referenced to the zero-phase cosinusoid shown as the dashed waveform; and (b) representation as a phasor on the complex plane where Re is the real part and Im is the imaginary part.

is called the phasor of $u(t)$. The phasor contains the amplitude and phase of the cosinusoid, and given the frequency of the cosinusoid, the original time-domain waveform can be reconstructed. The time-domain form of the complex function is

$$u(t) = \Re \{f(t)\} = \Re \{ze^{j\omega t}\} = \Re \{re^{j\phi}e^{j\omega t}\} = \Re \{re^{j(\omega t + \phi)}\} = r \cos(\omega t + \phi). \quad (1.114)$$

$\Re\{\}$ indicates that the real part of a complex number is taken, and similarly $\Im\{\}$ indicates that the imaginary part of a complex number is taken. The complex number can be represented in rectangular or magnitude-phase form so that

$$z = x + jy = r\angle\phi = re^{j\phi} = r(\cos\phi + j\sin\phi) \quad (1.115)$$

with the relationship shown in Figure 1-11(b). Note that in Equation (1.115), ϕ must be expressed in radians and anywhere it is used in calculations. Also

$$x = r \cos(\phi) \quad \text{and} \quad y = r \sin(\phi). \quad (1.116)$$

Basic calculations using the complex numbers

$$w = a + jb = q\angle\theta \quad \text{and} \quad z = c + jd = r\angle\phi \quad (1.117)$$

(with $a, b, c, d, \theta, \phi, r$, and q being real numbers) are

- $j \cdot j = j^2 = -1$
- Addition: $w + z = (a + jb) + (c + jd) = (a + c) + j(b + d)$
- Subtraction: $w - z = (a + jb) - (c + jd) = (a - c) + j(b - d)$
- Multiplication: $w \cdot z = (a + jb) \cdot (c + jd) = (ac - bd) + j(bc + ad)$
- Magnitude: $|w| = \sqrt{a^2 + b^2} = q$; $|z| = \sqrt{c^2 + d^2} = r$
- Angle: $\theta = \arctan(b/a) = \arccos(a/q) = \arcsin(b/q)$ (Correction may be required to get the phase in the right quadrant. This requires that the signs of a and b be examined.)
- Multiplication (alternative): $w \cdot z = qr\angle(\theta + \phi)$
- Division: $w/z = \frac{a + jb}{c + jd} = \frac{(a + jb)(c - jd)}{(c + jd)(c - jd)} = \left(\frac{ac + bd}{c^2 + d^2}\right) + j\left(\frac{bc - ad}{c^2 + d^2}\right)$
- Division (alternative): $w/z = q/r\angle(\theta - \phi)$
- Square root: $\sqrt{w} = \sqrt{q}\angle(\theta/2 + m\pi)$, $m = 0, 1$ (i.e. $\sqrt{w} = \sqrt{q}\angle(\theta/2)$ and $\sqrt{q}\angle(\theta/2 + \pi)$)
- n th root: $\sqrt[n]{w} = \sqrt[n]{q}\angle\left(\frac{\theta}{n} + 2\pi\frac{m}{n}\right)$, $m = 0, 1, \dots, (n - 1)$
- Negative: $-w = -q\angle\theta = q\angle(\theta + \pi)$
- Complex conjugate: $w^* = a - jb = q\angle(-\theta)$
- Squared magnitude: $|z|^2 = z \cdot z^*$
- Conjugate addition: $(w + z)^* = w^* + z^*$
- Conjugate power: $(z^n)^* = (z^*)^n$
- Conjugate multiplication: $(wz)^* = w^*z^*$
- Conjugate division: $(w/z)^* = w^*/z^*$
- Conjugate exponential: $\exp(z^*) = (\exp z)^*$

- Conjugate logarithm: $\log(z^*) = (\log z)^*$
- Conjugate conjugate: $(w^*)^* = w$
- Complex inverse: $z^{-1} = z^*/|z|^2$
- Complex magnitude: $|z^*| = |z|$

EXAMPLE 1.7 Complex numbers

Consider the complex numbers $w = -0.5 - j1.6$ and $z = 5 - j3$, and the waveform $v(t) = 2.3 \cos(2\pi 10t - 1.2)$.

- In polar form, $w = 1.676\angle(-1.874)$, where 1.874 is in radians; alternatively $w = 1.676\angle(-107.4)^\circ$.
- In polar form, $z = 5.831\angle(-0.54)$.
- $2w = -1 - j3.2 = 3.353\angle(-1.874)$.
- $z \cdot w = w \cdot z = w \cdot z = (1.676 \cdot 5.831)\angle(-1.874 - 0.54) = 9.774\angle(-2.414) = -7.3 - j6.5$.
- $\sqrt{z} = 2.327 - j0.645$.
- Alternatively $\sqrt{z} = \sqrt{5.831}\angle(-0.54/2) = 2.415\angle(-0.27)$.
- $w/z = (1.676/5.831)\angle[-1.874 - (-0.54)] = 0.287\angle-1.333 = 0.068 - j6.5$.
- The radian frequency of $v(t)$ is 20π rads/s.
- The frequency of $v(t)$ is 10 Hz.
- The phasor of $v(t)$ is $v = 2.3\angle(-1.2) = 2.3\angle(-68.755^\circ) = 0.833 - j2.144$.
- If w is a phasor and its frequency is 1 GHz, the waveform equivalent of w is $w(t) = 1.676 \cos(2\pi \cdot 10^9 t - 1.874)$ and the phase is -1.874 radians or -107.35° or 252.65° .

1.A.5 Vector Operators

Vector Multiplication

There are two types of operations that multiply vectors. **A**, **B**, and **C** are vectors with

$$\mathbf{A} = a_i \mathbf{i} + a_j \mathbf{j} + a_k \mathbf{k}, \quad (1.118)$$

where **i**, **j**, and **k**, are orthogonal vectors such as the unit vectors of the Cartesian coordinate system, that is, \hat{x} , \hat{y} , and \hat{z} in the x , y and z directions, respectively.

Dot Product

$\mathbf{A} \cdot \mathbf{B}$ is called the dot product, the scalar product or the inner product. It is read as “a dot b.”

$$\mathbf{A} \cdot \mathbf{B} = a_i b_i + a_j b_j + \dots + a_k b_k.$$

Commutative property: $\mathbf{A} \cdot \mathbf{B} = \mathbf{B} \cdot \mathbf{A}$.

Distributive property: $\mathbf{A} \cdot (\mathbf{B} + \mathbf{C}) = \mathbf{A} \cdot \mathbf{B} + \mathbf{A} \cdot \mathbf{C}$.

Bilinear property (r is a scalar): $\mathbf{A} \cdot (r\mathbf{B} + \mathbf{C}) = r(\mathbf{A} \cdot \mathbf{B}) + (\mathbf{A} \cdot \mathbf{C})$.

Scalar multiplication property (r and s are scalars): $(r\mathbf{A}) \cdot (s\mathbf{B}) = (rs)(\mathbf{A} \cdot \mathbf{B})$.

Orthogonal property: Two nonzero vectors **A** and **B** are orthogonal if and only if $\mathbf{A} \cdot \mathbf{B} = 0$.

Cross Product $\mathbf{A} \times \mathbf{B}$ is called the cross product. It is read as “a cross b.” Now the vector components of \mathbf{A} , \mathbf{B} , and \mathbf{C} need to be more tightly specified as orthogonal vectors, typically having unit amplitude, that have the property

$$\mathbf{i} \times \mathbf{j} = \mathbf{k}, \quad \mathbf{j} \times \mathbf{k} = \mathbf{i}, \quad \mathbf{k} \times \mathbf{i} = \mathbf{j}, \quad \text{and} \quad \mathbf{i} \times \mathbf{i} = 0 = \mathbf{j} \times \mathbf{j} = \mathbf{k} \times \mathbf{k} \quad (1.119)$$

$$\mathbf{j} \times \mathbf{i} = -\mathbf{k}, \quad \mathbf{k} \times \mathbf{j} = -\mathbf{i}, \quad \mathbf{i} \times \mathbf{k} = -\mathbf{j}. \quad (1.120)$$

The unit vectors of the Cartesian coordinate system have this property with \mathbf{i} , \mathbf{j} , and \mathbf{k} , corresponding to the unit vectors \hat{x} , \hat{y} , and \hat{z} in the x , y and z directions, respectively.

$$\begin{aligned} \mathbf{a} \times \mathbf{b} &= (a_i \mathbf{i} + a_j \mathbf{j} + a_k \mathbf{k}) \times (b_i \mathbf{i} + b_j \mathbf{j} + b_k \mathbf{k}) \\ &= a_i b_i \mathbf{i} \times \mathbf{i} + a_i b_j \mathbf{i} \times \mathbf{j} + a_i b_k \mathbf{i} \times \mathbf{k} + a_j b_i \mathbf{j} \times \mathbf{i} + a_j b_j \mathbf{j} \times \mathbf{j} + a_j b_k \mathbf{j} \times \mathbf{k} + \\ &\quad a_k b_i \mathbf{k} \times \mathbf{i} + a_k b_j \mathbf{k} \times \mathbf{j} + a_k b_k \mathbf{k} \times \mathbf{k} \\ &= (a_j b_k - a_k b_j) \mathbf{i} + (a_k b_i - a_i b_k) \mathbf{j} + (a_i b_j - a_j b_i) \mathbf{k}. \end{aligned} \quad (1.121)$$

Anticommutative property: $\mathbf{A} \times \mathbf{B} = -\mathbf{B} \times \mathbf{A}$.

Distributive property: $\mathbf{A} \times (\mathbf{B} + \mathbf{C}) = \mathbf{A} \times \mathbf{B} + \mathbf{A} \times \mathbf{C}$.

Bilinear property (r is a scalar): $\mathbf{A} \times (r\mathbf{B} + \mathbf{C}) = r(\mathbf{A} \times \mathbf{B}) + (\mathbf{A} \times \mathbf{C})$.

Scalar multiplication property (r and s are scalars): $(r\mathbf{A}) \times (s\mathbf{B}) = (rs)(\mathbf{A} \times \mathbf{B})$.

Lagrange's formula

$$\mathbf{A} \times (\mathbf{B} \times \mathbf{C}) = \mathbf{B}(\mathbf{B} \cdot \mathbf{C}) - \mathbf{C}(\mathbf{A} \cdot \mathbf{B}).$$

Del (∇) Vector Operator

Operations in Cartesian, Cylindrical, and Spherical Coordinate Systems

This section defines the del, or the nabla ∇ , a calculus operator that operates on vector quantities and also on a scalar to create a vector. The various del operators in the Cartesian (rectangular), spherical, and cylindrical coordinate systems are presented. Here a scalar is denoted by f and a vector by \mathbf{F} :

- grad, ∇ , is the gradient of a scalar with direction. ∇f is read as “grad f .”
- div, ∇ , is a measure of how a vector is spreading out from a point. $\nabla \cdot \mathbf{F}$ is read as “div \mathbf{F} .”
- curl, $\nabla \times$, is a measure of the rotation of a vector. $\nabla \times \mathbf{F}$ is read as “curl \mathbf{F} .”

Cartesian (rectangular) coordinates (x, y, z) :

\hat{x} is the unit vector in the x direction and F_x is the component of the field in the x -direction. Similarly for the other components.

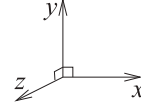


Figure 1-12

$$\mathbf{F} = F_x \hat{x} + F_y \hat{y} + F_z \hat{z} \quad (1.122)$$

$$\text{grad } \nabla f = \frac{\partial f}{\partial x} \hat{x} + \frac{\partial f}{\partial y} \hat{y} + \frac{\partial f}{\partial z} \hat{z} \quad (1.123)$$

$$\text{div } \nabla \cdot \mathbf{F} = \frac{\partial F_x}{\partial x} + \frac{\partial F_y}{\partial y} + \frac{\partial F_z}{\partial z} \quad (1.124)$$

$$\text{curl } \nabla \times \mathbf{F} = \left(\frac{\partial F_z}{\partial y} - \frac{\partial F_y}{\partial z} \right) \hat{x} + \left(\frac{\partial F_x}{\partial z} - \frac{\partial F_z}{\partial x} \right) \hat{y} + \left(\frac{\partial F_y}{\partial x} - \frac{\partial F_x}{\partial y} \right) \hat{z} \quad (1.125)$$

$$\nabla^2 \mathbf{F} = \frac{\partial^2 \mathbf{F}}{\partial x^2} + \frac{\partial^2 \mathbf{F}}{\partial y^2} + \frac{\partial^2 \mathbf{F}}{\partial z^2} \quad (1.126)$$

$$\text{differential length, } d\ell = dx \hat{x} + dy \hat{y} + dz \hat{z} \quad (1.127)$$

$$\text{differential normal area, } d\mathbf{s} = dy \, dz \hat{x} + dx \, dz \hat{y} + dx \, dy \hat{z} \quad (1.128)$$

$$\text{differential volume, } dv = dx \, dy \, dz. \quad (1.129)$$

Cylindrical coordinates (ρ, ϕ, z) :

The cylindrical coordinates are ρ for radius, ϕ for angle, and z for height. These are related to the Cartesian coordinates by

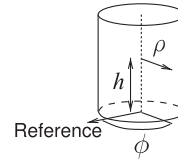


Figure 1-13

$$x = \rho \cos \phi, \quad y = \rho \sin \phi, \quad z = z \quad (1.130)$$

$$\rho = \sqrt{x^2 + y^2}, \quad \phi = \text{atan2}(y, x), \quad z = z \quad (1.131)$$

$$\text{vector } \mathbf{F} = F_\rho \hat{\rho} + F_\phi \hat{\phi} + F_z \hat{z} \quad (1.132)$$

$$\text{grad } \nabla f = \frac{\partial f}{\partial \rho} \hat{\rho} + \frac{1}{\rho} \frac{\partial f}{\partial \phi} \hat{\phi} + \frac{\partial f}{\partial z} \hat{z} \quad (1.133)$$

$$\text{div } \nabla \cdot \mathbf{F} = \frac{1}{\rho} \frac{\partial \rho F_\rho}{\partial \rho} + \frac{1}{\rho} \frac{\partial F_\phi}{\partial \phi} + \frac{\partial F_z}{\partial z} \quad (1.134)$$

$$\text{curl } \nabla \times \mathbf{F} = \left(\frac{1}{\rho} \frac{\partial F_z}{\partial \phi} - \frac{\partial F_\phi}{\partial z} \right) \hat{\rho} + \left(\frac{\partial F_\rho}{\partial z} - \frac{\partial F_z}{\partial \rho} \right) \hat{\phi} + \frac{1}{\rho} \left(\frac{\partial(\rho F_\phi)}{\partial \rho} - \frac{\partial F_\rho}{\partial \phi} \right) \hat{z} \quad (1.135)$$

$$\text{differential length, } d\ell = d\rho \hat{\rho} + \rho d\phi \hat{\phi} + dz \hat{z} \quad (1.136)$$

$$\text{differential normal area, } d\mathbf{s} = \rho d\phi \, dz \hat{\rho} + d\rho \, dz \hat{\phi} + \rho d\rho \, d\phi \hat{z} \quad (1.137)$$

$$\text{differential volume, } dv = \rho d\rho \, d\phi \, dz. \quad (1.138)$$

Spherical coordinates (ρ, θ, ϕ) :

The spherical coordinates are ρ for radius, θ for angle of the horizontal projection, and ϕ for the elevation angle. These are related to the Cartesian coordinates by

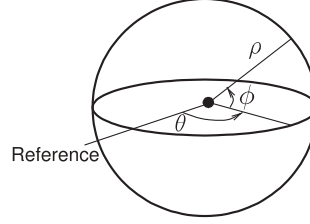


Figure 1-14

$$x = r \sin \theta \cos \phi, \quad y = r \sin \theta \sin \phi, \quad z = r \cos \theta \quad (1.139)$$

$$r = \sqrt{x^2 + y^2 + z^2}, \quad \theta = \arccos(z/r), \quad \phi = \text{atan2}(y, x) \quad (1.140)$$

$$\text{vector } \mathbf{F} = F_r \hat{\mathbf{r}} + F_\theta \hat{\boldsymbol{\theta}} + F_\phi \hat{\boldsymbol{\phi}} \quad (1.141)$$

$$\text{grad } \nabla f = \frac{\partial f}{\partial r} \hat{\mathbf{r}} + \frac{1}{r} \frac{\partial f}{\partial \theta} \hat{\boldsymbol{\theta}} + \frac{1}{r \sin \theta} \frac{\partial f}{\partial \phi} \hat{\boldsymbol{\phi}} \quad (1.142)$$

$$\text{div } \nabla \cdot \mathbf{F} = \frac{1}{r^2} \frac{\partial(r^2 F_r)}{\partial r} + \frac{1}{r \sin \theta} \frac{\partial(F_\theta \sin \theta)}{\partial \theta} + \frac{1}{r \sin \theta} \frac{\partial F_\phi}{\partial \phi} \quad (1.143)$$

$$\begin{aligned} \text{curl } \nabla \times \mathbf{F} = & \frac{1}{r \sin \theta} \left(\frac{\partial(F_\phi \sin \theta)}{\partial \theta} - \frac{\partial F_\theta}{\partial \phi} \right) \hat{\mathbf{r}} \\ & + \frac{1}{r} \left(\frac{1}{\sin \theta} \frac{\partial F_r}{\partial \phi} - \frac{\partial(r F_\phi)}{\partial r} \right) \hat{\boldsymbol{\theta}} + \frac{1}{r} \left(\frac{\partial(r F_\theta)}{\partial r} - \frac{\partial F_r}{\partial \theta} \right) \hat{\boldsymbol{\phi}} \end{aligned} \quad (1.144)$$

$$\text{differential length } d\ell = dr \hat{\mathbf{r}} + r d\theta \hat{\boldsymbol{\theta}} + r \sin \theta d\phi \hat{\boldsymbol{\phi}} \quad (1.145)$$

$$\text{differential area } ds = r^2 \sin \theta d\theta d\phi \hat{\mathbf{r}} + r \sin \theta dr d\phi \hat{\boldsymbol{\theta}} + r dr d\theta \hat{\boldsymbol{\phi}} \quad (1.146)$$

$$\text{differential volume } dv = r^2 \sin \theta dr d\theta d\phi. \quad (1.147)$$

Identities

Identities for the del, ∇ , operator:

$$\text{div grad } f = \nabla \cdot (\nabla f) = \nabla^2 f = \Delta f (\text{Laplacian}) \quad (1.148)$$

$$\Delta(fg) = f \Delta g + 2 \nabla f \cdot \nabla g + g \Delta f \quad (1.149)$$

$$\text{curl grad } f = \nabla \times (\nabla f) = 0 \quad (1.150)$$

$$\text{div curl } \mathbf{F} = \nabla \cdot (\nabla \times \mathbf{F}) = 0 \quad (1.151)$$

$$\text{curl curl } \mathbf{F} = \nabla \times (\nabla \times \mathbf{F}) = \nabla(\nabla \cdot \mathbf{F}) - \nabla^2 \mathbf{F} \quad (1.152)$$

$$\mathbf{A} \times (\mathbf{B} \times \mathbf{C}) = \mathbf{B}(\mathbf{A} \cdot \mathbf{C}) - \mathbf{C}(\mathbf{A} \cdot \mathbf{B}). \quad (1.153)$$

1.A.6 Hyperbolic Functions and Complex Numbers

$$\cosh(x) = \frac{1}{2}(e^x + e^{-x}) = \cos(jx) \quad (1.154)$$

$$\cosh(jx) = \frac{1}{2}(e^{jx} + e^{-jx}) = \cos(x) \quad (1.155)$$

$$\cosh(-x) = \cosh(x) \quad (1.156)$$

$$\sinh(x) = \frac{1}{2}(e^x - e^{-x}) = -j \sin(jx) \quad (1.157)$$

$$\sinh(jx) = \frac{1}{2}(e^{jx} - e^{-jx}) = j \sin(x) \quad (1.158)$$

$$\sinh(-x) = -\sinh(x) \quad (1.159)$$

$$\cosh^2(x) - \sinh^2(x) = 1 \quad (1.160)$$

$$\tanh(x) = \sinh(x) / \cosh(x) \quad (1.161)$$

$$\tanh(x) = -j \tan(jx) \quad (1.162)$$

$$\tanh(jx) = j \tan(x) \quad (1.163)$$

$$\tanh(-x) = -\tanh(x) \quad (1.164)$$

$$\sin(jx) = j \sinh(x) \quad (1.165)$$

$$\cos(jx) = \cosh(x) \quad (1.166)$$

$$\tan(jx) = j \tanh(x) \quad (1.167)$$

$$e^x = \cosh(x) + \sinh(x) \quad e^{-x} = \cosh(x) - \sinh(x) \quad (1.168)$$

$$e^{jx} = \cos(x) + j \sin(x) \quad e^{-jx} = \cos(x) - j \sin(x) \quad (1.169)$$

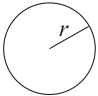
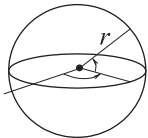
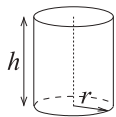

$$\sin(x + jy) = \sin(x) \cosh(y) + j \cos(x) \sinh(y) \quad (1.170)$$

$$\cos(x + jy) = \cos(x) \cosh(y) - j \sin(x) \sinh(y) \quad (1.171)$$

$$e^\gamma = e^{(\alpha + j\beta)} = e^\alpha e^{j\beta}, \text{ where } \gamma = \alpha + j\beta \quad (1.172)$$

$$\cot(x) = \frac{1}{2} [\cot(x/2) - \tan(x/2)]. \quad (1.173)$$

1.A.7 Volumes and Areas

	Circle	Sphere	Cylinder	Cone
	$r = \text{radius}$ 	$r = \text{radius}$ 	$r = \text{radius}$ $h = \text{height}$ 	$r = \text{radius of base}$ $h = \text{height}$ 
Area	πr^2	$4\pi r^2$	$2\pi r h$ (cylinder) $2\pi r^2$ (base & top)	
Volume		$4\pi r^3 / 3$	$\pi r^2 h$	$\pi r^2 h / 3$

1.A.8 Series Expansions

Square root:

$$\begin{aligned} \sqrt{1+x} &= \sum_{n=0}^{\infty} \frac{(-1)^n (2n)!}{(1-2n)(n!)^2 (4^n)} x^n \\ &= 1 + \frac{1}{2}x - \frac{1}{8}x^2 + \frac{1}{16}x^3 - \frac{5}{128}x^4 + \dots \text{ for } -1 < x \leq 1. \end{aligned} \quad (1.174)$$

Exponential function (the natural number e raised to a power):

$$e^x = \sum_{n=0}^{\infty} \frac{x^n}{n!} = 1 + x + \frac{x^2}{2!} + \frac{x^3}{3!} + \dots \text{ for all } x. \quad (1.175)$$

Natural logarithm:

$$\ln(1 - x) = - \sum_{n=1}^{\infty} \frac{x^n}{n} \text{ for } -1 \leq x < 1 \quad (1.176)$$

$$\ln(1 + x) = \sum_{n=1}^{\infty} (-1)^{n+1} \frac{x^n}{n} \text{ for } -1 < x \leq 1. \quad (1.177)$$

Binomial series:

$$(1 + x)^\alpha = \sum_{n=0}^{\infty} \binom{\alpha}{n} x^n \text{ for all } |x| < 1 \text{ and all complex } \alpha \quad (1.178)$$

where n is an integer and the binomial coefficient is

$$\binom{\alpha}{n} = \prod_{k=1}^n \frac{\alpha - k + 1}{k} = \frac{\alpha(\alpha - 1) \cdots (\alpha - n + 1)}{n!}. \quad (1.179)$$

If α is replaced by an integer N the binomial coefficient is

$$\binom{N}{n} = \frac{N!}{(N - n)!n!}. \quad (1.180)$$

Infinite geometric series:

$$\frac{1}{1 - x} = \sum_{n=0}^{\infty} x^n \text{ for } |x| < 1. \quad (1.181)$$

$$\frac{x}{(1 - x)^2} = \sum_{n=1}^{\infty} n x^n \text{ for } |x| < 1. \quad (1.182)$$

$$\frac{1}{(1 - x)^2} = \sum_{n=1}^{\infty} n x^{n-1} \text{ for } |x| < 1. \quad (1.183)$$

1.A.9 Trigonometric Series Expansions

$$\sin x = \sum_{n=0}^{\infty} \frac{(-1)^n}{(2n + 1)!} x^{2n+1} = x - \frac{x^3}{3!} + \frac{x^5}{5!} - \cdots \text{ for all } x \quad (1.184)$$

$$\cos x = \sum_{n=0}^{\infty} \frac{(-1)^n}{(2n)!} x^{2n} = 1 - \frac{x^2}{2!} + \frac{x^4}{4!} - \cdots \text{ for all } x \quad (1.185)$$

$$\tan x = x + \frac{x^3}{3} + \frac{2x^5}{15} + \cdots \text{ for } |x| < \frac{\pi}{2} \quad (1.186)$$

$$\sinh x = \sum_{n=0}^{\infty} \frac{x^{2n+1}}{(2n + 1)!} = x + \frac{x^3}{3!} + \frac{x^5}{5!} + \cdots \text{ for all } x \quad (1.187)$$

$$\cosh x = \sum_{n=0}^{\infty} \frac{x^{2n}}{(2n)!} = 1 + \frac{x^2}{2!} + \frac{x^4}{4!} + \cdots \text{ for all } x \quad (1.188)$$

$$\tanh x = \sum_{n=1}^{\infty} \frac{B_{2n} 4^n (4^n - 1)}{(2n)!} x^{2n-1} = x - \frac{1}{3} x^3 + \frac{2}{15} x^5 - \frac{17}{315} x^7 + \cdots \text{ for } |x| < \frac{\pi}{2} \quad (1.189)$$

$$\operatorname{arsinh}(x) = \sum_{n=0}^{\infty} \frac{(-1)^n (2n)!}{4^n (n!)^2 (2n+1)} x^{2n+1} \text{ for } |x| \leq 1 \quad (1.190)$$

$$\operatorname{artanh}(x) = \sum_{n=0}^{\infty} \frac{x^{2n+1}}{2n+1} \text{ for } |x| < 1. \quad (1.191)$$

1.A.10 Special Polynomials

Several polynomials have special properties of use in the design of filters and matching networks. Their arguments are put in terms of frequency and a transfer function of a two-port is expressed in terms on one of the special polynomials or its inverse.

Butterworth Polynomial

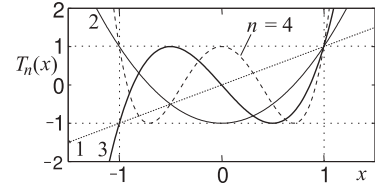
The Butterworth polynomials have the general form

$$B_n(x) = \begin{cases} \prod_{k=1}^{n/2} \left\{ x^2 - 2x \cos \left[\frac{(2k+n-1)\pi}{2n} \right] + 1 \right\} & \text{for } n \text{ even} \\ (x+1) \prod_{k=1}^{(n-1)/2} \left\{ x^2 - 2x \cos \left[\frac{(2k+n-1)\pi}{2n} \right] + 1 \right\} & \text{for } n \text{ odd} \end{cases} \quad (1.192)$$

These of course do not look like polynomials but their expansions are, see Table 1-5.

Chebyshev Polynomial

The n th-order Chebyshev polynomial of the first kind, $T_n(x)$, (often just called the Chebyshev polynomial) has the special property that the maximum absolute value of $T_n(x)$ for $-1 \leq x \leq 1$ is 1. This can be seen in the figure to the right where the first four Tchebyshev polynomials are plotted.



When x is frequency this means that the frequency response in a bandwidth has equal ripples across the passband and outside (both above and below) the value of $T_n(x)$ rapidly diverges (the magnitude becomes monotonically larger). For a filter or matching network the reflection coefficient is expressed in terms of $T_n(x)$ and so the skirts of the transmission response are steep. Normalization of x and scaling of the Chebyshev polynomials is used to scale the response in frequency and amplitude. The Chebyshev polynomial is obtained using the recursion formula

$$T_n(x) = 2xT_{n-1}(x) - T_{n-2}(x) \quad \text{with} \quad T_1(x) = x \quad \text{and} \quad T_2(x) = 2x^2 - 1. \quad (1.193)$$

For example, with $n = 3$,

$$T_3(x) = 2xT_{3-1}(x) - T_{3-2}(x) = 2x(2x^2 - 1) - x = 4x^3 - 2x - x = 4x^3 - 3x. \quad (1.194)$$

Table 1-5:
Butterworth
polynomials.

n	Butterworth polynomial $B_n(x)$
1	$x + 1$
2	$x^2 + 1.4142x + 1$
3	$(x + 1)(x^2 + x + 1)$
4	$(x^2 + 0.7564x + 1)(x^2 + 1.8478x + 1)$
5	$(x + 1)(x^2 + 0.1680x + 1)(x^2 + 1.6180x + 1)$
6	$(x^2 + 0.5176x + 1)(x^2 + 1.4142x + 1)(x^2 + 1.9319x + 1)$
7	$(x + 1)(x^2 + 0.4450x + 1)(x^2 + 1.2470x + 1)(x^2 + 1.8019x + 1)$
8	$(x^2 + 0.3902x + 1)(x^2 + 1.1111x + 1)(x^2 + 1.6629x + 1)(x^2 + 1.9616x + 1)$

Several useful expansions of Chebyshev polynomials are used in microwave engineering to relate the frequency response of a function or circuit to the Chebyshev characteristic. Generally the frequency is referred to the electrical length θ (which for a transmission line θ is proportional to frequency). Some of the more useful expansions used in the text follow:

$$T_n(\cos \theta) = \cos(n\theta) \quad (1.195)$$

and note that when $\theta = \pi/2$, $\cos(n\theta) = 0$ when n is odd and $\cos(n\theta) = \pm 1$ when n is even. From this identity two more useful identities are derived:

$$T_n(x) = \cos(n \cos^{-1} x) \text{ for } |x| \leq 1, \text{ and } T_n(x) = \cosh(n \cosh^{-1} x) \text{ for } |x| \geq 1. \quad (1.196)$$

A normalized argument $\cos \theta / \cos \theta_m$ is often used to define a passband as being between θ_m and $(\pi - \theta_m)$. That is that we can relate the Chebyshev response to frequency and define a frequency bandwidth. Then a useful Chebyshev polynomial expansion is

$$T_n(\cos \theta / \cos \theta_m) = T_n(\sec \theta_m \cos \theta) = \cos \{n [\cos^{-1}(\cos \theta / \cos \theta_m)]\}. \quad (1.197)$$

From Section 1.A.2 note that $\cos^2 \theta = \frac{1}{2}[1 + \cos(2\theta)]$, $\cos \theta \cos(n\theta) = \frac{1}{2} \cos[(n+1)\theta] \cos[(n-1)\theta]$, and $\sec(\theta_m) = 1/\cos \theta_m$. Then (after ingenious manipulation) Equation (1.193) becomes

$$\begin{aligned} T_1(\cos \theta / \cos \theta_m) &= \sec \theta_m \cos \theta \\ T_2(\cos \theta / \cos \theta_m) &= \sec^2 \theta_m [\cos(2\theta) + 1] - 1 = \sec^2 \theta_m \cos(2\theta) + (\sec^2 \theta_m - 1) \\ T_3(\cos \theta / \cos \theta_m) &= \sec^3 \theta_m [\cos(3\theta) + 3 \cos \theta] - 3 \sec \theta_m \cos \theta \\ &= \sec^3 \theta_m \cos(3\theta) + 3(\sec^3 \theta_m - \sec \theta_m) \cos \theta \\ T_4(\cos \theta / \cos \theta_m) &= \sec^4 \theta_m [\cos(4\theta) + 4 \cos(2\theta) + 3] - 4 \sec^2 \theta_m [\cos(2\theta) + 1] + 1 \\ &= \sec^4 \theta_m \cos(4\theta) + 4(\sec^4 \theta_m - \sec^2 \theta_m) \cos(2\theta) + (3 \sec^4 \theta_m - 4 \sec^2 \theta_m + 1) \\ K_5(\cos \theta / \cos \theta_m) &= \sec^5 \theta_m [\cos(5\theta) + 5 \cos(3\theta) + 7 \cos \theta] - \sec^3 \theta_m [5 \cos(3\theta) + 11 \cos \theta] \\ &\quad + 4 \sec \theta_m \cos \theta \\ &= \sec^5 \theta_m \cos(5\theta) + 5(\sec^5 \theta_m - \sec^3 \theta_m) \cos(3\theta) \\ &\quad + (7 \sec^5 \theta_m - 11 \sec^3 \theta_m + 4 \sec \theta_m) \cos \theta. \end{aligned} \quad (1.198)$$

1.A.11 Matrix Operations

A, **B**, and **C** are square matrices and **V** is a vector.

Determinant:

$$|\mathbf{A}| = \det(\mathbf{A}). \quad (1.199)$$

Transpose:

$$(\mathbf{ABC})^T = \mathbf{C}^T \mathbf{B}^T \mathbf{A}^T \quad (1.200)$$

$$(\mathbf{ABC}^T)^T = \mathbf{CB}^T \mathbf{A}^T. \quad (1.201)$$

Inverse:

$$(\mathbf{ABC})^{-1} = \mathbf{C}^{-1} \mathbf{B}^{-1} \mathbf{A}^{-1} \quad (1.202)$$

$$(\mathbf{ABC}^{-1})^{-1} = (\mathbf{C}^{-1})^{-1} \mathbf{B}^{-1} \mathbf{A}^{-1} = \mathbf{CB}^{-1} \mathbf{A}^{-1} \quad (1.203)$$

$$\mathbf{AA}^{-1} = \mathbf{A}^{-1} \mathbf{A} = \mathbf{I} = 1. \quad (1.204)$$

Two row square matrices and vectors

$$\mathbf{A} = \begin{bmatrix} a_{11} & a_{12} \\ a_{21} & a_{22} \end{bmatrix} \quad \mathbf{B} = \begin{bmatrix} b_{11} & b_{12} \\ b_{21} & b_{22} \end{bmatrix} \quad \mathbf{V} = \begin{bmatrix} v_1 \\ v_2 \end{bmatrix} \quad (1.205)$$

Multiplication:

$$\mathbf{AV} = \begin{bmatrix} a_{11} & a_{12} \\ a_{21} & a_{22} \end{bmatrix} \begin{bmatrix} v_1 \\ v_2 \end{bmatrix} = \begin{bmatrix} (a_{11}v_1 + a_{12}v_2) \\ (a_{21}v_1 + a_{22}v_2) \end{bmatrix} \quad (1.206)$$

$$\mathbf{AB} = \begin{bmatrix} a_{11} & a_{12} \\ a_{21} & a_{22} \end{bmatrix} \begin{bmatrix} b_{11} & b_{12} \\ b_{21} & b_{22} \end{bmatrix} = \begin{bmatrix} (a_{11}b_{11} + a_{12}b_{21}) & (a_{11}b_{12} + a_{12}b_{22}) \\ (a_{21}b_{11} + a_{22}b_{21}) & (a_{21}b_{12} + a_{22}b_{22}) \end{bmatrix}. \quad (1.207)$$

Determinant:

$$|\mathbf{A}| = \det(\mathbf{A}) = \det \begin{pmatrix} a & b \\ c & d \end{pmatrix} = \frac{1}{ad - bc}. \quad (1.208)$$

Transpose:

$$\mathbf{A}^T = \begin{bmatrix} a_{11} & a_{12} \\ a_{21} & a_{22} \end{bmatrix}^T = \begin{bmatrix} a_{11} & a_{21} \\ a_{12} & a_{22} \end{bmatrix} \quad (1.209)$$

Inverse:

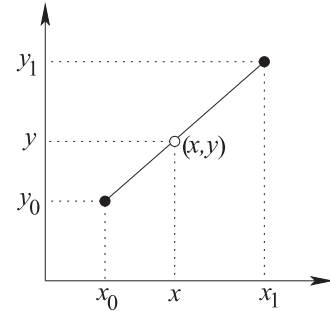
$$\mathbf{A}^{-1} = \begin{bmatrix} a & b \\ c & d \end{bmatrix}^{-1} = \frac{1}{|\mathbf{A}|} \begin{bmatrix} d & -b \\ -c & d \end{bmatrix} = \frac{1}{ad - bc} \begin{bmatrix} d & -b \\ -c & d \end{bmatrix}. \quad (1.210)$$

1.A.12 Interpolation

Linear Interpolation

Linear interpolation can be used to extract data from tables. In the table below there are two known points, (x_0, y_0) and (x_1, y_1) , and the linear interpolant is the straight line between them. The unknown point (x, y) is found by locating it on this straight line.

Variable	
Independent	Dependent
x_0	y_0
x	y
x_1	y_1



Thus

$$\frac{y - y_0}{y_1 - y_0} = \frac{x - x_0}{x_1 - x_0} \quad (1.211)$$

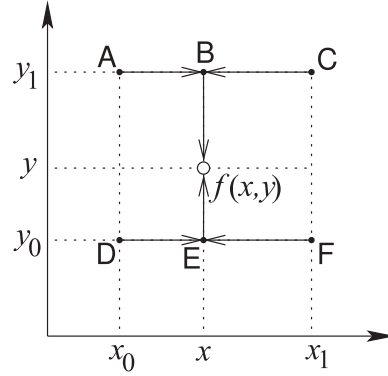
so that, given x ,

$$y = y_0 + (x - x_0) \frac{y_1 - y_0}{x_1 - x_0}. \quad (1.212)$$

Bilinear Interpolation

Bilinear interpolation is a two-dimensional generalization of linear interpolation. In the table below, $f(D) = f(x_0, y_0)$, $f(A) = f(x_0, y_1)$, $f(F) = f(x_1, y_0)$, and $f(C) = f(x_1, y_1)$ are known and $f(x, y)$ is to be found. The bilinear interpolation technique is illustrated in the figure.

Independent	Variable	
	Independent	Dependent
x_0	y_0	f_0
x	y	f
x_1	y_1	f_1



First, find the value of the function at point B from the values at Point A and Point C. Thus, from Equation (1.212),

$$f(B) = f(x, y_1) = f(A) + (x - x_0) \frac{f(C) - f(A)}{x_1 - x_0}. \quad (1.213)$$

Similarly

$$f(E) = f(x, y_0) = f(D) + (x - x_0) \frac{f(F) - f(D)}{x_1 - x_0}. \quad (1.214)$$

Linear interpolation between Point B and Point E yields

$$f(x, y) = f(E) + (y - y_0) \frac{f(B) - f(E)}{y_1 - y_0}. \quad (1.215)$$

Combining these, the function obtained from bilinear interpolation is

$$\begin{aligned} f(x, y) = & \frac{f(x_0, y_0)}{(x_1 - x_0)(y_1 - y_0)}(x_1 - x)(y_1 - y) + \frac{f(x_1, y_0)}{(x_1 - x_0)(y_1 - y_0)}(x - x_0)(y_1 - y) \\ & + \frac{f(x_0, y_1)}{(x_1 - x_0)(y_1 - y_0)}(x_1 - x)(y - y_0) + \frac{f(x_1, y_1)}{(x_1 - x_0)(y_1 - y_0)}(x - x_0)(y - y_0). \end{aligned} \quad (1.216)$$

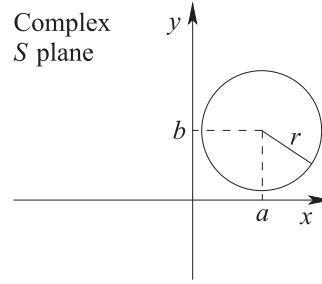
When interpolating from a table, choosing the points closest to the final point will yield greatest accuracy.

1.A.13 Circles on the Complex Plane

A common situation that occurs when working with complex numbers involves equating the magnitude of a complex number being equal to a real number. As will be shown, this defines a circle in the complex plane. Consider the relation

$$|S - c| = r, \quad (1.217)$$

Figure 1-15: A circle in the S plane defined by the relation $|S - c| = r$, where $c = a + jb$ and $S = x + jy$.



where $S = x + jy$ and $c = a + jb$ are complex numbers and r is a real number. Substituting for S and c in Equation (1.217) yields

$$|(x - a) + j(y - b)| = r, \quad (1.218)$$

that is, $[(x - a) + j(y - b)][(x - a) - j(y - b)] = r^2$ (1.219)

$$(x - a)^2 + (y - b)^2 = r^2. \quad (1.220)$$

The above is a general equation for a circle in the x - y plane with center (a, b) and radius r (see Figure 1-15).

1.A.14 Bilinear Transform

The bilinear transformation maps a circle in the complex plane onto another circle in the complex plane [19]. The bilinear transformation of a complex variable z is

$$w = \frac{Az + B}{Cz + 1}. \quad (1.221)$$

where A , B , and C are real numbers. In RF and microwave usage, z and w could be reflection coefficients or impedances. Rearranging Equation (1.221) results in

$$w = \frac{A}{C} + \frac{B - \frac{A}{C}}{Cz + 1}, \quad (1.222)$$

which can be rearranged again as $\frac{w - \frac{A}{C}}{B - \frac{A}{C}} = \frac{1}{Cz + 1}$. (1.223)

The complexity of the derivation is reduced by introducing the intermediate variables W and Z defined as

$$W = \frac{w - \frac{A}{C}}{B - \frac{A}{C}} \quad (1.224) \quad \text{and} \quad Z = Cz + 1, \quad (1.225)$$

and noting that, from Equation (1.223), $W = 1/Z$. (1.226)

If, in Equation (1.225), the locus of z describes a circle, then the locus of Z will also be a circle since C is a constant. If the center of the circle in Z space is C_Z and the distance from any point on the circle to the center is the radius R_Z , then

$$|Z - C_Z| = R_Z. \quad (1.227)$$

Considering Equation (1.225), then in z space, the center of the circle is

$$C_z = \frac{C_Z}{C} - \frac{1}{C} \quad (1.228)$$

and its radius is

$$R_z = R_Z/C. \quad (1.229)$$

Removing the magnitude signs in Equation (1.227) leads to

$$(Z - C_Z)(Z - C_Z)^* = (Z - C_Z)(Z^* - C_Z^*) = R_Z^2, \quad (1.230)$$

or

$$ZZ^* - C_Z Z^* - C_Z^* Z + (|C_Z|^2 - R_Z^2) = 0, \quad (1.231)$$

which is the general equation for a circle in the complex plane.

Now, the circle in the Z plane will be related to what happens in the W plane. Substituting Equation (1.226) into Equation (1.231) results in

$$\frac{1}{WW^*} - C_Z \frac{1}{W^*} - C_Z^* \frac{1}{W} + (|C_Z|^2 - R_Z^2) = 0, \quad (1.232)$$

and rearranging,

$$WW^* - \frac{C_Z}{(|C_Z|^2 - R_Z^2)} W - \frac{C_Z^*}{(|C_Z|^2 - R_Z^2)} W^* + \frac{1}{(|C_Z|^2 - R_Z^2)} = 0. \quad (1.233)$$

This is in the same form as Equation (1.231), so Equation (1.233) describes a circle in W space with center

$$C_W = \frac{C_Z^*}{(|C_Z|^2 - R_Z^2)} \quad (1.234)$$

and radius

$$R_W = \left| \frac{R_Z}{|C_Z|^2 - R_Z^2} \right|. \quad (1.235)$$

Now the locus of w will also be a circle. From Equation (1.224),

$$w = W \left(B - \frac{A}{C} \right) + \frac{A}{C} \quad (1.236)$$

so that W is scaled and a constant added. The center of the circle in w space is

$$C_w = C_W \left(B - \frac{A}{C} \right) + \frac{A}{C} = \frac{C_Z^* (B - A/C)}{(|C_Z|^2 - R_Z^2)} + \frac{A}{C} \quad (1.237)$$

and the radius is

$$R_w = R_W \left| B - \frac{A}{C} \right| = \left| \frac{(B - A/C)}{|C_Z|^2 - R_Z^2} \right|. \quad (1.238)$$

Substituting Equations (1.228) and (1.229) in the above relates the centers and radii in the w and z spaces:

$$C_w = \frac{(CC_z + 1)^*(B - A/C)}{(|CC_z + 1|^2 - |CR_z|^2)} + \frac{A}{C} \quad (1.239)$$

$$R_w = \left| \frac{(B - A/C)CR_z}{|CC_z + 1|^2 - |CR_z|^2} \right| = \left| \frac{(BC - A)R_z}{|CC_z + 1|^2 - |CR_z|^2} \right|. \quad (1.240)$$

Thus the bilinear transform, Equation (1.221), maps all points on a circle in the z plane to points on a circle in the w plane.

1.A.15 Quadratic and Cubic Equations

Quadratic Equation

The general form of the quadratic equation in x is (a , b , and c can be complex)

$$ax^2 + bx + c = 0, \quad (1.241)$$

where $a \neq 0$ There are two solutions, called roots, given by the quadratic formula, [20]

$$x = \frac{-b \pm \sqrt{b^2 - 4ac}}{2a}, \quad (1.242)$$

and \pm indicates two possible roots,

$$x_+ = \frac{-b + \sqrt{b^2 - 4ac}}{2a} \quad \text{and} \quad x_- = \frac{-b - \sqrt{b^2 - 4ac}}{2a}. \quad (1.243)$$

Even if a , b , and c are real, the roots may be complex and they could be degenerate, that is, the same. The factors of the quadratic equation come from the roots, that is,

$$ax^2 + bx + c = a(x - x_+)(x - x_-). \quad (1.244)$$

Cubic Equation

The general form of the cubic equation in x is (a , b , c and d can be complex)

$$ax^3 + bx^2 + cx + d = 0, \quad (1.245)$$

where $a \neq 0$ There are three solutions, called roots, given by the cubic formula, [20]

$$x_k = \frac{1}{3a} \left(b + u_k + \frac{\Delta_0}{u_k C} \right), \quad k \in \{1, 2, 3\} \quad (1.246)$$

where the u_k s are the cube roots of one: $u_1 = 1$, $u_2 = \frac{1}{2}(-1 + j\sqrt{3})$, $u_3 = \frac{1}{2}(-1 - j\sqrt{3})$, and

$$C = \left[\frac{1}{2} \left(\Delta_1 + \sqrt{\Delta_1^2 - 4\Delta_0^3} \right) \right]^{1/3} \quad (1.247)$$

with $\Delta_0 = b^2 - 3ac$ and $\Delta_1 = 2b^3 - 9abc + 27a^2d$. In Equation (1.247) any choice of the square or cube roots can be made as the effect is simply to exchange x_1 , x_2 and x_3 . Note that $ax^3 + bx^2 + cx + d = (x - x_1)(x - x_2)(x - x_3)$.

1.A.16 Kron's Method: Network Condensation

Kron's method [21–23] is also called network condensation and is used in developing simpler equivalent networks of large linear circuits with algebraic y parameters, that is, for resistive networks, or for general linear circuits in frequency-domain analysis where the y parameters are complex numbers. Network condensation is a numerical approach particular to circuits. It is of use in reduced-order modeling of linear circuits and in filter design.

The indefinite nodal admittance formulation of a network with four external terminals (see Figure 1-16) is

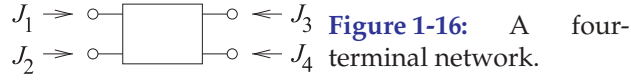


Figure 1-16: A four-terminal network.

$$\begin{bmatrix} y_{11} & y_{12} & \cdots & y_{1,k} & y_{1,k+1} \\ y_{21} & y_{22} & \cdots & y_{2,k} & y_{2,k+1} \\ \vdots & \vdots & \ddots & \vdots & \vdots \\ y_{k1} & y_{k2} & \cdots & y_{k,k} & y_{k,k+1} \\ y_{k+1,1} & y_{k+1,2} & \cdots & y_{k+1,k} & y_{k+1,k+1} \end{bmatrix} \begin{bmatrix} v_1 \\ v_2 \\ v_3 \\ v_4 \\ v_5 \\ \vdots \\ v_k \\ v_{k+1} \end{bmatrix} = \begin{bmatrix} J_1 \\ J_2 \\ J_3 \\ J_4 \\ 0 \\ \vdots \\ 0 \\ 0 \end{bmatrix}, \quad (1.248)$$

as there are no external current sources at the internal terminals $5, 6, \dots, k+1$. Since the $(k+1)$ th current source is zero, the $(k+1)$ th row and column of \mathbf{Y} can be eliminated, yielding

$$\begin{bmatrix} y'_{11} & y'_{12} & \cdots & y'_{1,k} \\ y'_{21} & y'_{22} & \cdots & y'_{2,k} \\ \vdots & \vdots & \ddots & \vdots \\ y'_{k1} & y'_{k2} & \cdots & y'_{k,k} \end{bmatrix} \begin{bmatrix} v'_1 \\ v'_2 \\ v'_3 \\ v'_4 \\ v'_5 \\ \vdots \\ v'_k \end{bmatrix} = \begin{bmatrix} J_1 \\ J_2 \\ J_3 \\ J_4 \\ 0 \\ \vdots \\ 0 \end{bmatrix}, \quad (1.249)$$

$$\text{where } y'_{ij} = y_{ij} - y_{k+1,j} \frac{y_{i,k+1}}{y_{k+1,k+1}} \quad \text{and} \quad v'_i = v_i - v_{k+1}. \quad (1.250)$$

It is of no concern that the terminal voltages have been altered, as they have all had the same quantity added to them. This has the same effect as choosing another reference terminal. The reference terminal is arbitrary until it is connected to the full circuit. The process can be continued until the network equations are reduced to that of a four-terminal element, that is

$$\begin{bmatrix} y''_{11} & y''_{12} & y''_{13} & y''_{14} \\ y''_{21} & y''_{22} & y''_{23} & y''_{24} \\ y''_{31} & y''_{32} & y''_{33} & y''_{34} \\ y''_{41} & y''_{42} & y''_{43} & y''_{44} \end{bmatrix} \begin{bmatrix} v''_1 \\ v''_2 \\ v''_3 \\ v''_4 \end{bmatrix} = \begin{bmatrix} J_1 \\ J_2 \\ J_3 \\ J_4 \end{bmatrix}. \quad (1.251)$$

The y -parameter matrix in Equation (1.251) is that of the four-terminal element shown in Figure 1-16.

Transmission Lines

2.1	Introduction	51
2.2	Transmission Line Theory	55
2.3	The Terminated Lossless Line	66
2.4	Special Cases of Lossless Terminated Lines	78
2.5	The Lossy Terminated Line	87
2.6	Reflections at Interfaces	92
2.7	Models of Transmission Lines	105
2.8	Two-Conductor Transmission Lines	110
2.9	Coaxial Line	111
2.10	Summary	115
2.11	References	116
2.12	Exercises	117
2.A	Appendix: Physical Constants and Material Properties	123

2.1 Introduction

A transmission line stores electric and magnetic energy, and for an alternating signal at a position on the line, energy is converted from one form to the other as time progresses. As such a line has a circuit form that combines inductors, L s (for the magnetic energy), capacitors, C s (for the electric energy), and resistors, R s (modeling losses), whose values depend on the line geometry and material properties.

The transmission lines considered in this chapter are restricted to just two parallel conductors, as shown in Figure 2-1, with the distance between the two wires (i.e., in the transverse direction) being substantially smaller than the wavelengths of the signals on the line. The correct physical interpretation is that the conductors of a transmission line confine and guide an EM field. The EM field contains the energy of the signal and not the current on the line.

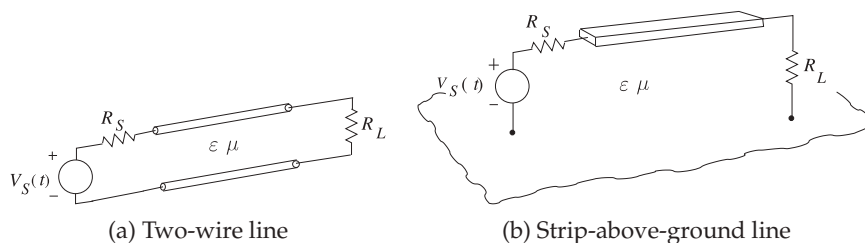


Figure 2-1: Two conductor transmission lines.

However, with electrically small transverse dimensions, a two conductor line may be satisfactorily analyzed on the basis of voltages and currents.

The earliest understanding of signal transmission led to telegraphy over distances. The critical theoretical step that enabled transmission over more than short distances was the development of an understanding of signal transmission on lines using phasor analysis [1]. This frequency-domain analysis is still the best way to understand transmission lines. This transmission line theory with modern developments is presented in Section 2.2 and useful formulas and concepts developed in Section 2.3 for lossless transmission lines. Section 2.4 presents several configurations of lossless lines that are particularly useful in microwave circuit design and used in many places in this book series. Section 2.5 repeats the analysis of lossless lines but now for lossy lines. Reflections and transmission of power at multiple interacting interfaces is considered in Section 2.6. Important network models for transmission lines are developed in Section 2.7. The last section, Section 2.8, presents summary formulas for many two-conductor transmission lines.

2.1.1 When Must a Line be Considered a Transmission Line

The key determinant of whether a transmission line can be considered as an invisible connection between two points is whether the signal anywhere along the interconnect has the same value at a particular instant. If the value of the signal (say, voltage) varies along the line (at an instant), then it may be necessary to consider transmission line effects. A typical criterion used is that if the length of the interconnect is less than 1/20th of the wavelength of the highest-frequency component of a signal, then transmission line effects can be safely ignored and the circuit can be modeled as a single *RLC* circuit [2]. The actual threshold used— $\lambda/20$, $\lambda/10$, or $\lambda/5$ —is based on experience and the particular application. For example, an interconnect carrying a digital signal clocking at 4 GHz has an appreciable frequency component at 20 GHz. Then the interconnect reaches the $\lambda/10$ threshold when it is 4.5 mm long. Thus it takes a finite time for the variation of a voltage at one end of the interconnect to impact the voltage at the other end. The ultimate limit is determined by the speed of light, c , but this is reduced by the relative permittivity and permeability of the material in which the fields exist. The relative permittivity and permeability describe the effect of excess potential energy storage in the material, above that of vacuum, in a manner that is analogous to storing mechanical energy in a spring.

2.1.2 Movement of a Signal on a Transmission Line

A **coaxial line** (Figure 2-2(a)) is the quintessential transmission line as it is one of the few transmission line structures that can be described exactly from first principles when there is no loss. This is because the cross section of a coaxial line matches the cylindrical coordinate system, an orthogonal coordinate system with boundary conditions that can be expressed in terms of just one coordinate (the radius). It is known how to solve Maxwell's equations, which are just differential equations, in an orthogonal coordinate system. This is done for a coaxial line in Section 2.9.

When a positive voltage pulse is applied to the center conductor of the

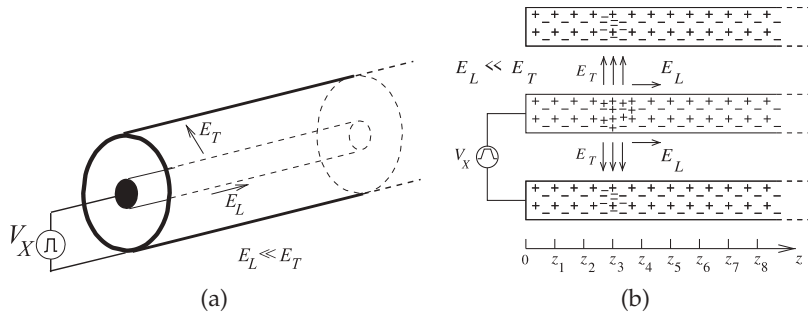


Figure 2-2: A coaxial transmission line: (a) three-dimensional view; (b) the line with pulsed voltage source showing the electric fields at an instant in time as a voltage pulse travels down the line. $E_L \ll E_T$.

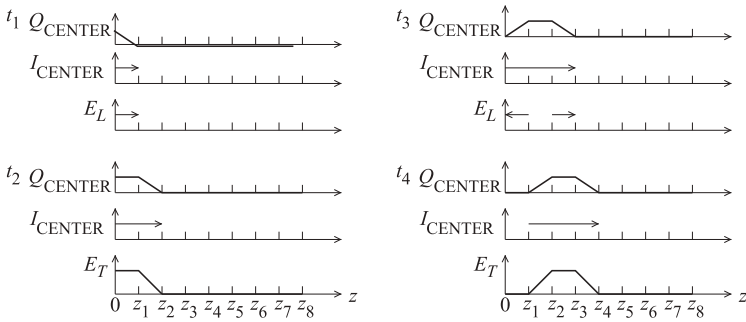


Figure 2-3: Fields, currents, and charges on the coaxial transmission line of Figure 2-2 at times $t_4 > t_3 > t_2 > t_1$. Q_{CENTER} is the net free charge on the center conductor. I_{CENTER} is the current on the center conductor.

coaxial line, as shown in Figure 2-2(a), an electric field results that is directed from the center conductor to the outer conductor. Referring to Figure 2-2(b), the component of the field that is directed along the shortest path from the center conductor to the outer conductor is denoted E_T , and the subscript T denotes the transverse component of the field with the transverse plane being perpendicular to the direction of propagation along the line. Figure 2-2(b) shows the fields in the structure after the pulse has started moving along the line. This is shown in another view in Figure 2-3 at four different times. The transverse voltage, V_T , is given by E_T integrated along a path between the inner and outer conductors: $V_T \approx E_T(a - b)$. This is a good measure, provided that the transverse dimensions are small compared to a wavelength (otherwise the integral is then path dependent). The voltage pulse exciting the line has a trapezoidal shape and Figure 2-3 shows the charge, Q_{CENTER} , and current, I_{CENTER} , on the center conductor and the transverse field, E_T . The voltage between the inner and outer conductor has the same form as E_T . As indicated by Maxwell's equations, a change in time of the electric field results in a spatial change in the magnetic field and hence current. As a result there is a variation of the current in time and this results in a spatial change of the electric field. The chasing from a time variation to a spatial variation and then back to a time variation causes the pulse to move down the line.

The pulse moves down the line at the **group velocity**, which for a lossless coaxial line is the same as the **phase velocity**, v_p .¹ This is determined by the physical properties of the region between the conductors. The permittivity,

¹ The phase velocity is the apparent velocity of a point of constant phase on a sinewave and is almost frequency independent for a low-loss coaxial line of small transverse dimensions (less than $\lambda/10$).

ε , describes energy storage associated with the electric field, E , and the energy storage associated with the magnetic field, H , is described by the permeability, μ . (Both ε and μ are properties of the medium—the material.) It has been determined that²

$$v_p = 1/\sqrt{\mu\varepsilon}. \quad (2.1)$$

In a vacuum $\varepsilon = \varepsilon_0$, the free-space permittivity, and $\mu = \mu_0$, the free-space permeability. These are physical constants and have the values

$$\text{Permittivity of free space: } \varepsilon_0 = 8.854 \times 10^{-12} \text{ F/m.}$$

$$\text{Permeability of free space: } \mu_0 = 4\pi \times 10^{-7} \text{ H/m.}$$

One conclusion here is that EM energy can be stored in **free space**, i.e. in a vacuum. In free space $v_p = c = 1/\sqrt{\mu_0\varepsilon_0} = 3 \times 10^8 \text{ m/s}$. The free-space wavelengths, $\lambda_0 = c/f$, at several frequencies, f , are

f	100 MHz	1 GHz	10 GHz
λ_0	3 m	30 cm	3.0 cm

Commonly λ_0 is used to indicate the wavelength in free space and λ_g , the guide wavelength, is used to denote the wavelength on a transmission line. It is convenient to use the relative permittivity (or the less commonly used term **dielectric constant**), ε_r , defined as

$$\varepsilon_r = \varepsilon/\varepsilon_0. \quad (2.2)$$

Similarly the relative permeability is

$$\mu_r = \mu/\mu_0, \quad (2.3)$$

and most materials have $\mu_r = 1$. The permittivity, permeability, and conductivity of materials used in RF and microwave circuits are given in Appendix 2.A.

EXAMPLE 2.1

Transmission Line Wavelength

A length of coaxial line is filled with a dielectric having a relative permittivity of 20 and is designed to be $1/4$ wavelength long at a frequency, f , of 1.850 GHz.

- What is the free-space wavelength?
- What is the wavelength of the signal in the dielectric-filled coaxial line?
- How long is the line?

Solution:

- $\lambda_0 = c/f = 3 \times 10^8 / 1.85 \times 10^9 = 0.162 \text{ m} = 16.2 \text{ cm}$.
- Note that for a dielectric-filled line with $\mu_r = 1$, $\lambda = v_p/f = c/(\sqrt{\varepsilon_r}f) = \lambda_0/\sqrt{\varepsilon_r}$, so $\lambda = \lambda_0/\sqrt{\varepsilon_r} = 16.2 \text{ cm}/\sqrt{20} = 3.62 \text{ cm}$.
- $\lambda_g/4 = 3.62 \text{ cm}/4 = 9.05 \text{ mm}$.

² This is derived from Maxwell's equations and describes the situation where the fields have a very simple structure, in general where the fields are solely directed in the transverse plane.

2.2 Transmission Line Theory

This section develops the theory of signal propagation on transmission lines. The first section, Section 2.2.1, makes the argument that a circuit with resistors, inductors, and capacitors is a good model for a transmission line. The complete development of transmission line theory is presented in Section 2.2.2, and Section 2.2.3 relates the RLGC transmission line model to the properties of a medium. The dimensions of some of the quantities that appear in transmission line theory are discussed in Section 2.2.4. Section 2.2.5 summarizes the important parameters of a lossless line and then two particularly important lines, coaxial lines and microstrip lines, are considered in Sections 2.2.6 and 2.2.7.

2.2.1 Transmission Line RLGC Model

Regardless of the actual structure, a segment of uniform transmission line (i.e., a line with constant cross section along its length) as shown in Figure 2-4(a) can be modeled by the circuit shown in Figure 2-4(b) with

$$\begin{array}{ll} \text{Resistance along the line} & = R \\ \text{Inductance along the line} & = L \\ \text{Conductance shunting the line} & = G \\ \text{Capacitance shunting the line} & = C \end{array} \left| \begin{array}{l} \text{all specified} \\ \text{per unit length.} \end{array} \right.$$

Thus R , L , G , and C are also referred to as resistance, inductance, conductance, and capacitance per unit length. (Sometimes p.u.l. is used as shorthand for **per unit length**.) In the metric system, ohms per meter (Ω/m), henries per meter (H/m), siemens per meter (S/m) and farads per meter (F/m), respectively, are used. The values of R , L , G , and C are affected by the geometry of the transmission line and by the electrical properties of the dielectrics and conductors. C describes the ability to store electrical energy and is mostly due to the properties of the dielectric. G describes loss in the dielectric which derives from conduction in the dielectric and from dielectric relaxation. Most microwave substrates have negligible conductivity so dielectric relaxation loss dominates. Dielectric relaxation loss results from the movement of charge centers which result in distortion of the dielectric lattice (if a crystal) or molecular structure. The periodic variation of the E field transfers energy from the EM field to mechanical vibrations. R is due to ohmic loss in the metal more than anything else. L describes the ability to store magnetic energy and is mostly a function of geometry, as most materials used with transmission lines have $\mu_r = 1$ (so no more magnetic energy is stored than in a vacuum).

For most lines the effects due to L and C dominate because of the relatively low series resistance and shunt conductance. The propagation characteristics of the line are described by its loss-free, or lossless, equivalent line, although in practice some information about R or G is necessary to determine power

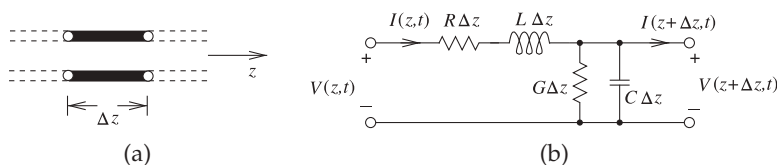


Figure 2-4: Transmission line segment: (a) of length Δz ; and (b) lumped-element model.

losses. The lossless concept is just a useful and good approximation.

2.2.2 Derivation of Transmission Line Properties

In this section the differential equations governing the propagation of signals on a transmission line are derived. These are coupled first-order differential equations and are akin to Maxwell's Equations in one dimension. Solution of the differential equations describes how signals propagate, and leads to the extraction of a few parameters that describe transmission line properties.

Applying **Kirchoff's laws** applied to the model in Figure 2-4(b) and taking the limit as $\Delta z \rightarrow 0$ the **transmission line equations** are

$$\frac{\partial v(z, t)}{\partial z} = -Ri(z, t) - L \frac{\partial i(z, t)}{\partial t} \quad (2.4)$$

$$\frac{\partial i(z, t)}{\partial z} = -Gv(z, t) - C \frac{\partial v(z, t)}{\partial t}. \quad (2.5)$$

$V(z)$ is a phasor and $v(z, t) = \Re\{V(z)e^{j\omega t}\}$. $\Re\{w\}$ denotes the real part of w , a complex number.

In sinusoidal steady-state using cosine-based phasors these become

$$\frac{dV(z)}{dz} = -(R + j\omega L)I(z) \quad (2.6) \quad \text{and} \quad \frac{dI(z)}{dz} = -(G + j\omega C)V(z). \quad (2.7)$$

Eliminating $I(z)$ in the above yields the wave equation for $V(z)$:

$$\frac{d^2 V(z)}{dz^2} - \gamma^2 V(z) = 0. \quad (2.8) \quad \text{Similarly} \quad \frac{d^2 I(z)}{dz^2} - \gamma^2 I(z) = 0, \quad (2.9)$$

where the propagation constant is

$$\gamma = \alpha + j\beta = \sqrt{(R + j\omega L)(G + j\omega C)}, \quad (2.10)$$

with SI units of m^{-1} and where α is the attenuation coefficient and has units of nepers per meter (Np/m), and β is the phase-change coefficient, or phase constant, and has units of radians per meter (expressed as rad/m or radians/m). Nepers and radians are dimensionless units, but serve as prompts for what is being referred to.

Equations (2.8) and (2.9) are second-order differential equations that have solutions of the form

$$V(z) = V_0^+ e^{-\gamma z} + V_0^- e^{\gamma z} \quad (2.11) \quad \text{and} \quad I(z) = I_0^+ e^{-\gamma z} + I_0^- e^{\gamma z}. \quad (2.12)$$

The physical interpretation of these solutions is that $V^+(z) = V_0^+ e^{-\gamma z}$ and $I^+(z) = I_0^+ e^{-\gamma z}$ are forward-traveling waves (moving in the $+z$ direction) and $V^-(z) = V_0^- e^{\gamma z}$ and $I^-(z) = I_0^- e^{\gamma z}$ are backward-traveling waves (moving in the $-z$ direction). $V(z)$, V_0^+ , V_0^- , $I(z)$, I_0^+ and I_0^- are all phasors. Substituting Equation (2.11) in Equation (2.6) results in

$$I(z) = \frac{\gamma}{R + j\omega L} [V_0^+ e^{-\gamma z} - V_0^- e^{\gamma z}]. \quad (2.13)$$

Then from Equations (2.13) and (2.12)

$$I_0^+ = \frac{\gamma}{R + j\omega L} V_0^+ \quad \text{and} \quad I_0^- = \frac{\gamma}{R + j\omega L} (-V_0^-). \quad (2.14)$$

The characteristic impedance is defined as

$$Z_0 = \frac{V_0^+}{I_0^+} = \frac{-V_0^-}{I_0^-} = \frac{R + j\omega L}{\gamma} = \sqrt{\frac{R + j\omega L}{G + j\omega C}}, \quad (2.15)$$

with the SI unit of ohms (Ω). Equations (2.11) and (2.12) can be rewritten as

$$V(z) = V_0^+ e^{-\gamma z} + V_0^- e^{\gamma z} \quad (2.16) \quad \text{and} \quad I(z) = \frac{V_0^+}{Z_0} e^{-\gamma z} - \frac{V_0^-}{Z_0} e^{\gamma z}. \quad (2.17)$$

Converting back to the time domain:

$$v(z, t) = |V_0^+| \cos(\omega t - \beta z + \varphi^+) e^{-\alpha z} + |V_0^-| \cos(\omega t + \beta z + \varphi^-) e^{\alpha z}, \quad (2.18)$$

where φ^+ and φ^- are phases of the forward- and backward-traveling waves, respectively. The phasors of the traveling voltage waves are

$$V_0^+(z) = |V_0^+| e^{j\varphi^+} e^{-j\beta z} \quad \text{and} \quad V_0^-(z) = |V_0^-| e^{j\varphi^-} e^{j\beta z}. \quad (2.19)$$

The following quantities are defined:

$$\text{Characteristic impedance: } Z_0 = \sqrt{(R + j\omega L)/(G + j\omega C)} \quad (2.20)$$

$$\text{Propagation constant: } \gamma = \sqrt{(R + j\omega L)(G + j\omega C)} \quad (2.21)$$

$$\text{Attenuation constant: } \alpha = \Re\{\gamma\} \quad (2.22)$$

$$\text{Phase constant: } \beta = \Im\{\gamma\} \quad (2.23)$$

$$\text{Wavenumber: } k = -j\gamma \quad (2.24)$$

$$\text{Phase velocity: } v_p = \omega/\beta \quad (2.25)$$

$$\text{Wavelength: } \lambda = \frac{2\pi}{|\gamma|} = \frac{2\pi}{|k|}, \quad (2.26)$$

where $\omega = 2\pi f$ is the radian frequency and f is the frequency with the SI units of hertz (Hz). The wavenumber k as defined here is used in electromagnetics and where wave propagation is concerned. Considering one of the traveling waves, the phase velocity refers to the apparent velocity of which a point of constant phase on the sinewave appears to move.

For low-loss materials, $\alpha \ll \beta$, and so $\beta \approx |k|$, then the following approximations are valid:

$$\text{Characteristic impedance: } Z_0 \approx \sqrt{L/C} \quad (2.27)$$

$$\text{Phase constant: } \beta \approx \omega\sqrt{LC} \quad (2.28)$$

$$\text{Wavenumber: } k \approx \beta \quad (2.29)$$

$$\text{Phase velocity: } v_p = \omega/\beta \quad (2.30)$$

$$\text{Wavelength: } \lambda \approx \frac{2\pi}{\beta} = v_p/f. \quad (2.31)$$

The important result here is that a voltage wave (and a current wave) can be defined on a transmission line. One more parameter needs to be introduced: the group velocity,

$$v_g = \frac{\partial \omega}{\partial \beta}. \quad (2.32)$$

The group velocity is the velocity of a modulated waveform's envelope and describes how fast information propagates. It is the velocity at which the energy (i.e. information) in the waveform moves. Thus group velocity can never be more than the speed of light in a vacuum, c . Phase velocity, however, can be more than c . If the speed at which information moves varies with frequency, then a signal such as a pulse will spread out. Such a line is said

to have dispersion. For a lossless, dispersionless line, the group and phase velocity are the same. If the phase velocity is frequency independent, then β is linearly proportional to ω .

Electrical length is used in designs with transmission lines prior to establishing the physical length of the line. The electrical length of a line is expressed either as a fraction of a wavelength or in degrees (or radians), where a wavelength corresponds to 360° (or 2π radians). So if β is the phase constant of a signal on the line and ℓ is its physical length, the electrical length of the line in radians is $\beta\ell$.

EXAMPLE 2.2**Physical and Electrical Length**

A transmission line is 10 cm long and at the operating frequency the phase constant β is 30 rad/m. What is the electrical length of the line?

Solution:

The physical length of the line is $\ell = 10 \text{ cm} = 0.1 \text{ m}$. Then the electrical length of the line is $\ell_e = \beta\ell = (30 \text{ rad/m}) \times 0.1 \text{ m} = 3 \text{ radians}$. The electrical length can also be expressed in terms of wavelength noting that 360° corresponds to 2π radians, which also corresponds to λ . Thus $\ell_e = (3 \text{ radians}) = 3 \times 360/(2\pi) = 171.9^\circ$ or $\ell_e = 3/(2\pi) \lambda = 0.477 \lambda$.

EXAMPLE 2.3**RLGC Parameters**

A transmission line has the *RLGC* parameters $R = 100 \Omega/\text{m}$, $L = 80 \text{ nH/m}$, $G = 1.6 \text{ S/m}$, and $C = 200 \text{ pF/m}$. Consider a traveling wave at 2 GHz on the line.

- What is the attenuation constant?
- What is the phase constant?
- What is the phase velocity?
- What is the characteristic impedance of the line?
- What is the group velocity?

Solution:

$$(a) \quad \alpha: \gamma = \alpha + j\beta = \sqrt{(R + j\omega L)(G + j\omega C)}; \quad \omega = 12.57 \cdot 10^9 \text{ rad/s}$$

$$\gamma = \sqrt{(100 + j\omega \cdot 80 \cdot 10^{-9})(1.6 + j\omega 200 \times 10^{-12})} = (17.94 + j51.85) \text{ m}^{-1}$$

$$\alpha = \Re\{\gamma\} = 17.94 \text{ Np/m}$$

$$(b) \quad \text{Phase constant: } \beta = \Im\{\gamma\} = 51.85 \text{ rad/m}$$

$$(c) \quad \text{Phase velocity:}$$

$$v_p = \frac{\omega}{\beta} = \frac{2\pi f}{\beta} = \frac{12.57 \times 10^9 \text{ rad} \cdot \text{s}^{-1}}{51.85 \text{ rad} \cdot \text{m}^{-1}} = 2.42 \times 10^8 \text{ m/s}$$

$$(d) \quad Z_0 = (R + j\omega L)/\gamma = (100 + j\omega \cdot 80 \cdot 10^{-9})/(17.94 + j51.85) = (17.9 + j4.3) \Omega$$

Note also that $Z_0 = \sqrt{(R + j\omega L)/(G + j\omega C)}$, which yields the same answer.

$$(e) \quad \text{Group velocity:}$$

$$v_g = \left. \frac{\partial \omega}{\partial \beta} \right|_{f=2 \text{ GHz}}$$

Numerical derivatives will be used, thus $v_g = \Delta\omega/\Delta\beta$. Now β is already known at 2 GHz. At 1.9 GHz, $\gamma = 17.884 + j49.397 \text{ m}^{-1}$, and so $\beta = 49.397 \text{ rad/m}$.

$$v_g = \frac{2\pi(2 \text{ GHz} - 1.9 \text{ GHz})}{\beta(2 \text{ GHz}) - \beta(1.9 \text{ GHz})} = \frac{2\pi(2 - 1.9)10^9 \text{ Hz}}{(51.85 - 49.397) \text{ m}^{-1}} = 2.563 \times 10^8 \text{ m/s}.$$

(Note that $\text{Hz} = \text{s}^{-1}$. Note that $v_g \neq v_p$, and so the transmission line has dispersion.)

2.2.3 Relationship of RLGC parameters to Permittivity and Permeability of a Medium

In the previous section the telegrapher's equations for a transmission line modeled as subsections of *RLGC* elements was derived. Very good accuracy is obtained if the length of a subsection is no more than one-twentieth of a wavelength. The full transmission line model is the cascade of many transmission line subsections (e.g. see Figure 2-5). In this section the *RLGC* parameters are related to the physical parameters of permittivity and permeability. The development does not go into much detail, as the derivation is involved and can only be derived analytically for a few regular transmission line structures. If you are curious, the development is done for a parallel plate waveguide and a rectangular waveguide in Chapter 6 and for a coaxial line in Section 2.9.

The main parameters describing propagation on a transmission line are Z_0 and γ , and these depend on the permeability and permittivity of the medium and the spatial variation of the E and H fields resulting from the geometry of the conductors. Only a few geometries permit analytic solution of the fields so in general a numerical field solution is required and Z_0 and γ derived. Very often equations are curve fit to the numerical solutions but the structure of the equations have a theoretical foundation. It is found that there can be a number of possible field solutions (not unusual for the solution of differential equations) each of which is called a mode. Modes that have all the fields in the transverse plane (perpendicular to the propagation direction) is called a transverse EM (TEM) mode and these modes exist at DC. The other modes are only possible above a cut-off frequency. It is found that the propagation constant has the form

$$\gamma^2 = -(k^2 - k_c^2), \quad (2.33)$$

where k_c is the cutoff wavenumber and for a particular line usually has a different value for each mode. The wavenumber of a homogeneous line is

$$k = j\omega\sqrt{\mu\epsilon}. \quad (2.34)$$

A mode can only exist and describe a propagating signal when $\beta = \Im\{\gamma\}$ is not zero which requires that γ^2 be negative. Thus a mode can support a propagating mode only if the wavenumber is greater than the cut-off wavenumber, i.e. when $k > k_c$. A TEM mode has $k_c = 0$ so a signal, other than DC can always propagate on the line in a TEM mode. A homogeneous line has just one type of medium supporting the EM fields. An example of a homogeneous line is a teflon-filled coaxial line. A non-homogeneous line has two or more dielectric mediums, such as air and a dielectric. For non-homogeneous lines the concept of an equivalent homogeneous line with an effective permittivity ϵ_{eff} and effective permeability μ_{eff} is used. Then

$$k = j\omega\sqrt{\mu_{\text{eff}}\epsilon_{\text{eff}}} \quad (2.35)$$

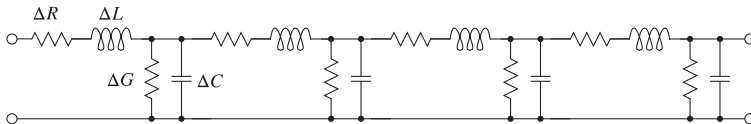


Figure 2-5: *RLGC* model of a transmission line.

Loss is incorporated in the imaginary parts of ε and μ for TEM modes. As before, for any mode,

$$\text{Attenuation constant: } \alpha = \Re\{\gamma\} \quad (2.36)$$

$$\text{Phase constant: } \beta = \Im\{\gamma\} \quad (2.37)$$

$$\text{Phase velocity: } v_p = \omega/\beta \quad (2.38)$$

$$\text{Wavelength: } \lambda = \frac{v_p}{f} = \frac{2\pi}{\beta}, \quad (2.39)$$

Comparing γ in Equations (2.10) and (2.35), an equivalence can be developed between the lumped-element form of transmission line propagation and the propagation of an EM wave in a medium. Specifically,

$$-\omega^2 \mu_{\text{eff}} \varepsilon_{\text{eff}} = (R + j\omega L)(G + j\omega C). \quad (2.40)$$

Lossless Medium

If the medium is lossless (μ and ε are real and $R = 0 = G$), then

$$\mu_{\text{eff}} \varepsilon_{\text{eff}} = LC. \quad (2.41)$$

When the medium is free space (a vacuum), then a subscript zero is used. Free space is also lossless, so the following results hold:

$$\alpha_0 = 0 \quad \text{and} \quad \beta_0 = -j\gamma = \omega\sqrt{\mu_0\varepsilon_0} = \omega\sqrt{LC}. \quad (2.42)$$

If frequency is specified in gigahertz (indicated by f_{GHz}), in free space

$$\beta_0 = 20.958 f_{\text{GHz}} \quad \text{units of rads/m.} \quad (2.43)$$

At 1 GHz, $\beta_0 = 20.958$ rad/m and $\lambda_0 = 29.98$ cm (use $\lambda_0 \approx 30$ cm at 1 GHz as a reference). In a lossless medium with **effective relative permeability** $\mu_e = \mu_{\text{eff}}/\mu_0 = 1$ and **effective relative permittivity** $\varepsilon_e = \varepsilon_{\text{eff}}/\varepsilon_0$,

$$\beta = \sqrt{\varepsilon_e} \beta_0. \quad (2.44)$$

Z_0 depends strongly on the spatial variation of the fields. When there is no variation in the plane transverse to the direction of propagation (i.e. for plane wave propagation)

$$Z_0 = \sqrt{\mu/\varepsilon}. \quad (2.45)$$

However, if there is variation of the fields

$$Z_0 = \kappa \sqrt{\mu_{\text{eff}}/\varepsilon_{\text{eff}}} = \kappa \sqrt{\mu_0/\varepsilon_0} \sqrt{\mu_e/\varepsilon_e}, \quad (2.46)$$

where κ captures the effect of geometric variation of the fields. Spatial variation of the fields stores additional energy in the E and H fields, affecting γ as well as Z_0 .

If the boundary conditions on a transmission line are such that a required spatial variation of the fields cannot be supported, then the signal cannot propagate. The critical frequency at which $k = j\omega\sqrt{\mu\varepsilon} = k_c$ is called the cutoff frequency, f_c . Signals cannot propagate on the line if the frequency is below f_c . For the rest of this chapter the only lines considered are those for which $k_c = 0$, (and $f_c = 0$), i.e. TEM modes on transmission lines. That is, the lines carry DC signals.

Low Loss Medium

Transmission line loss is due to the resistance of conductors, which is described by R , and loss in the dielectric described by G . For most dielectrics there is very little conductive loss and loss is due almost entirely to dielectric relaxation. (The most common exception is when the dielectric is silicon as there can be appreciable conduction in silicon.) In dielectric relaxation an electric field causes charge centers to move and these cause the lattice to vibrate which we know is heat so energy is transferred from the electric field to heat. The energy lost is proportional to frequency and so G is directly proportional to frequency and consequently, provided there is no conduction in the dielectric, the **loss tangent** of the transmission line is thus defined as:

$$\tan \delta = G/\omega C = \text{independent of frequency.} \quad (2.47)$$

One consequence of Equation (2.47), and noting that C is approximately independent of frequency, is that if G is known at one frequency then its value at another frequency can be quickly determined.

The loss tangent of the dielectric medium and the loss tangent of the transmission line may not be the same as the EM fields may not be confined just to the medium, e.g. fields are in air and in a dielectric.

2.2.4 Dimensions of γ , α , and β

The SI unit of γ are inverse meters (m^{-1}) and the attenuation constant, α , and the phase constant, β , have, strictly speaking, the same units. However, the convention is to introduce the dimensionless quantities Neper and radian to convey additional information. Thus the attenuation constant α has the units of Nepers per meter (Np/m) and the phase constant β has the units radians per meter (rad/m). The unit Neper comes from the name of the e ($= 2.7182818284590452354 \dots$) symbol (written in upright font and not italics since it is a constant), which is called the Neper. The Neper is used in calculating transmission line signal levels, as in Equations (2.11) and (2.12). The attenuation and phase constants are often separated and then the attenuation constant describes the decrease in signal amplitude as the signal travels down a transmission line. So when $\alpha\ell = 1$ Np, where ℓ is the length of the line, the signal has decreased to $1/e$ of its original value, and the power drops to $1/e^2$ of its original value. The decrease in signal level represents loss and the units of decibels per meter (dB/m) are used with $1 \text{ Np} = 20 \log e = 8.6858896381 \text{ dB}$. So expressing α as 1 Np/m is the same as saying that the attenuation loss is 8.6859 dB/m. To convert from dB to Np multiply by 0.1151. Thus $\alpha = x \text{ dB/m} = x \times 0.1151 \text{ Np/m}$.

The name for e derives from John **Napier**, who developed the theory of logarithms [3]. e is sometimes called Euler's constant.

In engineering
 $\log x \equiv \log_{10} x$ and
 $\ln x \equiv \log_e x$.

EXAMPLE 2.4

Transmission Line Characteristics

A line has an attenuation of 10 dB/m and a phase constant of 50 radians/m at 2 GHz.

- What is the complex propagation constant of the transmission line?
- If the capacitance of the line is 100 pF/m and the conductive loss is zero (i.e., $G = 0$), what is the characteristic impedance of the line?

Solution:

- $\alpha|_{\text{Np}} = 0.1151 \times \alpha|_{\text{dB}} = 0.1151 \times (10 \text{ dB/m}) = 1.151 \text{ Np/m}$, $\beta = 50 \text{ rad/m}$
 Propagation constant, $\gamma = \alpha + j\beta = (1.151 + j50) \text{ m}^{-1}$
- $\gamma = \sqrt{(R + j\omega L)(G + j\omega C)}$, and $Z_0 = \sqrt{(R + j\omega L)/(G + j\omega C)}$,
 therefore $Z_0 = \gamma/(G + j\omega C)$; $\omega = 2\pi \cdot 2 \times 10^9 \text{ s}^{-1}$; $G = 0$; $C = 100 \times 10^{-12} \text{ F}$,
 so $Z_0 = 39.8 - j0.916 \Omega$.

2.2.5 Lossless Transmission Line

If the conductor and dielectric are ideal (i.e., lossless), then $R = 0 = G$ and the equations for the transmission line characteristics simplify. The transmission line parameters from Equations (2.15) and (2.21)–(2.26) are then

$$Z_0 = \sqrt{\frac{L}{C}} \quad (2.48) \quad \alpha = 0 \quad (2.49)$$

$$\beta = \omega\sqrt{LC} \quad (2.50) \quad v_p = 1/\sqrt{LC} \quad (2.51)$$

$$\lambda_g = \frac{2\pi}{\omega\sqrt{LC}} = \frac{v_p}{f}. \quad (2.52)$$

Note that there is a distinction between a transmission line and an RLC circuit. When a transmission line is referred to as having an impedance of 50Ω , this is referring to the line having a characteristic impedance of 50Ω , the line cannot be replaced by a 50Ω resistor.

A line cannot be replaced by a lumped element except as follows:

1. When calculating the forward voltage wave of a line that is infinitely long (or there are no reflections from the load). Then the line can be replaced by an impedance equal to the characteristic impedance of the line. The total voltage is then only the forward-traveling component.
2. The characteristic impedance and load impedance are used to calculate the input impedance of the terminated line at a particular frequency.

2.2.6 Coaxial Line

The analytic calculation of the characteristic impedance of a transmission line from geometry is not always possible except for a few regular geometries (matching orthogonal coordinate systems). For a coaxial line, the electric fields extend in a radial direction from the center conductor to the outer conductor. So it is possible to calculate the voltage by integrating this E field from the center to the outer conductor. The magnetic field is circular, centered on the center conductor, so the current on the conductor can be calculated as the closed integral of the magnetic field. (Here the field lines and the conductor boundaries correspond to the cylindrical coordinate system.) Solving for the fields in the region between the center and outer conductors yields the following formula for the characteristic impedance of a coaxial line (the derivation is presented in Section 2.9):

$$Z_0 = 138\sqrt{\frac{\mu_r}{\varepsilon_r}} \log\left(\frac{b}{a}\right) \Omega = 60\sqrt{\frac{\mu_r}{\varepsilon_r}} \ln\left(\frac{b}{a}\right) \Omega, \quad (2.53)$$

where ε_r is the relative permittivity of the medium between the center and outer conductors, b is the inner diameter of the outer conductor, and a is the outer diameter of the inner conductor. With a higher ε_r , more energy is stored in the electric field and the capacitance per unit length of the line, C , increases. As the relative permittivity of the line increases, the characteristic impedance of the line reduces. Equation (2.53) is an exact formulation for the characteristic impedance of a coaxial line. Such a formula can only be approximated for nearly every other line.

Most coaxial cables have Z_0 of 50Ω , but different ratios of b and a yield special properties of the coaxial line. When the ratio is 1.65 for an air-filled line, $Z_0 = 30 \Omega$ and the line has **maximum power-carrying** capability. The

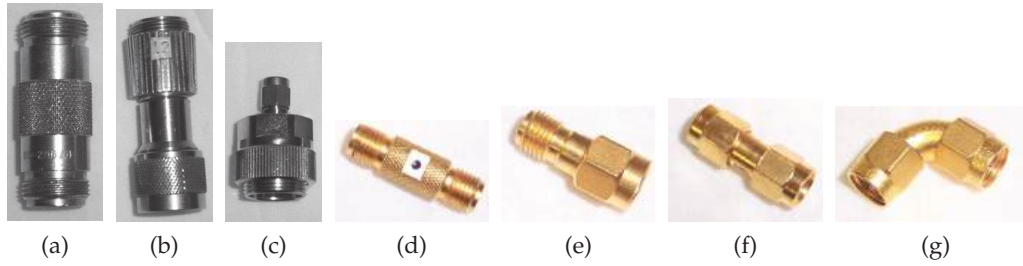


Figure 2-6: Coaxial line adaptors: (a) N-type female-to-female (N(f)-to-N(f)); (b) APC-7 to N-type male (APC-7-to-N(m)); (c) APC-7 to SMA-type male (APC-7-to-SMA(m)); SMA adaptors: (d) SMA-type female-to-female (SMA(f)-to-SMA(f)); (e) SMA-type male-to-female (SMA(m)-to-SMA(f)); (f) SMA-type male-to-male (SMA(m)-to-SMA(m)); and (g) SMA elbow. N, APC-7 and SMA are known as connector series.

ratio for maximum voltage breakdown is 2.7, corresponding to $Z_0 = 60 \Omega$ for an air-filled line. The characteristic impedance for minimum attenuation in an air-filled line is 77Ω , with a diameter ratio of 3.59. This optimum ratio of outer-to-inner conductors for **minimum loss** is independent of the dielectric and typical dielectrics have negligible loss with line loss due almost entirely due to the conductors. If the dielectric filling the coaxial line is polyethylene (which is most common) with $\epsilon_r = 2.3$, the characteristic impedance of the minimum loss line is 50.6Ω .

The velocity of propagation in a lossless coaxial line having uniform medium is the same as that for a plane wave in the medium, i.e. $v_g = c/\sqrt{\epsilon_r}$. There is one caveat. This is true for all transmission line structures supporting the minimum variation of the fields corresponding to a TEM mode. Higher-order modes, with greater spatial variations of the fields will travel more slowly (i.e. $v_g < c/\sqrt{\epsilon_r}$), will be considered in Chapter 4. The diameter of the outer conductor and the type of internal supports for the internal conductor determines the frequency range of coaxial components. At high frequencies, and hence short wavelengths, large internal dimensions of a large diameter cable can support more than one spatial variation of the EM fields, i.e. more than one mode. This is undesirable because two modes will travel at different speeds and a propagating signal divides energy between the two modes and, since the modes have different group velocities, the signal will become garbled. Thus the transverse dimensions of the cable determine its upper frequency limit for reliable signal transmission.

There are various coaxial lines with different diameters and different levels of attention given to the uniformity of the lines. Each type of line is called a series and it is necessary to convert between series using adaptors. Various adaptors are shown in Figure 2-6. Primarily these have different cost, loss, and uniformity of Z_0 . It is often necessary to convert between series and also to convert between the sexes (male and female) of connectors. Note that a plug (or jack) could be either female or male.

The different construction of connectors can be seen in Figure 2-7. With the APC-7 connector shown in Figure 2-7(a) the inside diameter of the outer conductor is 7 mm. The unique feature of this connector is that it is sexless, with the interface plate being spring-loaded. That is, an APC-7 connector can always be connected to another APC-7 connector. These are precision

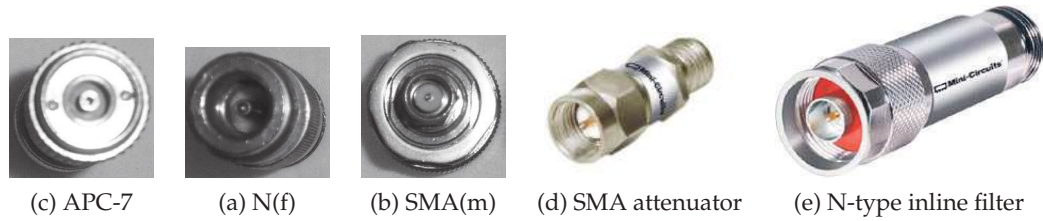


Figure 2-7: Various coaxial 50 Ω transmission line connectors: (a) APC-7 coaxial connector (7 mm outer conductor diameter); (b) female N-type (N(f)) coaxial connector (7 mm); (c) male SMA-type (SMA(m)) coaxial connector (3.5 mm); (d) DC to 26 GHz, 2-W SMA precision fixed attenuator; and (e) N-type inline 500 MHz lowpass filter. ((d) and (e) copyright 2012 Scientific Components Corporation d/b/a Mini-Circuits, used with permission [4]).

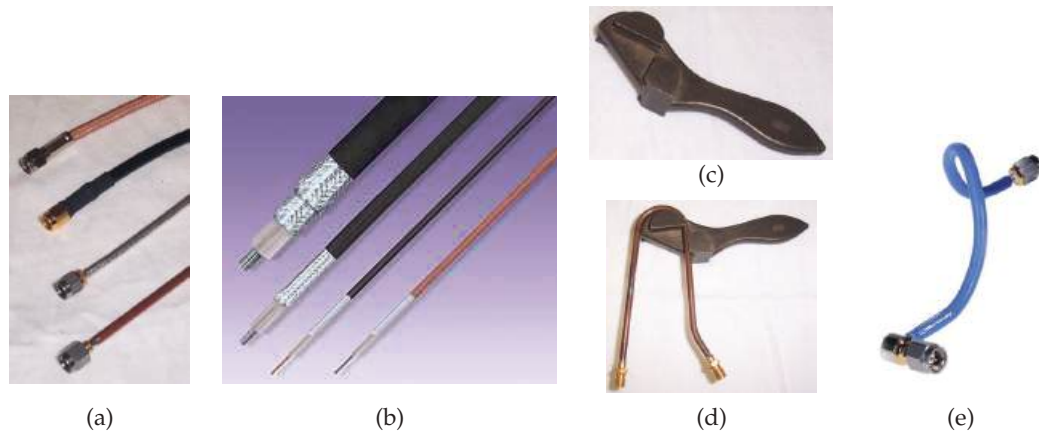


Figure 2-8: Coaxial lines: (a) SMA cables (from the top): flexible cable type I, type II, type III, and semirigid cable; (b) coaxial cables showing layers; (c) semirigid coaxial cable bender; (d) bender with line; and (e) hand-formable cable supporting tight radius with low return and insertion loss. ((b) Copyright Megaphase LLC, used with permission [5].) ((e) Copyright 2012 Scientific Components Corporation d/b/a Mini-Circuits, used with permission [4].)

connectors used in some microwave measurements. The N-type connector in Figure 2-7(b) and the SMA connector in Figure 2-7(c) are more common day-to-day connectors. Different views of these connectors are shown in Figures 2-7(d and e). Unlike an APC-7 connector, an N-type (or SMA) male connector, for example, can only be connected to a female N-type connector. There are a large number of different types or series of connectors for high-power applications, different frequency ranges, distortion levels, and cost.

There are also many types of coaxial cables, as shown in Figure 2-8(a). These are cables with SMA connectors (with 3.5 mm outer conductor diameter). Microwave cables without connectors are shown in Figure 2-8(b). These cables range in cost, flexibility, and the number of times they can be reliably flexed or bent. The semirigid cable shown at the bottom of Figure 2-8(a) must be bent using a bending tool, as shown in Figure 2-8(c), and in



Figure 2-9: Torque wrench used in making repeatable coaxial connections. Copyright MegaPhase LLC, used with permission [5].

use in Figure 2-8(d). The controlled bending radius ensures minimal change in the characteristic impedance and propagation constant of the cable. Semirigid cables can only be bent once however. The highest precision bend is realized using an elbow bend, shown in Figure 2-6(g). Various flexible cables have different responses to bending, with higher precision (and more expensive) cables having the least impact on characteristic impedance and phase variations as cables are flexed.

Precision measurements require that connectors be repeatably attached using a torque wrench, as shown in Figure 2-9. A torque wrench can be used in a conventional manner, but once the prescribed torque is obtained the wrench breaks just above the head. This ensures that two connectors are repeatably joined with the same force and so the contact resistance and quality of the connection is repeatable.

2.2.7 Microstrip Line

A microstrip line is shown in Figure 2-10(a). This is a commonly used transmission line, as it can be cheaply fabricated using printed circuit board techniques. This line consists of a metal-backed substrate of relative permittivity ϵ_r on top of which is a metal strip. Above that is air. The width of the strip determines the characteristic impedance of the line. The characteristic impedance of microstrip lines having various strip widths is shown in Figure 2-11 for several substrate permittivities. So the wider the strip and the higher the substrate permittivity, the lower the characteristic impedance of the line. The EM fields are partly in air and partly in the dielectric and an effective permittivity must be used when calculating the electrical length of the line. The results of field simulations of the effective permittivity of lines of various widths and with various substrate permittivities are shown in Figure 2-12, where it can be seen that the effective relative permittivity, ϵ_{eff} , increases for wide strips. This is because more of the EM field is in the substrate. Microstrip transmission line structures are often drawn showing just the layout of the strip, as shown in Figure 2-10(b), where

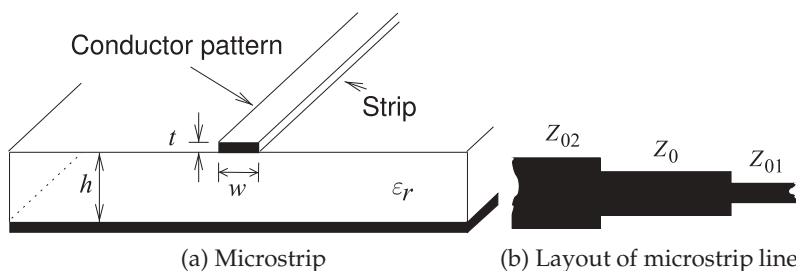


Figure 2-10: Microstrip transmission line. The layout (or top) view is commonly used with circuit designs using microstrip. This is the pattern of the strip where (b) shows three lines of different width.

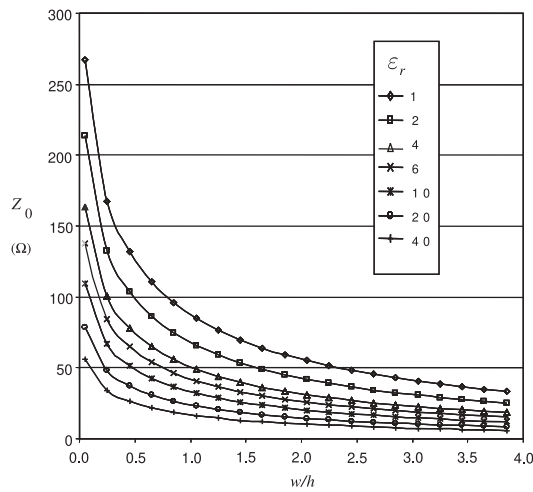


Figure 2-11: Dependence of Z_0 of a microstrip line at 1 GHz for various ϵ_r and aspect (w/h) ratios. Calculated using EM simulation.

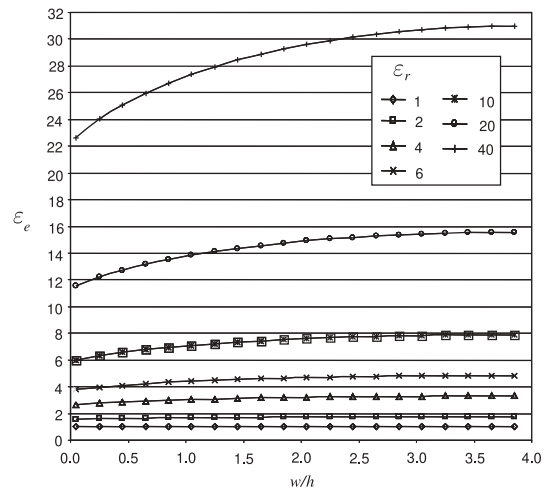


Figure 2-12: Dependence of effective relative permittivity ϵ_e of a microstrip line at 1 GHz for various permittivities and aspect ratios (w/h).

the three lines have different characteristic impedances. The next chapter presents detailed analyses of microstrip and other planar transmission lines.

2.2.8 Summary

The important takeaway from this section is that a signal moves on a transmission line as forward- and backward-traveling waves. The energy transferred is in the traveling waves. The total voltage and current at a point on the line is the sum of the traveling voltage and traveling current waves, respectively, but the total voltage/current view is not sufficient to describe how a transmission line works. Transmission line theory is expressed in terms of traveling voltage and current waves and these are akin to a one-dimensional form of Maxwell's equations. An argument was developed that posits a model of a line as cascaded sections of RLGC circuit and these circuit elements can be loosely related to the material properties of the medium in which the transmission line is embedded. There are a modification factors due to the actual orientation of the electric and magnetic fields and developing these requires detailed field analysis of the actual transmission line geometry. This can be done for a coaxial line but a microstrip line requires numerical analysis.

2.3 The Lossless Terminated Line

Microwave engineers want to work with total voltage and current when possible and the art of design synthesis usually requires relating the total voltage and current world of a lumped element circuit to the traveling voltage world of transmission lines. This section develops the important abstractions that enable the total voltage and current view of the world to be used with transmission lines. The first step in this process is in Section 2.3.1 where total voltages and currents are related to forward- and backward-

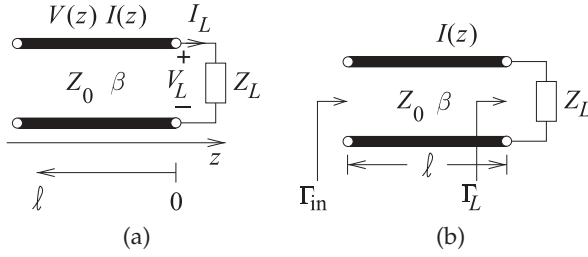


Figure 2-13: A terminated transmission line.

traveling voltages and currents. Insight into traveling waves and reflections is presented in Section 2.3.2. Important abstractions are presented first for the input reflection coefficient of a terminated lossless line in Section 2.3.3 and then for the input impedance of the line in Section 2.3.4. The last section, Section 2.3.5, presents a view of the total voltage on the transmission line and describes the voltage standing wave concept.

2.3.1 Total Voltage and Current on the Line

Consider the terminated line shown in Figure 2-13(a). Assume an incident or forward-traveling wave, with traveling voltage $V_0^+ e^{-j\beta z}$ and current $I_0^+ e^{-j\beta z}$ propagating toward the load Z_L at $z = 0$. The characteristic impedance of the transmission line is the ratio of the voltage and current traveling waves so that

$$\frac{V_0^+(z)}{I_0^+(z)} = \frac{V_0^+ e^{-j\beta z}}{I_0^+ e^{-j\beta z}} = \frac{V_0^+(0)}{I_0^+(0)} = \frac{V_0^+}{I_0^+} = Z_0. \quad (2.54)$$

The reflected wave has a similar relationship (but note the sign change):

$$\frac{V_0^- e^{j\beta z}}{-I_0^- e^{j\beta z}} = \frac{V_0^-}{-I_0^-} = Z_0. \quad (2.55)$$

The load Z_L imposes an additional constraint on the relationship of the total voltage and current at $z = 0$:

$$\frac{V_L}{I_L} = \frac{V(z=0)}{I(z=0)} = Z_L. \quad (2.56)$$

When $Z_L \neq Z_0$ there must be a reflected wave with appropriate amplitude to satisfy the above equations. Now the total voltage

$$V(z) = V_0^+ e^{-j\beta z} + V_0^- e^{j\beta z}, \quad (2.57)$$

and the total current, $I(z)$, is related to the traveling current waves by

$$I(z) = \frac{V_0^+}{Z_0} e^{-j\beta z} - \frac{V_0^-}{Z_0} e^{j\beta z} = I_0^+ e^{-j\beta z} + I_0^- e^{j\beta z}. \quad (2.58)$$

Thus at the termination of the line ($z = 0$),

$$\frac{V(0)}{I(0)} = Z_L = Z_0 \frac{V_0^+ + V_0^-}{V_0^+ - V_0^-}.$$

This can be rearranged as the ratio of the reflected voltage to the incident voltage:

$$\frac{V_0^-}{V_0^+} = \frac{Z_L - Z_0}{Z_L + Z_0}.$$

This ratio is defined as the voltage **reflection coefficient** at the load,

$$\Gamma_L = \Gamma_L^V = \frac{V_0^-(0)}{V_0^+(0)} = \frac{V_0^-}{V_0^+} = \frac{Z_L - Z_0}{Z_L + Z_0}. \quad (2.59)$$

That is, at the load

$$V_0^- = \Gamma_L V_0^+. \quad (2.60)$$

The relationship of the traveling waves on the line can also be described using the transmission coefficient T (this is the capital Greek letter tau which looks the same as the English letter 'T').

The voltage transmission coefficient from a port at position z to a port at position 0 is (for the transmission line)

$$T = T^V = \frac{V_0^+(\text{at end of line})}{V_0^+(\text{at start of line})} = \frac{V_0^+(0)}{V_0^+(z)} = \frac{V_0^+}{V_0^+ e^{-j\beta z}} = e^{j\beta z}. \quad (2.61)$$

The relationship in Equation (2.59) can be rewritten so that the input load impedance can be obtained from the reflection coefficient:

$$Z_L = Z_0 \frac{1 + \Gamma^V}{1 - \Gamma^V}. \quad (2.62)$$

Similarly, the current reflection coefficient can be written as

$$\Gamma^I = \frac{I_0^-}{I_0^+} = \frac{-Z_L + Z_0}{Z_L + Z_0} = -\Gamma^V. \quad (2.63)$$

The voltage reflection coefficient is used most of the time, so the reflection coefficient, Γ , on its own refers to the voltage reflection coefficient, $\Gamma^V = \Gamma$.

There are several special cases that are noteworthy. The most important of these is the case when there is no reflected wave and $\Gamma = 0$. To obtain $\Gamma = 0$, the value of load impedance, Z_L , is equal to Z_0 , the characteristic impedance of the transmission line as seen in Equation (2.59).

The total voltage and current waves on the line can be written as

$$V(z) = V_0^+[e^{-j\beta z} + \Gamma e^{j\beta z}] \quad (2.64) \quad I(z) = \frac{V_0^+}{Z_0}[e^{-j\beta z} - \Gamma e^{j\beta z}]. \quad (2.65)$$

From Equations (2.64) and (2.65) it can be seen that the total voltage and current on the line consist of superpositions of incident and reflected waves.

EXAMPLE 2.5**Forward- and Backward-Traveling Waves at an Open Circuit**

A lossless transmission line is terminated in an open circuit. What is the relationship between the forward- and backward-traveling voltage waves at the end of the line?

Solution:

At the end of the line the total current is zero, so that $I^+ + I^- = 0$ and so

$$I^- = -I^+. \quad (2.66)$$

The forward- and backward traveling voltages and currents are related to the characteristic impedance by

$$Z_0 = V^+/I^+ = -V^-/I^-, \quad (2.67)$$

Note the change in sign, as a result of the direction of propagation changing but the positive reference for current is in the same direction. Substituting for I^- at the termination,

$$V^+ = -V^-I^+/I^- = -V^-I^+/-I^+ = V^-. \quad (2.68)$$

Thus the total voltage at the end of the line, V_{TOTAL} , is $V^+ + V^- = 2V^+$. Note that the total voltage at the end of the line is twice the incident (forward-traveling) voltage.

EXAMPLE 2.6**Current Reflection Coefficient**

A load consists of a shunt connection of a capacitor of 10 pF and a resistor of 60 Ω . The load terminates a lossless 50 Ω transmission line. The operating frequency is 5 GHz.

- What is the impedance of the load?
- What is the normalized impedance of the load (normalized to Z_0 of the line)?
- What is the reflection coefficient of the load?
- What is the current reflection coefficient of the load?

Solution:

- $C = 10 \cdot 10^{-12}$ F; $R = 60$ Ω ; $f = 5 \cdot 10^9$ Hz; $\omega = 2\pi f$; $Z_0 = 50$ Ω

$$Z_L = R || C = (1/R + j\omega C)^{-1} = 0.168 - j3.174 \Omega.$$

- $z_L = Z_L/Z_0 = 3.368 \cdot 10^{-3} - j0.063$.
- This is the voltage reflection coefficient. $\Gamma_L = (z_L - 1)/(z_L + 1) = -0.985 - j0.126 = 0.993 \angle 187.3^\circ$.
- $\Gamma_L^I = -\Gamma_L = 0.985 + j0.126 = 0.993 \angle (187.3 - 180)^\circ = 0.993 \angle 7.3^\circ$.

2.3.2 Forward- and Backward-Traveling Pulses

Reflections at the end of a line produce a backward-traveling signal. Forward- and backward-traveling pulses are shown in Figure 2-14(a) for the situation where the resistance at the end of the line is lower than the characteristic impedance of the line ($Z_L < Z_0$). The voltage source is a step voltage that is zero for time $t < 0$. At time $t = 0$, the step is applied to the line and it begins traveling down the line, as shown at time $t = 1$. This voltage step moving from left to right is called the forward-traveling voltage wave.

At time $t = 2$, the leading edge of the step reaches the load, and as the load has lower resistance than the characteristic impedance of the line, the

total voltage across the load drops below the level of the forward-traveling voltage step. The reflected wave is called the backward-traveling wave and it must be negative, as it adds to the forward-traveling wave to yield the total voltage. Thus the voltage reflection coefficient, Γ , is negative and the total voltage on the line, which is all that can be directly observed, drops. A reflected, smaller, and opposite step signal travels in the backward direction and adds to the forward-traveling step to produce the waveform shown at $t = 3$. The impedance of the source matches the transmission line impedance so that the reflection at the source is zero. The signal on the line at time $t = 4$, the time for round-trip propagation on the line, therefore remains at the lower value. The easiest way to remember the polarity of the reflected pulse is to consider the situation with a short-circuit at the load. Then the total voltage on the line at the load must be zero. The only way this can occur when a signal is incident is if the reflected signal is equal in magnitude but opposite in sign, in this case $\Gamma = -1$. So whenever $|Z_L| < |Z_0|$, the reflected pulse will tend to subtract from the incident pulse.

The opposite situation occurs when the resistance at the load is higher than the characteristic impedance of the line (Figure 2-14(b)). In this case the reflected pulse has the same polarity as the incident signal. Again, to remember this, think of the open-circuited case. The voltage across the load doubles, as the reflected pulse has the same sign as well as magnitude as that of the incident signal, in this case $\Gamma = +1$. This is required so that the total current is zero.

A more illustrative situation is shown in Figure 2-15, where a more

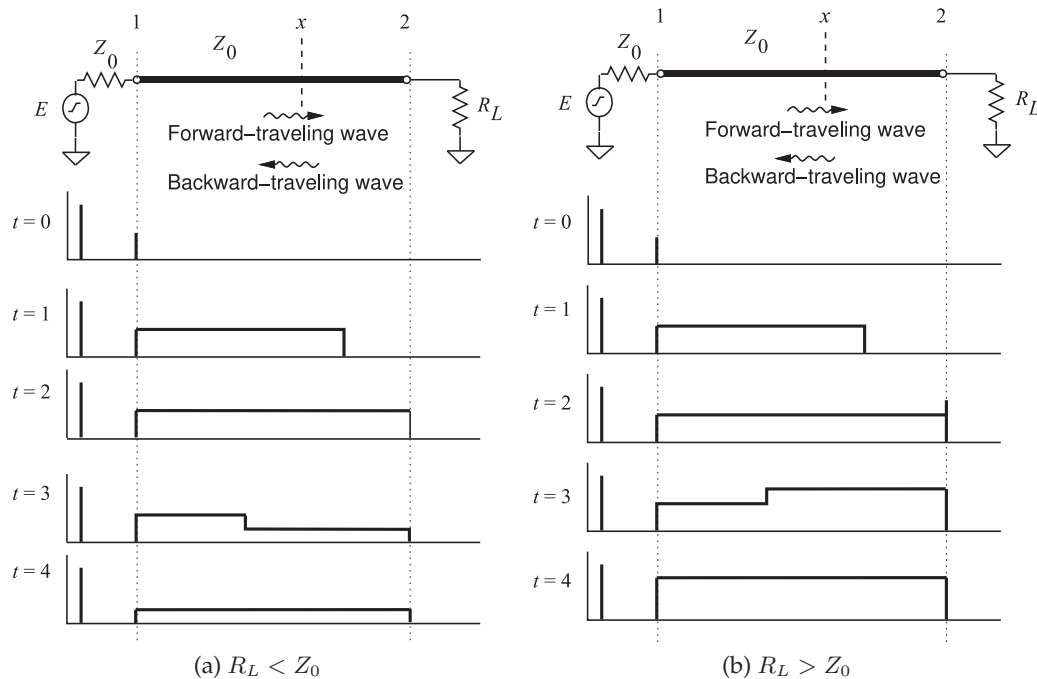


Figure 2-14: Reflection of a voltage pulse from a load: (a) when the resistance of the load, R_L is lower than the characteristic impedance of the line, Z_0 ; and (b) when R_L is greater than Z_0 .

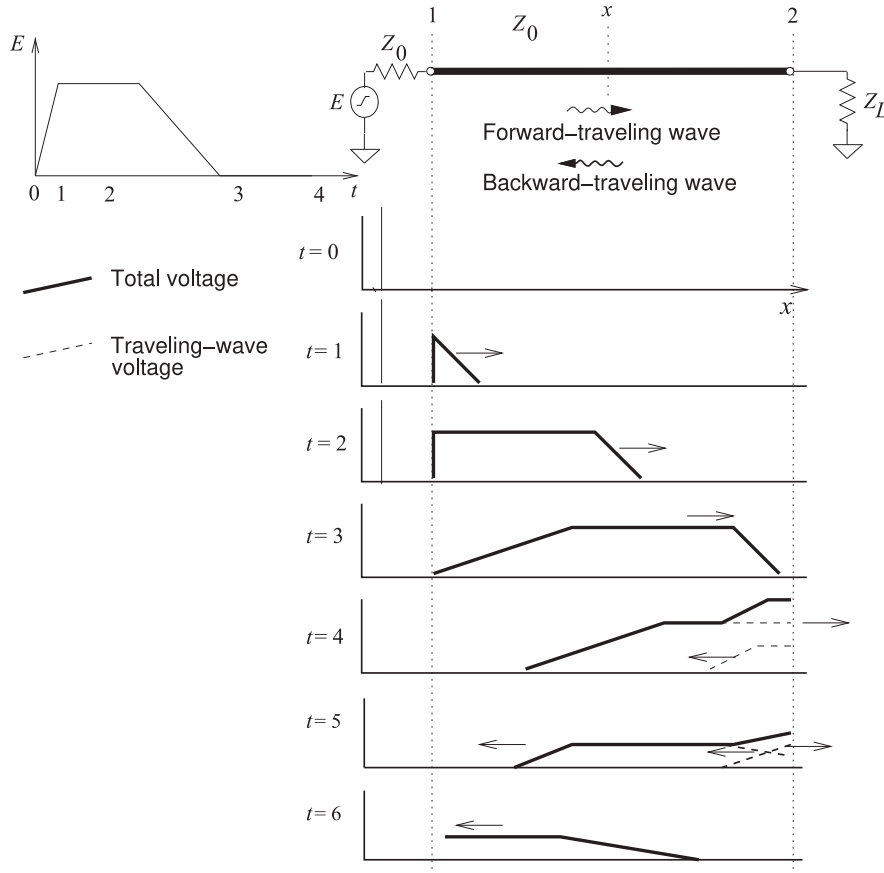


Figure 2-15: Reflection of a pulse on an interconnect showing forward- and backward-traveling pulses. $Z_L > Z_0$.

complicated signal is incident on a load that has a resistance higher than that of the characteristic impedance of the line. The peaking of the voltage that results at the load is typically the design objective in many long digital interconnects, as less overall signal energy needs to be transmitted down the line, or equivalently a lower current drive capability of the source is required to achieve first incidence switching. This is at the price of having reflected signals on the interconnects, but these are dissipated through a combination of line loss and absorption of the reflected signal at the driver.

2.3.3 Input Reflection Coefficient of a Lossless Line

The reflection coefficient looking into a line varies with position along the line as the forward- and backward-traveling waves change in relative phase. Referring to Figure 2-16, at a distance ℓ from the load (i.e., $z = -\ell$), the input

Figure 2-16: Terminated transmission line: (a) a transmission line terminated in a load impedance, Z_L , with an input impedance of Z_{in} ; and (b) a transmission line with source impedance Z_G and load Z_L .

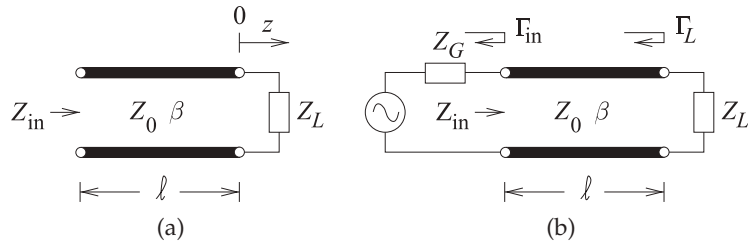
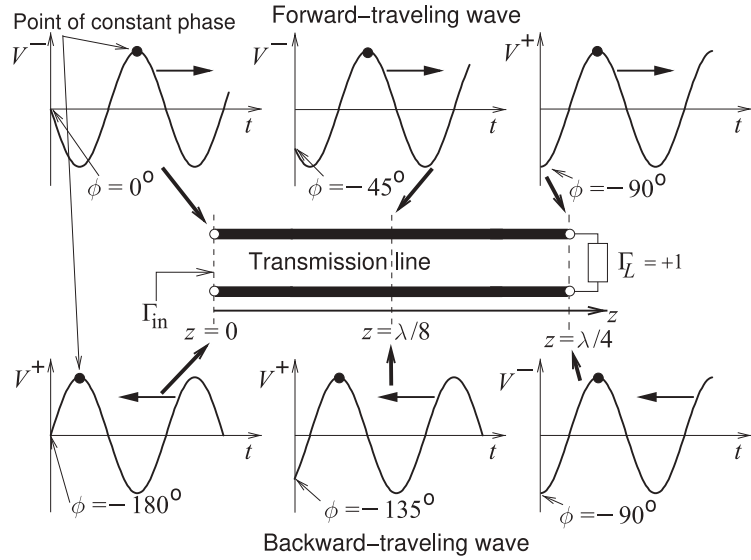


Figure 2-17: The forward-traveling wave $v^+(t, z) = |V^+| \cos(\omega t - \beta z) = |V^+| \cos(\omega t + \phi(z))$ and the backward-traveling wave $v^-(t, z) = |V^-| \cos(\omega t + \beta z) = |V^-| \cos[\omega t + \phi(z)]$. The phase, ϕ , of the forward-traveling wave becomes increasingly negative along the line as z increases, and when reflected the phase ϕ of the backward-traveling wave becomes increasingly negative as the wave moves away from the load (i.e. as z decreases).



reflection looking into a terminated lossless line is

$$\Gamma_{in}|_{z=-\ell} = \frac{V^-(z=-\ell)}{V^+(z=-\ell)} = \frac{V^-(z=0)e^{-j\beta\ell}}{V^+(z=0)e^{+j\beta\ell}} = \frac{V^-(z=0)e^{-j\beta\ell}}{V^+(z=0)e^{+j\beta\ell}} = \Gamma_L e^{-j2\beta\ell} \quad (2.69)$$

Note that Γ_{in} has the same magnitude as Γ_L but rotates in the clockwise direction (becomes increasingly negative) at twice the rate of increase of the electrical length $\beta\ell$.

It is important to graphical concepts introduced later that there be a full appreciation for the angle of Γ_{in} becoming increasingly negative at twice the rate at which the electrical length of the line increases. Figure 2-17 is a way of visualizing this. The transmission line here is $\lambda/4$ long with an electrical length of 90° and is terminated in a load with reflection coefficient $\Gamma_L = +1$. At position $z = 0$ the forward-traveling voltage wave is $v^+(t, 0) = |V^+| \cos(\omega t)$, and this then propagates down the line in the $+z$ direction. The forward-traveling voltage at point $z = \lambda/8$ at $t = 0$ will be the same as the voltage at $z = 0$ at a time one-eighth of a period in the past. The voltage at $z = \lambda/8$ is $v^+(t, \lambda/8) = |V^+| \cos(\omega t - 2\pi/8)$, i.e. there is a phase rotation of -45° . Then at $z = \lambda/4$, $v^+(t, \lambda/4) = |V^+| \cos(\omega t - 2\pi/4)$, i.e. at time $t = 0$ there is a phase rotation of -90° relative to $v^+(0, 0)$, and this is the negative of the electrical length of the line. The voltage wave reflects at the load and becomes a backward-traveling wave. Here $\Gamma_L = +1$ and so, at the load, the phase of the backward- and forward-traveling waves are the same. The backward-

traveling wave continues to travel in the $-z$ direction and its phase at $t = 0$ becomes increasingly negative as z gets closer to the input of the line. The phase of the backward-traveling wave at $z = 0$ is rotated -90° with respect to the backward-traveling wave at the load, and has rotated -180° relative to the forward-traveling wave at $z = 0$. For a lossless line, in general, the angle of $\Gamma_{in} = [\text{phase of } V^-(z = 0) \text{ relative to the phase of } V^+(z = 0)] + (\text{the phase of } \Gamma_L) = -2(\text{electrical length of the line}) + (\text{the phase of } \Gamma_L)$.

2.3.4 Input Impedance of a Lossless Line

The impedance looking into a lossless line varies with position, as the forward- and backward-traveling waves combine to yield position-dependent total voltage and current. At a distance ℓ from the load (i.e., $z = -\ell$), the input impedance seen looking toward the load is

$$Z_{in}|_{z=-\ell} = \frac{V(z = -\ell)}{I(z = -\ell)} = Z_0 \frac{1 + |\Gamma| e^{j(\Theta - 2\beta\ell)}}{1 - |\Gamma| e^{j(\Theta - 2\beta\ell)}} = Z_0 \frac{1 + \Gamma_L e^{j(-2\beta\ell)}}{1 - \Gamma_L e^{j(-2\beta\ell)}}. \quad (2.70)$$

Another form is obtained by substituting Equation (2.59) in Equation (2.70):

$$\begin{aligned} Z_{in} &= Z_0 \frac{(Z_L + Z_0)e^{j\beta\ell} + (Z_L - Z_0)e^{-j\beta\ell}}{(Z_L + Z_0)e^{j\beta\ell} - (Z_L - Z_0)e^{-j\beta\ell}} = Z_0 \frac{Z_L \cos(\beta\ell) + jZ_0 \sin(\beta\ell)}{Z_0 \cos(\beta\ell) + jZ_L \sin(\beta\ell)} \\ &= Z_0 \frac{Z_L + jZ_0 \tan \beta\ell}{Z_0 + jZ_L \tan \beta\ell}. \end{aligned} \quad (2.71)$$

This is the **lossless telegrapher's equation**. The electrical length, $\beta\ell$, is in radians when used in calculations.

2.3.5 Standing Waves and Voltage Standing Wave Ratio

The total voltage on a terminated line is the sum of forward- and backward-traveling waves. This sum produces what is called a standing wave. Figure 2-18 shows the total and traveling waveforms on a line terminated in a reactance and evaluated at times equal to multiples of an eighth of a period. Here the traveling waves have the same amplitude indicating that the termination of the line is reactive, $|\Gamma| = 1$. The interesting property here is that the total voltage appears as a standing wave with fixed points called nodes where the total voltage is always zero. This is more easily seen in Figure 2-19(a), where the total voltage is overlaid for many times. If the termination has resistance, then the magnitude of the backward-traveling wave will be less than that of the forward-traveling wave and the overlaid total voltage is as shown in Figure 2-19(b). This is still a standing wave, but the minima are now not zero. The envelope of this standing wave is shown in Figure 2-19(c), where there is a maximum amplitude V_{\max} and a minimum amplitude V_{\min} .

Now this situation will be examined mathematically to relate the standing wave to the reflection coefficient. If $\Gamma = 0$, then the magnitude of the total voltage on the line, $|V(z)|$, is equal to $|V_0^+|$ anywhere on the line. For this reason, such a line is said to be "flat." If there is reflection the magnitude of the total voltage on the line is not constant (see Figure 2-19(b)). Thus from Equations (2.64) and (2.65):

$$|V(z)| = |V_0^+| |1 + \Gamma e^{2j\beta z}| = |V_0^+| |1 + \Gamma e^{-2j\beta\ell}|, \quad (2.72)$$

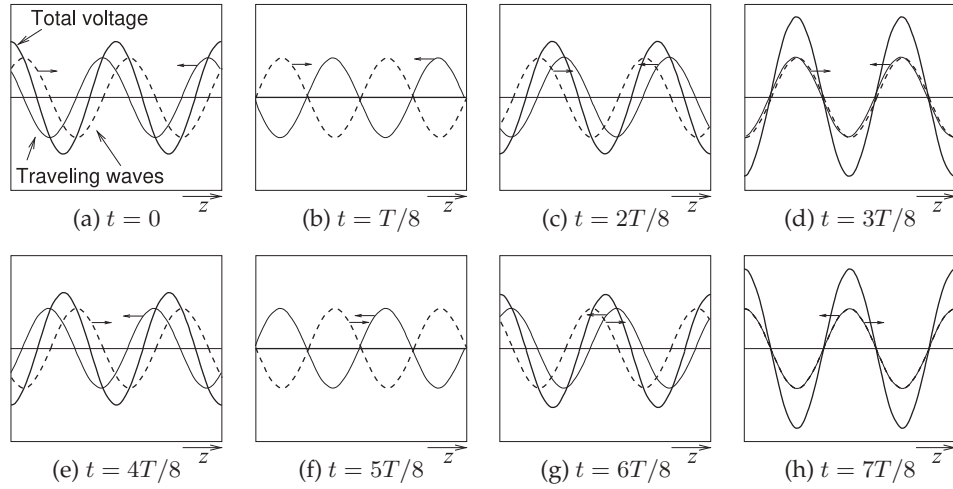


Figure 2-18: Evolution of a standing wave with a reactive load as the sum of forward- and backward-traveling waves (to the right and left, respectively) of equal amplitude evaluated at times t equal to eighths of the period T . At $t = T/8$ and $t = 5T/8$ the total voltage everywhere on the line is zero.

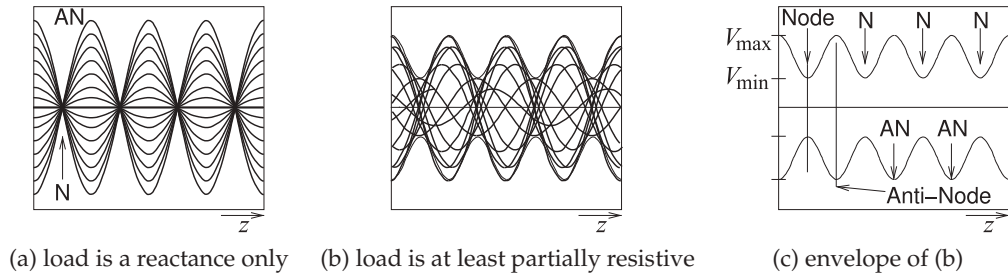


Figure 2-19: Standing waves as an overlay of waveforms at many times: (a) when the forward- and backward-traveling waves have the same amplitude; (b) when the waves have different amplitudes; and (c) the envelope of the standing wave. N is a node (a minimum) and AN is an antinode (a maximum). Nodes, N, are separated by $\lambda/2$. Antinodes, AN, are separated by $\lambda/2$.

where $z = -\ell$ is the positive distance measured from the load at $z = 0$ toward the generator. Or, setting $\Gamma = |\Gamma|e^{j\Theta}$,

$$|V(z)| = |V_0^+| \left| 1 + |\Gamma|e^{j(\Theta-2\beta\ell)} \right|, \quad (2.73)$$

where Θ is the phase of the reflection coefficient ($\Gamma = |\Gamma|e^{j\Theta}$) at the load. This result shows that the voltage magnitude oscillates with position z along the line. The maximum value occurs when $e^{j(\Theta-2\beta\ell)} = 1$ and is given by

$$V_{\max} = |V_0^+| (1 + |\Gamma|). \quad (2.74)$$

Similarly the minimum value of the total voltage magnitude occurs when

the phase term is $e^{j(\Theta-2\beta l)} = -1$, and is given by

$$V_{\min} = |V_0^+|(1 - |\Gamma|). \quad (2.75)$$

A mismatch can be defined by the **voltage standing wave ratio (VSWR)**:

$$\text{VSWR} = \frac{V_{\max}}{V_{\min}} = \frac{(1 + |\Gamma|)}{(1 - |\Gamma|)}. \quad (2.76) \quad \text{Also} \quad |\Gamma| = \frac{\text{VSWR} - 1}{\text{VSWR} + 1}. \quad (2.77)$$

Notice that in general Γ is complex, but VSWR is necessarily always real and $1 \leq \text{VSWR} \leq \infty$. For the matched condition, $\Gamma = 0$ and $\text{VSWR} = 1$, and the closer VSWR is to 1, the closer the load is to being matched to the line and the more power is delivered to the load. The magnitude of the reflection coefficient on a line with a short-circuit or open-circuit load is 1, and in both cases the VSWR is infinite.

To determine the position of the standing wave maximum, ℓ_{\max} , consider Equation (2.73) and note that at the maximum

$$\Theta - 2\beta\ell_{\max} = 2n\pi, \quad n = 0, 1, 2, \dots \quad (2.78)$$

Here Θ is the angle of the reflection coefficient at the load:

$$\Theta - 2n\pi = 2\frac{2\pi}{\lambda_g}\ell_{\max}. \quad (2.79)$$

Thus the position of the voltage maxima, ℓ_{\max} , normalized to wavelength is

$$\frac{\ell_{\max}}{\lambda_g} = \frac{1}{2} \left(\frac{\Theta}{2\pi} - n \right), \quad n = 0, -1, -2, \dots \quad (2.80)$$

Similarly the position of the voltage minima is (using Equation (2.73)):

$$\Theta - 2\beta\ell_{\min} = (2n + 1)\pi. \quad (2.81)$$

After rearranging the terms,

$$\frac{\ell_{\min}}{\lambda_g} = \frac{1}{2} \left(\frac{\Theta}{2\pi} - n + \frac{1}{2} \right), \quad n = 0, -1, -2, \dots \quad (2.82)$$

Summarizing from Equations (2.80) and (2.82):

1. The distance between two successive maxima is $\lambda_g/2$.
2. The distance between two successive minima is $\lambda_g/2$.
3. The distance between a maximum and an adjacent minimum is $\lambda_g/4$.
4. From the measured VSWR the magnitude of the reflection coefficient $|\Gamma|$ can be found. From the measured ℓ_{\max} the angle Θ of Γ can be found. Then from Γ the load impedance can be found.

In a similar manner to that above, the magnitude of the total current on the line is

$$|I(\ell)| = \frac{|V_0^+|}{Z_0} |1 - |\Gamma|e^{j(\Theta-2\beta\ell)}|. \quad (2.83)$$

Hence the standing wave current is maximum where the standing-wave voltage amplitude is minimum, and minimum where the standing-wave voltage amplitude is maximum.

Z_{in} in Equation 2.71 is a periodic function of length with period $\lambda/2$ and it varies between Z_{\max} and Z_{\min} , where

$$Z_{\max} = \frac{V_{\max}}{I_{\min}} = Z_0 \times \text{VSWR} \quad \text{and} \quad Z_{\min} = \frac{V_{\min}}{I_{\max}} = \frac{Z_0}{\text{VSWR}}. \quad (2.84)$$

EXAMPLE 2.7**Standing Wave Ratio**

In Example 2.6 the load consisted of a capacitor of 10 pF in shunt with a resistor of 60 Ω . The load terminated a lossless 50 Ω transmission line. The operating frequency is 5 GHz.

- What is the SWR?
- What is the current standing wave ratio (ISWR)? (When SWR is used on its own it is assumed to refer to VSWR.)

Solution:

- From Example 2.6 $\Gamma_L = 0.993\angle 187.3^\circ$ and so

$$\text{VSWR} = \frac{1 + |\Gamma_L|}{1 - |\Gamma_L|} = \frac{1 + 0.993}{1 - 0.993} = 285.$$

- ISWR = VSWR = 285.

EXAMPLE 2.8**Standing Waves**

A load has an impedance $Z_L = 45 + j75 \Omega$ and the system reference impedance, Z_0 , is 100 Ω .

- What is the reflection coefficient?
- What is the current reflection coefficient?
- What is the SWR?
- What is the ISWR?
- The power available from a source with a 100 Ω Thevenin equivalent impedance is 1 mW. The source is connected directly to the load, Z_L . Use the reflection coefficient to calculate the power delivered to Z_L .
- What is the total power absorbed by the Thevenin equivalent source impedance?
- Discuss the effect on power flow of inserting a lossless 100 Ω transmission line between the source and the load.

Solution:

- The voltage reflection coefficient is

$$\begin{aligned}\Gamma_L &= (Z_L - Z_0)/(Z_L + Z_0) = (45 + j75 - 100)/(45 + j75 + 100) \\ &= (93.0\angle(2.204 \text{ rads}))/ (163.2\angle(0.4773 \text{ rads})) \\ &= 0.570\angle(1.726 \text{ rads}) = 0.570\angle 98.9^\circ = -0.0881 + j0.563 = \Gamma^V.\end{aligned}\quad (2.85)$$

- The current reflection coefficient is

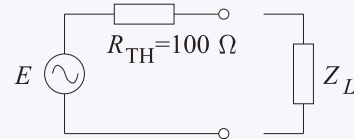
$$\Gamma^I = -\Gamma^V = 0.0881 - j0.563 = 0.570\angle(98.9^\circ - 180^\circ) = 0.570\angle 81.1^\circ. \quad (2.86)$$

- The SWR is the VSWR, so

$$\text{SWR} = \text{VSWR} = \frac{V_{\max}}{V_{\min}} = \frac{1 + |\Gamma^V|}{1 - |\Gamma^V|} = \frac{1 + 0.570}{1 - 0.570} = 3.65. \quad (2.87)$$

- The current SWR is ISWR = VSWR.

- To determine the reflection coefficient of the load, begin by developing the Thevenin equivalent circuit of the load. The power available from the source is $P_A = 1 \text{ mW}$, so the Thevenin equivalent circuit is



The power reflected by the load is

$$P_R = P_A |\Gamma_L|^2 = 1 \text{ mW} \cdot (0.570)^2 = 0.325 \text{ mW}$$

and the power delivered to the load is

$$P_D = P_A (1 - |\Gamma_L|^2) = 0.675 \text{ mW}.$$

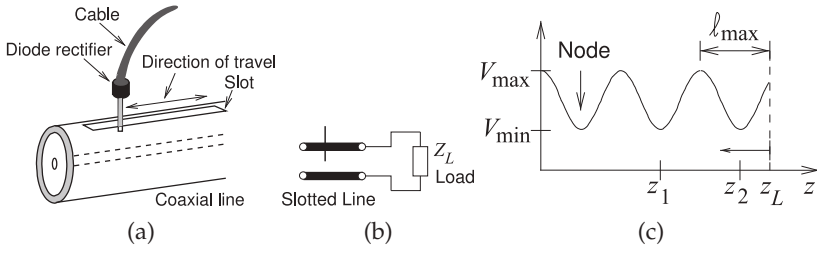


Figure 2-20: Measurement of standing waves: (a) coaxial slotted line; (b) schematic of slotted line; (c) measured standing wave.

- (f) It is tempting to think that the power dissipated in R_{TH} is just P_R . However, this is not correct. Instead, the current in R_{TH} must be determined and then the power dissipated in R_{TH} found. Let the current through R_{TH} be I , and this is composed of forward- and backward-traveling components:

$$I = I^+ + I^- = (1 + \Gamma_I)I^+,$$

where I^+ is the forward-traveling current wave. Thus

$$P_A = \frac{1}{2}|I^+|^2 R_{TH} = \frac{1}{2}|I^+|^2 \times 100 = 1 \text{ mW} = 10^{-3} \text{ W},$$

so $I^+ = 4.47 \text{ mA}$, and

$$I = (1 + \Gamma_I)I^+ = (1 + 0.0881 - j0.563) \times 4.47 \times 10^{-3} \text{ A}, \quad |I| = 5.48 \text{ mA}.$$

The power dissipated in R_{TH} is

$$P_{TH} = \frac{1}{2}|I|^2 R_{TH} = \frac{1}{2}(5.48 \times 10^{-3})^2 R_{TH} = 1.50 \text{ mW}. \quad (2.88)$$

The circuit is that shown in part (e) and so the current in R_{TH} is the same as the current in Z_L . Thus the power delivered to the load Z_L is due to the real part of Z_L :

$$P_D = \frac{1}{2}|I|^2 \Re(Z_L) = \frac{1}{2}(5.48 \times 10^{-3})^2 \times 45 = 0.676 \text{ mW} \quad (2.89)$$

- (g) Inserting a transmission line with the same characteristic impedance as the Thevenin equivalent impedance will have no effect on power flow.

VSWR Measurement

The measurement of standing waves can be used to calculate the impedance of a load. The device that does this measurement, called a slotted line, is shown in Figure 2-20(a). A probe is inserted a small distance into the transmission line to measure the electric field. The RF electric field produces an RF voltage on the probe that is rectified by the diode detector. The DC voltage at the output of the detector is proportional to the total voltage on the line. The probe can be moved along the line and the ratio of V_{\max} to V_{\min} determined. This is just the VSWR. To find the complex load impedance it is also necessary to determine the position of the node of the standing wave. From the measured VSWR the magnitude of the reflection coefficient $|\Gamma|$ can be found. From the measured l_{\max} the angle Θ of Γ can be found. From Γ the load impedance can be found. This is demonstrated in the next example.

EXAMPLE 2.9**Slotted Line Measurement of Impedance**

A slotted line is used to determine the properties of the standing wave on a terminated $50\ \Omega$ line see Figure 2-19(c). $V_{\max} = 5\text{ V}$ and $V_{\min} = 2\text{ V}$, and the first minimum is 2 cm from the load. The guide wavelength is 10 cm. What is the load impedance Z_L ?

Solution:

Now $\text{VSWR} = V_{\max}/V_{\min} = 5/2 = 2.5$. So from Equation (2.77)

$$|\Gamma| = |\Gamma_L| = \frac{\text{VSWR} - 1}{\text{VSWR} + 1} = \frac{2.5 - 1}{2.5 + 1} = 0.428. \quad (2.90)$$

Equation (2.82) and the position of the first node can be used to determine the angle of Γ_L . For the first node (minimum), $n = 0$ and

$$\frac{\ell_{\min}}{\lambda_g} = \frac{1}{2} \left(\frac{\Theta}{2\pi} + \frac{1}{2} \right). \quad (2.91) \quad \text{Rearranging, } \Theta = 2\pi \left(2\frac{\ell_{\min}}{\lambda_g} - \frac{1}{2} \right) \text{ radians.} \quad (2.92)$$

Now $\ell_{\min} = 2\text{ cm}$ and $\lambda_g = 10\text{ cm}$. So, in degrees,

$$\Theta = 360 \left(2\frac{\ell_{\min}}{\lambda_g} - \frac{1}{2} \right) = 360 \left(2\frac{2}{10} - \frac{1}{2} \right) = -36^\circ. \quad (2.93)$$

Thus $\Gamma_L = 0.428\angle(-36^\circ) = 0.3463 - j0.2516$, so the load impedance is (where $Z_0 = 50\ \Omega$)

$$Z_L = Z_0 \left(\frac{1 + \Gamma_L}{1 - \Gamma_L} \right) = 83.2 - j51.3\ \Omega. \quad (2.94)$$

2.3.6 Summary

This section related the physics of traveling voltage and current waves on lossless transmission lines to the total voltage and current view. First the input reflection coefficient of a terminated lossless line was developed and from this the input impedance, which is the ratio of total voltage and total current, derived. At any point along a line the amplitude of total voltage varies sinusoidally, tracing out a standing wave pattern along the line and yielding the VSWR metric which is the ratio of the maximum amplitude of the total voltage to the minimum amplitude of that voltage. This is an important metric that is often used to provide an indication of how good a match, i.e. how small the reflection is, with a $\text{VSWR} = 1$ indicating no reflection and a $\text{VSWR} = \infty$ indicating total reflection, i.e. a reflection coefficient magnitude of 1.

2.4 Special Lossless Line Configurations

The lossless transmission line configurations considered in this section are used as circuit elements in RF designs and are used elsewhere in this book series. The first element considered in Section 2.4.1 is a short length of short-circuited line which looks like an inductor. The element considered in Section 2.4.2 is a short length of open-circuited line which looks like a capacitor. Then lengths of short-circuited and open-circuited lines, called stubs, used nearly always as shunt elements to introduce an admittance in a circuit, are described in Sections 2.4.3 and 2.4.4. Another type of element, described in Section 2.4.5, is a short length of line with either high or low characteristic impedance realizing a small series inductor or capacitor respectively. The

final element described in Section 2.4.6 is a quarter-wave transformer, a quarter-wavelength long line with a particular characteristic impedance which is used in two ways. It can be used to provide maximum power transfer from a source to a load resistance, and it can invert an impedance, e.g. making a capacitor terminating the line look like an inductor.

2.4.1 Short Length of Short-Circuited Line

A transmission line terminated in a short circuit ($Z_L = 0$) has the input impedance (using Equation (2.71))

$$Z_{\text{in}} = jZ_0 \tan(\beta\ell). \quad (2.95)$$

So a short length of line, $\ell < \lambda_g/4$, looks like an inductor with inductance L_s ,

$$Z_0 \tan(\beta\ell) = \omega L_s, \quad \text{and so} \quad L_s = \frac{Z_0}{\omega} \tan \frac{2\pi\ell}{\lambda_g}. \quad (2.96)$$

From Equation (2.96) it can be seen that for a given ℓ , L_s is proportional to Z_0 . Hence, for larger values of L_s , sections of transmission line of high characteristic impedance are needed. So microstrip lines with narrow strips can be used to realize inductors in planar microstrip circuits.

2.4.2 Short Length of Open-Circuited Line

An open-circuited line has $Z_L = \infty$ and so (using Equation (2.71))

$$Z_{\text{in}} = -j \frac{Z_0}{\tan \beta\ell}. \quad (2.97)$$

For lengths ℓ such that $\ell < \lambda/4$, an open-circuited segment of line realizes a capacitor C_0 for which

$$\frac{1}{\omega C_0} = \frac{Z_0}{\tan \beta\ell} \quad \text{and so} \quad C_0 = \frac{1}{Z_0} \frac{\tan(\beta\ell)}{\omega}. \quad (2.98)$$

From the above relationship, it can be seen that C_0 is inversely proportional to Z_0 . Hence, for larger values of C_0 , sections of transmission line with low characteristic impedance need to be used.

2.4.3 Short-Circuited Stub

A stub is a section of open-circuited or short-circuited transmission line and is used as a series or shunt element in a microwave circuit. There are several representations. A shorted stub is shown in Figure 2-21(a) as a transmission line with characteristic impedance Z_{01} that is short circuited. The input impedance of the line is Z_1 . If the line is lossless, the usual assumption, then Z_{01} will be real and Z_1 will be imaginary. Stubs are commonly used in microwave circuits and generally all stubs in a network have the same length, such as $\lambda/4$ long or $\lambda/8$ long. Which it is is specified in the design. Realistically they do not need to have the same length but there are some special properties for certain lengths, as will become clearer. A cleaner way to indicate a shorted stub is shown in Figure 2-21(b), where the value of the stub is as indicated. The absence of a 0 subscript (which would indicate

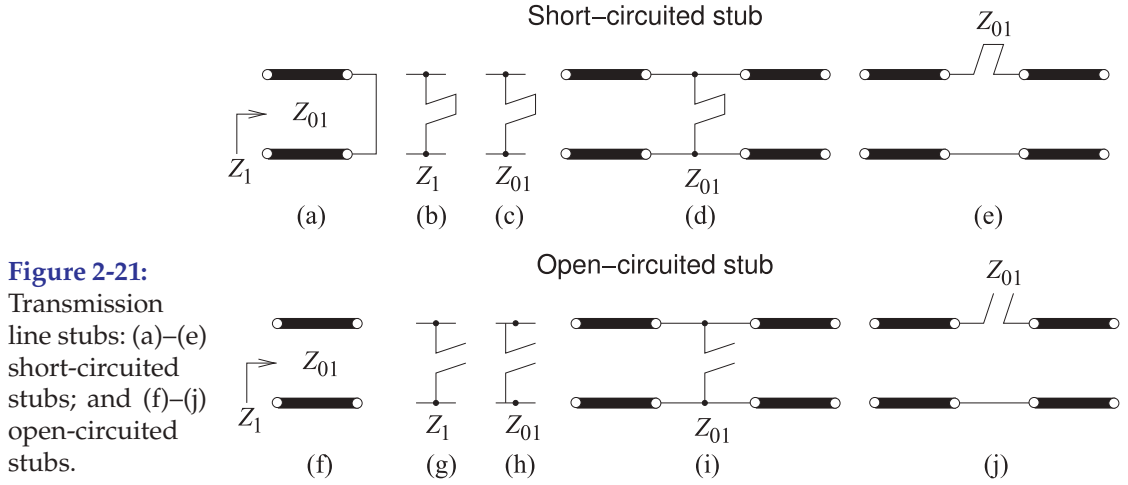


Figure 2-21: Transmission line stubs: (a)–(e) short-circuited stubs; and (f)–(j) open-circuited stubs.

characteristic impedance) means that this is the reactive input impedance of the stub. If a 0 subscript is used, as in Figure 2-21(c), the characteristic impedance of the stub is indicated. If a numerical value is given then an imaginary impedance indicates that the input impedance is being specified, whereas a real impedance indicates the characteristic impedance of the stub. The shorted stub is shown as a shunt element in Figure 2-21(d) and as a series element in Figure 2-21(e). However in nearly all transmission line technologies, including microstrip, only shunt stubs can be realized. The open-circuited stubs with annotations are shown in Figures 2-21(f–j) with similar assignments of meaning. The length of a stub is often indicated by its resonant frequency, f_r . This is the frequency at which the stub is $\lambda/4$ long.

The shorted stub in Figure 2-21(a) has the input impedance (from Equation (2.71))

$$Z_1 = jZ_{01} \tan \beta \ell, \quad (2.99)$$

where ℓ is the physical length of the line. Since the stub is $\lambda/4$ long at f_r , then at frequency f , the input impedance of the stub is

$$Z_1 = jZ_{01} \tan \left(\frac{\pi f}{2 f_r} \right). \quad (2.100)$$

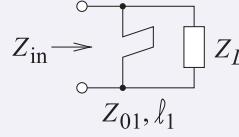
A special situation, and the most commonly used in design, is when the operating frequency is around one-half of the resonant frequency (i.e., $f \approx \frac{1}{2}f_r$). Then the stub is one-eighth of a wavelength long and the argument of the tangent function in Equation (2.100) is approximately $\pi/4$ and Z_1 becomes

$$Z_1 \approx jZ_{01} \tan \left(\frac{\pi}{4} \right) = jZ_{01}, \quad (2.101)$$

thus realizing an inductance at $f = f_r/2$ with a reactance equal to the characteristic impedance of the line.

EXAMPLE 2.10**Short-Circuited Stub**

Develop the electrical design of the shunt stub shown with a load of impedance $Z_L = 75 + j15 \Omega$ so that the total impedance of the load and stub is real.

**Solution:**

The short-circuited stub has characteristic impedance Z_{01} and length ℓ_1 . Choose $Z_{01} = 75 \Omega$ (generally this must be between 15Ω and 100Ω for most transmission line technologies). The stub needs to be designed so that the susceptances of the stub and load sum to zero. The admittance of the load $Y_L = 1/Z_L = 0.01282 - j0.002564 \text{ S}$. The required admittance of the stub is $Y_{\text{STUB}} = j0.002564 \text{ S}$ so, using Equation (2.99),

$$Z_{\text{STUB}} = 1/Y_{\text{STUB}} = jZ_{01} \tan \beta \ell_1 = -j390 \Omega.$$

Therefore, the electrical length of the stub is

$$\beta \ell_1 = \arctan(-j390/j75) = -1.381 + n\pi \text{ radians}, n = 0, 1, 2, \dots \quad (2.102)$$

The first positive angle is taken so the stub has the shortest length. So

$$\beta \ell_1 = 1.761 \text{ radians} = 100.9^\circ. \quad (2.103)$$

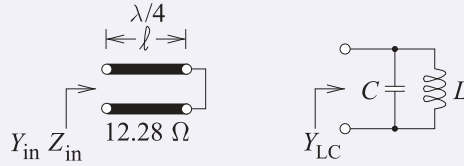
The complete electrical design of the stub is that it is a shunt short-circuited stub with a characteristic impedance of 75Ω and with an electrical length of 100.9° . The combined impedance of the stub and load is $Z_X = 1/(\Re\{Y_L\}) = 1/0.01282 = 78.00 \Omega$.

EXAMPLE 2.11**Model of a Resonant Shorted Transmission Line**

This example presents an analytic approach to developing the equivalent circuit of a shorted stub at resonance. Consider a shorted transmission line with characteristic impedance $Z_0 = 12.28 \Omega$ and resonant, i.e. a quarter-wavelength long, at 1850 MHz.

Solution:

At the first resonant frequency, $f_r = \omega_r/(2\pi)$, the transmission line presents an open circuit and the appropriate circuit model is shown on the right.



The strategy here is to develop the LC equivalent circuit by equating the derivatives of the resonator and the LC circuit. This is in addition to equating the input admittances of the two circuits at the resonant frequency $f_r = \omega_r/(2\pi)$. That is, at frequency f_r

$$Y_{\text{in}}(f_r) = 0 = Y_{\text{LC}}(f_r) = j[\omega_r C - 1/(\omega_r L)] \quad \text{and so} \quad \omega_r^2 = 1/(LC). \quad (2.104)$$

The input impedance of the line at frequency $f = \omega/(2\pi)$ is $Z_{\text{in}}(\omega) = jZ_0 \tan(\beta \ell)$, and so its input admittance is

$$Y_{\text{in}}(\omega) = \frac{-j}{Z_0} \cot(\beta \ell). \quad (2.105)$$

The derivative of the transmission line admittance is (using Equation (1.112))

$$\frac{\partial Y_{\text{in}}}{\partial \omega} = \frac{\partial \beta \ell}{\partial \omega} \frac{\partial Y_{\text{in}}}{\partial \beta \ell} = \frac{\partial \beta \ell}{\partial \omega} \left(\frac{-j}{Z_0} \right) [-\csc^2(\beta \ell)]. \quad (2.106)$$

Now β is proportional to ω for a lossless dispersionless line so

$$\frac{\partial Y_{\text{in}}}{\partial \omega} = \frac{\beta \ell}{\omega} \frac{j}{Z_0} \csc^2(\beta \ell).$$

Since the line is approximately $\lambda/4$ long near the resonant frequency, for $f \approx f_r$, $\beta\ell \approx \pi/2$, $\csc(\beta\ell) \approx 1$ (which is a good approximation since at f_r , $[\partial \csc(\beta\ell)]/(\partial\omega) = 0$), and

$$\left. \frac{\partial Y_{\text{in}}}{\partial \omega} \right|_{\omega_r} = \frac{j\beta\ell}{\omega_r Z_0}. \quad (2.107)$$

The input admittance of the parallel LC circuit is

$$Y_{\text{LC}} = j \left(\omega C - \frac{1}{\omega L} \right) \quad \text{and} \quad \frac{\partial Y_{\text{LC}}}{\partial \omega} = j \left(C + \frac{1}{\omega^2 L} \right). \quad (2.108)$$

At and near resonance $\omega^2 \approx 1/(LC)$ and so

$$\left. \frac{\partial Y_{\text{LC}}}{\partial \omega} \right|_{\omega_r} = j2C. \quad (2.109)$$

Equating the derivatives of Y_{in} , Equation (2.107), and of Y_{LC} , Equation (2.109), yields

$$\frac{-j\beta\ell}{\omega Z_0} = j2C. \quad (2.110)$$

Thus (since $\beta\ell \approx \pi/2$)

$$C = \frac{\pi}{4\omega_r Z_0} = \frac{\pi}{4 \cdot 2\pi \cdot 1850 \cdot 10^6 \cdot 12.28} = 5.502 \cdot 10^{-12} \text{ F} = 5.502 \text{ pF} \quad (2.111)$$

and, since $\omega_r^2 = 1/(LC)$,

$$L = \frac{1}{\omega_r^2 C} = \frac{1}{(2\pi \cdot 1850 \cdot 10^6)^2 \cdot 5.502 \cdot 10^{-12}} = 1.345 \cdot 10^{-9} \text{ H} = 1.345 \text{ nH}. \quad (2.112)$$

2.4.4 Open-Circuited Stub

An open-circuited transmission line is commonly used as a circuit element called an open stub shown in Figure 2-21(f-j). From Equation (2.71) and noting that $Z_L = \infty$, the open stub input impedance is

$$Z_1 = -jZ_{01} \frac{1}{\tan \beta\ell}. \quad (2.113)$$

With the stub one-quarter wavelength long at the frequency f_r , the input impedance at f_r is a short circuit and the stub is said to be resonant at f_r . Then at a frequency f , the input impedance of the stub is

$$Z_1 = -jZ_{01} \tan^{-1} \left(\frac{\pi f}{2 f_r} \right). \quad (2.114)$$

When $f = \frac{1}{2}f_r$ the stub is one-eighth wavelength long and

$$Z_1 = -jZ_{01} \frac{1}{\tan \left(\frac{\pi}{4} \right)} = -jZ_{01}. \quad (2.115)$$

So a $\lambda/8$ long open-circuited stub ($\lambda/4$ at f_r , $f = \frac{1}{2}f_r$) realizes a capacitance with a reactance equal to the characteristic impedance of the line.

If the length of a stub can be changed then the stub can be used as a tuning element. A common microstrip tuning technique is shown in Figure 2-22, where bonding to different pads enables a variable length stub to be realized.

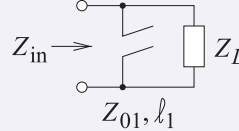


Figure 2-22: Open-circuited stub with variable length realized using wire bonding from the fixed stub to one of the bond pads. The bond pads are on the same layer as the strip metal layer and bonding to them extends the length of the open-circuited stub.

EXAMPLE 2.12

Open-Circuited Stub

Develop the electrical design of the open-circuit stub shown with a load of impedance $Z_L = 75 + j15 \Omega$ so that the total impedance of the load and stub is real.



Solution:

The open-circuited stub has characteristic impedance Z_{01} and length ℓ_1 . A good choice is to choose Z_{01} around the impedance level of the load as long as it can be realized; so choose $Z_{01} = 75 \Omega$. The stub needs to be designed so that the susceptances of the stub and load sum to zero. The admittance of the load $Y_L = 1/Z_L = 0.01282 - j0.002564 \text{ S}$. The required admittance of the stub is $Y_{\text{STUB}} = j0.002564 \text{ S}$, so, using Equation (2.113),

$$Z_{\text{STUB}} = 1/Y_{\text{STUB}} = -jZ_{01}/\tan \beta \ell_1 = -j390 \Omega.$$

Therefore, the electrical length of the stub is

$$\beta \ell_1 = \arctan(j75/j390) = 0.1900 + n\pi \text{ radians}, n = 0, 1, 2, \dots \quad (2.116)$$

The first positive angle is taken so the stub has the shortest length. Then

$$\beta \ell_1 = 0.1900 \text{ radians} = 10.89^\circ. \quad (2.117)$$

The complete electrical design of the stub is that it is a shunt open-circuited stub with a characteristic impedance of 75Ω and an electrical length of 10.89° . The combined impedance of the stub and load is $Z_X = 1/(\Re\{Y_L\}) = 1/0.01282 = 78.00 \Omega$.

2.4.5 Electrically Short Lossless Line

Consider the input impedance, Z_{in} , of an electrically short line (i.e., $\beta \ell$ is small) (see Figure 2-23). Using Equation (2.71),

$$Z_{\text{in}} \approx \frac{Z_L + jZ_0(\beta \ell)}{1 + j(Z_L/Z_0)(\beta \ell)} \approx [Z_L + jZ_0(\beta \ell)] \left[1 - j\frac{Z_L}{Z_0}(\beta \ell) \right]. \quad (2.118)$$

Since $Z_0\beta = \sqrt{L/C}(\omega\sqrt{LC}) = \omega L$ and $\beta/Z_0 = (\omega\sqrt{LC})/\sqrt{L/C} = \omega C$ (where L and C are the inductance and capacitance per unit length of the line), Equation (2.118) can be written as

$$Z_{\text{in}} \approx Z_L [1 + (\beta \ell)^2] + j[\omega(L\ell) - Z_L^2\omega(C\ell)]. \quad (2.119)$$

Since $\beta \ell$ is small, $(\beta \ell)^2$ is very small, and so the $(\beta \ell)^2$ term can be ignored. Then the input impedance of an electrically short line terminated in impedance Z_L is

$$Z_{\text{in}} \approx Z_L + j[\omega(L\ell) - Z_L^2\omega(C\ell)]. \quad (2.120)$$

Some special cases of this result will be considered in the following examples.

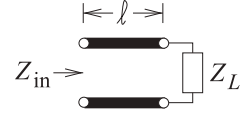
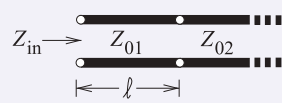


Figure 2-23: An electrically short line.

EXAMPLE 2.13**Capacitive Transmission Line Segment**

This example demonstrates that a predominantly capacitive behavior can be obtained from a short segment of transmission line, the Z_{01} line here, of low characteristic impedance. Consider the transmission line system shown below with lines having the characteristic impedances, Z_{01} and Z_{02} , $Z_{02} \gg Z_{01}$.



The value of Z_{in} is (treating Z_{02} as the load)

$$Z_{in} = Z_{01} \frac{Z_{02} + jZ_{01} \tan \beta \ell}{Z_{01} + jZ_{02} \tan \beta \ell}. \quad (2.121)$$

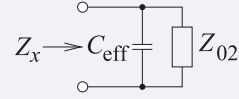
Now $(1 + jx)^{-1} \approx 1 - jx - x^2$. Thus for a short line (and so dropping the $\tan^2(\beta \ell)$ term)

$$Z_{in} \approx Z_{02} - j \frac{Z_{02}^2}{Z_{01}} \tan(\beta \ell) + jZ_{01} \tan(\beta \ell) = Z_{02} + jZ_{01} \tan(\beta \ell) \left[1 - \frac{Z_{02}^2}{Z_{01}^2} \right]. \quad (2.122)$$

For $Z_{02} \gg Z_{01}$ and for a short line, $\tan(\beta \ell) \approx \beta \ell$, and this becomes

$$Z_{in} \approx Z_{02} - j \frac{Z_{02}^2}{Z_{01}} \tan(\beta \ell) \approx Z_{02} - j \frac{Z_{02}^2}{Z_{01}} \beta \ell, \quad (2.123)$$

which is capacitive. Now consider the circuit to the right where an effective capacitance C_{eff} is in shunt with a load Z_{02} . This has the input impedance



$$Z_x = \left(j\omega C_{eff} + \frac{1}{Z_{02}} \right)^{-1} = \frac{Z_{02}}{1 + j\omega C_{eff} Z_{02}} = Z_{02} [1 - j\omega C_{eff} Z_{02} - (j\omega C_{eff} Z_{02})^2 + \dots]. \quad (2.124)$$

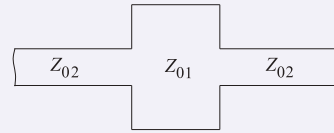
For $\omega C_{eff} Z_{02} \ll 1$ (i.e. an electrically short line)

$$Z_x \approx Z_{02} - j\omega C_{eff} Z_{02}^2 \quad (2.125)$$

Equating Equations (2.123) and (2.125), the effective value of the shunt capacitor realized by the short length of low-impedance line, the Z_{01} line, is

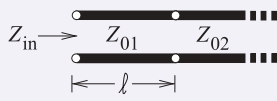
$$C_{eff} = \frac{1}{\omega Z_{02}^2} \frac{Z_{02}^2 \beta \ell}{Z_{01}} = \frac{\beta}{\omega} \frac{\ell}{Z_{01}}. \quad (2.126)$$

Thus a shunt capacitor can be realized approximately by a low-impedance line embedded between two high-impedance lines. The microstrip layout of this is shown in the figure on the right. Recall that a wide microstrip line has a low characteristic impedance.



EXAMPLE 2.14**Inductive Transmission Line Segment**

This example demonstrates that a (predominantly) inductive behavior can be obtained from a segment of transmission line. Consider the transmission line system shown below with lines having two different characteristic impedances, Z_{01} and Z_{02} , $Z_{02} \ll Z_{01}$.



The value of Z_{in} is (using Equation (2.71))

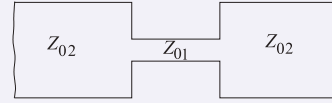
$$Z_{in} = Z_{01} \frac{Z_{02} + jZ_{01} \tan \beta \ell}{Z_{01} + jZ_{02} \tan \beta \ell}, \quad (2.127)$$

which for a short line can be expressed as

$$Z_{in} \approx Z_{02} [1 + \tan(\beta \ell)] + jZ_{01} \tan(\beta \ell). \quad (2.128)$$

Note that $jZ_{01} \tan(\beta \ell)$ is the dominant part for $\ell < \lambda/8$ and $Z_{02} \ll Z_{01}$.

Thus a microstrip realization of a series inductor is a high-impedance line embedded between two low-impedance lines. A top view of such a configuration in microstrip is shown in the figure. A narrow microstrip line has high characteristic impedance.



The previous two examples showed how a shunt capacitance or series inductance can be realized using short sections of line, the Z_{01} line here, with low or high characteristic impedance respectively. This enables realization of some lumped element circuits in microstrip form. A lumped element lowpass filter is shown in Figure 2-24(a) and this can be realized using wide and narrow microstrip lines, as shown in Figure 2-24(b).

2.4.6 Quarter-Wave Transformer

Figure 2-25(a) shows a resistive load R_L and a section of transmission line with length $\ell = \lambda_g/4$ (hence the name quarter-wave transformer). The input

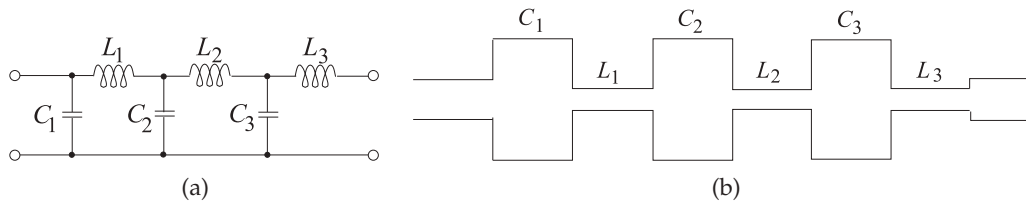


Figure 2-24: A lowpass filter: (a) in the form of an LC ladder network; and (b) realized using microstrip lines.

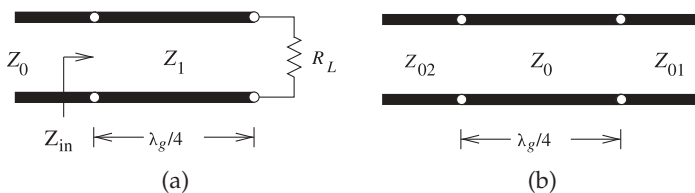


Figure 2-25: The quarter-wave transformer line: (a) transforming a load; and (b) interfacing two lines.



Figure 2-26: Layout of a microstrip quarter-wave transformer.

impedance of the line is

$$Z_{\text{in}} = Z_1 \frac{R_L + jZ_1 \tan(\beta\ell)}{Z_1 + jR_L \tan(\beta\ell)} = Z_1 \frac{R_L + jZ_1 \infty}{Z_1 + jR_L \infty} = \frac{Z_1^2}{R_L}. \quad (2.129)$$

The input impedance is matched to the transmission line Z_0 if

$$Z_{\text{in}} = Z_0^* = Z_0, \quad (2.130)$$

since here the characteristic impedance is real. Thus

$$Z_1 = \sqrt{Z_0 R_L} \quad (2.131)$$

and so the one-quarter wavelength long line acts as an ideal impedance transformer.

Another example of the quarter-wave transformer is shown in Figure 2-25(b). The input impedance looking into the quarter-wave transformer (from the left) is given by

$$Z_{\text{in}} = Z_0 \frac{Z_{01} + jZ_0 \tan(\beta\ell)}{Z_0 + jZ_{01} \tan(\beta\ell)} = Z_0 \frac{Z_{01} + jZ_0 \infty}{Z_0 + jZ_{01} \infty} = \frac{Z_0^2}{Z_{01}}. \quad (2.132)$$

Hence a section of transmission line of length $\ell = \lambda_g/4 + n\lambda_g/2$, where $n = 0, 1, 2, \dots$, can be used to match lines having different impedances, Z_{01} and Z_{02} , by constructing the line so that its characteristic impedance is

$$Z_0 = \sqrt{Z_{01} Z_{02}}. \quad (2.133)$$

Note that for a design center frequency f_0 , the matching section provides a perfect match only at the center frequency and at frequencies where $\ell = \lambda_g/4 + n\lambda_g/2$.

The layout of a microstrip quarter-wave transformer is shown in Figure 2-26, where $\ell = \lambda_g/4$ and the characteristic impedance of the transformer, Z_0 , is the geometric mean of the impedances on either side, that is, $Z_0 = \sqrt{Z_{01} Z_{02}}$.

A quarter-wave transformer has an interesting property that is widely used. Examine the final result in Equation (2.132), which is repeated here:

$$Z_{\text{in}} = \frac{Z_0^2}{Z_{01}}. \quad (2.134)$$

Equation (2.134) indicates that a one-quarter wavelength long line is an impedance inverter presenting, at Port 1, the inverse of the impedance presented at port 2, Z_{01} . This result also applies to complex impedances replacing Z_{01} . This impedance inversion is scaled by the square of the characteristic impedance of the line. This inversion holds in the reverse direction as well.

2.4.7 Summary

The lossless transmission line configurations considered in this section are those most commonly used in microwave circuit design. It is important to note that the stub line is almost always used in shunt configuration to provide an admittance in a circuit. Most transmission line technologies, including coaxial lines and microstrip, only permit shunt stubs. The quarter-wave transformer is a particularly interesting element enabling maximum power transfer from a source to a load that may be different. An interesting feature that is widely exploited is that the quarter-wave transformer inverts an impedance. For example, turning a small resistance into a large resistance, or even turning a small capacitor into a large inductance. These transformations are valid over a moderate bandwidth.

2.5 The Lossy Terminated Line

Previously Section 2.3 presented abstractions that enabled a total voltage and current view to be used with lossless transmission lines. A similar development is presented here for lossy lines. Important abstractions are presented first for the input reflection coefficient of a terminated lossy line in Section 2.5.1 and then for the input impedance of first a long lossy line in Section 2.5.2 and then for a finite length line in Section 2.5.3. Section 2.5.4 presents a simple approximation for the attenuation on a line if it is low loss. Power flow on a lossy line is considered in Section 2.5.5 and then the impact of dispersion on signal integrity considered in Section 2.5.6. The final section, Section 2.5.7, describes a technique for the design of a finite bandwidth dispersion-less line.

2.5.1 Input Reflection Coefficient of a Lossy Line

Γ_{in} of a lossy line can be developed by replacing $j\beta$ in Section 2.3.3 by γ . Referring to Figure 2-16, at a distance ℓ from the load (i.e., $z = -\ell$), the input reflection looking into a lossy line toward the load is

$$\begin{aligned}\Gamma_{\text{in}}|_{z=-\ell} &= \frac{V^-(z=-\ell)}{V^+(z=-\ell)} = \frac{V^-(z=0)e^{-\gamma\ell}}{V^+(z=0)e^{+\gamma\ell}} = \frac{V^-(z=0)}{V^+(z=0)} \frac{e^{-\gamma\ell}}{e^{+\gamma\ell}} \\ &= \Gamma_L e^{-2\gamma\ell} = \Gamma_L e^{-2\alpha\ell} e^{-2j\beta\ell}\end{aligned}\quad (2.135)$$

As the line becomes longer the magnitude of Γ_{in} decreases exponentially, approaching zero, because of attenuation described by the $e^{-2\alpha\ell}$ term.

2.5.2 Input Impedance of a Long Lossy Line

Figure 2-27(a) shows an infinitely long line with characteristic impedance Z_0 . The input impedance Z_{in} of the line is the ratio of the total voltage V_1 to the total current I_1 at the input of the line:

$$Z_{\text{in}} = \frac{V_1}{I_1}. \quad (2.136)$$

If the line is infinitely long or sufficiently lossy there is negligible reflected wave and thus the total voltage and current are just the forward-traveling

Figure 2-27: Transmission line networks: (a) an infinitely long line; and (b) with a finite-length line of characteristic impedance Z_{01} and an infinitely long transmission line of characteristic impedance Z_{02} .

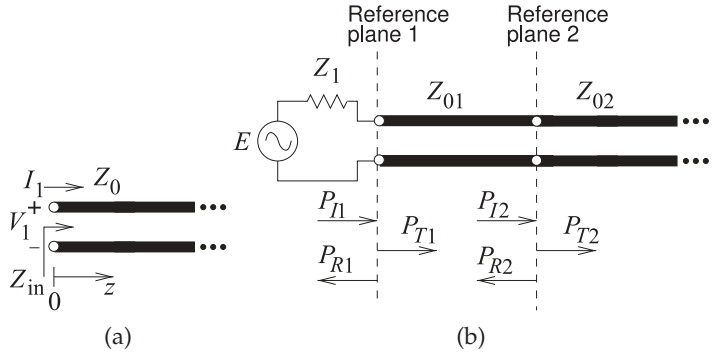
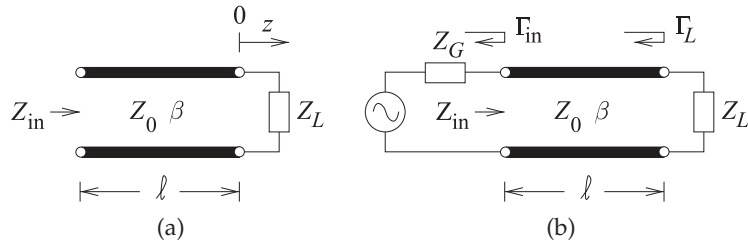


Figure 2-28: Terminated transmission line: (a) a transmission line terminated in a load impedance, Z_L , with an input impedance of Z_{in} ; and (b) a transmission line with source impedance Z_G and load Z_L .



voltage and current and

$$Z_{in} = \frac{V_1}{I_1} = \frac{V^+(0)}{I^+(0)} = Z_0. \quad (2.137)$$

The infinitely long line is approximated by a very long, slightly lossy, cable. It will not matter how the line is terminated (e.g., in a resistor, open circuit, or short circuit), there will be a negligible backward-traveling wave, and the input impedance of the cable will be its characteristic impedance.

2.5.3 Input Impedance of a Lossy Line

The impedance looking into the line varies with position, as the forward- and backward-traveling waves combine to yield position-dependent total voltage and current. At a distance ℓ from the load (i.e., $z = -\ell$), the input impedance seen looking toward the load is

$$Z_{in}|_{z=-\ell} = \frac{V(z = -\ell)}{I(z = -\ell)} = Z_0 \frac{1 + |\Gamma| e^{(j\Theta - 2\gamma\ell)}}{1 - |\Gamma| e^{(j\Theta - 2\gamma\ell)}} = Z_0 \frac{1 + \Gamma_L e^{-2\gamma\ell}}{1 - \Gamma_L e^{-2\gamma\ell}}. \quad (2.138)$$

Another form comes from substituting Equation (2.59) in Equation (2.138):

$$\begin{aligned} Z_{in} &= Z_0 \frac{(Z_L + Z_0)e^{\gamma\ell} + (Z_L - Z_0)e^{-\gamma\ell}}{(Z_L + Z_0)e^{\gamma\ell} - (Z_L - Z_0)e^{-\gamma\ell}} = Z_0 \frac{Z_L \cosh(\gamma\ell) + jZ_0 \sinh(\gamma\ell)}{Z_0 \cosh(\gamma\ell) + jZ_L \sinh(\gamma\ell)} \\ &= Z_0 \frac{Z_L + Z_0 \tanh \gamma\ell}{Z_0 + Z_L \tanh \gamma\ell}. \end{aligned} \quad (2.139)$$

This equation is also known as the **lossy telegrapher's equation**.

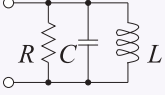
Note that Z_{in} is a quasi-periodic function of ℓ and approaches Z_0 for a long lossy line (i.e. provided that there is attenuation and the line's γ has a real part as then $\tanh \gamma\ell$ goes to one).

EXAMPLE 2.15**Transmission Line Resonator**

A shorted line is used as a resonator. The first resonance is a parallel resonance at 1 GHz.

- Draw the lumped-element equivalent circuit of the resonator.
- What is the impedance looking into the line at resonance?
- What is the electrical length of the resonator?
- If the resonator is $\lambda_g/4$ longer, what is the input impedance of the resonator now?

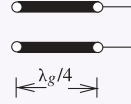
Solution:

- (a)  LC is an open circuit at resonance.
If the line is lossless, $R = 0$.

- (b) $Z_{in} = \infty$ (for a lossless line).

- (c) From Equation (2.71) and with $Z_L = 0$, $Z_{in} = jZ_0 \tan(\beta\ell)$.
 $Z_{in} = \infty$ when $\tan(\beta\ell) = \infty$, i.e. when $\beta\ell = \pi/2 = \lambda_g/4 = 90^\circ$.

- (d) $Z_{in} = 0 \Omega$.

**2.5.4 Attenuation on a Low-Loss Line**

Recall that γ , the propagation constant, is given by

$$\gamma = \sqrt{(R + j\omega L)(G + j\omega C)}. \quad (2.140)$$

This can be written as

$$\gamma = j\omega\sqrt{LC} \sqrt{\left(1 + \frac{R}{j\omega L}\right) \left(1 + \frac{G}{j\omega C}\right)}. \quad (2.141)$$

With a low-loss line, $R \ll \omega L$ and $G \ll \omega C$, and so, using a Taylor series approximation (see Equation (1.174)),

$$\left(1 + \frac{R}{j\omega L}\right)^{1/2} \approx 1 + \frac{1}{2} \frac{R}{j\omega L} \quad (2.142)$$

and $\left(1 + \frac{G}{j\omega C}\right)^{1/2} \approx 1 + \frac{1}{2} \frac{G}{j\omega C}, \quad (2.143)$

thus $\gamma \approx \frac{1}{2} \left(R\sqrt{\frac{C}{L}} + G\sqrt{\frac{L}{C}} \right) + j\omega\sqrt{LC}. \quad g \quad (2.144)$

Hence for low-loss lines (in Np/m if SI units are used),

$$\alpha \approx \frac{1}{2} \left(\frac{R}{Z_0} + GZ_0 \right) \quad (2.145) \quad \text{and} \quad \beta \approx \omega\sqrt{LC}. \quad (2.146)$$

What Equation (2.145) indicates is that for low-loss lines the attenuation constant, α , consists of dielectric- and conductor-related parts; that is,

$$\alpha = \alpha_d + \alpha_c \quad (2.147) \quad \alpha_d \approx GZ_0/2 \quad (2.148) \quad \text{and} \quad \alpha_c \approx R/(2Z_0) \quad (2.149)$$

where α_d is the attenuation contributed by dielectric loss and is called dielectric attenuation, and α_c is the attenuation contributed by the conductor loss and is called ohmic or conductive attenuation.

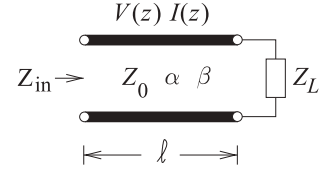


Figure 2-29: A low-loss transmission line. The propagation constant $\gamma = \alpha + j\beta$.

2.5.5 Power Flow on a Terminated Lossy Line

In this section a lossy transmission line with low loss is considered so that $R \ll \omega L$ and $G \ll \omega C$, and the characteristic impedance is $Z_0 \approx \sqrt{L/C}$. Figure 2-29 is a lossy transmission line and the total voltage and current at any point on the line are given by

$$V(z) = V_0^+ [e^{-\gamma z} + \Gamma e^{\gamma z}] \quad \text{and} \quad I(z) = \frac{V_0^+}{Z_0} [e^{-\gamma z} - \Gamma e^{\gamma z}]. \quad (2.150)$$

Section 2.5.3 derived the lossy telegrapher's equation:

$$Z_{\text{in}} = Z_0 \frac{Z_L + Z_0 \tanh \gamma \ell}{Z_0 + Z_L \tanh \gamma \ell}. \quad (2.151)$$

For a lossy transmission line not all of the power applied at the input will be delivered to the load as power will be lost on the line due to attenuation. The power delivered to the load (which is at position $z = 0$) is

$$P_L = \frac{1}{2} \Re \{V(0)I^*(0)\} = \frac{|V_0^+|^2}{2Z_0} (1 - |\Gamma_L|^2), \quad (2.152)$$

where Γ_L is the reflection coefficient of the load. Similarly the power at the input of the line (at position $z = -\ell$) is

$$P_{\text{in}} = \frac{1}{2} \Re \{V(-\ell)I^*(-\ell)\} = \frac{|V_0^+|^2}{2Z_0} [1 - |\Gamma_L|^2 e^{-4\alpha \ell}] e^{2\alpha \ell} \quad (2.153)$$

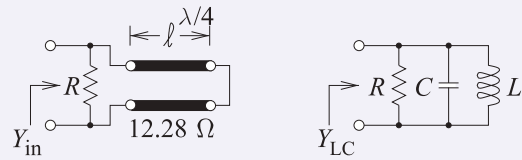
and the power lost in the line is

$$P_{\text{loss}} = P_{\text{in}} - P_L = \frac{|V_0^+|^2}{2Z_0} [(e^{2\alpha \ell} - 1) + |\Gamma_L|^2 (1 - e^{-2\alpha \ell})]. \quad (2.154)$$

EXAMPLE 2.16

Q of a Transmission Line Resonator Revisited

Energy is stored on a transmission line and this must be considered in deriving the Q of a transmission line resonator. Consider the $\lambda/4$ -long shorted transmission line examined in Examples 2.5 and 2.11. This line has a characteristic impedance of 12.28Ω , it is resonant at 1850 MHz, and a $10 \text{ k}\Omega$ resistor, R , is at the input as shown in the left figure.



Solution:

At resonance

$$Q = 2\pi \frac{\text{Peak energy stored}}{\text{Energy dissipated per cycle}} = \omega_r \frac{\text{Peak energy stored}}{\text{Power loss in the resistor}} \quad (2.155)$$

$$Q = 1/(\text{Fractional bandwidth}), \quad (2.156)$$

where ω_r is the radian frequency at resonance. So there are two fundamental ways that the Q can be determined: determining the peak energy stored and the power loss, and finding the fractional bandwidth. However, using the fractional bandwidth is only an approximate method, as Q is a measure of energy stored and energy dissipated.

For an RLC lumped-element resonator

$$Q = \begin{cases} \frac{1}{R} \sqrt{\frac{L}{C}} = \frac{\omega_r L}{R} & \text{for a series } RLC \text{ circuit} \\ R \sqrt{\frac{C}{L}} = \frac{\omega_r C}{G} & \text{for a shunt } RLC \text{ circuit.} \end{cases} \quad (2.157)$$

The narrowband lumped-element equivalent circuit of the resonator developed in Example 2.5, with $C = 5.503$ pF and $L = 1.345$ pH can be used. Thus

$$Q = R \sqrt{\frac{C}{L}} = 10 \cdot 10^3 \sqrt{\frac{5.503 \cdot 10^{-12}}{1.345 \cdot 10^{-9}}} = 640.$$

It is important to note that the input impedance of the transmission line at the resonant frequency cannot be used to find the Q of the transmission line resonator, as it does not convey any information about the energy stored. However, the narrowband model of the resonator at resonance does capture the energy storage information and so can be used to calculate the Q of the resonator, as was done here.

2.5.6 Lossy Transmission Line Dispersion

On a lossy line, phase velocity, group velocity, and attenuation constant are frequency dependent and so a lossy line is, in general, dispersive. That is, different frequency components of a signal travel at different speeds, and the phase velocity, v_p , and group velocity, v_g , are functions of frequency. As a result, the signal will spread out in time and, if the line is long enough, it will be difficult to extract the original information.

In the previous section it was seen, in Equation (2.146), that for a TEM line $\omega/\beta = v_p = v_g$ is approximately frequency independent for a low-loss line. This is true for most two-conductor lines (lines that support TEM modes), but not for all transmission line structures that guide EM waves (a rectangular waveguide is an example of where v_g and v_p differ significantly). Also, the conductive component of the attenuation constant, α_c in Equation (2.149), is approximately frequency independent. However, the dielectric component, α_d in Equation (2.148), is frequency dependent even for a low-loss line. This is because G is mostly due to energy loss when a material lattice or molecular components are distorted by the E field. So there is more loss and G increases linearly as the frequency increases. (Conductivity of the dielectric also affects G , but this is usually a much smaller effect except for a silicon substrate.) If the transmission line has moderate loss, all of the propagation parameters will be frequency dependent and the line is dispersive.

2.5.7 Design of a Dispersionless Lossy Line

Over a moderate bandwidth a lossy line can be designed to be dispersionless (i.e. $v_g \approx v_p \approx \text{constant}$). The parameters that are important in describing signal propagation on a transmission line are the propagation constant, γ , and the characteristic impedance, Z_0 . When considering dispersion it is more appropriate to examine α and $v_p \approx \omega/\beta$ (for a low loss line), as these parameters are generally frequency dependent for a lossy line. For a line to be dispersionless α , ω/β , and Z_0 should be independent of frequency.

For any low-loss line the propagation constant is

$$\gamma = \sqrt{(R + j\omega L)(G + j\omega C)} = j\omega\sqrt{LC} \left[\left(1 + \frac{R}{j\omega L}\right) \left(1 + \frac{G}{j\omega C}\right) \right]^{1/2}. \quad (2.158)$$

If the line is designed so that

$$R/L = G/C, \quad (2.159)$$

then
$$\gamma = \alpha + j\beta = j\omega\sqrt{LC} \left(1 + \frac{R}{j\omega L}\right) = R\sqrt{\frac{C}{L}} + j\omega\sqrt{LC}.$$

From this
$$\alpha = R\sqrt{\frac{C}{L}}, \quad \beta = \omega\sqrt{LC} \quad \text{and} \quad v_p = \omega/\beta = 1/\sqrt{LC}. \quad (2.160)$$

The analysis is completed by considering the characteristic impedance

$$Z_0 = \sqrt{\frac{R + j\omega L}{G + j\omega C}} = \sqrt{\frac{L}{C}} \sqrt{\frac{R/L + j\omega}{G/C + j\omega}}, \quad (2.161)$$

and, referring to Equation (2.159), note that the last square root term is 1, so

$$Z_0 = \sqrt{L/C}, \quad (2.162)$$

which is frequency independent. The important characteristics describing signal propagation are now frequency independent and the line is dispersionless. In practice a lossy dispersionless line can only be approximated over a small bandwidth since G is linearly dependent on frequency because of the frequency dependence of dielectric relaxation loss.

2.5.8 Summary

An earlier section developed the input reflection coefficient and input impedance of a lossless line. This section did the same thing but for a lossy line. Short-hand derivations were presented for the attenuation of a low loss line in terms of the per-unit-length resistance and characteristic impedance of the line. Dispersion on a line was discussed and a design technique presented for the design of a dispersionless line. This design is valid over a narrow or moderate bandwidth and this bandwidth limitation applies to all transmission line-based designs.

2.6 Reflections at Interfaces

Transmission lines transfer power from one point to another and there are often many interfaces at which power is reflected and transferred. This

section is focused on developing an intuitive understanding of reflection and transmission of power at interfaces and over a transmission line. Section 2.6.1 presents an understanding of power flow and introduces the return loss concept applying this analysis to a single interface in Section 2.6.3. Microwave engineering is greatly concerned with maximum power transfer and the analysis that supports design choices, the maximum power transfer theorem, is revisited in Section 2.6.2. Section 2.6.4 presents bounce diagram analysis which is concerned with reflection and transmission at multiple interfaces. This can be a confusing analysis but it provides the essential understanding for the development of intuition for how power flows, and understanding of situations where power flow may be disrupted. The final section, Section 2.6.5, presents the theory of small reflections, derived from bounce diagram analysis, which is used in several places in this book series in the synthesis of transmission line networks.

2.6.1 Power Flow and Return Loss

Now consider the power flow on the lossless line in Figure 2-13. The incident (forward-traveling) wave has the power

$$\begin{aligned} P^+ &= \frac{1}{2} \Re [V^+ (I^+)^*] = \frac{1}{2} \Re \left[V^+ \left(\frac{V^+}{Z_0} \right)^* \right] \\ &= \frac{1}{2} \Re \left\{ (V_0^+ e^{-j\beta z}) \left(\frac{V_0^+ e^{-j\beta z}}{Z_0} \right)^* \right\} = \frac{1}{2} \frac{|V_0^+|^2}{Z_0}, \end{aligned} \quad (2.163)$$

and the reflected wave has the power (using Equation (2.60))

$$P^- = \frac{1}{2} \frac{|V_0^-|^2}{Z_0} = \frac{|\Gamma|^2}{2} \frac{|V_0^+|^2}{Z_0}. \quad (2.164)$$

Considering conservation of power, the power delivered to the load, P_L , is the difference of the forward- and backward-traveling powers:

$$P_L = \frac{1}{2} \Re \{V_L I_L^*\} = P^+ - P^- = P^+ (1 - |\Gamma|^2). \quad (2.165)$$

Noteworthy cases are when there is an open circuit, a short circuit, or a purely reactive load at the end of a transmission line. These have $|\Gamma| = 1$. Thus all power is reflected back to the source and $P_L = 0$.

The power that is absorbed by the load appears as a loss as far as the incident and reflected waves are concerned. To describe this, the concept of return loss (RL) is introduced and defined as

$$\text{RL} = -20 \log |\Gamma| \text{ dB}. \quad (2.166)$$

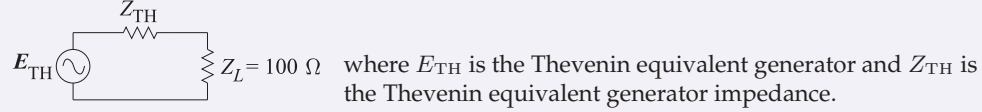
RL indicates the available power not delivered to the load. A matched load ($\Gamma = 0$) has $\text{RL} = \infty$ dB, and a total reflection ($|\Gamma| = 1$) has $\text{RL} = 0$ dB.

EXAMPLE 2.17**Transmission Line Model at the Load**

A transmission line with a characteristic impedance of $75\ \Omega$ supports a forward-traveling wave with a power of $1\ \mu\text{W}$. The line is terminated in a resistance of $100\ \Omega$. Draw the lumped-element equivalent circuit at the interface between the transmission line and the load.

Solution:

The equivalent circuit has the form

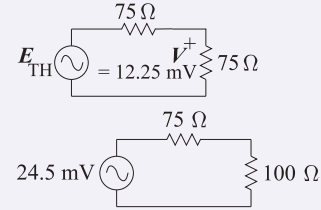


The amplitude of the forward-traveling voltage wave is obtained by calculating the power in the forward-traveling wave:

$$P^+ = \frac{1}{2}(V^+)^2/Z_0 = (V^+)^2/150 = 1\ \mu\text{W} = 10^{-6}\ \text{W}.$$

So $V^+ = \sqrt{150 \cdot 10^{-6}} = 12.25\ \text{mV}$. Note that V^+ is not E_{TH} . To calculate E_{TH} , consider the circuit to the right that results in maximum power transfer.

So $E_{\text{TH}} = 2V^+ = 24.5\ \text{mV}$. Since the line has a characteristic impedance of $75\ \Omega$, then $Z_{\text{TH}} = 75\ \Omega$. So the lumped-element equivalent circuit at the load is

**2.6.2 Maximum Power Transfer Theorem**

Many transmission line calculations can be solved using the concepts of maximum available power, incident power, and reflected power. At microwave frequencies the output impedance of sources, for example, cannot be ignored as can often be done at low frequencies. Thus the output of an RF source is defined in terms of maximum available power.

Consider the source shown in Figure 2-30 with an impedance $Z_S = R_S + jX_S$ driving a load $Z_L = R_L + jX_L$. The aim here is to find Z_L for maximum delivery of power to the load. The phasor current in the load is

$$I = \frac{E}{Z_S + Z_L} \quad (2.167)$$

and thus the average power in the load is

$$P_L = \frac{1}{2}|I|^2 R_L = \frac{1}{2} \left(\frac{|E|}{|Z_S + Z_L|} \right)^2 R_L = \frac{\frac{1}{2}|E|^2 R_L}{(R_S + R_L)^2 + (X_S + X_L)^2}. \quad (2.168)$$

The load required for maximum power transfer is obtained by first considering a fixed value of R_L and then finding the value of X_L required to minimize

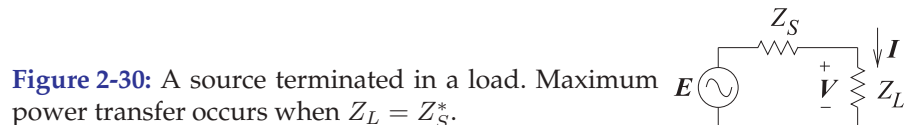


Figure 2-30: A source terminated in a load. Maximum power transfer occurs when $Z_L = Z_S^*$.

Equation (2.168). Since X_L only affects the denominator in Equation (2.168), it is clear that the denominator is minimized by making $X_L = -X_S$. So now Equation (2.168) reduces to

$$P_L = \frac{\frac{1}{2}|E|^2 R_L}{(R_S + R_L)^2} \quad (2.169) \quad \text{and} \quad P_L = \frac{\frac{1}{2}|E|^2}{(R_S^2/R_L + 2R_S + R_L)}. \quad (2.170)$$

Now the power delivered to the load is maximized by minimizing the denominator in Equation (2.170), which will occur when the derivative of the denominator in Equation (2.170) is zero. That is, when

$$\frac{d}{dR_L} (R_S^2/R_L + 2R_S + R_L)^2 = \frac{-R_S^2}{R_L^2} + 1 = 0. \quad (2.171)$$

The derivative is zero when

$$R_S^2/R_L^2 = 1, \quad \text{that is, when} \quad R_L = \pm R_S. \quad (2.172)$$

When the derivative is zero, the power transferred to the load is either the minimum or maximum power that can be delivered to the load. Clearly $R_L = -R_S$ is a nonsensical solution as the load and source resistance should be positive. In addition, the situations at the extremes need to be checked, that is, when R_L is very small, $R_L \rightarrow 0$, and when R_L is very large, $R_L \rightarrow \infty$. As $R_L \rightarrow 0$, Equation (2.169) becomes $P_L \rightarrow 0$, and as $R_L \rightarrow \infty$, Equation (2.169) becomes $P_L \rightarrow 0$. Clearly there will not be negative power dissipated in R_L , so when $R_L = R_S$ the maximum power, $P_L|_{\max}$, is dissipated in the load. Equation (2.169) becomes

$$P_L|_{\max} = \frac{1}{2} \frac{|E|^2 R_L}{(R_S + R_S)^2} = \frac{1}{8} \frac{|E|^2}{R_S}. \quad (2.173)$$

This is called the maximum available power, or simply the **available power** of the source. So the conditions for maximum power transfer are $R_L = R_S$ and $X_L = -X_S$; that is, the maximum power transfer from source to load requires

$$Z_L = Z_S^*. \quad (2.174)$$

Also note that if the source impedance in Figure 2-30 is resistive, $V = \frac{1}{2}E$ at maximum power transfer.

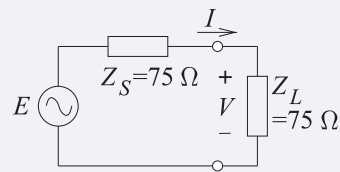
EXAMPLE 2.18

Available Power

A $75 \, \Omega$ source with an available power of 1 W is terminated in a short circuit. What is the power dissipated in the Thevenin equivalent resistance of the source?

Solution:

At RF, “ $75 \, \Omega$ source” refers to a source with a Thevenin equivalent resistance of $75 \, \Omega$ which here is Z_S . The condition for maximum power transfer, and when the full available power is delivered to the load, is when the load impedance, Z_L is the complex conjugate of $Z_S = 75 \, \Omega$. The circuit for maximum power transfer is as shown to the right.



To solve the problem we must determine E as this will not change even though the current through Z_S , I , will depend on the load impedance. The available power is

$$P_A = \frac{1}{2}|I|^2 \Re(Z_S) = \frac{1}{2}|I|^2 \times 75 = 1 \text{ W and so } I = \sqrt{2 \times 1/75} = 0.1633 \text{ A.}$$

From this the voltage across the load can be determined:

$$V = IZ_L = 0.1633 \times 75 = 12.25 \text{ V and from symmetry } E = 2V = 24.50 \text{ V.}$$

Now the condition with a short circuit, $Z_L = 0$, can be determined. Note that I and V will change but E will be fixed.

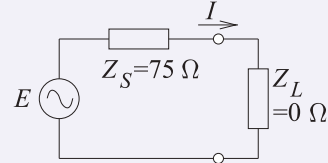
Considering the circuit to the right, now

$$I = E/(Z_S + Z_L) = 24.50/(75 + 0) = 0.3267 \text{ A.}$$

The power dissipated in Z_S is

$$P_S = \frac{1}{2}I^2 \Re(Z_S) = 0.3267 \times 75 = 4.002 \text{ W.}$$

Some comments on this result can be made. With a short circuit the current that flows in the circuit doubles compared to the maximum power transfer condition. Since the power dissipated in Z_S is proportion to the square of the current the power dissipated in the Thevenin equivalent resistance increases by a factor of 4 (P_S should be exactly 4 W). The ideal voltage source E can provide unlimited power. However no matter what the value of Z_L , the power dissipated in Z_L can never be more than the available power.



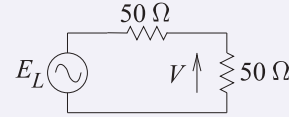
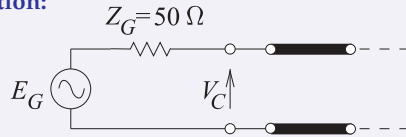
EXAMPLE 2.19

Forward-Traveling Wave Calculations

A transmission line is driven by a generator with a maximum available power of 20 dBm and a Thevenin equivalent impedance of 50Ω . The transmission line has a characteristic impedance of 50Ω .

- What is the Thevenin equivalent generator voltage?
- What is the magnitude of the forward-traveling voltage wave on the line? Assume that the line is infinitely long.
- What is the power of the forward-traveling voltage wave?

Solution:



- Maximum available power is delivered to the load when it is conjugately matched to the generator impedance (see right diagram). Then $P_{\text{LOAD}} = \frac{1}{2}V^2/R$ (V is peak voltage) (i.e., $P_{\text{LOAD}} = 20 \text{ dBm} = 0.1 \text{ W}$) and

$$V = \sqrt{2P_{\text{LOAD}} \cdot R} = \sqrt{2 \times 0.1 \times 50} \text{ V}_{\text{peak}} = 3.16 \text{ V,} \quad E_G = 2V = 6.32 \text{ V.}$$

- This is just V , so $V^+ = 3.16 \text{ V.}$
- $P^+ = 20 \text{ dBm.}$

2.6.3 A Single Interface

Many transmission line calculations are most conveniently addressed using the maximum available power concept. This is particularly so when there are multiple transmission lines. The concept is that the maximum available power from a source is incident on a load and if there is a mismatch, power is reflected and the rest of the power is transmitted. The circuits used to illustrate these calculations are shown in Figure 2-31. The available power of the source is P_{av} , which is incident on the reference plane shown in Figure 2-31(b) where it is called the incident power P_I . At the reference plane power

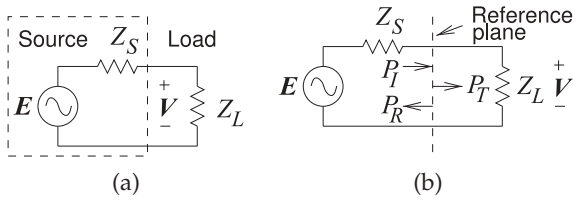


Figure 2-31: Calculations using incident and reflected power: (a) source terminated in a load; and (b) reference plane illustrating the use of incident and reflected power at a load.

is reflected, P_R , and power is transmitted, P_T . Using the reflection coefficient normalized to the impedance of the source (i.e., Z_S)

$$P_R = |\Gamma|^2 P_I, \quad (2.175) \quad \text{where} \quad \Gamma = \frac{Z_S - Z_L}{Z_S + Z_L} \quad (2.176)$$

and the transmitted power is

$$P_T = (1 - |\Gamma|^2) P_I. \quad (2.177)$$

EXAMPLE 2.20

Transmission Line Power Calculations

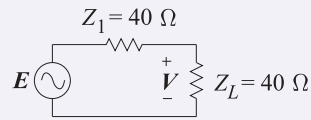
The transmission line shown in Figure 2-27(b) consists of a source with Thevenin impedance $Z_1 = 40 \, \Omega$ and source $E = 5 \, \text{V}$ (peak), connected to a $\lambda/4$ long line of characteristic impedance $Z_{01} = 40 \, \Omega$, which in turn is connected to an infinitely long line of characteristic impedance $Z_{02} = 100 \, \Omega$. The transmission lines are lossless. Two reference planes are shown in Figure 2-27(b). At reference plane 1 the incident power is P_{I1} (the maximum available power from the source), the reflected power is P_{R1} , and the transmitted power is P_{T1} . P_{I2} (the maximum available power from Z_{01}), P_{R2} , and P_{T2} are similar quantities at Reference Plane 2. P_{I1} , P_{R1} , P_{T1} , P_{I2} , P_{R2} , and P_{T2} are steady-state quantities.

- (a) What is P_{I1} ?
 (b) What is P_{T2} ?

Solution: Since the infinitely long line does not have a backward-traveling wave this problem reduces to a single transmission line interface problem.

First develop some expectations. This will be a sanity check during the problem. P_{I1} and P_{I2} are maximum available powers and since the Z_{01} line (this is a short way of talking about the line with a characteristic impedance Z_{01}) is lossless they should be equal: $P_{I1} = P_{I2}$. P_{T1} and P_{T2} are the total powers delivered to the right of the respective interfaces. Again since the Z_{01} line is lossless $P_{T1} = P_{T2}$. Also $P_{T1} \leq P_{I1}$ as power P_{R1} is reflected from the interface. Similarly $P_{T2} \leq P_{I2}$.

- (a) P_{I1} is the available power from the generator. Since the Thevenin impedance of the generator is $40 \, \Omega$, P_{I1} is the power that would be delivered to a matched load (the maximum available power). An equivalent problem is shown to the right where $V = \frac{1}{2}E = 2.5 \, \text{V}_{\text{peak}}$. So

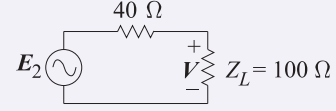


$$P_{I1} = \text{power in } Z_L = \frac{1}{2} (V)^2 \frac{1}{Z_L} = \frac{1}{2} (2.5)^2 \frac{1}{40} = 0.07813 \, \text{W} = 78.13 \, \text{mW}. \quad (2.178)$$

Note that the $\frac{1}{2}$ occurs because peak voltage is used in RF calculations.

- (b) Now the problem becomes interesting and there are many ways to solve it. One of the key observations is that the first transmission line has the same characteristic impedance as the Thevenin equivalent impedance of the generator, $Z_{01} = Z_1$, and so can be ignored where appropriate. This observation will be used in this example. One way to proceed is to directly calculate P_{T2} , and a second approach is to calculate the incident and reflected powers at reference plane 2 and then to determine P_{T2} .

- (i) First approach: looking to the left from reference plane 2, the circuit can be modeled as an equivalent circuit having a Thevenin equivalent resistance of 40Ω and a Thevenin equivalent voltage that has an available power of 78.13 mW. So in the circuit to the right, E_2 is just E or 5 V.



The load is 100Ω as the second transmission line is infinitely long. A reasonable question to ask is why E_2 is not 2.5 V, as this would be the voltage across $Z_L = 40 \Omega$ in part (a). However, 2.5 V is the voltage of the forward-traveling voltage wave on the first transmission line with characteristic impedance $Z_{01} = 40 \Omega$. It is not the Thevenin equivalent voltage of the source. The voltage across the load is

$$V = E_2 \frac{100}{40 + 100} = E \frac{100}{140} = 3.57 \text{ V}_{\text{peak}}. \quad (2.179)$$

The power transmitted at reference plane 2 is also the power delivered to the load:

$$P_{T2} = P_L = \frac{1}{2} (V)^2 \frac{1}{Z_L} = \frac{1}{2} (3.57)^2 \frac{1}{100} = 0.0638 \text{ W} = 63.8 \text{ mW}. \quad (2.180)$$

A quick check is that this is less than P_{I1} , as it should be.

- (ii) Second approach: This time P_{R2} , the reflected power at reference plane 2, will be calculated. The incident power at plane 2, P_{I2} , is just P_{I1} . P_{I2} is the maximum available power at reference plane 2 and not necessarily the power that is incident there. In general, to calculate P_{I2} the Thevenin equivalent source looking to the left from reference plane 2 would need to be calculated. However since here $Z_{01} = Z_1$, $P_{I2} = P_{I1} = 78.13 \text{ mW}$.

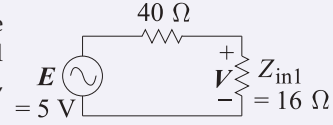
P_{R2} can be calculated from the voltage reflection coefficient at reference plane 2:

$$\Gamma_2 = \frac{Z_L - Z_{01}}{Z_L + Z_{01}} = \frac{100 - 40}{100 + 40} = 0.429 \quad (2.181)$$

$$P_{R2} = \Gamma_2^2 P_{I2} = 0.429^2 \times 78 \text{ mW} = 14.36 \text{ mW}. \quad (2.182)$$

So $P_{T2} = P_{I2} - P_{R2} = 78.13 \text{ mW} - 14.36 \text{ mW} = 63.7 \text{ mW}$, which is the same as the transmitted power calculated in the first approach, allowing for rounding error.

- (iii) A third approach is to calculate the input impedance looking to the right from reference plane 1, call this Z_{in1} . Using the lossless telegrapher's equation, Equation 2.71, Z_{in1} is calculated to be 16Ω .



The voltage across the 16Ω resistor is $16/(40 + 16)(5 \text{ V}) = 1.429 \text{ V}$. So the power dissipated in Z_{in1} is

$$P = \frac{1}{2} (1.429 \text{ V})^2 \frac{1}{16} = 0.0638 \text{ W} = 63.8 \text{ mW},$$

as before. All of this power must be transmitted to the infinitely long line, i.e. it is P_{T2} , as the system is otherwise lossless.

2.6.4 Bounce Diagram

A bounce diagram is a graphical representation of reflections at the interfaces between networks. A microwave network is shown in Figure 2-32 where there are two reference planes at boundaries between different parts of the network. At each boundary there are reflections and transmissions of what could be viewed as small packets of sinusoidal signals. While the bounce diagram yields a steady-state result such as the input impedance, the thought experiment is that small sinusoidal packets bounce around the transmission-line network. Bounce diagrams are used to explore the impact of multiple

reflections in a network leading to understanding, and from that to design decisions. Bounce diagrams are best illustrated through an example.

Reflection and Transmission Coefficients at a Boundary

Bounce diagram analysis requires that the reflection and transmission coefficients at a boundary be referenced to a common impedance. Figure 2-33(a) shows the interface of two transmission lines of characteristic impedance Z_{01} and Z_{02} at a reference plane. The problem is determining the reflection coefficient, Γ , and transmission coefficient, T , at the boundary referencing them to the same impedance. Here they will be referenced to Z_{01} . The reflection coefficient as seen from the Z_{01} line referenced to Z_{01} is

$$\Gamma = \frac{Z_{02} - Z_{01}}{Z_{02} + Z_{01}}. \quad (2.183)$$

Now the transmission coefficient referenced to Z_{01} is

$$T = {}^{Z_{01}}V_2^+ / V_1^+, \quad (2.184)$$

where ${}^{Z_{01}}V_2^+$ is the forward-traveling voltage wave on the Z_{02} line (traveling to the right) referenced to Z_{01} . It is not the actual forward-traveling voltage on the Z_{02} line. $V_1^+ = {}^{Z_{01}}V_1^+$ is the traveling voltage wave on the Z_{01} line that is incident at the boundary. It is obtained using the circuit in Figure 2-33(b). Figure 2-33(b) shows the maximum power transfer condition so that

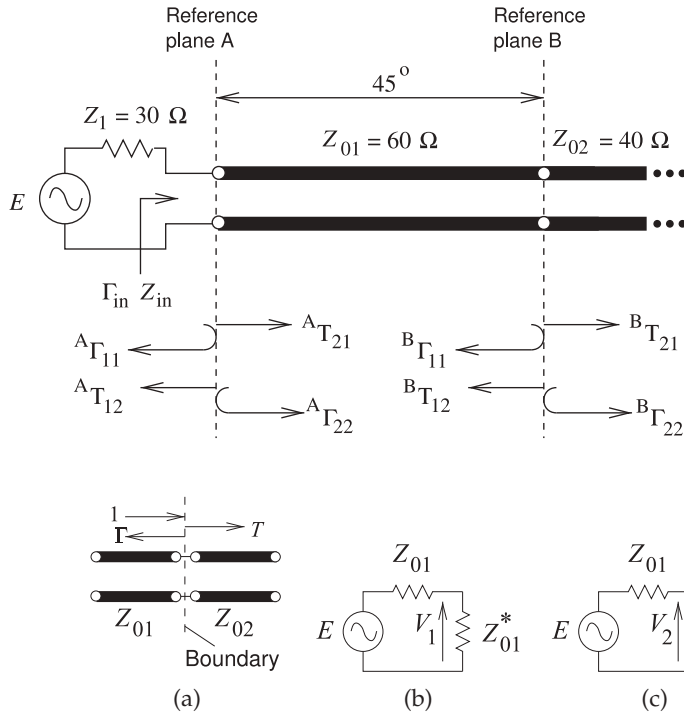


Figure 2-32: Transmission line network with a finite-length line of characteristic impedance Z_{01} and an infinitely long transmission line of characteristic impedance Z_{02} . ${}^A\Gamma_{1i}$ is the i th discrete reflection of an incident wave at the left-hand side of reference plane A. ${}^AT_{1i}$ is the transmission at reference plane A for the same event. ${}^A\Gamma_{2i}$ is the i th discrete reflection of an incident wave at the right-hand side of reference plane A.

Figure 2-33: Reflection (Γ) and transmission (T) at the boundary between two transmission lines of characteristic impedance Z_{01} and Z_{02} .

the forward-traveling wave on the Z_{01} line at the left of the boundary is

$$V_1^+ = V_1 = E \frac{Z_{01}}{Z_{01} + Z_{01}^*} = E \frac{Z_{01}}{2\Re(Z_{01})}. \quad (2.185)$$

(For real impedances $V_1^+ = \frac{1}{2}E$.)

The next parameter to determine is $^{Z_{01}}V_2^+$. This begins by determining the total voltage, V_2 , at the boundary using the circuit in Figure 2-33(c):

$$V_2 = E \frac{Z_{02}}{Z_{01} + Z_{02}}. \quad (2.186)$$

Now consider that the Z_{02} line is infinitely long, then it is clear that $V_2 = ^{Z_{02}}V_2^+$. This is the actual forward-traveling voltage on the Z_{02} line. Now the problem is how to change the reference impedance of V_2^+ . This is done by noting that the forward-traveling power wave is independent of the reference impedance, therefore the forward-traveling power wave on the Z_{02} line traveling to the right, away from the reference plane, is

$$P_{Z_{02}} = \frac{1}{2} \left[\frac{(^{Z_{02}}V_2^+)^2}{\Re(Z_{02})} \right] = \frac{1}{2} \left[\frac{(^{Z_{01}}V_2^+)^2}{\Re(Z_{01})} \right]. \quad (2.187)$$

So the desired forward-traveling voltage wave is (since $^{Z_{02}}V_2^+ = V_2$)

$$^{Z_{01}}V_2^+ = \sqrt{\frac{\Re(Z_{01})}{\Re(Z_{02})}} V_2 = E \sqrt{\frac{\Re(Z_{01})}{\Re(Z_{02})}} \left(\frac{Z_{02}}{Z_{01} + Z_{02}} \right). \quad (2.188)$$

So the transmission coefficient referenced to Z_{01} is

$$\begin{aligned} T = \frac{^{Z_{01}}V_2^+}{V_1^+} &= E \sqrt{\frac{\Re(Z_{01})}{\Re(Z_{02})}} \left(\frac{Z_{02}}{Z_{01} + Z_{02}} \right) \left(\frac{2\Re(Z_{01})}{Z_{01}} \frac{1}{E} \right) \\ &= \sqrt{\frac{\Re(Z_{01})}{\Re(Z_{02})}} \left[\frac{\Re(Z_{01})}{Z_{01}} \right] \left(\frac{2Z_{02}}{Z_{01} + Z_{02}} \right). \end{aligned} \quad (2.189)$$

An alternative way of determining T is to consider power conservation at the boundary. Then

$$|T|^2 = 1 - |\Gamma|^2, \quad \text{that is} \quad |T| = \pm \sqrt{1 - |\Gamma|^2}. \quad (2.190)$$

This can be used if T is expected to be real, which it will be if Z_{01} and Z_{02} are real. The positive sign should be taken. The more general formula, Equation (2.189), can be used with complex impedances.

EXAMPLE 2.21

Bounce Diagram

In the transmission line system in Figure 2-32 the electrical length of the Z_{01} line (i.e., the line with characteristic impedance Z_{01}) is 45° and the Z_{02} line is infinitely long. The aim here is to find the input impedance, Z_{in} . This will be arrived at in two ways. The first technique uses a bounce diagram approach and emphasizes reflection and transmission at the interface planes. The second approach uses the telegrapher's equation.

- (a) What are the reflection and transmission parameters at reference plane A?

${}^A\Gamma_{11}$ is the reflection coefficient of signals incident on Reference Plane A from the left. ${}^AT_{21}$ is the transmission coefficient at the plane for signals from the left. ${}^A\Gamma_{22}$ and ${}^AT_{12}$ are the corresponding parameters for scattering from signals coming from the right to the plane. So, normalizing to Z_1 ,

$${}^A\Gamma_{11} = \frac{Z_{01} - Z_1}{Z_{01} + Z_1} = 0.333; \quad {}^A\Gamma_{22} = -{}^A\Gamma_{11} = -0.333. \quad (2.191)$$

Using Equation (2.189),

$${}^AT_{21} = \sqrt{\frac{Z_1}{Z_{01}}} \left(\frac{2Z_{01}}{Z_1 + Z_{01}} \right) = \sqrt{\frac{30}{60}} \left(\frac{2 \cdot 60}{30 + 60} \right) = 0.943. \quad (2.192)$$

Similarly, ${}^AT_{12} = 0.943$, which is due to reciprocity. As an additional sanity check (this can only be done if Z_{01} and Z_{02} are real)

$${}^AT_{21} = \sqrt{1 - {}^A\Gamma_{11}^2} = 0.943, \quad {}^AT_{12} = \sqrt{1 - {}^A\Gamma_{22}^2} = 0.943. \quad (2.193)$$

- (b) What are the scattering parameters Γ_2 and T_2 at reference plane B?

The reference is Z_0 , and so the reflection coefficient going from the Z_{01} line to the Z_{02} line is

$${}^B\Gamma_{11} = \frac{Z_{02} - Z_0}{Z_{02} + Z_0}. \quad (2.194)$$

The question now is what system reference impedance to use? Should it be Z_1 , Z_{01} , or even Z_{02} ? The problem could be solved using any of these, but the simplest procedure is to use the same reference impedance throughout, and since the eventual aim is to calculate the overall input reflection coefficient, the appropriate choice is $Z_0 = Z_1$. Note, however, that the actual voltage levels on the lines are not being calculated (which would need to be referenced to the characteristic impedance of the lines being considered), but instead a traveling wave referenced to a universal system impedance. So the scattering parameters at reference plane B referenced to the impedance Z_1 are

$${}^B\Gamma_{11} = \frac{Z_{02} - Z_1}{Z_{02} + Z_1} = 0.143; \quad {}^B\Gamma_{22} = -{}^B\Gamma_{11} = -0.143 \quad (2.195)$$

$${}^BT_{21} = \sqrt{1 - {}^B\Gamma_{11}^2} = 0.990; \quad {}^BT_{12} = \sqrt{1 - {}^B\Gamma_{22}^2} = 0.990. \quad (2.196)$$

The second transmission line is infinitely long and so no signal from the line will be incident at reference plane B from the right.

- (c) What is the transmission coefficient of the Z_{01} transmission line referenced to Z_{01} ?

T_{01} is the ratio of the forward-traveling wave at the end of the line to its value at the start of the line. Using a reference impedance of Z_{01} , the magnitude of the transmission coefficient is one and it rotates by the line's electrical length $\Theta_1 = 45^\circ$ or 0.785 radians:

$$T_{01} = e^{-j\Theta_1} = \exp(-j0.785) = 0.707 - j0.707. \quad (2.197)$$

- (d) Draw the bounce diagram of the transmission line network.

The bounce diagram is shown in Figure 2-34.

- (e) What is Γ_{in} and hence what is Z_{in} ?

Γ_{in} is the steady-state input reflection coefficient and is obtained by adding all of the signals going to the left from reference plane A in Figure 2-34. So

$$\begin{aligned} \Gamma_{in} &= {}^A\Gamma_{11} + {}^AT_{12} {}^AT_{21} T_{01}^2 {}^B\Gamma_{11} \\ &\quad + {}^AT_{12} {}^AT_{21} T_{01}^4 {}^B\Gamma_{11} {}^A\Gamma_{22} + {}^AT_{12} {}^AT_{21} T_{01}^6 {}^B\Gamma_{11} {}^A\Gamma_{22}^2 \cdots \\ &= {}^A\Gamma_{11} + {}^AT_{12} {}^AT_{21} T_{01}^2 {}^B\Gamma_{11} [1 + x + x^2 + \cdots], \end{aligned} \quad (2.198)$$

where $x = T_{01}^2 {}^B\Gamma_{11} {}^A\Gamma_{22}$. Now $1/(1-x) = 1 + x + x^2 + \cdots$, and thus

$$\begin{aligned} \Gamma_{in} &= {}^A\Gamma_{11} + \frac{{}^AT_{12} {}^AT_{21} T_{01}^2 {}^B\Gamma_{11}}{1 - T_{01}^2 {}^B\Gamma_{11} {}^A\Gamma_{22}} \\ &= 0.333 + \frac{0.943 \times 0.943 \times (0.707 - j0.707)^2 \times (-0.2)}{1 - (0.707 - j0.707)^2 \times (-0.2) \times (-0.333)} \\ &= 0.345 - j0.177. \end{aligned} \quad (2.199)$$

Γ_{in} is the reflection at reference plane A and is referenced to $Z_1 = 30 \Omega$. So the input impedance is

$$Z_{in} = Z_1 \left(\frac{1 + \Gamma_{in}}{1 - \Gamma_{in}} \right) = 30 \left(\frac{1 + 0.345 - j0.177}{1 - 0.345 + j0.177} \right) = 55.39 + j23.08 \Omega. \quad (2.200)$$

- (f) Use the lossless telegrapher's equation, Equation (2.71), to find Z_{in} .

The infinitely long line presents an impedance Z_{02} to the 60Ω transmission line. So the input impedance looking into the 60Ω line at reference plane A is, using the lossless telegrapher's equation,

$$Z_{in} = Z_{01} \left(\frac{Z_{02} + jZ_{01} \tan \beta l}{Z_{01} + jZ_{02} \tan \beta l} \right),$$

where the electrical length βl is 45° or $\pi/4$ radians. So

$$Z_{in} = 60 \left(\frac{40 + j60 \tan(\pi/4)}{60 + j40 \tan(\pi/4)} \right) = 55.39 + j23.08 \Omega,$$

equivalent to the result obtained using the bounce diagram method (see Equation (2.200)).

The bounce diagram technique aids in physical understanding, however using the telegrapher's equation is a less error prone approach to solving transmission line problems.

2.6.5 Theory of Small Reflections

If the discontinuity at the boundary A in Figure 2-32 is small (i.e. Z_1 is close to Z_{01} instead of the $30 \Omega/60 \Omega$ discontinuity shown) then a useful approximation is obtained by noting that ${}^A\Gamma_{11}$ and ${}^A\Gamma_{22}$ are small and ${}^AT_{21} \approx {}^AT_{12} \approx 1$ so that in Equation (2.198) $x \approx 0$. Then Equation (2.198) becomes, using Equation (2.197), [6]

$$\Gamma_{in} \approx {}^A\Gamma_{11} + {}^AT_{12} {}^AT_{21} T_{01}^2 {}^B\Gamma_{11} \approx {}^A\Gamma_{11} + {}^B\Gamma_{11} e^{-2j\theta_1}. \quad (2.201)$$

That is, if the discontinuity at reference plane A is small then the input reflection coefficient is dominated by the initial reflection at A, from Z_1 to Z_{01} , and the initial reflection at B, from Z_{01} to Z_{02} , rotated by twice the electrical length, θ_1 , of the line.

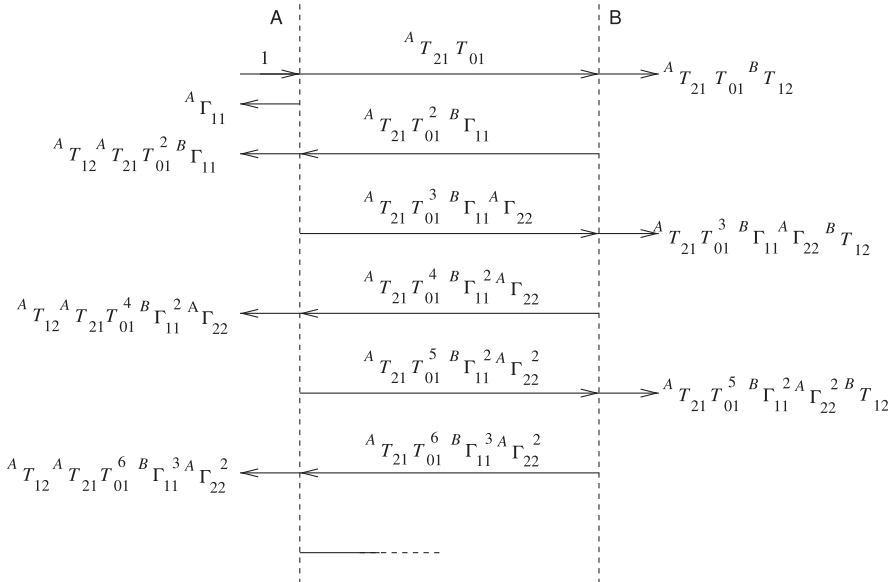


Figure 2-34:
Bounce
diagram of the
transmission line
network in
Figure 2-32.

EXAMPLE 2.22

Advanced Power Calculations

This example is similar to Example 2.20. Again, the transmission line network of Figure 2-27 is considered, but now the characteristic impedance of the first transmission line is not the same as the generator impedance and so the simplification used in the previous example can no longer be used. Now the generator has a Thevenin impedance $Z_1 = 40 \Omega$ and source $E = 5 \text{ V}_{\text{peak}}$, connected to a one-quarter wavelength long line of characteristic impedance $Z_{01} = 30 \Omega$ that in turn is connected to an infinitely long line of characteristic impedance $Z_{02} = 100 \Omega$. The transmission lines are lossless. Two reference planes are shown in Figure 2-27. At reference plane 1 the incident power is P_{I1} (the maximum available power from the source), the reflected power is P_{R1} and the transmitted power is P_{T1} . P_{I2} (the maximum available power from Z_{01}), P_{R2} , and P_{T2} are similar quantities at reference plane 2. P_{I1} , P_{R1} , P_{T1} , P_{I2} , P_{R2} , and P_{T2} are steady-state quantities.

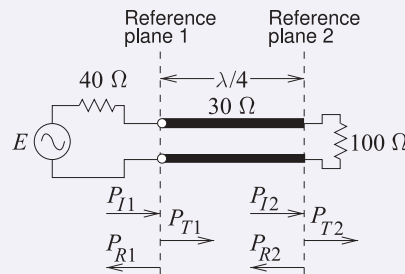
- What is P_{I1} ?
- What is P_{T2} ?
- Determine P_{T1} , P_{I2} , P_{R1} , and P_{R2} .

Solution:

One of the first things to note is that the infinitely long 100Ω transmission line is indistinguishable from a 100Ω resistor, so the reduced form of the problem is as shown to the right.

- P_{I1} was calculated in Example 2.20 in Equation (2.178):

$$P_{I1} = 78.13 \text{ mW}. \quad (2.202)$$



P_{I1} is the available power from the source and this is the power that would be delivered to a load that is conjugately matched to the Thevenin equivalent source impedance.

- The problem here is finding P_{T2} . Recall that the powers here are steady-state quantities so that multiple reflections of, say, a pulse are not being considered. Since the system is lossless, the power delivered by the generator must be the power delivered to the infinitely long transmission line Z_{02} (i.e., P_{T2}). The telegrapher's equation can be used to calculate the input impedance, Z_{in} , of the two transmission line system; that is, the input impedance of Z_{01} from the generator end. However, a simpler way to find this impedance is to realize that the Z_{01} line is a $\lambda/4$ transformer so that

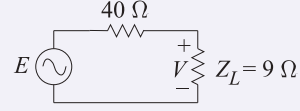
$$Z_{01} = 30 \Omega = \sqrt{Z_{in} Z_{02}} = \sqrt{100 Z_{in}}, \quad (2.203)$$

and so

$$Z_{in} = 9 \Omega. \quad (2.204)$$

The equivalent circuit is as shown to the right, where E is the original generator voltage of 5 V and

$$V = \frac{9}{40 + 9} 5 = 0.9184 \text{ V}. \quad (2.205)$$



The power delivered by the generator to the 9 Ω load is

$$P_{T2} = \frac{1}{2} V^2 / 9 = 0.04686 \text{ W} = 46.86 \text{ mW}. \quad (2.206)$$

- (c) The power transmitted into the system at reference plane 1, P_{T1} , is the same as the power transmitted to the 100 Ω load, as the first transmission line is lossless; that is,

$$P_{T1} = P_{T2} = 46.86 \text{ mW}. \quad (2.207)$$

Also $P_{R1} = P_{I1} - P_{T1} = (78.13 - 46.86) \text{ mW} = 31.27 \text{ mW}. \quad (2.208)$

The two remaining quantities to determine are P_{I2} and P_{R2} . There can be a number of interpretations of what these should be, but one thing that is certain is that

$$P_{T2} = P_{I2} - P_{R2} = 46.86 \text{ mW}. \quad (2.209)$$

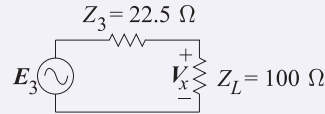
One interpretation that will be followed here is based on the equivalent circuit at reference plane 2. Let Z_{out} be the impedance looking to the left from reference plane 2. Again, using the property of a one-quarter wavelength long transmission line,

$$Z_{01} = 30 = \sqrt{Z_{out} \times 40} \quad (2.210)$$

and so

$$Z_{out} = Z_{01}^2 / 40 = 30^2 / 40 = 22.5 \Omega. \quad (2.211)$$

The equivalent circuit at reference plane 2 is then



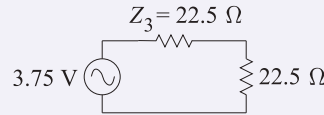
Now determine V_x that results in a power P_{T2} being delivered to the 100 Ω load, so

$$P_{T2} = \frac{1}{2} V_x^2 / 100 = 0.04686 \text{ W} \quad (2.212) \quad \text{and} \quad V_x = 3.06 \text{ V}. \quad (2.213)$$

From the circuit above,

$$V_x = \frac{100}{100 + 22.5} E_3 \quad (2.214) \quad \text{and so} \quad E_3 = 3.75 \text{ V}. \quad (2.215)$$

The available power from this source is obtained by considering



The available power at reference plane 2 is

$$P_{I2} = \frac{1}{2} \frac{(E_3/2)^2}{22.5} = \frac{1.875^2}{2 \times 22.5} = 0.07813 \text{ W} = 78.13 \text{ mW}. \quad (2.216)$$

From Equation (2.209),

$$P_{R2} = P_{I2} - P_{T1} = (78.13 - 46.86) \text{ mW} = 31.27 \text{ mW}. \quad (2.217)$$

Note that P_{R2} in Equation (2.217) is the same as P_{R1} in Equation (2.208), as expected.

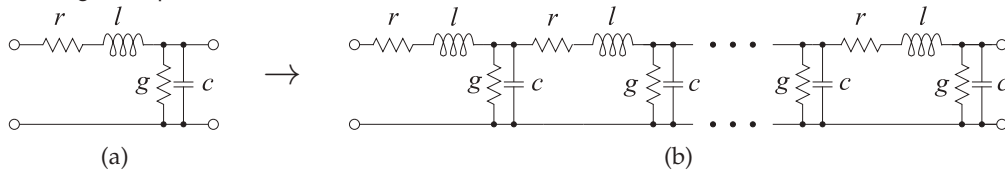
2.7 Models of Transmission Lines

Models of transmission lines enable lines to be incorporated in simulators and related to lumped-element circuits. Section 2.7.1 presents models used in circuit simulators such as Spice. Synthesis of microwave circuits often requires that a lumped-element design be realized using an equivalent transmission line network. The ABCD parameter technique described in Section 2.7.2 is the main means for relating these networks and thus synthesizing transmission line-based designs. This method is used many times in designs in this book series.

2.7.1 Circuit Models of Transmission Lines

Circuit models of transmission lines are required if they are to be used in a circuit simulator. RF and microwave engineering uses two types of simulators. Spice-like simulators use lumped-element transmission line models in which an $RLGC$ model of a short segment of line is replicated for the length of the line. If the ground plane is treated as a universal ground, then the model of a segment of length Δz is as shown in Figure 2-35(a). In this segment $r = R\Delta z$, $l = L\Delta z$, $g = G\Delta z$, and $c = C\Delta z$, where R , L , G , and C are the per unit length parameters of the line. Cascading the segments to get the length of the line yields the complete lumped-element model of the line, as shown in Figure 2-35(b). This model is adequate if there is a well-defined ground plane. Otherwise the more accurate form of the segment model shown in Figure 2-35(c) is used. The L and C of a two-conductor transmission line model relate to the fields between the conductors and not to the conductors themselves. So assigning them to just one conductor is not accurate. The capacitor is already shared between the two conductors in the original model, Figure 2-35(a), but the inductor was assigned to just one. The change in the distributed ground model of Figure 2-35(c) is that inductance

Common ground plane model



Distributed ground model

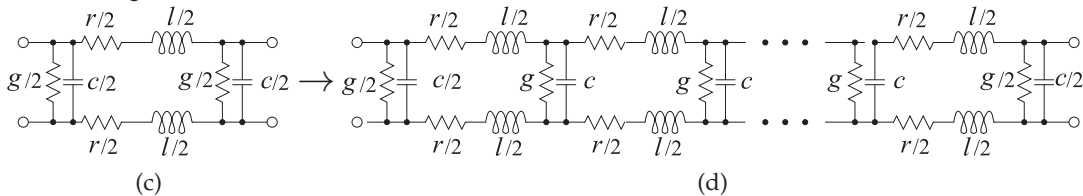


Figure 2-35: Lumped-element transmission line models: (a) model of a short segment (e.g. $\lambda/20$ long); (b) complete model of a transmission line; (c) more accurate model of a segment ; and (d) complete accurate model of a transmission line.

is assigned to each of the conductors.

One of the problems with the lumped-element model is that it is not possible to handle G correctly. G is largely due to dielectric relaxation loss and so is linearly dependent on frequency. Fortunately it is very small for RF and microwave substrates and so it can nearly always be ignored. An exception is a silicon integrated circuit where there is appreciable dielectric loss. Parasitic extraction software is used in silicon integrated circuit design to extract models similar to that in Figure 2-35(d) but account for coupling with other circuits. Especially in digital circuits, it is sometimes difficult to identify a ground plane (a current return path) except for critical interconnect networks such as clock and power distribution circuits.

EXAMPLE 2.23

Transmission Line Resonator

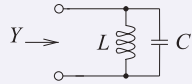
Communication filters are often constructed using several shorted transmission line resonators that are coupled to each other. Consider a coaxial line that is short-circuited at one end. The permittivity filling the coaxial line has $\varepsilon = 20$ and the resonator is to be designed to resonate at a center frequency, f_0 , of 1850 MHz when it is $\lambda/4$ long.

- What is the wavelength in the dielectric-filled coaxial line?
- What is the form of the equivalent circuit (in terms of inductors and capacitors) of the one-quarter wavelength long resonator if the coaxial line is lossless? Note that the input impedance of a shorted $\lambda/4$ -long line is infinite.
- What is the physical length of the resonator?

Solution:

The first thing to realize with this example is that the first resonance will occur when the length of the resonator is one-quarter wavelength ($\lambda/4$) long. Resonance generally means that the impedance is either an open or a short circuit and there is energy stored. When the shorted line is $\lambda/4$ long, the input impedance is an open circuit and also energy is stored.

- $\lambda_g = \lambda_0 / \sqrt{\varepsilon_r} = 16.2 \text{ cm} / \sqrt{20} = 3.62 \text{ cm}$. (Here $\lambda_0 = 30 \text{ cm}$ at 1 GHz was used. Thus at 1850 MHz $\lambda_0 = (30 \text{ cm}) / 1.85 = 16.2 \text{ cm}$.)

- 

$$Y = 0 \text{ at resonance}$$

$$Y = Y_L + Y_C = \frac{1}{j\omega L} + j\omega C = \frac{\omega^{-1}}{jL} + j\omega C.$$

- $\ell = (0.0362 \text{ m}) / 4 = 9.05 \text{ mm}$.

EXAMPLE 2.24

Resonator Model

This example builds on Example 2.23. RF communication filters are often constructed using several shorted transmission line resonators that are coupled to each other. Consider a coaxial line that is short-circuited at one end. The dielectric filling the coaxial line has a $\varepsilon = 20$ and the resonator is to be designed to resonate at a center frequency $f_0 = 1850 \text{ MHz}$.

- What is the wavelength in the dielectric-filled coaxial line?
- What is the form of the equivalent circuit (in terms of inductors and capacitors) of the one-quarter wavelength long resonator if the coaxial line is lossless?
- What is the physical length of the resonator?
- Determine the derivative with respect to frequency of the admittance of the LC equivalent circuit developed in (b). Determine an analytic expression for the derivative at the resonant frequency.

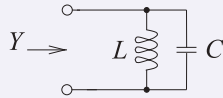
- (e) If the diameter of the inner conductor of the coaxial line is 2 mm and the inside diameter of the outer conductor is 5 mm, what is the characteristic impedance of the coaxial line?
- (f) Calculate the input admittance of the dielectric-filled coaxial line at $0.99f_0$, f_0 , and $1.01f_0$. Determine the numerical frequency derivative of the line admittance at f_0 .
- (g) Derive the numeric values of the equivalent circuit of the resonator at resonance.

Solution:

The first thing to realize is that the first resonance will occur when the length of the resonator is one-quarter wavelength ($\lambda/4$) long. Resonance generally means that the impedance is either an open or a short circuit and there is energy stored. When the shorted line is $\lambda/4$ long, the input impedance will be an open circuit. When the line is of zero length energy is not stored, so a zero-length line is not a resonator.

(a) $\lambda_g = \lambda_0 / \sqrt{\epsilon_r} = 16.2 \text{ cm} / \sqrt{20} = 3.62 \text{ cm}$.

(b)



$$Y = Y_L + Y_C = \frac{1}{j\omega L} + j\omega C = \frac{\omega^{-1}}{jL} + j\omega C.$$

$$Y = 0 \text{ at resonance.}$$

(c) $\ell = (0.0362 \text{ m})/4 = 9.05 \text{ mm}$.

(d) From (b),

$$\frac{\partial Y}{\partial \omega} = -\frac{\omega^{-2}}{jL} + jC = \frac{j}{\omega^2 L} + jC = j \left(\frac{1}{\omega^2 L} + C \right). \quad (2.218)$$

(e) From Equation (2.53), $Z_0 = 12.28 \Omega$.

(f) $Z_L = 0 \Omega$, $\ell = (0.0362 \text{ m})/4 = 9.05 \text{ mm}$, $\beta = \beta_0 \sqrt{\epsilon_r}$, where β_0 is the phase constant of free space. From Equations (2.43) and (2.44),

$$\beta = 20.958 \times f_0 |_{\text{GHz}} \times \sqrt{20} = 173.4 \text{ rad/m}.$$

At $0.99f_0$ and using Equation (2.71), $Z_{\text{in}} = j781.7 \Omega$; $Y_{\text{in}} = -j0.001279 \text{ S}$.

At f_0 , $Z_{\text{in}} = -j\infty \Omega$; $Y_{\text{in}} = 0 \text{ S}$. At $1.01f_0$, $Z_{\text{in}} = -j781.7 \Omega$; $Y_{\text{in}} = j0.001279 \text{ S}$.

So the derivative of the input admittance is

$$\frac{\partial Y}{\partial \omega} \approx \frac{\Delta Y_{\text{in}}}{\Delta \omega} = \frac{j(0.001279 + 0.001279)}{2\pi f_0(1.01 - 0.99)} = j1.101 \cdot 10^{-11} \text{ S} \cdot \text{s} = j1.101 \cdot 10^{-11} \text{ F}. \quad (2.219)$$

Note the SI unit equivalence $\text{S} \cdot \text{s} = \text{F}$ obtained by examining Table 2-1.

(g) The LC circuit resonates at $f_0 = 1.85 \text{ GHz}$ when $1/(j\omega_0 L) = -j\omega_0 C$; $\omega_0 = 2\pi f_0$. Thus

$$LC = \omega_0^{-2} = 0.7401 \times 10^{-20} \text{ s}^2. \quad (2.220)$$

Equating Equations (2.218) and (2.219):

$$\frac{1}{\omega_0^2 L} + C = 1.101 \times 10^{-11} \text{ F} \quad \text{and so} \quad C = 1.101 \times 10^{-11} - \frac{1}{\omega_0^2 L} \text{ F}. \quad (2.221)$$

Substituting this in Equation (2.220) (noting the SI unit equivalence $\text{S}^{-1} \cdot \text{s}^{-1} = \text{H}$):

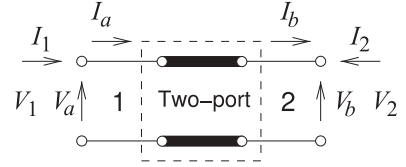
$$L \left(1.101 \times 10^{-11} - \frac{1}{\omega_0^2 L} \right) = 0.7401 \times 10^{-20} \text{ H}$$

$$1.101 \times 10^{-11} L = 1.4802 \times 10^{-20} \text{ H} \quad \text{and} \quad L = 1.345 \times 10^{-9} \text{ H} = 1.345 \text{ nH}. \quad (2.222)$$

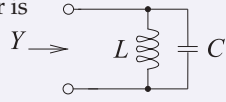
From Equation (2.221),

$$C = 0.7401 \times 10^{-20} / L = 5.503 \times 10^{-12} \text{ F} = 5.503 \text{ pF}. \quad (2.223)$$

Figure 2-36: Two-port network of a transmission line with cascable voltage and current definitions.



So the equivalent circuit of the resonator is



with $L = 1.345$ nH and $C = 5.503$ pF.

This equivalent circuit is valid for a range (say 5%–10%) of frequencies around 1.85 GHz. The broadband equivalence was obtained here by matching both the admittance and the derivative of the admittance.

2.7.2 ABCD (Chain) Parameters of a Transmission Line

ABCD parameters, also called chain parameters, are used in RF and microwave engineering to electrically equate two different structures such as a lumped-element network and a transmission line structure. Often the electrical design is undertaken using lumped elements and then these are converted to equivalent transmission line structures with the equivalence achieved using ABCD parameters.

Figure 2-36, shows the voltages and currents of a two-port in cascable form so that the input variables can be written in terms of the output variables:

$$\begin{bmatrix} V_a \\ I_a \end{bmatrix} = \begin{bmatrix} A & B \\ C & D \end{bmatrix} \begin{bmatrix} V_b \\ I_b \end{bmatrix}. \quad (2.224)$$

Note that the current at port 2 is in the opposite direction to the usual definition of the two-port current. So in terms of the port voltage and current at port 1, (V_1 and I_1), and the port voltage and current at port 2, (V_2 and I_2),

$$V_a = V_1, \quad I_a = I_1, \quad V_b = V_2, \quad \text{and} \quad I_b = -I_2. \quad (2.225)$$

In terms of traveling-wave voltages, the total voltage and current on a line of length ℓ , propagation constant γ , and characteristic impedance $Z_0 = 1/Y_0$ at position z are

$$V(z) = V_0^+ e^{-j\gamma(z-\ell)} + V_0^- e^{j\gamma(z-\ell)} \quad (2.226)$$

$$I(z) = Y_0 V_0^+ e^{-j\gamma(z-\ell)} - Y_0 V_0^- e^{j\gamma(z-\ell)}. \quad (2.227)$$

where V_0^+ and V_0^- are the traveling wave voltage phasors at $z = \ell$, (port 2), i.e.

$$V_0^+ = \frac{1}{2} (V_2 + Z_0 I_2) \quad \text{and} \quad V_0^- = \frac{1}{2} (V_2 - Z_0 I_2). \quad (2.228)$$

Substituting these into Equations (2.226) and (2.227),

$$V(z) = \frac{1}{2} (V_2 + Z_0 I_2) e^{-j\gamma(z-\ell)} + \frac{1}{2} (V_2 - Z_0 I_2) e^{j\gamma(z-\ell)} \quad (2.229)$$

$$I(z) = \frac{1}{2} (Y_0 V_2 + I_2) e^{-j\gamma(z-\ell)} - \frac{1}{2} (Y_0 V_2 - I_2) e^{j\gamma(z-\ell)}. \quad (2.230)$$

At Port 1 ($z = 0$)

$$V_1 = V(0) = \frac{1}{2} (V_2 + Z_0 I_2) e^{j\gamma\ell} + \frac{1}{2} (V_2 - Z_0 I_2) e^{-j\gamma\ell} \quad (2.231)$$

$$I_1 = I(0) = \frac{1}{2} (Y_0 V_2 + I_2) e^{j\gamma\ell} - \frac{1}{2} (Y_0 V_2 - I_2) e^{-j\gamma\ell}. \quad (2.232)$$

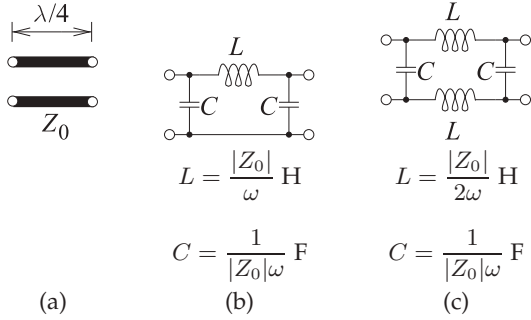


Figure 2-37: Lumped equivalent circuit of a one-quarter wavelength long line of characteristic impedance Z_0 which is the same as that of an impedance inverter (of $Z_0 \Omega$): (a) one-quarter wavelength long line segment; (b) lumped-element equivalent circuit; and (c) alternative lumped-element model.

Using the trigonometric identities in Section 1.A.2 (and noting that $I_2 = -I_b$),

$$V_a = V_1 = \cosh(\gamma\ell)V_2 - Z_0 \sinh(\gamma\ell)I_2 = \cosh(\gamma\ell)V_b + Z_0 \sinh(\gamma\ell)I_b \quad (2.233)$$

$$I_a = I_1 = Y_0 \sinh(\gamma\ell)V_2 - \cosh(\gamma\ell)I_2 = Y_0 \sinh(\gamma\ell)V_b + \cosh(\gamma\ell)I_b. \quad (2.234)$$

That is, the $ABCD$ parameters of a lossy line are

$$\begin{aligned} A &= \cosh(\gamma\ell) & B &= Z_0 \sinh(\gamma\ell) \\ C &= Y_0 \sinh(\gamma\ell) & D &= \cosh(\gamma\ell) \end{aligned} \quad (2.235)$$

and the $ABCD$ parameters of a lossless transmission line, where $\gamma = j\beta$, are

$$\begin{aligned} A &= \cos(\beta\ell) & B &= jZ_0 \sin(\beta\ell) \\ C &= jY_0 \sin(\beta\ell) & D &= \cos(\beta\ell) \end{aligned} \quad (2.236)$$

EXAMPLE 2.25

Lumped Element Model of a Quarter-Wavelength Long Line

Develop the lumped-element model of a one-quarter wavelength long lossless transmission line having characteristic impedance Z_0 .

Solution:

The model is developed by equating $ABCD$ parameters. The $ABCD$ parameters of a one-quarter wavelength long lossless line (with $\beta\ell = \pi/2$) are

$$A = \cos(\beta\ell) = 0 \quad (2.237) \quad C = jY_0 \sin(\beta\ell) = j/Z_0 \quad (2.239)$$

$$B = jZ_0 \sin(\beta\ell) = jZ_0 \quad (2.238) \quad D = \cos(\beta\ell) = 0. \quad (2.240)$$

The $ABCD$ parameters of a Pi network (see Table 2-1 of [7]) are

$$A = 1 + y_2/y_3 \quad (2.241) \quad C = y_1 + y_2 + y_1 y_2/y_3 \quad (2.243)$$

$$B = 1/y_3 \quad (2.242) \quad D = 1 + y_1/y_3. \quad (2.244)$$

$$\text{Equating Equations (2.238) and (2.242),} \quad y_3 = 1/(jZ_0), \quad (2.245)$$

and with Equations (2.237), (2.240), (2.241), and (2.244),

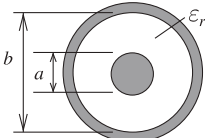
$$y_1 = y_2 = -y_3 = -1/(jZ_0). \quad (2.246)$$

The lumped equivalent circuit of the quarter-wave transformer in Figure 2-37(a) is shown in Figure 2-37(b). An alternative lumped-element model is shown in Figure 2-37(c). The lumped-element model of the 50Ω line at 400 MHz is shown in Figure 2-37(b) with $L = 19.89 \text{ nH}$ and $C = 7.968 \text{ pF}$. This is a simpler and more accurate model of a $\lambda/4$ long line than a model with multiple short line segments as in Figure 2-35.

2.8 Two-Conductor Transmission Lines

Nearly every two-conductor transmission line supports EM fields at frequencies down to DC. As a result, such lines can usually be characterized at DC and the properties of the lines will be essentially the same at RF frequencies. In the following, the characteristic impedances of the most common types of two-conductor lines are presented. For all of these lines the phase constant is the same as it would be in the medium without conductors (i.e., $\beta = \omega\sqrt{\mu\epsilon}$). The characteristic impedances are modifications of the free-space wave impedance $\eta_0 = \sqrt{\mu_0/\epsilon_0} = 120\pi \Omega = 376.73 \Omega$. The properties of many other transmission lines are given in [8].

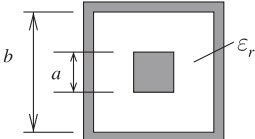
Coaxial line
Figure 2-38



$$Z_0 = \frac{\eta_0}{2\pi} \sqrt{\frac{\mu_r}{\epsilon_r}} \ln \left(\frac{b}{a} \right) = 60 \sqrt{\frac{\mu_r}{\epsilon_r}} \ln \left(\frac{b}{a} \right) \quad (2.247)$$

Exact. See derivation in Section 2.9.

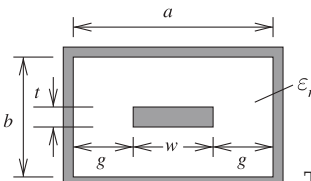
Square coaxial line
Figure 2-39



$$Z_0 \approx \eta_0 \sqrt{\frac{\mu_r}{\epsilon_r}} \left[4 \left(\frac{2a}{b-a} + 0.558 \right) \right]^{-1} \quad (2.248)$$

Typical accuracy: <1% for $b/a \leq 4$. Reference [9].

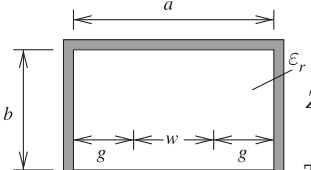
Rectangular coaxial line
Figure 2-40



$$Z_0 = \frac{\eta_0}{4} \sqrt{\frac{\mu_r}{\epsilon_r}} \left(\frac{w}{b-t} + \frac{1}{\pi} \left\{ \frac{b}{b-t} \ln \left(\frac{2b-t}{t} \right) + \ln \left[\frac{t(2b-t)}{(b-t)^2} \right] \right\} \frac{\ln [1 + \coth(\pi g/b)]}{\ln 2} \right)^{-1} \quad (2.249)$$

Typical accuracy: 1%. References [10–12].

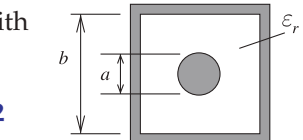
Rectangular coaxial line, thin strip
 $t \rightarrow 0$
Figure 2-41



$$Z_0 = \frac{\eta_0}{4} \sqrt{\frac{\mu_r}{\epsilon_r}} \left\{ \frac{w}{b} + \frac{2}{\pi} \ln \left[1 + \coth \left(\frac{\pi g}{b} \right) \right] \right\}^{-1} \quad (2.250)$$

Typical accuracy: 1%. Reference [10].

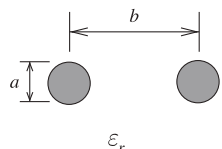
Square coax with circular inner conductor
Figure 2-42



$$Z_0 = \frac{\eta_0}{2\pi} \sqrt{\frac{\mu_r}{\epsilon_r}} \ln \left(\frac{1.0787b}{a} \right) \quad (2.251)$$

Typical accuracy: 1.5%. References [8, 13–15].

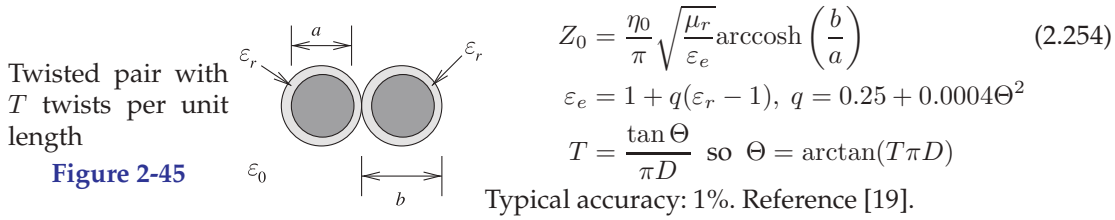
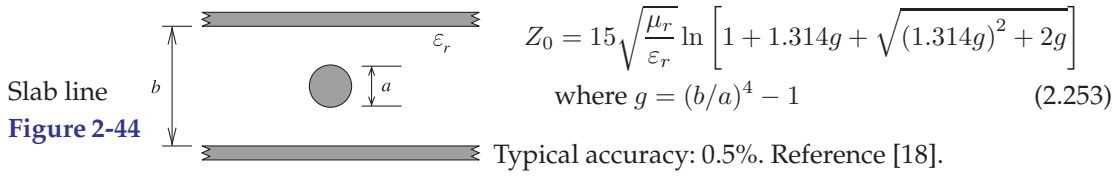
Parallel wires
Figure 2-43



$$Z_0 = \frac{\eta_0}{\pi} \sqrt{\frac{\mu_r}{\epsilon_r}} \operatorname{arccosh} \left(\frac{b}{a} \right) \quad (2.252)$$

Typical accuracy: 1%. References [16, 17].

Characteristics of two-conductor transmission lines.



Characteristics of two-conductor transmission lines.

2.9 Coaxial Line

In this section the characteristic impedance of a coaxial line is calculated. The technique assumes that the dynamic electric and magnetic fields will be the same as they would be at DC. This physical insight enables the problem to be solved relatively simply using the static field laws. Later the dynamic situation is considered when the fields on a realistic coaxial line are considered.

2.9.1 Characteristic Impedance of a Coaxial Line

In the following the per unit length parameters— R , L , G , and C —of a coaxial line are obtained. From these the characteristic impedance and propagation constant of the coaxial line are derived. The development is an example of how these parameters can be developed for any transmission line. The key is using a coordinate system that matches the structure being considered. Then Maxwell's equations can be expressed very simply, usually as one-dimensional ordinary differential equations. Very often the static electric and magnetic field laws can be used that make the development even simpler. If an orthogonal coordinate system does not coincide with the dimensions of the line, then sometimes it is possible to use a mathematical technique called conformal mapping to map a nonconforming shape such as a microstrip line into a shape that matches an orthogonal coordinate system [20]. Once the transmission line parameters are derived the result is mapped back to the original structure. Fortunately most transmission line structures conform to an orthogonal coordinate system.

The cross section of a coaxial line is shown in Figure 2-46(a) and it has two concentric conductors with the inner conductor having an outer radius of a and the inside of the outer conductor with a radius b . The fields between the conductors can be solved by expressing the field relations in cylindrical coordinates. The following is a simplification of the treatment in [21], which can be applied to a broader range of coaxial cables than just the circularly symmetrical conventional coaxial cable in Figure 2-46. The simplest possible field distribution is shown in Figure 2-46(b). The first parameter to be

developed is C . For this, the charge on one of the conductors is related to the voltage between the conductors. Consider a section of line of length Δz , then using Gauss's law, Equation (1.50), the electric flux is related to the total charge enclosed. So at radius r ,

$$\oint_s \bar{D} = Q_{\text{enclosed}} \\ 2\pi r D_r(r) \Delta z = \rho_\ell \Delta z \quad \text{and} \quad 2\pi r \varepsilon E_r(r) \Delta z = \rho_\ell \varepsilon \Delta z, \quad (2.255)$$

where ρ_ℓ is the charge on the inner conductor per unit length (in the z direction). So the radial electric field is

$$\bar{E} = E_r(r) \hat{\mathbf{r}} = \frac{\rho_\ell}{2\pi r \varepsilon} \hat{\mathbf{r}} \quad (2.256)$$

and \mathbf{r} is the unit vector in the radial direction. The voltage between the conductors is

$$V = \int_a^b E_r \cdot dr = \int_a^b \frac{\rho_\ell}{2\pi r \varepsilon} \cdot dr = \frac{\rho_\ell}{2\pi \varepsilon} \ln \left(\frac{b}{a} \right). \quad (2.257)$$

Now, the total capacitance of a section of line is

$$C_{\text{TOTAL}} = C \Delta z = \frac{Q}{V} = \frac{\rho_\ell \Delta z}{V}, \quad (2.258)$$

and so the capacitance per unit length of line is (with SI units of F/m)

$$C = \frac{2\pi \varepsilon}{\ln(b/a)}. \quad (2.259)$$

The conductance of the line is found beginning with the current density in the dielectric, which is

$$\mathbf{J} = \sigma \mathbf{E} + j\omega \varepsilon \mathbf{E}. \quad (2.260)$$

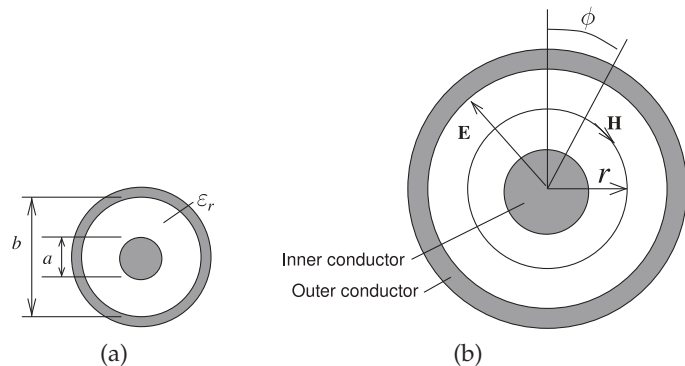
Integrating this over the volume of the dielectric,

$$I = GV + j\omega CV. \quad (2.261)$$

Using a similar development to that which led to Equation (2.259), the conductance per unit length is found to be (with the SI units of S/m)

$$G = \frac{2\pi \sigma}{\ln(b/a)}. \quad (2.262)$$

Figure 2-46: Coaxial line: (a) with inner an conductor of radius a and an outer conductor with inside radius b ; and (b) with cylindrical coordinates used in calculation.



The development of the expressions for L and R is more involved, as there will be current in the interior of the inner conductor. To simplify matters the high-frequency limit will be considered where the skin effect is fully established so that the currents on the inner and outer conductors are confined to a thin layer near the surfaces of the conductors at radius a for the inner conductor and at radius b for the outer conductor. Then the magnetic field will be confined to the region between the conductors. Using Ampere's circuital law, Equation (1.45),

$$\oint_{\ell} \vec{H} \cdot d\vec{\ell} = \oint_{\ell} H_{\phi} \hat{\phi} \cdot d\vec{\ell} = I_{\text{enclosed}} = I, \quad (2.263)$$

where the closed line integral is on a circle of constant radius. Noting that H_r is only a function of r , then for $a < r < b$,

$$I = 2\pi r H_r(r) \quad \text{and} \quad B_r = \mu H_r = \frac{\mu I}{2\pi r}. \quad (2.264)$$

This enables the line inductance to be calculated as the total magnetic flux (obtained by integrating over the cross section of the coaxial line between radii a and b) per unit current. So the inductance of the line per unit length is

$$L = \int_a^b \left(\frac{\mu}{2\pi r} \right) dr = \frac{\mu}{2\pi} \ln \left(\frac{b}{a} \right), \quad (2.265)$$

which has SI units of H/m.

The resistance of the lines is calculated using the surface resistance of the conductors, R_s . So the resistance of the line per unit length is

$$R = \frac{R_s}{2\pi} \left(\frac{1}{a} + \frac{1}{b} \right), \quad (2.266)$$

which has the SI units of Ω/m .

Then the lossless characteristic impedance of the coaxial line is

$$Z_0 = \sqrt{\frac{L}{C}} = \frac{1}{2\pi} \sqrt{\frac{\mu}{\epsilon}} \ln \left(\frac{b}{a} \right), \quad (2.267)$$

which has units of Ω s if all the quantities in the expression are in SI units. A complex characteristic impedance is derived using $Z_0 = \sqrt{(R + j\omega L)/(G + j\omega C)}$, but if the loss is small, this will be very close to the lossless characteristic impedance. Also

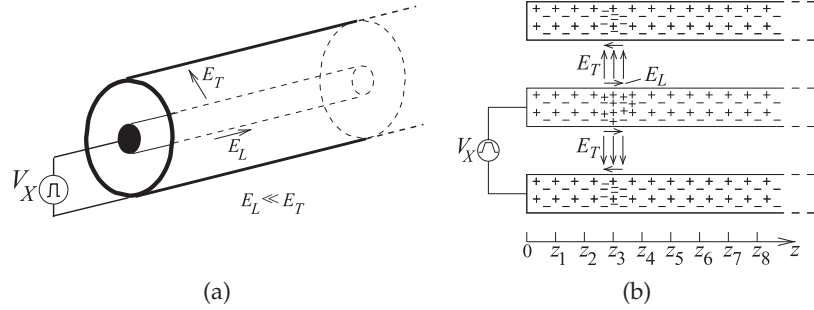
$$Z_0 = \sqrt{\frac{\mu_r}{\epsilon_r}} \frac{1}{2\pi} \sqrt{\frac{\mu_0}{\epsilon_0}} \ln \left(\frac{b}{a} \right) = 60 \sqrt{\frac{\mu_r}{\epsilon_r}} \ln \left(\frac{b}{a} \right). \quad (2.268)$$

Note that the 60 is exact and not an approximation.

For actual coaxial lines the dielectric has negligible loss and the resistance, R , is small. Using the results developed in Section 2.5.4 for a low-loss line, the attenuation coefficient for a low-loss coaxial line is, from Equation (2.149),

$$\alpha \approx \alpha_c = \frac{R}{2Z_0} = \frac{R_s}{2\pi} \left(\frac{1}{a} + \frac{1}{b} \right) \frac{2\pi}{\ln(b/a)} \sqrt{\frac{\epsilon}{\mu}} = \left(\frac{1}{a} + \frac{1}{b} \right) \frac{R_s}{\ln(b/a)} \sqrt{\frac{\epsilon}{\mu}} \quad (2.269)$$

Figure 2-47: A coaxial transmission line: (a) three-dimensional view; (b) the line with pulsed voltage source showing the electric fields at an instant in time as a voltage pulse travels down the line.



which is the attenuation due to the conductor, that is, due to ohmic or conductor loss. From Equation (2.269) it is seen that for a given characteristic impedance, and hence a fixed ratio b/a , the attenuation coefficient and thus loss, is minimized when the line has a large cross section (i.e., large a and b). With a fixed a , attenuation is minimized with $b/a = 3.59$ independent of μ and ϵ [17]. For an air-filled coaxial line with $\mu_r = 1 = \epsilon_r$, the characteristic impedance of this minimum-loss line is 76.7Ω . For a typically Teflon-filled coaxial line $\epsilon_r = 2.1$ and the characteristic impedance of a minimum loss line, from Equation (2.268), is 52.9Ω . The above result is when the conductivity of the inner and outer conductors is the same and the internal inductance of the conductors is negligible. If the internal inductance is not negligible, or the conductors have different conductivity, which happens when the conductors are not solid, then the optimum characteristic impedance could be higher or lower [17]. The choice of 50Ω for the characteristic impedance is a good compromise. Other optimum line dimensions can be derived for maximizing breakdown voltage and optimizing power transfer [22].

The upper operating frequency and dimensions of coaxial lines are chosen to ensure single-mode propagation [23–25]. A useful approximation to the cutoff frequency of the first higher-order mode is [23]

$$\lambda_c \approx \frac{\pi(a+b)}{2}, \quad (2.270)$$

which is the circumference of a circle halfway between the inner and outer conductors. Since b is several times a , then the radius of the outer conductor largely determines the upper operating frequency. Minimizing loss given a fixed cutoff frequency of the first higher-order mode yields another optimum value of b/a for minimum loss (see [22]).

2.9.2 Electromagnetic Fields on a Realistic Coaxial Line

In this section a realistic coaxial line is considered with conductors having a small amount of loss. This expands on the discussion in Section 2.1.2. When a positive voltage pulse is applied to the center conductor of the coaxial line, as shown in Figure 2-47(a), an electric field results that is essentially directed from the center conductor to the outer conductor. A much smaller component of the electric field will also be directed along the line. These fields are shown in Figure 2-47(b), where the direction of the electric field is the direction in which a positive charge would move if it was released into the field. The component of the field that is directed along the shortest path from the center conductor to the outer conductor (in the transverse plane)

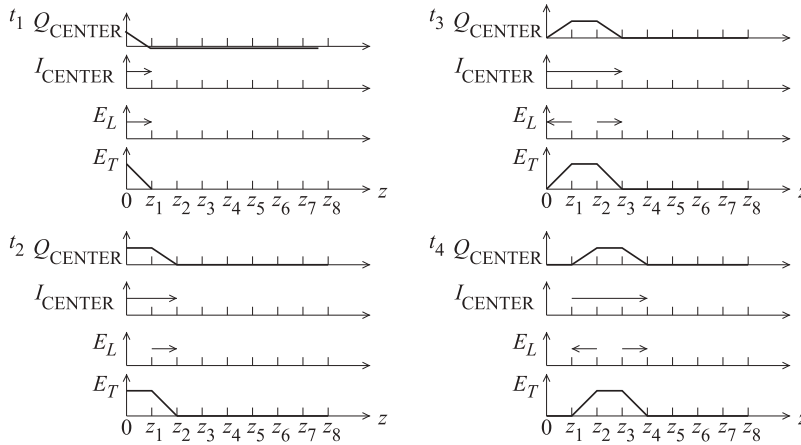


Figure 2-48: Fields, currents, and charges on the coaxial transmission line of Figure 2-2 at times $t_4 > t_3 > t_2 > t_1$. Q_{CENTER} is the net free charge on the center conductor. I_{CENTER} is the current on the center conductor.

is denoted E_T , and the component directed along the line is denoted E_L . (The subscripts T and L denote transverse and longitudinal components, respectively.) Thus, while $E_L \ll E_T$, it is necessary to accelerate electrons on the conductors and so give rise to current flow, and hence the movement of the pulse along the line. The electrons do not accelerate indefinitely, as they collide with atoms and scatter so that there is a net velocity of free electrons along the inner and outer conductors.

Snapshots of a pulse traveling along a line are shown in Figure 2-48 at four different times.

2.10 Summary

In this chapter a classical treatment of transmission lines was presented. Transmission lines are distributed elements and form the basis of microwave circuits. A distinguishing feature is that they support forward- and backward-traveling waves and they can be used to implement circuit functions. RF and microwave engineers are, of course, electrical engineers who learned how to design circuits using lumped elements. Distributed circuits can be made functionally equivalent to lumped-element circuits, at least over a narrow frequency range. The most important technique for establishing this is equating the $ABCD$ parameters of the distributed circuit and those of a lumped-element circuit. As will be seen, this technique will be exploited many times in the rest of this book. Distributed circuits enable an RF designer to realize functions that often have superior performance to their lumped-element analogs. At least at microwave frequencies, the loss of lumped elements can be significantly higher than those of distributed elements. Superior performance can be obtained by exploiting the intrinsic behavior of distributed structures. Sometimes functionality can only be conceived of using transmission-line structures, then, often, a low-frequency lumped-element equivalent can be developed. Exploiting the functionality of distributed structures requires a solid understanding of the behavior, modeling, and circuits that can be realized using transmission lines. The technology covered in this chapter provides the theoretical underpinning for all of the other topics covered in this book.

The most important of the formulas presented in this chapter are listed here. Reflection coefficients are referenced to an impedance Z_0 , the load

impedance is Z_L , and a line has a characteristic impedance Z_0 , physical length ℓ , and propagation constant γ (or electrical length in radians of $\beta\ell$ where ℓ is the physical length of the line).

Reflection coefficient of a load impedance Z_L :	Load impedance in terms of reflection coefficient Γ :	Input reflection coefficient of a lossless line of length ℓ
$\Gamma = \Gamma^V = \frac{Z_L - Z_{\text{REF}}}{Z_L + Z_{\text{REF}}}$ (2.59)	$Z_L = Z_{\text{REF}} \frac{1 + \Gamma}{1 - \Gamma}$ (2.62)	$\Gamma_{\text{in}} = \Gamma_L e^{-j2\beta\ell}$ (2.69)

Input reflection coefficient of a lossy line of length ℓ	Input impedance of a lossless line	Input impedance of a lossy line
$\Gamma_{\text{in}} = \Gamma_L e^{-2\gamma\ell}$ $= \Gamma_L e^{-2\alpha\ell} e^{-2j\beta\ell}$ (2.135)	$Z_{\text{in}} = Z_0 \frac{Z_L + jZ_0 \tan \beta\ell}{Z_0 + jZ_L \tan \beta\ell}$ (2.71)	$Z_{\text{in}} = Z_0 \frac{Z_L + Z_0 \tanh \gamma\ell}{Z_0 + Z_L \tanh \gamma\ell}$ (2.151)

Reflection coefficient in terms of VSWR	VSWR in terms of reflection coefficient
$ \Gamma = \frac{\text{VSWR} - 1}{\text{VSWR} + 1}$ (2.77)	$\text{VSWR} = \frac{(1 + \Gamma)}{(1 - \Gamma)}$ (2.76)

2.11 References

- [1] O. Heaviside, "Electromagnetic induction and its propagation," *Electrician*, Jun. 1887.
- [2] T. Edwards and M. Steer, *Foundations for Microstrip Circuit Design*. John Wiley & Sons, 2016.
- [3] C. Boyer and U. Merzbach, "Invention of logarithms," in *A History of Mathematics*, 2nd ed. John Wiley & Sons, 1991.
- [4] <http://www.minicircuits.com>.
- [5] <http://www.megaphase.com>.
- [6] G. Halford, "A wide-band waveguide phase-shifter," *Proc. IEE, Part III: Radio and Communication Engineering*, vol. 100, no. 65, pp. 117–124, 1953.
- [7] M. Steer, *Microwave and RF Design, Networks*, 3rd ed. North Carolina State University, 2019.
- [8] B. Wadell, *Transmission Line Design Handbook*. Artech House, 1991.
- [9] H. Green, "The numerical solution of transmission line problems," in *Advances in Microwaves*, L. Young, Ed. Academic Press, 1967.
- [10] T.-S. Chen, "Determination of the capacitance, inductance, and characteristic impedance of rectangular lines," *Microwave Theory and Techniques, IRE Trans. on*, vol. 8, no. 5, pp. 510–519, Sep. 1960.
- [11] J. Cruz and R. Brooke, "A variable characteristic impedance coaxial line (correspondence)," *IEEE Trans. on Microwave Theory and Techniques*, vol. 13, no. 4, pp. 477–478, Jul. 1965.
- [12] O. Cruzan and R. Garver, "Characteristic impedance of rectangular coaxial transmission lines," *IEEE Trans. on Microwave Theory and Techniques*, vol. 12, no. 5, pp. 488–495, 1964, also see "Correction to 'Characteristic impedance of rectangular coaxial transmission lines'," *IEEE Trans. Microwave Theory and Tech.*, Vol. 32, No. 2, pp. 219, Feb. 1984.
- [13] S. Cohen, "Beating a problem to death," *Microwave Journal*, vol. 12, no. 11, pp. 22–24, Nov. 1969.
- [14] S. Frankel, "Characteristic impedance of parallel wires in rectangular troughs," *Proc. of the IRE*, vol. 30, no. 4, pp. 182–190, Apr. 1942.
- [15] H. Green, "The characteristic impedance of square coaxial line (correspondence)," *IEEE Trans. on Microwave Theory and Techniques*, vol. 11, no. 6, pp. 554–555, Nov. 1963.
- [16] S. Ramo, J. Whinnery, and T. Van Duzer, *Fields and Waves in Communication Electronics*. John Wiley & Sons, 1965.
- [17] E. Green, F. Liebe, and H. Curtis, "The proportioning of shielded circuits for minimum high-frequency attenuation," *The Bell System Technical Journal*, 1936.
- [18] H. Wheeler, "Transmission-line properties of a strip line between parallel planes," *IEEE Trans. on Microwave Theory and Techniques*, vol. 26, no. 11, pp. 866–876, Nov. 1978.
- [19] P. Lefferson, "Twisted magnet wire transmission line," *IEEE Trans. on Parts, Hybrids, and Packaging*, vol. 7, no. 4, pp. 148–154, Dec. 1971, also see errata, *IEEE Trans. Parts, Hybrids, and Packaging*, Vol. 8, No. 2, p. 67, June 1972.
- [20] R. Collins, *Foundations for Microwave Engineering*. McGraw Hill, 1966.

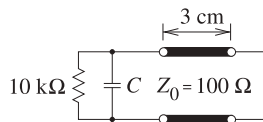
- [21] S. Schelkunoff, "The electromagnetic theory of coaxial transmission lines," *The Bell System Technical Journal*, vol. 13, no. 4, pp. 532–579, Oct. 1934.
- [22] T. Moreno, Ed., *Microwave Transmission Line Data*. Artech House, 1989.
- [23] J. Dimitros, "Exact cutoff frequencies of precision coax," *Microwaves*, pp. 28–31, Jun. 1965.
- [24] H. Green, "Determination of the cutoff of the first higher order mode in a coaxial line by the transverse resonance technique," *IEEE Trans. on Microwave Theory and Techniques*, vol. 37, no. 10, pp. 1652–1653, Oct. 1989.
- [25] N. Marcuvitz, *Waveguide Handbook*. McGraw-Hill, 1955.
- [26] "Standard Reference Data Database, U.S. National Institute of Standards and Technology and References," <http://www.nist.gov/srd>.
- [27] "International Council for Science: Committee on Data for Science and Technology." [Online]. Available: <http://www.codata.org/resources/databases/index.html>
- [28] "ISO/IEC 8000," international Standard Organization (ISO), International Electrotechnical Commission standard including standards on on letter symbols to be used in electrical technology. <http://www.iso.org>.
- [29] H. Haus, W. Atkinson, G. Branch, W. Davenport, W. Fonger, W. Harris, S. Harrison, W. McLeod, E. Stodola, and T. Talpey, "Representation of noise in linear twoports," *Proc. of the IRE*, vol. 48, no. 1, pp. 69–74, Jan. 1960.
- [30] J. Cox, D. Wagman, and V. Medvedev, *CO-DATA Key Values for Thermodynamics*. Hemisphere Publishing Corp., 1989.
- [31] G. Elert, "The physics hypertextbook," <http://hypertextbook.com>, 2007.
- [32] "Reference data for radio engineers, second edition, federal telephone and radio corporation," http://www.pmllett.com/Books/FTR_ref_data.pdf, 1946.
- [33] S. Uma, A. McConnell, M. Asheghi, K. Kurabayashi, and K. Goodson, "Temperature-dependent thermal conductivity of undoped polycrystalline silicon layers," *Int. J. Thermal Physics*, vol. 22, no. 2, pp. 605–616, Mar. 2001.

2.12 Exercises

1. A coaxial line is short-circuited at one end and is filled with a dielectric with a relative permittivity of 64. [Parallels Example 2.1]
 - (a) What is the free-space wavelength at 18 GHz?
 - (b) What is the wavelength in the dielectric-filled coaxial line at 18 GHz?
 - (c) The first resonance of the coaxial resonator is at 18 GHz. What is the physical length of the resonator?
2. A transmission line has the following *RLGC* parameters: $R = 100 \Omega/\text{m}$, $L = 85 \text{ nH/m}$, $G = 1 \text{ S/m}$, and $C = 150 \text{ pF/m}$. Consider a traveling wave on the transmission line with a frequency of 1 GHz. [Parallels Example 2.3]
 - (a) What is the attenuation constant?
 - (b) What is the phase constant?
 - (c) What is the phase velocity?
 - (d) What is the characteristic impedance of the line?
 - (e) What is the group velocity?
3. A transmission line has the per-unit length parameters $L = 85 \text{ nH/m}$, $G = 1 \text{ S/m}$, and $C = 150 \text{ pF/m}$. Use a frequency of 1 GHz. [Parallels Example 2.3]
 - (a) What is the phase velocity if $R = 0 \Omega/\text{m}$?
 - (b) What is the group velocity if $R = 0 \Omega/\text{m}$?
 - (c) If $R = 10 \text{ k}\Omega/\text{m}$ what is the phase velocity?
 - (d) If $R = 10 \text{ k}\Omega/\text{m}$ what is the group velocity?
4. A line is 10 cm long and at the operating frequency the phase constant β is 40 rad/m. What is the electrical length of the line? [Parallels Example 2.2]
5. A dielectric-filled lossless transmission line carrying a 1 GHz signal has the parameters $L = 80 \text{ nH/m}$ and $C = 200 \text{ pF/m}$. When the dielectric is replaced by air the line's capacitance is $C_{\text{air}} = 50 \text{ pF/m}$. What is the relative permittivity of the dielectric?
6. A coaxial transmission line is filled with lossy dielectric material with a relative permittivity of $5 - j0.2$. If the line is air-filled it would have a characteristic impedance of 100Ω . What is the input impedance of the line if it is 1 km long? Use reasonable approximations. [Hint: Does the termination matter?]
7. A transmission line has the per unit length parameters $R = 2 \Omega/\text{cm}$, $L = 100 \text{ nH/m}$, $G = 1 \text{ mS/m}$, $C = 200 \text{ pF/m}$.
 - (a) What is the propagation constant of the line at 5 GHz?
 - (b) What is the characteristic impedance of the line at 5 GHz?
 - (c) Plot the magnitude of the characteristic impedance versus frequency from 100 MHz to 10 GHz.

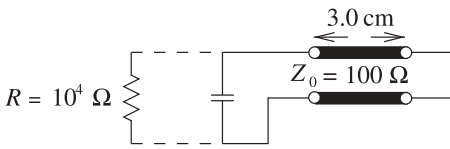
8. A line is 20 cm long and at 1 GHz the phase constant β is 20 rad/m. What is the electrical length of the line in degrees?
9. What is the electrical length of a line that is a quarter of a wavelength long,
 - (a) in degrees?
 - (b) in radians?
10. A lossless transmission line has an inductance of 8 nH/cm and a capacitance of 40 pF/cm.
 - (a) What is the characteristic impedance of the line?
 - (b) What is the phase velocity on the line at 1 GHz?
11. A 50 Ω coaxial airline is a coaxial line without a dielectric (i.e., it is air-filled) and with thin dielectric discs supporting the inner conductor have negligible effect. If the air is replaced by a dielectric having a relative permittivity of 20, what is the characteristic impedance of the dielectric-filled line?
12. A transmission line has an attenuation of 2 dB/m and a phase constant of 25 radians/m at 2 GHz. [Parallels Example 2.4]
 - (a) What is the complex propagation constant of the transmission line?
 - (b) If the capacitance of the line is 50 pF·m⁻¹ and $G = 0$, what is the characteristic impedance of the line?
13. A very low-loss microstrip transmission line has the following per unit length parameters: $R = 2 \Omega/\text{m}$, $L = 80 \text{ nH}/\text{m}$, $C = 200 \text{ pF}/\text{m}$, and $G = 1 \mu\text{S}/\text{m}$.
 - (a) What is the characteristic impedance of the line if loss is ignored?
 - (b) What is the attenuation constant due to conductor loss?
 - (c) What is the attenuation constant due to dielectric loss?
14. A lossless transmission line carrying a 1 GHz signal has the following per unit length parameters: $L = 80 \text{ nH}/\text{m}$, $C = 200 \text{ pF}/\text{m}$.
 - (a) What is the attenuation constant?
 - (b) What is the phase constant?
 - (c) What is the phase velocity?
 - (d) What is its characteristic impedance?
15. A transmission line has a characteristic impedance Z_0 and is terminated in a load with a reflection coefficient of $0.8\angle 45^\circ$. A forward-traveling voltage wave on the line has a power of 1 dBm.
 - (a) How much power is reflected by the load?
 - (b) What is the power delivered to the load?
16. A transmission line has an attenuation of 0.2 dB/cm and a phase constant of 50 radians/m at 1 GHz.
 - (a) What is the complex propagation constant of the transmission line?
 - (b) If the capacitance of the line is 100 pF/m and $G = 0$, what is the complex characteristic impedance of the line?
 - (c) If the line is driven by a source modeled as an ideal voltage and a series impedance, what is the impedance of the source for maximum transfer of power to the transmission line?
 - (d) If 1 W is delivered (i.e. in the forward-traveling wave) to the transmission line by the generator, what is the power in the forward-traveling wave on the line at 2 m from the generator?
17. The transmission line shown in Figure 2-27 consists of a source with Thevenin impedance $Z_1 = 40 \Omega$ and source $E = 5 \text{ V}$ (peak) connected to a $\lambda/4$ long line of characteristic impedance $Z_{01} = 50 \Omega$, which in turn is connected to an infinitely long line of characteristic impedance $Z_{02} = 100 \Omega$. The transmission lines are lossless. Two reference planes are shown in Figure 2-27. At reference plane 1 the incident power is P_{I1} , the reflected power is P_{R1} , and the transmitted power is P_{T1} . P_{I2} , P_{R2} , and (P_{T2}) are similar quantities at reference plane 2. [Parallels Examples 2.20 and 2.22]
 - (a) What is P_{I1} ?
 - (b) What is P_{T2} ?
18. A lossless, 10 cm-long, 75 Ω transmission line is driven by a 1 GHz generator with a Thevenin equivalent impedance of 50 Ω . The maximum power that can be delivered to a load attached to the generator is 2 W. The line is terminated in a load that has a complex reflection coefficient (referred to 50 Ω) of $0.65 + j0.65$. The effective relative permittivity, ϵ_e , of the non-magnetic transmission line is 2.0.
 - (a) Calculate the forward-traveling voltage wave (at the generator end of the transmission line). Ignore reflections from the load at the end of the 75 Ω line.
 - (b) What is the load impedance?
 - (c) What is the wavelength of the forward-traveling voltage wave?
 - (d) What is the VSWR on the line?
 - (e) What is line's propagation constant?
 - (f) What is the input reflection coefficient (at the generator end) of the line?
 - (g) What is the power delivered to the load?

19. The first resonance of a lossless non-magnetic open-circuited transmission line is at 30 GHz. The effective relative permittivity of the line is 12.
- What is the resonator's input impedance?
 - Draw its LC equivalent circuit.
 - What is its electrical length?
 - What is its physical length?
20. An open-circuited transmission line is used as a resonator. What is the electrical length of the line at its first resonance?
21. The second resonance of an open-circuited transmission line is used as a resonator.
- What is its input impedance?
 - What is its electrical length?
22. A lossless transmission line is driven by a 1 GHz generator having a Thevenin equivalent impedance of $50\ \Omega$. The transmission line is lossless, has a characteristic impedance of $75\ \Omega$, and is infinitely long. The maximum power that can be delivered to a load attached to the generator is 2 W.
- What is the total (phasor) voltage at the input to the transmission line?
 - What is the magnitude of the forward-traveling voltage wave at the generator side of the line?
 - What is the magnitude of the forward-traveling current wave at the generator side of the line?
23. A transmission line is terminated in a short circuit. What is the ratio of the forward- and backward-traveling voltage waves at the termination? [Parallels Example 2.5]
24. A $50\ \Omega$ transmission line is terminated in a $40\ \Omega$ load. What is the ratio of the forward- to the backward-traveling voltage waves at the termination? [Parallels Example 2.5]
25. A $50\ \Omega$ transmission line is terminated in an open circuit. What is the ratio of the forward- to the backward-traveling voltage waves at the termination? [Parallels Example 2.5]
26. The resonator below is constructed from a 3.0 cm length of $100\ \Omega$ air-filled coaxial line, shorted at one end and terminated with a capacitor at the other end.



- What is the lowest resonant frequency of this circuit without the capacitor (ignore the $10\ \text{k}\Omega$ resistor)?
 - What is the capacitor value to achieve the lowest-order resonance at 6.0 GHz (ignore the $10\ \text{k}\Omega$ resistor)?
 - Assume that loss is introduced by placing a $10\ \text{k}\Omega$ resistor in parallel with the capacitor. What is the Q of the circuit?
 - Approximately what is the bandwidth of the circuit?
27. A $50\ \Omega$ transmission line is terminated in a load that results in a reflection coefficient of $0.5 + j0.5$.
- What is the load impedance?
 - What is the VSWR on the line?
 - What is the input impedance if the line is one-half wavelength long?
28. Communication filters are often constructed using several shorted transmission line resonators that are coupled by passive elements such as capacitors. Consider a coaxial line that is short-circuited at one end. The dielectric filling the coaxial line has a relative permittivity of 64 and the resonator is to be designed to resonate at a center frequency, f_0 , of 800 MHz. [Parallels Example 2.24]
- What is the wavelength in the dielectric-filled coaxial line?
 - What is the form of the equivalent circuit (in terms of inductors and capacitors) of the one-quarter wavelength long resonator if the coaxial line is lossless?
 - What is the length of the resonator?
 - If the diameter of the inner conductor of the coaxial line is 2 mm and the inside diameter of the outer conductor is 5 mm, what is the characteristic impedance of the coaxial line?
 - Calculate the input admittance of the dielectric-filled coaxial line at $0.99f_0$, f_0 , and $1.01f_0$. Determine the numerical derivative of the line admittance at f_0 .
 - Derive the values of the equivalent circuit of the resonator at the resonant frequency and derive the equivalent circuit of the resonator. Hint: Match the derivative expression derived in (e) with the actual derivative derived in Example 2.24.
29. Develop an analytic formula relating a reflection coefficient (Γ_1) in one reference system (Z_{01}) to a reflection coefficient (Γ_2) in another reference system (Z_{02}).
30. A line has a characteristic impedance Z_0 and is terminated in a load with a reflection coefficient of 0.8. A forward-traveling voltage wave on the line has a power of 1 W.
- How much power is reflected by the load?
 - What is the power delivered to the load?

31. A load consists of a shunt connection of a capacitor of 10 pF and a resistor of 25 Ω . The load terminates a lossless 50 Ω transmission line. The operating frequency is 1 GHz. [Parallels Example 2.6]
 - (a) What is the impedance of the load?
 - (b) What is the normalized impedance of the load (normalized to the characteristic impedance of the line)?
 - (c) What is the reflection coefficient of the load?
 - (d) What is the current reflection coefficient of the load?
 - (e) What is the standing wave ratio (SWR)?
 - (f) What is the current standing wave ratio (ISWR)?
32. A 50 Ω air-filled transmission line is connected between a 40 GHz source with a Thevenin equivalent impedance of 50 Ω and a load. The SWR on the line is 3.5.
 - (a) What is the magnitude of the reflection coefficient, Γ_L , at the load?
 - (b) What is the phase constant, β , of the line?
 - (c) If the first minimum of the standing wave voltage on the transmission line is 2 mm from the load, determine the electrical distance (in degrees) of the SWR minimum from the load.
 - (d) Determine the angle of Γ_L at the load.
 - (e) What is Γ_L in magnitude-phase form?
 - (f) What is Γ_L in rectangular form?
 - (g) Determine the load impedance, Z_L .
33. A load consists of a resistor of 100 Ω in parallel with a 5 pF capacitor with an electrical signal at 2 GHz.
 - (a) What is the load impedance?
 - (b) What is the reflection coefficient in a 50 Ω reference system?
 - (c) What is the SWR on a 50 Ω transmission line connected to the load?
34. An amplifier is connected to a load by a transmission line matched to the amplifier. If the SWR on the line is 1.5, what percentage of the available amplifier power is absorbed by the load?
35. An output amplifier can tolerate a mismatch with a maximum SWR of 2.0. The amplifier is characterized by a Thevenin equivalent circuit with an impedance of 50 Ω and is connected directly to an antenna characterized by a load resistance R_L . Determine the tolerance limits on R_L so that the amplifier does not self-destruct.
36. A load has a reflection coefficient of 0.5 when referred to 50 Ω . The load is placed at the end of a 100 Ω -transmission line.
 - (a) What is the complex ratio of the forward-traveling wave to the backward-traveling wave on the 100 Ω line at the load end of the line?
 - (b) What is the VSWR on the 100 Ω line?
37. A load has a reflection coefficient of 0.5 when referred to 50 Ω . The load is at the end of a line with a 50 Ω characteristic impedance.
 - (a) If the line has an electrical length of 45°, what is the reflection coefficient calculated at the input of the line?
 - (b) What is the VSWR on the 50 Ω line?
38. A 100 Ω resistor in parallel with a 5 pF capacitor terminates a 100 Ω transmission line. Calculate the SWR on the line at 2 GHz.
39. A lossless 50 Ω transmission line has a 50 Ω generator at one end and is terminated in 100 Ω . What is the VSWR on the line?
40. A lossless 75 Ω line is driven by a 75 Ω generator. The line is terminated in a load that with a reflection coefficient (referred to 50 Ω) of $0.5 + j0.5$. What is the VSWR on the line?
41. A load with a 20 pF capacitor in parallel with a 50 Ω resistor terminates a 25 Ω line. The operating frequency is 5 GHz. [Parallels Example 2.7]
 - (a) What is the VSWR?
 - (b) What is ISWR?
42. A load $Z_L = 55 - j55 \Omega$ and the system reference impedance, Z_0 , is 50 Ω . [Parallels Example 2.8]
 - (a) What is the load reflection coefficient Γ_L ?
 - (b) What is the current reflection coefficient?
 - (c) What is the VSWR on the line?
 - (d) What is the ISWR on the line?
 - (e) Now consider a source connected directly to the load. The source has a Thevenin equivalent impedance $Z_G = 60 \Omega$ and an available power of 1 W. Use Γ_L to find the power delivered to Z_L .
 - (f) What is the total power absorbed by Z_G ?
43. A slotted line, as shown in Figure 2-19(c), is used to characterize a 50 Ω line terminated in a load Z_L . $V_{\max} = 1$ V and $V_{\min} = 0.1$ V, and the first minimum is 5 cm from the load. The guide wavelength is 30 cm. What is Z_L ? [Parallels Example 2.9]
44. A shorted coaxial line is used as a resonator. The first resonance is determined to be a parallel resonance and is at 1 GHz.
 - (a) Draw the lumped-element equivalent circuit of the resonator.
 - (b) What is the electrical length of the resonator?

- (c) What is the impedance looking into the line at resonance?
- (d) If the resonator is $\lambda/4$ longer, what is the impedance of the resonator now?
45. A load of $100\ \Omega$ is to be matched to a transmission line with a characteristic impedance of $50\ \Omega$. Use a quarter-wave transformer. What is the characteristic impedance of the quarter-wave transformer?
46. Determine the characteristic impedance of a quarter-wave transformer used to match a load of $50\ \Omega$ to a generator with a Thevenin equivalent impedance of $75\ \Omega$.
47. A transmission line is to be inserted between a $5\ \Omega$ line and a $50\ \Omega$ load so that there is maximum power transfer to the $50\ \Omega$ load at 20 GHz.
- (a) How long is the inserted line in terms of wavelengths at 20 GHz?
- (b) What is the characteristic impedance of the line at 20 GHz?
48. The resonator below is constructed from a 3.0 cm length of $100\ \Omega$ air-filled coaxial line shorted at one end and terminated with a capacitor at the other end:
- 
- (a) What is the lowest resonant frequency of this circuit without the capacitor (ignore the resistor)?
- (b) What is the capacitor value required to achieve resonance at 6.0 GHz?
- (c) Assume that loss is introduced by placing a $10\ \text{k}\Omega$ resistor in parallel with the capacitor. What is the Q of the circuit?
- (d) What is the bandwidth of the circuit?
49. A coaxial transmission line is filled with lossy material with a relative permittivity of $5 - j0.2$. If the line is air-filled it would have a characteristic impedance of $100\ \Omega$.
- (a) What is the characteristic impedance of the dielectric-filled line?
- (b) What is the propagation constant at 500 MHz?
- (c) What is the input impedance of the line if it has an electrical length of 280° and is terminated in a $35\ \Omega$ resistor?
50. A coaxial line is filled with a very slightly lossy material with a relative permittivity of 5. The line would have a characteristic impedance of $100\ \Omega$ if it was air-filled.
- (a) What is the characteristic impedance of the dielectric-filled line?
- (b) What is the propagation constant at 500 MHz? Use the fact that the velocity of an EM wave in a lossless air-filled line is the same as that of free-space propagation in air.
- (c) What is the input impedance of the line if it has an electrical length of 90° and it is terminated in a $35\ \Omega$ resistor?
- (d) What is the input impedance of the line if it has an electrical length of 180° and is terminated in an impedance $j35\ \Omega$?
- (e) What is the input impedance of the line if it is 1 km long? Use reasonable approximations.
51. A lossy transmission line with a characteristic impedance of $60 - j2\ \Omega$ is driven by a generator with a Thevenin equivalent impedance Z_g . If the line is infinitely long, what is Z_g for maximum power transfer from the generator to the line?
52. A $25\ \Omega$ -transmission line is driven by a generator with an available power of 23 dBm and a Thevenin equivalent impedance of $60\ \Omega$. [Parallels Example 2.19]
- (a) What is the Thevenin equivalent generator voltage?
- (b) What is the magnitude of the forward-traveling voltage wave on the line? Assume the line is infinitely long.
- (c) What is the power of the forward-traveling voltage wave?
53. A open-circuited coaxial line is used as a resonator. The first resonance is a series resonance at 2 GHz. [Parallels Example 2.15]
- (a) Draw the lumped-element equivalent circuit of the resonator.
- (b) What is the resonator's electrical length?
- (c) What is the impedance looking into the line at resonance?
- (d) If the resonator is $3\lambda_g/4$ longer, what is the input impedance of the resonator?
54. The forward-traveling wave on a $60\ \Omega$ line has a power of 2 mW. The line is terminated in a resistance of $50\ \Omega$. How much power is delivered to the $50\ \Omega$ load.
55. The forward-traveling wave on a $40\ \Omega$ line has a power of 2 mW. The line is terminated in a resistance of $60\ \Omega$. How much power is in the backward traveling wave?
56. The forward-traveling wave on a $60\ \Omega$ line has a power of 2 mW. The line is terminated in a resistance of $50\ \Omega$. Draw the lumped-element equivalent circuit.

- alent circuit at the interface of the line and the load. [Parallels Example 2.17]
57. A source is connected to a load by a one wavelength long transmission line having a loss of 1.5 dB. The source reflection coefficient (referred to the transmission line) is 0.2 and the load reflection coefficient is 0.5.
 - (a) What is the transmission coefficient?
 - (b) Draw the bounce diagram using the transmission and reflection coefficients. Determine the overall effective transmission coefficient from the source to the load. Calculate the power delivered to the load from a source with an available power of 600 mW.
 58. Consider a coaxial line that is short-circuited at one end. The dielectric filling the line has $\epsilon_r = 20$ and the line has its lowest frequency resonance at 2.4 GHz. [Parallels Example 2.23]
 - (a) What is the guide wavelength?
 - (b) Draw the resonator's equivalent circuit.
 - (c) What is the resonator's physical length?
 59. Consider a lossless coaxial line that is open-circuited at one end and is used as a resonator that is resonant at $f_0 = 2.4$ GHz. The line's dielectric has $\epsilon_r = 81$. [Parallels Example 2.24]
 - (a) What is the wavelength in the line?
 - (b) Draw the lumped-element equivalent circuit of a $\lambda_g/4$ long resonator?
 - (c) What is the resonator's physical length?
 - (d) What is the derivative with respect to frequency of the admittance of the LC equivalent circuit developed in (b).
 - (e) If the diameter of the inner conductor of the line is 1 mm and the inside diameter of the outer conductor is 3 mm, what is the characteristic impedance of the line?
 - (f) Determine the numerical frequency derivative of the line admittance at f_0 .
 - (g) Derive the values of the equivalent circuit of the resonator at resonance.
 60. Develop the lumped-element model of a half wavelength long line having characteristic impedance Z_0 . [Parallels Example 2.25]
 61. The diameter of the inner conductor of a coaxial line is 2 mm and the interior diameter of the outer conductor 8 mm. The coaxial line is filled with polyimide which has a relative permittivity of 3.2.
 - (a) What is the characteristic impedance of the line?
 - (b) Describe the conditions by which a non-TEM mode can be supported. Refer to two different families of higher-order modes.
 - (c) For the coaxial line here, at what frequency will a second propagating mode be first supported?

2.12.1 Exercises By Section

[†]challenging, [‡]very challenging

§2.1 1	23, 24, 25, 26 [†] , 27 [†] , 28 [†] , 29,	§2.5 48 [†] , 49 [†] , 50 [†] , 51, 52 [†] , 53
§2.2 2 [†] , 3, 4, 5, 6, 7, 8, 9, 10, 11,	30 [†] , 31 [†] , 32 [†] , 33 [†] , 34 [†] , 35 [†] ,	§2.6 54, 55, 56, 57 [†]
12, 13, 14 [†] , 15	36 [†] , 37, 38, 39, 40, 41, 42, 43	§2.7 58, 59 [†] , 60
§2.3 16 [†] , 17, 18 [†] , 19 [†] , 20, 21, 22,	§2.4 44 [†] , 45, 46, 47	§2.9 61

2.12.2 Answers to Selected Exercises

11 11.2 Ω	28(e) $j4.55 \cdot 10^{-11} \text{ S} \cdot \text{s}$	46 61.2 Ω
12 $0.23 + j25 \text{ m}^{-1}$	32(f) $0.544 + j0.116$	57 354.2 mW
17(b) 74.0 mW	33(f) 41.45	
28(c) 1.17 cm	35 $25 \Omega \leq Z_L \leq 100 \Omega$	

Appendix

2.A Physical Constants and Material Properties

2.A.1	SI Units	123
2.A.2	Greek Alphabet	127
2.A.3	Conductors, Dielectrics, and Magnetic Materials	127

2.A.1 SI Units

The main SI units used in RF and microwave engineering are given in Table 2-1. Symbols for SI units³ (from the French name *Système International d'Unités*) are written in upright roman font. (Source: U.S. National Institute of Standards and Technology (2006) [26], and 2002 CODATA recommended values of constants [27].)

The International Organization for Standardization (ISO) maintains the International System of Quantities (ISQ) defines the quantities that are measured in SI units [28]. These are set out in the ISO 8000 standard (which is jointly published with the International Electrotechnical Commission (IEC) as the IEC 8000).

- The fundamental units of the SI system are meter, kilogram, second, candela, mole, and Kelvin.
- The unit of length is spelled meter in the United States and metre in other countries.
- The unit designations, such as m for meter, is called a symbol and not an abbreviation.
- Symbols for units are written in lowercase unless the symbol is derived from the name of a person. For example, the symbol for the unit of force is N as it is named after Isaac Newton. An exception is the use of L for liter to avoid possible confusion with l, which looks like the numeral one and the letter i.
- A space separates a value from the symbol for the unit (e.g., 5.6 kg). There is an exception for degrees, with the symbol °. For example, 45 degrees is written 45°.

SI Unit Combinations

When SI units are multiplied a center dot is used. For example, newton meters is written N·m. When a unit is derived from the ratio of symbols then either a solidus (/) or a negative exponent is used; the symbol for velocity (meters per second) is either m/s or m·s⁻¹. The use of multiple solidi for a combination symbol is confusing and must be avoided. So the symbol for acceleration is m·s⁻² or m/s² and not m/s/s. Another example is the thermal conductivity of aluminum at room temperature which is $k = 237 \text{ kW} \cdot \text{m}^{-1} \cdot \text{K}^{-1}$ and not $k = 237 \text{ kW/m/K}$ or $237 \text{ kW/m} \cdot \text{K}$. However, $237 \text{ kW}/(\text{mK})$ is sometimes used.

Consider calculation of the thermal resistance of a rod of cross-sectional area A and length ℓ :

$$R_{\text{TH}} = \frac{\ell}{kA}. \quad (2.271)$$

If $A = 0.3 \text{ cm}^2$ and $\ell = 2 \text{ mm}$, the thermal resistance is

$$R_{\text{TH}} = \frac{(2 \text{ mm})}{(237 \text{ kW} \cdot \text{m}^{-1} \cdot \text{K}^{-1}) \cdot (0.3 \text{ cm}^2)} = \frac{(2 \cdot 10^{-3} \text{ m})}{237 \cdot (10^3 \cdot \text{W} \cdot \text{m}^{-1} \cdot \text{K}^{-1}) \cdot 0.3 \cdot (10^{-2} \cdot \text{m})^2} \quad (2.272)$$

$$= \frac{2 \cdot 10^{-3}}{237 \cdot 10^3 \cdot 0.3 \cdot 10^{-4}} \cdot \frac{\text{m}}{\text{W} \cdot \text{m}^{-1} \cdot \text{K}^{-1} \cdot \text{m}^2} \quad (2.273)$$

$$= 2.813 \cdot 10^{-4} \text{ K} \cdot \text{W}^{-1} = 281.3 \text{ } \mu\text{K/W}. \quad (2.274)$$

This would be an error-prone calculation if the thermal conductivity was taken as 237 kW/m/K .

The use of SI units initially means that calculations can be undertaken without the tedium of tracing units through calculations. This requires that the SI unit of the final result be known and assigned. Repeating the above calculation for the thermal resistance of a rod using Equation (2.271), first express the

³ The older metric systems used different fundamental units; for example, the mks metric system used meter, kilogram, and second as fundamental units; the cgs metric system used centimeter, gram, and second as fundamental units.

Table 2-1: Main SI units used in RF and microwave engineering. The SI units used in electromagnetics are given in Table 1-1.

SI unit	Name	Usage	In terms of fundamental units
A	ampere	current (abbreviated as amp)	Fundamental unit
cd	candela	luminous intensity	Fundamental unit
C	coulomb	charge	A·s
F	farad	capacitance	$\text{kg}^{-1} \cdot \text{m}^{-2} \cdot \text{A}^{-2} \cdot \text{s}^4$
g	gram	weight	=kg/1000
H	henry	inductance	$\text{kg} \cdot \text{m}^2 \cdot \text{A}^{-2} \cdot \text{s}^{-2}$
J	joule	unit of energy	$\text{kg} \cdot \text{m}^2 \cdot \text{s}^{-2}$
K	kelvin	thermodynamic temperature	Fundamental unit
kg	kilogram	SI fundamental unit	Fundamental unit
m	meter	length	Fundamental unit
mol	mole	amount of substance	Fundamental unit
N	newton	unit of force	$\text{kg} \cdot \text{m} \cdot \text{s}^{-2}$
Ω	ohm	resistance	$\text{kg} \cdot \text{m}^2 \cdot \text{A}^{-2} \cdot \text{s}^{-3}$
Pa	pascal	pressure	$\text{kg} \cdot \text{m}^{-1} \cdot \text{s}^{-2}$
s	second	time	Fundamental unit
S	siemen	admittance	$\text{kg}^{-1} \cdot \text{m}^{-2} \cdot \text{A}^2 \cdot \text{s}^3$
V	volt	voltage	$\text{kg} \cdot \text{m}^2 \cdot \text{A}^{-1} \cdot \text{s}^{-3}$
W	watt	power	$J \cdot \text{s}^{-1}$

quantities in SI units: $\ell = 2 \cdot 10^{-2} \text{ m}$; $k = 2.37 \cdot 10^5 \text{ W}/(\text{m} \cdot \text{K})$; and $A = 0.3 \cdot 10^{-4} \text{ m}^2$, then

$$R_{\text{TH}} = \frac{2}{2.37 \cdot 10^5 \cdot 0.3 \cdot 10^{-4}} = 2.813 \cdot 10^{-4}. \quad (2.275)$$

The SI unit of R_{TH} is K/W, so that $R_{\text{TH}} = 2.813 \cdot 10^{-4} \text{ K} \cdot \text{W}^{-1} = 281.3 \text{ } \mu\text{K/W}$.

SI Prefixes

A prefix before a unit indicates a multiple of a unit (e.g., 1 pA is 10^{-12} amps). (Source: 2015 ISO/IEC 8000 [28].) In 2009 new definitions of the prefixes for bits and bytes were adopted [28] removing the confusion over the earlier use of quantities such as kilobit to represent either 1,000 bits or 1,024 bits. Now kilobit (kbit) always means 1,000 bits and a new term kibibit (Kibit) means 1,024 bit. Also the now obsolete usage of kbps is replaced by kbit/s (kilobit per second). The prefix k stands for kilo (i.e. 1,000) and Ki is the symbol for the binary prefix kibi- (i.e. 1,024). (Note that “K” is sometimes used as an abbreviation for 1,024 but this is non-standard.) The symbol for byte (= 8 bits) is “B”.

Table 2-2: SI prefixes.

SI Prefixes			SI Prefixes			Prefixes for bits and bytes		
Symbol	Factor	Name	Symbol	Factor	Name	Name		
10^{-24}	y	yocto	10^1	da	deca	kilobit	kbit	1000 bit
10^{-21}	z	zepto	10^2	h	hecto	megabit	Mbit	1000 kbit
10^{-18}	a	atto	10^3	k	kilo	gigabit	Gbit	1000 Mbit
10^{-15}	f	femto	10^6	M	mega	terabit	Tbit	1000 Gbit
10^{-12}	p	pico	10^9	G	giga	kibibit	Kibit	1024 bit
10^{-9}	n	nano	10^{12}	T	tera	mebibit	Mibit	1024 Kibit
10^{-6}	μ	micro	10^{15}	P	peta	gibibit	Gibit	1024 Mibit
10^{-3}	m	milli	10^{18}	E	exa	tebibit	Tibit	1024 Gibit
10^{-2}	c	centi	10^{21}	Z	zetta	kilobyte	kB	1000 B
10^{-1}	d	deci	10^{24}	Y	yotta	kibibyte	KiB	1024 B

Physical and Mathematical Constants

Physical and mathematical constants in SI units. Source: U.S. National Institute of Standards and Technology (2006) [26], and 2002 CODATA recommended values of constants [27].

Table 2-3: Physical and mathematical constants.

Parameter	Value	Description
c	$299792458 \text{ m} \cdot \text{s}^{-1}$	Speed of light in a vacuum (free space)
e	$1.6021765310^{-19} \text{ C}$	Elementary charge (negative of an electron's charge)
e	2.718281828459045	Natural log base
γ	0.577215664901532	Euler's ratio
ϕ	1.618033988749894	Golden ratio
ϵ_0	$8.854187817 \times 10^{-12} \text{ F} \cdot \text{m}^{-1}$	Permittivity of a vacuum (free space)
h	$6.6260693 \times 10^{-34} \text{ J} \cdot \text{s}$	Planck constant (alt. $\hbar = h/(2\pi)$)
k	$1.3806505 \times 10^{-23} \text{ J} \cdot \text{K}^{-1}$	the Boltzmann constant
m_e	$9.1093826 \times 10^{-31} \text{ kg}$	Electron mass
μ_0	$12.566370614 \times 10^{-7} \text{ N} \cdot \text{A}^{-2}$	Permeability of free space = $4\pi \times 10^{-7} \text{ N} \cdot \text{A}^{-2}$
π	3.14159265358979323846264	Pi, ratio of circumference to diameter of a circle
η	101325 Pa	Standard atmosphere (pressure)
	376.730313461Ω	Characteristic impedance of vacuum (free space)
	$6.241509 \times 10^{18} \text{ eV}$	1 joule of energy in terms of electron-volts
	$1.602176 \times 10^{-19} \text{ J}$	1 eV of energy in joules (the energy required to move a charge e through a potential of 1 V)

Accuracy and Precision

Precision is a description of statistical variability or random error while accuracy includes systematic errors in a measurement or calculation (and these are not random) combined with statistical variability. For example, consider the calculation of the resistance of a uniform length of metal using dimensions (length ℓ , width w , thickness t , which are known accurately) and resistivity ρ where the ρ may not be known accurately. The resistance $R = \rho\ell/(wt)$.

The resistance calculation would not be accurate if the resistivity is not known accurately. However the calculation would be precise if the resistivity of the metal is known to be fixed (and not statistically variable). If the resistivity of the metal varies from place to place, i.e. it is not homogeneous, then there is statistical variability of the resistivity depending on the section of metal chosen and so both the precision and the accuracy of the resistance calculation would be poor. You can have a precise answer that is not accurate, but you cannot have an accurate result that is not precise.

The number of significant digits in a calculation or measurement implies the accuracy and/or precision of a number. Sometimes the accuracy is explicitly stated, for example $4.01 \pm 0.02 \text{ m}$, but more commonly in engineering the number of significant digits implies the accuracy and/or precision. Error is taken to be one half of the last significant digit. So 1200 m implies an accuracy of 0.5 m. While 1.2 km would imply an accuracy of 0.05 km or 20 m. Usually 4 is enough but there are departures from this.

One common situation is when we are talk about the center frequency of a carrier in a communication system. That is because we can precisely set the frequency of a carrier and can put communication bands very close together. For example, if we have frequency bands that are 25 kHz wide on a carriers near 900 MHz. We would need to indicate the frequency of the carrier to a fraction of a kilohertz. So there is a significant difference between specifying a carrier as being at 1.000000 GHz or at 1.000001 GHz. Sometimes however it is not important

to specify frequency so accurately. In the great majority of situations four digits of accuracy is enough, in any case it is very difficult to fabricate something with better than 0.1% accuracy.

When using decibels, a logarithmic scale, two digits after the decimal point is the usually sufficient and required. One digit after the decimal point is not enough accuracy. For example, 0 dB = $10^0 = 1.000$ and 0.1 dB = $10^{0.01} = 1.023$. So if there is only one digit after the decimal point is used then the accuracy implied is 1%. Now 0.01 dB = $10^{0.001} = 1.0023$ and so with two digits after the decimal point the implied accuracy is 0.1% which is about four digits of precision. With four digits after the decimal digit, 0.0001 dB = $10^{0.00001} = 1.000023$, which is the same as claiming around 6 digits of accuracy. Achieving this is highly unlikely except in circumstances involving frequency or when circuits are tuned after fabrication.

There are a few exceptions to the accuracy implied by the number of digits used with decibels. When a number is written as 0 dB or 10 dB, for example, with no digits after the decimal point, then the implication is that it is exactly 0 dB (= 1.00000000) or 10 dB (= 10.00000000). Another exception is a factor of 2 which in decibels is 3.01 dB. It is common to write this as 3 dB and when one sees 3 dB then most people automatically recognize this as a factor of exactly 2. Similarly for 6 dB the implication is that it refers to a factor of exactly 4.

Using more significant digits in a result than is justified can leave an impression of a lack of understanding, that the result was simply a matter of plugging numbers into a calculation rather than understanding what was being done. When an engineer presents results, the observer, usually another engineer, wants to develop trust for the engineering process. Engineering is pragmatic and abstractions are made, you always want to create an impression that you are in control and know what you are doing. Sure interim results can have many significant digits of accuracy but final results should have reasonable accuracy.

Standard Temperatures

Table 2-4: Temperature constants.

Description	Value	In Terms of Fundamental Units
Absolute zero temperature	0 K	Fundamental unit = -273.15°C
Room temperature	290–298 K	19–25°C, generally used as an imprecise measurement implying that properties are unchanged over a few degrees variation.
Standard temperature	290 K	In microwave engineering [29], different in other disciplines.
Available noise of a resistor at room temperature		–174 dBm/Hz. (e.g., in 2 Hz bandwidth the available noise of a resistor at room temperature is –171 dBm). (At 290 K the available noise power is –173.97 dBm/Hz, at 293 K it is –173.93 dBm/Hz, at 298 K it is –173.86 dBm/Hz.)

2.A.2 Greek Alphabet and Additional Characters

Greek alphabet			Greek alphabet			Additional characters	
Name	Upper-case	Lower-case	Name	Upper-case	Lower-case		
alpha	A	α	nu	N	ν	nabla	∇
beta	B	β	xi	Ξ	ξ	cross	\times
gamma	Γ	γ	omicron	O	o	times	\times
delta	Δ	δ	pi	Π	π	varepsilon	ε
epsilon	E	ϵ	rho	P	ρ	varphi	φ
zeta	Z	ζ	sigma	Σ	σ	varpi	ϖ
eta	H	η	tau	T	τ	varrho	ϱ
theta	Θ	θ	upsilon	Υ	υ	varsigma	ς
iota	I	ι	phi	Φ	ϕ	vartheta	ϑ
kappa	K	κ	chi	χ	χ	aleph	\aleph
lambda	Λ	λ	psi	Ψ	ψ		
mu	M	μ	omega	Ω	ω		

2.A.3 Conductors, Dielectrics, and Magnetic Materials

Electrical and thermal properties of RF and microwave materials are given in the tables below. A parameter listed as a range indicates that the parameter depend on the formulation of the alloy. \perp indicates the property in the direction perpendicular to the crystal axis. \parallel indicates the property in the direction parallel to the crystal axis.

Material data from several sources including the *Standard Reference Data* database of the U.S. National Institute of Standards and Technology [26], the CODATA databases of the International Council for Science, Committee on Data for Science and Technology [27], and references [30–33]. Electrical and especially thermal properties are functions of temperature; properties at temperatures other than 300 K should be researched.

Table 2-5:
Relative
permeability
of metals.

Material	Relative permeability μ_r	Material	Relative permeability μ_r
Aluminum	1.00000065	Nickel	50–600
Cobalt	60	Palladium	1.000 8
Copper	0.999 994	Permalloy 45	2 500
Ferrite (NiZn)	16–640	Platinum	1.000 265
Gold	0.999 998	Silver	0.99999981
Iron	5 000–6 000	Steel	100–40 000
Lead	0.999 983	Superconductors	0
Magnesium	1.000 006 93	Supermalloy	100 000
Manganese	1.000 125	Tungsten	1.000 068
Mumetal	20 000–1000 000	Wood (dry)	0.99999942

Some calculations require the use of volumetric heat capacity, c_v obtained from

$$c_v = c_p \rho \quad (2.276)$$

but ensure the use of SI units, i.e. convert the density ρ to $\text{kg} \cdot \text{m}^{-3}$.

The electrical resistivities listed in Table 2-8 for single-element metals are those of single-crystal metals. The resistivity of the best fabricated metal with multiple crystal grains tends to be up to 5% above that of a single-crystal. Poorly fabricated metals can have a resistivity twice as high.

Table 2-6: Electrical properties of dielectrics and nonconductors.

Material	Resistivity ($M\Omega \cdot m$ ρ_r at 300 K)	Relative permittivity (ϵ_r at 1 GHz)	Loss tangent ($\tan \delta$ at 1 GHz)
Air (dry, sea level)	4×10^7	1.0005	0.000
Alumina			
99.5%	$> 10^6$	9.8	0.0001–0.0002
96%	$> 10^6$	9.0	0.0006
85%	$> 10^6$	8.5	0.0015
Aluminum nitride	10^6	8.9	0.001
Bakelite	1–100	4.74	0.022
Beryllium oxide (toxic)	$> 10^8$	6.7	0.004
Diamond	10^5 – 10^{10}	5.68	< 0.0001
Ferrite (MnZn)	0.1 – $10 \Omega \cdot m$	13–16	0.0004
Ferrite (NiZn)	0.1–12.4	13–16	0.0004
FR-4 circuit board	8×10^5	4.3–4.5	0.01
GaAs	1.0	12.85	0.0006
InP	Up to 0.001	12.4	0.001
Glass	2×10^8	4–7	0.002
Mica	2×10^5	5.4	0.0006
Mylar	10^{10}	3.2	0.005
Paper, white	3.5×10^6	3	0.008
Polyethylene	$> 10^7$	2.26	0.0002
Polyimide	10^{10}	3.2	0.005
Polypropylene	$> 10^7$	2.25	0.0003
Quartz (fused)	7.5×10^{11}	3.8	0.00075
Sapphire			
//	$> 10^6$	11.6	0.00004–0.00007
\perp	$> 10^6$	9.4	0.00004–0.00007
Polycrystalline	$> 10^6$	10.13	0.00004–0.00007
Silicon (undoped)			
Low resistivity (used in CMOS)	$50 \mu\Omega \cdot m$	11.68	0.005
High resistivity	$300 m\Omega \cdot m$	11.68	0.005
Carbide (SiC)	100	10.8	0.002
Dioxide (SiO ₂)	5.8×10^7	3.7–4.1	0.001
Nitride (Si ₃ N ₄)	10^7	7.5	0.001
Poly	0.1–10 $k\Omega \cdot m$	11.7	0.005
Teflon (PTFE)	10^{10}	2.1	0.0003
Vacuum	∞	1	0
Water			
Distilled	182	80	0.1
Ice (273 K)	1	4.2	0.05
Wood (dry oak)	3×10^{11}	1.5–4	0.01
Zirconia (variable)	10^4	28	0.0009

Table 2-7: Thermal properties of dielectrics and nonconductors.

Material	Thermal conductivity, k ($\text{W} \cdot \text{m}^{-1} \cdot \text{K}^{-1}$) (at 300 K)	Specific heat capacity, c_p ($\text{kJ} \cdot \text{kg}^{-1} \cdot \text{K}^{-1}$) (at 25°C)	Density, ρ ($\text{g} \cdot \text{cm}^{-3}$) (at 25°C)	Speed of sound, c_s ($\text{m} \cdot \text{s}^{-1}$) (at 25°C)
Air (dry, sea level)	0.026	1.005	0.0018	343
Alumina (Al_2O_3)				9900–10520
100%	30	0.78	3.8	
99.5%	26.9–30	0.78	3.8	
96%	24.7	0.78	3.8	
85%	16	0.92	3.5	
Aluminum nitride	285	0.74	3.28	11000
Bakelite (wood filler)	0.2–1.4	1.38	1.25–1.36	
Beryllium oxide (toxic)	64–210	1.75 (@0°C)	1.85–2.85	
Diamond	1000–2000	0.52–0.63	3.50–3.53	12000
Ferrite (MnZn)	3.5–5	0.7–0.8	4.9	
Ferrite (NiZn)	3.5–5	0.75	4.5	
FR-4 circuit board	0.16–0.3	0.6	1.3–1.8	
Graphite	25–470	0.71–0.83	1.3–2.27	1200
GaAs	50–59	0.37	5.32	4730
InP	68	0.31	4.81	
Glass	0.8–1.2	0.5–0.84	2.0–8.0	3950–5640
Mica	260–750	0.5	0.72	
Mylar (polyethylene-terephthalate)	0.08	1.19	1.4	1900–2430
Paper (white bond)	40–90	1.4	0.72	
Polyethylene	0.42–0.51	2.3–2.9	2.30	1900–2430
Polyimide	0.12	1.09–1.15	1.43	
Polypropylene	0.35–0.40	1.7–2.0	0.855	2740
Quartz (fused)	1.30–1.44	0.67–0.74	2.2	5800
Sapphire				11100
//	35	0.74–0.78	4.05	
⊥	32	0.74–0.78	4.05	
Polycrystalline Silicon (undoped)	31–33	0.74–0.78	3.97–4.05	
low resistivity (CMOS)	149	0.705	2.34	8433
high resistivity	149	0.705	2.34	8433
carbide (SiC)	350–490	0.75	2.55	13060
dioxide (SiO_2)	1.4	1.0	2.27–2.63	
nitride (Si_3N_4)	28	0.711	3.44	11000
polysilicon	12.5–157	0.71–0.75	2.2–2.3	
Teflon (PTFE)	0.20–0.25	0.97	2.1–2.2	1400
Vacuum	0	0	0	
Water				
Distilled	580	4.18	0.997	1480
Ice (at 273 K)	2.22	2.05	0.917	4000
Wood (dry oak)	170	2	0.6–0.9	3960
Zirconia (variable)	1.7–2.2	0.40–0.50	5.6–6.1	

Table 2-8: Thermal and electrical properties of conductors.

Conductors						
Material	Electrical resistivity, ρ ($n\Omega \cdot m$) (at 20 °C)	Thermal conductivity, k ($W \cdot m^{-1} \cdot K^{-1}$) (at 300 K)	Specific heat capacity, c_p ($kJ \cdot kg^{-1} \cdot K^{-1}$) (at 25°C)	Density, ρ ($g \cdot cm^{-3}$) (at 25°C)	Thermal coefficient of resistance (K^{-1}) (at 20°C)	Speed of sound, c_s ($m \cdot s^{-1}$) (at 20°C)
Aluminum	26.50	237	0.897	2.70	0.004308	6420
Brass	Variable	120	0.38	8.4–8.7	0.0015	3500–4700
Bronze	Variable	110	0.38	7.4–8.9		
Chromium	125	93.9	0.450	7.15		5490
Constantan	500	19.5	0.39	8.9	± 0.00003	
Copper	16.78	401	0.39	8.94	0.004041	3560–4700
Gold	22.14	318	0.129	19.30	0.003715	3240
Graphite						
// c-axis	1 200	1 950	0.71	2.09–2.23	-0.0002	
\perp c-axis	41 000	5.7	0.71	2.09–2.23	-0.0002	
Iridium	47.1	147	0.131	22.6		
Iron (cast,hard)	96.1	80.2	0.449	7.87	0.005671	5600–5900
Lead	208	35.3	0.127	11.3		1160–2200
Manganin	430–480	22	0.406	8.4	± 0.000015	
Mercury	961	8.34	0.139	13.53	0.0089	
Nickel	69.3	90.9	0.445	8.90	0.0058–0.0064	5600
NiChrome	1 100	11.3	0.432	8.40	0.00017	
Palladium	105.4	71.8	0.244	12.0		3070
Platinum	105	71.6	0.133	21.5	0.0037–0.0038	3300
Silver	15.87	429	0.235	10.49	0.003819	3600–3650
Solder						
tin-lead Pb, Sn	17.2	34	0.167	8.89		
50% Pb						
lead-free	170	53.5	0.23	7.25		
77.2% Sn,						
2.8% Ag,						
20% In						
Steel, stainless	720	16	0.483	7.48–8.00		5740–5790
Steel, carbon						
(standard)	208	46	0.49	7.85	0.003–0.006	4880–5050
Tantalum	133	57.5	0.14	16.69	0.0038	
Tin	115	66.8	0.227	7.27		3300
Titanium	4 200	21.9	0.522	4.51		6070–6100
Tungsten	52.8	173	0.132	19.3	0.004403	5200
Zinc	59.0	116	0.388	7.14	0.0037–0.0038	4200

Planar Transmission Lines

3.1	Introduction	131
3.2	Substrates	132
3.3	Planar Transmission Line Structures	135
3.4	Modeling of Transmission Lines	138
3.5	Microstrip Transmission Lines	139
3.6	Microstrip Design Formulas	150
3.7	Stripline	151
3.8	Co-Planar Waveguide	155
3.9	Summary	159
3.10	References	160
3.11	Exercises	161

3.1 Introduction

The majority of transmission lines used in high-speed digital, RF, and microwave circuits are planar, as these can be defined using masks, photoresist, and etching of metal sheets. The most common planar transmission line is the microstrip line shown in Figure 3-1 and in cross section in Figure 3-2. This cross section is typical of what would be found on a semiconductor or **printed wiring board (PWB)**, which is also called a **printed circuit board (PCB)**. Current flows in both the top and bottom conductor, but in opposite directions. The physics is such that if there is a signal current on the top conductor, there must be a return signal current, which will tend to be as close to the signal current as possible to minimize stored energy. The provision of a signal return path close to the signal path is important in maintaining the integrity of (i.e., a predictable signal waveform on) an interconnect.

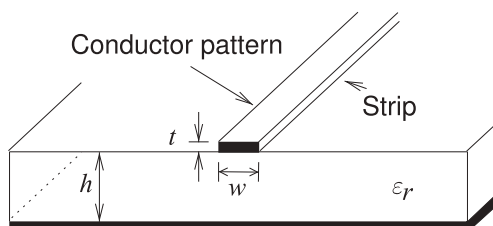


Figure 3-1: Microstrip transmission line.

Figure 3-2: Cross-sectional view of a microstrip line showing electric and magnetic field lines and current flow. The electric and magnetic fields are in two mediums—the dielectric and air. If the line is homogeneous (the same dielectric everywhere) the electric and magnetic fields are only in the transverse plane, a field configuration known as the transverse electromagnetic mode (TEM).

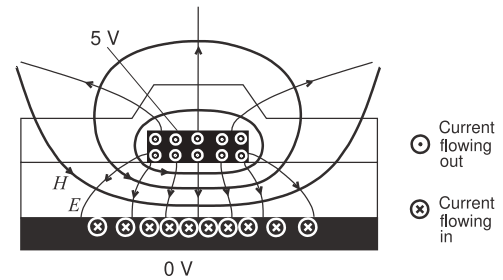
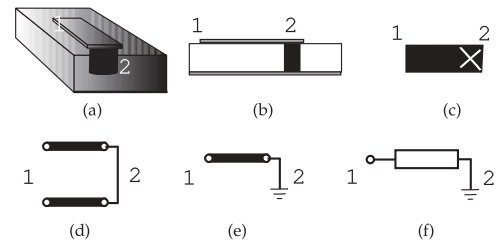


Figure 3-3: Representations of a shorted microstrip line with a short (or via) at port 2: (a) three-dimensional (3D) view indicating via; (b) side view; (c) top view with via indicated by X; (d) schematic representation of transmission line; (e) alternative schematic representation; and (f) representation as a circuit element.



In the microstrip line, electric field lines start on one of the conductors and finish on the other and are located almost entirely in the plane transverse to the long length of the line. The magnetic field is also mostly confined to the transverse plane, and so this line is referred to as a **transverse electromagnetic (TEM)** line. Integrating the electric field along a path gives the voltage. Since the voltage between the top and bottom conductors is more or less the same everywhere, longer E field lines correspond to lower levels of E field. The strength of the E field is also indicated by the density of the E field lines. This is a drawing convention for both electric and magnetic fields. A further comment is warranted for this line. This line is more accurately called a **quasi-TEM** line, as the longitudinal fields, particularly in the air region, are not negligible. The relative level of the longitudinal fields increases with frequency, but below about 10 GHz and for typical dimensions used, the line is still essentially TEM. In Figure 3-2 current flows in the strip and a return current flows in what is normally regarded as the ground conductor. Both the signal and return currents induce a magnetic field and the closed path integral of the magnetic field is equal to the current enclosed by the path.

Various schematic representations of a microstrip line are used. Consider the representations in Figure 3-3 of a length of microstrip line shorted by a via at the end denoted by “2” (specifically the “2” refers to Port 2). The views in Figure 3-3(a and b) provide perspectives. The representations shown in Figure 3-3(d–f) are symbols used in circuit diagrams with the one used depending on the number of microstrip lines in a circuit diagram. If a circuit diagram has many transmission line elements, then the simple representation of Figure 3-3(f) is most common. If there are few transmission line elements, then the representation of Figure 3-3(d) is most common.

3.2 Substrates

Planar transmission line design involves choosing both the transmission line structure to use and the substrate. In this section the electrical properties of materials will be discussed and then substrates commonly used with planar

interconnects will be considered.

3.2.1 Dielectric Effect

The presence of material between the conductors alters the electrical characteristics of the interconnect. With a dielectric, the application of an electric field moves the centers of positive and negative charge at the atomic and molecular level. Moving the charge centers changes the amount of energy stored in the electric field—a process akin to storing energy in a stretched spring. The extra energy storage property is described by the **relative permittivity**, ε_r , which is the ratio of the permittivity of the material to that of free space:

$$\varepsilon_r = \varepsilon / \varepsilon_0. \quad (3.1)$$

The relative permittivities of materials commonly used with interconnects range from 2.08 for TeflonTM, used in high-performance PCBs and coaxial cables, to 11.9 for silicon (Si), to 3.8–4.2 for silicon dioxide (SiO₂), and 12.4 for gallium arsenide (GaAs).

When the fields are in more than one medium (a **nonhomogeneous transmission line**), as for the microstrip line, the effective relative permittivity, $\varepsilon_{r,e}$ (or usually just $\varepsilon_e = \varepsilon_{r,e}$), is used. The characteristics of the nonhomogeneous line are then more or less the same as for the same structure with a uniform dielectric of permittivity, $\varepsilon_{\text{eff}} = \varepsilon_e \varepsilon_0$. The ε_{eff} changes with frequency as the proportion of energy stored in the different regions changes. This effect is called **dispersion** and causes a pulse to spread out as the different frequency components of the pulse want to travel at different speeds.

3.2.2 Dielectric Loss Tangent, $\tan \delta$

Loss in a dielectric comes from two sources: (a) **dielectric damping** (also called **dielectric relaxation**) and (b) conduction losses in the dielectric. Dielectric damping originates from the movement of charge centers resulting in mechanical distortion of the dielectric lattice. An alternating electric field results in vibrational (or phonon) energy in the dielectric, thus energy is lost from the electric field. It is easy to see that this loss increases linearly with frequency and is zero at DC. Because of this, in the frequency domain loss is described by incorporating an imaginary term in the **permittivity**. So now the permittivity of a dielectric becomes

$$\varepsilon = \varepsilon_r \varepsilon_0 = \varepsilon' - j\varepsilon'' = \varepsilon_0 (\varepsilon'_r - j\varepsilon''_r). \quad (3.2)$$

If there is no dielectric damping loss, $\varepsilon'' = 0$. The other type of loss that occurs in the dielectric is due to the movement of charge carriers in the dielectric. The ability to move charges is described by the conductivity, σ , and the loss due to current conduction is independent of frequency. So the energy lost in the dielectric is proportional to $\omega\varepsilon'' + \sigma$ and the energy stored in the electric field is proportional to $\omega\varepsilon'$. Thus a loss tangent is introduced:

$$\tan \delta = \frac{\omega\varepsilon'' + \sigma}{\omega\varepsilon'}. \quad (3.3)$$

Also the relative permittivity can be redefined as

$$\varepsilon_r = \varepsilon'_r - j \left(\varepsilon''_r + \frac{\sigma}{\omega \varepsilon_0} \right). \quad (3.4)$$

With the exception of silicon, the loss tangent is very small for dielectrics that are useful at RF and microwave frequencies and so most of the time

$$|\varepsilon_r| \approx \varepsilon'_r, \quad (3.5)$$

and this is what is quoted as the permittivity of a material. Thus

$$\varepsilon_r = \varepsilon'_r - j(\varepsilon''_r + \sigma/(\omega \varepsilon_0)) \approx \varepsilon'_r(1 - j \tan \delta). \quad (3.6)$$

3.2.3 Magnetic Material Effect

A similar effect on energy storage in the magnetic field occurs for a few materials. The magnetic properties of materials are due to the magnetic dipole moments that result from alignment of electron spins—an intrinsic property of electrons. In most materials the electron spins occur in pairs with opposite signs, with the result that there is no net **magnetic moment**. However, in magnetic materials, some of the electron spins are not canceled and there is a net magnetic moment. This net magnetic moment aligns itself with an applied H field and so provides a mechanism for additional storage of **magnetic energy**. The relative permeability, μ_r , describes this effect and

$$\mu = \mu_r \mu_0. \quad (3.7)$$

Most materials have $\mu_r = 1$. One notable exception is nickel, which has a high permeability, is a very convenient processing material, and is often used in electronic packaging for its desirable processing properties.

As with dielectrics, the effect of loss in a magnetic material can be described by its complex permeability:

$$\mu = \mu' - j\mu''. \quad (3.8)$$

Lossy magnetic effects are due to the movement of magnetic dipoles, which creates vibrations in a material and hence loss.

3.2.4 Substrates for Planar Transmission Lines

The properties of a number of common substrate materials are given in Table 3-1; more are given in Appendix 2.A. Crystal substrates such as sapphire, quartz, and semiconductors (Si, GaAs, and InP) have very good dimensional tolerances and uniformity of electrical properties. Many other substrates have high surface roughness and electrical properties that can vary. For example, FR4 is the most common type of printed circuit board substrate and is a weave of fiberglass embedded in resin. So the material is not uniform and in the assembly of a multilayer circuit board layers of FR4 are pressed together and the resin flows so that there is an unpredictable localized variation in the proportion of resin and glass. High-performance FR4 for microwave applications has a fine weave.

Material	$10^4 \tan \delta$ (at 10 GHz)	ϵ_r
Air (dry)	≈ 0	1
Alumina, 99.5%	1–2	10.1
Sapphire	0.4–0.7	9.4, 11.6
Glass, typical	20	5
Polyimide	50	3.2
Quartz (fused)	1	3.8
FR4 circuit board	100	4.3–4.5
RT-duroid 5880	5–15	2.16–2.24
RT-duroid 6010	10–60	10.2–10.7
AT-1000	20	10.0–13.0
Si (high resistivity)	10–100	11.9
GaAs	6	12.85
InP	10	12.4
SiO ₂ (on-chip)	—	4.0–4.2
LTCC (typical, green tape(TM) 951)	15	7.8

Table 3-1: Properties of common substrate materials. The dielectric loss tangent is scaled. For example, for glass, $\tan \delta$ is typically 0.002.

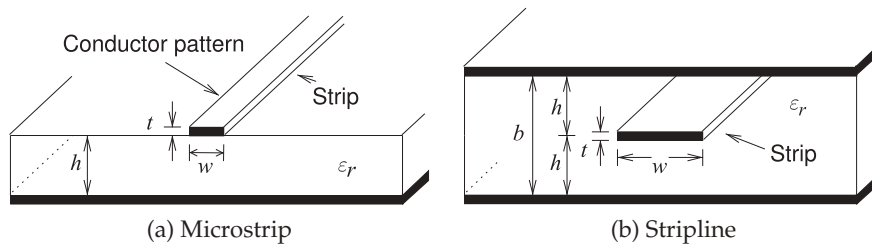


Figure 3-4: Planar transmission lines.

3.3 Planar Transmission Line Structures

Planar transmission lines are the most common transmission lines for high-speed digital, RF, and microwave circuits. Two planar transmission line structures are shown in Figure 3-4. The reason these are so popular is that they can be mass produced. For the microstrip line in Figure 3-4(a) the fabrication process begins with a dielectric sheet with solid metal layers on the top and bottom. One of these is covered with a photosensitive material, called a photoresist, exposed to a prepared pattern that defines the interconnect line network, then the photoresist is developed and the unexposed (or exposed, depending on whether the photoresist is positive or negative) metal on one side is etched away. The stripline in Figure 3-4(b) is fabricated similarly to microstrip but followed by one more step in which a dielectric sheet with a ground plane only is bonded on top.

There are two major categories of planar transmission lines that can be sorted according to the uniformity of the medium surrounding the transmission line conductors. When the embedding medium is uniform the transmission line structures are referred to as homogeneous. If there are two or more regions with different permittivity the transmission line is called inhomogeneous. The most important planar transmission line structures are shown in Figure 3-5. With the homogeneous lines virtually all of the fields are in the plane transverse to the direction of propagation (i.e., the longitudinal direction). Transmission lines where the longitudinal fields are

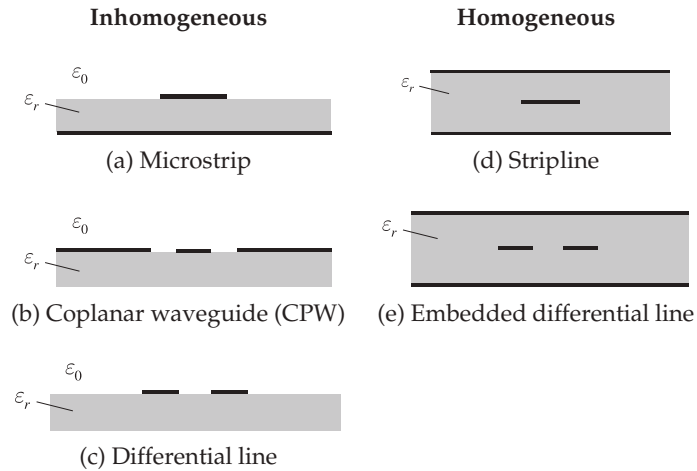


Figure 3-5: Cross sections of several homogeneous and inhomogeneous planar transmission line structures.

almost insignificant are referred to as supporting a TEM mode, and they are called TEM lines.

The most important inhomogeneous lines are shown in Figure 3-5(a–c). The main difference between the two sets of configurations (homogeneous and inhomogeneous) is the frequency-dependent variation of the EM field distributions with inhomogeneous lines. With inhomogeneous lines, the EM fields are not confined entirely to the transverse plane even if the conductors are perfect. However, they are largely confined to the transverse plane and so these lines are called **quasi-TEM lines**. The inhomogeneous lines are simpler to make. Each transmission line structure comprises a combination of metal (shown as dense black) and dielectric (indicated by the shaded region and having permittivity ϵ). It is common not to separately designate the permeability, μ , of the materials because, except for magnetic materials, $\mu = \mu_0$. The region with permittivity ϵ_0 is air. In most cases the dielectric principally supports the metal pattern, acting as a substrate, and clearly influences the wave propagation. The actual choice of structure depends on several factors, including operating frequency and the type of substrate and metallization system available.

3.3.1 Microstrip

Microwave circuits on compound semiconductor substrates (e.g. GaAs) are called **monolithic microwave integrated circuits (MMICs)**. Microwave circuits on silicon (Si) semiconductor substrates are called **radio frequency integrated circuits (RFICs)**. Microwave integrated circuits (MICs) are also called hybrid MICs.

Microstrip (Figure 3-5(a)) is the simplest structure to fabricate beginning with a thin dielectric substrate with metal on both sides. One metal sheet is kept as the electrical ground plane while the other is patterned using photolithography. The metal is chemically etched to form a microstrip transmission network. Although microstrip has a very simple geometric structure, the EM fields involved are complex and cannot be determined analytically. However, simple approaches to the field calculations combined with frequency-dependent expressions yield quite accurate designs. **Microwave integrated circuits (MICs)** using microstrip can be designed for frequencies up to several tens of gigahertz. At higher frequencies, particularly into the millimeter wavelength ranges (above 30 GHz), losses (including radiation) increase significantly, the transmission line characteristics vary greatly with frequency (called frequency dispersion), the field directions cannot be confined to the transverse plane, and fabrication tolerances become exceedingly difficult to meet as the required

substrate thickness becomes very thin. With monolithic ICs, fabrication tolerances are much finer than with hybrid MICs and the options available for both microstrip and other transmission structures are extended.

3.3.2 Coplanar Waveguide

Coplanar waveguide (CPW) (Figure 3-5(b)) [1] supports a quasi-TEM mode of propagation with the active metallization and the ground planes on the same side of the substrate. Each “side-plane” conductor is grounded and the center strip carries the signal, thus much less field enters the substrate when compared with microstrip. In conventional CPW the ground planes extend indefinitely, but in **finite ground CPW (FGCPW)**, the extent of the grounds is limited. It is important to connect the ground strips every tenth of a wavelength or so. This is done using wire bonds, via structures, or in integrated circuit form using air bridges. CPW does a good job of suppressing radiation, it has low frequency dispersion, and is preferred to microstrip for large spatially distributed circuits at frequencies above 20 GHz or so. It does have drawbacks, including the increased area required (compared with microstrip) and the need to use ground straps.

3.3.3 Coplanar Strip and Differential Line

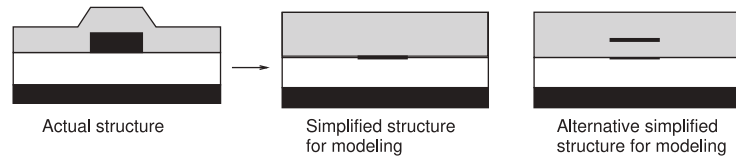
This simple transmission structure (Figure 3-5(c)) is formed by two conductors in the same plane. As with the embedded differential line, the possible existence of ground planes is incidental and ideally these should not influence the field pattern. In one realization, one of the conductors is grounded, and this form is called coplanar stripline or **coplanar strip (CPS)** [2–12]. In this configuration, CPS is used as an area-efficient variation of CPW. When neither of the conductors is grounded and the line is driven differentially, the interconnect is called a differential line. A differential line is used extensively with RFICs and in critical nets in high-speed digital ICs. The two forms have essentially identical electrical characteristics, with differences resulting from interaction with other metallic structures such as ground planes.

Silicon-based RFICs generally use differential signaling for analog signals to overcome the problem of field coupling in high-density circuits and problems due to the finite conductivity of the silicon substrate that results in high levels of circuit noise in the substrate. The currents on each of the differential signal paths balance each other and thus each provides the signal return path for the other. This design practice effectively eliminates RF currents that would occur on ground conductors.

3.3.4 Stripline

Stripline (Figure 3-5(d)) is a symmetrical structure somewhat like a coaxial line completely flattened out so that the center conductor is a rectangular metal strip and the outer grounded metal is an extended rectangular box. The entire structure is 100% filled with dielectric, and therefore transmission is TEM and completely dependent upon the relative permittivity, ϵ_r . Therefore the wavelength is simply the free-space value divided by the square root of ϵ_r . Stripline is fabricated similarly to microstrip, but now a substrate with a ground plane backing is placed on top.

Figure 3-6: A microstrip line modeled as a zero-thickness microstrip line. Also shown is a more accurate alternative simplified structure.



3.3.5 Embedded Differential Line

This simple transmission structure (Figure 3-5(e)) is formed by having just two conductors embedded in a substrate with no specific ground plane. In this structure the possible existence of ground planes is incidental, and ideally these should not influence the field pattern. Essentially the substrate acts as a mechanical supporting element and a quasi-TEM mode forms the main propagating field distribution.

3.4 Modeling of Transmission Lines

Describing the signal on a line in terms of E and H requires a description of the E and H fields in the transverse plane. This can be quite difficult. It is fortunate that current and voltage descriptions can be successfully used to describe the state of a transmission line at a particular position along the line. This is an approximation and the designer needs to be aware of situations where this breaks down. Such extraordinary effects are left to the next chapter. Once the transmission line descriptions have been simplified to current and voltage, R , L , G , and C models of the line can be developed. A range of models are used for transmission lines depending on the accuracy required and the frequency of operation.

Uniform interconnects (with regular cross section) can most accurately be modeled using EM modeling software. Most commonly a specialized type of software called $2\frac{1}{2}$ D EM is used, which only considers current flowing in the horizontal plane or in the vertical direction. A consequence is that planar interconnects are modeled as having zero thickness, as shown in Figure 3-6. This is reasonable for microwave interconnects, as the thickness of a planar strip is usually much less than the width of the interconnect. Many analytic formulas have also been derived for the characteristics of uniform interconnects. These formulas are important in arriving at synthesis formulas that can be used in design (i.e., arriving at the physical dimensions of an interconnect structure from its required electrical specifications). Just as importantly, the formulas provide insight into the effects of materials and geometry.

Simplification of the geometry of the type illustrated in Figure 3-6 for microstrip can lead to appreciable errors in some situations. More elaborate computer programs that capture the true geometry must still simplify the real situation. An example is that it is not possible to account for density variations of the dielectric. Consequently characterization of many RF and microwave structures requires measurements to “calibrate” simulations. Unfortunately it is also difficult to make measurements at microwave frequencies. Thus one of the paradigms in RF circuit engineering is requiring intuition, measurements, and simulations to develop self-consistent models of transmission lines and distributed elements.

3.5 Microstrip Transmission Lines

Transmission lines with conductors embedded in an inhomogeneous dielectric medium cannot support a pure TEM mode. This is the case even if the conductors are lossless. The most important member of this class is the microstrip transmission line (Figure 3-5(c)). Part of the field is in the air and part in the dielectric between the strip conductor and the ground. In most practical cases, the dielectric substrate is electrically thin, that is, $h \ll \lambda$. Then the transverse field is dominant and the fields are called quasi-TEM.

The original analysis of microstrip was based on the unfolding of a coaxial line [13].

3.5.1 Microstrip Line in the Quasi-TEM Approximation

In this section a number of relations are developed based on the principle that the phase velocity of an EM wave in an air-only homogeneous transmission with a TEM field line is just c . It is also shown that the static solutions for the transverse electric field alone can be used to calculate the characteristics of a transmission line. The procedure described is used in many EM computer programs to calculate the characteristics of transmission lines.

As a first step, the potential of the conductor strip is set to V_0 and Laplace's equation is solved using an EM simulator for the electrostatic potential everywhere in the dielectric. Then the per unit length (p.u.l.) electric charge, Q , on the conductor is determined. Using this in the following relation gives the line capacitance:

$$C = \frac{Q}{V_0}.$$

In the next step, the process is repeated with $\epsilon_r = 1$ to determine C_{air} (the capacitance of the line without a dielectric).

If the microstrip line is now an air-filled lossless TEM structure,

$$v_{p,\text{air}} = c = \frac{1}{LC_{\text{air}}} \quad (3.9) \quad \text{and so} \quad L = \frac{1}{c^2 C_{\text{air}}}. \quad (3.10)$$

L is not affected by the dielectric properties of the medium.¹ L calculated above is the desired p.u.l. inductance of the line with the dielectric as well as in free space. Once L and C have been found, the characteristic impedance can be found using

$$Z_0 = \sqrt{\frac{L}{C}}, \quad (3.11) \quad \text{rewritten as} \quad Z_0 = \frac{1}{c} \frac{1}{\sqrt{C C_{\text{air}}}}, \quad (3.12)$$

and the phase velocity is

$$v_p = \frac{1}{\sqrt{LC}} = c \sqrt{\frac{C_{\text{air}}}{C}}. \quad (3.13)$$

Now the field is distributed in the inhomogeneous medium and in free space, as shown in Figure 3-7(a). So the effective relative permittivity, ϵ_e , of the equivalent homogeneous microstrip line (see Figure 3-7(b)) is defined by

$$\sqrt{\epsilon_e} = \frac{c}{v_p}. \quad (3.14)$$

¹ The assumption that L is not affected by the dielectric is a good approximation. However, there is a small discrepancy as a change in the electric field orientation affects the magnetic field, but there is little additional magnetic energy storage.

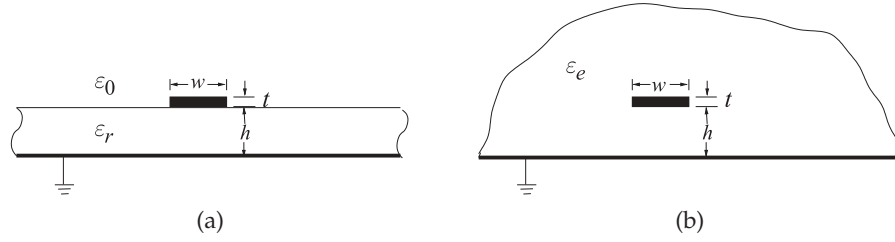


Figure 3-7: Microstrip (a) cross section; and (b) approximate equivalent structure where the strip is embedded in a dielectric of semi-infinite extent with effective relative permittivity ε_e .

Combining Equations (3.13) and (3.14), the effective relative permittivity (usually just the term effective permittivity is used) is obtained:

$$\varepsilon_e = \frac{C}{C_{\text{air}}}. \quad (3.15)$$

The effective permittivity can be interpreted as the permittivity of a homogeneous medium that replaces the air and the dielectric regions of the microstrip, as shown in Figure 3-7. Since some of the field is in the dielectric and some is in air, the effective relative permittivity must satisfy

$$1 < \varepsilon_e < \varepsilon_r. \quad (3.16)$$

However, the minimum ε_e will be greater than 1 as electrical energy will be distributed in air and dielectric. The wavelength on a transmission line, the guide wavelength λ_g , is related to the free space wavelength by $\lambda_g = \lambda_0 / \sqrt{\varepsilon_e}$.

EXAMPLE 3.1

Microstrip Calculations

A microstrip line has a characteristic impedance Z_0 of 50Ω derived from reflection coefficient measurements and an effective permittivity, ε_e , of 7 derived from measurement of phase velocity. What is the line's per-unit-length inductance, L , and capacitance, C ?

Solution: The key equations are $Z_0 = \sqrt{L/C}$, $\varepsilon_e = C/C_{\text{air}}$, and for the air-filled microstrip line (with a TEM mode) $v_p = 1/\sqrt{LC_{\text{air}}} = c$. Also assume that $\mu_r = 1$ which is the default if not specified otherwise and also that L does not change if only the dielectric is changed. Thus

$$C_{\text{air}} = \frac{C}{\varepsilon_e} \quad \text{and then} \quad L = \frac{\varepsilon_e}{c^2 C} \quad \text{so that} \quad Z_0 = \sqrt{\frac{L}{C}} = \frac{\sqrt{\varepsilon_e}}{cC}, \quad \text{that is} \quad C = \frac{\sqrt{\varepsilon_e}}{cZ_0}.$$

So $C = \sqrt{7}/(2.998 \cdot 10^8 \times 50) = 1.765 \cdot 10^{-10} = 176.5 \text{ pF/m}$ and $L = Z_0^2 C = 441.3 \text{ nH/m}$.

3.5.2 Input Impedance of a Shorted Microstrip Line Modeled using a Field Solver

In this example a shorted microstrip line is examined with the aid of a microwave computer-aided design tool. The specific tool used here is National Instruments AWR Design Environment (AWRDE), but most microwave analysis tools will provide the same insight. The project file for the AWR Design Environment is RFDesign_Shorted_Microstrip_Line.emp.

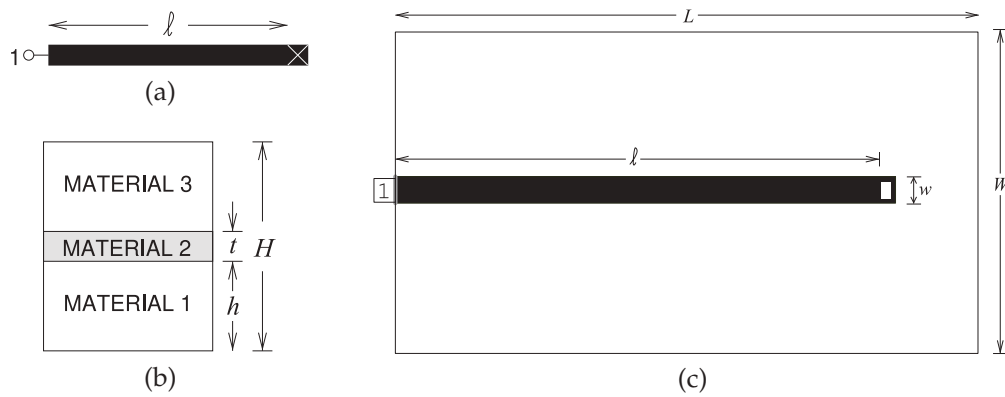


Figure 3-8: Microstrip line layout: (a) microstrip schematic; (b) stack-up of materials with material 1 being the substrate, material 2 being the metal of the strip, and Material 3 being vacuum; and (c) simulation layout. Dimensions are $w = 500 \mu\text{m}$, $\ell = 1 \text{ cm}$. The metal is $t = 6 \mu\text{m}$ thick gold (conductivity $\sigma = 42.6 \times 10^6 \text{ S/m}$) and the alumina substrate height is $h = 600 \mu\text{m}$ with relative permittivity $\epsilon_r = 9.8$ and loss tangent 0.001. The size of the simulation box is defined by $W = 6 \text{ mm}$, $L = 12 \text{ mm}$, and box height $H = 2.61 \text{ mm}$.

The schematic of the microstrip line is shown in Figure 3-8(a). This is what the microstrip looks like from above, with the black region indicating metal and the white cross indicating a via that connects the strip to the ground plane. The distance from the start of the line to the wall of the via is ℓ . The via has a finite length and it is important to take the length of the line up to the wall that terminates the propagating electric and magnetic fields of the microstrip line and not to the center point of the via. While vias are typically cylinders, and so there is not an electric wall across the microstrip, the part of the wall of the via that first encounters the EM fields guided by the microstrip line is a good approximation.

To perform an EM analysis of this line it is necessary to define an enclosure with the cross section shown in Figure 3-8(b) and the top view shown in Figure 3-8(c). The enclosure sets up the walls that terminate the EM field lines. Here the enclosure is a metal box length $L = 12 \text{ mm}$ and width $W = 6 \text{ mm}$. The height of the enclosure depends on the thicknesses assigned to the three materials that comprise the microstrip environment (see Figure 3-8(b)). The enclosure here is a metal box, but options are usually provided to define walls as electric or magnetic walls, and in addition the top walls of the box can be defined as absorbing walls. An absorbing or free-space wall presents an approximation to the free-space conditions. In this example six electric walls are used, with the side walls and top wall spaced a good distance from the line so that the fields are not perturbed by the presence of the side walls.

There are two main types of frequency-domain EM solvers used in microwave engineering. One type uses the finite element method (FEM), which solves for the fields at every grid point in a three-dimensional volume. This can provide a wealth of information and handle a broad range of microwave structures. However, it is very slow and runs into memory problems for all but the simplest structures. The other type of solver is called

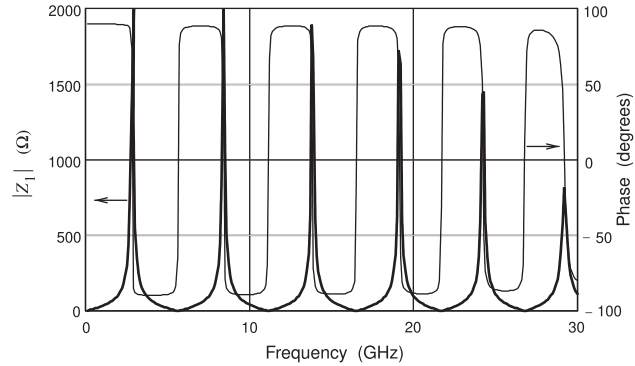


Figure 3-9: Magnitude and phase of the input impedance, Z_{in} , of the microstrip line in Figure 3-8.

a two-and-a-half dimensional (or $2\frac{1}{2}$ D) field solver. This type of solver uses what is called the method of moments to solve for the charges on the surfaces of metals. Fields are not found at every point in space and so a $2\frac{1}{2}$ D field solver is much faster than a 3D solver. The type of solver that will be used here is a $2\frac{1}{2}$ D field solver available in the AWRDE environment and also used in the Sonnet simulations used elsewhere in this book. The restriction that comes with using a $2\frac{1}{2}$ D field solver is that the conductors and dielectrics must be arranged in layers, as shown in Figure 3-8(b). Metals are treated as infinitely thin and, in some tools, dielectrics can be arranged as blocks, but still following the layering protocol.

The layout in the horizontal x - y plane in Figure 3-8(c) is very close to the schematic view shown in Figure 3-8(a). Port 1 (the only port) of the microstrip line is shown on the left in Figure 3-8(a) and in Figure 3-8(c) it is embedded in the left electric wall. As was mentioned, a $2\frac{1}{2}$ D field solver finds the charges on the metal. A grid of cells is established and most often the grid is a regular rectangular mesh and curves and oblique angles can only be approximated. Even when more sophisticated meshes are used, a curved shape is approximated by straight lines. In Figure 3-8(c) the via is inserted as a rectangular cuboid. Another restriction of $2\frac{1}{2}$ D field solvers is that currents must flow either in the x - y plane or in the vertical (z) direction. So as long as the via has a small (relative to a wavelength) dimension in the z direction and the x - y dimensions of the via are small, this is a small restriction in exchange for a simulation that can be thousands of times faster than full 3D methods.

The dimensions of the microstrip were chosen for a characteristic impedance of $50\ \Omega$ yielding $w = 500\ \mu\text{m}$ for the alumina dielectric with relative permittivity $\epsilon_r = 9.8$ and height $h = 600\ \mu\text{m}$. Also $\ell = 1\ \text{cm}$. Often it is necessary to include realistic loss for the materials to obtain physically meaningful results. Here the metal of the line and of the bottom wall is gold with conductivity $\sigma = 42.6 \times 10^6\ \text{S/m}$ and the loss tangent of the alumina is 0.001. The strip has a thickness $t = 6\ \mu\text{m}$. The metal strip is simulated as though it was infinitely thin, but the thickness is used in calculating the resistance of the strip. The dielectric above the strip is free space with permittivity ϵ_0 and with a thickness of 2 mm. So the height of the box $H = h + t + 2\ \text{mm} = 2.610\ \text{mm}$.

The input impedance, Z_{in} , of the shorted microstrip line is shown in Figure 3-9. The plots show the magnitude and phase of the input impedance. The phase is mostly $+90^\circ$ or -90° , indicating that Z_{in} is mostly reactive. At low frequencies near 0 GHz, the input impedance is inductive since

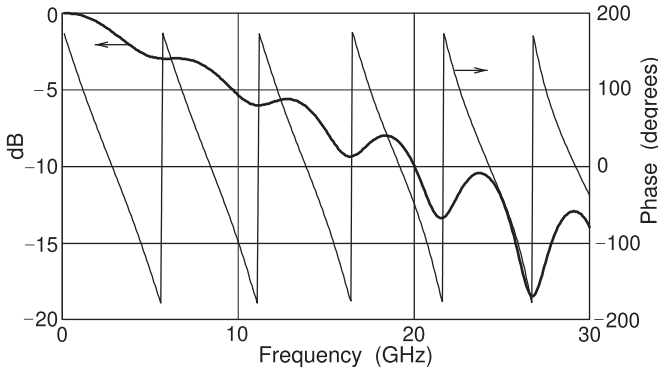


Figure 3-10: Magnitude and phase of the input reflection coefficient, Γ , of the microstrip line in Figure 3-8 but now with a high loss substrate with $\tan \delta = 0.1$.

the phase is approximately $+90^\circ$. Z_{in} increases as would be expected from the approximate model of a shorted line. At 3 GHz, Z_{in} changes from inductive to capacitive going through a near-open circuit. The transition is not instantaneous, as the line is lossy. Z_{in} continues to cycle as the excitation frequency increases.

It is interesting to view what happens when the loss is greatly increased. Here this is done by increasing the loss tangent of the dielectric, $\tan \delta$, to 0.1. This is much higher than that of any useful substrate. The reflection coefficient of the high loss line is shown in Figure 3-10. At very low frequencies $|\Gamma| \approx 0$ dB, i.e., $|\Gamma| \approx 1$. The phase of $\Gamma \approx 180^\circ$ so that $\Gamma \approx -1$ (i.e., a short circuit). As frequency increases $|\Gamma|$ decreases because of increasing dielectric loss and the phase of Γ monotonically decreases as the line becomes electrically longer.

3.5.3 Effective Permittivity and Characteristic Impedance

This section presents formulas for the effective permittivity and characteristic impedance of a microstrip line. These formulas are fits to the results of detailed EM simulations. Also, the form of the equations is based on good physical understanding. First, assume that the thickness, t , is zero. This is not a bad approximation, as $t \ll w, h$ for most microwave circuits.

Hammerstad and others provide well-accepted formulas for calculating the effective permittivity and characteristic impedance of microstrip lines [14–16]. Given ϵ_r , w , and h , the effective relative permittivity is

$$\epsilon_e = \frac{\epsilon_r + 1}{2} + \frac{\epsilon_r - 1}{2} \left(1 + \frac{10h}{w} \right)^{-a \cdot b}, \quad (3.17)$$

$$\text{where } a(u)|_{u=w/h} = 1 + \frac{1}{49} \ln \left[\frac{u^4 + \{u/52\}^2}{u^4 + 0.432} \right] + \frac{1}{18.7} \ln \left[1 + \left(\frac{u}{18.1} \right)^3 \right] \quad (3.18)$$

$$\text{and } b(\epsilon_r) = 0.564 \left[\frac{\epsilon_r - 0.9}{\epsilon_r + 3} \right]^{0.053}. \quad (3.19)$$

Mostly the term “effective permittivity” is used to mean effective relative permittivity (check the magnitude).

Take some time to interpret Equation (3.17), the formula for **effective relative permittivity**. If $\epsilon_r = 1$, then $\epsilon_e = (1 + 1)/2 + 0 = 1$, as expected. If ϵ_r is not that of air, then ϵ_e will be between 1 and ϵ_r , dependent on the geometry of the line, or more specifically, the ratio w/h . For a very wide line, $w/h \gg 1$, $\epsilon_e = (\epsilon_r + 1)/2 + (\epsilon_r - 1)/2 = \epsilon_r$, corresponding to the EM energy being confined to the dielectric. For a thin line $w/h \ll 1$, $\epsilon_e = (\epsilon_r + 1)/2$, the

average of the dielectric and air permittivities.

The characteristic impedance is given by

$$Z_0 = \frac{Z_{01}}{\sqrt{\varepsilon_e}}, \quad (3.20)$$

where the characteristic impedance of the microstrip line in free space is

$$Z_{01} = Z_0|_{(\varepsilon_r=1)} = 60 \ln \left[\frac{F_1 h}{w} + \sqrt{1 + \left(\frac{2h}{w} \right)^2} \right] \quad (3.21)$$

$$\text{and } F_1 = 6 + (2\pi - 6) \exp \left\{ - (30.666h/w)^{0.7528} \right\}. \quad (3.22)$$

The accuracy of Equation (3.17) is better than 0.2% for $0.01 \leq w/h \leq 100$ and $1 \leq \varepsilon_r \leq 128$. Also, the accuracy of Equation (3.21) is better than 0.1% for $w/h < 1000$. Note that Z_0 has a maximum value when w is small.

Now consider the special case where w is vanishingly small. Then ε_e has its minimum value:

$$\varepsilon_e = \frac{1}{2}(\varepsilon_r + 1). \quad (3.23)$$

This leads to an approximate (and convenient) form of Equation (3.17):

$$\varepsilon_e = \frac{(\varepsilon_r + 1)}{2} + \frac{(\varepsilon_r - 1)}{2} \frac{1}{\sqrt{1 + 12h/w}}. \quad (3.24)$$

This approximation has its greatest error of 1% for low and high ε_r and narrow lines, $w/h \ll 1$. Again, Equation (3.20) is used to calculate the characteristic impedance. A comparison of the line characteristics using the more precise formula for ε_e (Equation (3.17)) and the slightly less accurate fit (Equation (3.24)) is given in Table 3-2.

The more exact analysis, represented by Equation (3.17), was used to develop Table 3-3, which can be used in the design of microstrip on a silicon dioxide (SiO_2) substrate and on an FR4 printed circuit board that both have a relative permittivity of 4, on alumina with a permittivity of 10, on a silicon (Si) substrate with a relative permittivity of 11.9, and on a gallium arsenide (GaAs) substrate with a relative permittivity of 12.85.

EXAMPLE 3.2

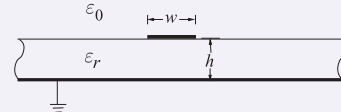
Microstrip Calculations

The strip of a microstrip line has a width of $600 \mu\text{m}$ and is fabricated on a lossless substrate that is $635 \mu\text{m}$ thick and has a relative permittivity of 4.1.

- What is the effective relative permittivity?
- What is the characteristic impedance?
- What is the propagation constant at 5 GHz ignoring any losses?

Solution:

Use the formulas for effective permittivity, characteristic impedance, and attenuation constant from Section 3.5.3 with $w = 600 \mu\text{m}$; $h = 635 \mu\text{m}$; $\varepsilon_r = 4.1$; $w/h = 600/635 = 0.945$.



ε_r	w/h	ε_e Eq. (3.17), 0.2%	Z_0 Eq. (3.17), 0.2%	ε_e Eq. (3.24), 1%	Z_0 Eq. (3.24), 1%
1	0.01	1	401.1	1	401.1
1	0.1	1	262.9	1	262.9
1	1	1	126.5	1	126.5
1	10	1	29.04	1	29.04
1	100	1	3.61	1	3.61
2	0.01	1.525	322.5	1.514	325.9
2	0.1	1.565	210.0	1.545	211.5
2	1	1.645	98.64	1.639	98.83
2	10	1.848	21.36	1.837	21.43
2	100	1.969	2.58	1.972	2.58
10	0.01	5.683	165.8	5.630	169.0
10	0.1	6.016	107.0	5.909	108.2
10	1	6.705	48.86	6.748	48.70
10	10	8.556	9.93	8.534	9.94
10	100	9.707	1.16	9.752	1.16
20	0.01	10.88	119.6	10.77	122.2
20	0.1	11.57	77.14	11.36	78.00
20	1	13.01	35.07	13.13	34.91
20	10	16.93	7.06	16.91	7.06
20	100	19.38	0.821	19.48	0.819
128	0.01	66.90	48.15	66.30	49.25
128	0.1	71.51	31.02	70.27	31.37
128	1	81.12	14.05	82.11	13.96
128	10	71.51	2.80	70.27	2.80
128	100	123.8	0.325	124.5	0.324

Table 3-2: Comparison of two fitted equations for the effective relative permittivity and characteristic impedance of a microstrip line. Equation (3.17) has an accuracy of better than 0.2% and Equation (3.24) has an accuracy of better than 1%.

(a)
$$\varepsilon_e = \frac{\varepsilon_r + 1}{2} + \frac{\varepsilon_r - 1}{2} \left(1 + \frac{10h}{w} \right)^{-a \cdot b}$$

From Equations (3.18) and (3.19),

$$a = 1 + \frac{1}{49} \ln \left[\frac{(w/h)^4 + \{w/(52h)\}^2}{(w/h)^4 + 0.432} \right] + \frac{1}{18.7} \ln \left[1 + \left(\frac{w}{18.1h} \right)^3 \right] = 0.991,$$

$$b = 0.564 \left[\frac{\varepsilon_r - 0.9}{\varepsilon_r + 3} \right]^{0.053} = 0.541.$$

From Equation (3.17), $\varepsilon_e = 2.967$.

(b) In free space,

$$Z_0|_{\text{air}} = 60 \ln \left[\frac{F_1 \cdot h}{w} + \sqrt{1 + \left(\frac{2h}{w} \right)^2} \right],$$

where $F_1 = 6 + (2\pi - 6) \exp \left\{ - (30.666h/\omega)^{0.7528} \right\}$, $Z_0 = Z_0|_{\text{air}} / \sqrt{\varepsilon_e}$

$$Z_0|_{\text{air}} = 129.7 \, \Omega \quad \text{and} \quad Z_0 = Z_0|_{\text{air}} / \sqrt{\varepsilon_e} = 75.3 \, \Omega.$$

(c) $f = 5 \, \text{GHz}$, $\omega = 2\pi f$, $\gamma = j\omega\sqrt{\mu_0\varepsilon_0\varepsilon_e} = j180.5/\text{m}$.

Table 3-3: Microstrip line normalized width $u (= w/h)$ and effective permittivity, ϵ_e , for specified characteristic impedance Z_0 . Data derived from the analysis in Section 3.5.3.

Z_0 (Ω)	$\epsilon_r = 4$ (SiO ₂ , FR4)		$\epsilon_r = 10$ (Alumina)		$\epsilon_r = 11.9$ (Si)	
	u	ϵ_e	u	ϵ_e	u	ϵ_e
140	0.171	2.718	0.028	5.914	0.017	6.907
139	0.176	2.720	0.029	5.917	0.018	6.910
138	0.181	2.722	0.030	5.919	0.019	6.914
137	0.185	2.723	0.031	5.922	0.020	6.919
136	0.190	2.725	0.032	5.924	0.021	6.923
135	0.195	2.727	0.033	5.927	0.022	6.925
134	0.201	2.729	0.035	5.931	0.022	6.927
133	0.206	2.731	0.036	5.933	0.023	6.930
132	0.212	2.733	0.037	5.936	0.024	6.934
131	0.217	2.734	0.038	5.939	0.025	6.937
130	0.223	2.736	0.040	5.942	0.026	6.941
129	0.229	2.738	0.043	5.949	0.028	6.948
128	0.235	2.740	0.044	5.951	0.029	6.951
127	0.241	2.742	0.046	5.955	0.030	6.954
126	0.248	2.744	0.048	5.958	0.031	6.957
125	0.254	2.746	0.050	5.962	0.033	6.963
124	0.261	2.748	0.052	5.966	0.034	6.966
123	0.268	2.750	0.054	5.970	0.035	6.969
122	0.275	2.752	0.056	5.973	0.038	6.977
121	0.283	2.755	0.058	5.977	0.039	6.980
120	0.290	2.757	0.061	5.982	0.041	6.985
119	0.298	2.759	0.063	5.985	0.043	6.990
118	0.306	2.761	0.066	5.990	0.045	6.995
117	0.314	2.763	0.068	5.993	0.047	6.999
116	0.323	2.766	0.071	5.998	0.049	7.004
115	0.331	2.768	0.074	6.003	0.051	7.008
114	0.340	2.771	0.077	6.007	0.053	7.013
113	0.349	2.773	0.080	6.012	0.055	7.017
112	0.359	2.776	0.083	6.016	0.057	7.022
111	0.368	2.778	0.086	6.021	0.060	7.028
110	0.378	2.781	0.089	6.025	0.062	7.032
109	0.389	2.783	0.093	6.031	0.065	7.038
108	0.399	2.786	0.097	6.036	0.068	7.044
107	0.410	2.789	0.100	6.040	0.071	7.050
106	0.421	2.791	0.104	6.046	0.074	7.055
105	0.432	2.794	0.109	6.052	0.077	7.061
104	0.444	2.797	0.113	6.057	0.080	7.066
103	0.456	2.800	0.117	6.062	0.084	7.073
102	0.468	2.803	0.122	6.069	0.087	7.079
101	0.481	2.806	0.127	6.075	0.091	7.085
100	0.494	2.809	0.132	6.081	0.095	7.092
99	0.507	2.812	0.137	6.087	0.099	7.099
98	0.521	2.815	0.143	6.094	0.103	7.105
97	0.535	2.819	0.148	6.100	0.108	7.113
96	0.550	2.822	0.154	6.106	0.112	7.120
95	0.565	2.825	0.160	6.113	0.117	7.127
94	0.580	2.829	0.167	6.121	0.122	7.135
93	0.596	2.832	0.173	6.127	0.128	7.144
92	0.612	2.836	0.180	6.134	0.133	7.151
91	0.629	2.839	0.187	6.142	0.139	7.159
90	0.646	2.843	0.195	6.150	0.145	7.168
89	0.664	2.847	0.202	6.157	0.151	7.176
87	0.701	2.855	0.219	6.173	0.164	7.193
86	0.721	2.859	0.228	6.182	0.171	7.203
85	0.740	2.863	0.237	6.190	0.179	7.213
84	0.761	2.867	0.246	6.198	0.187	7.223
83	0.782	2.872	0.256	6.208	0.195	7.233
82	0.804	2.876	0.266	6.216	0.203	7.242
81	0.826	2.881	0.277	6.226	0.212	7.253
80	0.849	2.885	0.288	6.235	0.221	7.263

Table 3-3 continued.

Z_0 (Ω)	$\epsilon_r = 4$ (SiO ₂ , FR4)	$\epsilon_r = 10$ (Alumina)	$\epsilon_r = 11.9$ (Si)	Z_0 (Ω)	$\epsilon_r = 4$ (SiO ₂ , FR4)	$\epsilon_r = 10$ (Alumina)	$\epsilon_r = 11.9$ (Si)
	u	u	u		u	u	u
79	0.873	2.890	0.299	44	2.518	3.131	1.047
78	0.898	2.895	0.311	43	2.609	3.140	1.096
77	0.923	2.900	0.324	42	2.703	3.150	1.147
76	0.949	2.905	0.337	41	2.803	3.160	1.201
75	0.976	2.910	0.350	40	2.908	3.171	1.259
74	1.003	2.915	0.364	39	3.019	3.181	1.319
73	1.032	2.921	0.379	38	3.136	3.192	1.384
72	1.062	2.926	0.394	37	3.259	3.203	1.452
71	1.092	2.932	0.410	36	3.390	3.214	1.524
70	1.123	2.937	0.426	35	3.528	3.226	1.600
69	1.156	2.943	0.444	34	3.675	3.237	1.682
68	1.190	2.949	0.462	33	3.831	3.250	1.769
67	1.224	2.955	0.480	32	3.997	3.262	1.862
66	1.260	2.961	0.500	31	4.174	3.275	1.961
65	1.298	2.968	0.520	30	4.364	3.288	2.067
64	1.336	2.974	0.541	29	4.567	3.301	2.181
63	1.376	2.980	0.563	28	4.785	3.315	2.304
62	1.417	2.987	0.586	27	5.020	3.329	2.436
61	1.460	2.994	0.610	26	5.273	3.344	2.579
60	1.504	3.001	0.635	25	5.547	3.359	2.734
59	1.551	3.008	0.661	24	5.845	3.374	2.902
58	1.598	3.015	0.688	23	6.169	3.390	3.086
57	1.648	3.022	0.717	22	6.523	3.407	3.287
56	1.700	3.030	0.746	21	6.912	3.424	3.508
55	1.753	3.037	0.777	20	7.341	3.441	3.752
54	1.809	3.045	0.809	19	7.815	3.459	4.022
53	1.867	3.053	0.843	18	8.344	3.478	4.323
52	1.927	3.061	0.878	17	8.936	3.497	4.661
51	1.991	3.069	0.915	16	9.603	3.517	5.043
50	2.056	3.077	0.954	15	10.361	3.538	5.476
49	2.125	3.086	0.995	14	11.229	3.559	5.972
48	2.197	3.094	1.037	13	12.233	3.581	6.547
47	2.272	3.103	1.081	12	13.407	3.604	7.219
46	2.350	3.112	1.128	11	14.798	3.628	8.016
45	2.432	3.121	1.177	10	16.471	3.652	8.975

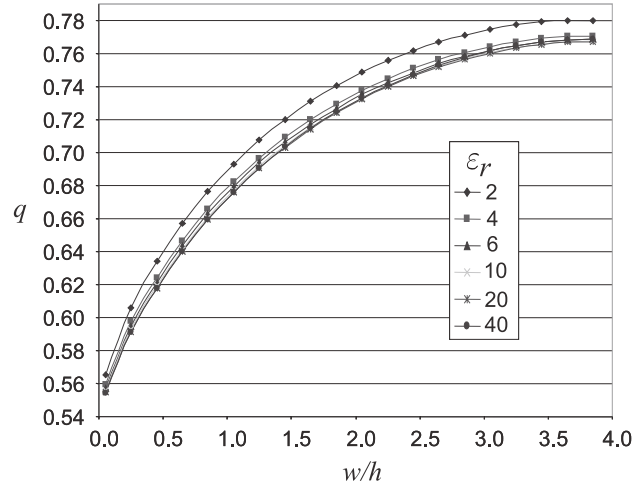


Figure 3-11: Dependence of the q factor of a microstrip line at 1 GHz for various permittivities and aspect (w/h) ratios. (Data obtained from EM field simulations using Sonnet.)

3.5.4 Filling Factor

Defining a filling factor, q , provides useful insight into the distribution of energy in an inhomogeneous transmission line. The effective microstrip permittivity is²

$$\varepsilon_e = 1 + q(\varepsilon_r - 1), \quad (3.25)$$

where for a microstrip line q has the bounds

$$\frac{1}{2} \leq q \leq 1. \quad (3.26)$$

The useful aspect of q is that it is almost independent of ε_r . A q factor of 1 would indicate that all of the fields are in the dielectric region. The dependence of the q of a microstrip line at 1 GHz for various permittivities and aspect (w/h) ratios is shown in Figure 3-11. The properties of a microstrip line, and uniform transmission lines in general, can be described very well by considering the geometric filling factor, q , and the dielectric permittivity separately. Fitting of the microstrip data yields a formula for q in terms of the geometry parameters [19]:

$$q = \frac{1}{2} \left(1 + \frac{1}{\sqrt{1 + 12h/w}} \right). \quad (3.27)$$

3.5.5 Microstrip Resistance

R for a microstrip line is the sum of the resistance of the strip and the resistance of the ground plane:

$$R = R_{\text{strip}} + R_{\text{ground}} \quad (3.28)$$

(with SI units of Ω/m). At low frequencies the current is uniformly distributed in the strip and so

$$R_{\text{strip}} = \frac{\rho}{wt} = \frac{R_s}{w}, \quad (3.29)$$

² The effective permittivity in Equation (3.25) is the upper bound on the permittivity of mixtures [17] and is known as the Maxwell Garnett mixing rule [18].

where ρ (with units of Ωm) is the resistivity of the strip metal, $R_s = \rho/t$ (with units of Ω but referred to as Ω/sq , ohms per square) is the **sheet resistance** (also called the **surface resistance**) of the strip, t is the thickness of the strip, and w is the width of the strip. The sheet resistance is used to indicate the resistance of a sheet of conductor without needing to factor in the thickness t in calculations.

At DC the current is distributed in the ground plane over the full width of the ground. At quite low frequencies this transitions so that the current is not uniformly distributed in the ground plane and the resistance of the ground plane is approximated as [19]

$$R_{\text{ground}} = \frac{R_{sg}}{w} \frac{w/h}{w/h + 5.8 + 0.03h/w}, \text{ for } 0.1 \leq w/h \leq 10, \quad (3.30)$$

where the sheet resistance of the ground plane is R_{sg} . The transition frequency from DC to the low-frequency approximation above has been found to be 1.3 MHz for a microstrip with $w = 200 \mu\text{m}$, $h = 100 \mu\text{m}$, $\epsilon_r = 4$, and a ground plane width of 2 mm (i.e., a very wide ground) [20]. So at RF and microwave frequencies Equation (3.30) should be used as the low-frequency value of R_{ground} . Both R_{strip} and R_{ground} will increase at higher frequencies as then the charges rearrange at much higher frequencies. This will be considered in the next chapter.

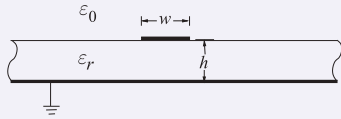
Finally, the attenuation due to the conductor loss, α_c , from Equation (2.149), is $R/2Z_0$ and so

$$\alpha_c = \frac{R_{\text{strip}} + R_{\text{ground}}}{2Z_0}. \quad (3.31)$$

EXAMPLE 3.3 Microstrip Attenuation

If the strip in Example 3.2 has a resistance of $1 \Omega/\text{cm}$ and the ground plane resistance can be ignored, what is the attenuation constant at 5 GHz?

Solution:



For a low-loss line, $\alpha = R/(2Z_0)$ (since there is no dielectric loss), $R = 1 \Omega/\text{cm}$, $Z_0 = 75.3 \Omega$, and so, using Equation (2.149),

$$\alpha = 0.664 \text{ Np/m}.$$

3.5.6 Microstrip Conductance

For a microstrip line, an estimate of G is [19]

$$G = \frac{\epsilon_e - 1}{\epsilon_r - 1} \omega (\tan \delta) \epsilon_r C_{\text{air}}, \quad (3.32)$$

where $\tan \delta$ is the loss tangent of the microstrip substrate and ω is the radian frequency. So from Equations (2.148), (3.12), and (3.32),

$$\alpha_d = \frac{GZ_0}{2} = \frac{1}{2} \frac{\epsilon_e - 1}{\epsilon_r - 1} \omega (\tan \delta) \epsilon_r C_{\text{air}} \frac{1}{c\sqrt{CC_{\text{air}}}}. \quad (3.33)$$

Or, using Equation (3.15), this can be written as

$$\alpha_d = \frac{\omega}{c} (\tan \delta) \frac{\epsilon_r(\epsilon_e - 1)}{2\sqrt{\epsilon_e}(\epsilon_r - 1)} \text{ Np/m.} \quad (3.34)$$

This formula can be used with any TEM transmission line, that is, any transmission line in which the fields are perpendicular to the direction of propagation.

EXAMPLE 3.4 Microstrip “Rule-Of-Thumb”

A rule of thumb is a guideline that is not intended to be accurate but can be easily applied. The accurate formulas for the characteristic impedance and effective permittivity of a microstrip line, Equations (3.20)–(3.24), indicate an underlying trend. The very approximate ‘rule of thumb,’ for characteristic impedance of a microstrip line is

$$Z_{0,\text{ROT}} = \frac{k}{\sqrt{\epsilon_r}} \sqrt{\frac{h}{w}}. \quad (3.35)$$

where k is a constant which is established for a reference line. Taking the reference as $\epsilon_r = 10$ and $w/h = 0.954$ then from Tables 3-2 and 3-3, $Z_{0,\text{REF}} = 50 \Omega$. For this reference $k = 154.4 \Omega$. The following table indicates the accuracy of this rule of thumb.

ϵ_r	w/h	actual $Z_0 (\Omega)$	approximate $Z_{0,\text{ROT}} (\Omega)$	error	ϵ_r	w/h	actual $Z_0 (\Omega)$	approximate $Z_{0,\text{ROT}} (\Omega)$	error
10	1	48.86	48.8	1%	4	2.056	50	53.8	8%
2	1	98.64	109	11%	10	0.954	50	50.0	0%
20	1	35.07	34.5	2%	11.9	0.800	50	50.0	0%
4	0.849	80	83.8	5%	4	4.364	30	37.0	23%
10	0.288	80	91.0	14%	10	2.355	30	31.8	6%
11.9	0.221	80	95.2	19%	11.9	2.067	30	31.1	4%

Thus the trends are correctly described. Even the worst case ($\epsilon = 4, w/h = 4.364$) has an error of 23% for a factor of 11 parameter change from the reference ($\epsilon = 10, w/h = 0.954$).

3.6 Microstrip Design Formulas

The formulas developed in Section 3.5.3 enable the electrical characteristics to be determined given the material properties and the physical dimensions of a microstrip line. In design, the physical dimensions must be determined given the desired electrical properties. Several people have developed procedures that can be used to synthesize microstrip lines [15, 21–24]. This subject is considered in much more depth in [19], and here just one approach is reported. The formulas are useful outside the range indicated, but with reduced accuracy. Again, these formulas are the result of curve fits, but starting with physically based equation forms.

3.6.1 High Impedance

For narrow strips, that is, when $Z_0 > (44 - 2\epsilon_r) \Omega$,

$$\frac{w}{h} = \left(\frac{\exp H'}{8} - \frac{1}{4 \exp H'} \right)^{-1}, \quad (3.36)$$

$$\text{where } H' = \frac{Z_0 \sqrt{2(\epsilon_r + 1)}}{119.9} + \frac{1}{2} \left(\frac{\epsilon_r - 1}{\epsilon_r + 1} \right) \left(\ln \frac{\pi}{2} + \frac{1}{\epsilon_r} \ln \frac{4}{\pi} \right). \quad (3.37)$$

For $Z_0 > (63 - 2\varepsilon_r) \Omega$, [24]

$$\varepsilon_e = \frac{\varepsilon_r + 1}{2} \left[1 + \frac{29.98}{Z_0} \left(\frac{2}{\varepsilon_r + 1} \right)^{1/2} \left(\frac{\varepsilon_r - 1}{\varepsilon_r + 1} \right) \left(\ln \frac{\pi}{2} + \frac{1}{\varepsilon_r} \ln \frac{4}{\pi} \right) \right]^2. \quad (3.38)$$

The formula for ε_e is accurate to better than 1% for $Z_0 > (44 - 2\varepsilon_r) \Omega$ (i.e. $w/h < 1.3$) for $8 < \varepsilon_r < 12$ [24]. Overall the synthesis of w/h has an accuracy of better than 1%.

3.6.2 Low Impedance

Strips with low Z_0 are relatively wide and the formulas below can be used when $Z_0 < (44 - 2\varepsilon_r) \Omega$. The cross-sectional geometry is given by

$$\frac{w}{h} = \frac{2}{\pi} [(d_{\varepsilon_r} - 1) - \ln(2d_{\varepsilon_r} - 1)] + \frac{(\varepsilon_r - 1)}{\pi \varepsilon_r} \left[\ln(d_{\varepsilon_r} - 1) + 0.293 - \frac{0.517}{\varepsilon_r} \right], \quad (3.39)$$

$$\text{where } d_{\varepsilon_r} = \frac{59.95\pi^2}{Z_0 \sqrt{\varepsilon_r}}. \quad (3.40)$$

For $Z_0 < (63 - 2\varepsilon_r) \Omega$ [24]

$$\varepsilon_e = \frac{\varepsilon_r}{0.96 + \varepsilon_r(0.109 - 0.004\varepsilon_r)[\log(10 + Z_0) - 1]}. \quad (3.41)$$

The expression for ε_e is accurate to better than 1% [24] for $8 < \varepsilon_r < 12$ and $8 \leq Z_0 \leq (63 - 2\varepsilon_r) \Omega$.

EXAMPLE 3.5

Microstrip Design

Design a microstrip line to have a characteristic impedance of 75Ω at 10 GHz. The microstrip a substrate that is $500 \mu\text{m}$ thick with a relative permittivity of 5.6. (a) What is the width of the line? (b) What is the effective permittivity of the line?

Solution:

(a) The high-impedance (or narrow-strip) formula (Equation (3.36)) is to be used for $Z_0 > (44 - \varepsilon_r) [= (44 - 5.6) = 38.4] \Omega$.

With $\varepsilon_r = 5.6$ and $Z_0 = 75 \Omega$, Equation (3.37) yields $H' = 2.445$. From Equation (3.36), $w/h = 0.704$, thus $w = w/h \times h = 0.704 \times 500 \mu\text{m} = 352 \mu\text{m}$.

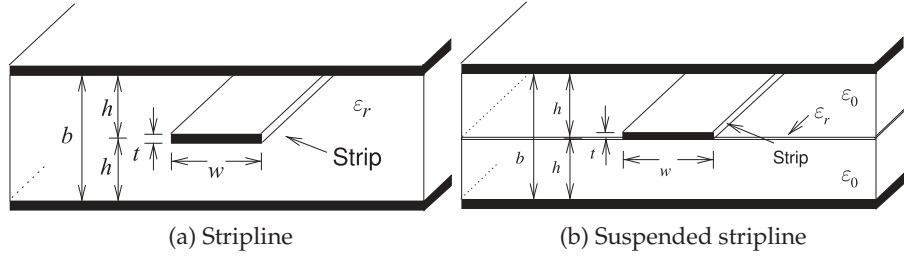
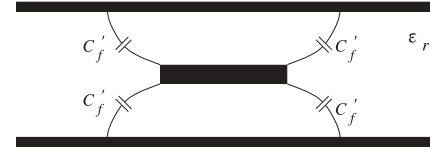
(b) The effective permittivity formula is Equation (3.38), and so $\varepsilon_e = 3.82$.

3.7 Stripline

A symmetrical stripline is shown in Figure 3-12(a). A stripline resembles a microstrip line and comprises a center conductor pattern symmetrically embedded completely within a dielectric, the top and bottom layers of which are conducting ground planes. The strip of width w is considered to have a thickness t that is very small so that the strip is a distance h from each of the ground planes and the ground planes are separated by $b = 2h$. The strip is completely surrounded by the dielectric and so this is a homogeneous medium and there is no need to introduce an effective permittivity.

Figure 3-12:

Stripline transmission lines. In the suspended stripline the strip is supported by a membrane.

**Figure 3-13:** Fringe capacitance at the corners of the strip in a stripline transmission lines.

3.7.1 Characteristic Impedance of a Stripline

Finite Thickness

The characteristic impedance of a stripline is [25, 26]

$$Z_0 = \left[\frac{30\pi}{\sqrt{\epsilon_r}} \right] \frac{(1 - t/b)}{(w_{\text{eff}}/b) + C_f}, \quad (3.42)$$

where the effective width of the strip, w_{eff} , is obtained from

$$\frac{w_{\text{eff}}}{b} = \begin{cases} \frac{w}{b} - \left[\frac{(0.35 - w/b)^2}{(1 + 12t/b)} \right] & \frac{w}{b} < 0.35 \\ \frac{w}{b} & \frac{w}{b} \geq 0.35 \end{cases} \quad (3.43)$$

$$\text{and } C_f = \frac{2}{\pi} \ln \left[\frac{1}{1 - (t/b)} + 1 \right] - \frac{t}{\pi b} \ln \left\{ \frac{1}{[1 - (t/b)]^2} - 1 \right\}. \quad (3.44)$$

C_f accounts for the fringing capacitance at the edges of the strip and incorporates the effect of the strip thickness for $t \ll b$. The fringing capacitance per unit length (e.g., F/m) at each corner of the strip is

$$C'_f = \frac{\epsilon_0 \epsilon_r C_f}{1 - t/b} \quad (3.45)$$

and is shown in Figure 3-13. The accuracy of these formulas is better than 1% for $W/(b - t) > 0.05$ and $t/b < 0.025$.

Zero Thickness

If the strip has zero thickness, the characteristic impedance of stripline is

$$Z_0 = \left[\frac{30\pi}{\sqrt{\epsilon_r}} \right] \frac{1}{(w_{\text{eff}}/b) + 2 \ln 2/\pi} = \frac{94.25}{\sqrt{\epsilon_r}} \frac{1}{(w_{\text{eff}}/b) + 0.441}, \quad (3.46)$$

where the effective width of the strip, w_{eff} , is obtained from

$$\frac{w_{\text{eff}}}{b} = \begin{cases} \frac{w}{b} - \left(0.35 - \frac{w}{b} \right)^2 & \frac{w}{b} < 0.35 \\ \frac{w}{b} & \frac{w}{b} \geq 0.35 \end{cases}. \quad (3.47)$$

The fringing capacitance per unit length at each corner of the strip is

$$C'_f = \frac{\epsilon_0 \epsilon_r 2 \ln 2}{\pi} = 0.441 \epsilon_0 \epsilon_r. \quad (3.48)$$

A stripline supports a purely TEM mode and there is no dielectric dispersion due to an effective permittivity change with frequency. Losses in a stripline are due to dielectric, conductor, and radiative losses. Radiative losses are confined to energy lost to excitation of the parallel plate waveguide mode, but this can be suppressed by shorting the ground planes together at regular intervals (say every tenth of a wavelength).

Formulas have also been developed for the characteristic impedance of asymmetrical stripline, that is, when the strip is not centered between the ground planes [27].

EXAMPLE 3.6 Stripline

A thin strip of a symmetrical stripline has a width of 0.5 mm, is embedded in a dielectric of relative permittivity 5.6, and is between ground planes separated by 1 mm. What is the characteristic impedance of the stripline?

Solution:

The structure is shown in Figure 3-12(a) with $w = 0.5$ mm and $b = 1$ mm. Since the strip is thin, consider that $t = 0$. So from Equations (3.43) and (3.44)

$$\frac{w_{\text{eff}}}{b} = 0.5 \quad \text{and} \quad C_f = 0.441, \quad (3.49)$$

and so

$$Z_0 = \frac{94.25}{\sqrt{5.6}} \frac{1}{(0.5 + 0.441)} = 42.77 \, \Omega. \quad (3.50)$$

3.7.2 Attenuation on a Stripline

For a low-loss stripline with radiation loss suppressed by vias between the ground planes, the attenuation, α , comprises two parts, the conductive attenuation, α_c , and the dielectric attenuation, α_d , so that $\alpha = \alpha_c + \alpha_d$. From Equation (2.149)

$$\alpha_c = \frac{R}{2Z_0}, \quad (3.51)$$

where R is the resistance per unit length of the line. R is the sum of the strip and ground resistances. At low frequencies the resistance of the strip is

$$R_{\text{strip}} = R_s/w, \quad (3.52)$$

where R_s is the sheet resistance of the strip and w is the width of the strip. The treatment for the ground resistance is similar to that described in Section 3.5.5 for microstrip. At low microwave frequencies

$$R_{\text{ground}} = \frac{1}{2} \frac{R_{\text{sg}}}{w} \frac{w/h}{w/h + 5.8 + 0.03h/w}, \quad \text{for } 0.1 \leq w/h \leq 10, \quad (3.53)$$

where the sheet resistance of the ground plane is R_{sg} . The factor of one-half arises because there are two grounds and the resistance from each is in parallel. The effect of the ground on the line resistance is small. Both R_{strip} and R_{ground} will increase at higher frequencies as the charges rearrange at much higher frequencies. This will be considered in the next chapter.

The formula for the dielectric attenuation comes from Equation (3.34). The general formula for the attenuation constant due to dielectric loss is, for a low-loss TEM line,

$$\alpha_d = \frac{\omega}{c} (\tan \delta) \frac{\epsilon_r(\epsilon_e - 1)}{2\sqrt{\epsilon_e}(\epsilon_r - 1)} \text{ Np/m.} \quad (3.54)$$

Since the effective permittivity of a stripline is just the relative permittivity of the substrate, $\epsilon_e = \epsilon_r$, then Equation (3.54) reduces to

$$\alpha_d = \frac{\omega}{2c} (\tan \delta) \sqrt{\epsilon_r} \text{ Np/m} = \frac{1}{2} \omega \sqrt{\mu_0 \epsilon_0 \epsilon_r} (\tan \delta) \text{ Np/m.} \quad (3.55)$$

(Note that here ω is the radian frequency and not the width w .)

The suspended stripline structure shown in Figure 3-12(b) has minimal dielectric and hence minimal dielectric loss. Resonators built using a suspended stripline have a high Q and this structure can be used to realize high-performance filters.

EXAMPLE 3.7

Stripline Attenuation

What is the attenuation of a symmetrical stripline at 1 GHz with $w = h = 0.5$ mm, a $t = 4$ μm -thick strip, silver metallization, and an FR-4 substrate. The ground planes are 4 μm thick. Assume that high frequency effects on line resistance can be ignored.

Solution:

The strip is very thin and the results of Example 3.6 can be used so $Z_0 = 42.77 \Omega$. The resistivity of silver is $\rho_{\text{Ag}} = 14.87 \text{ n}\Omega \cdot \text{m}$ and so the sheet resistivity of the strip, $R_s = \rho_{\text{Ag}}/t = (14.87 \text{ n}\Omega \cdot \text{m})/(4 \mu\text{m}) = 3.968 \text{ m}\Omega$. From Equation (3.52) the resistance of the strip is $R_{\text{strip}} = R_s/w = (3.968 \text{ m}\Omega)/(1 \text{ mm}) = 3.968 \Omega/\text{m}$. The sheet resistance of the grounds is the same as the strip so $R_{sg} = 3.968 \text{ m}\Omega$. From Equation (3.53) the resistance of the grounds is

$$\begin{aligned} R_{\text{ground}} &= \frac{1}{2} \frac{R_{sg}}{w} \frac{w/h}{w/h + 5.8 + 0.03h/w} \\ &= \frac{1}{2} \frac{(3.968 \text{ m}\Omega)}{(1 \text{ mm})} \frac{1}{1 + 5.8 + 0.03} = \frac{3.968 \Omega/\text{m}}{6.83} = 0.581 \Omega/\text{m} \end{aligned} \quad (3.56)$$

so that the total line resistance $R = R_{\text{strip}} + R_{\text{ground}} = 4.549 \Omega/\text{m}$. Thus the attenuation due to conductor loss is $\alpha_c = R/(2Z_0) = 0.1064 \text{ Np/m} = 0.924 \text{ dB/m}$.

FR-4 has negligible conductivity and loss in the dielectric is due to dielectric relaxation. FR-4 has a loss tangent at 1 GHz of 0.01 and a relative dielectric constant of 4.3. From Equation (3.55)

$$\alpha_d = \frac{1}{2} \omega \sqrt{\mu_0 \epsilon_0 \epsilon_r} (\tan \delta) \text{ Np/m.} = 0.2172 \text{ Np/m} = 1.886 \text{ dB/m.} \quad (3.57)$$

The total attenuation $\alpha = \alpha_c + \alpha_d = (0.924 + 1.886) \text{ dB/m} = 2.810 \text{ dB/m}$.

3.7.3 Design Formulas for a Stripline

The synthesis of a symmetrical stripline with a substrate having a relative permittivity ϵ_r and thickness b requires determination of the width of the strip for a particular characteristic impedance [25]. The width w is obtained from

$$\frac{w}{b} = \begin{cases} x & \text{for } Z_0 \leq 120/\sqrt{\epsilon_r} \Omega \\ 0.85 - \sqrt{0.6 - x} & \text{for } Z_0 > 120/\sqrt{\epsilon_r} \Omega, \end{cases} \quad (3.58)$$

where
$$x = \frac{30\pi}{\sqrt{\epsilon_r} Z_0} - \frac{2 \ln 2}{\pi} = \frac{94.25}{\sqrt{\epsilon_r} Z_0} - 0.441. \quad (3.59)$$

3.8 Coplanar Waveguide

Microstrip is the most popular medium for circuit design at frequencies ranging from several hundred megahertz to tens of gigahertz. However, the electrical characteristics of a microstrip line are sensitive to variations of substrate thickness, and radiation from a microstrip line increases when the substrate is thick. The substrate thickness is not well controlled and can vary by 1%–5% in many substrate technologies. As a result, the characteristic impedance will change by about the same amount. This is not acceptable in many designs where it is desirable that microstrip synthesis be accurate to 1% or so. The lateral dimensions, however, are well controlled being photolithographically defined and then etched.

A solution to the problems of microstrip is coplanar waveguide (CPW) shown in Figure 3-14(a). CPW consists of a central strip flanked by two metal half-planes that carry the return current. The outer conductors can be regarded as ground, but they do not need to be explicitly connected to ground. Provided that the substrate is sufficiently thick, in practice this means that the substrate thickness is two or three times greater than both the strip width w and the metal separation s , the electrical characteristics of CPW are entirely determined by the lateral dimensions, since all of the metallization is on one layer.

Of course, the infinite half-grounds of CPW cannot be produced so a more realistic implementation of CPW is **finite ground CPW (FGCPW)**, shown in Figure 3-14(b), where the signal return conductors are of finite width. For both the CPW and FGCPW lines, the vitalization and currents

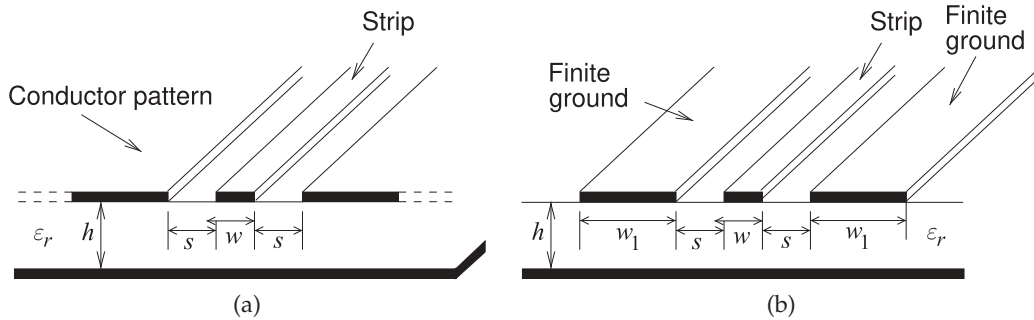


Figure 3-14: Coplanar waveguide (CPW): (a) conventional; and (b) finite ground CPW (FGCPW).

are confined to a single layer. However, the following discussion focuses on the idealized CPW structure in Figure 3-14(a) as this has been studied extensively. However, the characteristics of FGCPW are very close to those of CPW if $w_1 \geq 3w$ (see Figure 3-14(b)).

3.8.1 Effective Permittivity and Characteristic Impedance of CPW

The fields in CPW, and thus the EM energy, are almost equally divided between air and dielectric, especially when the gap is small relative to the thickness of the dielectric. The effective relative permittivity of CPW is [28]

$$\varepsilon_e = \varepsilon_{r,e} = 0.5(\varepsilon_r + 1) \{ \tanh[1.785 \log(h/s) + 1.75] + (ks/h)[0.04 - 0.7k + 0.01(1 - 0.1\varepsilon_r)(0.25 + k)] \}, \quad (3.60)$$

which is accurate to 1.5% for $h/s \geq 1$. In Equation (3.60)

$$k = \frac{w}{w + 2s}. \quad (3.61)$$

Simply taking the effective permittivity as $(\varepsilon_r + 1)/2$ is a good starting point in analysis and design.

The characteristic impedance of CPW is [29]

$$Z_0 = \frac{30\pi}{\sqrt{\varepsilon_e}} \frac{K'(k)}{K(k)}, \quad (3.62)$$

$$\text{where } k' = \sqrt{1 - k^2} \quad \text{and} \quad K'(k) = K(k'). \quad (3.63)$$

$K(k)$ and $K(k')$ are elliptic integrals, but the ratio, which is all that is required, is much simpler [30]:

$$\begin{aligned} \frac{K(k)}{K'(k)} &\approx \frac{1}{\pi} \ln \left(2 \frac{1 + \sqrt{k}}{1 - \sqrt{k}} \right) & 0 \leq k \leq 0.707 \\ \frac{K'(k)}{K(k)} &\approx \frac{1}{\pi} \ln \left(2 \frac{1 + \sqrt{k'}}{1 - \sqrt{k'}} \right) & 0.707 < k \leq 1 \end{aligned} \quad (3.64)$$

Note that with CPW, Z_0 is determined by the ratio of the center strip width w to the gap width s . This makes the design of a CPW line with a particular Z_0 non unique because an infinite range of w and s values will result in a specific Z_0 requirement. This provides additional design flexibility.

EXAMPLE 3.8

CPW

A CPW line is fabricated on a 500 μm thick GaAs substrate, has a strip with a width of 200 μm , and a gap of 200 μm between the strip and the ground planes. The relative permittivity of the substrate is 12.85 and the strip is 10 μm thick. What is the effective permittivity and characteristic impedance of the CPW line?

Solution:

The structure is that shown in Figure 3-14(a) with $w = 500 \mu\text{m}$, $s = 200 \mu\text{m}$, $h = 500 \mu\text{m}$, and $t = 10 \mu\text{m}$. From Equation (3.61),

$$k = \frac{w}{w + 2s} = \frac{500}{500 + 400} = 0.556. \quad (3.65)$$

From Equation (3.60),

$$\begin{aligned}\varepsilon_e &= 0.5(12.85 + 1) \{ \tanh[1.785 \log(500/200) + 1.75] \\ &\quad + (0.556 \cdot 200/500)[0.04 - 0.7 \cdot 0.556 + 0.01(1 - 0.1 \cdot 12.85)(0.25 + 0.556)] \} \\ &= 6.28.\end{aligned}\quad (3.66)$$

This compares to $\varepsilon_e = 6.925$ if the permittivities of air and the substrate are averaged.

Several quantities need to be calculated before calculating Z_0 . Since $0 \leq k \leq 0.707$,

$$\frac{K(k)}{K'(k)} = \frac{1}{\pi} \ln \left(2 \frac{1 + \sqrt{k}}{1 - \sqrt{k}} \right) = 0.833. \quad (3.67)$$

Thus from Equation (3.62),

$$Z_0 = \frac{30\pi}{\sqrt{\varepsilon_e}} \frac{K'(k)}{K(k)} = 45.1 \, \Omega. \quad (3.68)$$

3.8.2 Loss of CPW lines

Loss of a CPW line is primarily due to dielectric, radiative, and conductor losses. Dielectric loss is lower in a CPW line than in a microstrip line as the electric field lines are evenly divided between the air and dielectric, whereas with a microstrip line most of the field is concentrated in the dielectric. Also, radiation loss with CPW is much lower than with microstrip as the fields lines with a CPW line are much more tightly confined. In practice, when s/h is near to or greater than 1 the structure partially turns into a microstrip transmission line and it is of no use as a CPW line. This transfer of energy into the microstrip mode is another form of loss but can be avoided.

At low frequencies the strip resistance is

$$R_{\text{strip}} = R_s/w, \quad (3.69)$$

where R_s is the sheet resistance of the strip and w is the width of the central strip. The ground resistance can be ignored as the ground current spreads out considerably and the resistances of each ground are in parallel, thus further reducing the ground resistance.

Approximately, the dielectric and conductive components of the attenuation are (if ω , μ_0 , and ε_0 have SI units) [19]

$$\alpha_D = \frac{1}{2} \omega \sqrt{\mu_0 \varepsilon_0 \varepsilon_r} \tan \delta \, \text{Np/m} \quad \text{and} \quad \alpha_C = \frac{R_{\text{strip}}}{2Z_0} \, \text{Np/m}, \quad (3.70)$$

respectively. So α_D is almost entirely due to the choice of substrate material.

In summary, it is necessary to calculate the loss of CPW lines using EM simulation software to obtain the required accuracy. This is due to the more tightly confined fields and the greater variation of current densities compared to microstrip and stripline. A key attribute of CPW is the relative frequency independence of the effective permittivity, as this leads to almost dispersion-free transmission of signals. Also, devices can be connected along the signal path without using vias.

3.8.3 CPW Structures

The various CPW structures shown in Figure 3-15 are used to realize transmission line elements. The CPW-to-microstrip transition shown in

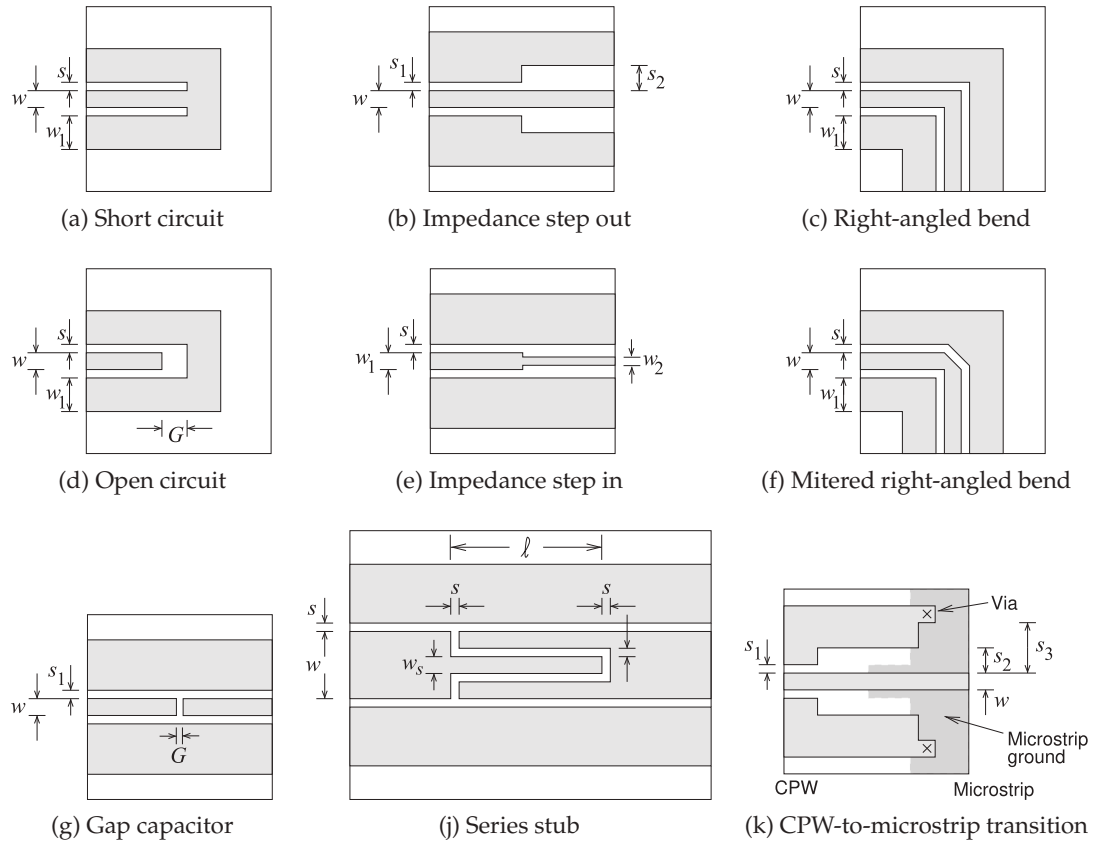


Figure 3-15: CPW structures.

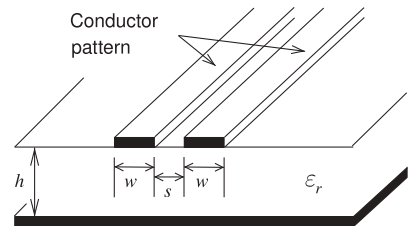


Figure 3-16: Differential line or coplanar strips (CPS).

Figure 3-15(k) requires vias to transfer the ground plane from the same surface as the strip in the CPW line to the second metal plane that forms the ground of microstrip.

3.8.4 Differential Line and Coplanar Strip

A coplanar strip (CPS) line is shown in Figure 3-16. CPS has only two conductors separated by a narrow longitudinal slot. It is a balanced line structure and is occasionally implemented in applications including radiating elements and transitions. CPS has become important for on-chip implementations, especially for RFICs and high-speed digital signal transmission, where it is usually referred to as differential line.

CPS is closely related to CPW, as the signal return path is well defined

and the electrical characteristics are independent of substrate thickness. CPS is a good structure to use instead of CPW when space is at a premium. Differential line is commonly used with RFICs, as the signal path on the IC is almost always differential since differential circuits on-chip remove many of the distortion and noise-coupling concerns. CPS suffers from relatively high radiation losses when realized on low-permittivity substrates. The radiation also results in substantial interaction and cross talk between adjacent circuits, although this is lower than with a microstrip line.

3.8.5 Summary

Coplanar waveguide is the transmission medium of choice above 20 GHz or so, although the threshold for the switch from microstrip to CPW is higher for on-chip lines. CPW confines the EM fields in a more localized manner than does microstrip, thus reducing spurious coupling, radiation, and dispersion. The electrical characteristics of CPW are defined by the lateral dimensions that can be accurately defined photolithographically. This is a significant advantage when the thickness of a substrate cannot be accurately controlled. CPW provides a precisely defined signal return path and this reduces capacitive coupling of signal lines. CPS lines are also used as digital interconnect mediums where the desirable attribute is the differential signaling. Differential lines, having the same structure as CPS, are commonly used as off-chip transmission lines connecting RFICs.

3.9 Summary

This chapter considered the most important planar transmission lines: microstrip, CPW and stripline. These lines can be produced using printed circuit board techniques. At frequencies below 1 GHz, economics require that standard FR4 circuit boards be used. The weave of a conventional FR4 circuit board can be a significant fraction of critical transmission line dimensions and so affect electrical performance. Nonwoven substrates and sometimes hard substrates such as alumina ceramic, sapphire, or silicon crystal wafers are often required. These also provide higher-dimensional tolerance than can be achieved using conventional woven FR4 substrates. In general, once a design has been optimized in fabrication so that the desired electrical characteristics are obtained, microwave circuits using planar transmission lines can be cheaply and repeatably manufactured in volume. This is true even with ceramic substrates that shrink when they are fired in a process performed after the transmission lines have been patterned. Microstrip and CPW are ideal transmission lines enabling surface modification in design optimization. Buried transmission line mediums such as stripline are difficult to rework, but of course allow more compact designs and thus lower unit costs. However, the rework difficulty results in higher design cost. Stripline does have an advantage over microstrip. Microstrip radiates, but with the fields confined between ground planes, stripline does not. Also stripline design enables multilayer circuit boards to be used, and thus results in smaller overall circuit size, at the price of higher design cost since design on-the-bench optimization are much more difficult.

3.10 References

- [1] C. Wen, "Coplanar waveguide: A surface strip transmission line suitable for nonreciprocal gyromagnetic device applications," *IEEE Trans. on Microwave Theory and Techniques*, vol. 17, no. 12, pp. 1087–1090, Dec. 1969.
- [2] R. Simons, N. Dib, and L. Katehi, "Modeling of coplanar stripline discontinuities," *IEEE Trans. on Microwave Theory and Techniques*, vol. 44, no. 5, pp. 711–716, May 1996.
- [3] D. Prieto, J. Cayrou, J. Cazaux, T. Parra, and J. Graffeuil, "Cps structure potentialities for mmics: a cps/cpw transition and a bias network," in *1998 IEEE MTT-S Int. Microwave Symp. Dig.*, Jun. 1998, pp. 111–114.
- [4] K. Goverdhanam, R. Simons, and L. Katehi, "Micro-coplanar striplines-new transmission media for microwave applications," in *1998 IEEE MTT-S Int. Microwave Symp. Dig.*, Jun. 1998, pp. 1035–1038.
- [5] —, "Coplanar stripline components for high-frequency applications," *IEEE Trans. on Microwave Theory and Techniques*, vol. 45, no. 10, pp. 1725–1729, Oct. 1997.
- [6] J. Knorr and K. Kuchler, "Analysis of coupled slots and coplanar strips on dielectric substrate," *IEEE Trans. on Microwave Theory and Techniques*, vol. 23, no. 7, pp. 541–548, Jul. 1975.
- [7] S. Pintz, "Full-wave spectral-domain analysis of coplanar strips," *IEEE Trans. on Microwave Theory and Techniques*, vol. 39, no. 2, pp. 239–246, Feb. 1991.
- [8] M. Gunston, *Microwave Transmission-line Impedance Data*. Van Nostrand Reinhold Company, 1973.
- [9] P. Holder, "X-band microwave integrated circuits using slotline and coplanar waveguide," *The Radio and Electronic Engineer*, vol. 48, no. 1/2, pp. 38–43, Jan./Feb. 1978.
- [10] K. Gupta, R. Garg, and I. Bahl, *Microstrip Lines and Slotlines*, 2nd ed. Artech House, 1996.
- [11] B. Spielman, "Computer-aided analysis of dissipation losses in isolated and coupled transmission lines for microwave and millimetre-wave applications," *NRL Formal Report*, no. 8009, 1976.
- [12] A. Ganguly and B. Spielman, "Dispersion characteristics for arbitrarily configured transmission media," *IEEE Trans. on Microwave Theory and Techniques*, vol. 25, no. 12, pp. 1138–1141, Dec. 1977.
- [13] R. Barrett, "Microwave printed circuits—a historical survey," *IRE Trans. on Microwave Theory and Techniques*, vol. 3, no. 2, pp. 1–9, Mar. 1955.
- [14] E. Hammerstad and O. Jensen, "Accurate models for microstrip computer-aided design," in *1980 IEEE MTT-S Int. Microwave Symp. Digest*, May 1980, pp. 407–409.
- [15] E. Hammerstad and F. Bekkadal, "A microstrip handbook, ELAB Report STF44 A74169," University of Trondheim, Norway, Tech. Rep., Feb. 1975.
- [16] E. O. Hammerstad, "Equations for microstrip circuit design," in *5th European Microwave Conf.*, Sep. 1975, pp. 268–272.
- [17] K. Karkkainen, A. Sihvola, and K. Nikoskinen, "Effective permittivity of mixtures: numerical validation by the fdtd method," *IEEE Trans. on Geoscience and Remote Sensing*, vol. 38, no. 3, pp. 1303–1308, May 2000.
- [18] J. Garnett, "Colors in metal glasses and metal films," *Trans. Royal Society*, vol. 53, pp. 385–420, 1904.
- [19] T. Edwards and M. Steer, *Foundations for Microstrip Circuit Design*. John Wiley & Sons, 2016.
- [20] A. Djordjevic and T. Sarkar, "Closed-form formulas for frequency-dependent resistance and inductance per unit length of microstrip and strip transmission lines," *IEEE Trans. on Microwave Theory and Techniques*, vol. 42, no. 2, pp. 241–248, Feb. 1994.
- [21] H. Wheeler, "Transmission-line properties of parallel wide strips by a conformal-mapping approximation," *IEEE Trans. on Microwave Theory and Techniques*, vol. 12, no. 3, pp. 280–289, May 1964.
- [22] —, "Transmission-line properties of parallel strips separated by a dielectric sheet," *IEEE Trans. on Microwave Theory and Techniques*, vol. 13, no. 2, pp. 172–185, Feb. 1965.
- [23] L. W. Cahill, "Approximate formulae for microstrip transmission lines," *Proc. Institute of Radio and Electrical Engineers*, vol. 35, pp. 317–321, Oct. 1974.
- [24] R. Owens, "Accurate analytical determination of quasi-static microstrip line parameters," *Radio and Electronic Engineer*, vol. 46, no. 7, pp. 360–364, Jul. 1976.
- [25] I. Bahl and R. Garg, "A designer's guide to stripline circuits," *Microwaves*, pp. 90–96, 1978.
- [26] S. Cohn, "Problems in strip transmission lines," *IRE Trans. on Microwave Theory and Techniques*, vol. 3, no. 2, pp. 119–126, Mar. 1955.
- [27] H. Howe, *Stripline Circuit Design*. Artech House, 1974.
- [28] W. Hilberg, "From approximations to ex-

- act relations for characteristic impedances," *IEEE Trans. on Microwave Theory and Techniques*, vol. 17, no. 5, pp. 259–265, May 1969.
- [29] C. Wen, "Coplanar waveguide: A surface strip transmission line suitable for nonreciprocal gyromagnetic device applications," *IEEE Trans. on Microwave Theory and Techniques*, vol. 17, no. 12, pp. 1087–1090, Dec. 1969.
- [30] M. Houdart, "Coplanar lines : Application to broadband microwave integrated circuits," in *6th European Microwave Conf.*, Sep. 1976, pp. 49–53.

3.11 Exercises

- At low frequencies a microstrip line has a capacitance of 1 nF/m and when the dielectric is replaced by air its capacitance is 0.5 nF/m. What is the phase velocity of signals on the line with the dielectric substrate in place? Consider that the relative magnetic permeability is 1.
- A non-magnetic microstrip line has a capacitance of 100 pF/m and when the dielectric is replaced by air it has a capacitance of 25 pF/m. What is the phase velocity of signals on the line with the dielectric?
- At low frequencies a non-magnetic microstrip transmission line has a capacitance of 10 nF/m and when the dielectric is replaced by air it has a capacitance of 2.55 nF/m. What is the effective permittivity of the microstrip line of signals on the line with the dielectric substrate in place?
- A microstrip line on 250 μm thick GaAs has a minimum and maximum strip widths of 50 μm and 250 μm respectively. What is the range of characteristic impedances that can be used in design?
- A microstrip line with a substrate having a relative permittivity of 10 has an effective permittivity of 8. What is the wavelength of a 10 GHz signal propagating on the microstrip?
- A microstrip line has a width of 500 μm and a substrate that is 635 μm thick with a relative permittivity of 20. What is the effective permittivity of the line?
- The strip of a microstrip has a width of 250 μm and is fabricated on a lossless substrate that is 500 μm thick and has a relative permittivity of 2.3. [Parallels Example 3.2]
 - What is the effective relative permittivity of the line?
 - What is the characteristic impedance of the line?
 - What is the propagation constant at 3 GHz ignoring any losses?
 - If the strip has a resistance of 0.5 Ω/cm and the ground plane resistance can be ignored, what is the attenuation constant of the line at 3 GHz?
- A microstrip line on a 250 μm -thick silicon substrate has a width of 200 μm . Use Table 3-3.
 - What is line's effective permittivity.
 - What is its characteristic impedance?
- A 600 μm -wide microstrip line on a 500 μm -thick alumina substrate. Use Table 3-3.
 - What is line's effective permittivity.
 - What is its characteristic impedance?
- A microstrip line on a 1 mm-thick FR4 substrate has a width of 0.497 mm. Use Table 3-3.
 - What is line's effective permittivity.
 - What is its characteristic impedance?
- Consider a microstrip line on a substrate with a relative permittivity of 12 and thickness of 1 mm.
 - What is the minimum effective permittivity of the microstrip line if there is no limit on the minimum or maximum width of the strip?
 - What is the maximum effective permittivity of the microstrip line if there is no limit on the minimum or maximum width of the strip?
- A microstrip line has a width of 1 mm and a substrate that is 1 mm thick with a relative permittivity of 20. What is the geometric filling factor of the line?
- The substrate of a microstrip line has a relative permittivity of 16 but the calculated effective permittivity is 12. What is the filling factor?
- A microstrip line has a strip width of 250 μm and a substrate with a relative permittivity of 10 and a thickness of 125 μm . What is the filling factor?
- A microstrip line has a strip width of 250 μm and a substrate with a relative permittivity of 4 and thickness of 250 μm . Determine the filling factor and thus the effective relative permittivity of the line?
- A microstrip line has a strip with a width of 100 μm and the substrate which is 250 μm thick and a relative permittivity of 8.
 - What is the filling factor, q , of the line?

- (b) What is the line's effective relative permittivity?
- (c) What is the characteristic impedance of the line?
17. An inhomogeneous transmission line is fabricated using a medium with a relative permittivity of 10 and has an effective permittivity of 7. What is the fill factor q ?
18. A microstrip technology uses a substrate with a relative permittivity of 10 and thickness of $400\ \mu\text{m}$. The minimum strip width is $20\ \mu\text{m}$. What is the highest characteristic impedance that can be achieved?
19. A microstrip transmission line has a characteristic impedance of $75\ \Omega$, a strip resistance of $5\ \Omega/\text{m}$, and a ground plane resistance of $5\ \Omega/\text{m}$. The dielectric of the line is lossless.
- (a) What is the total resistance of the line in Ω/m ?
- (b) What is the attenuation constant in Np/m ?
- (c) What is the attenuation constant in dB/cm ?
20. A microstrip line has a characteristic impedance of $50\ \Omega$, a strip resistance of $10\ \Omega/\text{m}$, and a ground plane resistance of $3\ \Omega/\text{m}$.
- (a) What is the total resistance of the line in Ω/m ?
- (b) What is the attenuation constant in Np/m ?
- (c) What is the attenuation constant in dB/cm ?
21. A microstrip line has $10\ \mu\text{m}$ -thick gold metallization for both the strip and ground plane. The strip has a width of $125\ \mu\text{m}$ and the substrate is $125\ \mu\text{m}$ thick.
- (a) What is the low frequency resistance (in Ω/m) of the strip?
- (b) What is the low frequency resistance of the ground plane?
- (c) What is the total low frequency resistance of the microstrip line?
22. A $50\ \Omega$ microstrip line has $10\ \mu\text{m}$ -thick gold metallization for both the strip and ground plane. The strip has a width of $250\ \mu\text{m}$ and the lossless substrate is $250\ \mu\text{m}$ thick.
- (a) What is the low frequency resistance (in Ω/m) of the strip?
- (b) What is the low frequency resistance of the ground plane?
- (c) What is the total low frequency resistance of the microstrip line?
- (c) What is the attenuation in dB/m of the line at low frequencies?
23. A $50\ \Omega$ microstrip line with a lossless substrate has a $0.5\ \text{mm}$ -wide strip with a sheet resistance of $1.5\ \text{m}\Omega$ and the ground plane resistance can be ignored. What is the attenuation constant at $1\ \text{GHz}$? [Parallels Example 3.3]
24. A microstrip line operating at $10\ \text{GHz}$ has a substrate with a relative permittivity of 10 and a loss tangent of 0.005. It has a characteristic impedance of $50\ \Omega$ and an effective permittivity of 7.
- (a) What is the conductance of the line in S/m ?
- (b) What is the attenuation constant in Np/m ?
- (c) What is the attenuation constant in dB/cm ?
25. A microstrip line has the per unit length parameters $L = 2\ \text{nH}/\text{m}$ and $C = 1\ \text{pF}/\text{m}$, also at $10\ \text{GHz}$ the substrate has a conductance G of $0.001\ \text{S}/\text{m}$. The substrate loss is solely due to dielectric relaxation loss and there is no substrate conductive loss. The resistances of the ground and strip are zero.
- (a) What is G at $1\ \text{GHz}$?
- (b) What is the magnitude of the characteristic impedance at $1\ \text{GHz}$?
- (c) What is the dielectric attenuation constant of the line at $1\ \text{GHz}$ in dB/m ?
26. A microstrip line has the per unit length parameters $L = 1\ \text{nH}/\text{m}$ and $C = 1\ \text{pF}/\text{m}$, also at $1\ \text{GHz}$ the substrate has a conductance G of $0.001\ \text{S}/\text{m}$. The substrate loss is solely due to dielectric relaxation loss and there is no substrate conductive loss. The resistance of the strip is $0.5\ \Omega/\text{m}$ and the resistance of the ground plane is $0.1\ \Omega/\text{m}$.
- (a) What is the per unit length resistance of the microstrip line at $1\ \text{GHz}$?
- (b) What is the magnitude of the characteristic impedance at $1\ \text{GHz}$?
- (c) What is the conductive attenuation constant in Np/m ?
- (d) What is the dielectric attenuation constant of the line at $1\ \text{GHz}$ in dB/m ?
27. A microstrip line operating at $2\ \text{GHz}$ has perfect metallization for both the strip and ground plane. The strip has a width of $250\ \mu\text{m}$ and the substrate is $250\ \mu\text{m}$ thick with a relative permittivity of 10 and a loss tangent of 0.001.
- (a) What is the filling factor, q , of the line?
- (b) What is the line's effective relative permittivity?
- (c) What is the line's attenuation in Np/m ?
- (d) What is the line's attenuation in dB/m ?
28. A $50\ \Omega$ microstrip line operating at $1\ \text{GHz}$ has perfect metallization for both the strip and ground plane. The substrate has a relative permittivity of 10 and a loss tangent of 0.001. Without the dielectric the line has a capacitance of $100\ \text{pF}/\text{m}$.

- (a) What is the line conductance in S/m?
 (b) What is the line's attenuation in Np/m?
 (c) What is the line's attenuation in dB/m?
29. Design a microstrip line having a $50\ \Omega$ characteristic impedance. The substrate has a permittivity of 2.3 and is $250\ \mu\text{m}$ thick. The operating frequency is 18 GHz. You need to determine the width of the microstrip line.
30. A load has an impedance $Z = 75 + j15\ \Omega$.
 (a) What is the load reflection coefficient, Γ_L , with reference impedance of $75\ \Omega$?
 (b) Design an open-circuited stub at the load that will make the impedance of the load plus the stub, call this Z_1 , be purely real. Choose a stub characteristic impedance of $75\ \Omega$. At this stage do an electrical design only. (This requires complete electrical information such as the electrical length of the stub.)
 (c) Following on from (b), now design a quarter-wave transformer between the source and the stub that will present $50\ \Omega$ at the input. (The design must include the characteristic impedance of the transmission line and its electrical length. Thus the structure is a $\lambda/4$ transformer, a stub, and the load.)
 (d) Now convert the electrical specifications of the design into a physical design at 1 GHz using microstrip technology with substrate thickness $h = 0.5\ \text{mm}$ and relative permittivity $\epsilon_r = 10$. You must design the widths and lengths of the stub and the quarter-wave transformer.
31. Design a microstrip line to have a characteristic impedance of $65\ \Omega$ at 5 GHz. The substrate is $635\ \mu\text{m}$ thick with a relative permittivity of 9.8. Ignore the thickness of the strip. [Parallels Example 3.5]
 (a) What is the width of the line?
 (b) What is the effective permittivity of the line?
32. Design a microstrip shorted stub at 10 GHz with the following characteristics:
 • Characteristic impedance of $60\ \Omega$.
 • A substrate with a relative permittivity of 9.6 and thickness of $500\ \mu\text{m}$.
 • Input impedance of $j60\ \Omega$.
 (a) What is the width of the microstrip line?
 (b) What is the length of the line in centimeters?
 (c) What is the effective permittivity of the line?
 (d) If the line is one-quarter wavelength longer than that calculated in (b), what will the input reactance be?
- (e) Regardless of your calculations above, what is the input admittance of a one-quarter wavelength long shorted stub?
33. Design a microstrip line to have a characteristic impedance of $20\ \Omega$. The microstrip is to be constructed on a substrate that is 1 mm thick with a relative permittivity of 12. [Parallels Example 3.5]
 (a) What is the width of the line? Ignore the thickness of the strip and frequency-dependent effects.
 (b) What is the effective permittivity of the line?
34. A load has an impedance $Z = 75 + j15\ \Omega$.
 (a) What is the load reflection coefficient, Γ_L , if the system reference impedance is $75\ \Omega$?
 (b) Design a shorted stub at the load that will make the impedance of the load plus the stub, call this Z_1 , be purely real; that is, the reflection coefficient of the effective load, Γ_1 , has zero phase. Choose a stub characteristic impedance of $75\ \Omega$. At this stage do an electrical design only. (This requires complete electrical information, e.g. the electrical length of the stub.)
 (c) Following on from (b), now design a quarter-wave transformer between the source and the stub that will present $50\ \Omega$ at the input. (The design must include the characteristic impedance of the transmission line and its electrical length. Thus the structure is a $\lambda/4$ transformer, a stub, and the load.)
 (d) Now convert the electrical design into a physical design at 1 GHz using microstrip technology with substrate thickness $h = 0.5\ \text{mm}$ and relative permittivity $\epsilon_r = 10$. You must design the widths and lengths of the stub and the quarter-wave transformer.
35. The strip of a symmetrical stripline has a width of 1 mm and the ground planes of the stripline are separated by 2 mm. The dielectric has a relative permittivity of 4.2. The strip has negligible thickness.
 (a) What is the effective permittivity of the stripline?
 (b) What is the characteristic impedance of the stripline at 1 GHz?
36. The strip of a symmetrical stripline has a width of $500\ \mu\text{m}$ and the ground planes of the stripline are separated by 1 mm. The dielectric has a relative permittivity of 10. The strip has a thickness of 0.1 mm.
 (a) What is the effective permittivity of the stripline?

- (b) What is the characteristic impedance of the stripline?
 (c) What is the total fringing capacitance in pF/m?
37. The strip of a symmetrical stripline has a width of $200\text{ }\mu\text{m}$ and the ground planes of the stripline are separated by 1 mm . The dielectric has a relative permittivity of 4. The strip has a thickness of 0.1 mm .
 (a) What is the effective permittivity of the stripline?
 (b) What is the characteristic impedance of the stripline?
 (c) What is the total fringing capacitance in pF/m?
38. The strip of a symmetrical stripline has a width of $50\text{ }\mu\text{m}$ and the ground planes of the stripline are separated by $300\text{ }\mu\text{m}$. The dielectric has a relative permittivity of 10. The strip has a thickness of $10\text{ }\mu\text{m}$. What is the characteristic impedance of the stripline?
39. The strip of a symmetrical stripline has a width of 0.25 mm and the ground planes of the stripline are separated by 1 mm . The dielectric has a relative permittivity of 80. What is the effective width of the strip?
40. The strip of a symmetrical stripline has a width of $100\text{ }\mu\text{m}$ and is embedded in a lossless medium that is $400\text{ }\mu\text{m}$ thick and has a relative permittivity of 13, thus the separation, h , from the strip to each of the ground planes is $200\text{ }\mu\text{m}$.
 (a) Draw the effective waveguide model of a stripline with magnetic walls and an effective strip width, w_{eff} .
 (b) What is the effective relative permittivity of the stripline waveguide model?
- (c) What is w_{eff} ?
41. A symmetrical stripline has a thin strip with a width of $200\text{ }\mu\text{m}$, is embedded in a dielectric of relative permittivity 12, and is between ground planes separated by $500\text{ }\mu\text{m}$. What is Z_0 of the line? [Parallels Example 3.6]
42. At 1 GHz a $60\text{ }\Omega$ stripline has the per unit parameters $R = 2\text{ }\Omega/\text{m}$ and $G = 1\text{ mS/m}$. What is the attenuation of the line in dB/m?
43. A $50\text{ }\Omega$ symmetrical stripline has a 0.5 mm -wide strip and the ground planes are separated by 1.2 mm . The strip has a sheet resistance of $1.5\text{ m}\Omega$ and each ground plane has a sheet resistance of $1\text{ m}\Omega$. (Ignore high frequency effects on resistance.) The substrate has a loss tangent of 0.005 and a relative permittivity of 6. [Parallels Example 3.7]
 (a) What is the line's effective permittivity?
 (b) What is its characteristic impedance?
 (c) What is the attenuation constant of the line in dB/m at 2 GHz ?
44. The strip of a CPW line has a width $w = 400\text{ }\mu\text{m}$ and separations from the in-plane grounds of $s = 250\text{ }\mu\text{m}$. The substrate is $h = 1000\text{ }\mu\text{m}$ thick and the thickness of the metal is $t = 5\text{ }\mu\text{m}$. What is the effective permittivity and characteristic impedance of the CPW line.
45. A CPW line with a $250\text{ }\mu\text{m}$ thick GaAs substrate, has a width of $125\text{ }\mu\text{m}$ and thickness of $3\text{ }\mu\text{m}$, and a gap of $125\text{ }\mu\text{m}$ between the strip and ground planes. [Parallels Example 3.8]
 (a) What is the line's effective permittivity?
 (b) is the Z_0 of the line?

3.11.1 Exercises by Section

[†]challenging, [‡]very challenging

§3.2 1, 2, 3	21, 22, 23, 24, 25 [†] , 26 [†] ,	§3.7 34 [‡] , 35 [†] , 36 [†] , 37 [†] , 38 [†] , 39 [†] ,
§3.5 4, 5, 6 [†] , 7 [†] , 8, 9, 10, 11, 12,	27, 28	40 [‡] , 41 [†] , 42, 43
13, 14, 15, 16, 17, 18, 19, 20,	§3.6 29 [†] , 30 [†] , 31 [†] , 32 [‡] , 33 [†]	§3.8 44, 45 [†]

3.11.2 Answers to Selected Exercises

6 12.75	25(b) 44.72 Ω	33(b) 9.17
7(c) $j84.1\text{ m}^{-1}$	31(a) $340\text{ }\mu\text{m}$	39 245.5 μm
19(c) 0.579 dB/m	34(b) 100.9° for open stub,	40(c) 969 μm
20(a) 13 Ω/m	10.89 $^\circ$ for shorted stub	

Extraordinary Transmission Line Effects

4.1	Introduction	165
4.2	Frequency-Dependent Characteristics	166
4.3	High-Frequency Properties of Microstrip Lines	174
4.4	Multimoding on Transmission Lines	178
4.5	Parallel Plate Waveguide	179
4.6	Microstrip Operating Frequency Limitations	183
4.7	Multimoding Considerations for Coplanar Waveguide	189
4.8	Multimoding Considerations for Stripline	190
4.9	Power Losses and Parasitic Effects	191
4.10	Lines on Semiconductor Substrates	192
4.11	Summary	195
4.12	References	196
4.13	Exercises	197

4.1 Introduction

Previous chapters discussed the low-frequency operation of transmission lines. This chapter describes the origins of, particularly of planar lines. Figure 4-1 shows the typical frequency dependence of a line's $RLGC$ parameters. The variations of R , L , and C are of most interest, and, except with some semiconductor substrates, G is usually negligible.

The major limitation on the dimensions and maximum operating frequency of a transmission line is determined by the origination of higher-order modes (i.e., orientations of the fields). Different modes on a transmission line travel at different velocities. Thus the problem is that if a signal on a line is split between two modes, then the information sent from one end of the line will reach the other end in two packets arriving at different times. The two modes have random partitioning of the signal

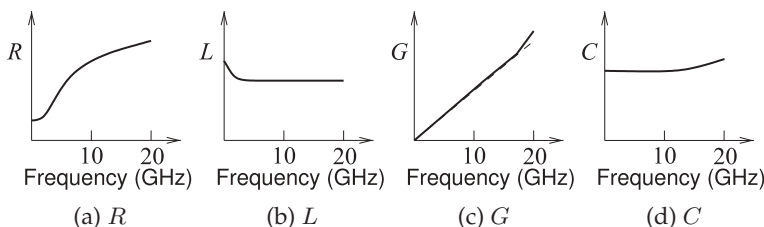


Figure 4-1: Frequency dependence of transmission line parameters.

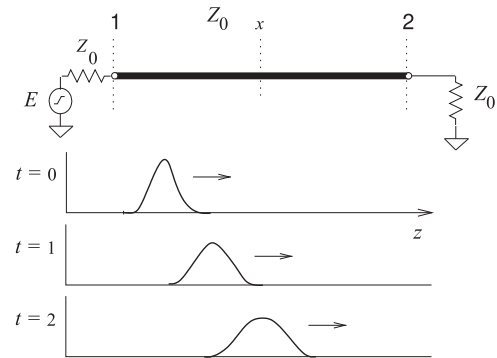


Figure 4-2: Dispersion of a pulse along a line.

energy and it is the combination that will be detected, and in general the information will be lost as the two modes combine in an incoherent manner. Multimoding must always be avoided.

4.2 Frequency-Dependent Characteristics

All interconnects have frequency-dependent behavior. In this section the origins of the frequency-dependent behavior of a microstrip line are examined because microstrip has the most significant frequency dependence among interconnects of general interest. Frequency-dependent behavior other than multimoding often results in dispersion. The effect can be seen in Figure 4-2 for a pulse traveling along a line. The pulse spreads out as the different frequency components travel at different speeds. For a long line, successive pulses will start merging and the signal will become unintelligible.

The most important frequency-dependent effects are

- changes of material properties (permittivity, permeability, and conductivity) with frequency (Section 4.2.1),
- current bunching (discussed in Section 4.2.3),
- skin effect (Sections 4.2.4 and 4.2.5),
- internal conductor inductance variation (Section 4.2.4),
- dielectric dispersion (Section 4.2.6), and
- multimoding (Section 4.4).

While the discussion focuses on microstrip lines, the effects occur with other planar and nonplanar transmission lines.

4.2.1 Material Dependency

Changes of permittivity, permeability, and conductivity with frequency are properties of the materials used. Fortunately the materials of interest in microwave technology have characteristics that are almost independent of frequency, at least up to 300 GHz or so.

4.2.2 Frequency-Dependent Charge Distribution

Skin effect, current bunching, and internal conductor inductance are all due to the necessary delay in transferring EM information from one location to another. This information cannot travel faster than the speed of light in the medium. In a dielectric material the speed of an EM wave will be slower

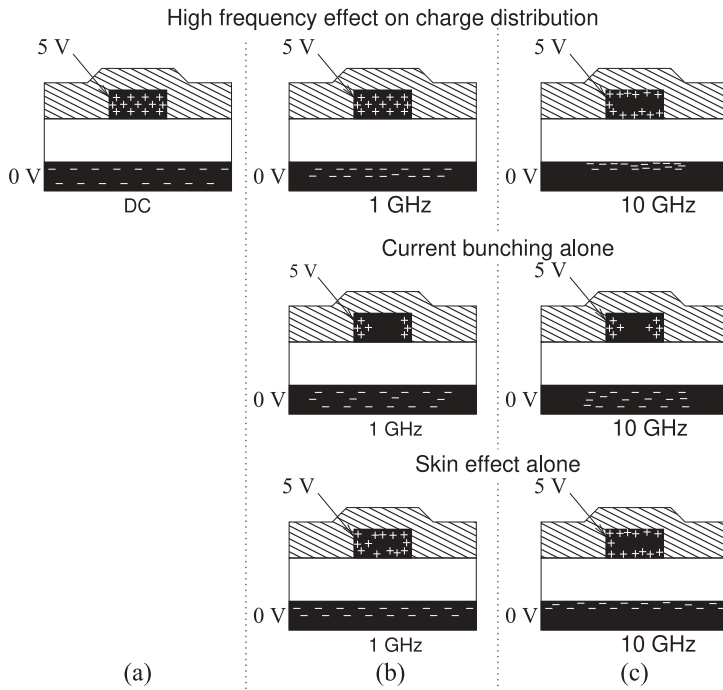


Figure 4-3: Cross-sectional view of the charge distribution on an interconnect at different frequencies. The + and - indicate charge concentrations of different polarity and corresponding current densities. There is no current bunching or skin effect at DC.

than that in free space by a factor of $\sqrt{\epsilon_r}$, where ϵ_r is the relative permittivity of the material. Thus the speed of an EM wave in microwave dielectrics is reduced typically by a factor ranging from just over 1 to 300. However, the velocity in a conductor is extremely low because of high conductivity. In brief, current bunching is due to changes related to the finite velocity of information transfer through the dielectric, and skin effect and variations of internal conductor inductance are due to the very slow speed of information transfer inside a conductor. As frequency increases, only limited information to rearrange charges can be sent before the polarity of the signal reverses and information is sent to reverse the changes. The skin and charge-bunching effects on a microstrip line are illustrated in cross section in Figure 4-3.

4.2.3 Current Bunching

Consider the charge distribution for a microstrip line shown in the cross-sectional views in Figure 4-3. The microstrip cross sections shown here are typical of an interconnect on a printed circuit board or a monolithically integrated circuit where the top dielectric is a **passivation** layer. The thickness of the microstrip is often a significant fraction of its width, although this is exaggerated in Figure 4-3.

The charge distribution shown in Figure 4-3(a) applies when there is a positive DC voltage on the strip (the top conductor). In this case there are positive charges on the top conductor arranged with a fairly uniform distribution. The individual positive charges (caused by the absence of balancing electrons exposing positively charged ions) tend to repel each other, but this has little effect on the charge distribution for practical conductors with finite conductivity. (If the conductor had zero resistance then these net charges would be confined to the surface of the conductor.) The bottom conductor is known as the ground plane and there are balancing

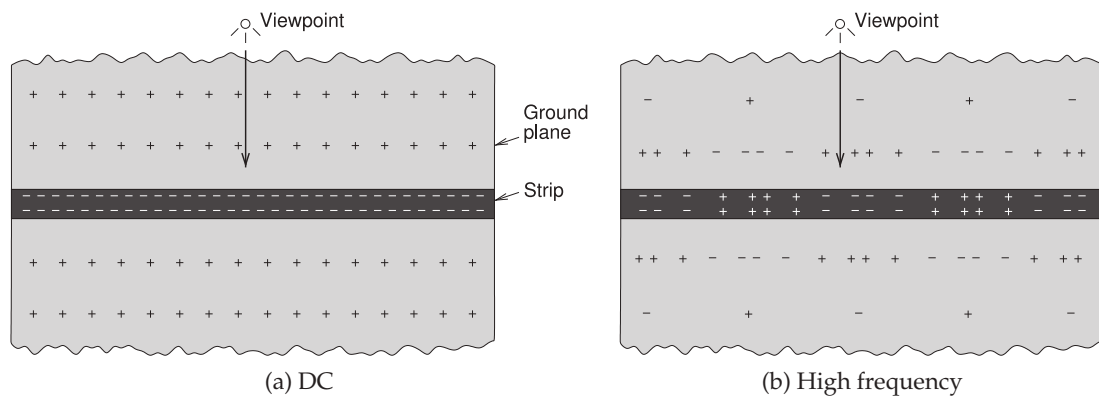


Figure 4-4: Current bunching effect in time. Positive and negative charges are shown on the strip and on the ground plane. The viewpoint is on the ground plane.

negative charges, or a surplus of electrons, so that electric field lines begin on the positive charges and terminate on the negative charges. The negative charges on the ground plane are uniformly distributed across the whole of the ground plane. An important point is that where there are unbalanced charges there can be current flow. So the charge distribution at DC, shown in Figure 4-3(a), indicates that for the top conductor, current would flow uniformly inside the conductors and the return current in the ground plane would be distributed over the whole of the ground plane.

The charge distribution becomes less uniform as frequency increases and eventually the signal changes so quickly that information to rearrange charges on the ground plane is soon (half a period later) countered by reverse instructions. Thus the charge distribution depends on how fast the signal changes. Another way of looking at this effect is to view the charges on the strip of the microstrip line at one time. This is shown in Figure 4-4 for a DC signal on the line and for a high-frequency signal. The DC situation is shown in Figure 4-4(a) where there is a uniform distribution of negative charges on the strip. This uniform distribution (in this case of negative charges) is seen from the viewpoint shown. The field then induces uniformly distributed positive charges on the ground plane. At a high frequency the charges on the strip alternate between negative and positive charges, as shown in Figure 4-4(b). Now the effective charge on the strip that is “seen” depends on how far the viewpoint is from the strip. When the viewpoint is at a large distance, it will seem as though the positive and negative charges cancel each other out. Thus on the ground plane at a large distance from the strip there will effectively be very little net charge on the strip. Consequently, at distance, there will be few matching charges on the ground plane that match the charges on the strip. Closer into the strip the ground will “see” a more concentrated charge on the strip and the charges on the ground plane will correspond more closely to the DC situation.

The electric field lines, which must originate and terminate on charges, will concentrate in the substrate more closely under the strip as frequency increases. There will be fewer electric field lines in the air that go out to the fewer distant charges in the ground plane. The two major effects are that

the effective permittivity of the microstrip line increases with frequency, and resistive loss increases as the average current density in the ground, which corresponds to the net charge density, increases. Thus the line resistance and capacitance increase with frequency (see Figure 4-1(a) and 4-1(d), respectively). For the majority of substrates G is due to dielectric relaxation rather than conduction in the dielectric. As such, G increases linearly with frequency with a superlinear increase at very high frequencies when the electric field is more concentrated in the dielectric (see Figure 4-1(c)).

In the frequency domain the current bunching effects are seen in the higher-frequency views shown in Figures 4-3(b and c). (The concentration of charges near the surface of the metal is a separate effect known as the skin effect.) The longitudinal impact of current or charge bunching alone is illustrated in Figures 4-5, 4-6, and 4-7. These figures present amplitudes of the current and charge phasors at various frequencies and were calculated using the **Sonnet** EM simulator. In interpreting these figures, take into account the magnitudes of the current and charge distributions as identified in the captions, as the scales are normalized. An alternative view (or time-domain view) is the instantaneous snapshot of current and charge shown in Figure 4-8.

This situation is not just confined to the transverse plane, and regions further along the interconnect also send instructions. The net effect is bunching of charges and hence of current on both the ground plane and the strip.

4.2.4 Skin Effect and Internal Conductor Inductance

At low frequencies, currents are distributed uniformly throughout a conductor. Thus there are magnetic fields inside the conductor and hence magnetic energy storage. As a result, there is internal conductor inductance. Transferring charge to the interior of conductors is particularly slow, and as the frequency of the signal increases, charges are confined closer to the surface of the metal. This effect is seen in Figure 4-9 where the current density inside the strip of a microstrip line is plotted at various frequencies. Thus time-varying EM fields are not able to penetrate the conductors as much as frequency increases. This phenomenon is known as the skin effect. With lower internal currents, the internal conductor inductance reduces and the total inductance of the line drops [1–4]. Thus the redistribution of the current results in a change of the inductance with frequency (see Figure 4-1(b)). Only above a few gigahertz or so can the line inductance be approximated as a constant for the transverse interconnect dimensions of a micron to several hundred microns.

The skin effect is characterized by the skin depth, δ_s , which is the distance at which the electric field, or equivalently the charge density, reduces to $1/e$ of its value at the surface. The skin depth is determined to be

$$\delta_s = 1/\sqrt{\pi f \mu_0 \sigma_2}. \quad (4.1)$$

Here f is frequency and σ_2 is the conductivity of the conductor. The conductivity is a measured quantity that is determined by the same physical phenomenon.¹ The permittivity and permeability of metals typically used

¹ This phenomenon is described by M. Born and E. Wolf [5]. In a conductor an electric field

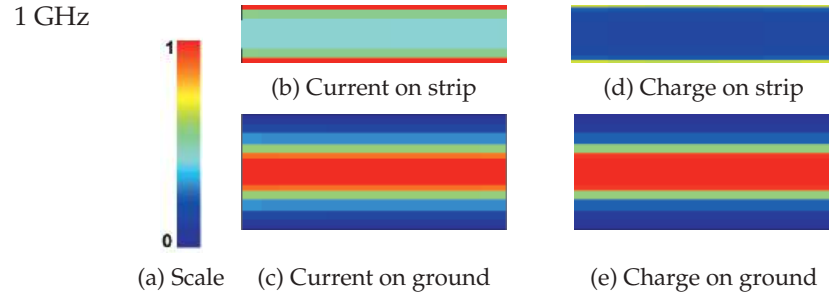


Figure 4-5: Normalized current and charge magnitudes on an alumina microstrip line at 1 GHz ($\epsilon_r = 10.0$): (a) scale; (b) longitudinal current, i_z , on the strip (10–26 A/m); (c) on the ground plane (0–3.2 A/m); (d) charge on the strip (80–400 nC/m²); and (e) on the ground (0–33 nC/m²). See inside the back cover for a color image.

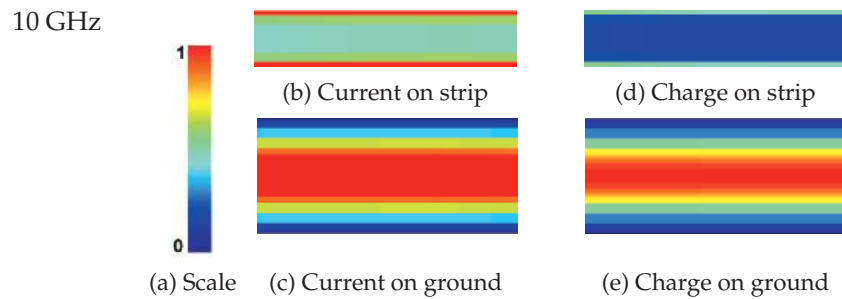


Figure 4-6: Normalized current and charge magnitudes on an alumina microstrip line at 10 GHz: (a) scale; (b) longitudinal current, i_z , on the strip (10–28 A/m); (c) on the ground plane (0–4.1 A/m); (d) charge on the strip (114–512 nC/m²); and (e) on the ground (0–39 nC/m²). See inside the back cover for a color image.

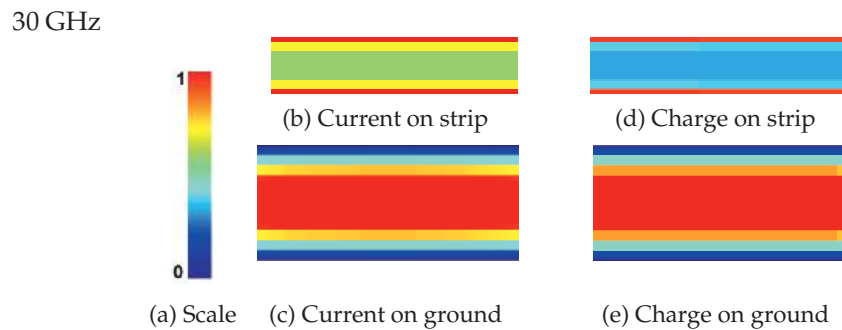


Figure 4-7: Normalized magnitudes of current and charge on an alumina microstrip line at 30 GHz: (a) scale; (b) longitudinal current, i_z , on the strip (10–31 A/m); (c) on the ground plane (0–6 A/m); (d) the charge on the strip (200–575 nC/m²); and (e) on the ground (0–68 nC/m²). See inside the back cover for a color image.

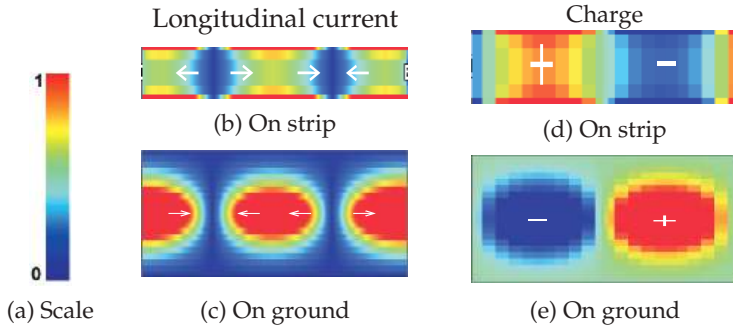


Figure 4-8: Normalized instantaneous current and charge on an alumina microstrip line at 30 GHz. Lighter regions have higher current density in (b) and (c), and more positive charge in (d) and (e).

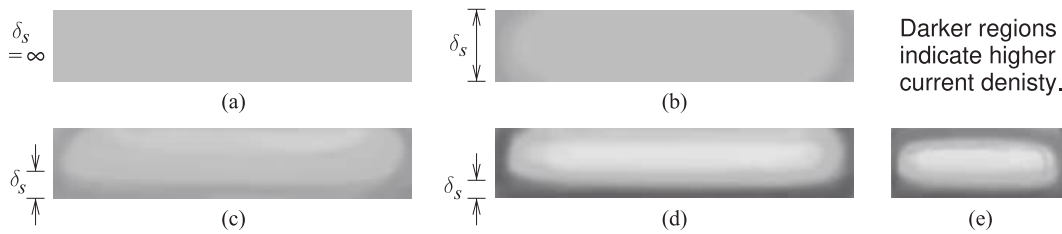


Figure 4-9: Cross sections of the strip of a microstrip line showing the impact of skin effect and current bunching on current density: (a) at dc (uniform current density); (b) the strip thickness, t , is equal to the skin depth, δ_s (i.e. at a low microwave frequency); (c) $t = 3\delta_s$; (d) $t = 5\delta_s$ (i.e. at a high microwave frequency); and (e) $t = 5\delta_s$ for a narrow strip. The plots are the result of 3D simulations of a microstrip line using internal conductor gridding.

for interconnects (e.g., gold, silver, copper, and aluminum) are that of free space, ϵ_0 and μ_0 , respectively, as there is no mechanism to store electric energy (there is no separation of charge centers) and, except for magnetic materials, no mechanism to store magnetic energy (no unbalanced magnetic moments).

4.2.5 Skin Effect and Line Resistance

The skin effect is illustrated in Figure 4-3(b) at 1 GHz. The situation is more extreme as the frequency continues to increase (e.g., to 10 GHz) as in Figure 4-3(c). There are several important consequences of this. On the top conductor, as frequency increases, current flow is mostly concentrated near the surface of the conductors and the effective cross-sectional area of the conductor, as far as the current is concerned, is less. Thus the resistance of the top conductor increases. A more dramatic situation exists for the charge distribution in the ground plane. From the previous discussion of current bunching it was noted that charge is not uniformly distributed over the whole of the ground plane, but instead becomes more concentrated under

accelerates free electrons that in turn radiate around the direction of motion. This process is repeated as the field penetrates the conductor. While the leading edge of the electric field propagates quickly through the conductor it rapidly diminishes in amplitude. The average field penetrates very slowly due to the large number of free electrons and multiple scattering of the field. A rough guide is that the effective velocity at microwave frequencies for transfer of the bulk of the energy is about $c/1000$. It is not possible to determine an accurate number.

the strip as frequency increases. In addition to this, charges and current are confined to the skin of the ground conductor so that the frequency-dependent relative change of ground plane resistance with increasing frequency is greater than that of the strip. On the strip, current bunching results in charges being concentrated on the edges of the strip. This effect is more pronounced the higher the permittivity of the substrate.

The skin effect and current bunching result in frequency dependence of the line resistance, R , with

$$R(f) = \begin{cases} R(0) & f \text{ such that } t \leq 3\delta_s \\ R(0) + R_{\text{skin}}(f) & f \text{ such that } t > 3\delta_s, \end{cases} \quad (4.2)$$

where $R(0) = R_{\text{strip}}(0) + R_{\text{ground}}(0)$ is the resistance of the line at low frequencies (see Equation (3.28)). $R(f)$ describes the frequency-dependent line resistance that is due to both the skin effect and current bunching. Approximately,

$$R_{\text{skin}}(f) = R(0)k\sqrt{f}. \quad (4.3)$$

Here k is a constant, and while Equation (4.3) indicates proportionality to \sqrt{f} , this is an approximation, but $R(f)$ always increases more slowly than frequency [4, 6–8]. The dominant breakpoint is indicated in Equation (4.2).

The increased resistance of the strip at high frequencies results from both current bunching, increasing the current density at the edges of the strip and reducing it in the middle with respect to the width of the strip, and skin effect, increasing the current density on the top and bottom surfaces of the strip and reducing it in the middle with respect to the thickness of the strip (this is of concern at frequencies where $t > 3\delta_s$ [4, 7]). At low frequencies the contribution of the ground to the resistance of the line is small, but because of current bunching the resistance of the ground becomes significant [8] at higher frequencies. The resistance of the ground further increases because of the skin effect and at high microwave frequencies the resistance of the ground can be comparable to that of the strip. Surface roughness of the metal also affects line resistance [9]. This is easy to imagine if the roughness is comparable to the skin depth as the current path is increased by the roughness. Roughness of the metal surface primarily reflects the roughness of the substrate for hard substrates. With soft substrates the underside of the metal is intentionally roughened so that the rough needle-like metal surface penetrates into and anchors to the dielectric when the metal and dielectric are pressed together. For these reasons it is not possible to develop a simple and accurate expression for the frequency-dependent resistance of a microstrip line, and EM simulation is also necessary, but even then roughness cannot be accounted for. EM simulation is necessary in any case to determine attenuation due to radiation. It is essential to incorporate measurements into the design cycle of circuits at high microwave frequencies to account for effects that cannot be modeled [10, 11]. One observation on the frequency dependence of resistance is that it is pointless to make the thickness of the strip or of the ground thicker than three times the skin depth.

EXAMPLE 4.1 Skin Depth

Determine the skin depth for copper (Cu), silver (Ag), aluminum (Al), gold (Au), and titanium (Ti) at 100 MHz, 1 GHz, 10 GHz, and 100 GHz.

Solution:

The skin depth is calculated using Equation (4.1) and the conductivity from Appendix 2.A.

Metal	Resistivity ($\text{n}\Omega \cdot \text{m}$)	Conductivity (MS/m)	Skin depth, δ_s (μm)			
			100 MHz	1 GHz	10 GHz	100 GHz
Copper (Cu)	16.78	59.60	6.52	2.06	0.652	0.206
Silver (Ag)	15.87	63.01	6.34	2.01	0.634	0.201
Aluminum (Al)	26.50	37.74	8.19	2.59	0.819	0.259
Gold (Au)	22.14	45.17	7.489	2.37	0.749	0.237
Titanium (Ti)	4200	0.2381	103.1	32.6	10.3	3.26

4.2.6 Dielectric Dispersion

Dispersion is principally the result of the propagation velocity of a sinusoidal signal being dependent on frequency. For a pulse on the line, dispersion manifests as the various frequency components of a signal traveling with different velocities.

The electric field lines shift as a result of the different distributions of charge, with more of the electric energy being in the dielectric as frequency increases. Thus the effective permittivity of a microstrip line increases with increasing frequency. At high frequencies, the fundamental result of the field rearrangement is that the capacitance of the line increases, but this change can be quite small—typically less than 10% over the range of DC to 100 GHz. (This effect is described by the frequency dependence of the effective permittivity of the transmission line.) To a lesser extent, dispersion is also the result of other transmission line parameters changing with frequency, such as an interconnect's resistance. For an IC where the interconnects can have very small transverse dimensions (e.g., microns) on digital ICs, the line resistance is the most significant source of dispersion. The qualitative effect of dispersion is the same whether it is related to the resistance (resistance-induced dispersion) or change in the effective permittivity (dielectric-inhomogeneity-induced dispersion).

Different interconnect technologies have different dispersion characteristics. For example, with a microstrip line the effective permittivity changes with frequency as the proportion of the EM energy in the air region to that in the dielectric region changes. Dispersion is reduced if the fields are localized and cannot change orientation with frequency. This is the case with coplanar interconnects—in particular, coplanar waveguide (CPW) and coplanar strip (CPS) lines. The stripline of Figure 3-5(k) also has low dispersion, as the fields are confined in one medium and the effective permittivity is just the permittivity of the medium. Thus interconnect choices can have a significant effect on the integrity of a signal being transmitted.

As discussed earlier, as the frequency is increased, the fields on a microstrip line become more concentrated in the region beneath the strip. Thus there is a frequency-dependent effective microstrip permittivity, $\epsilon_e(f)$. This quantity increases with frequency and the wave is progressively slowed

down. The effective microstrip permittivity is now

$$\varepsilon_e(f) = \{c/[v_p(f)]\}^2. \quad (4.4)$$

Fundamentally, characterizing the dispersion problem then consists of solving the transmission line fields for the frequency-dependent phase velocity, $v_p(f)$. The limits of $\varepsilon_e(f)$ are readily established; at the low-frequency extreme it reduces to the static TEM value ε_e (or $\varepsilon_e(0)$), while as frequency is increased indefinitely, $\varepsilon_e(f)$ approaches the substrate permittivity itself, ε_r . That is,

$$\varepsilon_e(f) \rightarrow \begin{cases} \varepsilon_e(0) & \text{as } f \rightarrow 0 \\ \varepsilon_r & \text{as } f \rightarrow \infty. \end{cases} \quad (4.5)$$

Between these limits $\varepsilon_e(f)$ changes smoothly.

4.2.7 Summary

Various transmission line technologies have different frequency dispersion characteristics. The two most important technologies for microwave circuits are coaxial lines and microstrip. With both the variation of resistance with frequency due principally to the skin effect are significant. However this has little effect on characteristic impedance and effective permittivity with the dominate effect being increased loss at higher frequencies. With microstrip, but not with a coaxial line, variations due to changing orientation of the EM fields is the most significant effect. With increasing frequency the proportion of signal energy in the air region reduces and the proportion in the dielectric increases. The overall trend with microstrip is for the fields to be more concentrated in the dielectric as frequency increases and this increases a microstrip line's effective relative permittivity and hence slows down propagation. The variation of characteristic impedance of microstrip with frequency is more complex as the increasingly tight transverse rotation, i.e. curl, of the fields tends to increase characteristic impedance but the increasing effective permittivity tends to decrease characteristic impedance. Thus following the initial design of a microstrip circuit, it is important to use EM simulations to adjust designs to account for dispersion.

4.3 High-Frequency Properties of Microstrip Lines

Here the high-frequency properties of microstrip lines are discussed and formulas incorporating frequency dependence are presented for effective permittivity, characteristic impedance, and attenuation loss. The effective permittivity at DC (as calculated in the previous chapter) is denoted $\varepsilon_e(0)$ and the characteristic impedance at DC is $Z_0(0)$. These are also called the quasi-static effective permittivity and quasi-static characteristic impedance. Detailed analysis [12] yields the following formula for the **frequency-dependent effective permittivity** of a microstrip line:

$$\varepsilon_e(f) = \varepsilon_r - \frac{\varepsilon_r - \varepsilon_e(0)}{1 + (f/f_a)^m}, \quad (4.6)$$

where

$$f_a = \frac{f_b}{0.75 + (0.75 - 0.332 \varepsilon_r^{-1.73}) (w/h)} \quad (4.7)$$

$$f_b = \frac{47.746 \times 10^6}{h \sqrt{\varepsilon_r - \varepsilon_e(0)}} \tan^{-1} \left\{ \varepsilon_r \sqrt{\frac{\varepsilon_e(0) - 1}{\varepsilon_r - \varepsilon_e(0)}} \right\} \quad (4.8)$$

$$m = \begin{cases} m_0 m_c & m_0 m_c \leq 2.32 \\ 2.32 & m_0 m_c > 2.32 \end{cases} \quad (4.9)$$

$$m_0 = 1 + \frac{1}{1 + \sqrt{w/h}} + 0.32 \left(1 + \sqrt{w/h} \right)^{-3} \quad (4.10)$$

$$m_c = \begin{cases} 1 + \frac{1.4}{1 + w/h} \{0.15 - 0.235 e^{-0.45 f/f_a}\}, & \text{for } w/h \leq 0.7 \\ 1, & \text{for } w/h > 0.7. \end{cases} \quad (4.11)$$

SI units are used in these equations. The accuracy of the equations is better than 0.6% for $0.1 \leq w/h \leq 10$, $1 \leq \varepsilon_r \leq 128$, and for any value of h/λ provided that $h < \lambda/10$.

The **frequency-dependent characteristic impedance** is, with reference to Equations (3.21) and (3.20),

$$Z_0(f) = \frac{Z_{01}}{\sqrt{\varepsilon_e(f)}} = Z_0(0) \frac{\sqrt{\varepsilon_e(0)}}{\sqrt{\varepsilon_e(f)}}. \quad (4.12)$$

The free-space wavelength is λ_0 , the wavelength in the medium is λ , and the guide wavelength (the wavelength on the line) is λ_g .

4.3.1 Frequency-Dependent Loss

The effect of loss on signal transmission is captured by the attenuation constant, α . There are two primary sources of loss: that resulting from the dielectric, captured by the dielectric attenuation constant, α_d , and that from the conductor loss, captured by the conductor attenuation constant, α_c . Thus

$$\alpha|_{dB} = \alpha_d|_{dB} + \alpha_c|_{dB}. \quad (4.13)$$

When dielectric loss is significant (e.g., the substrate is silicon which has appreciable conductivity), the previous formula for α_d (Equation (3.34)) provides a good estimate for the attenuation when ε_e is replaced by the frequency-dependent effective relative permittivity, $\varepsilon_e(f)$.

Frequency-dependent conductor loss, described by the conductor attenuation α_c , results from the concentration of current as frequency increases:

$$\alpha_c(f) = \frac{R(f)}{2 Z_0}, \quad (4.14)$$

where $R(f)$ is the frequency-dependent line resistance described in Section 4.2.5.

A third source of loss is radiation loss, leading to an attenuation factor, α_r . At the frequencies at which a transmission line is generally used, it is usually smaller than dielectric and conductor losses. So, in full,

$$\alpha(f) = \alpha_d(f) \cdot \alpha_c(f) \cdot \alpha_r(f), \quad (4.15)$$

and in decibels

$$\alpha(f)|_{dB} = \alpha_d(f)|_{dB} + \alpha_c(f)|_{dB} + \alpha_r(f)|_{dB}. \quad (4.16)$$

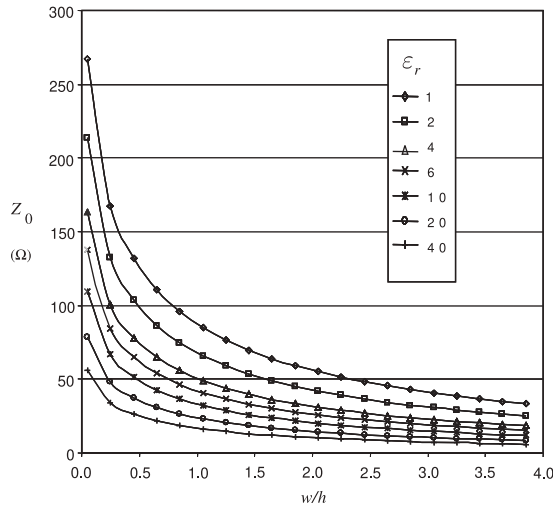


Figure 4-10: Dependence of Z_0 of a microstrip line at 1 GHz for various permittivities and aspect (w/h) ratios.

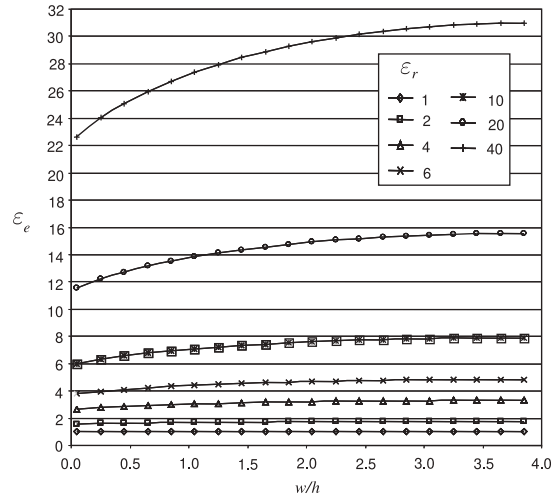


Figure 4-11: Dependence of effective relative permittivity, ϵ_e , of a microstrip line at 1 GHz for various permittivities and aspect ratios (w/h).

4.3.2 Field Simulations

In this section, results are presented for EM simulations of microstrip lines with a variety of parameters. These simulations were performed using the Sonnet EM simulator. Figure 4-10 presents calculations of Z_0 for various aspect ratios (w/h) and substrate permittivities (ϵ_r) when there is no loss. The key information here is that narrow strips and low-permittivity substrates have high Z_0 . Conversely, wide strips and high-permittivity substrates have low Z_0 . The dependence of permittivity on aspect ratio is shown in Figure 4-11, where it can be seen that the effective permittivity, ϵ_e , increases for wide strips. This is because more of the EM field is in the substrate.

When loss is incorporated, ϵ_e becomes complex and the imaginary components indicate loss mostly due to conductor loss. Figure 4-12 presents the frequency dependence of three microstrip lines with different substrates and aspect ratios. These simulations took into account finite loss in the conductors and in the dielectric. In Figure 4-12(a) it can be seen that the effective permittivity, ϵ_e , increases with frequency as the fields become confined more to the substrate. Also, the real part of the characteristic impedance is plotted with respect to frequency. Up to 20 GHz a drop-off in Z_0 is observed as frequency increases. This is due to both reduction of internal strip and ground inductances as charges move to the skin of the conductor and also to greater confinement of the EM fields in the dielectric as frequency increases. It is not long before the characteristic impedance increases. This effect is not due to the skin effect and current bunching that were previously described. Rather it is due to other EM effects that are only captured in EM simulation. It is a result of spatial variations being developed in the fields (related to the fact that not all parts of the fields are in instantaneous contact).

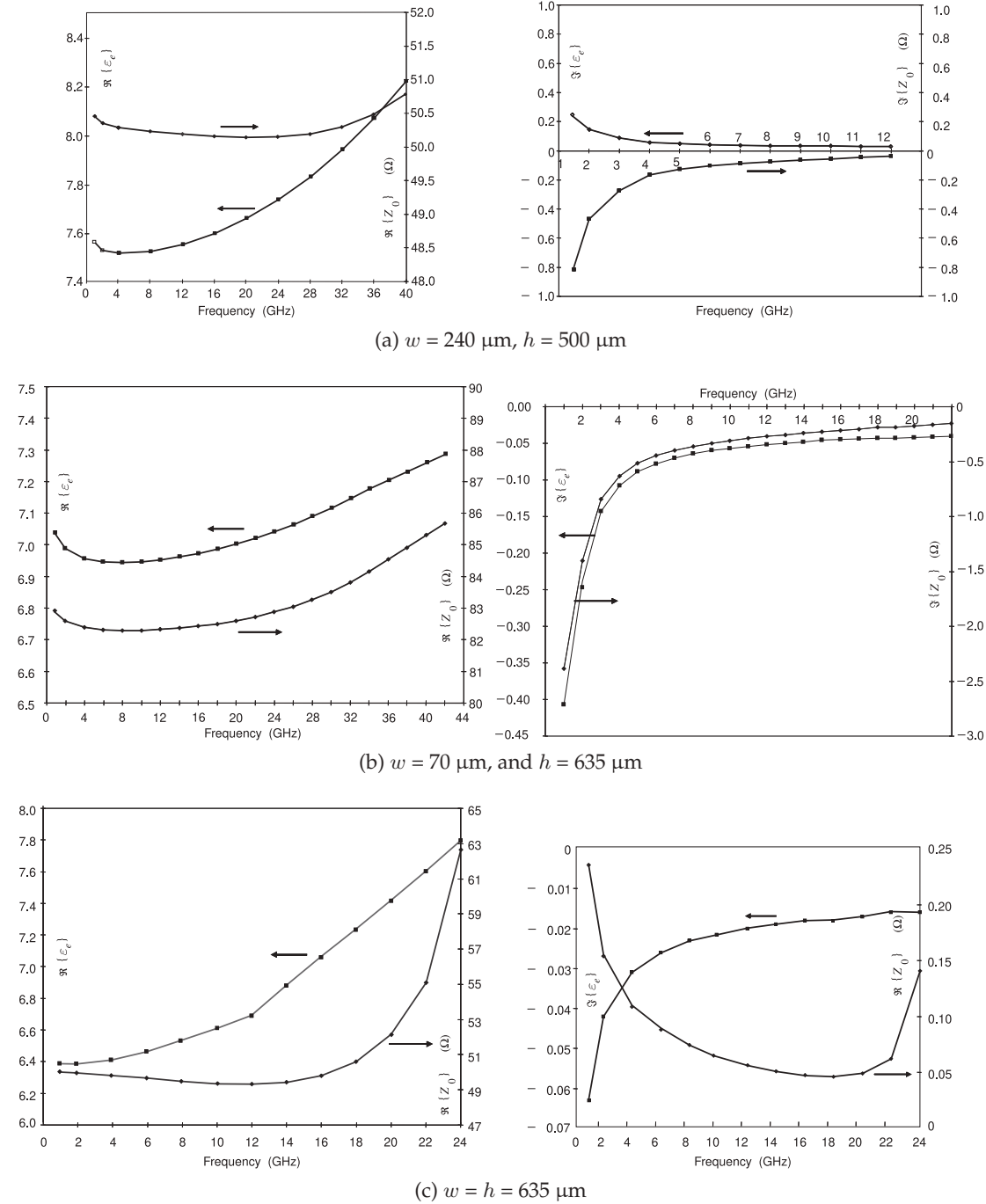


Figure 4-12: Frequency dependence of the real and imaginary parts of ϵ_e and Z_0 of a gold microstrip line on alumina with $\epsilon_r(\text{DC})$.

4.3.3 Summary

Today's microwave designer is indeed fortunate that in the 1980s considerable effort was put into developing frequency-dependent formulas for effective permittivity and characteristic impedance, Equations (4.6) and (4.12), and these can still be used. One effect that is not captured by these formulas is the increased transverse curl of the EM fields with increasing frequency and this tends to increase the characteristic impedance, e.g. see Section 4.3.2. But the frequency-dependence of effective relative permittivity is captured. To incorporate the geometric impact on frequency-dependent characteristic impedance it is necessary to optimize a design using EM field simulation following an initial design using the frequency-dependent formulas.

4.4 Multimoding on Transmission Lines

Multimoding is a phenomenon that affects the integrity of a signal as it travels on a transmission line. For transmission lines, multimoding occurs when there are two or more EM field configurations that can support a propagating wave. Different field configurations travel at different speeds so that the information traveling in two or modes would combine incoherently and, if the energy in the modes is comparable, it will be impossible to discern the intended information being sent. It is critical that the dimensions of transmission line structures be designed to avoid multimoding. The most common mode on a transmission line is when there is no, or the minimum possible, variation of the fields in the transverse direction (perpendicular to the direction of propagation).

The transmission structures of interest here are those that have conductors that establish boundary conditions to guide a wave along an intended path. For these lines the lowest-order mode with minimum transverse field variations is called the TEM mode. Higher-order modes occur when the fields can vary. From here the discussion necessarily invokes EM theory. If you need to do this, see Section 1.5, where EM theory is reviewed specifically with respect to multimoding. One of the important concepts is that electric and magnetic walls impose boundary conditions on the fields. Electric walls are conductors, whereas a magnetic wall is formed approximately at the interface of two regions having different permittivity.

It is the property of EM fields that spatial variations of the fields cannot occur too quickly. This comes directly from Maxwell's equations that relate the spatial derivative (the derivative with respect to distance) of the electric field to the time derivative of the magnetic field. The same is true for spatial variation of the magnetic field and time variation of the electric field. How fast a field varies with time depends on frequency. How fast an EM field changes spatially, its curl, depends on wavelength relative to geometry and on boundary conditions. Without electric and magnetic walls establishing boundary conditions, as in free space, a full wavelength is required to obtain the lowest-order variation of the fields. With electric or magnetic walls where the fields can terminate, a smaller distance is sufficient. Between two electric walls one-half wavelength of distance is required. The same is true for magnetic walls. With one electric wall and one magnetic wall, a quarter-wavelength separation of the walls will support a higher-order mode. A

	E field	H field
Electric wall	Normal	Parallel
Magnetic wall	Parallel	Normal

Table 4-1: Properties of the EM fields at electric and magnetic walls.

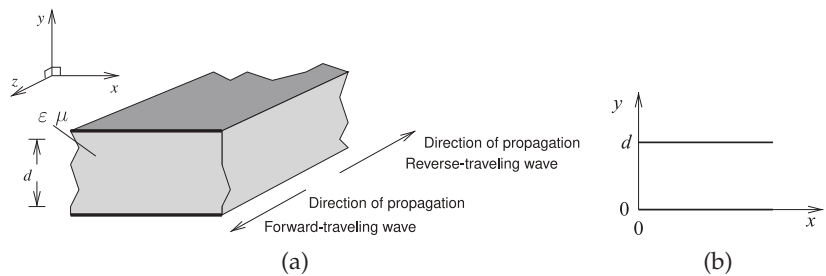


Figure 4-13: Parallel-plate waveguide: (a) three-dimensional view; and (b) cross-sectional (transverse) view.

general rule for avoiding multimoding is that critical transverse geometries must be kept to under a fraction of a wavelength (say, $< \lambda/2$ or $< \lambda/4$).

One type of multimoding has already been described. In the previous chapter it was seen that the signals on a regular transmission line have two simple solutions that are interpreted as the forward-traveling and backward-traveling modes. Each mode is a possible solution of the differential equations describing the signals. These are not the modes being referred to by the term multimoding. The boundary conditions in the longitudinal direction are established by the source and load impedances, and so the variation can be any fraction of a wavelength. This section is concerned with other solutions to the equations describing the fields on a transmission line structure. In general, the other solutions arise when the transverse dimensions, such as the distance between the two conductors of a two-conductor transmission line, permits a variation of the fields.

The boundary conditions established at electric and magnetic walls were derived in Section 1.8 and are summarized in Table 4-1. Circuit structures such as transmission lines, substrate thicknesses, and related geometries are nearly always chosen so that only one solution of Maxwell's equations is possible. In particular, if the cross-sectional dimensions of a transmission line are much less than a wavelength then it will be impossible for the fields to curl up on themselves and so perhaps there will be only one or, in some cases, no solutions to Maxwell's equations.

4.5 Parallel-Plate Waveguide

The parallel-plate waveguide shown in Figure 4-13 is the closest regular structure to planar transmission lines such as a microstrip line. The aim here is to develop design guidelines that will enable transmission line structures to be designed to avoid multimoding.

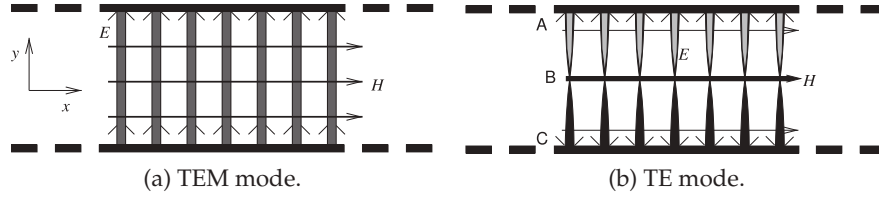


Figure 4-14: Parallel-plate waveguide showing electric, E , and magnetic, H , field lines. The electric (E) and magnetic (H) field lines are shown with the line thickness indicating field strength. The shading of the E field lines indicates polarity (+ or -) and the arrows indicate direction (and also polarity). The z direction is into the page.

4.5.1 Electromagnetic Derivation

The development of the wave equations begins with **Maxwell's equations** (Equations (1.1)–(1.4)). A simplification to the equations is to assume a linear, isotropic, and homogeneous medium, a uniform dielectric, so that ϵ and μ are independent of signal level and are independent of the field direction and position. Thus (in the time domain)

$$\nabla \times \bar{\mathcal{E}} = \frac{\partial \bar{\mathcal{B}}}{\partial t} \quad \nabla \times \bar{\mathcal{H}} = \bar{\mathcal{J}} + \frac{\partial \bar{\mathcal{D}}}{\partial t} \quad (4.17)$$

$$\nabla \cdot \bar{\mathcal{D}} = \rho_V \quad \nabla \cdot \bar{\mathcal{B}} = 0, \quad (4.18)$$

where ρ_V is the volume charge density and $\bar{\mathcal{J}}$ is the current density. $\bar{\mathcal{J}}$ and ρ_V will be zero except at an electric wall. The above equations do not include magnetic charge or magnetic current density. These do not actually exist and so a modified form of Maxwell's equations incorporating these is not necessary to solve the fields on a structure.

In the lateral direction, the x direction, the parallel-plate waveguide in Figure 4-13 extends indefinitely. For this regular structure, and with a few assumptions, the form of Maxwell's equations with multidimensional spatial derivatives can be simplified. One approach to solving differential equations is to assume a form of the solution and then test to see if it is a valid solution. The first solution to be considered is called the TEM mode and corresponds to the minimum possible variation of the fields. Also, it is assumed that the variation in the z direction is described by the traveling-wave equations. So the only fields of interest here are E and H in the transverse plane; all that is seen in Figure 4-13(b). If all the fields are in the xy plane, then it is sufficient to apply just the boundary conditions that come from the top and bottom ground planes. At first it appears that there are many possible solutions to the differential equations. This is simplified by assuming certain variational properties of the E_x , E_y , H_x , and H_y fields and then seeing if these solutions can be supported. The simplest solution is when there is no variation in the fields and then the only possible outcome is that $E_x = 0 = H_y$. This is the TEM mode indicated in Figure 4-14(a). At the boundaries, the top and bottom metal planes, there is a divergence of the electric field, as immediately inside the (ideal) conductor there is no electric field and immediately outside there is. This divergence is supported by the surface charge on the ground planes (see Equation (1.2)).

In Figure 4-14(a), the thickness of the lines indicates relative field strength

and there is no variation in field strength in either the electric or magnetic fields shown. The coefficients of the field components are determined by the boundary conditions. The trial solution used here has $E_x = 0 = H_y$ and $E_z = 0 = H_z$; that is, the trial solution has the electric field in the y direction and the magnetic field is in the x direction. Maxwell's equations (Equations (4.17) and (4.18)) become (note that $\bar{\mathcal{E}} = \bar{\mathcal{E}}_x \hat{x} + \bar{\mathcal{E}}_y \hat{y} + \bar{\mathcal{E}}_z \hat{z}$)

$$\nabla \times \bar{\mathcal{E}}_y \hat{y} = -\frac{\partial \bar{\mathcal{B}}_x \hat{x}}{\partial t} \quad \nabla \times \bar{\mathcal{H}}_x \hat{x} = \frac{\partial \bar{\mathcal{D}}_y \hat{y}}{\partial t} + \bar{\mathcal{J}} \quad (4.19)$$

$$\nabla \cdot \bar{\mathcal{D}}_y \hat{y} = \rho \quad \nabla \cdot \bar{\mathcal{B}}_x \hat{x} = 0. \quad (4.20)$$

Expanding the curl, $\nabla \times$, and div, $\nabla \cdot$, operators using Equations (1.21) and (1.22) these become (with $D = \varepsilon E$ and $B = \mu H$)

$$\hat{x} \frac{\partial \bar{\mathcal{E}}_y}{\partial z} = \frac{\partial \bar{\mathcal{B}}_x \hat{x}}{\partial t} = \frac{\partial \mu \bar{\mathcal{H}}_x \hat{x}}{\partial t} \quad (4.21)$$

$$\hat{y} \frac{\partial \bar{\mathcal{H}}_x}{\partial z} = \frac{\partial \bar{\mathcal{D}}_y \hat{y}}{\partial t} + \bar{\mathcal{J}} = \frac{\partial \varepsilon \bar{\mathcal{E}}_y \hat{y}}{\partial t} + \bar{\mathcal{J}} \quad (4.22)$$

$$\frac{\partial \bar{\mathcal{D}}_y}{\partial y} = \frac{\partial \varepsilon \bar{\mathcal{E}}_y}{\partial y} = \rho \quad (4.23)$$

$$\frac{\partial \bar{\mathcal{B}}_x}{\partial x} = \frac{\partial \mu \bar{\mathcal{H}}_x}{\partial x} = 0. \quad (4.24)$$

These equations describe what happens at each point in space.

Equation (4.21) indicates that if there is a time-varying component of the x -directed B field then there must be a z -varying component of the E_y field component. This is just part of the wave equation describing a field propagating in the z direction. Equation (4.22) indicates the same thing, but now the roles of the electric and magnetic fields are reversed. Equation (4.21) shows that the y component of the electric field can be constant between the plates, but at the plates there must be a charge on the surface of the conductors (see Equation (4.23)), to terminate the electric field (as indicated by Equation (4.23)), as there is no electric field inside the conductors. Equation (4.24) indicates that the x component of the magnetic field cannot vary in the x direction (i.e., B_x and H_x are constant). Thus the assumption behind the trial solution about the form of this mode is correct. The electric and magnetic field are uniform in the transverse plane, the xy plane, and the only variation is in the direction of propagation, the z direction (but there is no z -directed component of the fields). Thus the test solution satisfies Maxwell's equations. This is the TEM mode, as all field components are in the x and y directions and none are in the z direction. The TEM mode can be supported at all frequencies in the parallel-plate waveguide.

In exploring the existence of higher-order modes, Maxwell's equations need to be simplified further. Putting Equations (4.21)–(4.24) in phasor form, and considering the source free region between the plates (so $J = 0$ and $\rho = 0$), these become (note that E_x is the phasor of \mathcal{E}_x)

$$\frac{\partial E_y}{\partial z} = j\omega\mu H_x \quad \frac{\partial H_x}{\partial z} = j\omega\varepsilon E_y \quad (4.25)$$

$$\frac{\partial E_y}{\partial y} = 0 \quad \frac{\partial H_x}{\partial x} = 0 \quad (4.26)$$

and the solution becomes

$$\frac{\partial^2 E_y}{\partial z^2} = \gamma^2 E_y \quad \text{and} \quad \frac{\partial^2 H_x}{\partial z^2} = \gamma^2 H_x, \quad (4.27)$$

where $\gamma = j\omega\sqrt{\mu\epsilon}$ and there is no variation of the E_y component of the electric field in the y direction and no variation of the H_x component of the magnetic field in the x direction.

Another possible set of modes occurs when the electric field is only in the y direction, but then there must be a variation of the field strength, as shown in Figure 4-14(b). The simplest variation is when there is a half-sinusoidal spatial variation of the E_y field component. Applying the methodology described above, it is found that there must be a component of the magnetic field in the z direction to support this mode. Hence these modes are called **transverse electric** (TE) modes. (Interchanging the roles of the electric and magnetic fields yields the **transverse magnetic** (TM) modes where there is an electric field component in the z direction.) The half-sinusoidal variation still enables the charge to support the existence of an E_y electric field.

A key result from our previous discussion is that there must be enough distance for the field to curl and this is related to wavelength, λ . This transverse electric mode can only exist when $h \geq \lambda/2$. When h is smaller than one-half wavelength, this mode cannot be supported, and is said to be cut off. Only the TEM mode can be supported all the way down to DC, so modes other than TEM have a cutoff frequency, f_c , and a cutoff wavelength, λ_c . The concept of wavenumber $k (= 2\pi/\lambda = \omega\sqrt{\mu\epsilon})$ is also used. The cutoff wavelength, λ_c , and the cutoff wavenumber, k_c , are both related to the dimension below which a mode cannot “curl” sufficiently to be self-supporting. For the lowest TE mode, $k_c = 2\pi/\lambda_c$ with $\lambda_c = 2h$. In general, for TE modes, there can be n variations of the electric field, and n indicates the n th TE mode, denoted as TE_n , for which $k_{c,n} = n\pi/h$ and $\lambda_c = 2h/n$. The propagation constant of any mode in a uniform lossless medium (not just in a parallel-plate waveguide mode) is

$$\beta = \sqrt{k^2 - k_c^2}. \quad (4.28)$$

For the TEM mode, $k_c = 0$. High-order modes are described by their own k_c .

TM modes are similarly described, and again $k_c = n\pi/h$ for the TM_n mode. A mode can be supported at any frequency above the cutoff frequency of the mode, it just cannot be supported at frequencies below the cutoff frequency as it is not possible for the fields to vary (or curl) below cutoff.

4.5.2 Multimoding and Electric and Magnetic Walls

In the above discussion, the parallel-plate waveguide had two electric walls—the top and bottom metal walls. Here results will be presented when magnetic walls are introduced. A magnetic wall can only be approximated, as magnetic conductors do not exist (since magnetic charges do not exist). Whereas an electric wall appears as a short circuit, a magnetic wall is an open circuit. Maxwell’s equations and the electric and magnetic walls establish the following requirements on the fields:

Electric wall	Perpendicular electric field Tangential magnetic field
Magnetic wall	Perpendicular magnetic field Tangential electric field

Table 4-2: Requirements imposed on fields by electric and magnetic walls.

The lowest-order modes that can be supported by combinations of electric and magnetic walls are shown in Figure 4-15. With two electric or two magnetic walls, a TEM mode (having no field variations in the transverse plane) can be supported. Of course, there will be variations in the field components in the direction of propagation. The modes with the simplest geometric variations in the plane transverse to the direction of propagation establish the critical wavelength. In Figure 4-15 the distance between the walls is d . For the case of two like walls (Figures 4-15(a and c)), $\lambda_c = 2h$, as one-half sinusoidal variation is required. With unlike walls (see Figure 4-15(b)), the varying modes are supported with just one-quarter sinusoidal variation, and so $\lambda_c = 4h$.

EXAMPLE 4.2

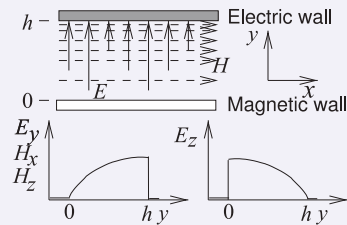
Modes and Electric and Magnetic Walls

A magnetic wall and an electric wall are 1 cm apart and are separated by a lossless material having $\varepsilon_r = 9$. What is the cut-off frequency of the lowest-order mode in this system?

Solution:

The EM field established by the electric and magnetic walls is described in Figure 4-15(b). There is no solution to the Maxwell's equations that has no variation of the EM fields since it is not possible to have a spatially uniform electric field which is perpendicular to an electric wall while also being perpendicular to a parallel magnetic wall. The other solutions of Maxwell's equations require that the fields vary spatially, i.e. curl. Without electric and magnetic walls the minimum distance over which the EM fields will fold back on to themselves is a wavelength. With parallel electric and magnetic wall separated by h the minimum distance for a solution of Maxwell's equations is a quarter wavelength, λ , of the walls as shown on the right in Figure 4-15(b). That is

$$h = \lambda/4 \quad \text{or} \quad \lambda = 4h = 4 \text{ cm} = \lambda_0/(\sqrt{\varepsilon_t \mu_r}). \quad (4.29)$$



Since the relative permeability has not been specified assume that $\mu_r = 1$ so

$$\lambda_0 = \lambda\sqrt{9} = 12 \text{ cm} = c/f$$

The cut-off frequency is

$$\begin{aligned} f &= (2.998 \times 10^8 \text{ m/s})/(0.12 \text{ m}) \\ &= 2.498 \text{ GHz} \end{aligned} \quad (4.30)$$

4.6 Microstrip Operating Frequency Limitations

Different types of higher-order modes can exist with microstrip and the two maximum operating frequencies of microstrip lines are (a) the lowest-order TM mode and (b) the lowest-order transverse microstrip resonance mode. In practice, **multimoding** is a problem when two conditions are met. First it must be possible for higher-order field variations to exist, and second, that energy can be effectively coupled into the higher-order mode. Generally this

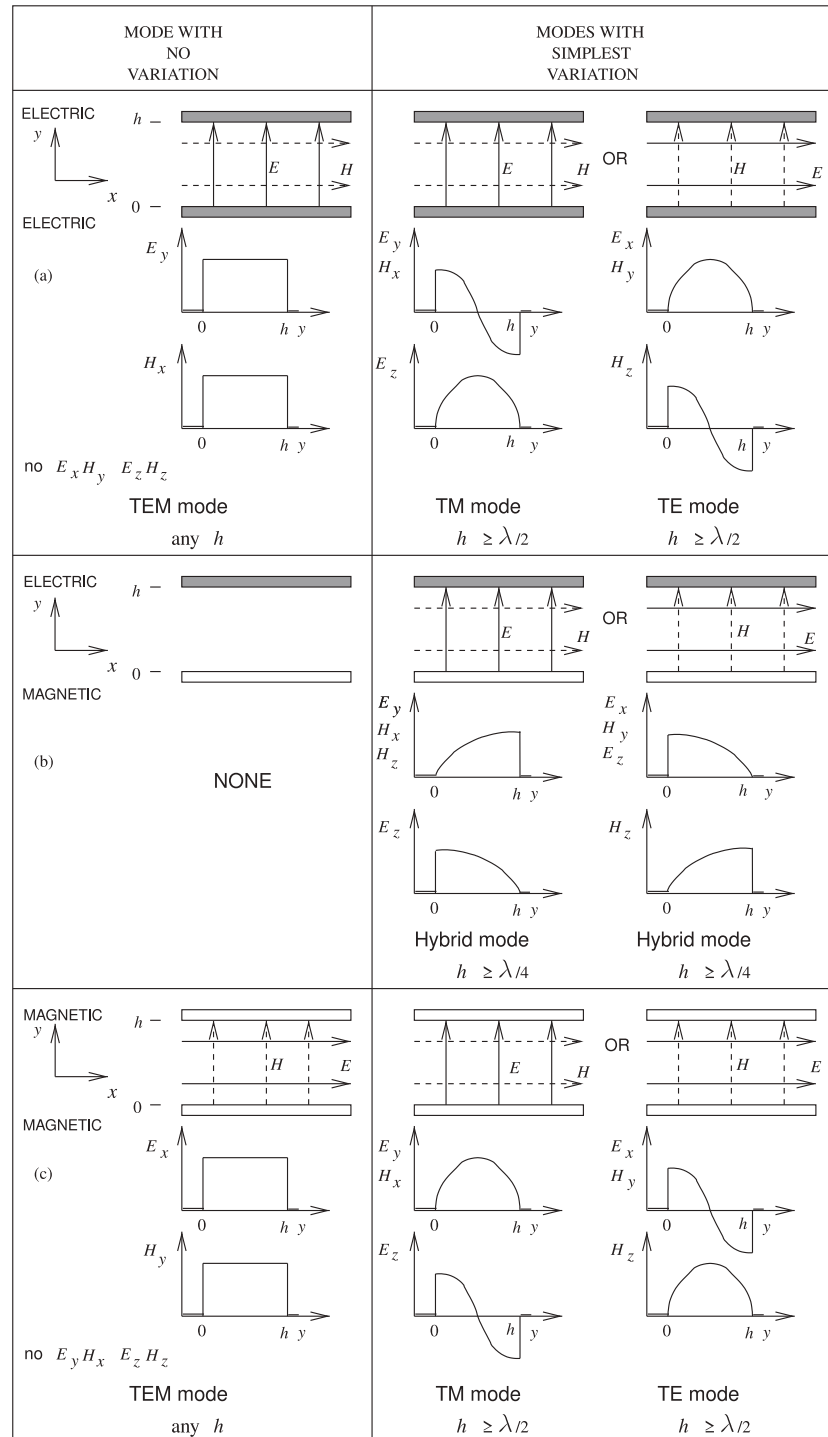


Figure 4-15: Lowest-order modes supported by combinations of electric and magnetic walls.

requires significant discontinuity on the line or that the phase velocities of two modes approximately coincide. An early discussion said that the phase velocities of two modes would be different and this is when the dielectric is uniform. However, with a nonhomogeneous line like microstrip, there can be frequencies where the phase velocities of two modes can coincide.

Since discontinuities are inevitable it is always a good idea to use only the first consideration. As was noted previously, the modal analysis that was possible with the parallel-plate waveguide cannot be repeated easily for the microstrip line because of the irregular cross section, but the phenomena is very similar. Instead of a TEM mode, there is a quasi-TEM mode and there are TE and TM modes.

4.6.1 Microstrip Dielectric Mode (Slab Mode)

A dielectric on a ground plane with an air region (of a wavelength or more above it) can support a TM mode, generally called a microstrip dielectric mode, **substrate mode**, **microstrip TM mode**, or slab mode. The microstrip dielectric mode is a problem for narrow microstrip lines. Whether this mode exists in a microstrip environment depends on whether energy can be coupled from the quasi-TEM mode (which is always generated) of the microstrip line into the TM dielectric mode. The critical frequency at which the TM mode becomes important is when there is significant coupling. Coupling is a problem with a microstrip line having a narrow strip, as the field orientations of the quasi-TEM mode and the dielectric mode align. Also, coupling occurs when the phase velocities of the two modes coincide. A detailed analysis reported in Chapter 11 of [12] and in [13] shows that this occurs at the first critical frequency,

$$f_{c1} = \frac{c \tan^{-1}(\epsilon_r)}{\sqrt{2\pi h} \sqrt{\epsilon_r - 1}}. \quad (4.31)$$

At f_{c1} the dielectric mode will be generated even if there is not a discontinuity. If there is a discontinuity, say a split of one microstrip line into two microstrip lines, multimoding will occur when the dielectric mode can exist. From Figure 4-15(b), the dielectric slab mode can be supported when $h > \lambda_g/4$, where λ_g is the wavelength in the dielectric. Now $\lambda_g = \lambda_0/\sqrt{\epsilon_r} = c/(f\sqrt{\epsilon_r})$, so the second critical frequency is

$$f_{c2} = \frac{c}{4h\sqrt{\epsilon_r}}. \quad (4.32)$$

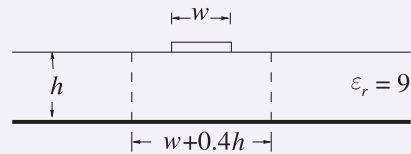
This development assumes that the interface between the dielectric and air forms a good magnetic wall. With a dielectric having a permittivity of 10, typical for microwave circuits, the effective value of h would be increased by up to 10%. However, it is difficult to place an exact value on this.

In summary, f_{c2} is the lowest frequency at which the dielectric mode will exist if there is a discontinuity, and f_{c1} is the lowest frequency at which the dielectric mode will exist if there is not a discontinuity.

EXAMPLE 4.3

Dielectric Mode

The strip of a microstrip has a width of 1 mm and is fabricated on a lossless substrate that is 2.5 mm thick and has a relative permittivity of 9. At what frequency does the substrate (or slab) mode first occur?



Solution:

Two frequencies must be considered. One that comes from the dimensions of the dielectric slab and the other from considerations of matching phase velocities. From phase velocity consideration used in developing Equation (4.31), the first critical frequency is

$$f_{c1} = \frac{c \tan^{-1}(\epsilon_r)}{\sqrt{2\pi h \sqrt{\epsilon_r - 1}}} = 13.9 \text{ GHz.}$$

The other critical frequency is when a

variation of the magnetic or electric field can be supported between the ground plane and the approximate magnetic wall supported by the dielectric/free-space interface. This is when $h = \frac{1}{4}\lambda = \lambda_0/(4\sqrt{9}) = 2.5 \text{ mm} \Rightarrow \lambda_0 = 3 \text{ cm}$. Thus the second slab mode critical frequency is

$$f_{c2} = 10 \text{ GHz.}$$

Since discontinuities cannot be avoided, f_{c2} is the critical frequency to use.

4.6.2 Higher-Order Microstrip Mode

If the cross-sectional dimensions of a microstrip line are smaller than a fraction of a wavelength, then the electric and magnetic field lines will be as shown in Figure 3-2. These field lines have the minimum possible spatial variation and the fields are almost entirely confined to the transverse plane; this mode is called the quasi-TEM microstrip mode. However, as the frequency of the signal on the line increases it is possible for these fields to have one-quarter or one-half sinusoidal variations. Deriving the frequency at which a higher-order microstrip mode is supported is involved.

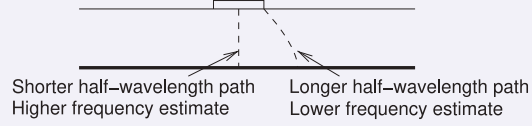
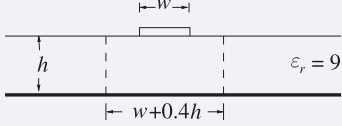
The following is a summary of a more complete discussion on operating frequency limitations in Section 7.8 of [12]. Some variations of the fields or modes do not look anything like the field orientations shown in Figure 3-2. However, the variations that are closest to the quasi-TEM mode are called higher-order microstrip modes and the one that occurs at the lowest frequency corresponds to a half-sinusoidal variation of the electric field between the edge of the strip and the ground plane. This path is a little longer than the path directly from the strip to the ground plane. However, for a wide strip, most of the EM energy is between the strip and the ground plane (both of which are electric walls) with approximate magnetic walls on the side of the strip. The modes are then similar to the parallel-plate waveguide modes described in Section 1.5. The next highest microstrip mode (or parallel-plate TE mode) occurs when there can be a half-sinusoidal variation of the electric field between the strip and the ground plane. This corresponds to Figure 4-15(a). However, for finite-width strips the first higher-order microstrip mode occurs at a lower frequency than implied by the parallel-plate waveguide model. This is because the microstrip fields are not solely confined to the dielectric region, and in fact the electric field lines do not follow the shortest distance between the strip and the ground plane. Thus the fields along the longer paths to the sides of the strip can vary at a lower frequency than on the direct path. With detailed EM modeling and with experimental support it has been established that the first higher-order microstrip mode can exist at frequencies greater than [12]

$$f_{\text{Higher-Microstrip}} = \frac{c}{4h\sqrt{\epsilon_r - 1}}. \quad (4.33)$$

This is, however, only an approximate guide.

EXAMPLE 4.4**Higher-Order Microstrip Mode**

The strip of a microstrip has a width of 1 mm and is fabricated on a lossless substrate that is 2.5 mm thick and has a relative permittivity of 9. At what frequency does the first higher microstrip mode first propagate?

**Solution:**

The higher-order microstrip mode occurs when a half-wavelength variation of the electric field between the strip and the ground plane can be supported. When $h = \lambda/2 = \lambda_0/(3 \cdot 2) = 2.5$ mm; that is, the mode will occur when $\lambda_0 = 15$ mm. So

$$f_{\text{Higher-Microstrip}} = 20 \text{ GHz.}$$

A better estimate of the frequency where the higher-order microstrip mode becomes a problem is given by Equation (4.33):

$$f_{\text{Higher-Microstrip}} = c/(4h\sqrt{\varepsilon_r - 1}) = 10.6 \text{ GHz.}$$

So two estimates have been calculated for the frequency at which the first higher-order microstrip mode can first exist. The first estimate is approximate and is based on a half-wavelength variation of the electric field confined to the direct path between the strip and the ground plane. The second estimate is more accurate as it considers that on the edge of the strip the fields follow a longer path to the ground plane. It is the half-wavelength variation on this longer path that determines if the higher-order microstrip mode will exist. Thus the more precise determination yields a lower critical frequency.

4.6.3 Transverse Microstrip Resonance

For a wide microstrip line, a transverse resonance mode can exist. This is the mode that occurs when EM energy bounces between the edges of the strip with the discontinuity at the strip edges forming a weak boundary. This is illustrated in Figure 4-16, where the microstrip shown in cross section in Figure 4-16(a) is approximated as a rectangular waveguide in Figure 4-16(b) with magnetic walls on the sides and an extended electrical wall on the top surface of the dielectric. Figure 4-16(b) is called the microstrip waveguide model. The transverse resonance mode corresponds to the lowest-order H field variation between the magnetic walls. At the cutoff frequency for this transverse-resonant mode, the equivalent circuit is a resonant transmission line of length $w + 2d$, as shown in Figure 4-17, where $d = 0.2h$ accounts for the microstrip side fringing. A half-wavelength must be supported by the length $w + 2d$. Therefore the cutoff half-wavelength is

$$\frac{\lambda_c}{2} = w + 2d = w + 0.4h, \quad \text{that is,} \quad \frac{c}{2f_c\sqrt{\varepsilon_r}} = w + 0.4h. \quad (4.34)$$

Hence the critical frequency for transverse resonance is

$$f_{c,\text{TRAN}} = \frac{c}{\sqrt{\varepsilon_r}(2w + 0.8h)}. \quad (4.35)$$

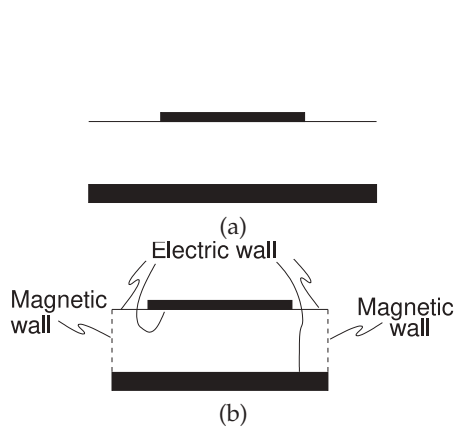


Figure 4-16: Approximation of a microstrip line as a waveguide: (a) cross section of microstrip; and (b) **microstrip waveguide model** having effective width $w + 0.4h$ with magnetic and electric walls.

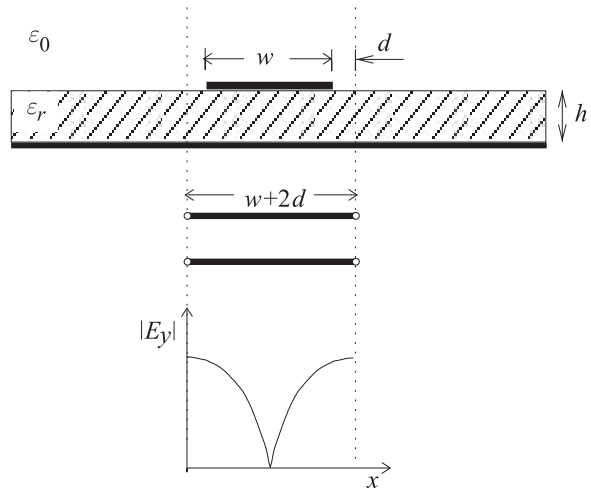


Figure 4-17: Transverse resonance: standing wave ($|E_y|$) and equivalent transmission line of length $w + 2d$, where $d = 0.2h$.

EXAMPLE 4.5

Transverse Resonance Mode

The strip of a microstrip has a width of 1 mm and is fabricated on a lossless substrate that is 2.5 mm thick and has a relative permittivity of 9.

- At what frequency does the transverse resonance first occur?
- What is the operating frequency range of the microstrip line?

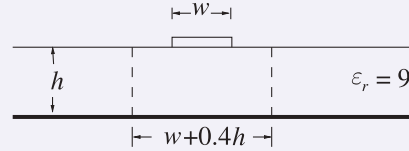
Solution:

$$h = 2.5 \text{ mm}, w = 1 \text{ mm}, \lambda = \lambda_0 / \sqrt{\epsilon_r} = \lambda_0 / 3$$

- The magnetic waveguide model of Figure 4-16 can be used in estimating the frequency at which this occurs. The frequency at which the first transverse resonance mode occurs is when there is a full half-wavelength variation of the magnetic field between the magnetic walls, that is, when $w + 0.4h = \lambda/2 = 2 \text{ mm}$:

$$\frac{\lambda_0}{3 \cdot 2} = 2 \text{ mm} \Rightarrow \lambda_0 = 12 \text{ mm}, \quad \text{and so} \quad f_{c, \text{TRAN}} = 25 \text{ GHz}. \quad (4.36)$$

- All of the critical multimoding frequencies must be considered here and the minimum taken: for the slab mode, f_{c1} (Equation (4.6.1)) and f_{c2} (Equation (4.6.1), see Example 4.3 for the calculation of these); for the higher-order microstrip mode, $f_{\text{High-Microstrip}}$ (Equation (4.33), see Example 4.4 for this calculation)); and for the transverse resonance mode (Equation (4.36), and calculated in this example). So the operating frequency range is DC to 10 GHz.



4.6.4 Summary

There are four principal higher-order modes that need to be considered with microstrip transmission lines:

Mode	Critical frequency
Dielectric (or substrate) mode with no discontinuity	Equation (4.31)
Dielectric (or substrate) mode with discontinuity	Equation (4.32)
Higher order microstrip mode	Equation (4.33)
Transverse resonance mode	Equation (4.35)

The lowest frequency determines the upper frequency of transmission line operation with a single mode.

4.7 High-Frequency Considerations for Coplanar Waveguide

The field orientation on CPW is little affected when frequency increases and as such the effective permittivity of CPW has little frequency dependence. (This is in marked contrast to microstrip.) Thus dielectric-related dispersion of CPW is minimal and this is one of the main advantages of using CPW over microstrip. CPW has the frequency-dependent line resistance

$$R(f) = \begin{cases} R(0) & f \text{ such that } t \leq 3\delta_s \\ R(0) + R_{\text{skin}}(f) & f \text{ such that } t > 3\delta_s, \end{cases} \quad (4.37)$$

where $R(0) (= R_{\text{strip}}(0) + R_{\text{ground}}(0))$ is the resistance of the line at low frequencies. $R(f)$ describes the frequency-dependent line resistance, which is due to both the skin effect and current bunching. Approximately,

$$R_{\text{skin}}(f) = R(0)k\sqrt{f}, \quad (4.38)$$

where k is a constant. As with microstrip, EM simulations are recommended to determine line loss. This is necessary in any case to determine attenuation due to radiation, which can be ignored at low microwave frequencies.

The discussion of multimoding on CPW will consider the finite ground CPW structure (FGCPW) shown in Figure 4-18. Most of the considerations pertaining to multimoding on microstrip apply to FGCPW. However, with CPW the fields penetrate into the substrate a lesser distance and so it is less likely that the substrate mode or microstrip mode will be excited. To avoid the microstrip mode the FGCPW should be a sufficient distance from the bottom ground plane. Generally a substrate height three or more times both the gap and strip width is sufficient. A mode that can exist on FGCPW that does not have an equivalent with microstrip occurs when the ground strips on either side of the center strip acquire different voltages. The correct functioning of FGCPW requires these to be at the same potential. The solution is to connect the two side strips together using grounding straps as shown in Figure 4-19(a). The straps are realized using bond wires if FGCPW is used on a circuit board, or using air bridges if the line is on a monolithic integrated circuit. Placing the strips at approximately one-quarter wavelength distances is appropriate, although this can be relaxed if the line

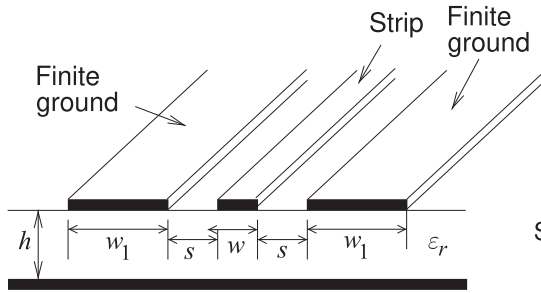


Figure 4-18: Finite ground CPW transmission line.

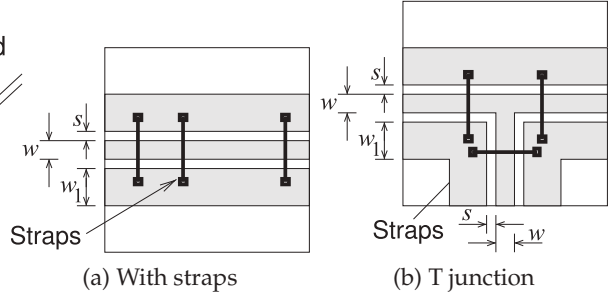
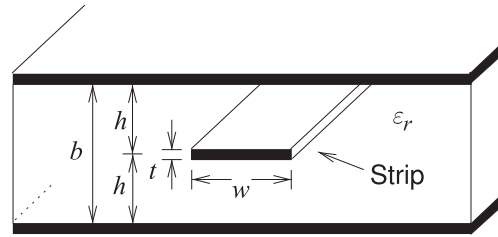


Figure 4-19: CPW structures with ground straps to suppress the parallel plate mode.

Figure 4-20: Stripline transmission line.



is fairly free of discontinuities. The straps should be placed randomly to avoid any filtering effect that could result from placing the straps at regular intervals. The straps should also be used whenever there is a discontinuity (see, e.g., the junction in Figure 4-19(b)).

4.8 High-Frequency Considerations for Stripline

A stripline transmission line is shown in Figure 4-20. Being a homogeneous line, stripline does not have a frequency-dependent permittivity until molecular effects become important at hundreds of gigahertz (depending on the substrate). Stripline has the frequency-dependent line resistance

$$R(f) = \begin{cases} R(0) & f \text{ such that } t \leq 3\delta_s \\ R(0) + R_{\text{skin}}(f) & f \text{ such that } t > 3\delta_s, \end{cases} \quad (4.39)$$

where $R(0) = R_{\text{strip}}(0) + R_{\text{ground}}(0)$ is the resistance of the line at low frequencies. $R(f)$ describes the frequency-dependent line resistance, which is due to both the skin effect and current bunching. Approximately,

$$R_{\text{skin}}(f) = R(0)k\sqrt{f}, \quad (4.40)$$

where k is a constant.

As with microstrip, EM simulations are recommended to determine line loss. However, provided that regular vias are used between the ground planes (and eliminating the TEM parallel plate mode), attenuation due to radiation loss is minimal.

The moding that is of most concern with stripline is the parallel plate waveguide mode that can be excited at stripline discontinuities. The simplest

parallel plate waveguide mode has no variation of the fields in the transverse direction, so there is a uniform electric field from the top plate to the bottom plate. This mode can propagate down to DC. In normal operation a stripline has an E field directed from the strip to the top ground plane and an oppositely directed E field from the strip to the bottom ground plane. Thus excitation of the parallel plate waveguide mode can be suppressed by making sure that the two ground planes are at the same potential. This is done by periodically shorting the two ground planes together using through-substrate vias. Apart from this consideration, the multimoding considerations presented for the microstrip should also be considered.

4.9 Power Losses and Parasitic Effects

Four separate mechanisms lead to power losses in microstrip lines:

- (a) Conductor losses.
- (b) Dissipation in the dielectric of the substrate.
- (c) Radiation losses.
- (d) Surface-wave propagation.

The first two items are dissipative effects, whereas radiation losses and surface-wave propagation are essentially parasitic phenomena. The reader is directed to Chapter 8 of [12] for an extensive treatment. Here, summary results are presented.

Conductor losses greatly exceed dielectric losses for most microstrip lines fabricated on low-loss substrates. Lines fabricated on low-resistivity silicon wafers, however, can have high dielectric loss. These wafers are most commonly used for digital circuits, and the interconnect transverse dimensions are generally very small so that line resistance is very high, and again, resistive losses dominate.

Radiation from a microstrip line results from asymmetric structures. In particular, discontinuities such as abruptly open-circuited microstrip (i.e., open ends), steps, and bends will all radiate to a certain extent. Such discontinuities form essential features of microwave circuits and therefore radiation cannot be avoided. Efforts must be made to reduce such radiation and its undesirable effects. In most cases, radiation can be represented by a shunt admittance.

Surface waves, trapped just beneath the surface of the substrate dielectric, will propagate away from microstrip discontinuities as TE and TM modes. The effect of surface waves can be treated as a shunt conductance.

Various techniques can be used to suppress radiation and surface waves:

- (a) Metallic shielding or “screening.”
- (b) The introduction of lossy (i.e., absorbent) material near any radiative discontinuity.
- (c) The utilization of compact, planar, inherently enclosed circuits such as inverted microstrip and stripline.
- (d) Reducing the current densities flowing in the outer edges of any metal sections and concentrate currents toward the center and in the middle of the microstrip.
- (e) Possibly shaping the discontinuity in some way to reduce the radiative efficiency.

4.10 Lines on Semiconductor Substrates

Propagation on transmission line structures fabricated on semiconductor substrates can have peculiar behavior. The interest in such lines is in relation to RF integrated circuits (RFICs) and monolithic microwave integrated circuits (MMICs) using both silicon and compound semiconductor technologies. More specifically, interconnects on **metal-oxide-semiconductor (MOS)** or **metal-insulator-semiconductor (MIS)** systems, where an insulating layer, such as oxide, exists between the conductor and the semiconductor wafer (see Figure 4-21(a)), are of particular interest due to their ability to support a **slow-wave mode**. A slow-wave mode propagates much slower than would be expected. In the case of a semiconductor substrate with intermediate conductivity, the magnetic field penetrates into the substrate but the electric field does not. This separation of magnetic and electric fields slows the wave. Slow-wave structures find major use in distributed elements on-chip at RF. In particular, a silicon substrate can have a significant impact on microstrip propagation that derives from the charge layer formed at the silicon-silicon dioxide interface. The slow-wave effect is utilized in delay lines, couplers, and filters. With Schottky contact lines, the effect is used in variable-phase shifters, voltage-tunable filters, and various other applications.

Now, an intuitive explanation of the propagation characteristics of microstrip lines on layered substrates can be based on the parallel-plate structure shown in Figure 4-22. For an exact EM analysis of the slow-wave effect with silicon substrates, see [14]. As well as developing a very useful approximation for the important situation of transmission lines on an insulator such as silicon oxide on a semiconductor, the treatment below indicates the type of approach that can be used to analyze unusual structures. In this structure, assume a quasi-TEM mode of propagation. In other words, the wave propagation parameters α , β , and Z_0 can be deduced from electrostatic and magnetostatic solutions for the per unit length parameters C , G , L , and R .

The analysis begins with a treatment of the classic **Maxwell-Wagner capacitor**. Figure 4-23(a) shows the structure of such a capacitor where there are two different materials between the parallel plates of the capacitor with different permittivities and conductivities. The equivalent circuit is shown in

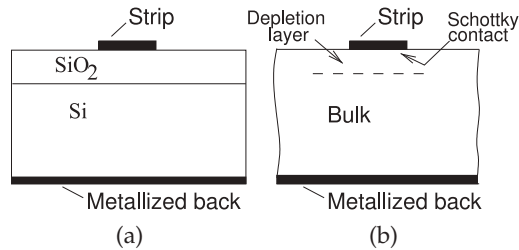


Figure 4-21: Transmission lines on silicon semiconductor: (a) silicon-silicon dioxide sandwich; and (b) bulk view.

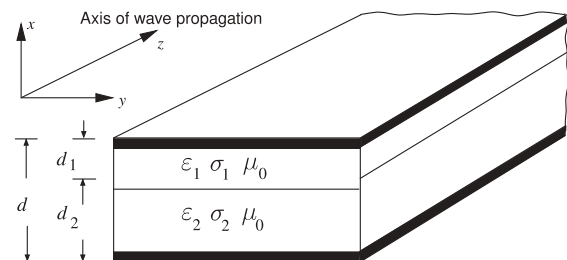


Figure 4-22: Parallel-plate transmission line structure.

Figure 4-23(b) with the elements given by (A is the plate area)

$$C_1 = \varepsilon_1 \frac{A}{d_1}, \quad R_1 = \frac{1}{\sigma_1} \frac{d_1}{A}, \quad C_2 = \varepsilon_2 \frac{A}{d_2}, \quad R_2 = \frac{1}{\sigma_2} \frac{d_2}{A} \quad (4.41)$$

$$\tau_1 = R_1 C_1 = \frac{\varepsilon_1}{\sigma_1}, \quad \tau_2 = R_2 C_2 = \frac{\varepsilon_2}{\sigma_2}. \quad (4.42)$$

The admittance of the entire structure at radian frequency ω is

$$Y(\omega) = \frac{1}{R_1 + R_2} \frac{(1 + j\omega\tau_1)(1 + j\omega\tau_2)}{1 + j\omega\tau}, \quad (4.43)$$

$$\text{where} \quad \tau = \frac{R_1\tau_2 + R_2\tau_1}{R_1 + R_2}. \quad (4.44)$$

$$\text{Introducing} \quad Y(\omega) = j\omega \left(\varepsilon_e \frac{A}{d} \right), \quad (4.45)$$

the effective complex permittivity, $\varepsilon_e = \varepsilon'_e - j\varepsilon''_e$, can be defined in terms of Equation (4.43). Using Equations (4.43) and (4.45) yields

$$\varepsilon'_e = \frac{\tau_1 + \tau_2 - \tau + \tau\tau_1\tau_2\omega^2}{(R_1 + R_2)[1 + (\omega\tau)^2]} \frac{d}{A}. \quad (4.46)$$

Consider now the case when R_1 goes to infinity (i.e., Layer 1, the top layer, in Figure 4-23 is an insulator). For this case, Equation (4.46) becomes

$$\varepsilon'_e = \frac{1 + \left(1 + \frac{d_2}{d_1} \frac{\varepsilon_1}{\varepsilon_2}\right) \left(\frac{\omega\varepsilon_2}{\sigma_2}\right)^2}{1 + \left(1 + \frac{d_2}{d_1} \frac{\varepsilon_1}{\varepsilon_2}\right)^2 \left(\frac{\omega\varepsilon_2}{\sigma_2}\right)^2} \left(\varepsilon_1 \frac{d}{d_1}\right). \quad (4.47)$$

It is clear from Equations (4.46) and (4.47) that the effective complex permittivity has a frequency-dependent component. Consider how this varies with a few cases of ω . For $\omega = 0$, the static value of the effective permittivity is

$$\varepsilon'_{e,0} = \varepsilon_1 \frac{d}{d_1}. \quad (4.48)$$

For the case where ω goes to infinity (the optical value), the real part of the effective permittivity is

$$\varepsilon'_{e,\infty} = \frac{\varepsilon_1\varepsilon_2(d_1 + d_2)}{\varepsilon_2d_1 + \varepsilon_1d_2}. \quad (4.49)$$

Note also that the value of $\varepsilon'_{e,\infty}$ can be approximately achieved for a large value of $\omega\varepsilon_2/\sigma_2$ (i.e., low-conductivity substrates can be used to ensure that the displacement currents dominate). In a similar way, it is clear that $\varepsilon'_{e,0}$ can be achieved by having a small value of $\omega\varepsilon_2/\sigma_2$. Also note that $\varepsilon'_{e,0}$ can be made very large by making d_1 much smaller than d .

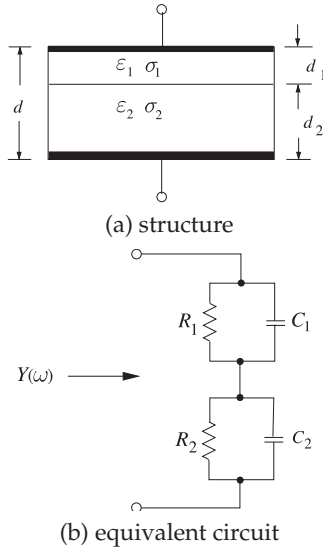


Figure 4-23: Maxwell-Wagner capacitor.

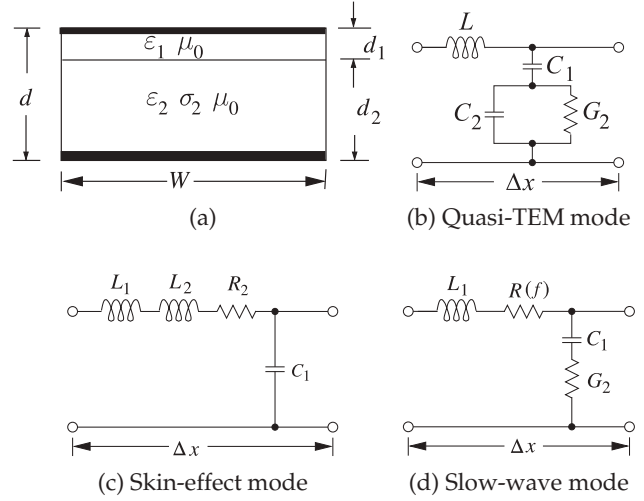


Figure 4-24: Modes on an MOS transmission line: (a) equivalent structure of the MOS line of Figure 4-21.

EXAMPLE 4.6

Two-Layer Substrate

Consider the structure in Figure 4-22. Determine the guide wavelength, λ_g , and the wavelength in the insulator, λ_1 , at a frequency of 1 GHz. SiO_2 and Si are the dielectrics, with permittivities $\epsilon_1 = 4\epsilon_0$ and $\epsilon_2 = 13\epsilon_0$ (the conductivities are zero). The depths d_2 and d_1 of the two dielectrics are $d_2 = 250 \mu\text{m}$ and $d_1 = 0.1 \mu\text{m}$.

Solution:

$$\lambda_1 = \frac{3 \times 10^8}{10^9 \sqrt{4}} = 0.15 \text{ m} = 15 \text{ cm},$$

$$\epsilon_e = \frac{\epsilon_1 \epsilon_2 (d_1 + d_2)}{\epsilon_1 d_2 + \epsilon_2 d_1} = 12.99 \epsilon_0, \quad \lambda_g = \frac{3 \times 10^8}{10^9 \sqrt{12.99}} = 0.0832 \text{ m} = 8.32 \text{ cm}. \quad (4.50)$$

4.10.1 Modes on the MIS (MOS) Line

The previous description of the properties of a Maxwell-Wagner capacitor leads to a discussion of the possible modes on the MIS (MOS) line. To make the problem tractable, the transmission line shown in Figure 4-21(a) will be approximated as having the cross section shown in Figure 4-24(a).

Dielectric Quasi-TEM Mode

The first possible mode is the dielectric quasi-TEM mode, for which the sectional equivalent circuit model of Figure 4-24(b) is applicable. In this mode $\sigma_2 \ll \omega \epsilon_2$. This implies from the earlier discussion that $\epsilon'_e = \epsilon'_{e,\infty}$ and $\mu'_e = \mu_0$. Thus the per unit length parameters are

$$L = \mu_0 \frac{d_1}{W}, \quad C_1 = \epsilon_1 \frac{W}{d_1}, \quad C_2 = \epsilon_2 \frac{W}{d_2}, \quad G_2 = \sigma_2 \frac{W}{d_2}. \quad (4.51)$$

These have the SI units H/m for L , F/m for C_1 , F/m for C_2 , and S/m for G_2 .

Skin-Effect Mode

The second possible mode is the **skin-effect mode**, for which the sectional equivalent circuit model of Figure 4-24(c) is applicable. Here, $\sigma_2 \ll \omega \varepsilon_2$ is such that the skin depth $\delta_s = 1/\sqrt{\pi f \mu_0 \sigma_2}$ in the semiconductor is much smaller than d_2 and

$$\varepsilon'_e = \varepsilon'_{e,0}, \quad \mu'_e = \frac{\mu_0}{d} \left(d_1 + \frac{\delta_s}{2} \right),$$

Thus

$$L_1 = \mu_0 \frac{d_1}{W}, \quad C_1 = \varepsilon_1 \frac{W}{d_1} \quad (4.52)$$

$$L_2 = \mu_0 \frac{1}{W} \left(\frac{\delta_s}{2} \right), \quad R_2 = 2\pi f \mu_0 \frac{1}{W} \left(\frac{\delta_s}{2} \right). \quad (4.53)$$

These have the SI units H/m for L_1 and L_2 , F/m for C_1 , and Ω/m for R_2 .

Slow-Wave Mode

The third possible mode of propagation is the slow-wave mode [15, 16], for which the sectional equivalent circuit model of Figure 4-24(d) is applicable. This mode occurs when f is not so large and the resistivity is moderate so that the skin depth, δ_s , is larger than (or on the order of) d_2 . Thus $\varepsilon'_e = \varepsilon'_{e,0}$, but $\mu'_e = \mu_0$. Therefore

$$v_p = \frac{1}{\sqrt{\varepsilon'_e \mu'_e}} = \frac{1}{\sqrt{\mu_0 \varepsilon_0}} \frac{1}{\sqrt{\varepsilon_1}} \sqrt{\frac{d_1}{d}} \quad (4.54)$$

(with SI units of m/s) and $\lambda_g = \lambda_1 \sqrt{d_1/d}$, where λ_1 is the wavelength in the insulator.

4.11 Summary

Design is an iterative process and initial RF design is based on frequency-independent characteristics. For a transmission line, quantities such as the characteristic impedance, effective permittivity, phase and group velocities, and the RLGC parameters are taken as fixed. The RLGC parameters are the basis of the simplest lumped-element circuit model of a transmission line. Each of the components of this model will vary with frequency. The resistance per unit length, R , increases with frequency as charges concentrate on the surface of conductors and charges bunch (i.e., become less spread out). Both of these effects are due to the finite time it takes to transmit the EM signal that rearranges charges to support an alternating wave.

An EM signal on a transmission line is described by Maxwell's equations and there can be many possible solutions depending on the boundary conditions. With transmission lines and other microwave structures such as resonators these are called modes. All transmission lines have at least two solutions, the forward- and backward-traveling waves. While strictly these are also modes, this classification is avoided by microwave engineers. Microwave engineers identify modes as different solutions to Maxwell's equations that, for transmission lines, are different orientations of the

fields largely in the transverse direction to propagation. Each mode will, in general, have forward- and backward-traveling components. A two-conductor transmission line is designed to have dimensions that are small enough that there is only one mode, or else special precautions are taken to avoid a second mode being established. Sometimes multimoding is desirable. If these multimoded structures are used there are strict design criteria that enable the special functionality that is made available to be exploited. Multimoding sets the upper bound on the frequency of operation of most transmission line structures.

The most popular microwave transmission lines—microstrip, stripline and CPW—can all support multiple modes, but most are cut off by keeping transverse dimensions small with respect to a wavelength. When it is possible for a second (or higher-order) mode to exist, whether that mode is generated depends on the coupling mechanism between modes. This coupling mechanism is a discontinuity, which of course is common if circuit structures are to be incorporated. Stripline and CPW can support a second mode at quite low frequencies. With stripline the dominant second mode is the parallel-plate waveguide mode supported by the two ground planes of stripline.

A microwave designer must always be aware of frequency dependence and multimoding and choose dimensions to avoid their occurrence except when the use is intentional and controlled.

4.12 References

- [1] C. Holloway and G. A. Hufford, "Internal inductance and conductor loss associated with the ground plane of a microstrip line," *IEEE Trans. on Electromagnetic Compatibility*, vol. 39, no. 2, pp. 73–78, May 1997.
- [2] G. Ponchak and A. Downey, "Characterization of thin film microstrip lines on polyimide," *IEEE Trans. on Components, Packaging, and Manufacturing Technology, Part B: Advanced Packaging*, vol. 21, no. 2, pp. 171–176, May 1998.
- [3] Hai-Young Lee and T. Itoh, "Phenomenological loss equivalence method for planar quasi-tem transmission lines with a thin normal conductor or superconductor," *IEEE Trans. on Microwave Theory and Techniques*, vol. 37, no. 12, pp. 1904–1909, Dec. 1989.
- [4] W. Heinrich, "Quasi-tem description of MMIC coplanar lines including conductor-loss effects," *IEEE Trans. on Microwave Theory and Techniques*, vol. 41, no. 1, pp. 45–52, Jan. 1993.
- [5] M. Born and E. Wolf, *Principles of Optics: Electromagnetic Theory of Propagation, Interference, and Diffraction of Light*, 7th ed. Cambridge University Press, 1999.
- [6] K. Coperich, J. Morsey, V. Okhmatovski, A. Cangellaris, and A. Ruehli, "Systematic development of transmission-line models for interconnects with frequency-dependent losses," *IEEE Trans. on Microwave Theory and Techniques*, vol. 49, no. 10, pp. 1677–1685, Oct. 2001.
- [7] W. Heinrich, "Full-wave analysis of conductor losses on MMIC transmission lines," *IEEE Trans. on Microwave Theory and Techniques*, vol. 38, no. 10, pp. 1468–1472, Oct. 1990.
- [8] R. Faraji-Dana and Y. Chow, "The current distribution and ac resistance of a microstrip structure," *IEEE Trans. on Microwave Theory and Techniques*, vol. 38, no. 9, pp. 1268–1277, Sep. 1990.
- [9] A. Djordjevic and T. Sarkar, "Closed-form formulas for frequency-dependent resistance and inductance per unit length of microstrip and strip transmission lines," *IEEE Trans. on Microwave Theory and Techniques*, vol. 42, no. 2, pp. 241–248, Feb. 1994.
- [10] B. Biswas, A. Glasser, S. Lipa, M. Steer, P. Franzon, D. Griffiths, and P. Russell, "Experimental electrical characterization of on-chip interconnects," in *IEEE 6th Topical Meeting on Electrical Performance of Electronic Packaging*, 1997, pp. 57–59.
- [11] A. Deutsch, R. Krabbenhoft, K. Melde, C. Surovic, G. Katopis, G. Kopcsay, Z. Zhou, Z. Chen, Y. Kwark, T.-M. Winkel, X. Gu, and T. Standaert, "Application of the short-pulse

- propagation technique for broadband characterization of pcb and other interconnect technologies," *IEEE Trans. on Electromagnetic Compatibility*, vol. 52, no. 2, pp. 266–287, May 2010.
- [12] T. Edwards and M. Steer, *Foundations for Microstrip Circuit Design*. John Wiley & Sons, 2016.
- [13] G. Vendelin, "Limitations on stripline Q," *Microwave Journal*, pp. 63–69, 1970.
- [14] H. Hasegawa, M. Furukawa, and H. Yanai, "Properties of microstrip line on si-sio2 system," *IEEE Trans. on Microwave Theory and Techniques*, vol. 19, no. 11, pp. 869–881, Nov. 1971.
- [15] D. Jager, "Slow-wave propagation along variable schottky-contact microstrip line," *IEEE Trans. on Microwave Theory and Techniques*, vol. 24, no. 9, pp. 566–573, Sep. 1976.
- [16] Y. K. et al, "Quasi-tem analysis of "slow-wave" mode propagation on coplanar microstructure mis transmission lines," *IEEE Trans. on Microwave Theory and Techniques*, vol. 35, no. 6, pp. 545–551, Jun. 1987.

4.13 Exercises

- Current bunching and the skin effect result in transmission line loss increasing with frequency.
 - Show current bunching on a transverse diagram of the microstrip line.
 - Describe the skin effect on a transverse diagram of the microstrip line.
- What is the skin depth on a copper microstrip line at 10 GHz? Assume that the conductivity of the deposited copper forming the strip is half that of bulk single-crystal copper. Use the data in the table on page 130.
- What is the skin depth on a silver microstrip line at 1 GHz? Assume that the conductivity of the fabricated silver conductor is 75% that of bulk single-crystal silver. Use the data in the table on page 130.
- What is the dominant source of dispersion on a microstrip transmission line?
- Using Figure 4-12, determine the complex characteristic impedance and complex effective permittivity of a microstrip line at 12 GHz. The line is fabricated on alumina with $\epsilon_r(0) = 9.9$, $w = 240 \mu\text{m}$, $h = 500 \mu\text{m}$.
- A magnetic wall and an electric wall are 2 cm apart and are separated by a lossless material having a relative permittivity of 10 and a relative permeability of 23. What is the cut-off frequency of the lowest-order mode in this system?
- Describe the transverse resonance mode on stripline. When can it occur?
- The strip of a microstrip has a width of $600 \mu\text{m}$ and is fabricated on a lossless substrate that is 1 mm thick and has a relative permittivity of 10.
 - Draw the microstrip waveguide model of the microstrip line. Put dimensions on your drawing.
 - Sketch the electric field distribution of the first transverse resonance mode and calculate the frequency at which the transverse resonance mode occurs.
- A microstrip line has a width of $352 \mu\text{m}$ and is constructed on a substrate that is $500 \mu\text{m}$ thick with a relative permittivity of 5.6.
 - Determine the frequency at which transverse resonance would first occur.
 - When the dielectric is slightly less than one-quarter wavelength in thickness the dielectric slab mode can be supported. Some of the fields will appear in the air region as well as in the dielectric, extending the effective thickness of the dielectric. Ignoring the fields in the air (use a one-quarter wavelength criterion), at what frequency will the dielectric slab mode first occur?
- The strip of a microstrip has a width of $600 \mu\text{m}$ and uses a lossless substrate that is $635 \mu\text{m}$ thick and has a relative permittivity of 4.1.
 - At what frequency will the first transverse resonance occur?
 - At what frequency will the first higher-order microstrip mode occur?
 - At what frequency will the slab mode occur?
 - Identify the useful operating frequency range of the microstrip.
- The design space for transmission lines in microstrip designs is determined by the design project leader to be 20–100 Ω . The preferred substrate has a thickness of $500 \mu\text{m}$ and a relative permittivity of 8. What is the maximum operating frequency range of designs supported by this technology choice. Ignore frequency disper-

sion effects (i.e., frequency dependence of effective permittivity and losses). [Hint: First determine the dimensions of the strip that will provide the required impedance range and then determine the frequency at which lowest-order multimoding occurs.]

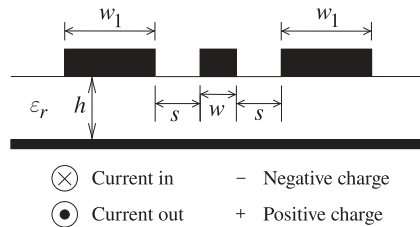
12. Consider the design of transmission lines in microstrip technology using a lossless substrate with a relative permittivity of 10 and thickness of 400 μm . You will want to use the formulas in Section 3.5.3.
 - (a) What is the maximum characteristic impedance that can be achieved for a transmission line fabricated in this technology?
 - (b) Plot the characteristic impedance versus strip width.
 - (c) From manufacturing tolerance considerations, the minimum strip width that can be manufactured is 20 μm . What is the maximum characteristic impedance that can be achieved in practice?
 - (d) If the operating frequency range is 1–10 GHz, determine the maximum width of the strip from higher-order mode considerations. You must consider the transverse resonance mode as well as higher-order microstrip modes.
 - (e) Identify the electrical design space (i.e., the achievable characteristic impedance range).
 - (f) Identify the physical design space (i.e., the range of acceptable strip widths).
 - (g) If the electrical design space requires that transmission line impedances be achieved within $\pm 2 \Omega$, what tolerance must be achieved in the manufacturing process if the substrate thickness can be achieved exactly? [Hint: First identify the critical physical process corner and thus the critical strip width that is most susceptible to width variations. Then determine the tolerance on the strip width to achieve the allowable characteristic impedance variation. That is, characteristic impedance is a function of strip width and height. If the substrate is perfect (no height variation), then how much can the strip width vary to keep the impedance within $\pm 2 \Omega$ of the desired value? You can solve this graphically using a plot of Z_0 versus width or you can iteratively arrive at the answer by recalculating Z_0 .]
 - (h) If the electrical design space requires that transmission line impedances be achieved within $\pm 2 \Omega$, what tolerance must be achieved in the manufacturing process if the substrate thickness tolerance is $\pm 2 \mu\text{m}$?

If the substrate is not perfect (the height variation is $\pm 2 \mu\text{m}$), then how much can the strip width vary to keep the impedance within $\pm 2 \Omega$ of the desired value? This problem is directly applicable to real-world process/design trade-offs.
13. The strip of a microstrip has a width of 500 μm and is fabricated on a lossless substrate that is 635 μm thick and has a relative permittivity of 12. [Parallels Examples 4.3, 4.4, and 4.5]
 - (a) At what frequency does the transverse resonance first occur?
 - (b) At what frequency does the first higher-order microstrip mode first propagate?
 - (c) At what frequency does the substrate (or slab) mode first occur?
14. The strip of a microstrip has a width of 250 μm and uses a lossless substrate that is 300 μm thick and has a relative permittivity of 15.
 - (a) At what frequency does the transverse resonance first occur?
 - (b) At what frequency does the first higher-order microstrip mode propagate?
 - (c) At what frequency does the substrate (or slab) mode first occur?
 - (d) What is the highest operating frequency of the microstrip?
15. A microstrip line has a strip width of 100 μm and is fabricated on a substrate that is 150 μm thick and has a relative permittivity of 9.
 - (a) Draw the microstrip waveguide model and indicate and calculate the dimensions of the model.
 - (b) Based only on the microstrip waveguide model, determine the frequency at which the first transverse resonance occurs?
 - (c) Based on the microstrip waveguide model, determine the frequency at which the first higher-order microstrip mode occurs?
 - (d) At what frequency will the slab mode occur? For this you cannot use the microstrip waveguide model.
16. A microstrip line has a strip width of 100 μm and is fabricated on a substrate that is 150 μm thick and has a relative permittivity of 9.
 - (a) Define the properties of a magnetic wall.
 - (b) Identify two situations where a magnetic wall can be used in the analysis of a microstrip line; that is, give two situations where a magnetic wall approximation can be used.
 - (c) Draw the microstrip waveguide model and indicate and calculate the dimensions of the model.

17. Consider the design of transmission lines in microstrip technology using a lossless substrate with relative permittivity of 20 and thickness of 200 μm .
 - (a) Using qualitative arguments, show that the maximum characteristic impedance that can be achieved for a transmission line fabricated in this technology is 116 Ω . The maximum is not actually 116 Ω , but a simple argument will bring you to this conclusion.
 - (b) Plot the characteristic impedance versus substrate width.
 - (c) From manufacturing tolerance considerations, the minimum strip width that can be manufactured is 20 μm . What is the maximum characteristic impedance that can be achieved in practice?
 - (d) If the operating frequency range is 2–18 GHz, determine the maximum width of the strip from higher-order mode considerations. You must consider the transverse resonance mode, the higher-order mode, and the slab mode.
 - (e) Identify the electrical design space (i.e., the characteristic impedance range).
 - (f) Identify the physical design space (i.e., the range of acceptable strip widths).
 - (g) If the electrical design space requires that transmission line impedances be achieved within $\pm 2 \Omega$, what tolerance must be achieved in the manufacturing process if the substrate thickness can be achieved exactly? [Hint: First identify the critical physical process corner and thus the critical strip width that is most susceptible to width variations. Then determine the tolerance on the strip width to achieve the allowable characteristic impedance variation.]
 - (h) If the electrical design space requires that transmission line impedances be achieved within $\pm 2 \Omega$, what tolerance must be achieved in the manufacturing process if the substrate thickness tolerance is $\pm 2 \mu\text{m}$?
18. The strip of a microstrip line has a width of 0.5 mm, and the microstrip substrate is 1 mm thick and has a relative permittivity of 9 and relative permeability of 1.
 - (a) Draw the microstrip waveguide model and calculate the dimensions of the model. Clearly show the electric and magnetic walls in the model.
 - (b) Use the microstrip waveguide model to calculate the cut off frequency of the transverse resonance mode?
 - (c) A substrate mode can also be excited but the cut off frequency of this mode cannot be calculated using the microstrip waveguide model. Provide a brief description of the substrate mode and calculate the lowest frequency at which it can exist.
19. A microstrip technology uses a substrate with a relative permittivity of 10 and thickness of 400 μm . If the operating frequency is 10 GHz, what is the maximum width of the strip from higher-order mode considerations.
20. A microstrip line operating at 18 GHz has a 200 μm thick substrate with a relative permittivity of 20.
 - (a) Determine the maximum width of the strip from higher-order mode considerations. Consider the transverse resonance mode, the higher-order microstrip mode, and the slab mode.
 - (b) Thus determine the minimum achievable characteristic impedance.
21. A microstrip line has a strip width of 100 μm and is fabricated on a 150 μm -thick lossless substrate with a relative permittivity of 9.
 - (a) Define the properties of a magnetic wall.
 - (b) Identify two situations where a magnetic wall can be used in determining multimoding on a microstrip line. That is, give two locations where a magnetic wall approximation can be used.
22. Two magnetic walls are separated by 1 mm in a lossless material having a relative permittivity of 9 and a relative permeability of 1.
 - (a) What is the wavelength of a 10 GHz signal in this material?
 - (b) Now consider a field variation, i.e. a mode and not constant, established by the magnetic walls. Describe this lowest order field variation. That is how does the H field vary or how does the E field vary (one is sufficient)?
 - (c) What is the lowest frequency at which a field variation can be supported by those walls in the specified medium?
23. A microstrip line has a strip width of 250 μm and a 300 μm thick substrate with a relative permittivity of 15. At what frequency can the substrate mode first occur?
24. A microstrip line has a strip width of 250 μm and a 300 μm thick substrate with a relative permittivity of 15. At what frequency can a higher-order microstrip mode first propagate?
25. A microstrip line has a strip width of 200 μm and a substrate that is 400 μm thick and has a rela-

tive permittivity of 4. Use the microstrip waveguide model to determine the lowest frequency at which higher-order microstrip mode can occur.

26. A microstrip line has a strip width of $250\text{ }\mu\text{m}$ and a $300\text{ }\mu\text{m}$ thick substrate with a relative permittivity of 15. At what frequency can transverse resonance first occur?
27. The figure below is the cross section of a finite ground coplanar waveguide (FGCPW) transmission line over a ground plane. The FGCPW consists of the ground strips of width w_1 and the strip of width w . Now $w_1 = 2.5 \times s$, $w = 1.3 \times s$, and $h = 4 \times s$. The thickness is $t = 0.3 \times s$.



- (a) Ignore the bottom ground plane for now. Redraw the structure and indicate the charge and current distributions at microwave frequencies using the convention shown. On the strip the current flows in and the charge is positive.
- (b) Does this structure support a transverse EM mode?
- (c) Again ignoring the bottom ground plane, redraw the structure and indicate the region where the energy is concentrated.
- (d) Now consider the complete structure. If the guide wavelength is λ_g , and the wavelength in the dielectric is λ , indicate the criterion for the lowest frequency at which transverse resonance will become a problem.
28. Use a diagram to show the E and H fields of the microstrip mode on finite ground CPW.
29. Does finite ground CPW support a transverse resonance mode? Explain.
30. For a finite ground CPW line illustrate the following modes and the conditions under which they occur.
- The microstrip mode.
 - The cross mode (the ground planes not at the same potential).
 - The transverse mode mode.
31. Consider a symmetrical stripline with the following parameters: total substrate thickness, $d = 1.7\text{ mm}$; strip width, $w = 2.5\text{ mm}$; relative permittivity of the substrate = 9; and operating frequency = 30 GHz.
- What is the value of the effective permittivity?
 - What is the value of the free-space wavelength?
 - What is the value of the guide wavelength?
32. What is the dominant cause of dispersion on a stripline? That is, what is most likely to cause frequency dependence of the characteristic impedance and propagation constant of the line.
33. The strip of a microstrip line has a width of $200\text{ }\mu\text{m}$ and the substrate is $400\text{ }\mu\text{m}$ thick and has a relative permittivity of 4.
- Draw the effective waveguide model of a microstrip line with magnetic walls and an effective strip width, w_{eff} .
 - What is the effective relative permittivity of the microstrip waveguide model?
 - What is w_{eff} ?
 - Can the lowest frequency at which the transverse resonance mode first occurs be determined from the microstrip waveguide model?
34. The strip of a symmetrical stripline has a width of $200\text{ }\mu\text{m}$ and is embedded in a lossless medium that is $400\text{ }\mu\text{m}$ thick and has a relative permittivity of 13, thus the separation, h , from the strip to each of the ground planes is $200\text{ }\mu\text{m}$.
- Draw the waveguide model of a stripline with magnetic walls and an effective strip width, w_{eff} , which will be approximately the same as with a microstrip line.
 - What is the effective relative permittivity of the stripline waveguide model?
 - What is w_{eff} ?
 - At what frequency will the first transverse resonance occur?
 - At what frequency will the first higher-order stripline mode occur?
 - At what frequency will the first parallel-plate waveguide mode occur? Do not consider the mode with no field variation, as this cannot be excited.
 - Identify the useful operating frequency range of the stripline.
35. Describe the parallel-plate mode on stripline.
36. Consider the structure in Figure 4-22. Determine the guide wavelength, λ_g , and the wavelength in the top insulator, λ_1 , at a frequency of 20 GHz. The permittivities are $\epsilon_1 = 3.9\epsilon_0$ and $\epsilon_2 = 13\epsilon_0$. The depths of the dielectrics are $d_2 = 100\text{ }\mu\text{m}$ and $d_1 = 1.0\text{ }\mu\text{m}$. [Parallels Example 4.6]
37. Consider a metal-oxide-semiconductor transmission medium as examined in Section 4.10.

The structure in the form of a Maxwell–Wagner capacitor is shown in Figure 4-23(a) with $d_1 = 100 \mu\text{m}$, $d_2 = 500 \mu\text{m}$, and relative permittivities $\varepsilon_{r1} = 3.9$ and $\varepsilon_{r2} = 13$. Ignore the finite con-

ductivity. What is the capacitance model of this structure (see Figure 4-23(b)) and what are the values of the capacitances?

4.13.1 Exercises by Section

[†]challenging, [‡]very challenging

§4.2 1[†], 2, 3

§4.3 4[†]

§4.4 5

§4.5 6, 7

§4.6 8[†], 9[†], 10[†], 11[‡], 12[‡], 13[†], 14[†], §4.8 31[‡], 32[†], 33[†], 34[‡], 35

15[†], 16[†], 17[‡], 18[†], 19, 20, 21, §4.10 36, 37[†]

22, 23, 24, 25, 26

§4.7 27[‡], 28, 29, 30

4.13.2 Answers to Selected Exercises

3 2.315 μm

6 247 MHz

8(c) 25 GHz

9(c) DC to 63.4 GHz

10(d) $\text{DC} \leq f \leq 48.6 \text{ GHz}$

14 104.6 GHz

17(a) 116 Ω

17(f) $20 \mu\text{m} < w < 1.96 \text{ mm}$

18(b) 55.6 GHz

34 207.9 GHz

Coupled Lines and Applications

5.1	Introduction	203
5.2	Physics of Coupling	204
5.3	Coupled Transmission Line Theory	208
5.4	Low Frequency Capacitance Model of Coupled Lines	210
5.5	Symmetric Coupled Transmission Lines	213
5.6	Formulas for Impedance of Coupled Microstrip Lines	217
5.7	Terminated Coupled Lines	223
5.8	Directional Coupler	227
5.9	Models of Parallel Coupled Lines	235
5.10	Differential and Common Modes	243
5.11	Common Impedance Coupling	246
5.12	Summary	246
5.13	References	248
5.14	Exercises	249

5.1 Introduction

This chapter describes what happens when two transmission lines are so close together that the fields produced by one line interfere with the other line. Then a portion of the signal energy on one line is transferred to the other resulting in coupling. For microstrip lines the coupling reduces as the lines separate and usually the coupling is small enough to be ignored if the separation is at least three times the height of the strips. Transmission line coupling may be undesirable in many situations, but the phenomenon is exploited to realize many novel RF and microwave elements such as filters. A coupled pair of transmission lines also enables the forward- and backward-traveling waves on a line to be separately measured.

The chapter begins with a discussion of the physics of coupling which leads to the preferred description of propagation on a pair of **parallel coupled lines (PCLs)** as supporting an even mode and an odd mode, and forward- and backward-traveling versions of each. Many microwave circuit elements are based on PCL elements such as PCL filters. The separation of the fields into even and odd modes comes naturally from a consideration of the fields. This leads to a low-frequency circuit model described in Section 5.4. Section 5.4.1 presents a high frequency

model of a PCL with the L and C model of a single transmission line replaced by multiple inductances, capacitances, and mutual inductances and capacitances. As with single microstrip lines, formulas have been developed for the propagation characteristics of a pair of coupled microstrip lines, and these are presented in Section 5.6. The rest of the chapter builds up design concepts and presents some particular applications on the way.

Section 5.7 presents the analysis used to determine reflection coefficients of terminated coupled lines. The next section, Sections 5.8, describe two types of couplers that use a pair of coupled lines to selectively separate and tap off a portion of the power in either the forward-traveling wave, the backward-traveling wave, or both. A design technique for synthesizing them is presented and this is key to nearly all design using a pair of coupled lines as a circuit element. Section 5.9 presents the circuit models for various coupled line configurations and these models are essential to the synthesis of PCL-based microwave components. There are other ways to partition the modes on a pair of coupled lines and with RFICs the preferred description uses differential and common modes as described in Section 5.10. The difference between these modes and odd and even modes comes down to bookkeeping with a preference to use differential and common modes with circuits, and a preference to use odd and even modes when relating to fields. The final section, Section 5.11, describes another type of coupling, common impedance coupling. This is not always related to PCLs but this is the appropriate place to consider this phenomenon.

5.2 Physics of Coupling

If the fields of one transmission line intersect the region around another transmission line, then some of the energy propagating on the first line appears on the second. This coupling discriminates in terms of forward- and backward-traveling waves. In particular, consider the coupled microstrips shown in Figure 5-1. The direction of propagation comes from $\vec{E} \times \vec{H}$. Using the right-hand rule, the direction of propagation of the signal on the left-hand strip is out of the page. This is called the forward-traveling direction. Now consider the fields around the right-hand strip, the inactive line, and note the direction of the E field. The H field immediately to the left of the right-hand strip is stronger than on the right of the strip. So effectively there is a clockwise circulation of the H field around the right hand strip. By applying $\vec{E} \times \vec{H}$ to the signal induced on the right-hand strip, it is seen that the induced signal travels into the page, or in the backward-traveling direction. The coupling with parallel-coupled microstrip lines is called backward-wave coupling. This is, of course, a frequency-domain view of coupling. In practice, there is also a small component of forward coupling.

In digital systems the forward coupling is of most importance because of the way traveling waves are reinforced. To appreciate this, consider a voltage step traveling in the forward direction on one strip. The step edge couples across to the neighboring line, producing a large backward-traveling pulse and a smaller forward-traveling pulse (approximately the derivative of the original step signal). The coupled forward-traveling pulse travels at the same velocity as the step signal so that the coupled forward-traveling signal integrates over time, whereas the backward-traveling signal does not.

The discussion now returns to the frequency-domain view, as this is the

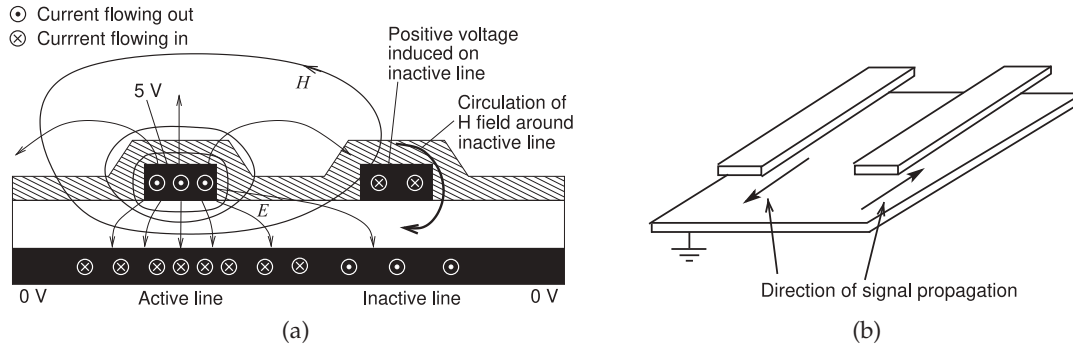


Figure 5-1: Edge-coupled microstrip lines with the left line driven with the forward-traveling field coming out of the page: (a) cross section of microstrip lines as found on a printed circuit board showing a conformal top passivation or solder resist layer; and (b) in perspective showing the direction of propagation of the driven line (left) and the direction of propagation of the main coupled signal on the victim line (right).

required orientation in designing narrowband systems (i.e., most RF and microwave circuits). Previously forward- and backward-traveling waves on an individual transmission line were introduced as separate modes; each mode is a self-sustaining and propagating field orientation on a transmission line. By analogy, in understanding coupled line behavior, and to facilitate design using transmission line coupling, it is a good idea to treat a pair of coupled lines as a single transmission structure. This structure supports two families of modes called the even mode and the odd mode, and both have forward- and backward-traveling components (see Figure 5-2).

In the even mode (Figures 5-2(a and b)), the amplitude and polarity of the voltages on the two signal conductors are the same. In the odd mode (Figures 5-2(c and d)), the voltages on the two signal conductors are equal but have opposite polarity. Any EM field orientation on the coupled lines can be represented as a weighted addition of the even-mode and odd-mode field configurations.

It is just as valid to consider the field orientations based on each of the lines (taken one at a time) and to consider the effect of the other line as a perturbation of the fields of the first line. However, the odd- and even-mode view of the fields assists in understanding and quantitatively describing coupling. This view facilitates the design of components that exploit coupling. The configuration of the fields supported by the coupled lines depends on how the lines are driven and terminated. The actual fields will be a superposition of the even and odd modes. Also, at any instant the voltages on the lines are composed of even and odd components.

The characteristic impedances of the even and odd modes will differ because of the different field orientations. These are termed the even-mode and odd-mode characteristic impedances, denoted by Z_{0e} and Z_{0o} , respectively. Here the e subscript identifies the even mode and the o subscript identifies the odd mode. With coupled microstrip lines, the phase velocities

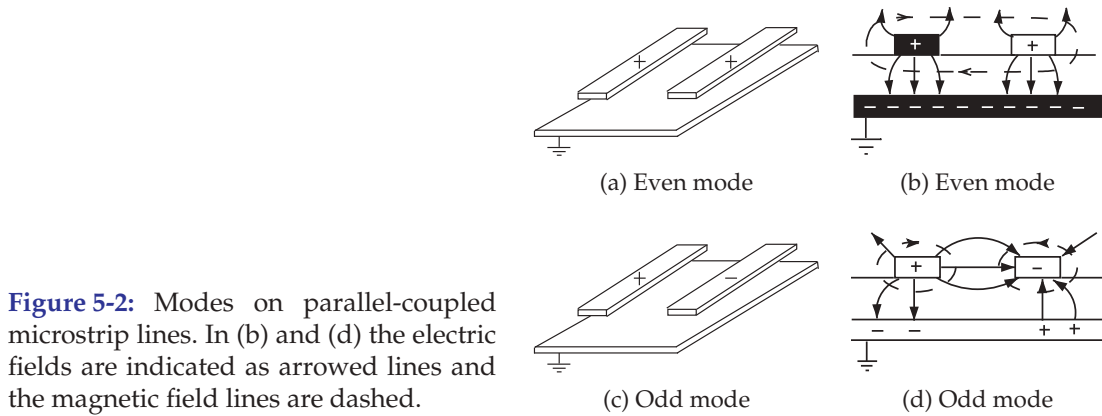


Figure 5-2: Modes on parallel-coupled microstrip lines. In (b) and (d) the electric fields are indicated as arrowed lines and the magnetic field lines are dashed.

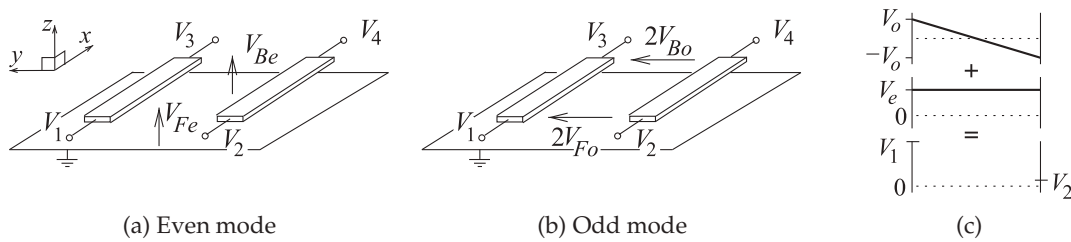


Figure 5-3: Definitions of total voltages and even- and odd-mode voltage phasors on a pair of coupled microstrip lines: (a) even-mode voltage definition; (b) odd-mode voltage definition; (c) depiction of how even- and odd-mode voltages combine to yield the total voltages on individual lines. *F* indicates front and *B* indicates back.

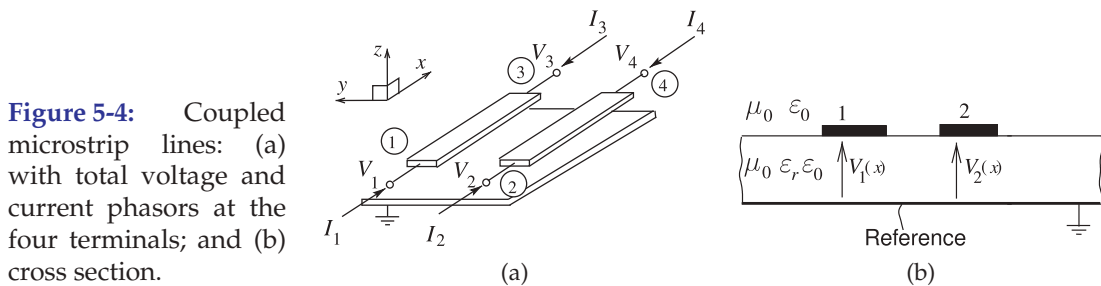


Figure 5-4: Coupled microstrip lines: (a) with total voltage and current phasors at the four terminals; and (b) cross section.

of the two modes will differ since the two modes have different amounts of energy in the air and in the dielectric, resulting in different effective permittivities of the two modes.

Coupled lines are modeled by determining the propagation characteristics of the even and odd modes. Also, at the circuit level, coupling can be described by network parameters that relate total voltage and current. Using the definitions shown in Figures 5-3 and 5-4, the total voltage and current phasors on the original structure are a superposition of the even- and odd-mode solutions:

$$\left. \begin{aligned} V_1 &= V_{Fe} + V_{Fo} & I_1 &= I_{Fe} + I_{Fo} \\ V_2 &= V_{Fe} - V_{Fo} & I_2 &= I_{Fe} - I_{Fo} \\ V_3 &= V_{Be} + V_{Bo} & I_3 &= I_{Be} + I_{Bo} \\ V_4 &= V_{Be} - V_{Bo} & I_4 &= I_{Be} - I_{Bo} \end{aligned} \right\}, \quad (5.1)$$

with the subscripts F and B indicating the front and back, respectively, of the even- and odd-mode components. Also

$$\left. \begin{aligned} V_{Fe} &= (V_1 + V_2)/2 & I_{Fe} &= (I_1 + I_2)/2 \\ V_{Fo} &= (V_1 - V_2)/2 & I_{Fo} &= (I_1 - I_2)/2 \\ V_{Be} &= (V_3 + V_4)/2 & I_{Be} &= (I_3 + I_4)/2 \\ V_{Bo} &= (V_3 - V_4)/2 & I_{Bo} &= (I_3 - I_4)/2 \end{aligned} \right\}. \quad (5.2)$$

The forward-traveling components can be written as

$$\left. \begin{aligned} V_1^+ &= V_{Fe}^+ + V_{Fo}^+ & I_1^+ &= I_{Fe}^+ + I_{Fo}^+ \\ V_2^+ &= V_{Fe}^+ - V_{Fo}^+ & I_2^+ &= I_{Fe}^+ - I_{Fo}^+ \\ V_3^+ &= V_{Be}^+ + V_{Bo}^+ & I_3^+ &= I_{Be}^+ + I_{Bo}^+ \\ V_4^+ &= V_{Be}^+ - V_{Bo}^+ & I_4^+ &= I_{Be}^+ - I_{Bo}^+ \end{aligned} \right\}. \quad (5.3)$$

The backward-traveling components are written similarly so that the total front and back even- and odd-mode voltages are

$$\left. \begin{aligned} V_{Fe} &= V_{Fe}^+ + V_{Fe}^- & V_{Be} &= V_{Be}^+ + V_{Be}^- \\ V_{Fo} &= V_{Fo}^+ + V_{Fo}^- & V_{Bo} &= V_{Bo}^+ + V_{Bo}^- \end{aligned} \right\}. \quad (5.4)$$

With an ideal voltmeter the V_1 , V_2 , V_3 , and V_4 voltages would be measured from a point on the strip to a point on the ground plane immediately below. The voltages $2V_{Fo}$ and $2V_{Bo}$ are the voltages that would be measured between the strips at the front and back of the lines, respectively (see Figure 5-2). It would not be possible to directly measure V_{Fe} and V_{Be} .

One set of network parameters describing a pair of coupled lines is the port-based admittance matrix equation relating the port voltages, V_1 – V_4 , to the port currents, I_1 – I_4 :

$$\begin{bmatrix} I_1 \\ I_2 \\ I_3 \\ I_4 \end{bmatrix} = \begin{bmatrix} y_{11} & y_{12} & y_{13} & y_{14} \\ y_{21} & y_{22} & y_{23} & y_{24} \\ y_{31} & y_{32} & y_{33} & y_{34} \\ y_{41} & y_{42} & y_{43} & y_{44} \end{bmatrix} \begin{bmatrix} V_1 \\ V_2 \\ V_3 \\ V_4 \end{bmatrix}. \quad (5.5)$$

These are port-based y parameters as the currents and voltages are defined for ports. Since microstrip lines are fabricated (most of the time) on non-magnetic dielectrics, then they are reciprocal so that $y_{ij} = y_{ji}$. Coupling from one line to another is described by the terms y_{12} ($=y_{21}$) and y_{34} ($=y_{43}$).

Summary

The important concept introduced in this section is that fields and the propagating waves on a pair of parallel coupled lines can be described as a combination of odd and even modes each of which has forward- and backward-wave versions.

5.3 Coupled Transmission Line Theory

In this section coupled transmission line theory is developed in terms of the quantities shown in Figure 5-4. The voltages and currents shown here are phasors that vary along the line and are functions of x .

The quasi-TEM mode of propagation is also assumed, and the transmission line system is completely lossless with perfect conductors and insulators. In phasor form, the generalized telegrapher's equations for a pair of coupled lines are¹

$$\frac{dV_1(x)}{dx} = -j\omega L_{11}I_1(x) - j\omega L_{12}I_2(x) \quad (5.6)$$

$$\frac{dV_2(x)}{dx} = -j\omega L_{21}I_1(x) - j\omega L_{22}I_2(x) \quad (5.7)$$

$$\frac{dI_1(x)}{dx} = -j\omega C_{11}V_1(x) - j\omega C_{12}V_2(x) \quad (5.8)$$

$$\frac{dI_2(x)}{dx} = -j\omega C_{21}V_1(x) - j\omega C_{22}V_2(x). \quad (5.9)$$

These are generalizations of the telegrapher's equations of a single transmission line, and for reciprocity, $C_{12} = C_{21}$ and $L_{12} = L_{21}$. Compaction of the equations is obtained by introducing the per unit length inductance matrix, \mathbf{L} , and the per unit length capacitance matrix, \mathbf{C} , defined as

$$\mathbf{L} = \begin{bmatrix} L_{11} & L_{12} \\ L_{12} & L_{22} \end{bmatrix} \quad \text{and} \quad \mathbf{C} = \begin{bmatrix} C_{11} & C_{12} \\ C_{12} & C_{22} \end{bmatrix}. \quad (5.10)$$

The next step is to express the voltage on the pair of coupled transmission lines in vector form as

$$\mathbf{V}(x) = \begin{bmatrix} V_1(x) \\ V_2(x) \end{bmatrix} = [V_1(x) \ V_2(x)]^T, \quad (5.11)$$

where T indicates transpose and converts the row vector into a column vector. Similarly the vector of currents on the coupled transmission lines is

$$\mathbf{I}(x) = [I_1(x) \ I_2(x)]^T. \quad (5.12)$$

Using the above relations, the telegrapher's equation, from Equations (5.6)–(5.9), is represented in matrix form as

$$\frac{d}{dx}\mathbf{V}(x) = -j\omega\mathbf{L}\mathbf{I}(x) \quad (5.13) \quad \text{and} \quad \frac{d}{dx}\mathbf{I}(x) = -j\omega\mathbf{C}\mathbf{V}(x). \quad (5.14)$$

Rearranging Equations (5.13) and (5.14), taking derivatives, and after substitution, the final wave-equation form is obtained:

$$\frac{d^2}{dx^2}\mathbf{V}(x) + \omega^2\mathbf{LCV}(x) = 0 \quad (5.15) \quad \text{and} \quad \frac{d^2}{dx^2}\mathbf{I}(x) + \omega^2\mathbf{LCI}(x) = 0. \quad (5.16)$$

Solving these second-order differential equations yields descriptions of the

¹ In Figure 5-4(a) V_1 and V_2 are the voltages at terminals 1 and 2 of lines 1 and 2. They are also port voltages referenced to the ground immediately below the appropriate terminal. $V_1(x)$ and $V_2(x)$ are the total voltage anywhere on lines 1 and 2, respectively, as shown in Figure 5-4(b). Similar notation will be used for voltages and traveling-wave components.

propagation characteristics. With confidence, a solution in the form of propagating waves can be assumed:

$$\mathbf{V}(x) = \mathbf{V}_0 \boldsymbol{\beta} = \mathbf{V}_0 \text{diag}(e^{-j\beta_1 x}, e^{-j\beta_2 x}) = \mathbf{V}_0 \begin{bmatrix} e^{-j\beta_1 x} & 0 \\ 0 & e^{-j\beta_2 x} \end{bmatrix}. \quad (5.17)$$

Substituting this into Equation (5.15) yields

$$-\boldsymbol{\beta}^2 \mathbf{V}_0 + \omega^2 \mathbf{L} \mathbf{C} \mathbf{V}_0 = 0. \quad (5.18)$$

For a nontrivial solution of Equation (5.18), the determinant of the matrix equation should be zero:

$$\det \left(\mathbf{L} \mathbf{C} - \frac{\boldsymbol{\beta}^2}{\omega^2} \mathbf{U} \right) = 0, \quad \text{where the unit matrix } \mathbf{U} = \begin{bmatrix} 1 & 0 \\ 0 & 1 \end{bmatrix}. \quad (5.19)$$

Equation (5.19) is the characteristic equation that can be solved to determine the phase constant, β . There are many possible solutions, and weighted linear combinations of the solutions are also solutions.

If only the quasi-TEM modes are considered, then there are two possible sets of solutions for the phase constant, with one set of solutions being

$$\beta_1 = \pm \omega S_1 \quad (5.20) \quad \text{and the other} \quad \beta_2 = \pm \omega S_2. \quad (5.21)$$

The different signs here are physically interpreted as referring to the forward- and backward-traveling waves. Thus the coupled pair of conductors supports two unique families of modes (each family comprising forward- and backward-traveling waves) with each family relating to a particular field configuration on the coupled line system.² That is, S_1 and S_2 are each single numbers and, just considering the forward-traveling waves, ωS_1 is the propagation constant of one mode and ωS_2 is the propagation constant of the second mode.

The circuit-level model of a coupled line pair is developed by considering the calculation of the \mathbf{L} and \mathbf{C} matrices. The elements of the capacitance matrix are obtained in two simulations in which the line charge is calculated. A variety of commercially available software packages exist for the extraction of the per unit length \mathbf{L} and \mathbf{C} matrices. The matrix \mathbf{C} is calculated, in most packages, from the solutions of a two-dimensional electrostatic problem. The steps involve solving for the charges on the lines with voltages set on the conductors. With total voltages V_1 and V_2 on lines 1 and 2, the charges on lines Q_1 and Q_2 are

$$Q_1 = C_{11}V_1 + C_{12}V_2 \quad (5.22) \quad \text{and} \quad Q_2 = C_{12}V_1 + C_{22}V_2. \quad (5.23)$$

Simulation 1: With $V_1 = 1$ and $V_2 = 0$, the charges are calculated with the result that

$$C_{11} = Q_1 > 0 \quad (5.24) \quad \text{and} \quad C_{12} = Q_2 < 0. \quad (5.25)$$

(Note that $C_{ij}, i \neq j$, is negative.)

² Also it is up to the user to decide the form of the families to use. The most convenient family in microwave analysis is to use even and odd modes. In general, a system with N active conductors (and one reference conductor) will support $2 \times N$ (quasi-) TEM modes.

Simulation 2: With $V_1 = 0$ and $V_2 = 1$, the charges are recalculated, and now

$$C_{22} = Q_2 \quad \text{and} \quad C_{12} = Q_1. \quad (5.26)$$

The characterization of the lines is completed by determining the elements of the inductance matrix. This is done by calculating the capacitances with and without the dielectric. The principle effect of the dielectric is to alter the configuration and magnitude of the electric field. The dielectric has little effect on the magnitude and orientation of the magnetic field. With the same current on the coupled lines, the same magnetic energy is stored, and the inductances of the coupled line are unchanged by the dielectric. The other assumption is that with a TEM mode on the lines, and in the absence of a dielectric, the velocity of propagation is $c = 1/\sqrt{LC}$. Specifically, the assumption is that for a TEM mode and without a dielectric, the phase velocity is just c . This is a very good approximation and is exact if the conductors have infinite conductivity. (If the conductors have finite conductivity there would be field inside the conductors, and the wave slows down slightly.) Determining the capacitance matrix without the dielectric enables the inductance matrix to be calculated:

$$\mathbf{L} = \mathbf{L}_0 = \frac{1}{c^2} \mathbf{C}_0^{-1}, \quad (5.27)$$

where the subscript 0 indicates free space (but a subscript 0 on Z , e.g., Z_0 , indicates characteristic impedance).

5.3.1 Summary

This section introduced the telegrapher's equations for a pair of coupled lines in a form that is an extension of the telegrapher's equations of a single line but with the L and C of a single line replaced by 2×2 \mathbf{L} and \mathbf{C} matrices. It is no longer necessary to deal with fields and a circuit model can be used.

5.4 Low-Frequency Capacitance Model of Coupled Lines

The low-frequency model of a pair of lossless coupled lines comprises only capacitances. A pair of coupled lines, as shown in Figure 5-5(a), has four terminals. At very low frequencies V_1 and V_3 are identical as are voltages V_2 and V_4 . So the low-frequency model of the pair of coupled lines has just two terminals in addition to ground, as shown in Figure 5-5(b).

The capacitances in Figure 5-5(b) are the shunt capacitance C_1 and C_2 and the mutual capacitance C_g . In the even mode, the voltages at terminals 1 and 2 are the same so that C_g vanishes and the low-frequency capacitance model of the pair of coupled lines in the even mode comprises just the self-capacitances C_1 and C_2 (see Figure 5-5(c)). In the odd mode, the voltage at terminal 2 is the negative of the voltage at terminal 1. The result is that there is a virtual ground between the terminals. Now a better circuit model is that shown in Figure 5-5(d). This is where the restriction that the lines are of equal width is used. This assumption places the virtual ground between equal-value capacitances. The symmetrical case is the one of most interest. If asymmetrical coupled lines are to be analyzed, the analysis departs at this point and EM simulation is required.

To proceed, the capacitance model must be put in the form of per unit length capacitances and put in terms of the elements of a capacitance matrix.

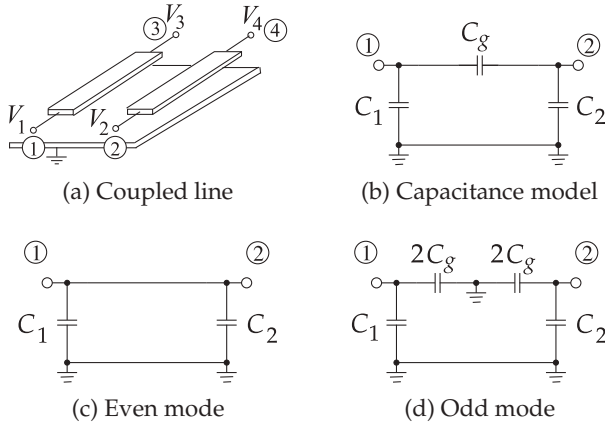


Figure 5-5: Very low frequency models of a pair of coupled lines.

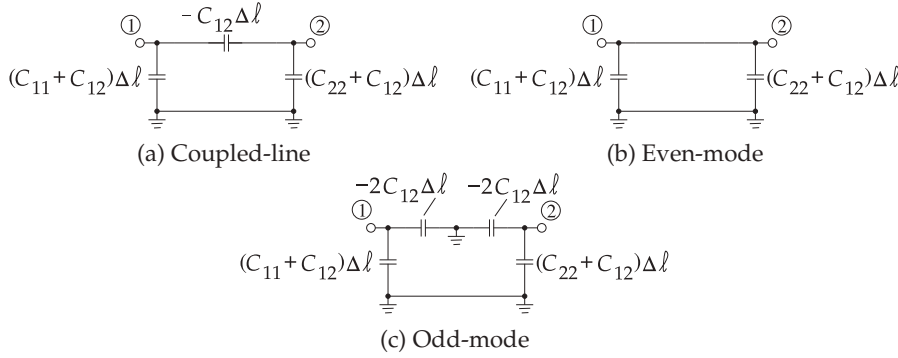


Figure 5-6: Low frequency capacitance models of a pair of coupled lines of length $\Delta\ell$.

The indefinite nodal admittance matrix of the low-frequency coupled-line model of Figure 5-5(b) is

$$\mathbf{Y} = j\omega \begin{bmatrix} C_1 + C_g & -C_g \\ -C_g & C_2 - C_g \end{bmatrix} = j\omega \mathbf{C} \Delta\ell, \quad (5.28)$$

where $\Delta\ell$ is the length of the coupled lines, and \mathbf{C} is the per unit length capacitance matrix (see Equation (5.10)). Thus the low-frequency capacitance model of a pair of coupled lines of length $\Delta\ell$ and equal width is as shown in Figure 5-6(a). It is found in analysis that C_{12} is negative.

For symmetrical coupled lines (the strips having the same width) the per unit length even- and odd-mode capacitances, as defined in the definition of odd and even modes in Section 5.2, are

$$C_e = C_{11} + C_{12} \quad \text{and} \quad C_o = C_{11} - C_{12}. \quad (5.29)$$

$$\text{That is, } \mathbf{C} = \begin{bmatrix} C_{11} & C_{12} \\ C_{12} & C_{22} \end{bmatrix} = \begin{bmatrix} \frac{1}{2}(C_e + C_o) & \frac{1}{2}(C_e - C_o) \\ \frac{1}{2}(C_e - C_o) & \frac{1}{2}(C_e + C_o) \end{bmatrix}. \quad (5.30)$$

5.4.1 Capacitance Matrix Extraction

This section describes a general procedure for the extraction of the capacitance matrix of a number of coupled conductors [1]. Either measurements or measurement-like simulations can be used. This is done by evaluating one capacitance at a time for different connections of interconnects to each other.

Without loss of generality, consider the three-line structure shown in Figure 5-7, where there are four conductors, including ground. A 3×3 capacitance matrix is extracted from the capacitances of pairs of connected conductors. There are seven possible combinations, as shown on the left-hand side of Figure 5-8. However, because of reciprocity, $C_{ij} = C_{ji}$, there are only six capacitances (C_{11} , C_{12} , C_{13} , C_{22} , C_{23} , and C_{33}) to be determined, and only six sets of connections are required. The seventh set serves as a check.

In an EM simulation, the connections are conveniently realized by holding the black group at one voltage (e.g., 1 V) and the white group at 0 V. The corresponding capacitance connections are shown on the right in the figure: the seven individual capacitance measurements are C_A , C_B , C_C , C_D , C_E , C_F , and C_G . Thus the elements of the capacitance matrix are

$$\left. \begin{aligned} C_{11} &= C'_{11} + C'_{12} + C'_{13} & C_{12} &= C_{21} = -C'_{12} \\ C_{22} &= C'_{22} + C'_{12} + C'_{23} & C_{13} &= C_{31} = -C'_{13} \\ C_{33} &= C'_{33} + C'_{13} + C'_{23} & C_{23} &= C_{32} = -C'_{23} \end{aligned} \right\}. \quad (5.31)$$

Figure 5-7: Three-line structure with four conductors labeled 1, 2, 3, and 4.

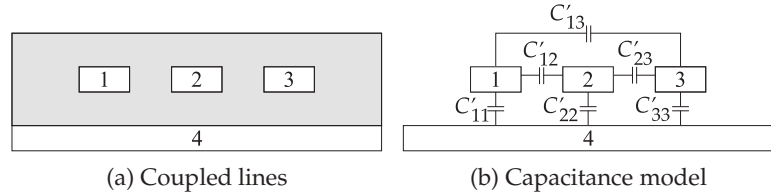
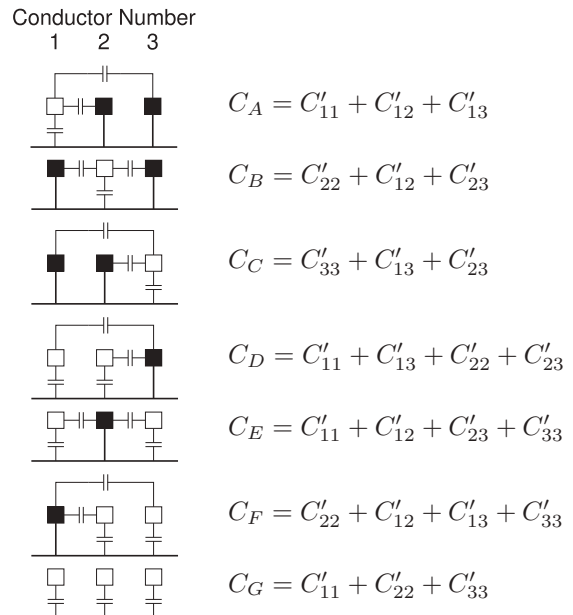


Figure 5-8: Combinations of conductors leading to various capacitance measurements. The capacitances C_A, \dots, C_G are measured between the conductor identified by the open square and the ground that is connected to the conductors, indicated by the closed squares.



Using the first six measurements in Figure 5-8,

$$\left. \begin{aligned} C_A &= C_{11} & C_D &= C_{11} + 2C_{12} + C_{22} \\ C_B &= C_{22} & C_E &= C_{11} + 2C_{13} + C_{33} \\ C_C &= C_{33} & C_F &= C_{22} + 2C_{23} + C_{33} \end{aligned} \right\}. \quad (5.32)$$

$$\text{Thus} \quad \left. \begin{aligned} C_{11} &= C_A & C_{12} &= C_{21} = \frac{1}{2}(C_D - C_A - C_B) \\ C_{22} &= C_B & C_{13} &= C_{31} = \frac{1}{2}(C_E - C_A - C_C) \\ C_{33} &= C_C & C_{23} &= C_{32} = \frac{1}{2}(C_F - C_B - C_C) \end{aligned} \right\}. \quad (5.33)$$

This extraction does not require the widths of the strips to be the same.

5.5 Symmetric Coupled Transmission Lines

In this section, even and odd modes are considered as defining independent transmission lines. The development is restricted to a symmetrical pair of coupled lines; that is, each transmission line of the pair is identical. Thus the strips have the same self-inductance, $L_s = L_{11} = L_{22}$, and self-capacitance, $C_s = C_{11} = C_{22}$, where the subscript s stands for "self." $L_m = L_{12} = L_{21}$ and $C_m = C_{12} = C_{21}$ are the mutual inductance and capacitance of the lines, and the subscript m stands for "mutual." Equations (5.6)–(5.9) can thus be written as

$$\frac{dV_1(x)}{dx} = -j\omega L_s I_1(x) - j\omega L_m I_2(x) \quad (5.34)$$

$$\frac{dV_2(x)}{dx} = -j\omega L_m I_1(x) - j\omega L_s I_2(x) \quad (5.35)$$

$$\frac{dI_1(x)}{dx} = -j\omega C_s V_1(x) - j\omega C_m V_2(x) \quad (5.36)$$

$$\frac{dI_2(x)}{dx} = -j\omega C_m V_1(x) - j\omega C_s V_2(x). \quad (5.37)$$

The even mode is defined as the mode corresponding to both conductors being at the same potential and carrying the same currents:³

$$V_1 = V_2 = V_e \quad \text{and} \quad I_1 = I_2 = I_e. \quad (5.38)$$

The odd mode is defined as the mode corresponding to the conductors being at opposite potentials relative to the reference conductor and carrying currents of equal amplitude but of opposite sign:⁴

$$V_1 = -V_2 = V_o \quad \text{and} \quad I_1 = -I_2 = I_o. \quad (5.39)$$

The characteristics of the two possible modes of the coupled transmission lines are now described. For the even mode, from Equations (5.34) and (5.35),

$$\frac{d}{dx} [V_1(x) + V_2(x)] = -j\omega [L_m + L_s] [I_1(x) + I_2(x)], \quad (5.40)$$

which becomes

$$\frac{dV_e(x)}{dx} = -j\omega (L_s + L_m) I_e(x). \quad (5.41)$$

³ Here $I_e = (I_1 + I_2)/2$ and $V_e = (V_1 + V_2)/2$. The reason for the supposedly equally valid definition $I_e = I_1 + I_2$ not being used is that the adopted definition results in the desirable form of the even-mode characteristic impedance.

⁴ Here $I_o = (I_1 - I_2)/2$ and $V_o = (V_1 - V_2)/2$.

Similarly, using Equations (5.36) and (5.37),

$$\frac{d}{dx} [I_1(x) + I_2(x)] = -j\omega (C_s + C_m) [V_1(x) + V_2(x)], \quad (5.42)$$

which in turn becomes

$$\frac{dI_e(x)}{dx} = -j\omega (C_s + C_m) V_e(x). \quad (5.43)$$

Defining the even-mode inductance and capacitance, L_e and C_e , respectively, as

$$L_e = L_s + L_m = L_{11} + L_{12} \quad \text{and} \quad C_e = C_s + C_m = C_{11} + C_{12} \quad (5.44)$$

leads to the **even-mode telegrapher's equations**:

$$\frac{dV_e(x)}{dx} = -j\omega L_e I_e(x) \quad (5.45) \quad \text{and} \quad \frac{dI_e(x)}{dx} = -j\omega C_e V_e(x). \quad (5.46)$$

From these, the even-mode characteristic impedance can be found,

$$Z_{0e} = \sqrt{\frac{L_e}{C_e}} = \sqrt{\frac{L_s + L_m}{C_s + C_m}}, \quad (5.47)$$

and also the even-mode phase velocity,

$$v_{pe} = \frac{1}{\sqrt{L_e C_e}}. \quad (5.48)$$

The characteristics of the odd-mode operation of the coupled transmission line can be determined in a similar procedure to that used for the even mode. Using Equations (5.34)–(5.37), the **odd-mode telegrapher's equations** become

$$\frac{dV_o(x)}{dx} = -j\omega (L_s - L_m) I_o(x) \quad \text{and} \quad \frac{dI_o(x)}{dx} = -j\omega (C_s - C_m) V_o(x). \quad (5.49) \quad (5.50)$$

Defining L_o and C_o for the odd mode such that

$$L_o = L_s - L_m = L_{11} - L_{12} \quad \text{and} \quad C_o = C_s - C_m = C_{11} - C_{12}, \quad (5.51)$$

then the odd-mode characteristic impedance is

$$Z_{0o} = \sqrt{\frac{L_o}{C_o}} = \sqrt{\frac{L_s - L_m}{C_s - C_m}} \quad (5.52)$$

and the odd-mode phase velocity is

$$v_{po} = \frac{1}{\sqrt{L_o C_o}}. \quad (5.53)$$

Now for a sanity check. If the individual strips are widely separated, L_m and C_m will become very small and Z_{0e} and Z_{0o} will be almost equal. As the strips become closer, L_m and C_m will become larger and Z_{0e} and Z_{0o} will diverge. This is as expected.

5.5.1 Odd-Mode and Even-Mode Capacitances

The previous section used the even- and odd-mode capacitances for two coupled microstrip lines with the strips having equal cross section so that each strip had the same self-capacitances. In this section this restriction is removed and the results apply to any pair of coupled lines in any technology and of any cross section. The results enable the capacitances of the capacitance matrix to be determined from calculations of the charges on the lines. Repeating Equations (5.22) and (5.23),

$$Q_1 = C_{11}V_1 + C_{12}V_2 \quad \text{and} \quad Q_2 = C_{21}V_1 + C_{22}V_2, \quad (5.54)$$

the capacitance matrix is

$$\mathbf{C} = \begin{bmatrix} C_{11} & C_{12} \\ C_{21} & C_{22} \end{bmatrix}. \quad (5.55)$$

In the even mode $V_1 = V_2 = V_e$ and so the even-mode charges on strip 1 and strip 2 are

$$Q_{1e} = (C_{11} + C_{12})V_e \quad \text{and} \quad Q_{2e} = (C_{21} + C_{22})V_e, \quad (5.56)$$

respectively. Defining the even-mode charge as

$$Q_e = (Q_{1e} + Q_{2e})/2, \quad (5.57)$$

then the even-mode charge becomes

$$Q_e = V_e(C_{11} + C_{22} + C_{12} + C_{21})/2. \quad (5.58)$$

This leads to the even-mode per unit length capacitance,

$$C_e = Q_e/V_e = (C_{11} + C_{22} + C_{12} + C_{21})/2. \quad (5.59)$$

Similarly, in the odd mode, $V_o = V_1 = -V_2$, and the odd-mode charges on strip 1 and strip 2 are

$$Q_{1o} = (C_{11} - C_{12})V_o \quad \text{and} \quad Q_{2o} = (C_{21} - C_{22})V_o, \quad (5.60)$$

respectively. The odd-mode charge is then

$$Q_o = (Q_{1o} - Q_{2o})/2 = (C_{11} + C_{22} - C_{12} - C_{21})V_o/2. \quad (5.61)$$

The odd-mode capacitance is

$$C_o = Q_o/V_o = (C_{11} + C_{22} - C_{12} - C_{21})/2. \quad (5.62)$$

EXAMPLE 5.1

Parallel Line Capacitance

EM software can be used to determine the even- and odd-mode parameters of a coupled line. This is usually done by setting the phasor voltages on the coupled line and evaluating the phasor charges. Consider a pair of coupled microstrip lines as in Figure 5-4. The voltage applied to the left strip is designated as V_1 and the voltage applied to the right strip is V_2 . The phasor charge on the strips are Q_1 and Q_2 , respectively. The analysis is repeated, but this time with the substrate removed, and so establishing the free-space situation. In this case the charges are denoted by Q_{01} and Q_{02} . The matrix of (computer-based) measurements is as follows:

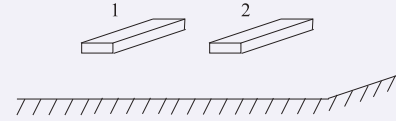
Case	V_1 (V)	V_2 (V)	Q_1 (pC/m)	Q_2 (pC/m)	Q_{01} (pC/m)	Q_{02} (pC/m)
A	1	-1	70	-80	22.2	-24.7
B	1	1	30	40	2.82	5.32

- What is the two-port capacitance matrix?
- What is the even-mode capacitance?

- (c) What is the odd-mode capacitance?
- (d) What is the free-space (no dielectric) two-port capacitance matrix?
- (e) What is the free-space even-mode capacitance?
- (f) What is the free-space odd-mode capacitance?
- (g) What is the even-mode effective relative permittivity?
- (h) What is the odd-mode effective relative permittivity?
- (i) Note that both the odd mode and even mode are TEM modes, so the phase velocity in the free-space situation is c . Determine the odd-mode and even-mode inductances per unit length in free space.
- (j) Note that the inductances do not change when the dielectric is replaced. What is the even-mode impedance?
- (k) What is the odd-mode impedance?
- (l) What is the even-mode phase velocity?
- (m) What is the odd-mode phase velocity?

Solution:

- (a) Begin by considering the cross section of a coupled line shown to the right and use the basic equations relating the charges on the line to the voltages on them:



$$Q_1 = C_{11}V_1 + C_{12}V_2 \quad \text{and} \quad Q_2 = C_{21}V_1 + C_{22}V_2,$$

and consider two sets of voltage conditions.

Case A: This is the odd excitation, $V_1 = 1$ V and $V_2 = -1$ V and the charges are

$$Q_{1A} = C_{11} - C_{12} \quad (5.63) \quad \text{and} \quad Q_{2A} = C_{21} - C_{22}. \quad (5.64)$$

Case B: This is the even excitation, $V_1 = V_2 = 1$ V and the charges are

$$Q_{1B} = C_{11} + C_{12} \quad (5.65) \quad \text{and} \quad Q_{2B} = C_{21} + C_{22}. \quad (5.66)$$

Adding Equations (5.63) and (5.65) results in

$$Q_{1A} + Q_{1B} = 2C_{11}, \quad \text{thus} \quad C_{11} = \frac{1}{2}(Q_{1A} + Q_{1B}) = (70 + 30)/2 \text{ pF/m} = 50 \text{ pF/m}. \quad (5.67)$$

Subtracting Equation (5.63) from Equation (5.65) yields

$$Q_{1B} - Q_{1A} = 2C_{12}, \quad \text{thus} \quad C_{12} = \frac{1}{2}(Q_{1B} - Q_{1A}) = \frac{1}{2}(30 - 70) \text{ pF/m} = -20 \text{ pF/m}. \quad (5.68)$$

Because of reciprocity, $C_{21} = C_{12} = -20$ pF/m.

Subtracting Equation (5.64) from Equation (5.66) results in

$$Q_{2B} - Q_{2A} = 2C_{22}, \quad \text{thus} \quad C_{22} = \frac{1}{2}(Q_{2B} - Q_{2A}) = \frac{1}{2}(40 + 80) \text{ pF/m} = 60 \text{ pF/m}. \quad (5.69)$$

Thus the per unit length capacitance matrix of the coupled line is

$$\mathbf{C} = \begin{bmatrix} C_{11} & C_{21} \\ C_{12} & C_{22} \end{bmatrix} = \begin{bmatrix} 50 & -20 \\ -20 & 60 \end{bmatrix} \text{ pF/m}. \quad (5.70)$$

- (b) Even-mode capacitance, C_e :

The even mode has $V_1 = V_2$ and the even-mode voltage is $V_e = (V_1 + V_2)/2$.

The even-mode charge is $Q_e = (Q_1 + Q_2)/2 = (30 + 40)/2 \text{ pC/m} = 35 \text{ pC/m}$, so

$$C_e = Q_e/V_e = 35 \text{ pF/m}. \quad (5.71)$$

(c) Odd-mode capacitance, C_o :

The odd-mode voltage is $V_o = (V_1 - V_2)/2$ and the odd-mode charge is $Q_o = (Q_1 - Q_2)/2$. With $V_1 = +1V$ and $V_2 = -1V$, $V_o = 1$,

$$Q_o = \frac{1}{2} [70 - (-80)] \text{ pC/m} = 75 \text{ pC/m, thus } C_o = Q_o/V_o = 75 \text{ pF/m.} \quad (5.72)$$

(d) Using a similar procedure to that in (a), but now using the free-space charge calculations, Q_{o1} and Q_{o2} results in the unit capacitance matrix:

$$\mathbf{C}_0 = \begin{bmatrix} 12.5 & -9.69 \\ -9.69 & 15.0 \end{bmatrix} \text{ pF/m.} \quad (5.73)$$

(e) $C_{e0} = 4.07 \text{ pF/m}$.

(f) $C_{o0} = 23.5 \text{ pF/m}$.

(g) $\varepsilon_{re} = C_e/C_{e0} = 35/4.07 = 8.6$.

(h) $\varepsilon_{ro} = C_o/C_{o0} = 75/23.5 = 3.2$.

(i) Phase velocity, $v_p = 1/\sqrt{LC}$. With no dielectric, the phase velocity is c :

$$v_p = c = 1/\sqrt{L_o C_o} \rightarrow L_o = 1/(c^2 C_o),$$

and the odd-mode free-space inductance is

$$L_{o0} = 1/(c^2 C_{o0}) = 1/[(3 \cdot 10^8)^2 \cdot 23.5 \cdot 10^{-12}] \text{ H/m} = 473 \text{ nH/m.} \quad (5.74)$$

The free-space even-mode inductance is

$$L_{e0} = 1/(c^2 C_{e0}) = 1/[(3 \cdot 10^8)^2 \cdot 4.07 \cdot 10^{-12}] \text{ H/m} = 2.73 \text{ } \mu\text{H/m.} \quad (5.75)$$

(j) $Z_o = \sqrt{L_o/C_o}$; $L_o = L_{o0}$ $Z_o = \sqrt{473 \cdot 10^{-9}/(75 \cdot 10^{-12})} \Omega = 79.4 \Omega$.

(k) $Z_e = \sqrt{L_e/C_e} \Rightarrow Z_e = \sqrt{2.73 \cdot 10^{-6}/(35 \cdot 10^{-12})} \Omega = 279 \Omega$.

(l) $v_{pe} = 1/\sqrt{L_e C_e} = (2.73 \cdot 10^{-6} \cdot 35 \cdot 10^{-12})^{-\frac{1}{2}} = 1.023 \cdot 10^8 \text{ m/s}$.

(m) $v_{po} = 1/\sqrt{L_o C_o} = (473 \cdot 10^{-9} \cdot 75 \cdot 10^{-12})^{-\frac{1}{2}} = 1.68 \cdot 10^8 \text{ m/s}$.

5.6 Formulas for Characteristic Impedance of Coupled Microstrip Lines

Formulas for the characteristic impedance and effective permittivity of symmetric coupled microstrip lines, with the cross section shown in Figure 5-9, were developed by Hammerstad and Jensen [2] based on the concept of even and odd modes. The formulas are accurate to better than 1% for $0.1 \leq u \leq 10$ and $g > 0.01$, where u is the normalized width, and g is the normalized gap:

$$u = w/h, \quad g = s/h. \quad (5.76)$$

In the following, Z_o and ε_e refer to the characteristic impedance and effective permittivity of an individual microstrip line with a normalized width of u on a substrate with a relative dielectric constant of ε_r .

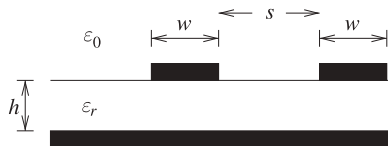


Figure 5-9: Cross section of symmetrically coupled microstrip lines.

5.6.1 Even-Mode Coupled-Line Parameters

The even-mode characteristic impedance is

$$Z_{0e}(u, g) = Z_{01e}(u, g) / \sqrt{\varepsilon_{ee}(u, g, \varepsilon_r)}, \quad (5.77)$$

where ε_{ee} is the effective relative permittivity of the even mode and Z_{01e} is the even-mode characteristic impedance with the dielectric replaced by free space:

$$Z_{01e}(u, g) = \frac{Z_0(u)}{1 - Z_0(u)\phi_e(u, g)/\eta_0}, \quad (5.78)$$

$$\text{where } \phi_e(u, g) = \frac{\varphi(u)}{\psi(g) \{ \alpha(g)u^{m(g)} + [1 - \alpha(g)]u^{-m(g)} \}} \quad (5.79)$$

and $\eta_0 = 376.73 \Omega \approx 377 \Omega$ is the characteristic impedance of a TEM wave in a vacuum (i.e., free space). Now $Z_0(u)$ is the free-space characteristic impedance of an individual microstrip line and is given by Equation (3.21). In Equations (5.77) and (5.78), the effective permittivity of the even mode is

$$\varepsilon_{ee}(u, g, \varepsilon_r) = \frac{\varepsilon_r + 1}{2} + \frac{\varepsilon_r - 1}{2} F_e(u, g, \varepsilon_r), \quad (5.80)$$

where

$$F_e(u, g, \varepsilon_r) = \left[1 + \frac{10}{\mu(u, g)} \right]^{-a(u)b(\varepsilon_r)} \quad (5.81)$$

$$a(u) = 1 + \frac{1}{49} \ln \left[\frac{u^4 + \{u/52\}^2}{u^4 + 0.432} \right] + \frac{1}{18.7} \ln \left[1 + \left(\frac{u}{18.1} \right)^3 \right] \quad (5.82)$$

$$b(\varepsilon_r) = 0.564 \left[\frac{\varepsilon_r - 0.9}{\varepsilon_r + 3} \right]^{0.053} \quad (5.83)$$

$$\varphi(u) = 0.8645u^{0.172} \quad (5.84)$$

$$\psi(g) = 1 + \frac{g}{1.45} + \frac{g^{2.09}}{3.95} \quad (5.85)$$

$$\alpha(g) = 0.5 \exp(-g) \quad (5.86)$$

$$m(g) = 0.2175 + \left[4.113 + \left(\frac{20.36}{g} \right)^6 \right]^{-0.251} + \frac{1}{323} \ln \left[\frac{g^{10}}{1 + (g/13.8)^{10}} \right] \quad (5.87)$$

$$\mu(u, g) = g \exp(-g) + \frac{u(20 + g^2)}{10 + g^2}. \quad (5.88)$$

5.6.2 Odd-Mode Coupled-Line Parameters

The odd-mode characteristic impedance is

$$Z_{0o}(u, g) = Z_{01o}(u, g) / \sqrt{\varepsilon_{eo}(u, g, \varepsilon_r)}, \quad (5.89)$$

where ε_{eo} is the effective relative permittivity of the odd mode and Z_{01o} is the odd-mode characteristic impedance with the dielectric replaced by free-space:

$$Z_{01o}(u, g) = \frac{Z_0(u)}{1 - Z_0(u)\phi_o(u, g)/\eta_0}. \quad (5.90)$$

$Z_0(u)$ is the free-space characteristic impedance of an individual microstrip line and is given by Equation (3.21). In Equations (5.89) and (5.90), the effective permittivity of the odd mode is

$$\varepsilon_{eo}(u, g, \varepsilon_r) = \frac{\varepsilon_r + 1}{2} + \frac{\varepsilon_r - 1}{2} F_o(u, g, \varepsilon_r), \quad (5.91)$$

where

$$F_o(u, g, \varepsilon_r) = f_o(u, g, \varepsilon_r) (1 + 10/u)^{-a(u)b(\varepsilon_r)} \quad (5.92)$$

$$\phi_o(u, g) = \phi_e(u, g) - \frac{\theta(g)}{\psi(g)} \exp \left[\beta(g) u^{n(g)} \ln(u) \right] \quad (5.93)$$

$$\theta(g) = 1.729 + 1.175 \ln \left(1 + \frac{0.627}{g + 0.327g^{2.17}} \right) \quad (5.94)$$

$$\begin{aligned} \beta(g) = & 0.2306 + \frac{1}{301.8} \ln \left[\frac{g^{10}}{1 + (g/3.73)^{10}} \right] \\ & + \frac{1}{5.3} \ln (1 + 0.646g^{1.175}) \end{aligned} \quad (5.95)$$

$$\begin{aligned} n(g) = & \left\{ \frac{1}{17.7} + \exp \left[-6.424 - 0.76 \ln(g) - (g/0.23)^5 \right] \right\} \\ & \times \ln \left(\frac{10 + 68.3g^2}{1 + 32.5g^{3.093}} \right) \end{aligned} \quad (5.96)$$

$$f_o(u, g, \varepsilon_r) = f_{o1}(g, \varepsilon_r) \exp \left[p(g) \ln(u) + q(g) \sin \left(\pi \frac{\ln u}{\ln 10} \right) \right] \quad (5.97)$$

$$p(g) = \exp(-0.745g^{0.295}) / \cosh(g^{0.68}) \quad (5.98)$$

$$f_{o1}(g, \varepsilon_r) = 1 - \exp \left\{ -0.179g^{0.15} - \frac{0.328g^{r(g, \varepsilon_r)}}{\ln[\exp(1) + (g/7)^{2.8}]} \right\} \quad (5.99)$$

$$r(g, \varepsilon_r) = 1 + 0.15 \left\{ 1 - \frac{\exp[1 - (\varepsilon_r - 1)^2/8.2]}{1 + g^{-6}} \right\} \quad (5.100)$$

$$q(g) = \exp(-1.366 - g), \quad (5.101)$$

and $a(u)$, $b(\varepsilon_r)$, and $\psi(g)$ are the same as for the even mode (see Section 5.6.1).

5.6.3 System Impedance of Coupled Lines

The system impedance of a pair of coupled lines is

$$Z_{0S} = \sqrt{Z_{0e}Z_{0o}}. \quad (5.102)$$

This is derived in Section 5.7.1 where it is shown that there will be no odd-mode reflections, and even-mode reflections will be small, at the ports of a symmetrical coupled-line pair if each line of the directional coupler is terminated in an impedance Z_{0S} . That is, Z_{0S} is the impedance required for matching. Z_0 is the characteristic impedance of an individual line of the symmetrical coupled-line pair (when there is no coupling) and is only close to Z_{0S} when the separation, s , of the lines is large.

5.6.4 Discussion

Normalized even- and odd-mode characteristic impedances of a pair of coupled lines are plotted in Figure 5-10 for various normalized widths u

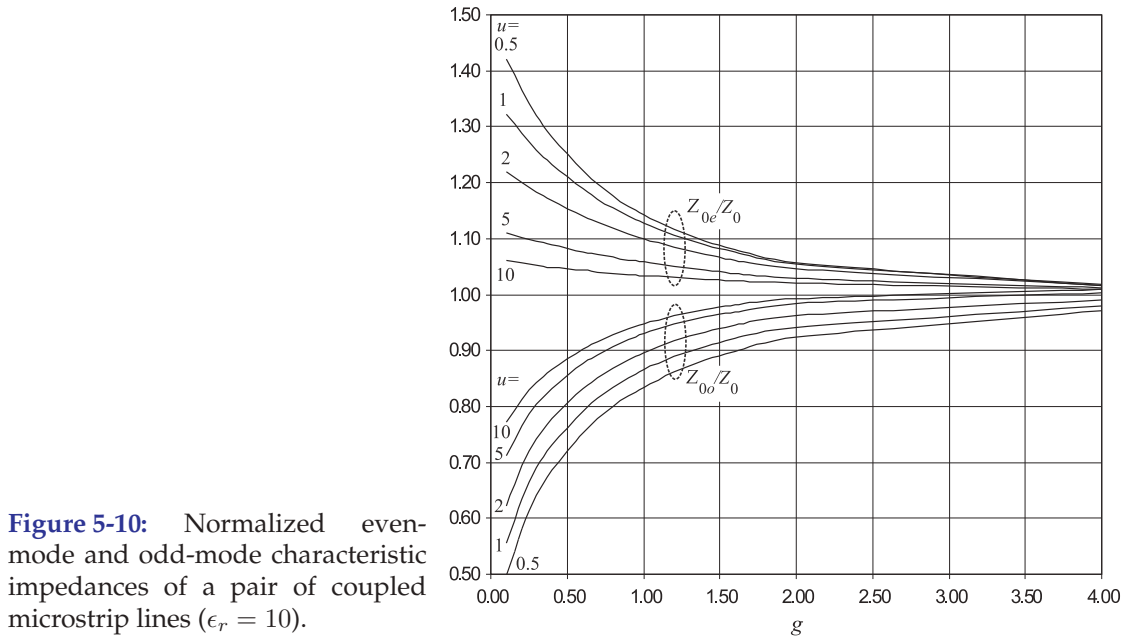


Figure 5-10: Normalized even-mode and odd-mode characteristic impedances of a pair of coupled microstrip lines ($\epsilon_r = 10$).

($= w/h$) and as a function of normalized gap width g ($= s/h$). This plot illustrates the utility of using even- and odd-mode descriptions. In Figure 5-10, the even- and odd-mode impedances are normalized to the characteristic impedance of an individual line, Z_0 . When the lines are far apart (i.e., g is large), the even- and odd-mode impedances converge to the characteristic impedance of a single line. As the lines get closer, the gap narrows, and the even- and odd-mode impedances diverge in opposite directions. To obtain the characteristic impedances of a coupled line the characteristic impedance of a single microstrip line must be found. This was given in Section 3.5.3 and the key result is repeated in Figure 5-11.

In the even mode, more of the field is in the dielectric than with the odd mode. It is therefore not surprising that the effective permittivities of the two modes differ. The normalized coupled-line effective permittivities are shown in Figure 5-12. The deviation of the even- and odd-mode permittivities as the gap between the lines narrows is not as large as the change in the characteristic impedance. Also, there is a difference in the phase velocities of the two modes along the line, and this has an appreciable effect on the performance of components such as filters that use coupled lines as a functional component. At the first reading of the plot (Figure 5-12) it would seem that there is nonmonotonic behavior at low g . This is an artifact of the normalization used, and the unnormalized permittivities are indeed monotonic with respect to both u and g .

Figure 5-13 plots, as a function of normalized separation, g , and for substrate permittivities ranging from 4 to 20, the even-mode and odd-mode characteristic impedances normalized to the characteristic impedance of a single strip for extremes of normalized widths ($u = 0.5$ and $u = 5$). The figure highlights that the split of the even- and odd-mode characteristic impedances is almost solely dependent on geometry (i.e., the separation of the strips) and not the permittivity of the substrate. In the figure appropriate normalization is used to highlight this fact. There are four families of curves,

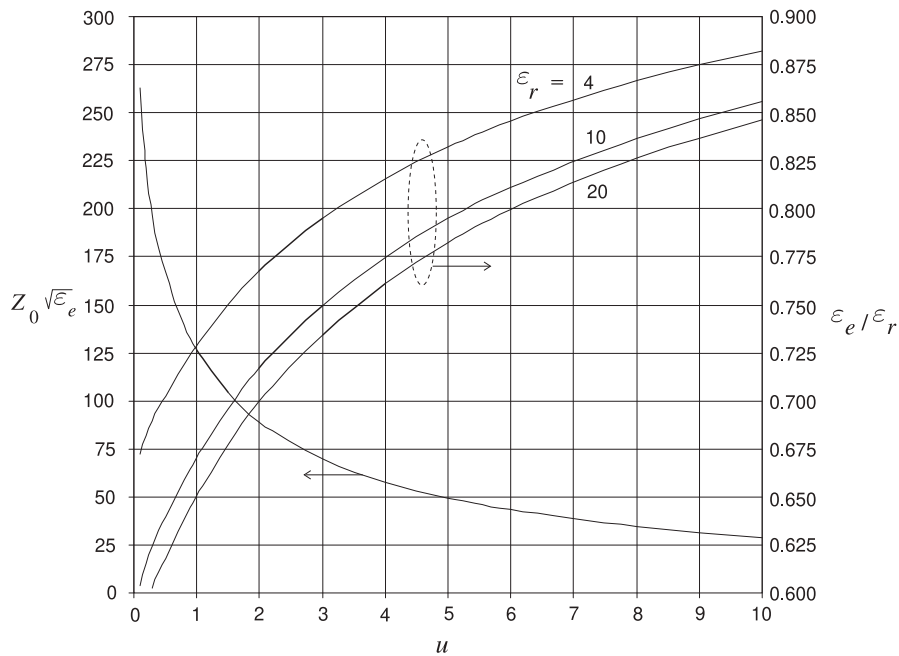


Figure 5-11: Normalized characteristic impedance and normalized effective permittivity of a microstrip line as a function of $u = w/h$. For example, if $u = 1$ and $\epsilon_r = 10$, then from the figure, $Z_0 \sqrt{\epsilon_e} = 126 \, \Omega$ and $\epsilon_e / \epsilon_r = 0.671$; thus $Z_0 = 48.6 \, \Omega$ and $\epsilon_e = 6.71$.

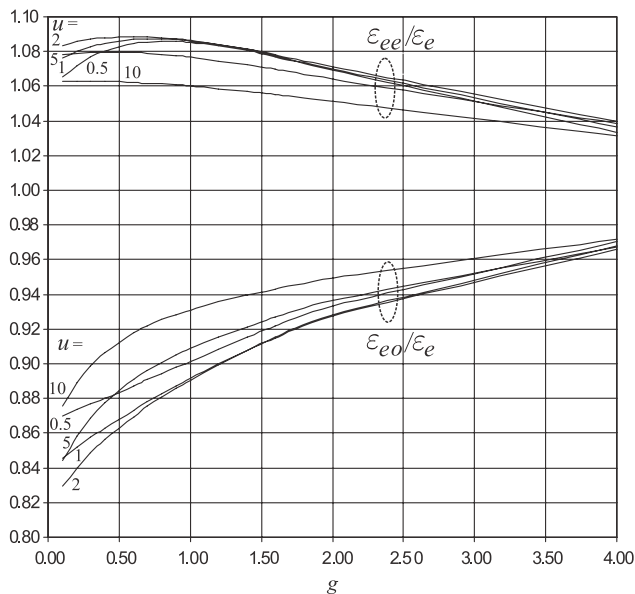


Figure 5-12: Normalized even-mode and odd-mode effective permittivity of a pair of coupled microstrip lines. The effective permittivity of an individual microstrip line with the same normalized width u is ϵ_e .

two for the even-mode characteristic impedances and two for the odd-mode characteristic impedances. Each family comprises the results for three widely different permittivities of the dielectric (specifically $\epsilon_r = 4, 10$, and 20).

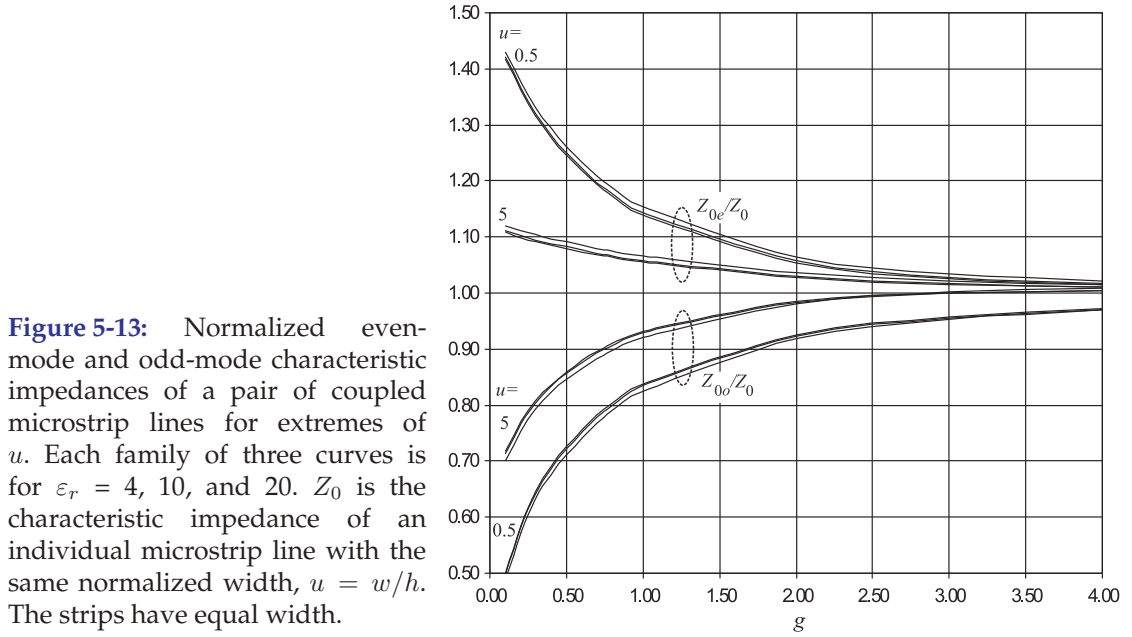


Figure 5-13: Normalized even-mode and odd-mode characteristic impedances of a pair of coupled microstrip lines for extremes of u . Each family of three curves is for $\epsilon_r = 4, 10$, and 20 . Z_0 is the characteristic impedance of an individual microstrip line with the same normalized width, $u = w/h$. The strips have equal width.

EXAMPLE 5.2

Even- and Odd-Mode Parameters

A coupled line is constructed on an alumina substrate of thickness $500 \mu\text{m}$ and relative permittivity $\epsilon_r = 10$. The lines are $500 \mu\text{m}$ wide and the gap separation is $250 \mu\text{m}$. What are the even- and odd-mode characteristic impedances and effective permittivities of the coupled line?

Solution:

The odd-mode characteristic impedance, Z_{0o} , and even-mode characteristic impedance, Z_{0e} , can be found using Figures 5-10 and 5-11. Now

$$u = w/h = (500 \mu\text{m})/(500 \mu\text{m}) = 1 \quad \text{and} \quad g = s/h = (250 \mu\text{m})/(500 \mu\text{m}) = 0.5.$$

From Figure 5-10,

$$Z_{0e}/Z_0 = 1.21 \quad \text{and} \quad Z_{0o}/Z_0 = 0.76, \quad (5.103)$$

where Z_0 is the characteristic impedance of an individual line. From Figure 5-11, and using the curve for $\epsilon_r = 10$,

$$\epsilon_e/\epsilon_r = 0.671, \quad \text{and so} \quad \epsilon_e = 10 \times 0.671 = 6.71. \quad (5.104)$$

Also from Figure 5-11,

$$Z_0\sqrt{\epsilon_e} = 126, \quad \text{and so} \quad Z_0 = 126/\sqrt{6.71} = 48.6 \Omega. \quad (5.105)$$

Consequently, combining Equations (5.103) and (5.105),

$$Z_{0o} = 37 \Omega \quad \text{and} \quad Z_{0e} = 59 \Omega. \quad (5.106)$$

The effective odd-mode and even-mode permittivities are obtained from Figure 5-12. The normalized even-mode effective permittivity is $\epsilon_{ee}/\epsilon_e = 1.086$ and the normalized odd-mode effective permittivity is $\epsilon_{eo}/\epsilon_e = 0.868$. Since $\epsilon_e = 6.71$, the final result is

$$\epsilon_{ee} = 7.28 \quad \text{and} \quad \epsilon_{eo} = 5.82.$$

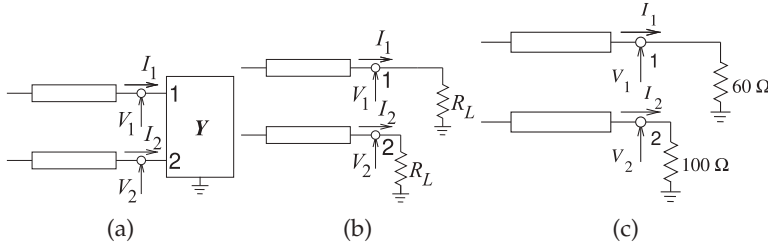


Figure 5-14: Terminated coupled lines: (a) with a load described by the y-parameter matrix Y ; (b) symmetrical loads; (c) loads considered in example.

5.6.5 Summary

This section presented formulas and graphs for determining the frequency-independent parameters of coupled lines given their dimensions. Frequency dependence of these electrical parameters are discussed in [3, 4]. The effect of finite metallization thickness is also discussed in [3]. Synthesis of coupled lines, i.e. determining their physical dimensions given their desired electrical parameters, is undertaken in the context of their use and is generally based on approximate, but reasonably accurate, models of a pair of coupled lines. This will be considered in Section 5.9.

5.7 Terminated Coupled Lines

A pair of coupled lines supports even and odd modes and these can be coupled by the terminations at the end of a line. Thus at a termination, such as that shown in Figure 5-14(a), where the termination is general and represented by a port-based admittance matrix Y , the reflected even and odd modes will have contributions from both incident even and odd modes:

$$V_e^- = \Gamma_{Le} V_e^+ + C_{eo} V_o^+ \quad \text{and} \quad V_o^- = \Gamma_{Lo} V_o^+ + C_{oe} V_e^+ \quad (5.107)$$

where Γ_{Le} and Γ_{Lo} are even- and odd-mode reflection coefficients and C_{oe} and C_{eo} describe coupling first from the odd mode to the even mode and then from the even mode to the odd mode. The derivation of the reflection coefficients and coupling coefficients is left for an example at the end of this section. The summary results are

$$\Gamma_{Le} = \frac{2 + Z_{0o} Y_{\Delta} - Z_{0e} Y_{\Sigma} - 2Z_{0e} Z_{0o} Y_D}{2 + Z_{0o} Y_{\Delta} + Z_{0e} Y_{\Sigma} + 2Z_{0e} Z_{0o} Y_D} \quad (5.108)$$

$$C_{eo} = \frac{2Z_{0e} Y_E}{2 + Z_{0o} Y_{\Delta} + Z_{0e} Y_{\Sigma} + 2Z_{0e} Z_{0o} Y_D} = -C_{oe} \quad (5.109)$$

$$\Gamma_{Lo} = \frac{1 + Z_{0o}(y_{12} + y_{21}) - Z_{0e} Z_{0o} Y_D}{1 + Z_{0o} Y_{\Delta} + Z_{0e} Y_{\Sigma} + Z_{0e} Z_{0o} Y_D} \quad (5.110)$$

$$\left. \begin{aligned} \text{where } Y_{\Sigma} &= (y_{11} + y_{12} + y_{21} + y_{22}), \quad Y_{\Delta} = (y_{11} - y_{12} - y_{21} + y_{22}) \\ Y_D &= (y_{11} y_{22} - y_{12} y_{21}) \quad \text{and } Y_E = (y_{11} - y_{12} + y_{21} - y_{22}). \end{aligned} \right\} \quad (5.111)$$

Controlling the coupling can be used in filter design based on parallel coupled lines.

5.7.1 Reflectionless Condition

In design of many coupled line sections it is important to minimize reflections of coupled lines. One quasi-reflectionless condition is to terminate individual lines of the coupled line in the system reference impedance

$Z_{0S} = \sqrt{Z_{0e}Z_{0o}}$. Then $y_{11} = 1/Z_{0S} = y_{22}$, and $y_{12} = 0 = y_{21}$ and referring to Equation (5.111), $Y_{\Sigma} = Y_{\Delta} = 2/Z_{0S} = 2/\sqrt{Z_{0e}Z_{0o}}$, $Y_E = 0$, and $Y_D = 1/Z_{0e}Z_{0o}$ and Equation (5.108) becomes

$$\Gamma_{Le} = \frac{2 + 2\sqrt{Z_{0o}Z_{0e}} - 2\sqrt{Z_{0e}Z_{0o}} - 2}{2 + 2\sqrt{Z_{0o}Z_{0e}} + 2\sqrt{Z_{0e}Z_{0o}} + 2} = \frac{\sqrt{Z_{0o}Z_{0e}} - 2\sqrt{Z_{0e}Z_{0o}}}{2 + \sqrt{Z_{0o}Z_{0e}} + \sqrt{Z_{0e}Z_{0o}}} \quad (5.112)$$

which is small and

$$\Gamma_{Lo} = \frac{1 + 0 - 1}{D} = 0. \quad (5.113)$$

Also note that the mode couplings C_{oe} and C_{eo} are both zero. So terminating the individual lines of a pair of coupled lines in Z_{0S} results in the odd-mode reflection coefficient Γ_{Lo} being zero and the odd-mode reflection coefficient Γ_{Le} being small.

The even and odd-mode reflection coefficients can both be set to zero by simultaneously setting the numerators of Equations (5.108) and (5.108) to zero while maintaining symmetry, i.e. $y_{11} = y_{22}$, and because of reciprocity $y_{12} = y_{21}$ thus ensuring that $Y_E = 0$ and coupling is zero.

EXAMPLE 5.3

Reflection at the End of a Pair of Coupled Lines

A pair of coupled lines with even- and odd-mode characteristic impedances Z_{0e} and Z_{0o} respectively is loaded as shown in Figure 5-14(a) where the load has the two-port y -parameter matrix, \mathbf{Y} . Find the even and odd-mode reflections.

Solution:

The analysis begins by writing out the expressions relating the traveling-wave and total voltages and currents at the termination.

$$\begin{aligned} V_e &= \frac{1}{2}(V_1 + V_2) & V_o &= \frac{1}{2}(V_1 - V_2) & I_e &= \frac{1}{2}(I_1 + I_2) & I_o &= \frac{1}{2}(I_1 - I_2) \\ V_1 &= (V_1^+ + V_1^-) & V_2 &= (V_2^+ + V_2^-) & I_1 &= (I_1^+ + I_1^-) & I_2 &= (I_2^+ + I_2^-) \\ V_1^+ &= (V_e^+ + V_o^+) & V_2^+ &= (V_e^+ - V_o^+) & I_1^+ &= (I_e^+ + I_o^+) & I_2^+ &= (I_e^+ - I_o^+) \\ V_1^- &= (V_e^- + V_o^-) & V_2^- &= (V_e^- - V_o^-) & I_1^- &= (I_e^- + I_o^-) & I_2^- &= (I_e^- - I_o^-) \\ I_e^+ &= V_e^+/Z_{0e} & I_e^- &= -V_e^-/Z_{0e} & I_o^+ &= V_o^+/Z_{0e} & I_o^- &= -V_o^-/Z_{0e} \end{aligned}$$

At the termination

$$\begin{aligned} \begin{bmatrix} I_1 \\ I_2 \end{bmatrix} &= \begin{bmatrix} I_e^+ + I_o^+ + I_e^- + I_o^- \\ I_e^+ - I_o^+ + I_e^- - I_o^- \end{bmatrix} = \mathbf{Y} \begin{bmatrix} V_1 \\ V_2 \end{bmatrix} = \begin{bmatrix} y_{11} & y_{12} \\ y_{21} & y_{22} \end{bmatrix} \begin{bmatrix} V_1 \\ V_2 \end{bmatrix} \\ \begin{bmatrix} (V_e^+ - V_e^-)/Z_{0e} + (V_o^+ - V_o^-)/Z_{0o} \\ (V_e^+ - V_e^-)/Z_{0e} - (V_o^+ - V_o^-)/Z_{0o} \end{bmatrix} &= \begin{bmatrix} y_{11} & y_{12} \\ y_{21} & y_{22} \end{bmatrix} \begin{bmatrix} V_e^+ + V_o^+ + V_e^- + V_o^- \\ V_e^+ - V_o^+ + V_e^- - V_o^- \end{bmatrix} \quad (5.114) \end{aligned}$$

The reflected even and odd modes have contributions from incident even and odd modes:

$$V_e^- = \Gamma_{Le} V_e^+ + C_{eo} V_o^+ \quad \text{and} \quad V_o^- = \Gamma_{Lo} V_o^+ + C_{oe} V_e^+ \quad (5.115)$$

where Γ_{Le} and Γ_{Lo} are even- and odd-mode reflection coefficients, C_{oe} and C_{eo} describe coupling, and

$$\Gamma_{Le} = \left. \frac{V_e^-}{V_e^+} \right|_{V_o^+ = 0}, \Gamma_{Lo} = \left. \frac{V_o^-}{V_o^+} \right|_{V_e^+ = 0}, C_{eo} = \left. \frac{V_e^-}{V_o^+} \right|_{V_e^+ = 0} \quad \text{and} \quad C_{oe} = \left. \frac{V_o^-}{V_e^+} \right|_{V_o^+ = 0}. \quad (5.116)$$

Γ_{Le} and C_{eo} are obtained by expanding Equation (5.114) with $V_o^+ = 0$:

$$\begin{aligned} (V_e^+ - V_e^-)/Z_{0e} - V_o^-/Z_{0o} &= y_{11}(V_e^+ + V_e^- + V_o^-) + y_{12}(V_e^+ + V_e^- - V_o^-) \\ \text{i.e. } \frac{V_e^-}{Z_{0e}}(1 + y_{11}Z_{0e} + y_{12}Z_{0e}) &= \frac{V_e^+}{Z_{0e}}(1 - y_{11}Z_{0e} - y_{12}Z_{0e}) - \frac{V_o^-}{Z_{0o}}(1 + y_{11}Z_{0o} - y_{12}Z_{0o}) \end{aligned} \quad (5.117)$$

$$\begin{aligned} (V_e^+ - V_e^-)/Z_{0e} + V_o^-/Z_{0o} &= y_{21}(V_e^+ + V_e^- + V_o^-) + y_{22}(V_e^+ + V_e^- - V_o^-) \\ \text{i.e. } \frac{V_o^-}{Z_{0o}}(-1 + y_{21}Z_{0o} - y_{22}Z_{0o}) &= \frac{V_e^+}{Z_{0e}}(1 - y_{21}Z_{0e} - y_{22}Z_{0e}) + \frac{V_e^-}{Z_{0e}}(-1 - y_{21}Z_{0e} - y_{22}Z_{0e}) \end{aligned} \quad (5.118)$$

Γ_{Le} is obtained by eliminating V_o^- by multiplying Equation (5.118) by $(1 + y_{11}Z_{0o} - y_{12}Z_{0o})$ and subtracting it from Equation (5.117) multiplied by $(-1 + y_{21}Z_{0o} - y_{22}Z_{0o})$:

$$V_e^- \frac{a}{Z_{0e}} = V_e^+ \frac{b}{Z_{0e}} \Big|_{V_o^+ = 0}. \quad \text{Thus } \Gamma_{Le} = \frac{b}{a} \quad (5.119)$$

where

$$\begin{aligned} a &= (1 + y_{11}Z_{0e} + y_{12}Z_{0e})(-1 + y_{21}Z_{0o} - y_{22}Z_{0o}) - (1 + y_{21}Z_{0e} + y_{22}Z_{0e})(1 + y_{11}Z_{0o} - y_{12}Z_{0o}) \\ &= -2 - Z_{0o}Y_{\Delta} - Z_{0e}Y_{\Sigma} - 2Z_{0e}Z_{0o}Y_D \end{aligned} \quad (5.120)$$

$$\begin{aligned} b &= (1 - y_{11}Z_{0e} - y_{12}Z_{0e})(-1 + y_{21}Z_{0o} - y_{22}Z_{0o}) - (1 - y_{21}Z_{0e} - y_{22}Z_{0e})(1 + y_{11}Z_{0o} - y_{12}Z_{0o}) \\ &= -2 - Z_{0o}Y_{\Delta} + Z_{0e}Y_{\Sigma} + 2Z_{0e}Z_{0o}Y_D \end{aligned} \quad (5.121)$$

$$Y_{\Sigma} = (y_{11} + y_{12} + y_{21} + y_{22}), Y_{\Delta} = (y_{11} - y_{12} - y_{21} + y_{22}), \text{ and } Y_D = (y_{11}y_{22} - y_{12}y_{21}) \quad (5.122)$$

$$\Gamma_{Le} = \frac{b}{a} = \frac{2 + Z_{0o}Y_{\Delta} - Z_{0e}Y_{\Sigma} - 2Z_{0e}Z_{0o}Y_D}{2 + Z_{0o}Y_{\Delta} + Z_{0e}Y_{\Sigma} + 2Z_{0e}Z_{0o}Y_D} \quad (5.123)$$

As a sanity check, if the load is symmetrical $y_{11} = y_{22} = Y_L = 1/Z_L$, the differential load impedance is infinite $y_{12} = 0 = y_{21}$, if the lines are far apart $Z_{0e} = Z_{0o} = Z_0$, then $Y_{\Sigma} = 2Y_L$, $Y_{\Delta} = 2Y_L$, and $Y_D = Y_L^2$ and Equation (5.123) becomes

$$\begin{aligned} \Gamma_{Le} &= \frac{2 + 2Z_0Y_L - 2Z_0Y_L - 2Z_0^2Y_L^2}{2 + 2Z_0Y_L + 2Z_0Y_L + 2Z_0^2Y_L^2} = \frac{1 - Z_0^2Y_L^2}{1 + 2Z_0Y_L + Z_0^2Y_L^2} = \frac{(1 - Z_0Y_L)(1 + Z_0Y_L)}{(1 + Z_0Y_L)(1 + Z_0Y_L)} \\ &= \frac{1 - Z_0Y_L}{1 + Z_0Y_L} = \frac{Z_L - Z_0}{Z_L + Z_0}. \end{aligned} \quad (5.124)$$

This is the reflection coefficient of a transmission line of characteristic impedance Z_0 terminated in a load Z_L as expected.

Find C_{eo} by expanding Equation (5.114) with $V_e^+ = 0$:

$$\begin{aligned} -V_e^-/Z_{0e} + (V_o^+ - V_o^-)/Z_{0o} &= y_{11}(V_o^+ + V_e^- + V_o^-) + y_{12}(-V_o^+ + V_e^- - V_o^-) \\ \text{i.e. } \frac{V_e^-}{Z_{0e}}(1 + y_{11}Z_{0e} + y_{12}Z_{0e}) &= \frac{V_o^+}{Z_{0o}}(1 - y_{11}Z_{0o} + y_{12}Z_{0o}) - \frac{V_o^-}{Z_{0o}}(1 + y_{11}Z_{0o} - y_{12}Z_{0o}) \end{aligned} \quad (5.125)$$

$$\begin{aligned} -V_e^-/Z_{0e} - (V_o^+ - V_o^-)/Z_{0o} &= y_{21}(V_o^+ + V_e^- + V_o^-) + y_{22}(-V_o^+ + V_e^- - V_o^-) \\ \text{i.e. } \frac{V_o^-}{Z_{0o}}(-1 + y_{21}Z_{0o} - y_{22}Z_{0o}) &= -\frac{V_o^+}{Z_{0o}}(1 + y_{21}Z_{0o} - y_{22}Z_{0o}) - \frac{V_e^-}{Z_{0e}}(1 + y_{21}Z_{0e} + y_{22}Z_{0e}) \end{aligned} \quad (5.126)$$

To eliminate V_o^- multiply Equation (5.126) by $(1 + y_{11}Z_{0o} - y_{12}Z_{0o})$ and subtract it from Equation (5.125) multiplied by $(-1 + y_{21}Z_{0o} - y_{22}Z_{0o})$:

$$\frac{V_e^-}{Z_{0e}}a = \frac{V_o^+}{Z_{0o}}c \quad \text{so that} \quad C_{eo} = \frac{c}{a} \frac{Z_{0e}}{Z_{0o}} \quad (5.127)$$

where a is as in Equation (5.120) and

$$c = (1 - y_{11}Z_{0o} + y_{12}Z_{0o})(-1 + y_{21}Z_{0o} - y_{22}Z_{0o}) + (1 + y_{21}Z_{0o} - y_{22}Z_{0o})(1 + y_{11}Z_{0o} - y_{12}Z_{0o}) \\ = -2Z_{0o}Y_E \quad \text{where} \quad Y_E = (y_{11} - y_{12} + y_{21} - y_{22}). \quad (5.128)$$

$$C_{eo} = \frac{2Z_{0o}Y_E}{2 + Z_{0o}Y_\Delta + Z_{0e}Y_\Sigma + 2Z_{0e}Z_{0o}Y_D} \quad (5.129)$$

Now for a sanity check. If the load is symmetrical $y_{11} = y_{22}$ and $y_{12} = y_{21}$, then $Y_E = 0$ and $C_{eo} = 0$ indicating that a signal is not converted from odd mode to even mode with reflection from a symmetrical load, as expected.

The analysis is now repeated to find Γ_{Lo} and C_{oe} . Γ_{Lo} is found by eliminating V_e^- from Equations (5.125) and (5.126) by multiplying Equation (5.126) by $(1 + y_{11}Z_{0e} + y_{12}Z_{0e})$ and subtracting it from Equation (5.125) multiplied by $(1 + y_{21}Z_{0e} + y_{22}Z_{0e})$:

$$\frac{V_o^+}{Z_{0o}}d = \frac{V_o^-}{Z_{0o}}e \Big|_{V_e^+=0} \quad \text{and} \quad \Gamma_{Lo} = \frac{V_o^-}{V_o^+} \Big|_{V_e^+=0} = \frac{d}{e} \quad (5.130)$$

$$d = (1 - y_{11}Z_{0o} + y_{12}Z_{0o})(1 + y_{21}Z_{0e} + y_{22}Z_{0e}) + (1 + y_{21}Z_{0o} - y_{22}Z_{0o})(1 + y_{11}Z_{0e} + y_{12}Z_{0e}) \\ = 2 + 2Z_{0o}(y_{12} + y_{21}) - 2Z_{0e}Z_{0o}Y_D \quad (5.131)$$

$$e = (1 + y_{11}Z_{0o} - y_{12}Z_{0o})(1 + y_{21}Z_{0e} + y_{22}Z_{0e}) - (-1 + y_{21}Z_{0o} - y_{22}Z_{0o})(1 + y_{11}Z_{0e} + y_{12}Z_{0e}) \\ = 2 + 2Z_{0o}Y_\Delta + 2Z_{0e}Y_\Sigma + 2Z_{0e}Z_{0o}Y_D \quad (5.132)$$

$$\Gamma_{Lo} = \frac{1 + Z_{0o}(y_{12} + y_{21}) - Z_{0e}Z_{0o}Y_D}{1 + Z_{0o}Y_\Delta + Z_{0e}Y_\Sigma + Z_{0e}Z_{0o}Y_D}. \quad (5.133)$$

C_{oe} is found by eliminating V_e^- achieved by multiplying Equation (5.118) by $(1 + y_{11}Z_{0e} + y_{12}Z_{0e})$ and subtracting it from Equation (5.117) multiplied by $(1 + y_{21}Z_{0e} + y_{22}Z_{0e})$:

$$V_o^- \frac{f}{Z_{0o}} = V_e^+ \frac{g}{Z_{0e}} \Big|_{V_o^+=0}. \quad \text{Thus} \quad C_{oe} = \frac{g}{f} \frac{Z_{0o}}{Z_{0e}} \quad \text{where} \quad (5.134)$$

$$g = -(1 - y_{11}Z_{0e} - y_{12}Z_{0e})(1 + y_{21}Z_{0e} + y_{22}Z_{0e}) + (1 - y_{21}Z_{0e} - y_{22}Z_{0e})(1 + y_{11}Z_{0e} + y_{12}Z_{0e}) \\ = 2Z_{0e}(y_{11} + y_{12} - y_{21} - y_{22}) = 2Z_{0e}Y_E \quad (5.135)$$

$$f = -(1 + y_{11}Z_{0o} - y_{12}Z_{0o})(1 + y_{21}Z_{0e} + y_{22}Z_{0e}) + (-1 + y_{21}Z_{0o} - y_{22}Z_{0o})(1 + y_{11}Z_{0e} + y_{12}Z_{0e}) \\ = -2 - Z_{0o}Y_\Delta - Z_{0e}Y_\Sigma - 2Z_{0e}Z_{0o}Y_D \quad (5.136)$$

$$C_{oe} = \frac{-2Z_{0o}Y_E}{2 + Z_{0o}Y_\Delta - Z_{0e}Y_\Sigma + 2Z_{0e}Z_{0o}Y_D} = -C_{eo}. \quad (5.137)$$

EXAMPLE 5.4

Even and Odd Mode Loads

A pair of coupled lines is loaded as shown in Figure 5-14(a). The even-mode characteristic impedance is $Z_{0e} = 90 \Omega$ and the odd-mode characteristic impedance is $Z_{0o} = 45 \Omega$.

- (a) What is the even-mode reflection coefficient?

To simplify calculations let the forward-traveling even-mode voltage at the load $V_e^+ = 1 \text{ V}$, and there is no forward-traveling odd-mode voltage. V_e^- and V_o^- are the backward-traveling even- and odd-mode voltages and I_e^+ , I_e^- and I_o^- are the corresponding currents. At Port 1

$$I_1 = \frac{1}{60}V_1 = V_e^+ + V_o^+ + V_e^- + V_o^- = \frac{1}{60}(1 + 0 + V_e^- + V_o^-) \\ I_1 = I_e^+ + I_o^+ + I_e^- + I_o^- = \frac{V_e^+}{Z_{0e}} + 0 - \frac{V_e^-}{Z_{0e}} - \frac{V_o^-}{Z_{0o}} = \frac{1}{90} - \frac{V_e^-}{90} - \frac{V_o^-}{45} \\ \text{Equating these and multiplying by } 180 \quad 1 + 5V_e^- + 7V_o^- = 0 \quad (5.138)$$

At Port 2

$$I_2 = \frac{1}{100} V_1 = \frac{1}{100} (V_e^- V_o^+ + V_e^- - V_o^-) = \frac{1}{100} (1 + 0 + V_e^- - V_o^-)$$

$$I_2 = I_e^+ - I_o^+ + I_e^- - I_o^- = \frac{V_e^+}{Z_{0e}} + 0 - \frac{V_e^-}{Z_{0e}} + \frac{V_o^-}{Z_{0o}} = \frac{1}{90} - \frac{V_e^-}{90} + \frac{V_o^-}{45}$$

$$\text{Equating these and multiplying by 900: } 1 - 19V_e^- + 29V_o^- = 0 \quad (5.139)$$

Multiplying Equation (5.139) by 7 and subtracting it from Equation (5.138) times 29:

$$(29 - 7) + (145 + 133)V_e^- + (203 - 203)V_o^- = 0 \Rightarrow V_e^- = -0.07914 \text{ V}$$

$$\text{Thus } \Gamma_{Le} = V_e^- / V_e^+ = V_e^- / 1 = -0.07914. \quad (5.140)$$

Alternatively the general formula, Equation (5.108), can be used noting that $Z_{0e} = 90 \Omega$, $Z_{0o} = 45 \Omega$, $y_{11} = 1/60$, $y_{22} = 1/100$, and $y_{12} = 0 = y_{21}$. Then $y_\Delta = 0.026667 \text{ S}$, $y_\Sigma = 0.026667 \text{ S}$, $y_D = 0.00016667 \text{ S}$:

$$\Gamma_{Le} = \frac{2 + 45 \cdot 0.026667 - 90 \cdot 0.026667 - 2 \cdot 45 \cdot 90 \cdot 0.00016667}{2 + 45 \cdot 0.026667 + 90 \cdot 0.026667 + 2 \cdot 45 \cdot 90 \cdot 0.00016667} = -0.07914 \quad (5.141)$$

The two evaluations of Γ_{Le} are in agreement.

(b) What is the effective even-mode load resistance R_{Le} ?

R_{Le} is the resistance that yields Γ_{Le} when referred to Z_{0e} . Thus

$$R_{Le} = Z_{0e} \frac{1 + \Gamma_{Le}}{1 - \Gamma_{Le}} = 90 \frac{1 + (-0.07914)}{1 - (-0.07914)} = 76.80 \Omega \quad (5.142)$$

(c) What is the odd-mode reflection coefficient?

Calculating this directly using Equation (5.110):

$$\Gamma_{Lo} = \frac{1 + 0 - 45 \cdot 90 \cdot 0.00016667}{1 + 45 \cdot 0.026667 + 90 \cdot 0.026667 + 45 \cdot 90 \cdot 0.00016667} = 0.06180 \quad (5.143)$$

(d) What is the effective odd-mode load resistance R_{Lo} ?

$$R_{Lo} = Z_{0o} \frac{1 + \Gamma_{Lo}}{1 - \Gamma_{Lo}} = 45 \frac{1 + 0.06180}{1 - 0.06180} = 50.92 \Omega \quad (5.144)$$

5.8 Directional Coupler

Coupling can be exploited to realize a new type of element called a directional coupler. The schematic of a directional coupler is shown in Figure 5-15(a) and a microstrip realization is shown in Figure 5-15(b). The microstrip realization is typical of most directional couplers in that it comprises two parallel signal lines with the electric and magnetic fields of a signal on one line inducing currents and voltages on the other. A usable directional

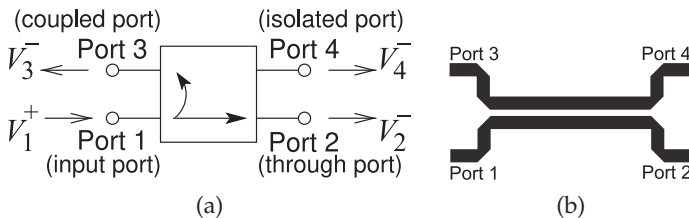


Figure 5-15: Directional couplers: (a) schematic; and (b) backward-coupled microstrip coupler. (Note that not all couplers are backward-wave couplers as shown in (a).)

Table 5-1: Ideal and typical parameters of a directional coupler.

Parameter	Ideal	Ideal (dB)	Typical
Coupling, C	-	-	3–40 dB
Transmission, T	$ \sqrt{1 - 1/C^2} $	$20 \log \sqrt{1 - 1/C^2} $	–0.5 dB
Directivity, D	∞	∞	40 dB
Isolation, I	∞	∞	40 dB

coupler has a coupled line length of at least one-quarter wavelength, with longer lengths of line resulting in broader bandwidth operation. Directional couplers are used to sample a traveling wave on one line and to induce a usually much smaller image of the wave on another line. That is, the forward- and backward-traveling waves are separated. Here a prescribed amount of the incident power is coupled out of the system. Thus, for example, a 20 dB microstrip coupler is a pair of coupled microstrip lines in which 1/100 of the power input is coupled from one microstrip line onto the another.

Referring to Figure 5-15, a coupler is specified in terms of the following parameters (always check the magnitude of the factors, as some papers and books on couplers use the inverse of the C used here):

- Coupling factor:
 $C = V_1^+ / V_3^- =$ inverse of the voltage fraction “transferred” (coupled) across to the opposite arm ($C > 1$).
- Transmission factor (inverse of insertion loss):
 $T = V_2^- / V_1^+ =$ transmission directly through the “primary” arm of the structure ($T < 1$).
- Directivity factor:
 $D = V_3^- / V_4^- =$ measure of the undesired coupling from Port 1 to Port 4 relative to the signal level at Port 3 ($D > 1$).
- Isolation factor:
 $I = V_1^+ / V_4^- =$ isolation between Port 4 and Port 1 ($I > 1$).

It is usual to quote these quantities in decibels. For example, the coupling factor in decibels is $C|_{\text{dB}} = 20 \log C$. So 20 dB coupling indicates that the coupling factor is 10. An ideal quarter-wave coupler has $D = \infty$ (i.e., infinite directivity) and

$$C = \frac{Z_{0e} + Z_{0o}}{Z_{0e} - Z_{0o}}. \quad (5.145)$$

This result comes from a detailed derivation for the case when the coupled-line section is one-quarter wavelength long—the length when the coupling is maximum. The derivation is given in Section 11.4 of [5]. In decibels the coupling is

$$C|_{\text{dB}} = 20 \log \left(\frac{Z_{0e} + Z_{0o}}{Z_{0e} - Z_{0o}} \right). \quad (5.146)$$

Typical and ideal parameters of a directional coupler are given in Table 5-1. Since an ideal coupler does not dissipate power, the magnitude of the transmission coefficient is

$$|T| = |\sqrt{1 - 1/C^2}|. \quad (5.147)$$

There are many types of directional couplers, and the phases of the traveling waves at the ports will not necessarily coincide. The microstrip

coupler shown in Figure 5-15(b) has maximum coupling when the lines are one-quarter wavelength long.⁵ At the frequency where they are one-quarter wavelength long, the phase difference between traveling waves entering at Port 1 and leaving at Port 2 will then be 90°.

EXAMPLE 5.5 Directional Coupler Isolation

A lossless directional coupler has coupling $C = 20$ dB, transmission factor 0.8, and directivity 20 dB. What is the isolation? Express your answer in decibels.

Solution:

Coupling factor: $C = V_1^+ / V_3^-$

Transmission factor: $T = V_2^- / V_1^+$

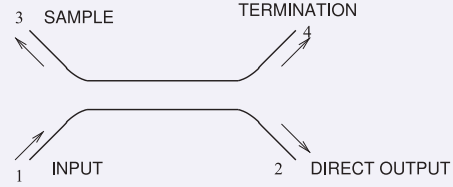
Directivity factor: $D = V_3^- / V_4^-$

Isolation factor: $I = V_1^+ / V_4^-$

$$D = 20 \text{ dB} = 10 \quad \text{and} \quad C = 20 \text{ dB} = 10,$$

so the isolation is

$$I = \frac{V_1^+}{V_4^-} = \frac{V_3^-}{V_4^-} \cdot \frac{V_1^+}{V_3^-} = D \cdot C = 10 \cdot 10 = 100 = 40 \text{ dB}.$$



5.8.1 Design Equations for a Directional Coupler

In the previous section the coupling factor was expressed in terms of the even- and odd-mode impedances. However, design starts with the specification of the coupling level, and from this the required physical dimensions are derived. A one-quarter wavelength long coupler will be considered, as this is the optimum coupling length. From Equation (5.145), the desired coupling factor is

$$C = \frac{Z_{0e} + Z_{0o}}{Z_{0e} - Z_{0o}}, \quad (5.148)$$

where the coupling factor is an absolute voltage-referenced quantity and usually must be derived from the coupling factor in decibels; let this be $C|_{\text{dB}}$:

$$C = 10^{C|_{\text{dB}}/20}. \quad (5.149)$$

The system impedance comes from

$$Z_{0S}^2 \approx Z_{0e} Z_{0o}. \quad (5.150)$$

Z_{0S} is introduced here because Z_0 is used for the characteristic impedance of the individual lines of the coupler; note that Z_0 is not equal to Z_{0S} . Z_{0S} should match the characteristic impedance of the transmission lines connected to the coupler. From these expressions, the even- and odd-mode impedances required are

$$Z_{0e} \approx Z_{0S} \sqrt{\frac{C+1}{C-1}} \quad (5.151)$$

$$Z_{0o} \approx Z_{0S} \sqrt{\frac{C-1}{C+1}}, \quad (5.152)$$

and the ratio of impedances is

$$Z_{0e}/Z_{0o} \approx \frac{C+1}{C-1}. \quad (5.153)$$

⁵ This is shown in a detailed derivation provided in Section 11.4 of [5].

EXAMPLE 5.6**Directional Coupler Electrical Design**

Develop the electrical design of a 15 dB directional coupler in a 50 Ω system.

Solution:

The electrical design of a directional coupler comes down to determining the even- and odd-mode characteristic impedances required. Now the coupling factor, C , is $(Z_{0e} + Z_{0o}) / (Z_{0e} - Z_{0o})$ and

$$Z_{0e} = Z_{0S} \sqrt{\frac{C+1}{C-1}}.$$

For a 15 dB directional coupler, $C = 15 \text{ dB} = 5.618$ and, since $Z_{0S} = 50 \Omega$,

$$Z_{0e} = 50 \sqrt{\frac{5.618+1}{5.618-1}} = 59.9 \Omega \quad \text{and} \quad Z_{0o} = Z_{0S}^2 / Z_{0e} = 50^2 / 59.9 = 41.7 \Omega.$$

The above are the required electrical design parameters.

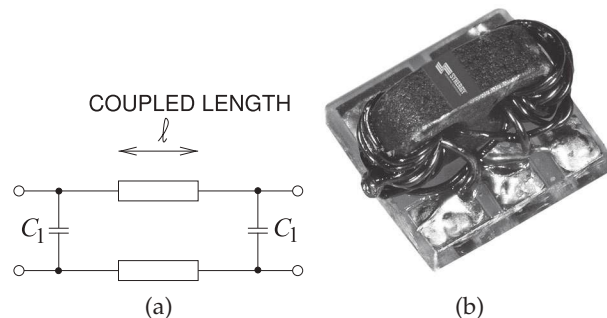
5.8.2 Directional Coupler With Lumped Capacitors

Directional couplers using only coupled transmission lines can be large at low frequencies, as the minimum length is approximately one-quarter of a wavelength. This can be a problem at RF and low microwave frequencies, say, below 3 GHz. The length of the line can be reduced by incorporating lumped elements, as shown in Figure 5-16(a). The equivalence is established using $ABCD$ parameters. Figure 5-16(b) shows a hybrid directional coupler using a ferrite core, forming a magnetic transformer, to provide enhanced coupling of the coupled lines at low frequencies with a frequency range of 1–700 MHz. At high frequencies the ferrite core is a magnetic open circuit and the line coupling dominates.

5.8.3 Physical Design of a Pair of Coupled Lines

Equations (5.151)–(5.153) are the basic design expressions, as Z_{0e} and Z_{0o} can be related to physical dimensions. When the two strips of a microstrip directional coupler are close, the orientation of the field lines and hence the characteristic impedances of the individual lines change. That is, the characteristic impedance of each line on its own, Z_0 , will differ from the system impedance, Z_{0S} . For a normalized line width of $u = (w/h)$, this effect is shown in Figure 5-17. Here Z_{0S} is the geometric mean of the even- and odd-mode impedances.

Figure 5-16: Parallel coupled lines with lumped capacitors bridging the ends to provide compensation: (a) schematic illustration; and (b) using a hybrid transformer to provide enhanced coupling of the coupled lines at low frequencies (Model GC6-2, copyright Synergy Microwave Corporation, used with permission [6]).



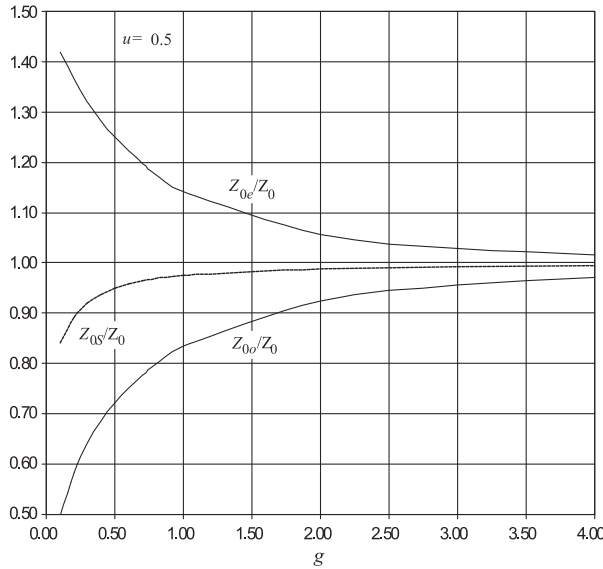


Figure 5-17: Normalized even- and odd-mode characteristic impedances of coupled microstrip lines with normalized width, $u = 0.5$, versus normalized gap spacing, g .

Microstrip coupler design proceeds as follows. The first step is to examine the specifications and determine the substrate permittivity, ϵ_r , coupling factor, C , and the system characteristic impedance, Z_{0S} . From C find Z_{0e}/Z_0 ; the data in Tables 5-2 and 5-3 enable some of the physical parameters to be determined, including the normalized gap coupling parameter, g , and the normalized strip width, u . The next step is to design the dimensions of the individual microstrip lines connecting the directional coupler using Table 3-3. At this stage the widths and spacings of the microstrip circuit are normalized. Using the substrate height, these are unnormalized to obtain the actual physical dimensions. Finally, the coupler is one-quarter wavelength long, as this was the basis for the formula relating the even- and odd-mode impedances to the coupling factor in Equation (5.145). The even and odd modes have different effective permittivities and the $\lambda_g/4$ length should apply to both the even and odd modes. Clearly both cannot be satisfied. It is reasonable to use the average of the even- and odd-mode permittivities to establish the coupler length. The length is not a very sensitive parameter anyway. The connection of the individual lines to the coupler is not specifically part of the synthesis described, but if designed they should have the system characteristic impedance.

A comment on this design procedure is in order. The design procedure above yields a narrowband directional coupler. A broadband directional coupler, and indeed any component that is desired to have a broad bandwidth, should be designed using filter principles. Another comment is that the design flow is one of synthesis. An alternative procedure that is often used is to start with an approximate design and rely on optimization tools to obtain the desired characteristics. This works in many cases, but does lead to novel design. Having said that, the synthesis procedure does not yield a perfect design, as parasitic and dispersive effects are not taken into account. Optimization from the synthesized design usually requires only a small adjustment. In practice, the uncertainties of physical structures (e.g., variations in the effective permittivity of actual materials) require experimental iteration as well.

Table 5-2: Design parameters for coupled lines for $\varepsilon_r = 4$. The normalized gap, g , is chosen to obtain the desired coupled-line mode impedance ratio, Z_{0e}/Z_{0o} . Data are derived from the analysis in Section 5.6. Z_0 is the characteristic impedance of an individual microstrip line with a normalized width, u . For $Z_{0S} = 50 \Omega$, $w/h = 2.056$, from Table 3-3.

$\varepsilon_r = 4$ (SiO ₂ and FR4), $Z_{0S} = 50 \Omega$							
g	Z_{0e}/Z_{0o}	u	Z_{0e} (Ω)	Z_{0o} (Ω)	ε_{ee}	ε_{eo}	Z_0 (Ω)
0.1	2.20	1.57	74.12	33.72	3.20	2.61	58.60
0.2	1.87	1.72	68.38	36.52	3.23	2.65	55.60
0.3	1.70	1.80	65.26	38.37	3.25	2.68	54.10
0.4	1.59	1.86	62.93	39.66	3.26	2.70	53.10
0.5	1.50	1.90	61.26	40.74	3.27	2.72	52.20
0.6	1.44	1.93	59.93	41.63	3.27	2.74	52.00
0.7	1.39	1.95	58.90	42.42	3.27	2.76	51.60
0.8	1.35	1.97	57.95	43.05	3.28	2.78	51.30
0.9	1.31	1.98	57.25	43.67	3.28	2.79	51.20
1.0	1.28	1.99	56.61	44.20	3.27	2.80	51.00
1.2	1.23	2.01	55.46	45.03	3.27	2.82	50.70
1.4	1.19	2.02	54.64	45.76	3.27	2.84	50.50
1.6	1.16	2.03	53.93	46.32	3.26	2.85	50.40
1.8	1.14	2.03	53.48	46.88	3.25	2.87	50.40
2.0	1.12	2.04	52.94	47.21	3.25	2.88	50.20
2.5	1.09	2.05	52.08	47.91	3.23	2.91	50.10
3	1.07	2.05	51.62	48.46	3.20	2.93	50.10
4	1.04	2.06	50.93	48.98	3.17	2.96	49.90
5	1.03	2.06	50.64	49.35	3.15	2.98	49.90
10	1.00	2.07	50.06	49.89	3.10	3.02	49.80

Table 5-3: Design parameters for a microstrip coupler on a substrate with ε_r of 10. Data are derived from the analysis in Section 5.6. Z_0 is the characteristic impedance of an individual microstrip line with a normalized width, u . For $Z_{0S} = 50 \Omega$, $w/h = 0.954$, from Table 3-3.

$\varepsilon_r = 10$ (Alumina), $Z_{0S} = 50 \Omega$							
g	Z_{0e}/Z_{0o}	u	Z_{0e} (Ω)	Z_{0o} (Ω)	ε_{ee}	ε_{eo}	Z_0 (Ω)
0.1	2.72	0.65	82.26	30.25	6.95	5.59	59.40
0.2	2.18	0.75	73.90	33.82	7.06	5.64	55.90
0.3	1.91	0.81	69.06	36.10	7.13	5.69	54.00
0.4	1.74	0.84	66.19	37.96	7.17	5.73	53.10
0.5	1.62	0.87	63.66	39.29	7.20	5.77	52.20
0.6	1.53	0.89	61.79	40.42	7.22	5.81	51.70
0.7	1.46	0.90	60.45	41.47	7.23	5.85	51.40
0.8	1.40	0.91	59.25	42.32	7.23	5.88	51.10
0.9	1.35	0.92	58.17	43.01	7.24	5.92	50.90
1.0	1.31	0.93	57.19	43.57	7.24	5.95	50.60
1.2	1.25	0.94	55.78	44.59	7.23	6.01	50.30
1.4	1.21	0.94	54.90	45.55	7.21	6.06	50.30
1.6	1.17	0.94	54.19	46.30	7.19	6.11	50.30
1.8	1.14	0.95	53.34	46.66	7.17	6.16	50.10
2.0	1.12	0.95	52.87	47.14	7.14	6.20	50.10
2.5	1.09	0.95	52.05	47.97	7.08	6.29	50.10
3	1.06	0.95	51.54	48.50	7.02	6.36	50.10
4	1.04	0.95	50.97	49.08	6.92	6.46	50.10
5	1.03	0.95	50.69	49.39	6.85	6.53	50.10
10	1.03	0.95	50.26	49.94	6.73	6.62	50.10

EXAMPLE 5.7 Physical Design of a 10 dB Microstrip Coupler

Design a microstrip directional coupler with the following specifications:

Transmission line technology	Microstrip
Coupling coefficient	C = 10 dB
Microstrip characteristic impedance	Z_0 = 50 Ω
Substrate permittivity	ϵ_r = 10.0
Substrate thickness	h = 1 mm
System center frequency (midband for the coupler)	f_0 = 5 GHz

The cross-sectional dimensions that must be determined are the strip width, w , and the strip separation, s , as shown in Figure 5-18. The procedure is to first determine the coupling factor:

$$C = 10^{(C_{\text{dB}}/20)} = 10^{(10/20)} = 3.162. \quad (5.154)$$

The ratio of the even- and odd-mode impedances required to achieve the desired coupling is derived from Equation (5.153):

$$Z_{0e}/Z_{0o} = \frac{C + 1}{C - 1} = \frac{3.162 + 1}{3.162 - 1} = 1.925. \quad (5.155)$$

Solution:

The problem now is to determine the physical geometry (i.e., the line widths and spacing). The data in Table 5-3 apply here (as $\epsilon_r = 10$), enabling the normalized gap, $g = s/h$, and normalized line width, $u = w/h$, to be determined for a specified impedance ratio, Z_{0e}/Z_{0o} . The table does not contain a line for $Z_{0e}/Z_{0o} = 1.925$ and so the table must be interpolated (e.g. using linear or bilinear interpolation as described in Appendix 1.A.12). The line for $Z_{0e}/Z_{0o} = 2.15$ has $g = 0.2$, and the line for $Z_{0e}/Z_{0o} = 1.90$ has $g = 0.3$. So for $Z_{0e}/Z_{0o} = 1.925$,

$$g = \left(\frac{0.3 - 0.2}{1.9 - 2.15} \right) \cdot (1.925 - 2.15) + 0.2 = 0.290, \quad (5.156)$$

$$\text{thus } s = g \cdot h = 0.290 \text{ mm}. \quad (5.157)$$

The value of u must also be interpolated from Table 5-3 and $u = 0.805$ is obtained; thus

$$w = u \cdot h = 0.805 \text{ mm}. \quad (5.158)$$

The coupler should be one-quarter wavelength long, so the effective relative permittivity of the even and odd modes is required. From Table 5-3, the interpolated values are

$$\epsilon_{ee} = 7.124 \quad \text{and} \quad \epsilon_{eo} = 5.686. \quad (5.159)$$

These effective permittivities are different, so determination of the optimum length of the coupler is not straightforward. The only choice is to use the average of the permittivities:

$$\epsilon_{e,\text{avg}} = (\epsilon_{ee} + \epsilon_{eo})/2 = 6.405. \quad (5.160)$$

$$\text{Thus the average wavelength is } \lambda_g = \frac{c}{f\sqrt{\epsilon_{e,\text{avg}}}} = \frac{3 \cdot 10^8}{5 \cdot 10^9 \sqrt{6.405}} = 2.37 \text{ cm} \quad (5.161)$$

$$\text{and the length of the coupler is } L = \lambda_g/4 = 5.93 \text{ mm}. \quad (5.162)$$

Finally, the widths of the feed lines must be determined. The system impedance is 50 Ω and, from Table 3-3, the width, w' , is found to be 0.954 mm. The final layout of the coupler is shown in Figure 5-19. The realization of a microstrip directional coupler as a laboratory component is shown in Figure 5-20.

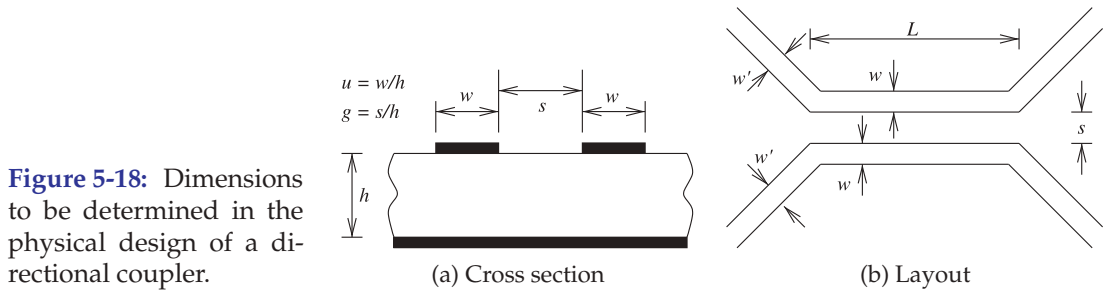


Figure 5-18: Dimensions to be determined in the physical design of a directional coupler.

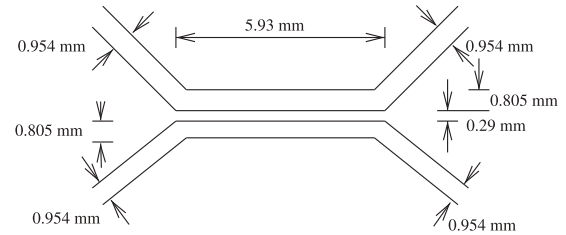
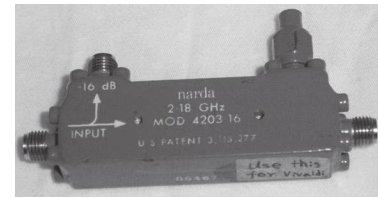


Figure 5-19: Final coupler layout for Example 5.7.

Figure 5-20: Connectorized directional couplers: (a) a microstrip directional coupler with SMA connectors connected to internal microstrip lines, the top right-hand connector has a $50\ \Omega$ termination; (b) a 250 W, 0.9–9 GHz coupler with N-type connectors on the through line and an SMA connector on the coupled port, insertion loss is less than 0.1 dB. Copyright 2012 Scientific Components Corporation d/b/a Mini-Circuits, used with permission [7].



(a)



(b)

EM analysis is often used to refine this synthesized coupler. There are two main uncertainties in the design. One is the uncertainty in the length of the coupler (due to the different even- and odd-mode effective permittivities). The other uncertainty is that the coupled-line equations come from low-frequency analysis—EM analysis will capture the frequency-dependent effects. However, only minor iteration would normally be required.

5.8.4 The Lange Coupler

A directional coupler comprised of two parallel microstrip lines cannot achieve a coupling of 3 dB, which corresponds to splitting the power of a traveling wave into two equal components. Lange [8] introduced a coupler, now known as the Lange coupler, in 1969. The Lange coupler (see Figure 5-21) has a coupling factor of around 3 dB. In this design, true quadrature coupling over an octave bandwidth is realized as a consequence of the interdigital coupling section, which also compensates for the differences of the even- and odd-mode phase velocities over the wide frequency range. Note the use of the center bond wires—this was the key invention. The bonding wires should look, electrically, as close as possible to a short-

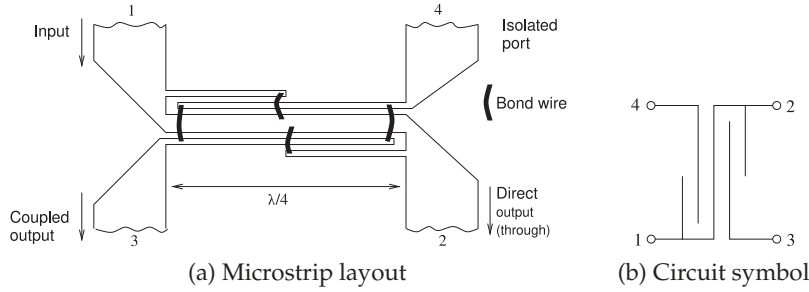


Figure 5-21: A four-finger Lange coupler.

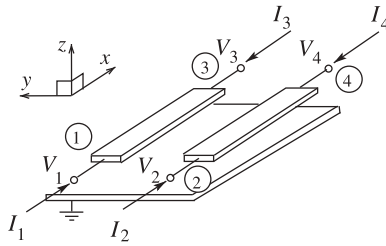


Figure 5-22: Coupled microstrip lines with total voltage and current phasors at the four terminals.

circuit. This means that their lengths, l_s , must be kept as short as possible: $l_s \ll \lambda_{gm}/4$, where λ_{gm} is the midband wavelength. In semiconductor technologies, these bond wires are replaced by air bridges, and in structures with two or more metal layers the wirebonds are replaced by vias to another metal layer and a short connection on the second metal layer. In some designs, six coupling fingers are used instead of the four shown in Figure 5-21. Note that the input-to-direct-output link meanders through the structure and this DC connection identifies the through connection.

The physical length of the coupler is approximately one-quarter wavelength long at the center frequency of the coupling band. As with many distributed components, this element was invented using intuition and empirical iterations. Since then, analytic design formulas have been developed to enable synthesis of the electrical parameters of the coupler (see [5]). The synthesis is based on even- and odd-mode impedances analogous to those developed in Section 5.8 for a coupler comprised of coupled microstrip lines. Synthesis leads to a design that is close to ideal, and subsequent modeling in an EM simulator can be used to obtain an optimized design accounting for frequency-dependent and parasitic effects.

5.9 Models of Parallel Coupled Lines

5.9.1 Chain Matrix Model of Coupled Lines

The chain matrix of a pair of coupled lines is the multiport version of the two-port $ABCD$ parameters and relates the input currents and voltages at one end of a pair of coupled lines to the voltages and currents at the other end. The chain matrix is derived here following the development in [9]. The terminal characteristics of the coupled lines shown in Figure 5-22 can be expressed in terms of the even and odd modes. For the even mode

$$\begin{bmatrix} \frac{1}{2}(V_1 + V_2) \\ \frac{1}{2}(I_1 + I_2) \end{bmatrix} = \begin{bmatrix} \cos \theta_e & jX_{0e} \sin \theta_e \\ jY_{0e} \sin \theta_e & \cos \theta_e \end{bmatrix} \begin{bmatrix} \frac{1}{2}(V_3 + V_4) \\ \frac{1}{2}(I_3 + I_4) \end{bmatrix} \quad (5.163)$$

and for the odd mode

$$\begin{bmatrix} \frac{1}{2}(V_1 - V_2) \\ \frac{1}{2}(I_1 - I_2) \end{bmatrix} = \begin{bmatrix} \cos \theta_o & jX_{0o} \sin \theta_o \\ jY_{0o} \sin \theta_o & \cos \theta_o \end{bmatrix} \begin{bmatrix} \frac{1}{2}(V_3 - V_4) \\ -\frac{1}{2}(I_3 - I_4) \end{bmatrix}, \quad (5.164)$$

where $Y_{0e} = 1/Z_{0e}$ is the even-mode characteristic admittance and $Y_{0o} = 1/Z_{0o}$ is the characteristic admittance of the odd mode. Also, θ_e is the electrical length of the lines for the even mode, and θ_o is the odd-mode electrical length of the lines. Grouping Equations (5.163) and (5.164),

$$\begin{bmatrix} V_1 \\ V_2 \\ I_1 \\ I_2 \end{bmatrix} = \begin{bmatrix} a_{11} & a_{12} & b_{11} & b_{12} \\ a_{21} & a_{22} & b_{21} & b_{22} \\ c_{11} & c_{12} & d_{11} & d_{12} \\ c_{21} & c_{22} & d_{21} & d_{22} \end{bmatrix} \begin{bmatrix} V_3 \\ V_4 \\ -I_3 \\ -I_4 \end{bmatrix}, \quad (5.165)$$

$$\text{where } a_{11} = a_{22} = d_{11} = d_{22} = \frac{1}{2}(\cos \theta_e + \cos \theta_o) \quad (5.166)$$

$$a_{12} = a_{21} = d_{12} = d_{21} = \frac{1}{2}(\cos \theta_e - \cos \theta_o) \quad (5.167)$$

$$b_{11} = b_{22} = j\frac{1}{2}(Z_{0e} \sin \theta_e + Z_{0o} \sin \theta_o) \quad (5.168)$$

$$b_{12} = b_{21} = j\frac{1}{2}(Z_{0e} \sin \theta_e - Z_{0o} \sin \theta_o) \quad (5.169)$$

$$c_{11} = c_{22} = j\frac{1}{2}(Y_{0e} \sin \theta_e + Y_{0o} \sin \theta_o) \quad (5.170)$$

$$c_{12} = c_{21} = j\frac{1}{2}(Y_{0e} \sin \theta_e - Y_{0o} \sin \theta_o). \quad (5.171)$$

Similarly the admittance equation for a pair of coupled lines is derived as

$$\begin{bmatrix} V_1 \\ V_2 \\ V_3 \\ V_4 \end{bmatrix} = \begin{bmatrix} y_{11} & y_{12} & y_{13} & y_{14} \\ y_{21} & y_{22} & y_{23} & y_{24} \\ y_{31} & y_{32} & y_{33} & y_{34} \\ y_{41} & y_{42} & y_{43} & y_{44} \end{bmatrix} \begin{bmatrix} I_1 \\ I_2 \\ I_3 \\ I_4 \end{bmatrix}, \quad (5.172)$$

$$\text{where } y_{11} = y_{22} = y_{33} = y_{44} = -j\frac{1}{2}(Y_{0e} \cot \theta_e + Y_{0o} \cot \theta_o) \quad (5.173)$$

$$y_{12} = y_{21} = y_{34} = y_{43} = -j\frac{1}{2}(Y_{0e} \cot \theta_e - Y_{0o} \cot \theta_o) \quad (5.174)$$

$$y_{13} = y_{31} = y_{24} = y_{42} = j\frac{1}{2}(Y_{0e} \csc \theta_e + Y_{0o} \csc \theta_o) \quad (5.175)$$

$$y_{14} = y_{41} = y_{23} = y_{32} = j\frac{1}{2}(Y_{0e} \csc \theta_e - Y_{0o} \csc \theta_o). \quad (5.176)$$

5.9.2 ABCD Parameters of Coupled-Line Sections

The chain matrix of a pair of coupled lines, Equation (5.165), can be used to develop the $ABCD$ parameters of two-port coupled line networks [9]. Several networks that are commonly used in realizing filters and other microwave circuits are shown in Table 5-4 with

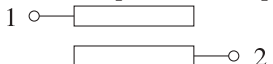
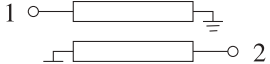
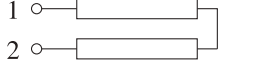
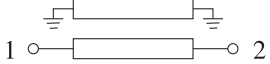
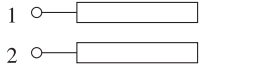
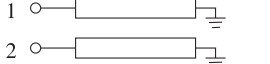
$$\begin{bmatrix} V_1 \\ I_1 \end{bmatrix} = \begin{bmatrix} A & B \\ C & D \end{bmatrix} \begin{bmatrix} V_2 \\ -I_2 \end{bmatrix}. \quad (5.177)$$

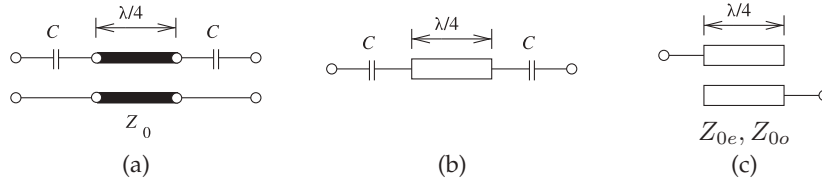
One approach to developing the physical layout of microwave circuits from the electrical design equates the $ABCD$ parameters of the coupled-line networks to the $ABCD$ of the synthesized lumped-element circuit.

5.9.3 Synthesis of Specific Coupled-Line Connections

The equivalence of $ABCD$ parameters can be used in microwave network synthesis to transform uncoupled transmission line structures into a

Table 5-4: $ABCD$ parameters of coupled-line sections. Usage described in [10–13].

<p>(a) Open-circuited interdigital coupled-line section (bandpass/bandstop networks)</p>  $A = D = (Z_{0e} \cot \theta_e + Z_{0o} \cot \theta_o) / \Delta$ $B = \frac{j}{2\Delta} [Z_{0e}^2 + Z_{0o}^2 - 2Z_{0e}Z_{0o} (\cot \theta_e \cot \theta_o + \csc \theta_e \csc \theta_o)]$ $C = 2j/\Delta$ $\Delta = Z_{0e} \csc \theta_e - Z_{0o} \csc \theta_o \quad (5.178)$	<p>(b) Short-circuited interdigital coupled-line section (bandpass/bandstop networks)</p>  $A = D = (Y_{0e} \cot \theta_e + Y_{0o} \cot \theta_o) / \Delta$ $B = 2j/\Delta$ $C = \frac{j}{2\Delta} [Y_{0e}^2 + Y_{0o}^2 - 2Y_{0e}Y_{0o} (\cot \theta_e \cot \theta_o + \csc \theta_e \csc \theta_o)]$ $\Delta = Y_{0e} \csc \theta_e - Y_{0o} \csc \theta_o \quad (5.179)$
<p>(c) Meander coupled-line section (lowpass networks)</p>  $A = D = (Z_{0e} \cot \theta_e - Z_{0o} \cot \theta_o) / \Delta$ $B = 2j2Z_{0e}Z_{0o} \cot \theta_e \tan \theta_o / \Delta$ $C = 2j/\Delta$ $\Delta = Z_{0e} \cot \theta_e + Z_{0o} \tan \theta_o \quad (5.180)$	<p>(d) Shorted symmetric coupled-line section (lowpass networks)</p>  $A = D = (Y_{0e} \cot \theta_e + Y_{0o} \cot \theta_o) / \Delta$ $B = 2j/\Delta$ $C = [j/(2\Delta)] [Y_{0e}^2 + Y_{0o}^2 + 2Y_{0e}Y_{0o} (\csc \theta_e \csc \theta_o - \cot \theta_e \cot \theta_o)]$ $\Delta = Y_{0e} \csc \theta_e + Y_{0o} \csc \theta_o \quad (5.181)$
<p>(e) Open-circuited combline coupled-line section (bandpass/bandstop networks)</p>  $A = D = (Z_{0e} \cot \theta_e + Z_{0o} \cot \theta_o) / \Delta$ $B = -j2Z_{0e}Z_{0o} \cot \theta_e \cot \theta_o / \Delta$ $C = 2j/\Delta$ $\Delta = Z_{0e} \cot \theta_e - Z_{0o} \cot \theta_o \quad (5.182)$	<p>(f) Short-circuited combline coupled-line section (bandpass/bandstop networks)</p>  $A = D = (Y_{0o} \cot \theta_o + Y_{0e} \cot \theta_e) / \Delta$ $B = 2j/\Delta$ $C = -j2Y_{0e}Y_{0o} \cot \theta_e \cot \theta_o / \Delta$ $\Delta = Y_{0o} \cot \theta_o - Y_{0e} \cot \theta_e \quad (5.183)$

**Figure 5-23:** Coupled line equivalence: (a) a one-quarter wavelength long line with input and output series capacitance; (b) microstrip layout; and (c) equivalent coupled lines laid out in microstrip. The network in (a) is equivalent to the network in (c) if $Z_{0e} = (1/C + 2Z_0)$ and $Z_{0o} = Z_0$.

coupled-line section. As an example, consider the capacitively coupled one-quarter wavelength long line shown in both Figures 5-23(a) and 5-23(b). This configuration often occurs in filter design and an equivalent structure using coupled lines and not requiring discrete capacitors is shown in Figure 5-23(c). The equivalence is developed by equating the $ABCD$ parameters of the two

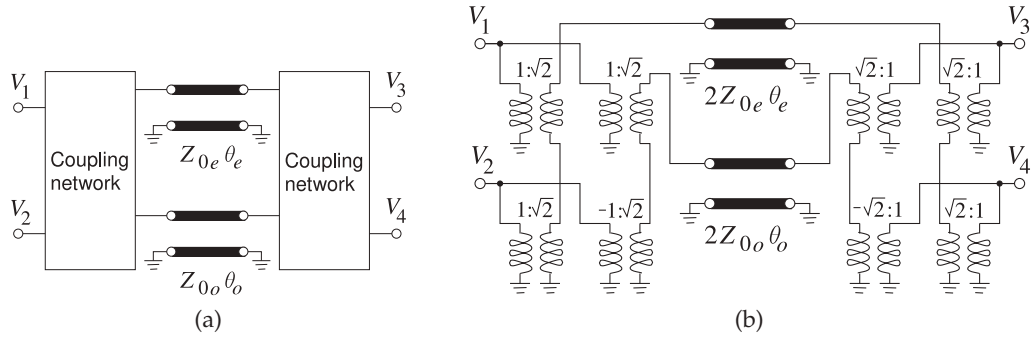


Figure 5-24: Models of a pair of coupled lines using even- and odd-mode lines: (a) with coupling network; and (b) with transformer-based coupling.

structures. The $ABCD$ matrix of the coupled-line network of Figure 5-23(c) is given in Table 5-4(a):

$$A = \frac{Z_{0e} \cot \theta_e + Z_{0o} \cot \theta_o}{Z_{0e} \csc \theta_e - Z_{0o} \csc \theta_o} = D \quad C = \frac{2j}{Z_{0e} \csc \theta_e - Z_{0o} \csc \theta_o}$$

$$B = \frac{j}{2} \frac{Z_{0e}^2 + Z_{0o}^2 - 2Z_{0e}Z_{0o}(\cot \theta_e \cot \theta_o + \csc \theta_e \csc \theta_o)}{Z_{0e} \csc \theta_e - Z_{0o} \csc \theta_o}, \quad (5.184)$$

where Z_{0e} and Z_{0o} are the modal impedances, and θ_e and θ_o are the even- and odd-mode electrical lengths.

Developing the $ABCD$ parameters of the capacitively loaded one-quarter wavelength long line in Figure 5-23(a) and equating them with the $ABCD$ parameters in Equation (5.184) leads to an equivalence between the loaded line (Figure 5-23(b)) and the coupled line shown in Figure 5-23(c), where

$$Z_{0e} = (1/C + 2Z_0) \quad \text{and} \quad Z_{0o} = Z_0. \quad (5.185)$$

5.9.4 Model Using Even- and Odd-Mode Lines

The pair of coupled lines in Figure 5-22 can be modeled using even- and odd- mode transmission lines as shown in Figure 5-24(a). While the partitioning of the terminal voltages and currents of the coupled lines into even- and odd-mode components is simple to describe mathematically (e.g., the odd-mode voltage $V_o = \frac{1}{2}(V_1 - V_2)$), there is not a simple way to represent the partitioning in circuit form. Instead, in a circuit simulator the coupling network in Figure 5-24(a) is modeled using voltage-controlled current sources [14]. A circuit model that is more convenient to use in the analysis of a coupled line networks is shown in Figure 5-24(b). The equivalence of this network to a coupled line is demonstrated by showing that the chain matrix parameters of the circuit in Figure 5-24(b) are the same as those in Equations (5.165)–(5.171), see Example 5.8.

Coupled lines are an important element in many microwave circuits, including filters, matching networks, and biasing networks. Very often the circuit development leads to a particular topology that can be implemented using coupled-line networks. For example, the structure at the top in Figure 5-25(a) is known as an open-circuited interdigital section. The equivalent

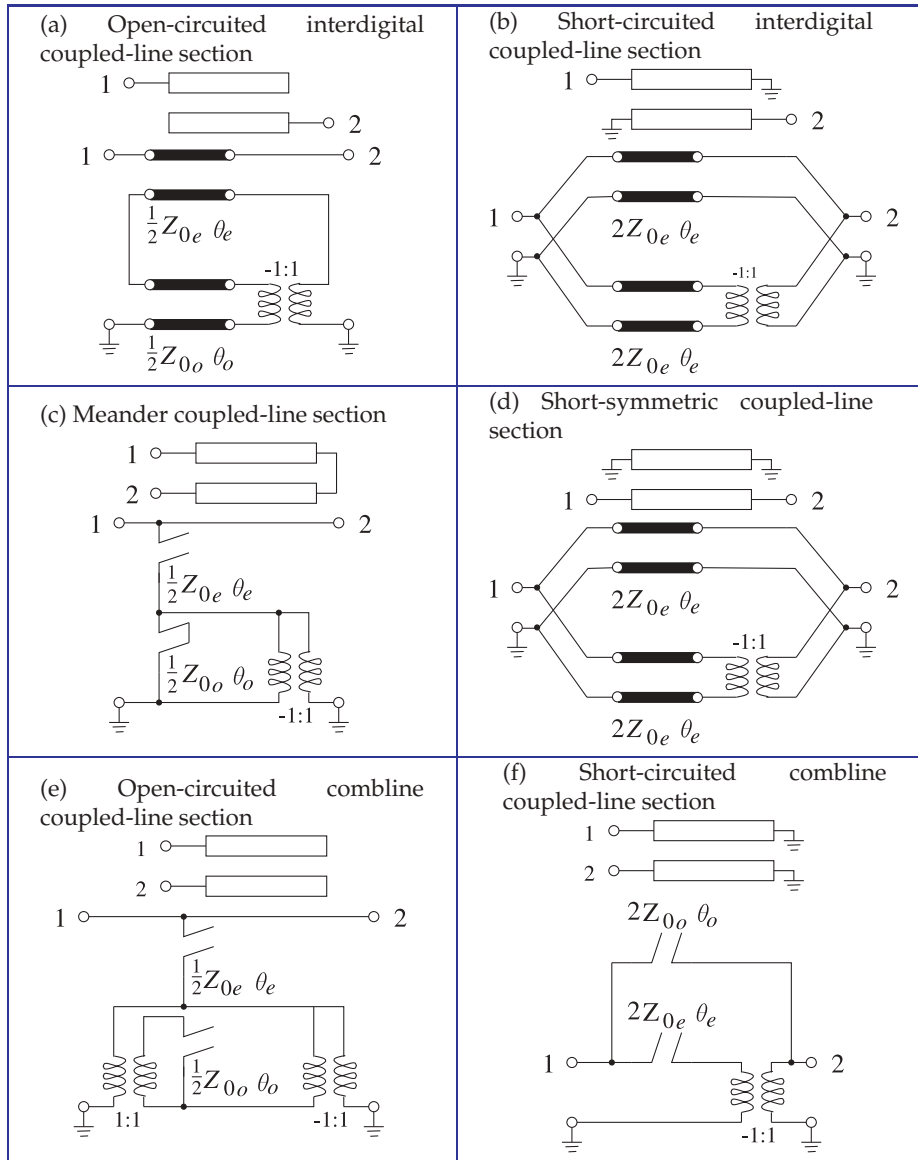


Figure 5-25: Coupled-line sections with models comprising individual transmission lines corresponding to the even- and odd-modes.

circuit of this network, shown at the bottom in Figure 5-25(a), is derived from the coupled-line equivalent circuit shown in Figure 5-24(b).

EXAMPLE 5.8**Chain Matrix Parameters of Coupled Lines**

Develop the chain matrix of the coupled-line model shown in Figure 5-24(b) and show that these are the chain matrix parameters of a coupled line.

Solution:

The coupled-line model is annotated with voltages and currents in Figure 5-26. Using Table 2-1 of [15], the even- and odd-mode lines have the following $ABCD$ parameters:

$$\begin{bmatrix} V_W \\ I_W \end{bmatrix} = \begin{bmatrix} \cos \theta_e & j2Z_e \sin \theta_e \\ j\frac{1}{2}Y_e \sin \theta_e & \cos \theta_e \end{bmatrix} \begin{bmatrix} V_Y \\ I_Y \end{bmatrix} \quad (5.186)$$

$$\text{and } \begin{bmatrix} V_X \\ I_X \end{bmatrix} = \begin{bmatrix} \cos \theta_o & j2Z_o \sin \theta_o \\ j\frac{1}{2}Y_o \sin \theta_o & \cos \theta_o \end{bmatrix} \begin{bmatrix} V_Z \\ I_Z \end{bmatrix}. \quad (5.187)$$

While the $ABCD$ parameters of the transformers could be used, it is more convenient to write down the terminal characteristics of the transformers directly. First, the transformers on the right-hand side are described by

$$\begin{aligned} V_Y &= \frac{1}{\sqrt{2}}(V_3 + V_4), & I_Y &= \frac{1}{2\sqrt{2}}[(-I_3) + (-I_4)] \\ V_Z &= \frac{1}{\sqrt{2}}(V_3 - V_4), & I_Z &= \frac{1}{2\sqrt{2}}[(-I_3) - (-I_4)]. \end{aligned} \quad (5.188)$$

Combining Equations (5.186)–(5.188) yields

$$\begin{bmatrix} V_W \\ V_X \\ I_W \\ I_X \end{bmatrix} = \begin{bmatrix} \sqrt{2} \cos \theta_e & \sqrt{2} \cos \theta_o & j\sqrt{2}Z_{0e} \sin \theta_e & j\sqrt{2}Z_{0e} \sin \theta_e \\ \sqrt{2} \cos \theta_o & -\sqrt{2} \cos \theta_e & j\sqrt{2}Z_{0o} \sin \theta_o & -j\sqrt{2}Z_{0o} \sin \theta_o \\ j\frac{1}{2\sqrt{2}}Y_{0e} \sin \theta_e & j\frac{1}{2\sqrt{2}}Y_{0e} \sin \theta_e & \frac{1}{2\sqrt{2}} \cos \theta_e & \frac{1}{2\sqrt{2}} \cos \theta_e \\ j\frac{1}{2\sqrt{2}}Y_{0o} \sin \theta_o & -j\frac{1}{2\sqrt{2}}Y_{0o} \sin \theta_o & -\frac{1}{2\sqrt{2}} \cos \theta_o & -\frac{1}{2\sqrt{2}} \cos \theta_o \end{bmatrix} \begin{bmatrix} V_3 \\ V_4 \\ -I_3 \\ -I_4 \end{bmatrix}. \quad (5.189)$$

The development is completed by using the voltage and current relations determined by the transformers on the left-hand side:

$$\begin{aligned} V_1 &= \frac{1}{2\sqrt{2}}(V_W + V_X), & I_1 &= \sqrt{2}(I_W + I_X) \\ V_2 &= \frac{1}{2\sqrt{2}}(V_W - V_X), & I_2 &= \sqrt{2}(I_W - I_X). \end{aligned} \quad (5.190)$$

Combining Equations (5.189) and (5.190):

$$\begin{bmatrix} V_1 \\ V_2 \\ I_1 \\ I_2 \end{bmatrix} = \begin{bmatrix} a'_{11} & a'_{12} & b'_{11} & b'_{12} \\ a'_{21} & a'_{22} & b'_{21} & b'_{22} \\ c'_{11} & c'_{12} & d'_{11} & d'_{12} \\ c'_{21} & c'_{22} & d'_{21} & d'_{22} \end{bmatrix} \begin{bmatrix} V_3 \\ V_4 \\ -I_3 \\ -I_4 \end{bmatrix}, \quad (5.191)$$

where

$$\begin{aligned} a'_{11} &= a'_{22} = d'_{11} = d'_{22} = \frac{1}{2}(\cos \theta_e + \cos \theta_o) & a'_{12} &= a'_{21} = d'_{12} = d'_{21} = \frac{1}{2}(\cos \theta_e - \cos \theta_o) \\ b'_{11} &= b'_{22} = j\frac{1}{2}(Z_{0e} \sin \theta_e + Z_{0o} \sin \theta_o) & b'_{12} &= b'_{21} = j\frac{1}{2}(Z_{0e} \sin \theta_e - Z_{0o} \sin \theta_o) \\ c'_{11} &= c'_{22} = j\frac{1}{2}(Y_{0e} \sin \theta_e + Y_{0o} \sin \theta_o) & c'_{12} &= c'_{21} = j\frac{1}{2}(Y_{0e} \sin \theta_e - Y_{0o} \sin \theta_o), \end{aligned}$$

which is identical to the chain matrix of the coupled transmission line, Equation (5.165). Thus Figure 5-24(b) is an accurate circuit model of a pair of coupled transmission lines.

5.9.5 Alternative Coupled-Line Model

The previous section developed a model of a pair of coupled lines and it was shown how the model related to various coupled-line sections. While $ABCD$ parameters can be used to equate two different implementations, it is useful to have a topology that can be visualized and used to guide synthesis.

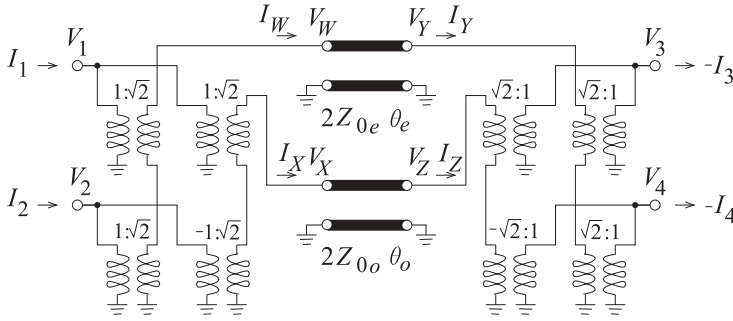


Figure 5-26: Annotated coupled-line model used in Example 5.4.

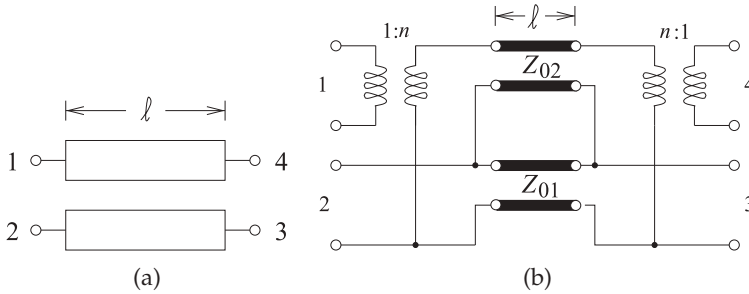


Figure 5-27: A pair of symmetrical coupled lines: (a) physical layout; and (b) its approximate equivalent circuit model in a form that appears in network synthesis. $n = (Z_{0e} + Z_{0o}) / (Z_{0e} - Z_{0o})$.

The accurate form of the coupled-line model developed in the previous section does not often occur in network synthesis. (In synthesis, such as when designing a filter using coupled lines, a mathematical description can sometimes be converted into circuit form which includes transmission lines that are coupled.) An alternative but approximate model that has the same topology as many synthesized networks is shown in Figure 5-27(b).

A physical pair of coupled lines is shown in Figure 5-27(a) with even-mode characteristic impedance, Z_{0e} , and odd-mode impedance, Z_{0o} , with the coupling coefficient⁶

$$K = \frac{Z_{0e} - Z_{0o}}{Z_{0e} + Z_{0o}}. \quad (5.192)$$

The corresponding approximate equivalent network model of the coupled line in Figure 5-27(a) was developed by Malherbe [16] and is shown in Figure 5-27(b) with

$$Z_{01} = \frac{Z_{0S}}{\sqrt{1 - K^2}} \quad (5.193) \quad Z_{02} = Z_{0S} \frac{\sqrt{1 - K^2}}{K^2} \quad (5.194)$$

$$n = \frac{1}{K} = \frac{Z_{0e} + Z_{0o}}{Z_{0e} - Z_{0o}} \quad (5.195) \quad Z_{0S} = \sqrt{Z_{0e} Z_{0o}}. \quad (5.196)$$

The electrical length of the Z_{01} and Z_{02} lines is the electrical length of the coupled line. The reason this model is approximate is it assumes that the coupled lines are symmetrical (e.g., equal width for the microstrip lines) and uses a low-frequency capacitor-based development. Also a pair of coupled lines has two electrical lengths, the electrical length of the even mode and

⁶ This is the inverse of the coupling factor, C used previously, see Equation (5.145). However using C introduces confusion since $ABCD$ parameters are often used in synthesis of coupled line networks. Note that here $K = 1/(\text{coupling factor})$, that is, $K = 1/C$.

the electrical length of the odd mode. So the best that can be done is to take the electrical lengths of the Z_{01} and Z_{02} lines as the average electrical lengths of the even and odd modes. Never-the-less this model is commonly used in developing the initial design of coupled-line networks that must then be followed by adjustment in a microwave circuit simulator.

5.9.6 Approximate Synthesis from the Coupled-Line Model

The electrical design of networks of coupled lines commonly leads to the parameters of the coupled-line model shown in Figure 5-27(b). From these the physical layout can be derived. That is, given $n = 1/K$, Z_{01} , and Z_{02} , the coupled-line parameters Z_{0S} , Z_{0e} , and Z_{0o} are found. Equations (5.193) and (5.194) lead to two equations for Z_{0S} :

$$Z_{0S,(5.197)} = Z_{01} \sqrt{1 - K^2} \quad (5.197)$$

$$Z_{0S,(5.198)} = Z_{02} \frac{K^2}{\sqrt{1 - K^2}}. \quad (5.198)$$

These could be different and this is a result of the model being approximate. If so, then the proper course forward is to use the geometric mean:

$$Z_{0S} = \sqrt{Z_{0S,(5.197)} Z_{0S,(5.198)}}. \quad (5.199)$$

Rearranging Equation (5.195),

$$\begin{aligned} 1 + n &= 1 + \frac{Z_{0e} + Z_{0o}}{Z_{0e} - Z_{0o}} = \frac{Z_{0e} - Z_{0o} + Z_{0e} + Z_{0o}}{Z_{0e} - Z_{0o}} = \frac{2Z_{0e}}{Z_{0e} - Z_{0o}} \\ 1 - \frac{2}{n+1} &= \frac{n-1}{n+1} = 1 - \frac{Z_{0e} - Z_{0o}}{Z_{0e}} = \frac{Z_{0o} - Z_{0e} + Z_{0e}}{Z_{0e}} = \frac{Z_{0o}}{Z_{0e}}. \end{aligned} \quad (5.200)$$

That is,

$$\frac{Z_{0e}}{Z_{0o}} = \frac{n+1}{n-1}. \quad (5.201)$$

Combining this with Equation (5.196),

$$Z_{0o} = Z_{0S} \sqrt{\frac{n-1}{n+1}} \quad \text{and} \quad Z_{0e} = \frac{Z_{0S}^2}{Z_{0o}}. \quad (5.202)$$

These equations can be used in physical synthesis. For example, if Z_{0S} is close to 50Ω and the substrate is alumina, then the ratio Z_{0e}/Z_{0o} can be used to find the physical dimensions from Table 5-3. Otherwise the formulas described in Section 5.6 can be used iteratively.

The physical length of the coupled line is determined by using the geometric mean of the even- and odd-mode effective permittivities to convert from the electrical length (in degrees or wavelengths). This initial design is followed by adjustment in a microwave circuit simulator.

5.10 Differential and Common Modes

In working with RFICs it is convenient to use differential and common mode definitions, rather than odd and even mode definitions, as these directly relate to the differential circuits most commonly used in CMOS design. There are several reasons for this and one is that the most common type of amplifier with CMOS circuits is a differential amplifier where there are two input signal lines and two output signal lines and the actual signal is the differential signal which, in terms of voltage, is the difference of the two voltages on the lines. The situation is as shown in Figure 5-28(a) where there are two signal conductors and a ground plane (at 0 V). Here the differential voltage is $V_d = (V_1 - V_2)$. The common mode voltage is $V_c = \frac{1}{2}(V_1 + V_2)$ which will normally consist of a DC voltage and a usually small, and ideally zero, common mode signal which is the non-DC part of V_c . Most CMOS circuits are designed so that the DC component of $V_d = 0$. It is a quirk of history that microwave engineering and thus EM analysis used even- and odd-mode signals whose definitions differ by a factor of two from the definitions of common- and differential-mode signals. This section relates the two groups of signals and parameters for the common/differential mode group and the even/odd mode group.

The differential- and common-mode parameters of coupled lines can be derived from the odd- and even-mode parameters. The difference is in the definition of the voltage and currents in the modes as shown in Figure 5-28. The even mode is defined with $V_1 = V_2 = V_e$ and $I_1 = I_2 = I_e$, while for the common mode $V_1 = V_2 = V_c$ and $I_1 + I_2 = I_c$. Thus, in terms of the even-mode characteristic impedance, Z_{0e} , the common-mode characteristic impedance is

$$Z_{0c} = \frac{1}{2}Z_{0e}. \quad (5.203)$$

The odd mode is defined with $V_1 = -V_2 = V_o$ and $I_1 = -I_2 = I_o$, while for the differential mode $V_1 - V_2 = V_d$ and $I_1 = -I_2 = I_d$. Thus, in terms of the odd-mode characteristic impedance, Z_{0o} , the differential-mode characteristic impedance is

$$Z_{0d} = 2Z_{0o}. \quad (5.204)$$

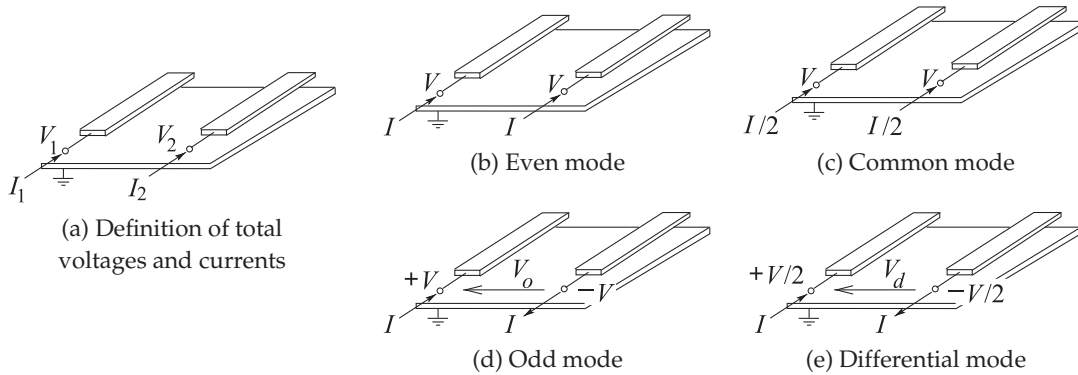
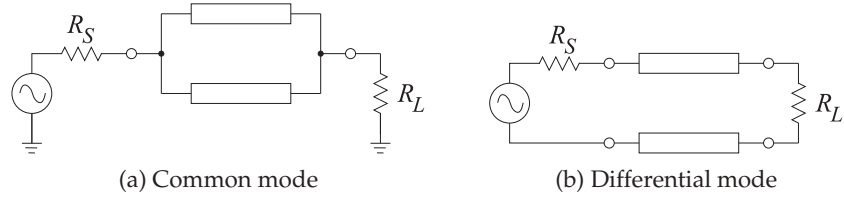


Figure 5-28: Definition of coupled-line modes.

Figure 5-29:
Driving
configurations.



Other parameters remain unchanged. That is, the propagation constant, phase and group velocities, and wavelengths are the same for common and even modes, as they are for the differential and odd modes.

The driving and termination configurations for differential and common mode signals are shown in Figure 5-29. The reflectionless (i.e. matched) termination of coupled lines used in common mode is

$$R_L = Z_{0c} = \frac{1}{2}Z_{0e}, \quad (5.205)$$

as in Figure 5-29(a). The reflectionless termination of a differential line is

$$R_L = Z_{0d} = 2Z_{0o}, \quad (5.206)$$

as shown in Figure 5-29(b).

EXAMPLE 5.9

Common and Differential Mode Reflections at the End of Coupled Lines

A pair of coupled lines with common- and differential-mode characteristic impedances Z_{0c} and Z_{0d} respectively is loaded as shown in Figure 5-14(a) where the load has the two-port y -parameter matrix, \mathbf{Y} . Find the common and differential-mode reflections. This example parallels Example 5.3 where even and odd modes were considered.

Solution:

The analysis begins by writing out the expressions relating the traveling-wave and total voltages and currents at the termination.

$$\begin{aligned} V_c &= \frac{1}{2}(V_1 + V_2) & V_d &= (V_1 - V_2) & I_c &= (I_1 + I_2) & I_d &= \frac{1}{2}(I_1 - I_2) \\ V_1 &= (V_1^+ + V_1^-) & V_2 &= (V_2^+ + V_2^-) & I_1 &= (I_1^+ + I_1^-) & I_2 &= (I_2^+ + I_2^-) \\ V_1^+ &= (V_c^+ + \frac{1}{2}V_d^+) & V_2^+ &= (V_c^+ - \frac{1}{2}V_d^+) & I_1^+ &= (\frac{1}{2}I_c^+ + I_d^+) & I_2^+ &= (\frac{1}{2}I_c^+ - I_d^+) \\ V_1^- &= (V_c^- + \frac{1}{2}V_d^-) & V_2^- &= (V_c^- - \frac{1}{2}V_d^-) & I_1^- &= (\frac{1}{2}I_c^- + I_d^-) & I_2^- &= (\frac{1}{2}I_c^- - I_d^-) \\ I_c^+ &= V_c^+/Z_{0c} & I_c^- &= -V_c^-/Z_{0c} & I_d^+ &= V_d^+/Z_{0d} & I_d^- &= -V_d^-/Z_{0d} \end{aligned}$$

At the termination

$$\begin{aligned} \begin{bmatrix} I_1 \\ I_2 \end{bmatrix} &= \begin{bmatrix} \frac{1}{2}I_c^+ + I_d^+ + \frac{1}{2}I_c^- + I_d^- \\ \frac{1}{2}I_c^+ - I_d^+ + \frac{1}{2}I_c^- - I_d^- \end{bmatrix} = \mathbf{Y} \begin{bmatrix} V_1 \\ V_2 \end{bmatrix} = \begin{bmatrix} y_{11} & y_{12} \\ y_{21} & y_{22} \end{bmatrix} \begin{bmatrix} V_1 \\ V_2 \end{bmatrix} \\ \begin{bmatrix} \frac{1}{2}(V_c^+ - V_c^-)/Z_{0c} + (V_d^+ - V_d^-)/Z_{0d} \\ \frac{1}{2}(V_c^+ - V_c^-)/Z_{0c} - (V_d^+ - V_d^-)/Z_{0d} \end{bmatrix} &= \begin{bmatrix} y_{11} & y_{12} \\ y_{21} & y_{22} \end{bmatrix} \begin{bmatrix} V_c^+ + \frac{1}{2}V_d^+ + V_c^- + \frac{1}{2}V_d^- \\ V_c^+ - \frac{1}{2}V_d^+ + V_c^- - \frac{1}{2}V_d^- \end{bmatrix} \end{aligned} \quad (5.207)$$

The reflected even and odd modes have contributions from incident common and differential modes:

$$V_c^- = \Gamma_{Lc}V_c^+ + C_{cd}V_d^+ \quad \text{and} \quad V_d^- = \Gamma_{Ld}V_d^+ + C_{dc}V_c^+ \quad (5.208)$$

where Γ_{ce} and Γ_{Ld} are common- and differential-mode reflection coefficients, C_{dc} and C_{cd} describe coupling, and

$$\Gamma_{Lc} = \left. \frac{V_c^-}{V_c^+} \right|_{V_d^+=0}, \quad \Gamma_{Ld} = \left. \frac{V_d^-}{V_d^+} \right|_{V_c^+=0}, \quad C_{cd} = \left. \frac{V_c^-}{V_d^+} \right|_{V_c^+=0} \quad \text{and} \quad C_{dc} = \left. \frac{V_d^-}{V_c^+} \right|_{V_d^+=0}. \quad (5.209)$$

Γ_{Lc} and C_{ed} are obtained by expanding Equation (5.207) with $V_d^+ = 0$

$$\begin{aligned} (V_c^+ - V_c^-)/Z_{0c} - 2V_d^-/Z_{0d} &= y_{11}(2V_c^+ + 2V_c^- + V_d^-) + y_{12}(2V_c^+ + 2V_c^- - V_d^-) \\ \text{i.e. } \frac{V_c^-}{Z_{0c}}(1 + 2y_{11}Z_{0c} + 2y_{12}Z_{0c}) &= \frac{V_c^+}{Z_{0c}}(1 - 2y_{11}Z_{0c} - 2y_{12}Z_{0c}) - \frac{V_d^-}{Z_{0d}}(2 + y_{11}Z_{0d} - y_{12}Z_{0d}) \end{aligned} \quad (5.210)$$

$$\begin{aligned} (V_c^+ - V_c^-)/Z_{0c} + 2V_d^-/Z_{0d} &= y_{21}(2V_c^+ + 2V_c^- + V_d^-) + y_{22}(2V_c^+ + 2V_c^- - V_d^-) \\ \text{i.e. } \frac{V_d^-}{Z_{0d}}(-2 + y_{21}Z_{0d} - y_{22}Z_{0d}) &= \frac{V_c^+}{Z_{0c}}(1 - 2y_{21}Z_{0c} - 2y_{22}Z_{0c}) + \frac{V_c^-}{Z_{0c}}(-1 - 2y_{21}Z_{0c} - 2y_{22}Z_{0c}) \end{aligned} \quad (5.211)$$

Γ_{Lc} is obtained by eliminating V_d^- by multiplying Equation (5.211) by $(2 + y_{11}Z_{0d} - y_{12}Z_{0d})$ and subtracting it from Equation (5.210) multiplied by $(-2 + y_{21}Z_{0d} - y_{22}Z_{0d})$:

$$V_c^- \frac{a}{Z_{0d}} = V_c^+ \frac{b}{Z_{0c}} \Big|_{V_d^+=0}. \quad \text{Thus } \Gamma_{Le} = \frac{b}{a} \quad (5.212)$$

where

$$\begin{aligned} a &= (1 + 2y_{11}Z_{0c} + 2y_{12}Z_{0c})(-2 + y_{21}Z_{0d} - y_{22}Z_{0d}) - (1 + 2y_{21}Z_{0c} + 2y_{22}Z_{0c})(2 + y_{11}Z_{0d} - y_{12}Z_{0d}) \\ &= -2 - Z_{0d}Y_{\Delta} - 4Z_{0c}Y_{\Sigma} - 4Z_{0c}Z_{0d}Y_D \end{aligned} \quad (5.213)$$

$$\begin{aligned} b &= (1 - 2y_{11}Z_{0c} - 2y_{12}Z_{0c})(-2 + y_{21}Z_{0d} - y_{22}Z_{0d}) - (1 - 2y_{21}Z_{0c} - 2y_{22}Z_{0c})(2 + y_{11}Z_{0d} - y_{12}Z_{0d}) \\ &= -4 - Z_{0d}Y_{\Delta} + 4Z_{0c}Y_{\Sigma} + 4Z_{0c}Z_{0d}Y_D \end{aligned} \quad (5.214)$$

$$Y_{\Sigma} = (y_{11} + y_{12} + y_{21} + y_{22}), Y_{\Delta} = (y_{11} - y_{12} - y_{21} + y_{22}), \text{ and } Y_D = (y_{11}y_{22} - y_{12}y_{21}) \quad (5.215)$$

$$\Gamma_{Lc} = \frac{b}{a} = \frac{4 + Z_{0d}Y_{\Delta} - 4Z_{0c}Y_{\Sigma} - 4Z_{0c}Z_{0d}Y_D}{4 + Z_{0d}Y_{\Delta} + 4Z_{0c}Y_{\Sigma} + 4Z_{0c}Z_{0d}Y_D} \quad (5.216)$$

Compare this to the even-mode reflection coefficient, Γ_{Le} , found in Example 5.3. Substituting $Z_{0d} = 2Z_{0o}$ and $Z_{0c} = \frac{1}{2}Z_{0e}$ in Equation (5.216)

$$\Gamma_{Lc} = \frac{4 + 2Z_{0o}Y_{\Delta} - 2Z_{0e}Y_{\Sigma} - 4Z_{0c}Z_{0d}Y_D}{4 + 2Z_{0o}Y_{\Delta} + 4Z_{0c}Y_{\Sigma} + 4Z_{0c}Z_{0d}Y_D} = \Gamma_{Le}. \quad (5.217)$$

Find C_{cd} by expanding Equation (5.207) with $V_c^+ = 0$:

$$\begin{aligned} -V_c^-/Z_{0c} + (2V_d^+ - 2V_d^-)/Z_{0d} &= y_{11}(V_d^+ + 2V_c^- + V_d^-) + y_{12}(-V_d^+ + 2V_c^- - V_d^-) \\ \text{i.e. } \frac{V_c^-}{Z_{0c}}(1 + 2y_{11}Z_{0c} + 2y_{12}Z_{0c}) &= \frac{V_d^+}{Z_{0d}}(2 - y_{11}Z_{0d} + y_{12}Z_{0d}) - \frac{V_d^-}{Z_{0d}}(2 + y_{11}Z_{0d} - y_{12}Z_{0d}) \end{aligned} \quad (5.218)$$

$$\begin{aligned} -V_c^-/Z_{0c} - (2V_d^+ - 2V_d^-)/Z_{0d} &= y_{21}(V_d^+ + 2V_c^- + V_d^-) + y_{22}(-V_d^+ + 2V_c^- - V_d^-) \\ \text{i.e. } \frac{V_d^-}{Z_{0d}}(-2 + y_{21}Z_{0d} - y_{22}Z_{0d}) &= -\frac{V_d^+}{Z_{0d}}(2 + y_{21}Z_{0d} - y_{22}Z_{0d}) - \frac{V_c^-}{Z_{0c}}(1 + 2y_{21}Z_{0c} + 2y_{22}Z_{0c}) \end{aligned} \quad (5.219)$$

To eliminate V_d^- multiply Equation (5.219) by $(2 + y_{11}Z_{0d} - y_{12}Z_{0d})$ and subtract it from Equation (5.218) multiplied by $(-2 + y_{21}Z_{0d} - y_{22}Z_{0d})$:

$$\frac{V_c^-}{Z_{0c}}a = \frac{V_d^+}{Z_{0d}}c \quad \text{so that} \quad C_{eo} = \frac{c}{a} \frac{Z_{0c}}{Z_{0d}} \quad (5.220)$$

where a is as in Equation (5.213) and

$$c = (2 - y_{11}Z_{0d} + y_{12}Z_{0d})(-2 + y_{21}Z_{0d} - y_{22}Z_{0d}) + (2 + y_{21}Z_{0d} - y_{22}Z_{0d})(2 + y_{11}Z_{0d} - y_{12}Z_{0d}) \\ = -2Z_{0d}Y_E \quad \text{where} \quad Y_E = (y_{11} - y_{12} + y_{21} - y_{22}). \quad (5.221)$$

$$C_{cd} = \frac{4Z_{0c}Y_E}{4 + Z_{0d}Y_{\Delta} + 4Z_{0c}Y_{\Sigma} + 4Z_{0c}Z_{0d}Y_D} = C_{eo} \quad (5.222)$$

(which can be verified using the substitutions $Z_{0d} = 2Z_{0o}$ and $Z_{0c} = \frac{1}{2}Z_{0e}$).

Similarly,

$$\Gamma_{Ld} = \frac{2 + Z_{0d}(y_{12} + y_{21}) - 2Z_{0c}Z_{0d}Y_D}{2 + Z_{0d}Y_{\Delta} + 4Z_{0c}Y_{\Sigma} + 2Z_{0c}Z_{0d}Y_D} = \Gamma_{Lo} \quad (5.223)$$

$$\text{and} \quad C_{dc} = \frac{-4Z_{0c}Y_E}{4 + Z_{0d}Y_{\Delta} + 4Z_{0c}Y_{\Sigma} + 4Z_{0c}Z_{0d}Y_D} = C_{cd} = C_{oe}, \text{ and} \quad (5.224)$$

5.11 Common Impedance Coupling

So far coupling has been discussed in terms of the EM fields shared by two transmission lines. This is not the only way coupling of signals occurs. Sharing of a return path results in coupling, often called common impedance coupling, as there is a circuit element common to two or more transmission lines. The simplest situation is a shared impedance rather than a shared transmission line return, so that the return current attributed to one interconnect induces a voltage across the common impedance element. This signal then appears as though it is on the victim line. The common impedance could be the inductance or resistance of the ground conductor in the case of microstrip lines. In general, however, common impedance coupling will occur whenever the current return path is common.

5.12 Summary

Coupling from one transmission line to a nearby neighbor may often be undesirable. However, the coupling can be controlled and coupled lines have become an important circuit component in distributed microwave circuits. One example is a directional coupler, which is little more than a pair of coupled lines, and this device forms the special function of separating forward- and backward-traveling waves. Another example of the application of coupled lines is their use in microwave filters. Bandpass filters are essentially coupled resonators. In a filter that uses coupled lines, each individual line becomes a resonator and the coupling of the resonators is controlled by how far they are spaced.

The analysis and circuit model of a pair of coupled lines is based on describing the voltages and currents on the lines as the linear combination of an even mode and an odd mode. Each of these modes will have forward- and backward-traveling wave components. Separating the signals on a coupled-line pair into even and odd modes facilitates extraction of the coupled-line parameters from simulation and measurement. It also enables a model of the coupled line to be developed that consists of individual lines that are coupled by transformers.

With the differential circuits used with RFICs it is more convenient to consider the signals on a pair of coupled lines as comprising common and differential modes. These can be directly related to even and odd modes and the difference comes down to definitions of average voltage (i.e., the common- and even-mode voltages) and the definition of the difference

voltage (i.e., the differential- and odd-mode voltages). There is a similar difference for the currents.

The suite of microwave elements that exploit distributed effects available to a microwave designer is surprisingly large. Coupled lines comprise a large proportion of these elements. This chapter concludes with an example of the broadband response of a pair of coupled microstrip lines.

EXAMPLE 5.10**Shorted Coupled Lines**

 Design Environment Project File: RFDesign_Coupled_Shorted_Microstrip_Lines.emp

In this example a pair of shorted coupled microstrip lines are examined using EM analysis. The layout of the coupled lines is shown in Figure 5-30. The box used in simulation has electric side and top walls. The bottom of the box (below the strips) is an electric wall and forms the ground plane. The ground plane is specified as gold and the finite conductivity of gold is used for the strips and the ground plane. The coupled lines here are arranged as a two-port structure. Scattering (S) parameters are used to describe the characteristics of microwave structures. The transmission coefficient is S_{21} , and for a matched structure S_{11} is the reflection coefficient. The coupled-line structure is symmetrical, as the widths of the strips are the same so that $S_{11} = S_{22}$ and $S_{12} = S_{21}$. Each microstrip line on its own was designed to have a characteristic impedance of $50\ \Omega$.

The calculated two-port S parameters are plotted in Figure 5-31. The loss of 0 dB corresponds to an S parameter absolute value of 1. Large S_{21} responses are centered at 1.5 GHz, 7.5 GHz, and 13 GHz and are shaped as bandpass filter responses. This suggests that coupled-line sections could be used as the basis of microwave bandpass filters. The passband frequencies are related to the lengths of the lines. The effective dielectric constant for one of the microstrip lines is 6.5 (from Table 3-2) and so at 1.5 GHz the 1 cm line length is $\lambda/8$ long, at 7.5 GHz it is $5\lambda/8$ long, and at 13 GHz it is $9\lambda/8$ long. The round-trip lengths are $\lambda/4$, $5\lambda/4$, and $9\lambda/4$ long at the respective frequencies. Thus the round-trip lengths are separated by λ and so the addition of half-wavelength sections of lossless line has no impact on the reflection and transmitted response amplitudes.

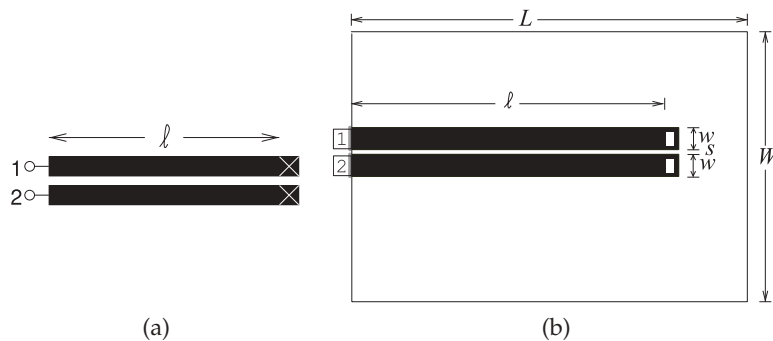


Figure 5-30: Coupled microstrip line layout: (a) schematic; and (b) layout in an EM field solver. Dimensions of the coupled lines are $w = 500\ \mu\text{m}$, $s = 100\ \mu\text{m}$, $\ell = 1\ \text{cm}$, $W = 6\ \text{mm}$, $L = 12\ \text{mm}$. The metal is $6\ \mu\text{m}$ thick gold (conductivity $\sigma = 42.6 \times 10^6$) and the alumina substrate height is $600\ \mu\text{m}$ with relative permittivity $\epsilon_r = 9.8$ and a loss tangent of 0.001.

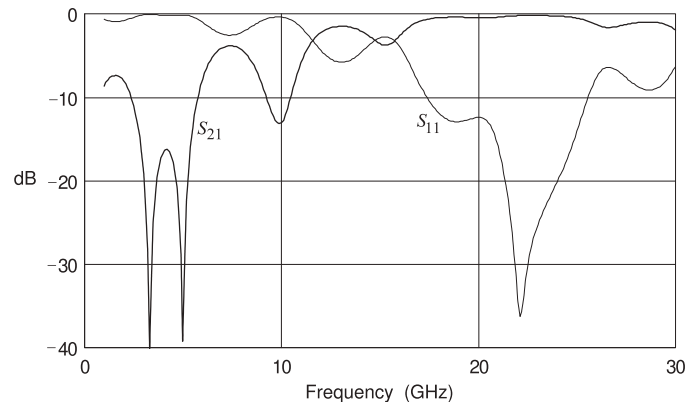


Figure 5-31: Insertion loss (S_{21}) and return loss (S_{11}) of the coupled line of Figure 5-30.

5.13 References

- [1] B. Biswas, "Modeling and simulation of high speed interconnects," Master's thesis, North Carolina State University, 1998.
- [2] E. Hammerstad and O. Jensen, "Accurate models for microstrip computer-aided design," in *1980 IEEE MTT-S Int. Microwave Symp. Digest*, May 1980, pp. 407–409.
- [3] M. Kirschning and R. Jansen, "Accurate wide-range design equations for the frequency-dependent characteristic of parallel coupled microstrip lines," *IEEE Trans. on Microwave Theory and Techniques*, vol. 32, no. 1, pp. 83–90, Jan. 1984.
- [4] —, "Accurate wide-range design equations for the frequency-dependent characteristic of parallel coupled microstrip lines," *IEEE Trans. on Microwave Theory and Techniques*, vol. 32, no. 1, pp. 83–90, Jan. 1984.
- [5] T. Edwards and M. Steer, *Foundations for Microstrip Circuit Design*. John Wiley & Sons, 2016.
- [6] <http://www.synergymwave.com>.
- [7] <http://www.minicircuits.com>.
- [8] J. Lange, "Interdigitated strip-line quadrature hybrid," in *1969 G-MTT Int. Microwave Symp.*, May 1969, pp. 10–13.
- [9] A. Johnson and G. Zysman, "Coupled transmission line networks in an inhomogeneous dielectric medium," in *1969 G-MTT Int. Microwave Symp.*, May 1969, pp. 329–337.
- [10] R. Mongia, I. Bahl, and P. Bhartia, *RF and Microwave Coupled-line Circuits*. Artech House, 1999.
- [11] J.-S. Hong and M. Lancaster, *Microstrip Filters for RF/Microwave Applications*. John Wiley & Sons, 2001.
- [12] E. Jones, "Coupled-strip-transmission-line filters and directional couplers," *Microwave Theory and Techniques, IRE Trans. on*, vol. 4, no. 2, pp. 75–81, Apr. 1956.
- [13] I. Hunter, *Theory and Design of Microwave Filters*. IEE Press, 2001.
- [14] V. Tripathi and J. Rettig, "A spice model for multiple coupled microstrips and other transmission lines," *IEEE Trans. on Microwave Theory and Techniques*, vol. 33, no. 12, pp. 1513–1518, Dec. 1985.
- [15] M. Steer, *Microwave and RF Design, Networks*, 3rd ed. North Carolina State University, 2019.
- [16] J. Malherbe, *Microwave Transmission Line Filters*. Artech House, 1979.

5.14 Exercises

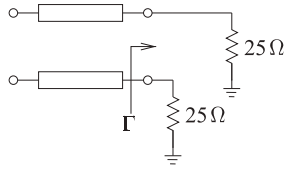
- Consider the cross section of a coupled transmission line, as shown in Figure 5-1, with even and odd modes both traveling out of the page.
 - For an even mode on the coupled line, consider a phasor voltage of 1 V on each of the lines above the ground plane at 0 V. Sketch the directed electric field in the transverse plane, i.e. show the direction of the electric field.
 - For the even mode, sketch the directed magnetic fields in the transverse plane (the plane of the cross section).
 - For an odd mode on the coupled line, consider a phasor voltage of +1 V on the left line and a phasor voltage of -1 V on the right line. Sketch the directed electric fields in the transverse plane (the plane of the cross section).
 - For the odd mode, sketch the directed magnetic fields in the transverse plane (the plane of the cross section).
- EM software can be used to determine the even- and odd-mode parameters of a coupled line. This is usually done by setting the phasor voltage on the coupled line and evaluating the phasor charge for each condition. The voltage applied to the left strip is V_1 and the voltage applied to the right strip is V_2 . The phasor charges on the strips are Q_1 and Q_2 , respectively. The analysis is repeated with the substrate replaced by free space. In this case, the charges are denoted by Q_{01} and Q_{02} . The (computer-based) measurements follow. [Parallels Example 5.1]
- Two 50 Ω microstrip lines are to be run parallel to each other on a 1 mm-thick printed circuit board with a relative permittivity $\epsilon_r = 4$. The signal on the lines is 3 GHz. The effective permittivity of the lines is 3.1 and it is determined that the approximate distance over which the lines will be parallel is 1.42 cm. The coupling of the signals on the lines must be at least 30 dB down.
 - What is the free-space wavelength, λ_0 , of the signal?
 - What is the guide wavelength, λ_g , of the signal?
 - How long is the parallel run of the microstrip lines in terms of λ_g ?
 - What is the required maximum parallel-line coupling factor? Explain your reasoning.
 - What is the minimum separation of the lines? Explain your reasoning.
- A pair of coupled lines has an even-mode effective permittivity, ϵ_{ee} , of 4.9 and an odd-mode effective permittivity of 5.2.
 - What is the even-mode phase velocity?
 - What is the odd-mode phase velocity?
- A directional coupler using coupled lines is constructed on an alumina substrate of thickness 300 μm and $\epsilon_r = 10$. The lines are 250 μm wide and the gap separation is 100 μm . What are (a) the characteristic impedances, (b) the effective permittivities, and (c) the phase velocities of the even and odd mode of the coupled line. (Hint: If you use a table you need to use interpolation as described in Section 1.A.12.)
- An ideal directional coupler is lossless and there are no reflections at the ports. If the coupling factor is 10, what is the magnitude of the transmission coefficient?
- A directional coupler has the following characteristics: coupling factor $C = 20$, transmission factor 0.9, and directivity factor 25 dB. Also, the coupler is matched so that there is no reflection at any of the ports. What is the isolation in decibels?
- A lossy 6 dB directional coupler is matched so that there is no reflection at any of the ports. The insertion loss (considering the through path) is 2 dB. If 1 mW is input to the directional coupler, what is the power in microwatts dissipated in the directional coupler? Ignore power leaving the isolated port.
- A 1 GHz microstrip directional coupler has a coupling factor of 20 dB. The coupler must have a system impedance of 50 Ω .

Charge	$V_1 = 1 \text{ V};$ $V_2 = -1 \text{ V}$	$V_1 = 1 \text{ V};$ $V_2 = 1 \text{ V}$
Q_1 (pC/m)	40	20
Q_2 (pC/m)	-50	30
Q_{01} (pC/m)	13.25	6
Q_{02} (pC/m)	-10	2.75

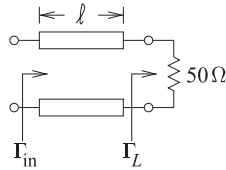
- What is the two-port capacitance matrix?
- What is the even-mode capacitance?
- What is the odd-mode capacitance?
- What is the free-space (no dielectric) two-port capacitance matrix?
- What is the free-space even-mode capacitance?
- What is the free-space odd-mode capacitance?
- What is the even-mode effective relative permittivity?
- What is the odd-mode effective relative permittivity?

- (a) Draw the layout of the directional coupler.
 - (b) What is the even-mode impedance of the coupler?
 - (c) What is the odd-mode impedance of the coupler?
 - (d) What is the optimum electrical length of the directional coupler in degrees at the design center frequency?
 - (e) If, in addition, the isolation of the directional coupler is 40 dB, what is its directivity in decibels?
10. A directional coupler comprising a coupled pair of microstrip lines is to be designed in a $75\ \Omega$ system. The coupling factor is 10.
 - (a) What is the system impedance Z_{0S} ?
 - (b) What is the odd-mode impedance of the coupler?
 - (c) What is the even-mode impedance of the coupler?
11. A matched directional coupler has a coupling factor C of 20, transmission factor 0.9, and directivity of 25 dB. What is the power dissipated in the directional coupler if the input power to Port 1 is 1 W.
12. Develop the design of a 10 dB directional coupler using coupled microstrip lines and a substrate with a permittivity of 10, a substrate thickness, h , of $600\ \mu\text{m}$, and a center frequency of 1 GHz. Develop the electrical design of the coupler (i.e., find the even- and odd-mode impedances required) and then develop the physical design (with widths and lengths) of the directional coupler. Use a system impedance of $50\ \Omega$.
13. Design a microstrip directional coupler with the following specifications:

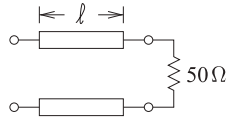
Transmission line technology: Microstrip
Coupling coefficient, C : 20 dB
Characteristic impedance, Z_{0S} : $50\ \Omega$
Substrate permittivity, ϵ_r : 4.0
Substrate thickness, h : $635\ \mu\text{m}$
Center frequency, f_0 : 10 GHz.
14. A directional coupler using coupled lines is constructed on an alumina substrate of thickness $300\ \mu\text{m}$. The lines are $250\ \mu\text{m}$ wide and the gap separation is $100\ \mu\text{m}$. What are the characteristic impedances, effective permittivities, and phase velocities of the even- and odd-modes of the coupled line? Port 1 is the input, Port 2 is the through output, and Port 3 is the coupled output. (Hint: See Table 5-3.)
 - (a) Draw the schematic of the directional coupler and label the ports.
 - (b) What is the transmission coefficient of the coupler?
 - (c) Can the directivity of the coupler be determined? If so, what is the directivity, D , of the coupler?
15. Consider a pair of parallel microstrip lines separated by a spacing, s , of $100\ \mu\text{m}$.
 - (a) What happens to the coupling factor of the lines as s reduces?
 - (b) What happens to the system impedance as s reduces and no other dimensions change?
 - (c) In terms of wavelengths, what is the optimum length of the coupled lines for maximum coupling?
16. What is the coupling factor of a Lange coupler in decibels?
17. Consider the open-circuited interdigital coupled-line section in Table 5-4. If the coupled line is $\lambda/4$ long, write down the simplified $ABCD$ parameters. Assume that $\theta_o = \theta_e$.
18. Consider the shorted symmetric coupled-line section in Table 5-4. If the coupled line is $\lambda/4$ long, write down the simplified $ABCD$ parameters. Assume that $\theta_o = \theta_e$.
19. Consider the open-circuited combline coupled-line section in Table 5-4. If the coupled line is $\lambda/4$ long, write down the simplified $ABCD$ parameters. Assume that $\theta_o = \theta_e$.
20. Consider the short-circuited interdigital coupled-line section in Table 5-4. If the coupled line is $\lambda/4$ long, write down the simplified $ABCD$ parameters. Assume that $\theta_o = \theta_e$.
21. A coupled microstrip line has an odd-mode impedance of $30\ \Omega$ and an even-mode impedance of $65\ \Omega$.
 - (a) What is the differential characteristic impedance of the coupled lines?
 - (b) What is the common-mode characteristic impedance of the coupled lines?
22. A pair of coupled microstrip lines has odd- and even-mode characteristic impedances of $60\ \Omega$ and $70\ \Omega$ respectively. If a load resistance, R_L , is placed at the end of the lines from one strip to the other, what is the value of R_L for no reflection of the even mode?
23. The coupled lines below have odd- and even-mode characteristic impedances of $30\ \Omega$ and $60\ \Omega$ respectively.



- (a) What is the odd-mode reflection coefficient Γ ?
- (b) What is the common-mode characteristic impedance of the coupled lines?
24. The coupled lines below have odd- and even-mode characteristic impedances of $60\ \Omega$ and $100\ \Omega$ respectively. The coupled lines have a length ℓ and this is $\lambda/4$ long for the odd mode.



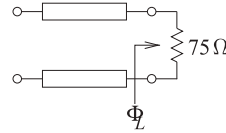
- (a) What is the odd-mode reflection coefficient at the load, call this Γ_{Lo} ?
- (b) What is the odd-mode reflection coefficient at the input to the coupled lines?
25. The coupled microstrip lines below have an odd-mode characteristic impedance of $40\ \Omega$ and an even-mode characteristic impedance of $75\ \Omega$.



- (a) What is the differential-mode characteristic impedance?

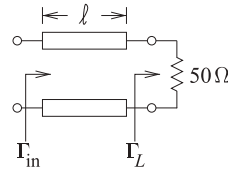
- (b) What is the common-mode characteristic impedance?

26. The coupled lines below have odd- and even-mode characteristic impedances of $40\ \Omega$ and $75\ \Omega$ respectively.



- (a) What is the differential-mode characteristic impedance, Z_{0d} ?
- (b) What is the differential-mode load resistance, Z_{Ld} ?
- (c) What is the differential-mode reflection coefficient, Γ_{Ld} , at the load?
- (d) What is the odd-mode reflection coefficient, Γ_{Lo} , at the load?

27. The coupled lines below have odd- and even-mode characteristic impedances of $60\ \Omega$ and $100\ \Omega$ respectively. The coupled lines have a length ℓ and this is $\lambda/4$ long for the odd mode.



- (a) What is the differential-mode reflection coefficient, Γ_d , at the load?
- (b) What is Γ_d at the input of the lines?

5.14.1 Exercises by Section

[†]challenging, [‡]very challenging

§5.2 1[†]

§5.5 2[†], 3[‡]

§5.6 4, 5,

§5.8 6, 7, 8, 9[†], 10[†], 11, 12[†], 13[†],

14[†], 15[†], 16

§5.9 17, 18, 19, 20

§5.10 21, 22, 23, 24, 25, 26, 27

5.14.2 Answers to Selected Exercises

2(h) 3.87

5(c) $v_{po} = 1.256 \cdot 10^8\ \text{m/s}$

6 0.9950

7(b) 187 mW

9(e) $D = 10\ \text{dB}$

10 $Z_{0e} = 67.84\ \Omega$

17 $C = 2j/(Z_{0e} - Z_{0o})$

21 $32.5\ \Omega$

24 0.4118

26 -0.0323

Waveguides

6.1	Introduction	253
6.2	The Rectangular Wave Equation	254
6.3	Parallel-Plate Waveguide	257
6.4	Rectangular Waveguide	262
6.5	Summary	274
6.6	References	275
6.7	Exercises	276

6.1 Introduction

Rectangular waveguides are used to route millimeter-wave signals and high power microwave signals. The rectangular waveguide, often called just waveguide, shown in Figure 6-1 has metal walls forming a rectangular pipe. Charges and currents induced in the conductive walls guide propagating EM fields in the $+z$ and $-z$ directions. The rectangular waveguide has very little loss compared to a coaxial line because the EM field is away from the walls and there is little current in the walls, and what is there is spread out resulting in low current density. All of the waveguide loss, as with the loss of most transmission systems, is resistive loss so minimizing current density minimizes loss.

This chapter begins with Section 6.2 where symmetries and restricting

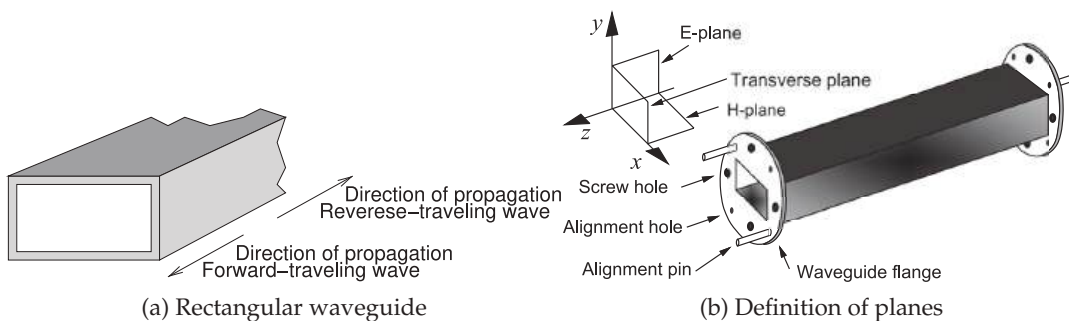
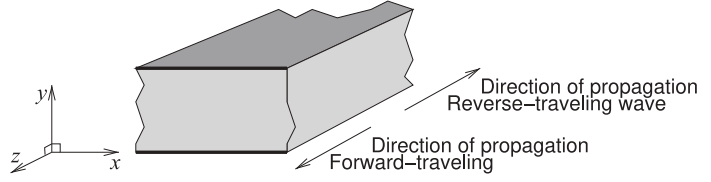


Figure 6-1: Rectangular waveguide.

Figure 6-2: Parallel-plate waveguide.



propagation to only the $\pm z$ direction are applied to Maxwell's equations to yield the rectangular wave equation. These are then used in Section 6.3 to describe propagation between two metal planes forming what is called a parallel-plate waveguide, see Figure 6-2. Then the rectangular wave equations are applied to a rectangular waveguide in Section 6.4 to derive the field distribution inside a rectangular waveguide.

6.2 The Rectangular Wave Equation

Maxwell's equations will be put in a form that can be used in establishing the field descriptions in parallel-plate and rectangular waveguides. The EM fields in these structures vary sinusoidally with respect to both position and time so the first simplification of Maxwell's equations is to use phasors. Boundary conditions are established by the metal walls, and these walls match the Cartesian coordinate system. So Maxwell's equations are put in Cartesian coordinate form. Simplifications of the fields can be made that relate to the positions of the metal walls. Another simplification is made by assuming that there can only be propagation in the $\pm z$ direction. When the wave propagates in the $+z$ direction it is called the forward-traveling wave, and when it propagates in the $-z$ direction it is called the reverse-traveling wave.

The development begins with Maxwell's equations (Equations (1.1)–(1.4)) in a source-free region ($\rho = 0$ and $J = 0$). A simplification comes from assuming a linear, isotropic, and homogeneous medium so that ϵ and μ are independent of signal level and are independent of the field direction and of position, thus

$$\nabla \times \bar{\mathcal{E}} = -\frac{\partial \bar{\mathcal{B}}}{\partial t} = -\mu \frac{\partial \bar{\mathcal{H}}}{\partial t} \quad (6.1) \quad \nabla \times \bar{\mathcal{H}} = \frac{\partial \bar{\mathcal{D}}}{\partial t} = \epsilon \frac{\partial \bar{\mathcal{E}}}{\partial t} \quad (6.3)$$

$$\nabla \cdot \bar{\mathcal{D}} = 0 = \nabla \cdot \bar{\mathcal{E}} \quad (6.2) \quad \nabla \cdot \bar{\mathcal{B}} = 0 = \nabla \cdot \bar{\mathcal{H}}. \quad (6.4)$$

Taking the curl of Equation (6.1) leads to

$$\nabla \times \nabla \times \bar{\mathcal{E}} = -\nabla \times \mu \frac{\partial \bar{\mathcal{H}}}{\partial t} = -\mu \frac{\partial (\nabla \times \bar{\mathcal{H}})}{\partial t}. \quad (6.5)$$

Applying the identity $\nabla \times \nabla \times \bar{\mathcal{A}} = \nabla(\nabla \cdot \bar{\mathcal{A}}) - \nabla^2 \bar{\mathcal{A}}$ to the left-hand side of Equation (6.5), and replacing $\nabla \times \bar{\mathcal{H}}$ with the right-hand side of Equation (6.3), the equation above becomes

$$-\nabla^2 \bar{\mathcal{E}} + \nabla(\nabla \cdot \bar{\mathcal{E}}) = -\mu \frac{\partial}{\partial t} \left(\epsilon \frac{\partial \bar{\mathcal{E}}}{\partial t} \right) = -\mu \epsilon \frac{\partial^2 \bar{\mathcal{E}}}{\partial t^2}. \quad (6.6)$$

Using Equation (6.2) this reduces to

$$\nabla^2 \bar{\mathcal{E}} = \mu \epsilon \frac{\partial^2 (\bar{\mathcal{E}})}{\partial t^2}, \quad (6.7)$$

where $\nabla^2 \bar{\mathcal{E}} = \frac{\partial^2 \bar{\mathcal{E}}}{\partial x^2} + \frac{\partial^2 \bar{\mathcal{E}}}{\partial y^2} + \frac{\partial^2 \bar{\mathcal{E}}}{\partial z^2} = \nabla_t^2 \bar{\mathcal{E}} + \frac{\partial^2 \bar{\mathcal{E}}}{\partial z^2}$. (6.8)

and $\nabla_t^2 \bar{\mathcal{E}} = \frac{\partial^2 \bar{\mathcal{E}}}{\partial x^2} + \frac{\partial^2 \bar{\mathcal{E}}}{\partial y^2}$ (6.9)

is used for fields propagating in the $\pm z$ direction and the subscript t indicates the transverse plane (the x - y plane here). Equation (6.9) can be put into the form of its components. Since

$$\bar{\mathcal{E}} = \mathcal{E}_x \hat{\mathbf{x}} + \mathcal{E}_y \hat{\mathbf{y}} + \mathcal{E}_z \hat{\mathbf{z}}, \quad (6.10)$$

then $\nabla^2 \bar{\mathcal{E}} = \left(\frac{\partial^2 \mathcal{E}_x}{\partial x^2} \hat{\mathbf{x}} + \frac{\partial^2 \mathcal{E}_y}{\partial x^2} \hat{\mathbf{y}} + \frac{\partial^2 \mathcal{E}_z}{\partial x^2} \hat{\mathbf{z}} \right) + \left(\frac{\partial^2 \mathcal{E}_x}{\partial y^2} \hat{\mathbf{x}} + \frac{\partial^2 \mathcal{E}_y}{\partial y^2} \hat{\mathbf{y}} + \frac{\partial^2 \mathcal{E}_z}{\partial y^2} \hat{\mathbf{z}} \right) + \left(\frac{\partial^2 \mathcal{E}_x}{\partial z^2} \hat{\mathbf{x}} + \frac{\partial^2 \mathcal{E}_y}{\partial z^2} \hat{\mathbf{y}} + \frac{\partial^2 \mathcal{E}_z}{\partial z^2} \hat{\mathbf{z}} \right)$ (6.11)

$$= \left(\frac{\partial^2 \mathcal{E}_x}{\partial x^2} + \frac{\partial^2 \mathcal{E}_x}{\partial y^2} + \frac{\partial^2 \mathcal{E}_x}{\partial z^2} \right) \hat{\mathbf{x}} + \left(\frac{\partial^2 \mathcal{E}_y}{\partial x^2} + \frac{\partial^2 \mathcal{E}_y}{\partial y^2} + \frac{\partial^2 \mathcal{E}_y}{\partial z^2} \right) \hat{\mathbf{y}} + \left(\frac{\partial^2 \mathcal{E}_z}{\partial x^2} + \frac{\partial^2 \mathcal{E}_z}{\partial y^2} + \frac{\partial^2 \mathcal{E}_z}{\partial z^2} \right) \hat{\mathbf{z}}, \quad (6.12)$$

and $\nabla_t^2 \bar{\mathcal{E}} = \left(\frac{\partial^2 \mathcal{E}_x}{\partial x^2} + \frac{\partial^2 \mathcal{E}_x}{\partial y^2} \right) \hat{\mathbf{x}} + \left(\frac{\partial^2 \mathcal{E}_y}{\partial x^2} + \frac{\partial^2 \mathcal{E}_y}{\partial y^2} \right) \hat{\mathbf{y}} + \left(\frac{\partial^2 \mathcal{E}_z}{\partial x^2} + \frac{\partial^2 \mathcal{E}_z}{\partial y^2} \right) \hat{\mathbf{z}}$. (6.13)

Invoking the phasor form, $\partial/\partial t$ is replaced by $j\omega$, and with propagation only in the $\pm z$ direction there is an assumed $e^{(j\omega t - \gamma z)}$ dependence of the fields. Development is now simplified by introducing the phasor \bar{E} defined so that

$$\bar{\mathcal{E}} = \bar{E} e^{-\gamma z}. \quad (6.14)$$

Now Equation (6.7) further reduces to

$$\nabla^2 \bar{E} = \left(\nabla_t^2 \bar{E} + \frac{\partial^2 \bar{E}}{\partial z^2} \right) = \nabla_t^2 \bar{E} + \gamma^2 \bar{E} = (j\omega)^2 \mu \epsilon \bar{E} = -k^2 \bar{E}, \quad (6.15)$$

where $k = \omega \sqrt{\mu \epsilon}$ is the **wavenumber** (with SI units of m^{-1}). Rearranging Equation (6.15) yields

$$\nabla_t^2 \bar{E} = -(\gamma^2 + k^2) \bar{E}. \quad (6.16)$$

A similar expression can be derived for the magnetic field:

$$\nabla_t^2 \bar{H} = -(\gamma^2 + k^2) \bar{H}. \quad (6.17)$$

Equations (6.16) and (6.17) are called wave equations, or Helmholtz equations, for phasor fields propagating in the z direction. Equations (6.16) and (6.17) are usually written as

$$\nabla_t^2 \bar{E} = -k_c^2 \bar{E} \quad (6.18) \quad \nabla_t^2 \bar{H} = -k_c^2 \bar{H}, \quad (6.19)$$

where the **cutoff wavenumber** is

$$k_c^2 = \gamma^2 + k^2. \quad (6.20)$$

Equations (6.18) and (6.19) describe the transverse fields (the fields in the x - y plane) between the conducting plates of the parallel-plate as well as within the walls of the rectangular waveguide having a $e^{(j\omega t - \gamma z)}$ dependence. The general form of the solution of these equations is a sinusoidal wave moving in the z direction. For propagating waves in a lossless medium, $\gamma = j\beta$, where β is the phase constant:

$$\beta = \pm \sqrt{k^2 - k_c^2}. \quad (6.21)$$

If β is not real, which occurs when $|k_c| < |k|$, then an EM wave cannot propagate and such modes are called evanescent modes. These are like fringing fields. If they are generated, say at a discontinuity, they will store reactive energy locally.

Boundary conditions, resulting from the charges and current on the plates, further constrain the solutions. Equation (6.1) with Equation (1.125) becomes

$$\nabla \times \bar{E} = j\omega\mu\bar{H}. \quad (6.22)$$

In rectangular coordinates, $\bar{E} = E_x\hat{x} + E_y\hat{y} + E_z\hat{z}$ and $\bar{H} = H_x\hat{x} + H_y\hat{y} + H_z\hat{z}$, and Equation (6.22) becomes

$$\left. \begin{aligned} \frac{\partial E_z}{\partial y} + \gamma E_y &= -j\omega\mu H_x, & -\frac{\partial E_z}{\partial x} - \gamma E_x &= -j\omega\mu H_y, \\ \frac{\partial E_y}{\partial x} - \frac{\partial E_x}{\partial y} &= -j\omega\mu H_z \end{aligned} \right\}. \quad (6.23)$$

Similarly for $\nabla \times \bar{H} = j\omega\varepsilon\bar{E}$:

$$\left. \begin{aligned} \frac{\partial H_z}{\partial y} + \gamma H_y &= j\omega\varepsilon E_x, & -\frac{\partial H_z}{\partial x} - \gamma H_x &= j\omega\varepsilon E_y, \\ \frac{\partial H_y}{\partial x} - \frac{\partial H_x}{\partial y} &= j\omega\varepsilon E_z \end{aligned} \right\}. \quad (6.24)$$

Solving Equations (6.23) and (6.24) yields the rectangular wave equations for $k_c \neq 0$ ($k_c^2 = k^2 + \gamma^2$ and if there is no loss $k_c^2 = \omega^2\mu\varepsilon - \beta^2$):

$$\left. \begin{aligned} E_x &= \frac{-1}{k_c^2} \left(\gamma \frac{\partial E_z}{\partial x} + j\omega\mu \frac{\partial H_z}{\partial y} \right) & E_y &= \frac{1}{k_c^2} \left(-\gamma \frac{\partial E_z}{\partial y} + j\omega\mu \frac{\partial H_z}{\partial x} \right) \\ H_x &= \frac{1}{k_c^2} \left(-\gamma \frac{\partial H_z}{\partial x} + j\omega\varepsilon \frac{\partial E_z}{\partial y} \right) & H_y &= \frac{-1}{k_c^2} \left(\gamma \frac{\partial H_z}{\partial y} + j\omega\varepsilon \frac{\partial E_z}{\partial x} \right) \\ E_z &= \frac{-j}{\omega\varepsilon} \left(\frac{\partial H_y}{\partial x} - \frac{\partial H_x}{\partial y} \right) & H_z &= \frac{j}{\omega\mu} \left(\frac{\partial E_y}{\partial x} - \frac{\partial E_x}{\partial y} \right). \end{aligned} \right\} \quad (6.25)$$

The solution for $k_c = 0$ is arrived at separately. Since $k_c = 0$ there is no loss. Also propagation at DC is a solution and the phasor fields at $\omega = 0$ will also be the field descriptions at any frequency. At $\omega = 0$, $\gamma = j\beta = 0$ and $k = 0$. Equations (6.23)–(6.24) are now written as

$$\left. \begin{aligned} \frac{\partial E_z}{\partial y} + 0 \cdot E_y &= 0 \cdot H_x = 0, & -\frac{\partial E_z}{\partial x} - 0 \cdot E_x &= 0 \cdot H_y = 0, \\ \frac{\partial E_y}{\partial x} - \frac{\partial E_x}{\partial y} &= -0 \cdot H_z = 0, & \frac{\partial H_z}{\partial y} + 0 \cdot H_y &= 0 \cdot E_x = 0, \\ -\frac{\partial H_z}{\partial x} - 0 \cdot H_x &= 0 \cdot E_y = 0, & \frac{\partial H_y}{\partial x} - \frac{\partial H_x}{\partial y} &= 0 \cdot E_z = 0. \end{aligned} \right\}. \quad (6.26)$$

The only solutions to these with $\partial/\partial x = 0$ that also satisfies boundary conditions are that $E_z = 0 = H_z = E_x = H_y$, and H_y and E_x are constants.

Now that the fields are in the appropriate forms, classification of possible solutions (i.e. modes) can be developed for the parallel-plate and rectangular waveguides. At this stage the following simplifications have been made to Maxwell's equations to get them into the form of Equation (6.25):

- Using phasors
- Restriction of propagation to the $+z$ and $-z$ directions
- Assuming that ε and μ are constants
- Putting the wave equations in rectangular form so that boundary conditions established by the metal walls can be easily applied.

6.3 Parallel-Plate Waveguide

This section derives the propagating EM fields for the parallel-plate waveguide shown in Figure 6-3. The parallel-plate waveguide shown in Figure 6-3(a) has conducting planes at the top and bottom that (as an approximation) extend infinitely in the x direction. Electromagnetic fields introduced between the plates, say by a sinusoidally varying voltage generator across the plates, will be guided by the charges and currents induced in the conductors.

The parallel-plate waveguide structure occurs in many planar circuits, such as between the ground and power planes of circuit boards. Understanding the EM propagation supported by parallel-plate waveguides enables design choices to be made that suppress unwanted propagation modes.

6.3.1 TEM Mode

In the transverse EM (TEM) mode, all of the E and H field components are in the plane transverse to the direction of propagation, that is, $E_z = 0 = H_z$. Thus Equation (6.26) requires that E_x , E_y , H_x , and H_y cannot vary with position in the transverse plane (i.e., with respect to x and y). Thus E_x , E_y , H_x , and H_y must be constant between the plates. Furthermore, boundary conditions require that $H_y = 0$ and $E_x = 0$ at the conductors. So in the TEM parallel-plate mode, only E_y and H_x exist, and they are constant. Equation

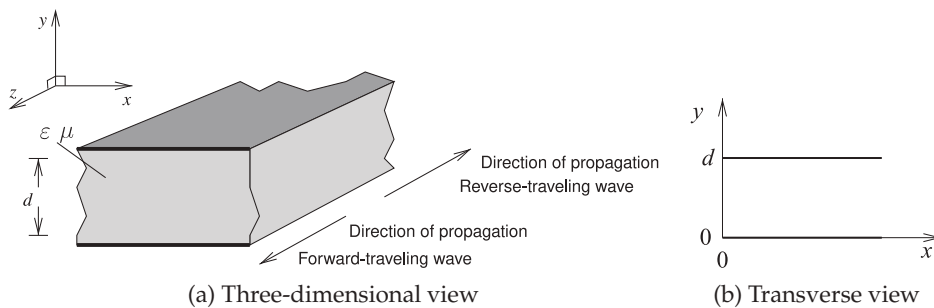
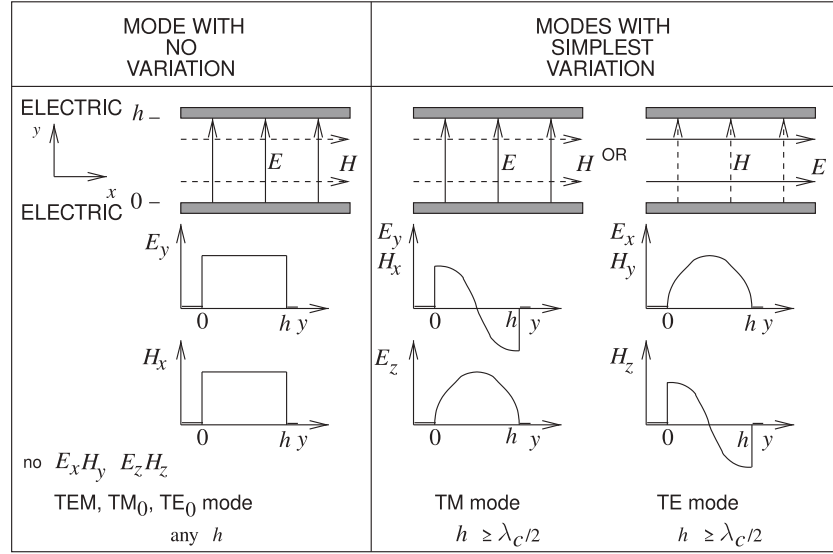


Figure 6-3: Parallel-plate waveguide.

Figure 6-4: Lowest-order modes supported by combinations of electric and magnetic walls for the TEM ($= \text{TM}_0 = \text{TE}_0$), TM_1 , and TE_1 modes.



(6.25) leads to

$$H_x = \frac{\gamma E_y}{j\omega\mu} = \pm \frac{j\omega\sqrt{\mu\epsilon}}{j\omega\mu} E_y = \pm \sqrt{\frac{\epsilon}{\mu}} E_y = \pm \frac{1}{\eta} E_y, \quad (6.27)$$

where the plus sign describes forward-traveling fields (propagating in the $+z$ direction) and the minus sign describes backward-traveling fields (propagating in the $-z$ direction). The quantity $\eta = \sqrt{\mu/\epsilon}$ is called the **wave impedance**, it is the **intrinsic impedance** of the medium between the parallel plates. This field variation is shown on the left in Figure 6-4(a). The TEM mode exists down to DC.

To determine the characteristic impedance of the parallel-plate waveguide first calculate the voltage of the top plate with respect to the bottom plate. This voltage is the integral of the electric field between the plates:

$$V = - \int_{y=0}^d E_y e^{-\gamma z} dy = E_y d e^{-\gamma z} \quad (6.28)$$

since E_y is a constant. The current on the top plate in the z direction is obtained by integrating the surface current density in the x direction. Assuming that the plates have a width W in the x direction then the current on the top plate is

$$I = - \int_{x=0}^W J_s \cdot \hat{z} dx = H_x W e^{-\gamma z} \quad (6.29)$$

since E_y is a constant. In terms of voltage and current (and hence treating the parallel-plate waveguide as a transmission line) the characteristic impedance of the TEM mode is

$$Z_0 = \frac{V}{I} = \frac{E_y d}{H_x W} = \frac{\eta d}{W}. \quad (6.30)$$

Here η is the intrinsic impedance of a TEM mode in the medium. Since we are considering a TEM mode, the wave impedance of the TEM mode is just

the intrinsic impedance, that is,

$$Z_{\text{TEM}} = E_y / H_x = Z_0|_{\text{free-space}} = \eta. \quad (6.31)$$

With $\eta_0 = \sqrt{\mu_0/\epsilon_0}$ being the free-space impedance, the characteristic impedance can be written

$$Z_0 = \frac{\eta_0 d}{W} \sqrt{\frac{\mu_r}{\epsilon_r}} \quad \text{and} \quad Z_{\text{TEM}} = \eta = \eta_0 \sqrt{\frac{\mu_r}{\epsilon_r}}. \quad (6.32)$$

The phase velocity ($= \omega/\beta$) is just the speed of light in the medium:

$$v_p = \frac{1}{\sqrt{\mu_0 \epsilon_0}} = \frac{c}{\sqrt{\mu_r \epsilon_r}}. \quad (6.33)$$

Formulas for attenuation are developed in [1] and the conductor attenuation

$$\alpha_c = \frac{R_s}{\eta d} \quad (\text{with SI units of Np/m}) \quad (6.34)$$

where $R_s = 1/(\sigma \delta_s)$ is the surface resistance of the conductor, σ is the conductivity of the conductor, and δ_s is the skin depth in the conductor. The attenuation due to dielectric loss is

$$\alpha_d = \frac{k^2 \tan \delta}{2\beta} \quad (\text{with SI units of Np/m}). \quad (6.35)$$

6.3.2 TM Mode

The **Transverse Magnetic Mode (TM)** is characterized by $H_z = 0$. Another restriction that will be used here in developing the field equations is that there is no variation of the fields in the x direction. Examining Equation (6.25) the only components of the field that could exist are E_y , E_z , and H_x . Everywhere E_y is perpendicular, and H_x is parallel, to the electrical walls so boundary conditions are satisfied for E_y and H_x . E_z will be parallel to the electrical walls at the walls so boundary conditions need to be applied in deriving E_z .

The boundary conditions are that the E field parallel to the conducting walls is zero. Considering E_z only, Equation (6.18) becomes

$$\frac{d^2 E_z}{dy^2} = -k_c^2 E_z. \quad (6.36)$$

The solution to Equation (6.36) is

$$E_z = [E_0 \sin(k_c y) + E_1 \cos(k_c y)] e^{-\gamma z}. \quad (6.37)$$

To find the coefficients E_0 and E_1 boundary conditions are applied so that E_z is zero at $y = 0$ and $y = d$ (since the E field parallel to the conductors must be zero), that is,

$$E_z|_{y=0} = 0 = E_1 \quad \text{and} \quad E_z|_{y=d} = 0 = E_0 \sin(k_c d). \quad (6.38)$$

This requires that $\sin(k_c d) = 0$, and thus requiring that there are discrete values of k_c :

$$k_c = m\pi/d \quad m = 1, 2, 3, \dots \quad (6.39)$$

(Note that $m = 0$ is also a solution but requires a separate derivation, see the summary for this section.) Each value of k_c identifies a different mode and m is the mode index. The m th mode is the TM_m mode and m indicates the number of half-sinusoidal variations of the fields in the y direction. The TM_m mode propagates if the wavelength of the signal is such that $\lambda \geq \lambda_c$, where λ_c is the critical wavelength of the m th mode.

Substituting the above results and assumptions (e.g., $\partial/\partial x = 0$) in Equation (6.25),

$$H_z = 0 \quad E_x = 0 \quad H_y = 0 \quad (6.40)$$

$$E_z = E_0 \sin(k_c y) e^{-\gamma z} \quad (6.41)$$

$$E_y = -\frac{\gamma}{k_c^2} \frac{dE_z}{dy} = -\frac{\gamma}{k_c} E_0 \cos(k_c y) e^{-\gamma z} \quad (6.42)$$

$$H_x = \frac{j\omega\epsilon}{k_c^2} \frac{dE_z}{dy} = \frac{j\omega\epsilon}{k_c} E_0 \cos(k_c y) e^{-\gamma z}. \quad (6.43)$$

These are the complete field descriptions of the TM parallel-plate waveguide modes with zero variation in the x direction. Recall that the wavenumber $k = \omega\sqrt{\mu\epsilon}$.

There are an infinite number of TM modes identified by the index m , which determines the cutoff wavenumber, k_c , of the particular mode. The propagation constant of the m th mode, i.e. the TM_m mode, is

$$\gamma = \sqrt{k_c^2 - k^2} = \sqrt{(m\pi/d)^2 - \omega^2\mu\epsilon}. \quad (6.44)$$

Propagation is only possible if γ has an imaginary component. Thus in a lossless medium $\gamma = j\beta$ and $\beta = \sqrt{k^2 - k_c^2}$. The cutoff frequency below which propagation is not possible is

$$f_c = \frac{1}{2\pi} \frac{k_c}{\sqrt{\mu\epsilon}} = \frac{1}{2\pi} \frac{m\pi}{d\sqrt{\mu\epsilon}} = \frac{m\nu}{2d}, \quad (6.45)$$

where $\nu = 1/\sqrt{\mu\epsilon}$ is the velocity of a TEM mode in the medium. The cutoff wavelength can also be defined as

$$\lambda_c = \frac{\nu}{f_c} = \frac{2d}{m}. \quad (6.46)$$

where ν is the speed of light in the medium. The wavelength of the TM_m mode, at a particular frequency, is the guide wavelength

$$\lambda_g = \frac{2\pi}{\beta} = \frac{\lambda}{\sqrt{1 - (f_c/f)^2}}, \quad (6.47)$$

where λ is the wavelength of a TEM mode in the medium: $\lambda = \nu/f$ (so $\lambda_g = \lambda$ when $k_c = 0$). The phase velocity of the modes is dependent on the mode index m through the cutoff frequency:

$$v_p = \frac{\omega}{\beta} = \frac{\nu}{\sqrt{1 - (f_c/f)^2}}, \quad (6.48)$$

and the group velocity is

$$v_g = \frac{d\omega}{d\beta} = \nu \sqrt{1 - (f_c/f)^2}. \quad (6.49)$$

The phase velocity, v_p , of a TM mode is greater than ν while the group velocity, v_g , is slower than ν . The group velocity is the velocity at which energy is transmitted and thus can never be faster than the speed of light, c . The phase velocity, however, can be greater than c . The TM mode field variation is shown on the right in Figure 6-4.

The wave impedance of the TM_m mode is

$$Z_{\text{TM}} = -E_y/H_x = \frac{\beta}{\omega\epsilon} = \frac{\beta\eta}{k}. \quad (6.50)$$

Formulas for attenuation are developed in [1] and the conductor attenuation

$$\alpha_c = \frac{2kR_s}{\beta\eta d} \quad (\text{with SI units of Np/m}) \quad (6.51)$$

where $R_s = 1/(\sigma\delta_s)$ is the surface resistance of the conductor, σ is the conductivity of the conductor, and δ_s is the skin depth in the conductor. The attenuation due to dielectric loss is

$$\alpha_d = \frac{k^2 \tan \delta}{2\beta}. \quad (\text{with SI units of Np/m}) \quad (6.52)$$

6.3.3 TE Mode

The **transverse electric (TE) mode** is characterized by $E_z = 0$. Following the same development as for the TM modes, the TE_n mode fields with n variations of the H_z are

$$E_z = 0, \quad E_y = 0, \quad H_x = 0 \quad (6.53)$$

$$H_z = H_0 \cos(k_c y) e^{-\gamma z} \quad (6.54)$$

$$E_x = \frac{j\omega\mu}{k_c} H_0 \sin(k_c y) e^{-\gamma z} \quad (6.55)$$

$$H_y = \frac{\gamma}{k_c} H_0 \sin(k_c y) e^{-\gamma z}. \quad (6.56)$$

The equations for k_c , v_p , v_g , f_c , λ_c , and λ_g of the TE_n mode are the same as for the TM_m mode considered in the previous section with the replacement of the mode index m by n , $n = 1, 2, 3, \dots$ (Note that $n = 0$ is also a solution but requires a separate derivation, see the summary for this section.) The TE mode field variation is shown on the right in Figure 6-4.

The wave impedance of the TE mode is

$$Z_{\text{TE}} = \frac{k\eta}{\beta}. \quad (6.57)$$

Formulas for attenuation are developed in [1] and the conductor attenuation

$$\alpha_c = \frac{2k_c^2 R_s}{k\beta\eta d} \quad (\text{with SI units of Np/m}) \quad (6.58)$$

where $R_s = 1/(\sigma\delta_s)$ is the **surface resistance**, η , of the conductor, σ is the conductivity of the conductor, and δ_s is the skin depth of the conductor. The attenuation due to dielectric loss is

$$\alpha_d = \frac{k^2 \tan \delta}{2\beta} \quad (\text{with SI units of Np/m}). \quad (6.59)$$

6.3.4 Summary

The TEM mode (where $k_c = 0$) is the same as the TM_0 mode and the TE_0 mode. Here derivations of the TE and TM modes began with from Equation (6.25) and were only solutions for $k_c \neq 0$. Development of the 0th order TE and TM modes requires derivation from Equation (6.26) but this was done for the TEM mode and so was not repeated for the TE_0 and TM_0 modes.

6.4 Rectangular Waveguide

A rectangular waveguide is shown in Figure 6-5(a). Rectangular waveguides guide EM energy between four connected electrical walls, and there is little current created on the walls. As a result, resistive losses are quite low, much lower than can be achieved using coaxial lines for example. One of the major uses of a rectangular waveguide is when losses must be kept to a minimum, so that a rectangular waveguide is used in very high-power situations such as radar, and at a few tens of gigahertz and above. At higher frequencies the loss of coaxial lines becomes very large, and it also becomes difficult to build small-diameter coaxial lines at 100 GHz and above. As a result, a rectangular waveguide is nearly always used above 100 GHz. There are many low- to medium-power legacy systems that use rectangular waveguides down to 1 GHz.

A rectangular waveguide supports many different modes, but it does not support the TEM mode. The modes are categorized as being either TM or TE, denoting whether all of the magnetic fields are perpendicular to the direction of propagation (these are the transverse magnetic fields) or whether all of the electric fields are perpendicular to the direction of propagation (these are the transverse electric fields). Dimensions of the waveguide can be chosen so that only one mode can propagate for a range of frequencies. With more than one mode propagating, the different components of a signal would travel at different speeds and thus combine at a load incoherently, since the ratio of the energy in the modes would vary (usually) randomly.

The TE and TM field descriptions are derived from the solution of differential equations—Maxwell's equations—subject to boundary conditions. The general solutions for rectangular systems are sinewaves and there are possibly many discrete solutions. The nomenclature that has developed over

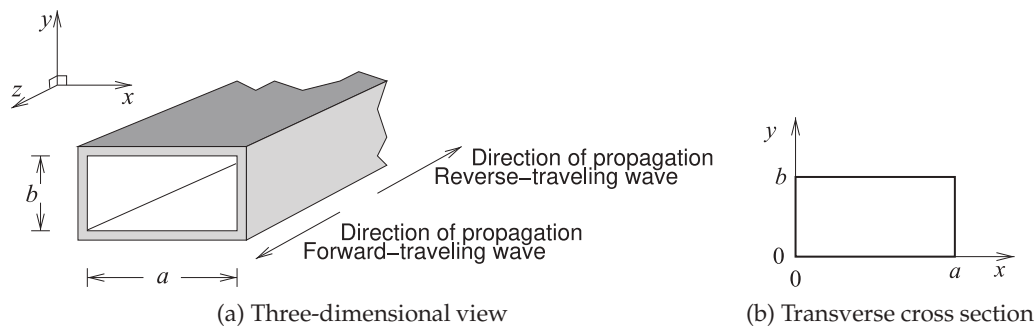


Figure 6-5: Rectangular waveguide with internal dimensions of a and b .

the years to classify modes references the number of variations in the x direction, using the index m , and the number of variations in the y direction, using the index n . So there are TE_{mn} and TM_{mn} modes, and dimensions are usually selected so that only the TE_{10} mode can propagate.

6.4.1 TM Modes

The development of the field descriptions for the TM modes begins with the rectangular wave equations derived in Section 6.2. Transverse magnetic waves have zero H_z , but nonzero E_z . The differential equation governing E_z is, in rectangular coordinates (from Equations (6.13) and (6.16)),

$$\nabla_t^2 E_z = \frac{\partial^2 E_z}{\partial x^2} + \frac{\partial^2 E_z}{\partial y^2} = -k_c^2 E_z. \quad (6.60)$$

Using a separation of variables procedure, this equation has the solution

$$E_z = [A' \sin(k_x x) + B' \cos(k_x x)] [C' \sin(k_y y) + D' \cos(k_y y)] e^{-\gamma z}, \quad (6.61)$$

$$\text{where } k_x^2 + k_y^2 = k_c^2. \quad (6.62)$$

The perfectly conducting boundary at $x = 0$ requires $B' = 0$ to produce $E_z = 0$ there. Similarly the ideal boundary at $y = 0$ requires $D' = 0$. Replacing $A'C'$ by a new constant A , then

$$E_z = A \sin(k_x x) \sin(k_y y) e^{-\gamma z}. \quad (6.63)$$

The axial electric field, E_z , must also be zero at $x = a$ and $y = b$. This can only be so (except for the trivial solution $A = 0$) if $k_x a$ is an integral multiple of π so that $\sin(k_x a) = 0$:

$$k_x a = m\pi, \quad m = 1, 2, 3, \dots \quad (6.64)$$

Similarly, for E_z to be zero at $y = b$, $\sin(k_y b) = 0$ and $k_y b$ must also be a multiple of π :

$$k_y b = n\pi, \quad n = 1, 2, 3, \dots \quad (6.65)$$

So the cutoff frequency of the TM wave with m variations in x and with n variations in y (i.e., the TM_{mn} mode) is, from Equation (6.62),

$$f_{c_{m,n}} = \frac{k_{c_{m,n}}}{2\pi\sqrt{\mu\epsilon}} = \frac{1}{2\pi\sqrt{\mu\epsilon}} \left[\left(\frac{m\pi}{a} \right)^2 + \left(n \frac{\pi}{b} \right)^2 \right]^{1/2}. \quad (6.66)$$

The remaining field components of the TM_{mn} wave are found with $H_z = 0$ and E_z from Equation (6.63) and Equation (6.25)):

$$E_x = -\frac{\gamma k_x}{k_{c_{m,n}}^2} A \cos(k_x x) \sin(k_y y) e^{-\gamma z} \quad (6.67)$$

$$E_y = -\frac{\gamma k_y}{k_{c_{m,n}}^2} A \sin(k_x x) \cos(k_y y) e^{-\gamma z} \quad (6.68)$$

$$H_x = \frac{j\omega\epsilon k_y}{k_{c_{m,n}}^2} A \sin(k_x x) \cos(k_y y) e^{-\gamma z} \quad (6.69)$$

$$H_y = -\frac{j\omega\epsilon k_x}{k_{c_{m,n}}^2} A \cos(k_x x) \sin(k_y y) e^{-\gamma z}. \quad (6.70)$$

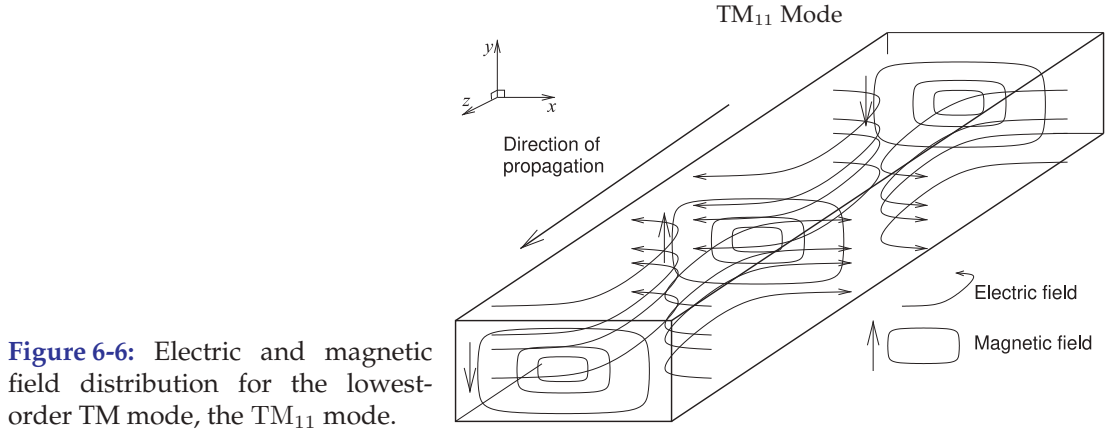


Figure 6-6: Electric and magnetic field distribution for the lowest-order TM mode, the TM_{11} mode.

The spatial field variations depend on the x and y cutoff wavenumbers, k_x and k_y , which in turn depend on the mode indexes and the cross-sectional dimensions of the waveguide. The cutoff wavenumber, k_c , is a function of the m and n indexes, and so $k_{c_{m,n}}$ is often used for the cutoff wavenumber with

$$k_{c_{m,n}}^2 = k_{x,m}^2 + k_{y,n}^2 = \left(\frac{m\pi}{a}\right)^2 + \left(\frac{n\pi}{b}\right)^2. \quad (6.71)$$

The lowest-order TM mode is the TM_{11} mode, with $m = 1$ and $n = 1$, and this has the minimum variation of the fields (of any TM mode); these are shown in Figure 6-6.

In summary, a mode can propagate only at frequencies above the cutoff frequency. Another quantity that defines when cutoff occurs is the cutoff wavelength, defined as

$$\lambda_c = \frac{\nu}{f_{c_{m,n}}}, \quad (6.72)$$

where $\nu = 1/\sqrt{\mu\epsilon}$ is the velocity of a TEM mode in the medium (and of course this is not a rectangular waveguide mode). The cutoff wavelength is the wavelength in the medium (without the waveguide walls) at which cutoff occurs. Since k_c^2 is $k^2 - \beta^2$, the attenuation constant of a given mode for frequencies below the cutoff frequency is

$$\alpha = \sqrt{k_{c_{m,n}}^2 - k^2} = k_{c_{m,n}} \sqrt{1 - \left(\frac{f}{f_{c_{m,n}}}\right)^2}, \quad f < f_{c_{m,n}}. \quad (6.73)$$

The phase constant for frequencies above the cutoff frequency is

$$\beta = \sqrt{k^2 - k_{c_{m,n}}^2} = k \sqrt{1 - \left(\frac{f_{c_{m,n}}}{f}\right)^2}, \quad f > f_{c_{m,n}}. \quad (6.74)$$

For a propagating mode (i.e., $f > f_{c_{m,n}}$) the wavelength of the mode, called the guide wavelength, is

$$\lambda_g = \frac{2\pi}{\beta} = \frac{\lambda}{\sqrt{1 - (f_c/f)^2}}, \quad (6.75)$$

where λ is the wavelength of a TEM mode in the medium (but of course not in the waveguide): $\lambda = \nu/f$. The phase velocity of the mode is also dependent on the mode indexes m and n through the cutoff frequency,

$$v_p = \frac{\omega}{\beta} = \frac{\nu}{\sqrt{1 - (f_{c_{m,n}}/f)^2}}, \quad (6.76)$$

and the group velocity is

$$v_g = \frac{d\omega}{d\beta} = \nu \sqrt{1 - (f_{c_{m,n}}/f)^2}. \quad (6.77)$$

6.4.2 TE Modes

Transverse electric waves have zero E_z and nonzero H_z so that, in rectangular coordinates,

$$\nabla_t^2 H_z = \frac{\partial^2 H_z}{\partial x^2} + \frac{\partial^2 H_z}{\partial y^2} = -k_c^2 H_z. \quad (6.78)$$

Solving using the separation of variables technique gives

$$H_z = [A'' \sin(k_x x) + B'' \cos(k_x x)] [C'' \sin(k_y y) + D'' \cos(k_y y)] e^{-\gamma z}, \quad (6.79)$$

$$\text{where } k_x^2 + k_y^2 = k_c^2. \quad (6.80)$$

Imposition of a boundary condition in this case is a little less direct, but the electric field components are

$$E_x = -\frac{j\omega\mu}{k_c^2} \frac{\partial H_z}{\partial y} \quad (6.81)$$

$$= -\frac{j\omega\mu k_y}{k_c^2} [A'' \sin(k_x x) + B'' \cos(k_x x)] [C'' \cos(k_y y) - D'' \sin(k_y y)] e^{-\gamma z}$$

$$E_y = \frac{j\omega\mu}{k_c^2} \frac{\partial H_z}{\partial x} \quad (6.82)$$

$$= \frac{j\omega\mu k_x}{k_c^2} [A'' \cos(k_x x) - B'' \sin(k_x x)] [C'' \sin(k_y y) + D'' \cos(k_y y)] e^{-\gamma z}.$$

For E_x to be zero at $y = 0$ for all x , $C'' = 0$; and for $E_y = 0$ at $x = 0$ for all y , $A'' = 0$. Defining $B''D'' = B$, then

$$H_z = B \cos(k_x x) \cos(k_y y) \quad (6.83)$$

$$E_x = \frac{j\omega\mu k_y}{k_c^2} B \cos(k_x x) \sin(k_y y) e^{-\gamma z} \quad (6.84)$$

$$E_y = -\frac{j\omega\mu k_x}{k_c^2} B \sin(k_x x) \cos(k_y y) e^{-\gamma z}. \quad (6.85)$$

E_y is zero at $x = a$, that is, $\sin(k_x a) = 0$, so that $k_x a$ must be a multiple of π :

$$k_x a = m\pi, \quad m = 1, 2, 3, \dots \quad (6.86)$$

Also, E_x is zero at $y = b$, that is, $\sin(k_y b) = 0$, so that $k_y b$ must be zero (so that E_x is always zero) or that it is a multiple of π . Therefore

$$k_y b = n\pi \quad n = 0, 1, 2, 3, \dots \quad (6.87)$$

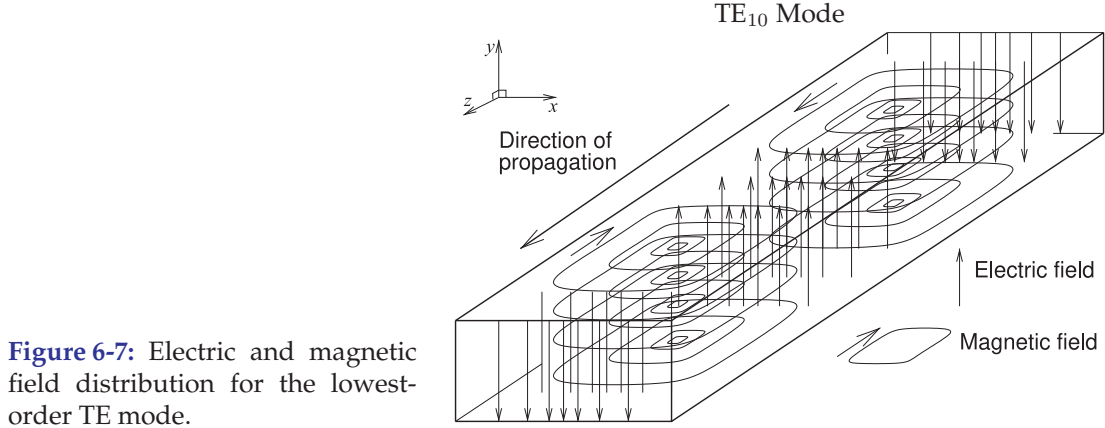


Figure 6-7: Electric and magnetic field distribution for the lowest-order TE mode.

The forms of the transverse electric field are then

$$E_x = \frac{j\omega\mu k_y}{k_{c_{m,n}}^2} B \cos(k_x x) \sin(k_y y) e^{-\gamma z} \quad (6.88)$$

$$E_y = -\frac{j\omega\mu k_x}{k_{c_{m,n}}^2} B \sin(k_x x) \cos(k_y y) e^{-\gamma z}, \quad (6.89)$$

and the corresponding transverse magnetic field components are

$$H_x = \frac{\gamma k_x}{k_{c_{m,n}}^2} B \sin(k_x x) \cos(k_y y) e^{-\gamma z} \quad (6.90)$$

$$H_y = \frac{\gamma k_y}{k_{c_{m,n}}^2} B \cos(k_x x) \sin(k_y y) e^{-\gamma z}. \quad (6.91)$$

Here the use of $k_{c_{m,n}}$ emphasizes that the cutoff wavenumber is a function of the m and n indexes:

$$k_{c_{m,n}}^2 = k_{x,m}^2 + k_{y,n}^2 = \left(\frac{m\pi}{a}\right)^2 + \left(\frac{n\pi}{b}\right)^2. \quad (6.92)$$

The lowest-order TE mode is the TE_{10} mode (with $m = 1$ and $n = 0$) and this has the minimum variation of the fields; these are shown in Figure 6-7.

6.4.3 Practical Rectangular Waveguide

The dimensions and operating frequencies of a rectangular waveguide are chosen to support only one propagating mode. The operating frequency is between the cutoff frequency of the mode with the lowest cutoff frequency and the cutoff frequency of the mode with the next lowest cutoff frequency. Thus only one mode propagates.

Referring to Figure 6-5, if the dimensions are chosen so that b is greater than a , then the lowest-order TE mode (the TE_{10} mode) has one variation of the fields in the x direction, while the lowest-order TM mode (the TM_{11} mode) has one variation of the field in the x direction and one variation in the y direction. Thus the cutoff frequency of the TM_{11} mode will be higher than the cutoff frequency of the TE_{10} mode. Below the cutoff frequency the modes will not propagate (i.e., β (the imaginary part of the propagation constant) is zero). The propagation constants of the rectangular waveguide

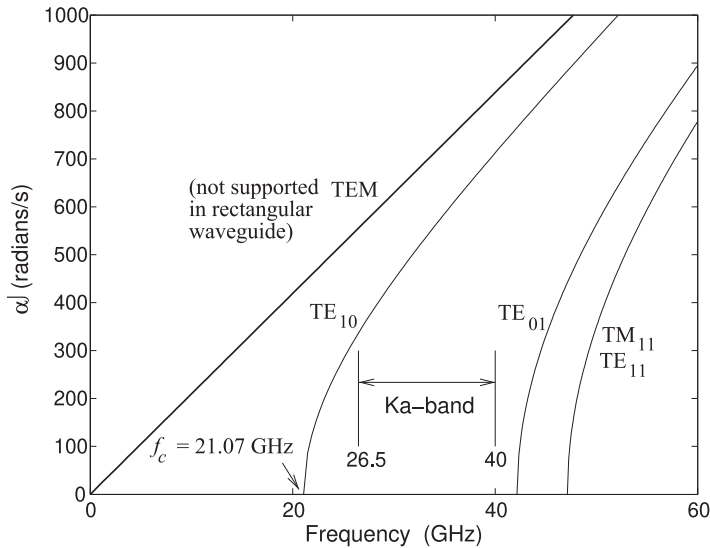


Figure 6-8: Dispersion diagram of waveguide modes in air-filled Ka-band rectangular waveguide with internal dimensions of 0.280×0.140 inches ($7.112 \text{ mm} \times 3.556 \text{ mm}$). Ka-band waveguide is used between 26.5 GHz and 40 GHz. Over this frequency range only the TE_{10} mode propagates.

Mode	Cut-off frequency (GHz)
TEM	not supported
TE_{10}	21.07 GHz
TE_{01}	42.15 GHz
TE_{11}	47.13 GHz
TM_{10}	not supported
TM_{01}	not supported
TM_{11}	47.13 GHz

Table 6-1: Cut-off frequencies of several modes in Ka-Band waveguide nominally used between 26.5 GHz and 40 GHz.

modes with the lowest cutoff frequencies are shown in Figure 6-8 for a Ka-band waveguide having internal dimensions of $a = 0.280$ inches and $b = 0.140$ inches. This figure is known as a dispersion diagram and is sometimes plotted as β versus k . There are four modes supported below 60 GHz and the line corresponding to the TEM mode is provided for reference, as the TEM mode is not supported in a rectangular waveguide.

Not all possible low-order modes can be supported in rectangular waveguide as the boundary conditions cannot be satisfied (see Table 6-1). The cutoff frequency of the TE_{10} mode is 21.07 GHz and the next lowest cutoff mode, the TE_{01} mode, has a cutoff frequency of 42.15 GHz. The mode has a cutoff frequency which is the frequency when the wavelength (in the medium, or free-space wavelength if the guide is air-filled) is twice the a dimension of the waveguide (see Figure 6-5). The next higher-order mode appears when it is possible for a variation in the y direction. This occurs at a frequency corresponding to the b dimension being one-half wavelength in the medium. The TE_{11} mode and TM_{11} modes have the same cutoff frequency of 47.13 GHz. In determining the operating frequency range both the phase and group velocity variations are considered. These are shown in Figure 6-9 for the TE_{10} mode, where they are normalized to c as the waveguide is air-filled. The group velocity, v_g , varies substantially, especially near the cutoff frequency of the mode. As a result, the lower operating frequency of the mode is chosen to be substantially above the cutoff frequency. The upper limit of the operating frequency is chosen to be about 5% below the cutoff frequency of the second propagating mode. This

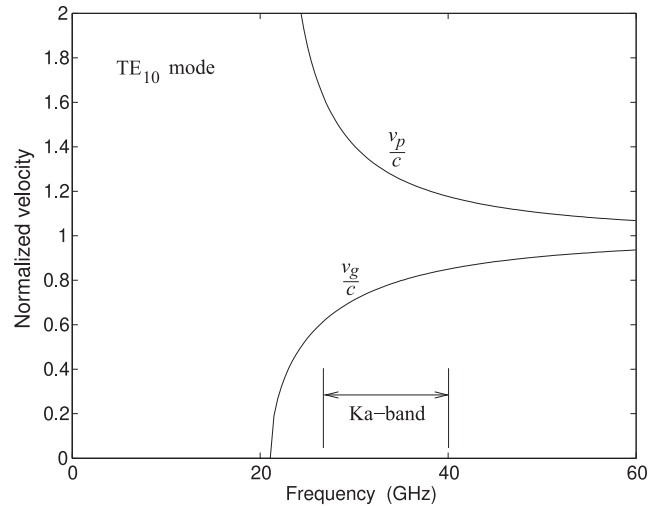


Figure 6-9: Normalized phase and group velocities of the TE_{10} mode in air-filled Ka-band waveguide.

is because small discontinuities can launch the higher-order mode. Thus the operating frequency of a Ka-band waveguide is 26.5 GHz–40 GHz, providing a margin of 5.4 GHz at the low end, and 2.2 GHz margin at the high end. So approximately one-half octave of bandwidth is supported by a rectangular waveguide if the wide dimension is twice the height of the waveguide. Since a rectangular waveguide is useful over a relatively narrow frequency range, standard dimensions have been developed, as listed in Table 6-2. A waveguide is referred to by its waveguide standard number (its WR designation), however, the old letter designations of bands are commonly used.

At times it is necessary to have a rectangular waveguide that can be used over more than one-half octave of bandwidth. This is achieved by reducing the height, b , of the waveguide, producing what is called a reduced-height waveguide. By reducing b to one-quarter of a , an octave of bandwidth can be obtained [2–4].

6.4.4 Rectangular Waveguide Components

Rectangular waveguide components require considerable machining, but the equivalents of many of the components that are available in microstrip can be realized. Invariably the lowest-order TE mode is used. This is the TE_{10} mode, with the field configuration shown in Figure 6-7. The characteristic of this mode is that the E-field is transverse to the direction of propagation. Many components have particular orientations to the planes of the E and H fields. Consider the rectangular waveguide bends shown in Figure 6-10. The bend in Figure 6-10(a) is called an H-plane bend, or H-bend, as the axis of the waveguide (which is in the direction of propagation) always remains parallel to the H field. With the E-plane bend, or E-bend, in Figure 6-10(b), the axis of the waveguide remains parallel to the E field. The flat sections at the end of the waveguide sections are called flanges. The pins in the flanges are alignment pins that insert into holes in the opposite flange.

In building circuits using rectangular waveguides, it is frequently necessary to rotate and twist the waveguide so that sections can be joined. Bends enable this, but **twists** (as shown in Figure 6-11) are also used.

Band	EIA waveguide band	Operating frequency (GHz)	Internal dimensions ($a \times b$, inches)	TE ₁₀ Cutoff (GHz)
	WR-2300	0.32–0.49	23.000×11.500	0.257
	WR-2100	0.35–0.53	21.000×10.500	0.281
	WR-1800	0.43–0.62	18.000×9.000	0.328
	WR-1500	0.49–0.74	15.000×7.500	0.393
	WR-1150	0.64–0.96	11.500×5.750	0.513
	WR-1000	0.75–1.1	9.975×4.875	0.592
	WR-770	0.96–1.5	7.700×3.385	0.766
	WR-650	1.12–1.70	6.500×3.250	0.908
R	WR-430	1.70–2.60	4.300×2.150	1.37
D	WR-340	2.20–3.30	3.400×1.700	1.74
S	WR-284	2.60–3.95	2.840×1.340	2.08
E	WR-229	3.30–4.90	2.290×1.150	2.58
G	WR-187	3.95–5.85	1.872×0.872	3.15
F	WR-159	4.90–7.05	1.590×0.795	3.71
C	WR-137	5.85–8.20	1.372×0.622	4.30
H	WR-112	7.05–10.00	1.122×0.497	5.26
X	WR-90	8.2–12.4	0.900×0.400	6.56
Ku	WR-62	12.4–18.0	0.622×0.311	9.49
K	WR-51	15.0–22.0	0.510×0.255	11.6
K	WR-42	18.0–26.5	0.420×0.170	14.1
Ka	WR-28	26.5–40.0	0.280×0.140	21.1
Q	WR-22	33–50	0.224×0.112	26.3
U	WR-19	40–60	0.188×0.094	31.4
V	WR-15	50–75	0.148×0.074	39.9
E	WR-12	60–90	0.122×0.061	48.4
W	WR-10	75–110	0.100×0.050	59.0
F	WR-8	90–140	0.080×0.040	73.8
D	WR-6	110–170	0.0650×0.0325	90.8
G	WR-5	140–220	0.0510×0.0255	116
	WR-4	170–260	0.0430×0.0215	137
	WR-3	220–325	0.0340×0.0170	174
Y	WR-2	325–500	0.0200×0.0100	295
	WR-1.5	500–750	0.0150×0.0075	393
	WR-1	750–1100	0.0100×0.0050	590

Table 6-2: Waveguide bands, operating frequencies, and internal dimensions. Waveguide dimensions specified in inches (use 25.4 mm/inch to convert to millimeters). The number in the WR designation is the long internal dimension of the waveguide in hundreds of an inch. The TE₁₀ mode cutoff frequency is when the long dimension is one-half wavelength long (the free-space wavelength if vacuum- or air-filled, or modified by the square root of the permittivity if the waveguide is dielectric filled).

Waveguide **tees** are used to split and combine signals. There are both E-plane and H-plane versions, as there were for **bends** (see Figure 6-12).

There is a wide variety of waveguide components. The components are developed from EM field considerations and not derived from current and voltage circuits. For example, a **termination** in a rectangular waveguide is realized using a resistive wedge of material as shown in Figure 6-13(a). This provides a termination with a lower reactive component than would be obtained with a lumped resistor placed at the end of the line. The matched load absorbs all of the power in the traveling wave incident on it. The functional component is a lossy material, often shaped as a wedge or tall pyramid, that absorbs power over a distance corresponding, perhaps, to one-half wavelength or longer. So while the characteristic impedance of a wave in the rectangular waveguide varies with frequency, the termination is always matched to this impedance. A high-power waveguide matched load is shown in Figure 6-13(b). This component uses the structure illustrated in Figure 6-13(a) and has fins for the dissipation of heat. A **waveguide**

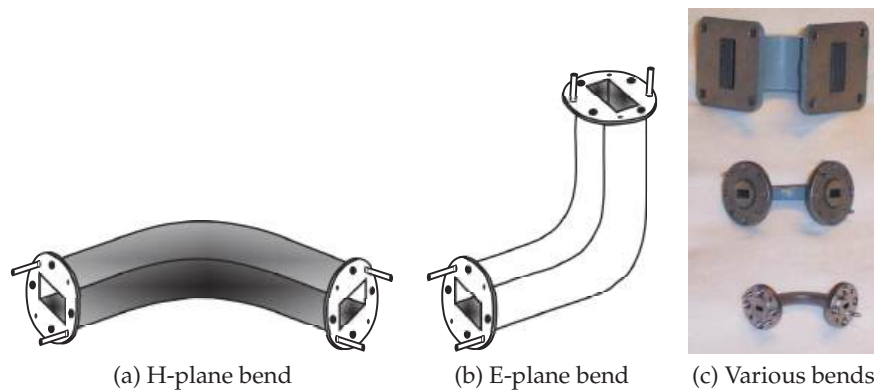


Figure 6-10: Rectangular waveguide bends. In (c), top is X-band (8–12 GHz), middle is Ku-band (12–18 GHz), and bottom is Ka-band (26–40 GHz).



Figure 6-11: Rectangular waveguide twist.

(a) Diagrammatic view

(b) Photograph

attenuator is realized by introducing resistive material, as shown in Figure 6-13(c). This introduces a section of line with a high attenuation coefficient. By controlling the depth of the resistive vane, as shown in Figure 6-13(d), a **variable attenuator** is obtained.

Discontinuities in the waveguide introduce inductive, capacitive, and resonant elements. Several discontinuities that are used to realize these elements are shown in Figure 6-14. These illustrate most clearly the use of E and H field disturbances to realize capacitive and inductive components. An E-plane discontinuity (Figure 6-14(a)) is modeled approximately by a frequency-dependent capacitor. H-plane discontinuities (Figure 6-14(b and c)) resemble inductors, as does the circular iris of Figure 6-14(d). The resonant waveguide iris of Figure 6-14(e) disturbs the E and H fields and is modeled by a parallel LC resonant circuit near the frequency of resonance. Posts in the waveguide are used as reactive elements (Figure 6-14(f)) and to mount active devices (Figure 6-14(g)). The equivalent circuits of waveguide discontinuities are modeled by capacitive elements if the E field is interrupted and by inductive elements if the H field (or current) is disturbed. Many papers (e.g., [5–8]) have been devoted to analytic field solutions that lead to equivalent lumped element representations of waveguide discontinuities that can then be used in synthesis.

A rectangular waveguide circulator is shown in Figure 6-15. A **circulator** uses a special property of magnetized ferrites that provides a preferred direction of EM propagation.

It is sometimes necessary to interface between waveguide series, and one component to do this is the tapered waveguide section shown in Figure 6-16(a). Alternatively the one-quarter wavelength long impedance transformer

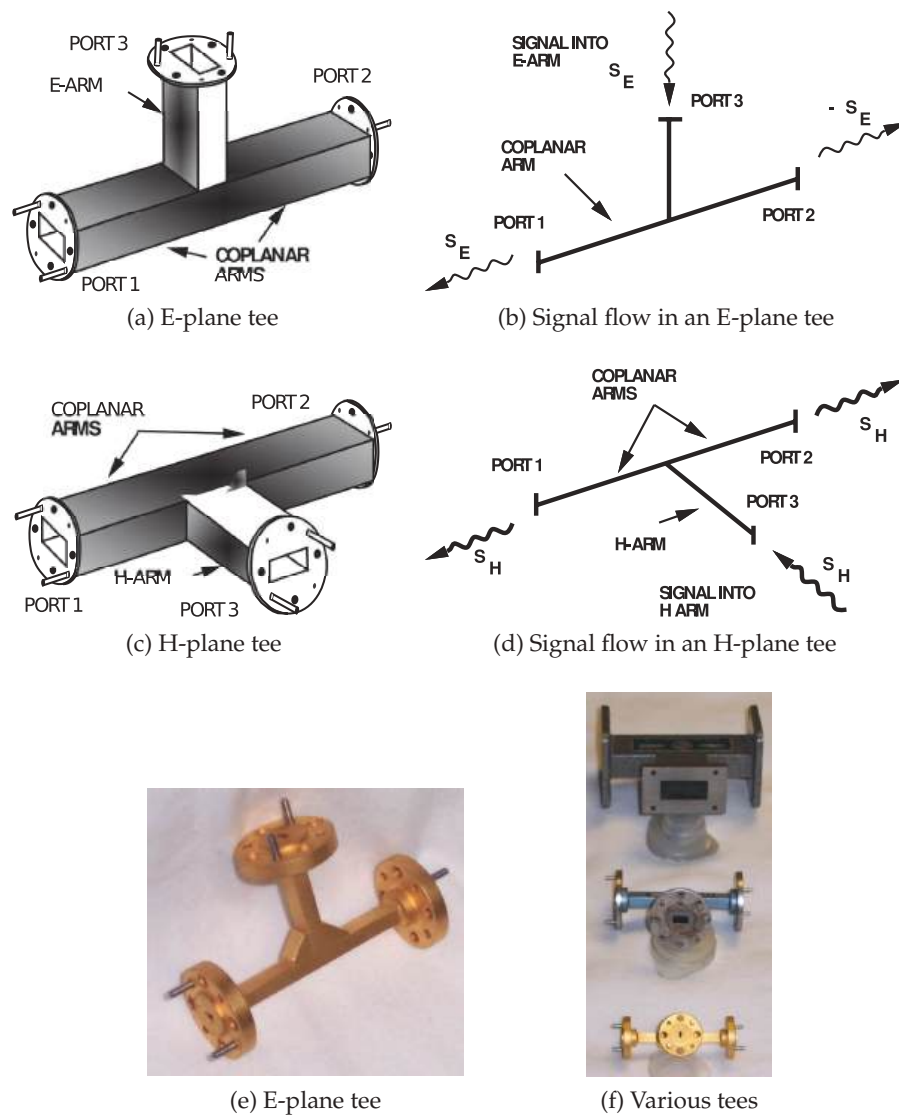


Figure 6-12: Rectangular waveguide tees: (a) three-dimensional representation of an E-plane tee; (b) description of the signal flow in an E-plane tee; (c) three-dimensional representation of an H-plane tee; (d) description of the signal flow in an H-plane tee; (e) photograph of an E-plane tee; and (f) photograph of waveguide tees for different waveguide bands (top, X-band H-plane tee; middle, Ku-band H-plane tee; bottom, Ka-band E-plane tee).

shown in Figure 6-16(b) could be used. This section can be shorter than the tapered waveguide section, which, however, has higher bandwidth.

Other components commonly encountered are the waveguide switch (see Figure 6-16(c)), the **coaxial-to-waveguide adaptor** (see Figure 6-17), and the waveguide horn antenna (see Figure 6-16(d)).

Distributed directional couplers are realized by two coupled transmission lines. A **rectangular waveguide directional coupler** is shown in Figure 6-18.

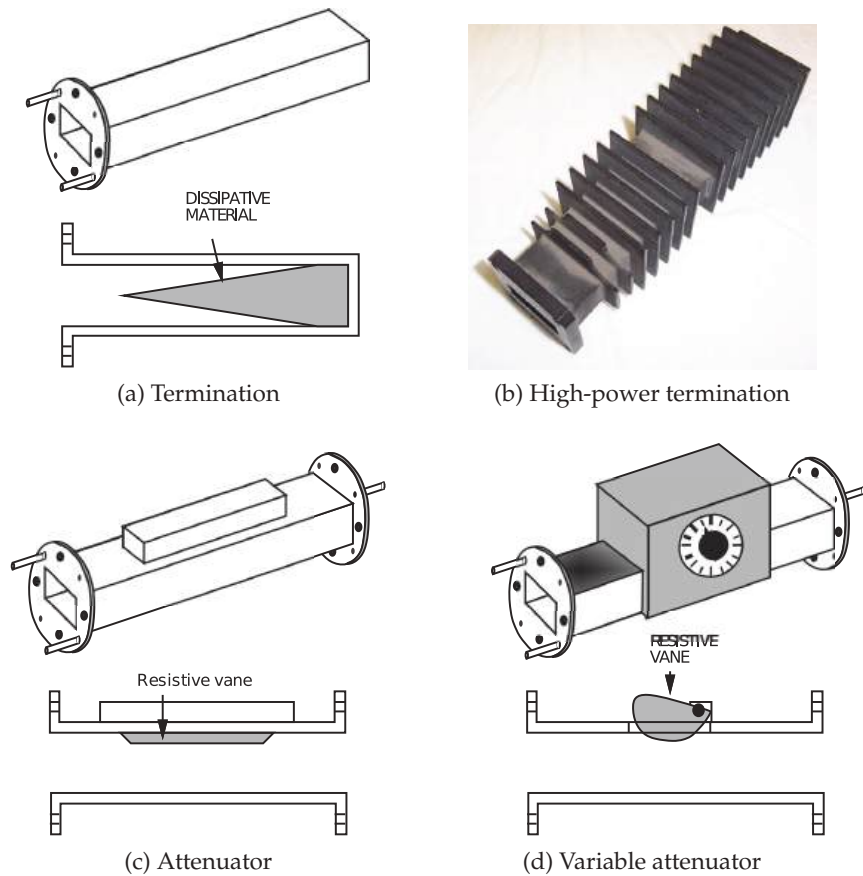
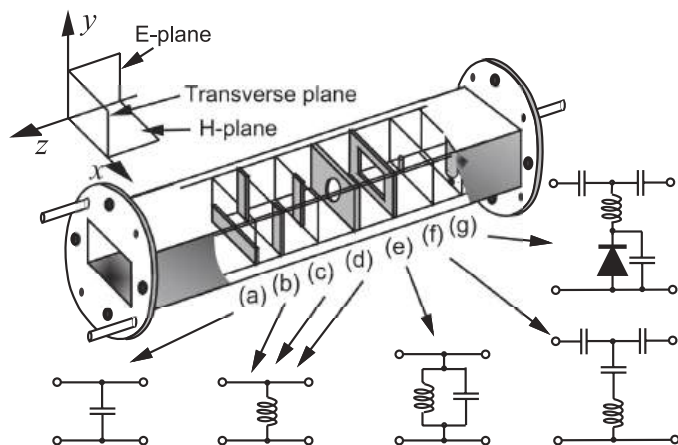


Figure 6-13: Terminations and attenuators in a rectangular waveguide.

Figure 6-14: Rectangular waveguide discontinuities and their lumped equivalent circuits: (a) capacitive E-plane discontinuity; (b) inductive H-plane discontinuity; (c) symmetrical inductive H-plane discontinuity; (d) inductive post discontinuity; (e) resonant window discontinuity; (f) capacitive post discontinuity; and (g) diode post mount.



Here the two transmission lines, the rectangular waveguides, are coupled by slots in the common wall of the guides. In Figure 6-18(b) the EM wave from the bottom waveguide leaks into the top waveguide through the coupling slots. A quick check on phasing indicates that the coupled wave in the reverse direction is canceled. Meanwhile, in the forward-traveling direction there is constructive interference of the coupled EM wave.

Variable elements available in a rectangular waveguide include the micrometer **tuner**, shown in Figure 6-19. The tuner shown in Figure 6-19(a)

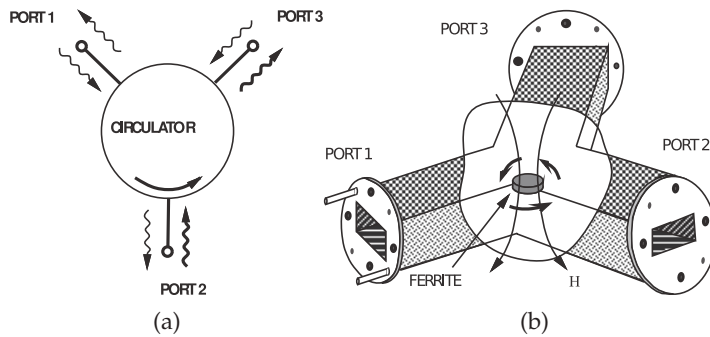


Figure 6-15: Waveguide circulator: (a) schematic; and (b) three-dimensional representation showing H field lines magnetizing a ferrite disk.

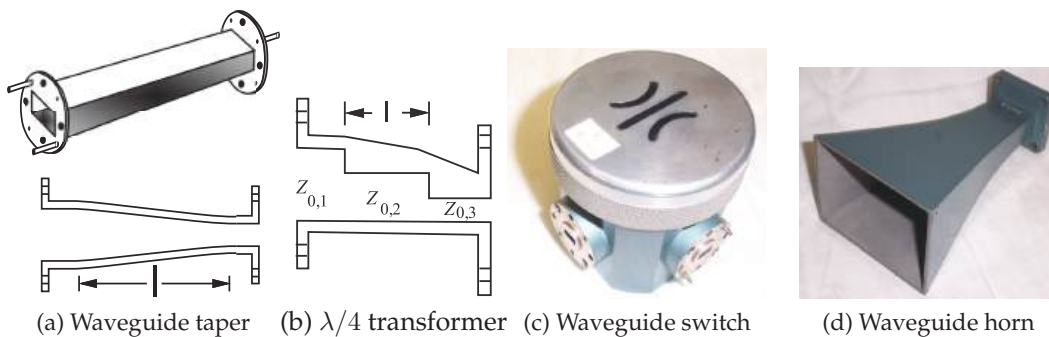


Figure 6-16: Waveguide components: (a) waveguide switch; (b) rectangular waveguide quarter-wavelength impedance transformer; (c) rectangular waveguide taper connecting one waveguide series to another; and (d) waveguide horn antenna.

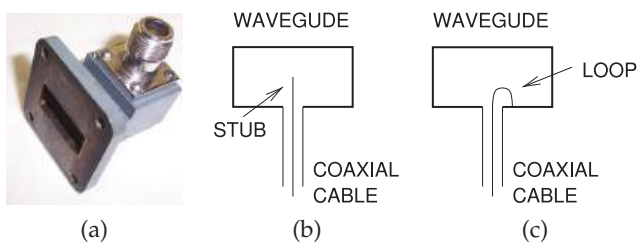


Figure 6-17: Coaxial transmission line to rectangular waveguide adaptor: (a) photograph; (b) adaptor using a coupling stub; and (c) adaptor using a coupling loop.

typically moves a reactive element along the waveguide. One example is the movable short circuit shown in Figure 6-19(b). Another variable element used in tuning is the waveguide slide tuner, shown in Figure 6-19(c). Here a slot is cut in the wide wall of the waveguide and a metal probe is inserted. The slot is in a region where the currents in the waveguide wall are minimum, so little discontinuity is introduced. The probe introduces a reactive discontinuity, and the reactance can be varied by changing the depth of penetration of the probe using the knob seen on top. The probe can move up-and-down along the slot to further increase the impedance range that can be presented.

Hybrids in waveguides (Figure 6-20) do not look anything like their microstrip equivalents.

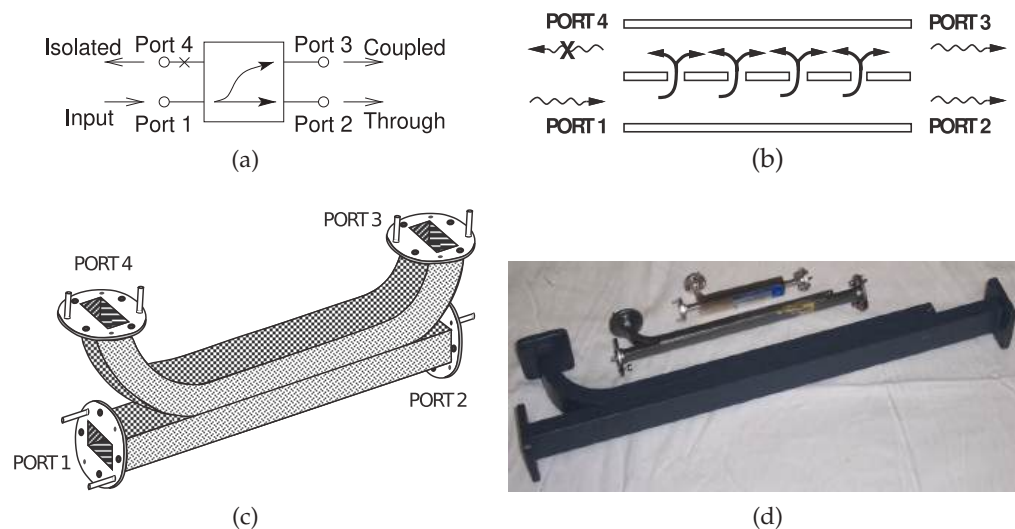


Figure 6-18: Rectangular waveguide directional couplers: (a) schematic; (b) and (c) waveguide directional coupler showing coupling slots; and (d) three directional couplers with the fourth port terminated in an integral matched load. In (d), from top to bottom: W-band, 10 cm long; Ka-band, 15 cm long, and X-band, 35 cm long.

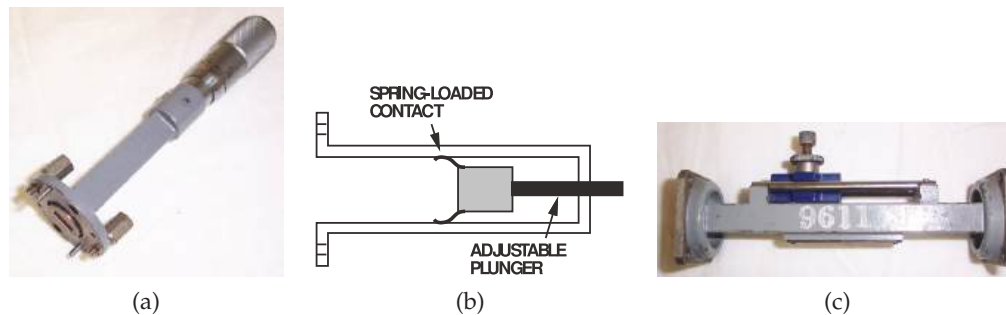


Figure 6-19: Waveguide tuners: (a) micrometer-driven variable short circuit; (b) internal details of a variable short circuit; and (c) waveguide slide tuner.

6.5 Summary

Rectangular waveguides guide EM fields in a rectangular pipe. Parallel plate waveguides are unintentional but are approximated by the planar conductors found in printed circuit boards. Rectangular wave equations describe propagation in these structures and are derived from Maxwell's equations by applying multiple simplifications such as using phasors, restricting propagation to just one direction, and applying symmetries. Important concepts that flow from the rectangular wave equations are that rectangular and parallel-plate waveguides support multiple modes, i.e. variations of the EM field, with all but the TEM mode having a finite cut-off frequency below which a particular mode cannot propagate. The

rectangular waveguide does not support a TEM mode, a mode with no variations of the field between boundaries, so the rectangular waveguide cannot support a propagating mode below the lowest cut-off frequency. A mode with more variations of the field will have a higher cut-off frequency. A separate physical result is that if two modes can propagate the EM energy will be equally partitioned between them. Thus if two or more modes can propagate the information will become garbled since different modes travel at different speeds. This is observed in practice so for example, with rectangular waveguide the useful frequency range of operation is between the cut-off frequency of the mode with the simplest field variation, and hence the lowest cut-off frequency, and the cut-off frequency of the next higher-order mode.

6.6 References

- [1] R. E. Collin, *Foundations for Microwave Engineering*. John Wiley & Sons, 2007.
- [2] H.-S. Oh and K.-W. Yeom, "A full ku-band reduced-height waveguide-to-microstrip transition with a short transition length," *IEEE Trans. on Microwave Theory and Techniques*, vol. 58, no. 9, pp. 2456–2462, Sep. 2010.
- [3] A. Tribak, J. Cano, A. Mediavilla, and M. Boussouis, "Octave bandwidth compact turnstile-based orthomode transducer," *IEEE Microwave and Wireless Components Letters*, vol. 20, no. 10, pp. 539–541, Oct. 2010.
- [4] N. Erickson, "High efficiency submillimeter frequency multipliers," in *1990 IEEE MTT-S Int. Microwave Symp. Dig.*, May 1990, pp. 1301–1304.
- [5] R. Eisenhart and P. Khan, "Theoretical and experimental analysis of a waveguide mounting structure," *IEEE Trans. on Microwave Theory and Techniques*, vol. 19, no. 8, pp. 706–719, Aug. 1971.
- [6] J. Bornemann and R. Vahldieck, "Characterization of a class of waveguide discontinuities using a modified te_{mn}^x mode approach," *IEEE Trans. on Microwave Theory and Techniques*, vol. 38, no. 12, pp. 1816–1822, Dec. 1990.
- [7] T. Rozzi and W. Mecklenbrauker, "Wide-band network modeling of interacting inductive irises and steps," *IEEE Trans. on Microwave Theory and Techniques*, vol. 23, no. 2, pp. 235–245, Feb. 1975.
- [8] P. Khan and M. Steer, "Analysis of bias-pin resonator diode mounts for millimeter-wave oscillators," *Proc. IEEE*, vol. 67, no. 11, pp. 1556–1557, Nov. 1979.

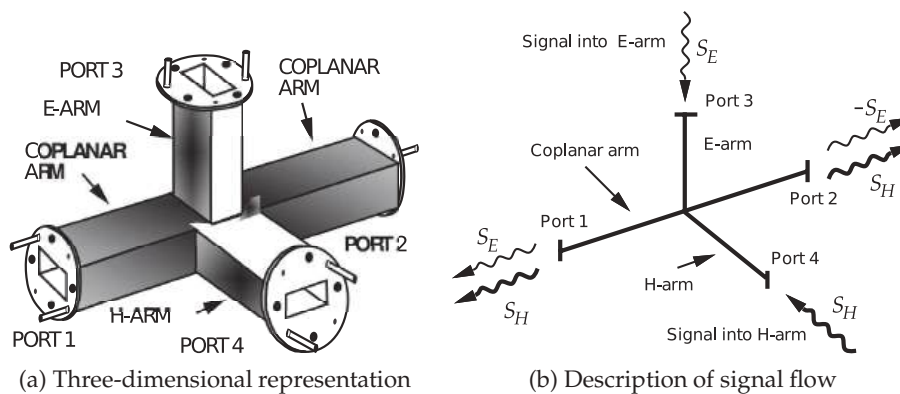


Figure 6-20: Rectangular waveguide hybrid.

6.7 Exercises

1. A four-layer circuit board has four levels of metalization with the two inner layers being supply and ground planes are RF grounds. The top layer has a very dense concentration of signal lines and for the purposes of understanding the fields in the dielectric between the top two layers of metalization both layers of metalization can be considered to be solid. The situation now reduces to a parallel plate waveguide which allows signals to travel in the dielectric from one region of the circuit board to another. The dielectric has a relative permittivity of 4 and the thickness of the dielectric between the metal layers is 1 mm.
 - (a) What is the mode that propagates at the lowest frequency and what is the cut-off wavenumber and cut-off frequency of this mode?
 - (b) What is the wave impedance of this mode at 1 GHz?
 - (c) What is the phase velocity of this mode at 1 GHz?
2. A multi-layer circuit board forms a parallel plate waveguide between the metal planes (even if they are broken up a little). Thus EM energy propagates around the circuit board and not all of the energy is confined by the circuit board lines.
 - (a) What is the EM mode that is mostly to propagate?
 - (b) Draw the E and H fields of the mode in cross section.
 - (c) If the distance between the plates is 1 mm, what is the lowest frequency at which this lowest order mode can propagate.
3. Two adjacent layers of a circuit board are continuous ground planes separated by a 0.5 mm-thick dielectric having a relative permittivity of 4.
 - (a) What is the lowest frequency at which the TEM mode propagates.
 - (b) What is the wave impedance of the TEM mode at 10 GHz.
4. Two adjacent layers of a circuit board are continuous ground planes separated by a 0.5 mm-thick dielectric having a relative permittivity of 4. What is the lowest frequency at which the TM_1 mode propagates.
5. Two adjacent layers of a circuit board are continuous ground planes separated by a 0.5 mm-thick dielectric having a relative permittivity of 4. What is the lowest frequency at which the TE_1 mode propagates.
6. An air-filled W-band waveguide has a 75–100 GHz operating frequency, extends in the z direction and has internal dimensions of $\Delta x = 0.100$ in. by $\Delta y = 0.050$ in. f_c is the cut-off frequency, and k_c is the cutoff wavenumber.
 - (a) Does the waveguide support a transverse electromagnetic (TEM) mode provide your reasons?
 - (b) What is the distinguishing feature of the TE waveguide modes?
 - (c) What is the distinguishing feature of the TM waveguide modes?
 - (d) What modes other than TEM, TE, and TM modes propagate in rectangular waveguide?
 - (e) Are TE_{00} and TM_{00} modes supported in the waveguide and why?
 - (f) What is k_c of the TE_{10} mode?
 - (g) What is k_c of the TE_{01} mode?
 - (h) What is k_c of the TE_{11} mode?
 - (i) What is f_c of the TE_{10} mode?
 - (j) What is f_c of the TE_{01} mode?
 - (k) What is the wavenumber of the TE_{01} mode at 90 GHz, discuss if your answer is not real?
 - (l) What is the wavenumber of the TE_{10} mode at 90 GHz, discuss if your answer is not real?
 - (m) What is f_c of the TE_{11} mode?
 - (n) What is k_c of the TM_{10} mode?
 - (o) What is k_c of the TM_{01} mode?
 - (p) What is k_c of the TM_{11} mode?
 - (q) What is k_c of the TM_{10} mode?
 - (r) What is f_c of the TM_{01} mode?
 - (s) What is f_c of the TM_{11} mode?
 - (t) What can you say about the relative cut-off frequency of the TE_{mn} and TM_{mn} , $m + n \geq 2$, modes relative to the cutoff frequencies of the TE_{mn} and TM_{mn} , $m + n = 1$, modes?
 - (u) Sketch and label the dispersion curves for the TE_{mn} and TM_{mn} , $m, n = 0, 1$, modes, i.e. β versus frequency over the frequency range 0 to 200 GHz.
 - (v) What is the frequency range over which only one mode can propagate?
 - (w) Why is it desirable that only one mode propagate?
 - (x) Why is the operating frequency range specified for this waveguide less than the frequency range over which only one mode can exist.
7. An air-filled E-band waveguide has a 60–90 GHz operating frequency and has internal dimensions of 0.122 in by 0.061 in.
 - (a) What is the phase velocity of the TE_{10} mode

- at 60 GHz.
- (b) What is the phase velocity of the TE_{10} mode at 90 GHz.
 - (c) What is the wave impedance of the TE_{10} mode at 60 GHz.
 - (d) What is the wave impedance of the TE_{10} mode at 90 GHz.
 - (e) What is the difference between characteristic impedance and wave impedance for the waveguide?
8. An X-band waveguide has the dimensions $0.9 \text{ in} \times 0.4 \text{ in}$. Calculate the cut-off frequencies for the TE_{10} , TE_{01} , and TM_{11} , modes.
 9. An X-band waveguide has the dimensions $0.9 \text{ in} \times 0.4 \text{ in}$. Calculate the cut-off frequencies for the TE_{10} , TE_{01} , and TM_{11} , modes.
 10. A W-band waveguide has the dimensions $0.1 \text{ in} \times 0.05 \text{ in}$ and the cut-off frequency of the TE_{10} mode is 59.0 GHz. Verify this.
 - (a) What is the cut-off frequencies of the TE_{01} mode?
 - (b) What is the cut-off frequencies of the TM_{11} mode?
 - (c) What is the the operating frequency range over which only one mode can exist?
 11. An E-band waveguide has the dimensions $0.122 \text{ in} \times 0.061 \text{ in}$ and the cut-off frequency of the TE_{10} mode is 48.4 GHz. Verify this.
 - (a) What is the cut-off frequency of the TE_{01} mode?
 - (b) What is the cut-off frequency of the TM_{11} mode?
 - (c) What is the the frequency range over which only one mode can exist?
 12. A W-band waveguide has the dimensions $0.1 \text{ in} \times 0.05 \text{ in}$. At 100 GHz only the TE_{10} mode can propagate. At 100 GHz and for the TE_{10} mode
 - (a) what is the wave impedance?
 - (b) what is the phase velocity?
 - (c) what is the group velocity?
 13. An E-band waveguide has the dimensions $0.1 \text{ in} \times 0.05 \text{ in}$. At 38 GHz only the TE_{10} mode can propagate. At 38 GHz and for the TE_{10} mode
 - (a) what is the wave impedance?
 - (b) what is the phase velocity?
 - (c) what is the group velocity?
 14. A communication system at 60 GHz has a bandwidth of 4 GHz so that the operating frequency range is 58 GHz to 62 GHz. Waveguide is to be used to route the millimeter-wave signal to an antenna. What waveguide should be used to justify your answer.
 15. A communication system 15 GHz has a bandwidth of 1 GHz so that the operating frequency range is 14.5 GHz to 15.5 GHz. Waveguide is to be used to route the millimeter-wave signal to an antenna. What waveguide should be used to justify your answer.

6.7.1 Exercises by Section

§6.2 1, 2, 3, 4, 5

§6.4 6, 7, 8, 9, 10, 11, 12, 13, 14, 15

Index

- η , 260, 263
- ∇ , 37
- $\nabla \cdot$, 12
- $\nabla \times$, 12
- α , 57, 61
- β , 57, 61
- γ , 56, 61
- δ , 171
- ε , 54, 138
- ε_0 , 12, 54
- ε' , 135
- ε_0 , 125
- ε'' , 135
- ε_e , 145
- ε_r , 54, 135
- ε_{ee} , 220
- ε_{eo} , 220
- η_0 , 220
- μ , 54, 138
- μ_0 , 10, 54, 125, 138
- μ_r , 54
- λ , 52, 57
- λ_0 , 54
- λ_g , 54
- π , 125
- ρ_V , 8
- ρ_{mV} , 8
- σ , 135
- σ , 171
- χ_e , 12
- ω , 57
- A, 123
- ABCD parameters
 - coupled line, 238
 - lossless transmission line, 109
 - lossy transmission line, 109
 - transmission line, 108
- absolute zero temperature, 126
- adaptor
 - coax to waveguide, 273
- air bridge, 237
- air, electrical properties, 137
- alumina
 - electrical properties, 137
 - microstrip, 146, 148
- ampere, 123
- Ampere's law, 16
- anisotropy, dielectric, 12
- APC-7, 63
- arcsinh series expansion, 41
- artanh series expansion, 41
- area
 - formula, 40
 - incremental, 9
- atmospheric pressure, 125
- attenuation
 - coefficient, 56
 - low-loss line, 89
 - conductive, 89
 - constant, 60–62, 89, 91, 177
 - definition, 57
 - dielectric, 89
 - low-loss line, 89
 - ohmic, 89
- attenuator, 276
 - rectangular waveguide, 272
- available
 - power, 93, 95
- B, 8
- backward-traveling wave, 56, 69
- bend
 - rectangular waveguide, 271
- bilinear
 - interpolation, 45
 - transformation, 46
- binomial
 - coefficients, 41
 - series expansion, 41
- Biot–Savart law, 16
- Boltzmann constant, 125
- Born, 19
- bounce diagram, 98
 - small reflections, 102
- boundary
 - transmission and reflection, 99
- Butterworth
 - polynomial, 42
- C, 123
- C , 51, 230
- c , 52, 125
- candela, 123
- capacitance matrix, 214
- capacitor
 - Maxwell–Wagner, 194
- Cartesian coordinates, 38
- cd, 123
- chain
 - parameters
 - transmission line, 108
- characteristic
 - impedance, 56, 62, 67, 69, 145, 146
 - effective, 145
 - free space, 220
 - medium, 28
 - microstrip, 146
 - parallel wires, 110
 - rectangular coaxial line, 110
 - slabline, 111
 - square coaxial line, 110
 - stripline, 154
 - twisted pair, 111
- charge
 - density, 9
 - magnetic, 9
 - surface, 9
 - electric, 8, 9
 - magnetic, 8, 9
- Chebyshev
 - polynomial, 42
- circle
 - area, 40
 - on complex plane, 45
- circulator
 - rectangular waveguide, 272
- closed
 - contour, 9
 - surface, 9
- coaxial
 - line, 52, 53, 62, 111, 114
 - characteristic impedance derivation, 111
 - maximum power-carrying, 62
 - minimum loss, 63
 - rectangular, 110
 - RLGC, 111
 - square, 110
 - waveguide adaptor, 275
- coefficient
 - attenuation, 56
 - phase-change, 56
- comblines
 - section, 238
- common
 - impedance coupling, 248
 - mode, 245
- complex
 - number, 34
 - hyperbolic function, 39
 - plane
 - circle, 45
- complex permittivity, 24
- conductive loss, 25
- conductivity, 24, 135
 - electrical, table, 127
 - of materials, 127
 - thermal, 127
 - thermal, table, 127
- conductor
 - and EM fields, 20
 - attenuation, 89
 - loss, microstrip, 193
 - lossy, 26
- cone, area and volume, 40
- constants
 - physical, 125
- contour, closed, 9
- coordinates
 - Cartesian, 38
 - cylindrical, 38
 - rectangular, 38
 - spherical, 39
- coplanar
 - strip, 139, 160
 - waveguide, *see* CPW, 157
 - modes, 191
- cos, 34, 39
 - series expansion, 41
- cosh, 39
 - series expansion, 41
- coulomb, 9, 123
- Coulomb's law, 18
- coupled lines, 205, 206, 221
 - ABCD parameters, 238
 - capacitance matrix, 214
 - extraction, 214
- characteristic impedance, 219
- comblines section, 238
- common mode, 245
- differential mode, 245

- directional coupler, 229, 230
 even mode, 207, 220–222
 even-mode capacitance, 217
 interdigital section, 238
 meander section, 238
 model, 237, 242
 low frequency, 212
 modes, 207, 208
 odd mode, 207, 220–222
 effective permittivity, 220
 odd-mode capacitance, 217
 physics, 206
 symmetric, 215
 synthesis, 244
 system impedance, 221
 theory, 210, 211
 traveling waves, 207
 coupler, 229
 20 dB, 230
 Lange, 236
 optimum length, 230
 slow wave, 194
 coupling
 common impedance, 248
 factor, 229–231
 directional coupler, 230
 CPS, 139, 160
 crosstalk, 161
 dispersion, 161, 175
 radiation, 161
 CPW, 138, 139, 157
 dispersion, 175
 finite ground, 139, 157
 high frequency, 191
 loss, 159
 modes, 191
 multimoding, 191
 cross product, vector, 37
 cubic equation, 48
 curl, 12
 operator, 37
 current
 bunching, 169
 density
 electric, 9
 magnetic, 9
 electric, 8, 9
 magnetic, 8, 9
 cutoff wavenumber, 257
 cylinder
 area and volume, 40
 cylindrical coordinates, 38

D, 230
D, 8
 dB
 Np equivalence, 61
 del operator, 37
 identities, 39
 delay line, slow wave, 194
 density, 127
 dielectric, 62, 135
 and EM fields, 19
 anisotropy, 12
 attenuation, 89
 constant, 54
 damping, 24, 135
 dispersion, 175
 effect of, 135
 isotropy, 12
 loss, 135
 microstrip, 193
 lossy, 24
 mode, 187
 refractive index, 19
 relaxation, 135
 differential
 interconnect, 160
 line, 138–140, 160
 embedded, 138, 140
 mode, 245
 directional
 coupler, 229, 230, 233
 coupling factor, 230
 design equations, 231
 design example, 231, 235
 hybrid, 232
 isolation, 230
 Lange, 236
 optimum length, 230
 rectangular waveguide, 273
 transmission factor, 230
 with lumped capacitors, 232
 directivity, 230
 directional coupler, 230
 factor, 229
 discontinuity
 rectangular waveguide, 272
 dispersion, 91, 135, 175
 dielectric, 175
 resistance, 175
 dispersionless line, lossy, 92
 div, 12
 operator, 37
 divergence theorem, 16
 dot product, vector, 36
 duroid, electrical
 properties, 137
 dyadic, 11
 permittivity, 12

E, 8
 e, natural number, 40, 125
 series expansion, 40
 E_L , 115
 E_T , 53, 114
 effective
 characteristic impedance, 145
 permittivity, 141, 145
 relative permeability, 60
 relative permittivity, 60, 145
 electric
 charge, 8, 9
 current, 8, 9
 density, 9
 field, 8
 intensity, 9
 flux, 8, 9
 polarization, 12
 susceptibility, 12, 24
 wall, 21, 184, 186, 260
 electrical length, 58
 EM
 fields
 in a dielectric material, 19
 in a lossy material, 24
 in a magnetic material, 10
 in a metal, 20
 embedded differential line, 140
 energy storage
 electric, 135
 magnetic, 136
 equation
 cubic, 48
 Helmholtz, 257
 Laplace, 141
 Maxwell's, 182, 256
 quadratic, 48
 wave, 56, 257
 even-mode, 207
 capacitance, 217
 characteristic impedance, 207
 coupled lines, 207
 effective permittivity, 220
 expansions
 series, 40
 trigonometric, 41
 exponential, 39
 series expansion, 40

 Faraday's law, 18
 farads, 9
 ferrite, 272
 electrical properties, 137
 FGCPW, 139, 157
 field
 electric, 8
 intensity
 electric, 9
 magnetic, 9
 magnetic, 8
 filling factor, 150
 filter
 slow wave, 194
 finite ground CPW, 157
 flux
 density
 electric, 9
 magnetic, 9
 electric, 8, 9
 magnetic, 8, 9
 formulas
 area, 40
 cubic, 48
 hyperbolic, 39
 quadratic, 48
 tanh, 39
 telegrapher's equation, 56
 volume, 40
 forward
 traveling wave, 56, 69
 FR4
 electrical properties, 137
 microstrip, 146, 148
 free space, 54, 60, 146
 frequency, 57
 radian, 57
 fundamental units, 123

 g, 123
 GaAs, 194
 electrical properties, 137
 gallium arsenide, 194
 electrical properties, 137
 Gauss's law, 17
 magnetism, 18
 Gbps, 124
 geometric series
 expansion, 41
 GiB, 124
 gibi, 124
 gibibit, 124
 Gibit, 124
 gigabit, 124
 glass, electrical properties, 137
 grad operator, 37
 gram, 123
 Greek alphabet, 127
 Greek letters, 127
 group
 velocity, 53, 57, 91
 and phase velocity, 57
 guide wavelength, *see* λ_g

- H**, 8
 h , 125
 Hammerstad, 219
 heat capacity
 specific, 127
 volumetric, 127
 Helmholtz equations, 257
 henry, 9
 homogeneous line, 137, 138
 hybrid
 directional coupler, 232
 hyperbolic function, 39

 I , 230
 identities
 ∇ , 39
 del operator, 39
 trigonometric, 34
 $\Im \{ \}$, 56
 impedance
 intrinsic, 260
 wave, 260
 incremental
 area, 9
 length, 9
 volume, 9
 index of refraction, 19
 inductance
 internal conductor, 171
 inhomogeneous
 line, 138
 medium, 141
 InP
 electrical properties, 137
 input
 impedance
 lossy line, 87
 reflection coefficient
 lossless line, 71
 lossy line, 87
 interconnect, 133, 135
 interdigital section, 238
 interpolation
 bilinear, 45
 linear, 44
 intrinsic impedance, 260
 inverse, matrix, 43, 44
 inverter
 lumped-element
 model, 109
 isolation, 230
 directional coupler, 230
 isotropy, dielectric, 12

 J , 123
J, 8
 j , 34
 Jensen, 219
 Joule, 123

 K, 123
 k, 257
 k , 184
 k_c , 184
 kbps, 124
 Kelvin, 123
 kg, 123
 KiB, 124
 kibi, 124
 kibibit, 124
 Kibit, 124
 kilo, 124
 kilobit, 124
 kilogram, 123
 Kirchhoff's laws, 56
 Kron's method, 48

 L , 51
 Lagrange's formula, 37
 Lange coupler, 236
 Laplace, 141
 law of cosines, 33
 length
 electrical, 58
 incremental, 9
 line
 characteristic impedance
 rectangular coaxial line,
 110
 square coaxial line, 110
 coaxial line, 111
 lossless
 input reflection
 coefficient, 71
 lossy
 input impedance, 87
 parallel wires, 110
 rectangular coaxial line,
 110
 slabline, 111
 square coaxial line, 110
 twisted pair, 111
 wire-in-box, 110
 linear
 interpolation, 44
 ln
 series expansion, 41
 logarithm
 series expansion, 41
 longitudinal field, 115, 134
 loss
 dielectric, 25
 tangent, 25, 135
 transmission line, 61
 lossless
 line
 input impedance, 73, 88
 medium, 60
 lossy
 conductor, 26

 dielectric, 24
 line
 input reflection
 coefficient, 87
 mediums
 and EM fields, 24
 low-loss line
 attenuation
 coefficient, 89
 lowpass filter, 85
 LTCC
 electrical properties, 137
 lumped element
 inverter, 109
 quarter-wavelength line,
 109

m, 8
 m , 123
 m_e , 125
 magnetic
 charge, 8, 9
 density, 9
 current, 8, 9
 density, 9
 energy, 10
 field, 8
 intensity, 9
 flux, 8, 9
 density, 9
 material, 136, 138
 and EM fields, 10
 moment, 136
 wall, 23, 184, 186, 260
 magnetostatic, 194
 matching
 network
 coupled lines, 221
 material, 135
 dielectric and EM fields,
 19
 lossy mediums and EM
 fields, 24
 magnetic and EM fields,
 10
 metal and EM fields, 20
 properties, 127
 mathematical
 foundations, 33
 matrix
 inverse, 43
 operations, 43
 transpose, 43
 maximum
 available power, 94
 power transfer
 theorem, 94
 Maxwell, 7
 Maxwell's equations, 7,
 182, 256

 integral form, 15
 phasor form, 14, 15
 point form, 7
 Maxwell-Wagner
 capacitor, 194, 196
 Mbps, 124
 meander section, 238
 mebi, 124
 mebibit, 124
 medium, 59, 136, 137
 lossless, 60
 megabit, 124
 metal
 -insulator-
 semiconductor,
 194
 -oxide-semiconductor,
 194
 and EM fields, 20
 meter, 123
 metric system, 123
 MiB, 124
 Mibit, 124
 MIC, 138
 microstrip, 133, 134, 137,
 138, 150, 151
 alumina, 146, 148
 characteristic impedance
 frequency-dependent,
 177
 conductor loss, 193
 coupler, 230
 design formulas, 152
 dielectric loss, 193
 dielectric mode, 187
 discontinuity
 open-circuit, 193
 effective permittivity
 frequency-dependent,
 176
 FR4, 146, 148
 frequency-dependent,
 168
 frequency-dependent
 characteristic
 impedance, 177
 frequency-dependent
 effective permittivity,
 176
 GaAs, 146
 high-frequency, 176
 higher-order mode, 185,
 188
 model, 140
 multimoding, 184, 185,
 187
 operating frequency
 limits, 185
 parasitic effects, 193
 PCB, 146, 148
 permittivity

- frequency-dependent, 176
- power losses, 193
- quasi-TEM, 141, 187
 - mode, 187
- radiation, 193
 - loss, 193
- resistance, 150
- Si, 146, 148
- silicon substrate, 194
- SiO₂, 146, 148
- slab mode, 187
- substrate mode, 187
- surface wave, 193
- TE, 187
 - mode, 187
- TM, 187
 - mode, 185, 187
- TM mode, 187
- transverse
 - resonance, 187, 189
 - resonance mode, 185
- via, 134
- waveguide model, 190
- wide strip, 153, 188
- microwave
 - integrated circuit MIC, 138
- MIS, 194, 196
- MMIC, 138, 194
- mode, 181
 - dielectric, 196
 - quasi-TEM, 139
 - skin-effect, 197
 - slow-wave, 197
 - TE, 184, 193, 263
 - TEM, 259
 - TM, 184, 193, 261
 - transverse
 - electric, 184
 - magnetic, 184
- model
 - lumped element inverter, 109
 - quarter-wavelength line, 109
- modes, 186, 260
- mol, 123
- mole, 123
- monolithic microwave
 - integrated circuit, 194
- MOS, 194
- multimoding, 180, 184
 - microstrip, 185
- multiplication, vector, 36
- N, 123
- nabla, 37
- Napier, 61
- natural
 - logarithm
 - series expansion, 41
 - number
 - series expansion, 40
- Neper, 56, 61
- network
 - condensation, 48
- newton, 123
- nickel, 136
- noise
 - room temperature resistor, 126
- nonhomogeneous
 - line, 135
 - medium, 135
- Np, 56, 61
 - dB equivalence, 61
 - definition, 61
- odd-mode, 207
 - capacitance, 217
 - characteristic impedance, 207
 - coupled lines, 207
 - effective permittivity, 220
- ohmic attenuation, 89
- operations
 - matrix, 43
- operator
 - vector, 36
- p.u.l. parameters, 55
 - P_A , 76
- Pa, 123
- parallel
 - lines, 205
 - plate waveguide, 256, 259
- parallel coupled line, 205
- parallel wires, 110
- parameters
 - ABCD
 - lossless transmission line, 109
 - lossy transmission line, 109
 - transmission line, 108
- chain
 - transmission line, 108
- pascal, 123
- passivation, 169
- PCB, 135, 169
 - microstrip, 146, 148
- PCL, 205
 - ABCD parameters, 240
- P_D , 76
- per unit length parameters, 55
- permeability, 8–10, 52, 54
 - complex, 136
 - effective relative, 60
 - free space, 54
 - of materials, 127
 - relative, 12, 54
 - RLGC relationship, 59
- permittivity, 8, 9, 12, 19, 52, 54, 135, 145
 - anisotropy, 12
 - complex, 135
 - dyadic, 12
 - effective, 141, 145, 147
 - effective relative, 60
 - free space, 54
 - imaginary part, 19, 135
 - of materials, 127
 - real part, 19, 135
 - refractive index, 20
 - relative, 12, 54, 135
 - RLGC relationship, 59
- phase
 - change coefficient, 56
 - coefficient, 56
 - constant, 56, 60–62
 - definition, 57
 - velocity, 53, 60, 62, 91, 141
 - and group velocity, 57
 - definition, 57
- phasor, 34, 35, 56
- phonon, 135
- physical constants, 125
- planar
 - interconnect, 133
- Planck constant, 125
- polarization, electric, 12
- polyimide, electrical
 - properties, 137
- polynomial
 - Butterworth, 42
 - Chebyshev, 42
- polynomial equation
 - cubic, 48
 - quadratic, 48
- power
 - available, 76
 - delivered, 76
 - flow, 93
- Poynting vector, 28
- printed
 - circuit board, 135
 - wiring board, 133, 135
- propagation
 - constant, 56, 89, 92
- properties, material, 127
- pulse, 135
 - q , 150
- quadratic equation, 48
- quarter-wave
 - transformer, 85
- quarter-wavelength line
 - lumped-element model, 109
- quartz, electrical
 - properties, 137
- quasi-TEM, 134
 - line, 138–140
 - mode, 194
- R , 51
- R_s , 174
- radian, 56, 61
- radiation, 138
 - loss, microstrip, 193
- radio
 - frequency integrated circuit, 139
- $\Re \{ \}$, 56
- rectangular
 - coordinates, 38
 - waveguide, 255, 264
- attenuator, 272
- bend, 271
- circulator, 272
- coaxial adaptor, 273
- components, 270
- directional coupler, 273
- discontinuity, 272
- tee, 271, 273
- termination, 271
- tuner, 274
- twist, 270
- variable attenuator, 272
- reflection
 - coefficient, 99
 - current, 68
 - electric field, 28
 - formula, 68
 - magnetic field, 28
 - voltage, 68
 - diagram, 98
- refractive index, 19
 - complex, 20
 - permittivity conversion, 20
- relative permeability, 136
- relaxation loss, 24
- resistance
 - sheet, 151, 155, 159
 - surface, 151, 263
- resistivity of materials, 127
- resistor
 - noise at room temperature, 126
- return loss, 93
- RFIC, 138, 139, 194
- RL, 93
- RLGC
 - permeability relationship, 59

- permittivity relationship, 59
- RLGC* model, 59
- room temperature, 126
 - noise of a resistor, 126
- R_{TH} , 77
- s, 123
- sapphire, electrical
 - properties, 137
- Schottky, 194
- semiconductor
 - lines, 194
- series
 - expansion, 40
 - binomial series, 41
 - e, 40
 - exponential, 40
 - exponential function, 40
 - geometric series, 41
 - ln, 41
 - natural logarithm, 41
 - natural number, 40
 - square root, 40
 - trigonometric, 41
 - trigonometric functions, 41
- sheet resistance, 151, 155, 159
- short circuit, 70
- SI, 61, 125
 - prefix, 124
 - unit combinations, 123
 - units, 123
- Si, 135, 194
 - electrical properties, 137
 - microstrip, 148
- silicon
 - dioxide, *see* SiO₂
- sin, 34, 39
 - series expansion, 41
- sinh, 39
 - series expansion, 41
- SiO₂, 135
 - electrical properties, 137
 - microstrip, 148
- skin
 - depth, 171
 - effect, 171, 173, 197
 - mode, 197
 - resistance, 174
- slab mode, 187
- slabline, 111
- slotline
 - radiation, 161
- slow-wave
 - effect, 194
 - mode, 197
- SMA, 64
- Sonnet, 171, 178
- sound speed, 127
- speed of light, *see* c, 125
- speed of sound, 127
- sphere
 - area and volume, 40
- spherical coordinates, 39
- square root
 - series expansion, 40
- standard
 - atmosphere, 125
 - temperature, 126
- Stoke's theorem, 16
- strip, 51
- stripline, 138, 139, 153
 - attenuation, 155
 - characteristic impedance, 154
 - high frequency, 192
 - modes, 192
 - multimoding, 192
 - suspended substrate, 156
 - TEM, 139
- stub
 - open, 82
- substrate, 134, 136
 - properties, 137
- substrate mode, 187
- surface, 9
 - charge
 - density, 9
 - density, magnetic, 9
 - current
 - density, electric, 9
 - density, magnetic, 9
 - resistance, 151
 - wave, 193
 - microstrip, 193
- surface resistance, 263
- susceptibility
 - electric, 12, 24
- symbols, 127
- system
 - impedance
 - coupled lines, 221
- Système International, *see* SI
- T , 230
- tan, 34, 39
 - series expansion, 41
- $\tan \delta$, 135
 - dielectric, 25
 - transmission line, 61
- tanh, 39
 - series expansion, 41
- Tbps, 124
- TE mode, 184, 263
- tebi, 124
- tebibit, 124
- tee, rectangular
 - waveguide, 271, 273
- telegrapher's equation, 210, 216
 - coupled lines, 210
 - even mode, 216
 - generalized, 210
 - lossless, 73
 - lossy, 88
 - odd mode, 216
- TEM, 134, 139, 141, 180, 182
 - line, 138
 - mode, 259
- temperature
 - absolute zero, 126
 - room, 126
 - standard, 126
- tensor, 11
- terabit, 124
- termination
 - rectangular waveguide, 271
- theory of small reflections, 102
- thermal conductivity, 127
- Thevenin, 76
 - resistance, *see* R_{TH}
- TiB, 124
- Tibit, 124
- TM mode, 184, 261
- total
 - current, 67
 - voltage, 67
- transformation
 - bilinear, 46
- transformer
 - quarter-wave, 85
- transmission
 - coefficient, 99
 - coupled lines, 230
 - voltage, 68
 - factor, 229, 230
 - directional coupler, 230
 - line, 51, 52, 70
 - ABCD parameters, 108
 - chain parameters, 108
 - coaxial, 52
 - coaxial, derivation of Z_0 , 111
 - current bunching, 169
 - dispersion, 91
 - dispersionless, 92
 - equations, 56
 - homogeneous, 137
 - loss, 193
 - low-loss approximation, 89
 - microstrip, *see* microstrip
 - mode, 181
- model, 140
- multimoding, 180, 184
- non-TEM, 110, 141
- nonhomogeneous, 135
- open-circuited, 79
- parallel wires, 110
- planar, 137
- quasi-TEM, 141
- rectangular coaxial line, 110
- schematic, 134
- semiconductor, 194
- short circuited, 79
- slabline, 111
- square coaxial line, 110
- TEM, 110
- terminated, 67, 72, 88
- terminated lossy, 90
- theory, 55, 56
- transformer, 85
- twisted pair, 111
- two conductor, 110
- wire-in-box, 110
- Z_0 of parallel wires, 110
- Z_0 of rectangular coaxial line, 110
- Z_0 of slabline, 111
- Z_0 of square coaxial line, 110
- Z_0 of twisted pair, 111
- line, lossless, 62, 66, 83
- input impedance, 73, 88
- input reflection
 - coefficient, 71
- line, lossy, 87, 90, 91
- input impedance, 87
- input reflection
 - coefficient, 87
- line, lossless, 78
- transpose, matrix, 43
- transverse
 - direction, 180
 - electric mode, 184, *see* TE mode
 - electromagnetic, 134
 - field, 53, 115, 141
 - magnetic mode, 184, *see* TM mode
 - plane, 114
 - resonance, 189, 190
- traveling
 - pulse, 69
 - step, 70
 - wave, 67, 69
- triangle, relationship of angles, 33
- trigonometric
 - derivatives, 34
 - identity, 34
 - series expansions, 41
- tuner

-
- rectangular waveguide, 274
 - twist
 - rectangular waveguide, 270
 - twisted pair, 111
 - two-wire line, 51
 - unit
 - amount of substance, 123
 - cgs, 123
 - charge, 123
 - current, 123
 - energy, 123
 - force, 123
 - length, 123
 - luminous intensity, 123
 - metric, 123
 - mks, 123
 - power, 123
 - SI, 123
 - time, 123
 - V, 123
 - v_g , definition, 57
 - v_p , definition, 57
 - vector
 - cross product, 37
 - dot product, 36
 - multiplication, 36
 - operator, 36
 - ∇ , 37
 - curl, 37
 - del, 37
 - div, 37
 - grad, 37
 - velocity
 - group, 53, 57, 91
 - phase, 53, 57, 91
 - volt, 123
 - voltage
 - reflection coefficient, 68
 - standing wave ratio, 75
 - transmission coefficient, 68
 - volume, 9
 - formula, 40
 - incremental, 9
 - integral, 9
 - VSWR, 73, 75
 - W, 123
 - wall
 - electric, 21
 - magnetic, 23
 - watt, 123
 - wave
 - equation, 56, 257
 - rectangular, 256
 - impedance, 28, 260
 - waveguide
 - attenuator, 274
 - bands, 271
 - bend, 271
 - circulator, 272
 - coaxial adaptor, 275
 - horn antenna, 275
 - hybrid, 277
 - impedance transformer, 272, 275
 - parallel-plate, 181, 256, 259
 - rectangular, 255, 264
 - switch, 273, 275
 - taper, 275
 - termination, 274
 - wavelength, 13, 60, 62, 181
 - definition, 57
 - wavenumber, 184, 257
 - cutoff, 184, 257
 - definition, 57
 - weber, 9
 - wirebond, 237
 - Z_0 , free-space impedance (use η_0), 220
 - Z_0 , 56
 - Z_{0o} , *see* odd-mode impedance
 - Z_{0e} , *see* even-mode impedance

Microwave and RF Design: Transmission Lines builds on the concepts of forward- and backward-traveling waves. Many examples are included of advanced techniques for analyzing and designing transmission line networks with microstrip lines primarily used in design examples. Coupled-lines are an important functional element in microwave circuits, and circuit equivalents of coupled lines are introduced as fundamental building blocks in design. The text and examples introduce the often hidden design requirements of mitigating parasitic effects and eliminating unwanted modes of operation. This book is suitable as both an undergraduate and graduate textbook, as well as a career-long reference book.

KEY FEATURES

- The second volume of a comprehensive series on microwave and RF design
- Open access ebook editions are hosted by NC State University Libraries at:
<https://repository.lib.ncsu.edu/handle/1840.20/36776>
- 56 worked examples
- An average of 31 exercises per chapter
- Answers to selected exercises
- Focus on planar lines including microstrip
- A companion book, *Fundamentals of Microwave and RF Design*, is suitable as a comprehensive undergraduate textbook on microwave engineering

ABOUT THE AUTHOR

Michael Steer is the Lampe Distinguished Professor of Electrical and Computer Engineering at North Carolina State University. He received his B.E. and Ph.D. degrees in Electrical Engineering from the University of Queensland. He is a Fellow of the IEEE and is a former editor-in-chief of *IEEE Transactions on Microwave Theory and Techniques*. He has authored more than 500 publications including twelve books. In 2009 he received a US Army Medal, "The Commander's Award for Public Service." He received the 2010 Microwave Prize and the 2011 Distinguished Educator Award, both from the IEEE Microwave Theory and Techniques Society.

OTHER VOLUMES

Microwave and RF Design
Radio Systems
Volume 1
ISBN 978-1-4696-5690-8

Microwave and RF Design
Networks
Volume 3
ISBN 978-1-4696-5694-6

Microwave and RF Design
Modules
Volume 4
ISBN 978-1-4696-5696-0

Microwave and RF Design
Amplifiers and Oscillators
Volume 5
ISBN 978-1-4696-5698-4

ALSO BY THE AUTHOR

Fundamentals of Microwave
and RF Design
ISBN 978-1-4696-5688-5